TA 350 .T58
C3
00826
3 1735 008 794 889

UNIVERSITY
OF PITTSBURGH

LIBRARIES

Digitized by the Internet Archive
in 2023 with funding from
No Sponsor

https://archive.org/details/bwb_P8-ALV-466

APPLIED ELASTICITY

BY

S. TIMOSHENKO
Formerly Professor of Mechanics in Kiev and Petrograd Polytechnical Institutes
Research Engineer, Research Dept., Westinghouse Electric and Mfg. Co.

AND

J. M. LESSELLS, B.Sc., A.M.I.Mech.E.
Mechanical Engineer, Research Dept., Westinghouse Electric and Mfg. Co.

First Edition

WESTINGHOUSE TECHNICAL NIGHT SCHOOL PRESS
EAST PITTSBURGH, PA.
1925

Copyright, 1925
Westinghouse Technical Night School Press

PRINTED IN THE UNITED STATES OF AMERICA

THE MAPLE PRESS COMPANY, YORK, PA.

PREFACE

The trend of modern industrial development is more and more towards the free acceptance and application of the teachings of pure science. Today those countries which have made the greatest industrial progress in the last decade are those which, having accepted these principles, are now characterized by the intensive application of scientific thought.

This tendency is making itself felt also in the field of education by the stimulation of the development of technical instruction. It has furthermore been influential in the founding of special institutions for undertaking and applying scientific research. The time was when it was generally considered that an engineer required principally a practical training without a very deep scientific education. This, however, is past and gone, and now it is necessary for him to have a training in the branches of science nearest to his specialty and the curricula of modern technical institutions are so arranged that provision is now made for studying those subjects. On the other hand, pure scientific institutions no longer consider the real problems as outside of their interest. For example, two famous Universities, Cambridge in England, and Göttingen in Germany have created chairs of engineering for the study of the applications of pure science. This attempt to bridge over the gap between pure science and engineering can have a high practical significance, and good results must be expected to accrue from such an understanding. In a word, the importance of scientific research in the solution of technical problems has been generally accepted by industry, and not only do we see in existence large central laboratories, such as the Bureau of Standards in this country, but private research laboratories as well, and we firmly believe that the role of such research establishments will become more and more important, as the years go by, in the dissemination of knowledge beneficial alike to industry and to science.

The reason for the increased recognition of the importance of pure science lies in the rapid development in modern industry itself. The engineer of the past had sufficient time to arrive at a solution of technical problems in an empirical manner by a slow step by step progress. In such a manner the engineer of old used his structure as an example for experiment, and this may have been justified by the very slow development of the industry; but this is not adequate now where there is not sufficient time to get the necessary data and where this kind of experiment would become very expensive. It is clear that in such cases the development of experimental laboratories for obtaining the necessary data for solving design problems is of first importance. New branches of industry developed principally during the last 25 years such as, for example, electro-technique, electric traction, aircraft, steam turbines and internal combustion engines are characterized by the intensive use of the weapon of science and owe to it their very existence and meteoric progress.

This general tendency can be seen also in the increased use of the mathematical theory of elasticity for solving technical problems. The importance of preliminary analyses in structures and in modern machine design continues to increase. In many cases of modern design the elementary solutions given by the strength of materials are insufficient and recourse has to be made to the mathematical theory of elasticity in order to obtain a more fundamental solution. Take, for instance, such important questions as concentration of stresses produced by holes, notches or sharp variation in cross-section of bars. Many failures in machines can be attributed to these high localized stresses, especially in cases where variable forces and vibrations are encountered. Elementary theory is useless in providing a method for calculating these stresses and only by using the general theory of elasticity is it possible to find a solution for this kind of problems.

Another type of problem where mathematical analysis becomes of practical importance is that where dynamic stresses are produced. In the cases of high speed machines where vibrations and impact are encountered it is not possible to obtain good results by a mere increase in dimensions. In these cases analysis alone can contribute toward finding a satisfactory solution. In this way solutions of problems on stress distribution in rotating discs, drums, or flywheels, critical speed for rotating shafts, torsional vibrations in shafts and in geared systems can be obtained. Not only can the application of theory assist in finding a solution of practical problems, but the continued use of such theory contributes to the progress in the theory itself by the development of approximate methods. Great progress has been made in recent times in developing these methods for solving the differential equations encountered in elasticity. Special graphical and numerical methods of solving these equations have been developed.

In cases where analysis is insufficient to procure an adequate solution, experimental methods of studying stress-distribution have been found. For instance, the photo-elastic method of determining stresses by experimenting with models of transparent material has now attained great practical importance. The determination of stresses in twisted bars by using the so-called "membrane analogy" represents another conspicuous example where success has been obtained by the application of scientific methods to the solution of these problems. Furthermore, the convincing results obtained by using the known hydrodynamical analogy in the solution of complicated problems of local stresses occuring in twisted prisms are well known. All this shows us what advantages can be expected from cooperation between the pure and applied sciences.

What is true for analysis is also true for experimental work in elasticity. There was a time when plain carbon steels were the only ones used in construction. Now there are a great variety of special materials employed and these can be intelligently applied only by a careful study of the characteristics of each. That this has been fully appreciated can be seen at once by considering the progress of metallurgical science and testing of materials during the last two decades and contrasting this with the fact that the first Congress on testing materials was held only about 50 years ago. Today all good technical institutions have a well developed laboratory for the testing of materials. Not only do the above facts make it essential to know the characteristics of the materials being used but also industrial establishments are being compelled to face greater and greater competition. This drives the designer to higher stress values and renders it still more imperative for him to have a knowledge of the materials he uses.

There is again the factor of weight. In the olden times the designer of stationary steam engines was not troubled about the total weight of the prime mover. This is not true today with regard to the design of aircraft or submarine engines. Here the consideration of weight is of prime importance. Development in the testing of materials has also shown that the static test does not tell the whole story and that recourse has to be made to dynamic forms of testing for material selection.

Following the general tendency about which we have spoken we have decided to give a contribution in this direction. In the first part of this volume we give some advanced chapters on the analysis of stresses and in the second part some on the mechanical properties of materials, principally metals, used in modern construction. The work was divided in such a manner that the analytical part was done by S. Timoshenko and the experimental part by J. M. Lessells. During the development each chapter was jointly discussed with the object in view of having complete continuity between the two parts of the book. Whether this work will be satisfactory we will leave to our readers to judge, but of this we are certain, the time is here when the analysis of stresses and the study of the mechanical properties of materials has become a positive necessity as an initial step in design work.

S. TIMOSHENKO.
J. M. LESSELLS.

RESEARCH DEPT., WESTINGHOUSE
ELECTRIC & MFG. CO.,
EAST PITTSBURGH.

PREFACE TO PART I

Following the general idea outlined in the preface, the intention is to develop in the analytical part of the volume, some advanced chapters devoted to the theory of strength of materials, which may be of practical interest to the designer in mechanical engineering. It is also the intention to bring to the attention of engineers, some solutions based on the mathematical theory of elasticity for those cases of stress distribution where elementary methods cannot give satisfactory results. New methods such as application of trigonometrical series in obtaining deflexion curves and application of Raileigh-Ritz method in considering vibration problems, are also discussed in this volume. In order to simplify the use of the book, a short review of the usual elementary theories is given in the first chapters, and several numerical examples with complete solutions. In developing this book, the author has followed very closely, the content of his previously published book on the strength of materials.*

The contents of the book in general are as follows:

In Chap. I the general formulae for tension and compression of prismatical bars are developed and afterwards, the more complicated problems are discussed, such as tension of non-prismatical bars, concentration of stresses produced by holes and notches, stresses in thin vessels submitted to internal pressure, and local stresses at the surface of contact of balls and rollers submitted to compression.

Chapter II includes a review of the usual theory of circular shafts, torsion of shafts of non-circular cross sections, a detail discussion of the method of applying the hydrodynamical and membrane analogies to the solution of such problems. The important problem of twist of shafts of variable cross section and the consideration of the effect of fillets on stress concentration have likewise found a place in this chapter.

Chapter III contains a recapitulation of the usual theory of stresses in beams. Comparison is made of the usual formulae for the normal and shearing stresses with exact solutions based on the theory of elasticity.

---

*"Strength of Materials" first edition, Kieff, 1911, Russia. 5th edition, St. Petersburg, 1923.

In Chap. IV various methods are developed for obtaining deflection curves. The grapho-analytical method combined with the principle of superposition, are discussed in detail. This method is usually much shorter and clearer than the analytical method. Its importance in the solution of beam problems cannot be over emphasized. The deflection of beams of variable cross section and the deflection due to shearing force, are discussed in the latter part of the chapter.

Statically undeterminate cases of bending are discussed in Chap. V. The principle of superposition and general theorems such as Castigliano theorem, theorem of least work, and reciprocal theorem, are used in the solution of this kind of problems.

Chapter VI contains the theory of bending of bars on elastic foundation. This theory can be applied to the solution of many practical problems such as deflection of railway tracks, stresses in circular tubes when the deformation is symmetrical about the axis, rotating drums, thermal stresses in thin cylinders, and many others of a similar nature. Several problems of this kind are considered in detail in this chapter.

In Chap. VII the theory of bending combined with longitudinal loading is developed. Such problems as struts and tie-rods having lateral loads are discussed in detail. The application of trigonometrical series to the solution of these problems is analyzed and simple approximate formulae for deflections are given. The latter part of the chapter is devoted to the column theory. A new approximate method for solving column problems is developed and applied in many important cases, such as column theory of bars uniformly loaded in axial direction, column theory of latticed bars, and bars of variable cross section.

Chapter VIII contains the theory of combined bending and torsion. After reviewing the usual theory of circular shafts, the theory of bending and twist of crank shafts on many supports is developed. The problem of deformation of open coiled helical springs is placed in this chapter.

In Chap. IX the general theory of bending of curved bars is developed and several applications of the theory in the solution of practical problems are explained. Such problems as those dealing with the deformation of circular rings, deformation of thin cylinders submitted to internal and external pressure, the collapse of cylindrical tubes submitted to external pressure, and the bending of curved tubes, are considered in detail.

Chapter X deals with the theory of bending of plates. The bending of rectangular plates when deflected under the action of uniformly distributed load, is considered in detail. Several numerical tables facilitating the determination of deflexions and stresses are given. Subsequent to the discussion of a common theory on the bending of circular plates, some new data on the buckling of plates under pressure and shear in their middle plane is given.

The important problems on dynamical stresses produced in moving machine parts by inertia and vibrations are considered in the last chapter. After a review of the general theory of vibration of elastic systems several practical problems are discussed such as stresses in rotating turbine discs, critical speed of shafts, torsional vibrations of shafts, and stresses produced during impact.

The author takes this opportunity of thanking numerous friends who have assisted him by suggestions, reading of manuscript, or checking examples; particularly his co-author John M. Lessells who has read over the complete manuscript. Credit is also due to Mr. R. H. Bailey of Metropolitan Vickers, Manchester, for reading over the manuscript of Chap. XI and to the members of the Mechanical Design School of the Westinghouse Elec. & Mfg. Co. (1924), for assistance in checking a part of the work.

S. TIMOSHENKO.

PREFACE TO PART II

In presenting this work on the experimental side of the subject of elasticity the author has not only given his own views, supported as far as possible by results obtained by him, but has made reference in the text to the results obtained by other investigators in that particular sphere. These references cover publications made in this country, England, Germany, and France. Some of the points, while not new, are brought into a text book for the first time, while others, on the other hand, are new.

In Chap. XII the author has tried to give a clear conception of definitions realizing to the fullest extent how important these are to the engineer. It is conceivable that paradoxial situations may arise due to the fact that an interpretation is put on a particular physical value not intended by the definition. The importance of the reduction of area value is discussed and some new methods of measuring this on particular geometrical shapes are given. A paragraph on the effects of chemical analysis contains data presented in such a way that it can be easily interpreted by the designer. Other important points such as speed of testing and temperature effects are also given.

In Chap. XIII a discussion with numerical results is made of the effects of cold work and overstrain. A general consideration is also made here on the factors which tend to influence the shape of the tensile test diagram and certain theories are advanced regarding the effects of internal stress.

Chapter XIV is devoted to the dynamic form of testing by impact. An endeavor is made here to explain just what the designer can expect of high impact values. A certain amount of space is given to the discussion of the results obtained from repeated impact tests and certain conclusions are made regarding their value.

Hardness, a rather indefinite term, according to our modern conceptions comes under review in Chap. XV. In addition to discussing the importance of being able to measure certain forms of hardness a review is made of new literature on the subject which includes the more recently developed pendulum method.

The next chapter is devoted to the subject of fatigue. Since this is the phase in which the author at present is most interested, there *is* much data given, certain of which *is* new on the fatigue properties of a variety of steels, including cast material. A considerable portion of the chapter is devoted to a discussion of the value of short time methods for determining the endurance limit, especially the one involving the measurement of deflection of the test bar. Experimental data is given, showing in a manner what may be expected from such tests.

Chapter XVI is devoted to the theory of strengths. This is possibly the first time that a full chapter has been given to such a subject in an engineering text book. The discussion of the various theories will be of value to the engineer in dealing with the solution of combined stress problems.

The culmination of the whole experimental part of the work appears in the final chapter on working stresses. Here the numerical data obtained for commonly used and special steels, presented *so* that it can be immediately used, together with the various methods of so proportioning the limiting stress values in design, forms a fitting conclusion to this work.

In presenting this work the author has been ably assisted by his co-author, S. Timoshenko. Not only does this refer to the critical survey made of each chapter especially Chap. XVIII but also to the help given in reviewing German publications. The author wishes to record his appreciation of this assistance. Mr. R. H. Bailey of Metropolitan Vickers, Manchester has also read over this part of the work and his suggestions have been very helpful. Acknowledgment must also be made to Dr. L. Aitchison for his review of Chap. XIII, to Sir Robert Hadfield for reviewing Chap XIV and XV and to Prof. H. F. Moore for his criticisms of Chap. XVI. Mr. P. Irwin and Mr. R. Wilhelm also have the authors thanks for the experimental data they have contributed. To the latter worker especial thanks are due for his criticisms in general. The best thanks of the author are also extended to the following Technical Societies from whose proceedings the author has obtained many figures: The Institution of Mechanical Engineers London, The Institution of Automobile Engineers London, The Iron and Steel Institute, The American Society for Testing Materials and The American Society for Steel Treating.

J. M. Lessells.

CONTENTS OF PART I

CHAPTER I

TENSION AND COMPRESSION

1. Tension and Compression of Prismatical Bars 1
2. Tension and Compression of Bars of Variable Cross-section 8
3. Combined Stress 11
4. Graphical Representation of Combined Stress, by Mohr's Circle 13
5. General Case of Stresses 16
6. Vessels Subjected to Internal Pressure 17
7. Compression of Balls and Rollers 21

CHAPTER II

TORSION

8. Shafts of Constant Circular Cross-section 26
9. Helical Spring Close Coiled 30
10. Shafts of Non Circular Cross-section 32
11. Torsion of Circular Shafts of Variable Cross-section 35
12. Hydrodynamical Analogy 42
13. Membrane Analogy 44

CHAPTER III

STRESSES IN BEAMS

14. Pure Bending 50
15. Bending Moment and Shearing Force 59
16. Normal Stresses 62
17. Shearing Stresses 63
18. Principal Stresses in Beams 67
19. Beams of Variable Section 68

CHAPTER IV

DEFLECTION OF BEAMS

20. Deflection Due to Bending Moment 71
21. Principle of Superposition 77
22. Graphical Method 82
23. Grapho-analytical Method 84
24. Deflection of Beams of Variable Cross-section 90
25. Deflection Due to Shearing Force 94

CHAPTER V

STATICALLY INDETERMINATE CASES OF BENDING

26. General Considerations 98
27. Beams—One End Built In and the Other Simply Supported 99
28. Beams with Built in Ends 102
29. Frames 105
30. Beams on Three Supports 110
31. Continuous Beams 112
32. Potential Energy of Deformation 117
33. Theorem of Castigliano 119
34. Theorem of Least Work 123
35. Reciprocal Theorem 126
36. Deflection Curve Represented by a Trigonometrical Series 129

CHAPTER VI

BENDING OF BARS ON ELASTIC FOUNDATION

37. General Equation of Deflection Curve 133
38. Infinitely Long Bar 134
39. Stresses in Railway Track 141
40. Deformation of a Cylindrical Tube Symmetrical about the Axis 143
41. Thermal Stresses in Hollow Cylinders Due to Non-uniform Heating along the axis of the Cylinder 146

CHAPTER VII

DIRECT AND BENDING STRESSES

42. Eccentric Longitudinal Load 153
43. Struts with Lateral Loads 156
44. Tie-rod with Lateral Loading 159
45. Application of Trigonometrical Series 161
46. Column Theory 164
47. Energy Method 169
48. Buckling of Bars of Variable Cross-section 175
49. Buckling of Latticed Struts 177

CHAPTER VIII

COMBINED BENDING AND TWIST

50. Circular Shafts 183
51. Single Throw Crankshaft 188
52. The Multi-throw Crankshaft 199
53. Application of Equations to a Three-throw Crankshaft 203
54. Open Coiled Helical Spring 209

CHAPTER IX

CURVED BARS

55. Theory of Bending 216
56. Particular Cases 220
57. Deflections of Curved Bars. 226
58. Circular Ring 232
59. Symmetrical Ring Submitted to Uniform Pressure 242
60. The Buckling of Circular Rings and Tubes under External Pressure . . 245
61. Thick Cylinder. 249
62. Bending of Curved Tubes 255

CHAPTER X

THIN PLATES

63. Bending of a Plate to a Cylindrical Surface. 260
64. Combination of Pure Bending in Two Perpendicular Directions 268
65. Bending of Circular Plates. 273
66. Uniformly Loaded Circular Plate 276
67. Circular Plate Loaded in the Center. 279
68. Circular Plate Uniformly Loaded along a Concentric Circle. 281
69. Deflection of a Circular Plate having a Circular Hole at the Center. . . . 284
70. Bending of Rectangular Plates. 288
71. Buckling of Rectangular Plates. 291

CHAPTER XI

STRESSES PRODUCED BY DYNAMICAL CAUSES

72. Effect of Inertia Forces 296
73. Rotating Discs. 301
74. Vibrations of Elastic Systems. 312
75. Free Vibrations. 313
76. Approximate Methods for Calculating Frequency of Natural Vibrations of a System 318
77. Rayleigh-Ritz Method 322
78. Damped Vibrations. 324
79. Forced Vibrations. 328
80. Torsional Vibrations 337
81. Impact 344

CONTENTS OF PART II

CHAPTER XII

Tension and Compression

Tension

82. General 352
83. Definitions: Elastic and Transition Stages 356
Elastic Limit—Proportional Limit—Yield Point—Elasticity.
84. Definitions: Plastic and Breaking Stage 360
Ultimate Stress—Elongation—Reduction of Area.
85. Significance of Tensile Test to Designers 364

Compression

86. General 364
87. Compression of Ductile Materials 365
88. Compression of Brittle Materials 366

Chemical Analysis

89. General 370
90. Carbon Steel 371
Annealed or Normalized—Heat-treated.
91. Alloy Steels 376
Annealed or Normalized—Heat-treated.
92. Light Alloys 379

Effect of Speed

93. General 380
94. Brittle Material 380
95. Ductile Material 380
96. Very Ductile Materials 381
97. Conclusions 382

Effects of High Temperature

98. General 383
99. Steels 383
Effect on Elastic Properties—Effect on Ultimate Stress and Ductility
100. Non-ferrous Alloys 389
101. Cast Iron 391
102. Conclusions 391

CHAPTER XIII

THE ELASTIC STAGE MODIFICATIONS

103. Overstrain 392
General—Low and Medium Carbon Steels—High Carbon and Alloy Steels—Conclusions.
104. Cold Work and Quenching Effects 396
Cold Work—Quenching—Practical Application.
105. Time Effect—Stresses within Elastic Limit 401
General—Elastic after Effects.
106. Time Effect—Stresses beyond Elastic Limit 402
General—Geiss Theory—Effect of Internal Stress.
107. Hysteresis 406
Hysteresis looping in Metals—Hysteresis Looping in Crystals—Conclusions.
108. Internal Stress 411
General—Annealed State—Rolled, Cast, and Normalized States—Heat-treated States—Overstrained States.
109. Amorphous Theory 414

CHAPTER XIV

IMPACT TESTS

110. General 418
Importance of Dynamic Tests—Un-notched Bar Tests—Importance of Stress Measurement.
111. Notched Bar Tests 421
Scope—Effect of Dimensions—Effect of Speed—Effect of Temperature—Carbon Steel—Alloy Steel—Notch Brittleness—Appearance of Fractures.
112. Repeated Blow Tests 434
General—Results—Discussion—Effect of Temperature.
113. Significance of Impact Test to the Designer 443

CHAPTER XV

HARDNESS

114. Introduction 444
115. Indentation Hardness 444
Material tested with itself—Ball Method—Cone Method.
116. Dynamic Tests 452
General—Sclerescope—Pendulum.
117. Scratch Tests 454
118. Significance of Hardness Test to the Designer 458

CHAPTER XVI

FATIGUE

119. General. 460
120. Looping during Cyclical Stress. 462
121. Changes in Crystals 465
122. Cycle of Complete Stress Reversal 466
Preliminary Statements—Carbon Steel—Alloy Steel—Steel Castings —Cold Worked Material—Non Ferrous Metals.
123. Cycle of Stress Variation 477
124. Effect of Form 480
125. Effect of Surface Finish. 482
126. Effect of Speed 485
127. Effect of Temperature 486
128. Short Time Methods. 487
General—Strain Method—Rise in Temperature Method—Repeated Blow Tests.
129. Significance to the Designer. 496

CHAPTER XVII

THEORY OF STRENGTHS

130. General. 497
Simple Stress—Combined Stress.
131. Variety and Scope of Theories. 498
132. Maximum Stress Theory 498
133. Maximum Strain Theory 500
134. Maximum Shear Theory 501
135. Mohr Theory 503
136. Other Theories 504
137. Limitations. 506
138. Conclusions. 507
Simple Torsion—Bending and Twist—Thick Cylinder—Application of Mohr Theory.

CHAPTER XVIII

WORKING STRESSES

139. Introduction 513
140. Static Loading. 515
Simple Stress—Combined Stress.
141. Dynamic Loading 516
General—Reversal of Stress —Variation of Stress—Combined Stress.
142. Other Types of Loading 520
Buckling—Vibrations—Impact.
143. Tables of Tensile and Fatigue Values. 522

APPLIED ELASTICITY
PART I

APPLIED ELASTICITY

CHAPTER I

TENSION AND COMPRESSION

1. Tension and Compression of Prismatical Bars.—Considering the simple extension of a prismatical bar of homogeneous material caused by forces acting along the axis of the bar as in Fig. 1, let:

P = tensile force in lbs.

A = area of cross section in sq. inch.

l = length of the bar in inches.

δ = extension of the bar in inches.

e_x, e_y = unit elongation in the direction of the X axis and of the Y axis respectively.

p = stress in lbs. per sq. inch.

q = pressure, in lbs. per sq. inch.

$\frac{1}{m}$ = Poisson's ratio.

E = Modulus of Elasticity.

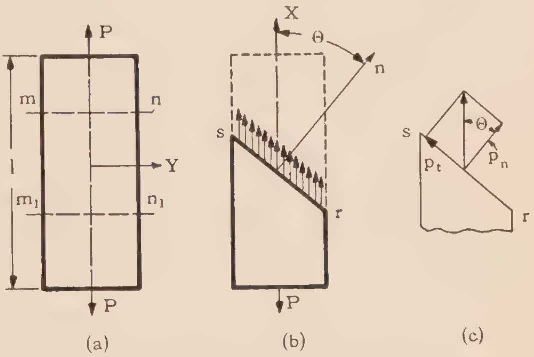

Fig. 1.—Stress distribution in simple tension.

Cross-section Perpendicular to Load.—On the assumption that every cross-section of the bar remains plane and perpendicular to the axis of the bar after extension, it can be concluded that the unit elongations of all longitudinal fibres are the same. Therefore the *stresses* are uniformly distributed over every cross-section of the bar, such as *mn*, and are determined as follows:

$$p = \frac{P}{A}. \qquad (1)$$

The extension of the bar within the elastic limit is represented by the well-known *Hooke's law,*

$$\delta = \frac{Pl}{AE}, \tag{2}$$

and the *unit elongation* becomes

$$e_x = \frac{\delta}{l} = \frac{p}{E}. \tag{3}$$

Plane Inclined at θ° to Load.—For any inclined section such as *s-r* (Fig. 1 (b)) the area of the section is $A_\theta = \frac{A}{\cos\theta}$, and the corresponding stress in the direction of tension,

$$p_\theta = \frac{P}{A_\theta} = p\cos\theta. \tag{4}$$

Resolving this stress into two components at right angles as shown in Fig. 1 (c), the following expressions for the *normal* and the *tangential stresses* across the section under consideration are obtained:

$$p_n = p\cos^2\theta \tag{5}$$

$$p_t = p\cos\theta\sin\theta = \frac{p\sin 2\theta}{2}, \tag{6}$$

from which it will be noted that the maximum normal stress acts across the section perpendicular to the axis of the bar and the maximum tangential stress acts across the section inclined at 45° to the axis of the bar.

Lateral Contraction.—From experimental evidence, it is well known that a longitudinal extension of a bar is always accompanied by lateral *contraction.* This contraction is only a fraction of the longitudinal extension and can be calculated from the formula

$$e_y = -\frac{1}{m}e_x \tag{7}$$

in which $1/m$ is a constant (*Poisson's ratio*), depending on the elastic property of the material. In the case of steel, $1/m$ is usually taken as .30. The minus sign would show that e_y is contraction.

In the case of compression, the foregoing formula can be used by considering the force and its corresponding deformation as negative.

Thermal Stress.

When a bar is heated from a temperature t_0 to t, the unit elongation is $e = \alpha(t - t_0)$, where α denotes the *coefficient of expansion* of the material. If this expansion is prevented by fastening the ends of the bar, compressive *thermal stresses* will be produced. The magnitude of these stresses can easily be determined from the equation

$$\frac{p}{E} = \alpha(t - t_0) \tag{8}$$

The application of this equation is shown in some numerical examples below.

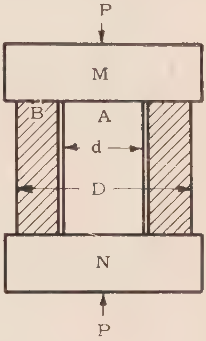

FIG. 2.

Example 1.—Referring to Fig. 2, if a steel cylinder A and copper tube B are compressed between the blocks M and N, determine the stresses in steel and copper and also the unit compression, if $P = 100{,}000$ lbs., $d = 4$ ins., $D = 8$ ins., $E_{\text{steel}} = 30 \times 10^6$ lbs. per sq. inch, $E_{\text{copper}} = 15 \times 10^6$ lbs. per sq. inch.

Solution.—Assuming that original cross-sections of the cylinder and of the tube remain *plane*, the unit compression in the steel and in the copper will be equal, therefore the stresses of each material will be in the same ratio as their moduli (Eq. 3, p. 2), i.e., the compressive stress in the steel will be twice as great as the compressive stress in the copper. The stress p in copper will be found from the equation of statics:

$$P = \frac{\pi d^2}{4} \cdot 2p + \frac{\pi}{4}(D^2 - d^2)p$$

Substituting numerical values:

compressive stress in copper, $p = 1{,}590$ lbs. per sq. inch;
compressive stress in steel, $2p = 3{,}180$ lbs. per sq. inch;

unit compression $\dfrac{p}{E_{\text{copper}}} = .000{,}106.$

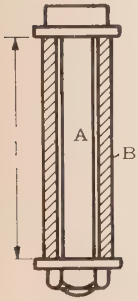

FIG. 3.

Example 2.—Referring to Fig. 3, what stresses will be produced in a steel bolt A and in copper tube B by ¼ of a turn of the screw, if the length of the bolt $l = 30$ ins., pitch of the bolt thread $h = \frac{1}{8}$ ins., area of the cross-section of the bolt $A_s = 1$ sq. inch, area of the cross-section of the tube $A_c = 2$ sq. inches?

Solution.—The moduli are the same as in example 1. By turning the screw, tension in the bolt and compression in the tube will be produced.

Let X denote the unknown tensile force in the bolt and the compressive force in the tube. The magnitude of X will be found from the condition that the extension of the bolt plus the compression of the tube are equal to the displacement of the nut along the bolt. In our case,

$$\frac{Xl}{E_sA_s} + \frac{Xl}{E_cA_c} = \frac{1}{4}h$$

from which,

$$X = \frac{hA_sE_s}{4l\left(1 + \dfrac{E_sA_s}{E_cA_c}\right)} = \frac{1}{32 \times 30}\,\frac{1 \times 30 \times 10^6}{(1 + 1)} = 15{,}600 \text{ lbs.}$$

The tensile stress in the bolt is $p_s = \frac{15,600}{1} = 15,600$ lbs. per sq. inch.

The compressive stress in the tube is $p_c = \frac{15,600}{2} = 7,800$ lbs. per sq. inch.

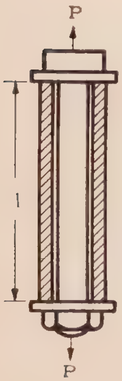

FIG. 4.

Example 3.—What change in stresses calculated in Example 2 will be produced by tensile forces $P = 5,000$ lbs., applied to the ends of the bolt as shown in Fig. 4?

Solution.—Let X denote the increase of tensile force in the bolt, and Y the decrease of compressive force in the tube. Then from the condition of equilibrium,

$$X + Y = P. \tag{a}$$

The second equation can be written down on the consideration that the unit elongation of the bolt and tube under the application of the forces P, must be equal, i.e.,

$$\frac{X}{A_sE_s} = \frac{Y}{A_cE_c} \text{ or } \frac{X}{Y} = \frac{A_sE_s}{A_cE_c} \tag{b}$$

In this case, $A_sE_s = A_cE_c$, therefore

$$X = Y = \tfrac{1}{2}P = 2,500 \text{ lbs.}$$

The increase of tensile stress in steel is 2,500 lbs. per sq. inch. The decrease of compressive stress in copper is 1,250 lbs. per sq. inch. From (b) it can be seen that in the case when A_s is small in comparison with A_c, the forces P produce only a small change in the stresses initially produced in the bolt.

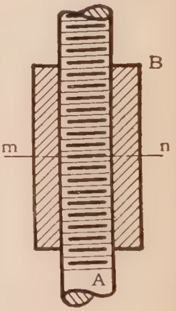

FIG. 5.

Example 4.—Referring to Fig. 5, a steel rod A is screwed into a copper tube B at room temperature $t = 15°C$. Determine the stresses which will act across the cross-section mn if the temperature be increased to 215°C.

Take the coefficient of expansion of copper $\alpha_c = 165 \times 10^{-7}$,
and that of steel $\alpha_s = 125 \times 10^{-7}$.
The area of the cross-section of the bolt, $A_s = 1$ sq. in.;
and that of the tube, $A_c = 3$ sq. in.

Solution.—Due to the fact that $\alpha_c > \alpha_s$, the increasing temperature produces compression in copper and tension in steel. Assuming that cross-sections distant from the ends of the copper tube remain *plane* under increase of temperature, the unit elongations of the copper and of the steel become equal. If X denotes the tensile force in the bolt and the compressive force in the copper tube, the equality of unit elongation will be represented by the equation

$$\alpha_s(t - t_0) + \frac{X}{A_sE_s} = \alpha_c(t - t_0) - \frac{X}{A_cE_c} \tag{a}$$

from which

$$X = \frac{(\alpha_c - \alpha_s)(t - t_0)A_sE_s}{1 + \frac{A_sE_s}{A_cE_c}}, \tag{b}$$

or substituting numerical values, given previously,

$$X = \frac{40 \times 10^{-7} \times 200 \times 1 \times 30 \times 10^6}{1 + \frac{1 \times 30 \times 10^6}{3 \times 15 \times 10^6}} = 14,400 \text{ lbs.},$$

which gives a tensile stress in steel,

$$p_s = \frac{X}{A_s} = 14{,}400 \text{ lbs. per sq. inch}$$

and a compressive stress in copper,

$$p_c = \frac{14{,}400}{A_c} = 4{,}800 \text{ lbs. per sq. inch.}$$

Example 5.—What change of stresses will be produced in the case represented in Fig. 3 by increasing the temperature from 15°C to 115°C?

Solution.—This can easily be obtained by using equation (b) of Example 4.

Example 6.—Suppose a copper tube is fitted over a steel tube at a temperature of 365°C., (Fig. 6) the fit being such that no pressure exists between tubes at this temperature. Determine the stresses which will be produced in the copper and in the steel when cooled to room temperature, 15°C., if the outer diameter of steel tube, $d = 4$ in., the thickness of the steel tube, $t_s = \frac{1}{8}$ in., and the thickness of the copper tube, $t_c = \frac{3}{16}$ in.

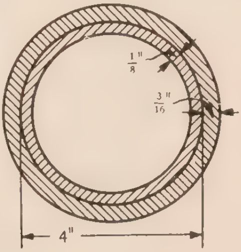

FIG. 6.

Solution.—Due to the difference in coefficients of expansion α_c and α_s, the outer copper tube will produce, when cooled, a pressure on inner steel tube. Let x denote this pressure, then the tensile stress in the copper tube will be given by*

$$p_c = \frac{xd}{2t_c}$$

The stress in steel is $p_s = -\frac{xd}{2t_s}$

The pressure x will be found from the equation

$$\alpha_c(t - t_0) - \frac{xd}{2t_cE_c} = \alpha_s(t - t_0) + \frac{xd}{2t_sE_s}$$

from which

$$p_c = \frac{xd}{2t_c} = \frac{(\alpha_c - \alpha_s)(t - t_0)E_c}{1 + \frac{t_c}{t_s}\frac{E_c}{E_s}} = \frac{40 \times 10^{-7} \times 350 \times 15 \times 10^6}{1.75} =$$

$$= 12{,}000 \text{ lbs. per sq. inch.}$$

Example 7.—Refer to Fig. 7. The weight W is supported by a vertical steel bar OA and two equal copper bars OB and OC. Determine the stress in these bars if the cross-sectional area of the steel bar is A_s and that of each copper bar is A_c.

Solution.—Let δ denote the displacement (OO_1) of the point O produced by the weight W, then the extension $\delta_1(=DO_1)$ of the copper bars is approximately equal to $\delta \cos \phi$. The unit elongation of the steel bar and the tensile force produced are δ/l and δ/lE_sA_s, respectively; while the unit elongation of the copper bars and the tensile force produced are $\delta \cos^2 \phi/l$ and $\delta \cos^2 \phi/lE_cA_c$, respectively.

---

* The thicknesses of tubes are considered as very small in comparison with the diameter.

The sum of the vertical components of these tensile forces in the three bars must be equal and opposite to W, i.e.,

$$W = \frac{\delta}{l}E_sA_s + 2\frac{\delta}{l}\cos^3\phi E_cA_c$$

from which

$$\frac{\delta}{l}E_sA_s = \frac{W}{1 + 2\cos^3\phi\frac{E_cA_c}{E_sA_s}}.$$

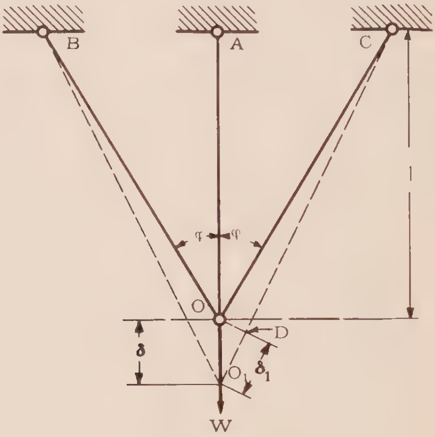

FIG. 7.

Example 8.—What stresses will be produced in the bars of Fig. 7 if the temperature be raised from t_0 to t? t_0 = assembly temperature.

Solution.—Let X denote the tensile force produced in the steel bar by an increase in temperature. Then from the condition of equilibrium, it can be seen that in the copper bars compressive forces act, equal to $X/2\cos\phi$; consequently the elongation of the steel bar becomes

$$\delta = \alpha_s(t - t_0)l + \frac{Xl}{E_sA_s}$$

and the elongation of copper bars is

$$\delta_1 = \alpha_c(t - t_0)\frac{l}{\cos\phi} - \frac{Xl}{2\cos\phi\cos\phi \cdot E_c \cdot A_c};$$

furthermore from previous consideration (see Example 7),

$$\delta_1 = \delta\cos\phi;$$

therefore,

$$\alpha_s(t - t_0)l + \frac{Xl}{E_sA_s} = \alpha_c(t - t_0)\frac{l}{\cos^2\phi} - \frac{Xl}{2\cos^3\phi E_cA_c}$$

from which

$$X = \frac{(t - t_0)\left(\frac{\alpha_c}{\cos^2\phi} - \alpha_s\right)E_sA_s}{1 + \frac{1}{2\cos^3\phi}\frac{E_sA_s}{E_cA_c}}.$$

Example 9.—Referring to Fig. 8, determine the form of the copper nut so that the force P will be uniformly distributed along the thread of the bolt throughout the distance a.

A_s = area of the cross-section of the steel bolt.

A_c = variable area of the cross-section of the nut.

Notations are as shown in Fig. 8.

Solution.—Assuming that a uniform distribution of the force P along the distance a has been obtained, the tensile force in the bolt across any section mn will be

$$P - \frac{Px}{a}$$

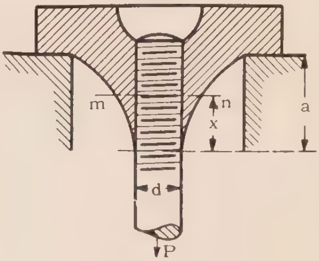

FIG. 8.

and the tensile force in the same cross-section of the nut will be

$$\frac{Px}{a}.$$

The unit elongation for copper and steel must be the same;* therefore

$$\frac{P}{E_s A_s}\left(1 - \frac{x}{a}\right) = \frac{Px}{aE_c A_c}$$

from which

$$A_c = \frac{x}{(a - x)} \cdot \frac{E_s}{E_c} \cdot A_s.$$

It will be seen that the theoretical magnitude of the area of the cross-section of the nut increases indefinitely as x approaches a.

Example 10.—Referring to Fig. 9, two equal horizontal bars AC and BC attached to end supports by pins A and B and connected between them with a pin C are subjected to the action of a vertical force P. Determine how the vertical displacement δ changes with the force P.

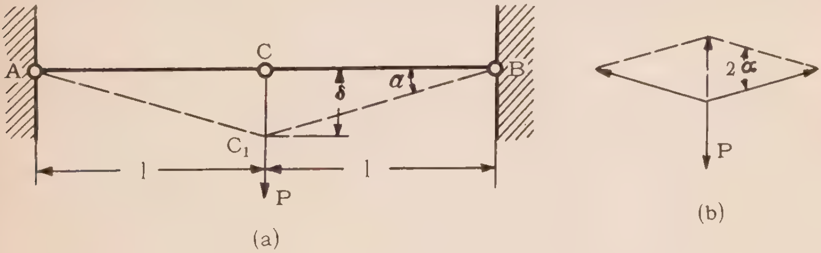

FIG. 9.

Solution.—If α be the very small angle of inclination of the bars after deformation, the vertical displacement of C will be represented by $CC_1 = \delta = \alpha l$, and $\alpha = \delta/l$.

---

* It is assumed that stresses are uniformly distributed over the cross-sections of the bolt and of the nut.

The unit elongation of the bars will be

$$\frac{BC_1 - BC}{BC} = \frac{\dfrac{l}{\cos\alpha} - l}{l} = \frac{\alpha^2}{2}$$

and the tensile force in the bars will be

$$\frac{\alpha^2}{2}EA.$$

These forces must be in equilibrium with P as shown in Fig. 9 (b); therefore

$$2\alpha \cdot \frac{\alpha^2}{2}EA = P,$$

or

$$\alpha = \sqrt[3]{\frac{P}{EA}}$$

and

$$\delta = l\alpha = l\sqrt[3]{\frac{P}{EA}}.$$

2. Tension and Compression of Bars of Variable Cross-section.—The formula (1) page 1 given for prismatical bars is applied frequently to the consideration of stresses in bars of variable cross-section. This gives sufficiently accurate results for all cases where a rapid variation of cross-section does not occur. Otherwise, the results obtained in such manner are entirely misleading. In order to show the limits of the application of formula (1) page 1, some results are given below which have been deduced from the mathematical theory of elasticity.

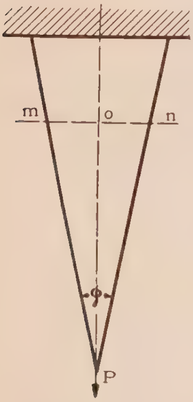

FIG. 10.—Extension of a symmetrical wedge.

Tension Member of Uniformly Varying Cross-section.—For the extension of a symmetrical wedge (Fig. 10), the exact solution based on the theory of elasticity shows that the *normal stresses* across any cross-section *mn* are not distributed uniformly, as assumed in formula (1). The maximum stress takes place at *O* and the minimum at the edges in points *m* and *n*. The difference between the maximum and minimum stress across any cross-section increases with the increase of the angle ϕ. When $\phi = 10°$, this difference is about 1.3% of the average stress as obtained from formula (1). When $\phi = 30°$, this difference is about 13%. From this it can be seen that formula (1) is accurate enough in cases of wedges or conical bars provided the angle ϕ is not large.

Tension Member with Sharp Variation in Cross-section.—As an example of the effect of a sharp variation in cross-section the standard tensile test specimen for concrete will now be considered (Fig. 11). In this case stress distribution across the cross-section *mn* is very far from uniform. Measurement by the *photo-elastic method*[*] shows that the maximum stress occurs at points *m* and *n* and that this stress is 1.75 times the average stress obtained from equation (1) page 1.

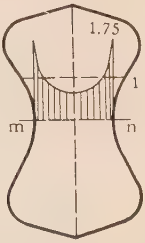

Fig. 11.—Stress distribution for concrete test bar in tension.

Another example of similar nature is met in considering stress in bolts (Fig. 12). Due to the *sharp variation* in sections near the head of the bolt, *concentration of stress* takes place at the points *m* and *n*, the beginning of the fillet. This concentration of stress increases as the radius of the fillets is decreased.

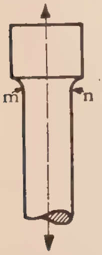

Fig. 12. Tension of a bolt.

Tension Members with Holes or Notches.—The effect of holes and notches on stress concentration will now be considered.

A *circular hole* of small radius ρ in a thin plate produces a very high stress concentration at points *m* and *n* (Fig. 13). The maximum stress becomes three times the stress calculated from formula (1). The normal stress p_1 at any point of the cross-section through the centre of the hole may be obtained from the formula[†]

$$p_1 = \frac{p}{2}\left(2 + \frac{\rho^2}{r^2} + 3\frac{\rho^4}{r^4}\right)$$

in which p denotes the average normal stress neglecting the hole and r the distance of the point considered from the centre of the hole. The stress distribution over the cross-section considered is shown in Fig. 13.

In the case of an *elliptical hole* the maximum stress at points *m* and *n* (Fig. 14) is

$$p_{\max} = p\left(1 + 2\frac{a}{b}\right).$$ [‡]

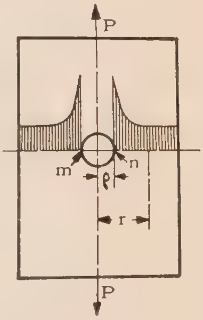

Fig. 13.—Stress distribution in tension member with circular hole.

---

[*] See E. Coker, *Proceedings of International Assoc. for Testing Materials*, New York Congress, 1913.

[†] Kirsch, *Zeit. d. Ver. Deutsch. Ing.*, 1898.

[‡] G. Kolosoff, Dissertation (1910) (Petrograd); see also, C. E. Inglis, *Engineering*, Vol. 95, p. 415, 1913. See also *Transaction Inst. of Naval Architects*, Meeting, March, 1913.

A semi-circular groove in a strip subjected to tension (Fig. 15) also produces very high stress-concentration. The experiments made* show that at points m and n the stresses are about twice as great as the average stress calculated from formula (1), provided that the radius of the groove is small in comparison with the width of the strip. All the conclusions on stress distribution made above assume that the maximum stresses are within the *elastic limit* of the material. Beyond the elastic limit, stress distribution depends on the *ductility* of the material. In the case of a *ductile material*, a considerable extension beyond the elastic limit can be obtained without great increase in stress. Due to this fact, the stress distribution beyond the elastic limit becomes more and more uniform with increase of extension. This explains why, in the case of ductile materials, holes and notches do not affect the *ultimate strength* when the notched piece is tested statically.

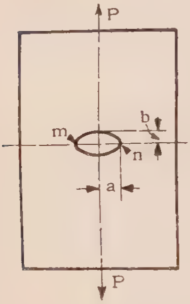

Fig. 14.—Stress distribution in tension member with elliptical hole.

On the other hand, in the case of a *brittle material*, such as glass, the high stress concentration remains right up to the point of breaking This causes a substantial weakening effect, as will be observed by the decreased ultimate strength of any notched bar of brittle material.

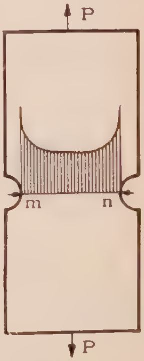

Fig. 15.—Stress distribution in tension member with groove.

It will be seen, therefore, that the adoption of notches in design work is a matter of judgment. They may have no effect on constructional work where soft steel is used, but for harder materials this consideration may become of great importance.

For the case of members subjected to repeated variation of stress, the effect of stress concentration becomes more severe for such cases as have been considered here. Under stress fluctuations and with high stress concentration, cracks are liable to develop, and, while with static members a certain stress concentration may not be accompanied with serious results, it will readily be seen that with members subjected to such stress variation the case is entirely different due to the possibility of these cracks being propagated through the entire section. This explains why holes, notches, and sharp variations of cross-section are so frequently the cause of failure in machine parts submitted to reversal of stress and vibration.*

---

* Preuss, *Zeit. d. Ver. Deutsch. Ing.*, p. 664, 1913.

3. Combined Stress.—The extension of a rectangular parallelopiped in the direction of the X and Y axes will now be considered (Fig. 16). Let P_x and P_y denote the tensile forces and A_x and A_y the corresponding cross-sectional areas perpendicular to the X and Y axes, respectively. Then the stresses across these cross-sections are

$$p_x = \frac{P_x}{A_x}, \qquad p_y = \frac{P_y}{A_y}$$

The stresses over any section perpendicular to the plane xy and inclined at the angle θ to the Y axis,† (Fig. 16 (b)), can easily be obtained by considering the action of the forces P_x and P_y separately and using the *principle of superposition.* The stresses produced by P_x are given by formulae (5) and (6) page 2. In order to determine the stresses produced by P_y it is only necessary to insert in the same formulae $-(90 - \theta)$ instead of θ. Combining the effects of P_x and P_y, the following formulae for normal and tangential stresses are obtained:

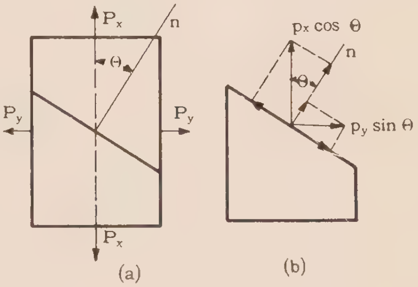

Fig. 16.—Stress distribution for combined stress conditions.

$$\left.\begin{aligned} p_n &= p_x \cos^2 \theta + p_y \sin^2 \theta \\ p_t &= \frac{p_x - p_y}{2} \sin 2\theta \end{aligned}\right\} \qquad (9)$$

By using formulae (3) and (7) and combining the effects of P_x and P_y, the *formulae for unit elongation* in X and Y directions can be obtained as follows:

---

* Some experimental data on the effect of notches on the endurance limit at fatigue test—see *University of Illinois Bulletin* #124, 1921, paper by H. F. Moore and T. B. Kommers. See also A. Foeppl, *Mitt. aus dem Mech. Techn. Laboratorium, Muenchen* #31. Several methods for determining the stress concentration produced by fillets and holes are discussed in a paper by the writer and Mr. W. Dietz, read before the Spring Meeting of A.S.M.E., May 20, 1925.

The effect of scratches on the ultimate strength was considered by Griffith, see *Philosophical Trans.*, V. 221 (1920). See also W. N. Thomas, *Engineering*, Vol. CXVI, p. 483, 1923.

† The angle is taken as positive if the external normal n to the cross-section considered is moving from X to Y in a clockwise direction as shown in Fig. 16 (b).

$$\left.\begin{aligned} e_x &= \frac{p_x}{E} - \frac{1}{m}\cdot\frac{p_y}{E} \\ e_y &= \frac{p_y}{E} - \frac{1}{m}\cdot\frac{p_x}{E} \end{aligned}\right\} \tag{10}$$

from which

$$\left.\begin{aligned} p_x &= \frac{\left(e_x + \frac{1}{m}e_y\right)E}{1 - \frac{1}{m^2}} \\ p_y &= \frac{\left(e_y + \frac{1}{m}e_x\right)E}{1 - \frac{1}{m^2}} \end{aligned}\right\} \tag{10a}$$

These expressions can also be used for cases where one or both of the stresses p_x and p_y are compressive. In such cases it is only necessary to consider compression as a negative tension.

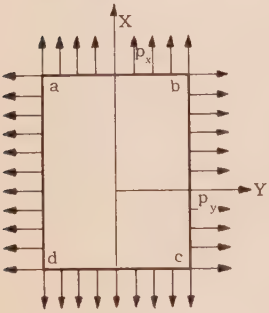

FIG. 17.

Example 11.—Determine what must be the magnitude of the stresses p_y distributed along the edges of a strip *abcd* (Fig. 17) in order to prevent lateral contraction. Determine also the unit elongation in the direction of X axis.

Solution.—From equation (10)

$$p_y = \frac{1}{m}p_x$$

and also, from (10a),

$$e_x = \frac{p_x}{E}\left(1 - \frac{1}{m^2}\right).$$

Example 12.—A steel ring while hot is assembled on a copper disc (Fig. 18). Determine the unit compression in the disc and the tensile stress in the ring, if d = 10 ins., b = 1 in. and the shrinkage 0.001 in. per inch of diameter d.

Solution.—Due to shrinkage, a pressure x lbs. per sq. inch will be produced between the ring and the disc. The tensile stress in the ring will be $xd/2b$. The increase in the internal diameter of the ring will be

$$\frac{xd^2}{2bE_s}$$

The decrease in the diameter of the disc, from equation (10), will be

$$\frac{xd}{E_c}\left(1 - \frac{1}{m}\right)$$

The pressure x can be now calculated from the equation

$$\frac{xd^2}{2bE_s} + \frac{xd}{E_c}\left(1 - \frac{1}{m}\right) = .001d.$$

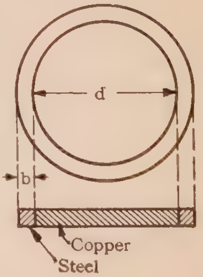

FIG. 18.

Putting $1/m = .3$ and substituting the numerical values given above,

$$\frac{5x}{E_s} + \frac{.7x}{E_c} = .001$$

from which

$$x = \frac{.001E_s}{5 + .7\frac{E_s}{E_c}} = \frac{30{,}000}{6.4} = 4{,}690 \text{ lbs. per sq. inch.}$$

Tensile stress in the ring is given by $\frac{xd}{2b} = 5x = 23{,}450$ lbs. per sq. inch.

and unit contraction in the disc by

$$\frac{x\cdot\left(1 - \frac{1}{m}\right)}{E_c} = \frac{4{,}690 \times .7}{15 \times 10^6} = .000{,}219$$

4. Graphical Representation of Combined Stress, by Mohr's Circle.—So far, combined stresses have been considered in a purely analytical manner. Since a diagram gives a clearer conception of the results of combined stresses, we shall consider *Mohr's diagram* by which problems involving combinations of stresses can be solved in a graphical manner. Let OA and OB represent stresses p_x and p_y (Fig. 19). Then the circle having AB as a diameter represents variation of stresses p_n and p_t with variations in the angle θ (Fig. 16). It is only necessary for a given θ to draw radius CD, making with the X axis the angle equal to 2θ. This angle is measured from X in a counter-clockwise direction. It is easy to show that the abscissa OF of the point D of the circle represents the normal stress p_n and the ordinate DF represents the *shearing* stress p_t. From Fig. 19,

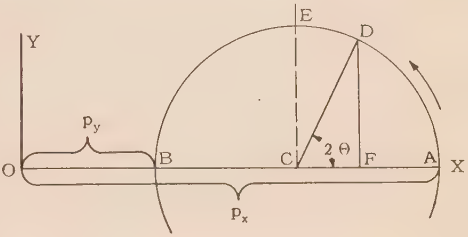

FIG. 19.—Mohr's circle for combined tension.

$$OF = OC + CF = \frac{p_x + p_y}{2} + \frac{p_x - p_y}{2}\cos 2\theta\,]$$

$$= p_x \cos^2\theta + p_y \sin^2\theta$$

$$DF = CD \sin 2\theta = \frac{p_x - p_y}{2}\sin 2\theta$$

which is in agreement with equations (9) page 11. Therefore, OF represents the stress normal to the section, and DF represents the corresponding tangential stress. This graphical representation gives a complete picture of variation of stresses with the angle θ. The maximum normal stress is represented by the point A of the circle and is equal to p_x. Maximum tangential stress, corresponding to the point E, is equal to $\frac{p_x - p_y}{2}$ and acts across the section, corresponding to $2\theta = 90°$, or $\theta = 45°$.

Simple Tension ($p_y = 0$).—In the case of a simple tension, ($p_y = 0$) the circle of Mohr is as shown in Fig. 20. It is easy to see that the coordinates of any point D represent equations (5) and (6).

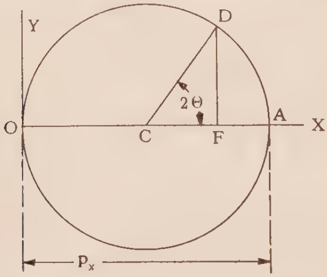

FIG. 20.—Mohr's circle for simple tension.

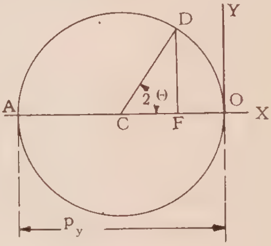

FIG. 21.—Mohr's circle for simple compression.

Simple Compression ($p_x = 0$).—Figure 21 represents the case of simple compression in the direction of the Y axis.

Pure Shear.—The case of a tension in the x direction accompanied by an equal compression in the y direction is represented by the circle in Fig. 22.

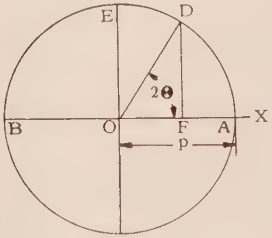

FIG. 22.—Graphical representation of pure shear.

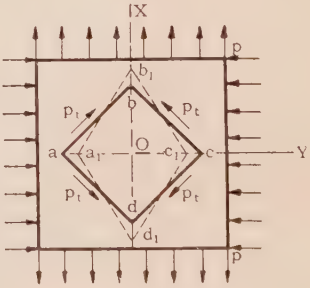

FIG. 23.—Case of pure shear.

In this case $p_x = -p_y = p$ and equations (9) page 11 give $p_n = p \cos 2\theta$, $p_t = p \sin 2\theta$

These equations represent the coördinates of the point D. The stresses over the cross-section for $\theta = 45°$ are represented by the point

E. It is seen that the normal stress over this section is equal to zero and the tangential stress is equal to the stress p.

Consider a rectangular parallelopiped with square base *abcd* as shown in Fig. 23. From the explanation given above it follows at once that over lateral faces of this element tangential stresses alone are acting. This state of stress is known as *pure shear*. The corresponding strain consists in angular distortion. After deformation the square *abcd* becomes the rhombus $a_1b_1c_1d_1$. The angular change β (angle abc − angle $a_1b_1c_1$) determining the distortion of square *abcd* is taken as a measure of the shear. This shear can be found from the unit elongations e_x and e_y as follows. The angle of rhombus $a_1b_1c_1d_1$ at b_1 is $\frac{\pi}{2} - \beta$, and from the triangle oc_1b_1,

$$\tan\left(\frac{\pi}{4} - \frac{\beta}{2}\right) = \frac{oc_1}{ob_1} = \frac{1 + e_y}{1 + e_x} \tag{a}$$

In this case, from equation (10) page 12,

$$e_x = \frac{p}{E} + \frac{1}{m}\frac{p}{E} = \frac{p}{E}\left(1 + \frac{1}{m}\right)$$

$$e_y = -\frac{p}{E} - \frac{1}{m}\frac{p}{E} = -\frac{p}{E}\left(1 + \frac{1}{m}\right).$$

Substituting in (a) and noting that β is a small quantity, it therefore follows,

$$\tan\left(\frac{\pi}{4} - \frac{\beta}{2}\right) = \frac{1 - \frac{\beta}{2}}{1 + \frac{\beta}{2}}$$

and

$$\frac{1 - \frac{\beta}{2}}{1 + \frac{\beta}{2}} = \frac{1 - \frac{p}{E}\left(1 + \frac{1}{m}\right)}{1 + \frac{p}{E}\left(1 + \frac{1}{m}\right)}$$

or

$$\beta = \frac{2\left(1 + \frac{1}{m}\right)p}{E} = \frac{2\left(1 + \frac{1}{m}\right)}{E}p_t \tag{b}$$

i.e., the shear is proportional to the shearing stress p_t and depends on the magnitude of the quantity given below:

$$G = \frac{E}{2\left(1 + \frac{1}{m}\right)} \tag{11}$$

The value G is known as the *modulus of rigidity*.

Substituting (11) in (b),

$$\beta = \frac{p_t}{G} \tag{12}$$

5. General Case of Stresses.—In general the state of stress at any point in a body can be represented by tension or compression in three mutually perpendicular directions (Fig. 24). The normal stresses over all cross-sections perpendicular to X, Y, and Z axes are respectively:

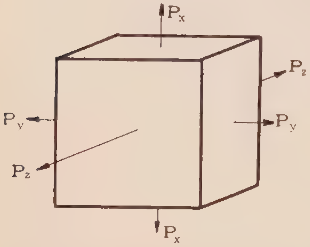

FIG. 24.—Representation of three mutually perpendicular stresses.

$$p_x = \frac{P_x}{A_x}, \quad p_y = \frac{P_y}{A_y}, \quad p_z = \frac{P_z}{A_z}.$$

It is assumed below that $p_x > p_y > p_z$. Combining the effects of the forces P_x, P_y and P_z, it can be concluded that over a section through the Z axis only the forces P_x and P_y produce stresses and therefore these stresses may be calculated from equation (9) and represented graphically in the way as described in the preceding paragraph. In Fig. 25, Mohr's circle with a diameter AB represents these stresses. In the same manner the stresses over any section through the X axis can be represented by a circle having BC as a diameter. The circle with the diameter AC represents stresses over any section through the Y axis. The three circles of Mohr represent stresses over three series of sections through the X, Y, and Z axes. For any section inclined to X, Y, and Z, the stress may be represented by the coordinates of a point located in the shaded area of Fig. 25.* This conclusion is very important and will be used later in the consideration of the different strength theories (Chap. XVII, Part II).

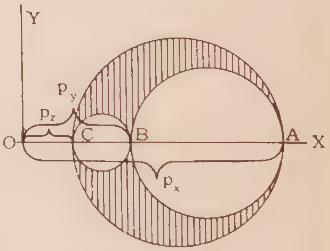

FIG. 25. Graphical representation of stresses in general case.

The equations for calculating the *unit elongations* in directions of X, Y and Z axes may be obtained by combining the effects of P_x, P_y, and P_z:

---

[*] The proof of this statement can be found in the book by A. Foeppl, "Technische Mechanik," Vol. 5, p. 18, 1918.

$$\left.\begin{aligned} e_x &= \frac{p_x}{E} - \frac{1}{mE}(p_y + p_z) \\ e_y &= \frac{p_y}{E} - \frac{1}{mE}(p_x + p_z) \\ e_z &= \frac{p_z}{E} - \frac{1}{mE}(p_x + p_y) \end{aligned}\right\} \qquad (13)$$

By adding these equations an expression for calculating the **unit** *volume expansion* Δ is obtained:

$$\Delta = e_x + e_y + e_z = \frac{1 - \dfrac{2}{m}}{E}(p_x + p_y + p_z) \qquad (14)$$

Example 13.—Determine the decrease in the volume of a solid steel sphere of 10 inches diameter submitted to a uniform hydraulic pressure $p = 1{,}000$ lbs. per sq. inch.

Solution.—From Equation (14),

$$\Delta = -\frac{3p\left(1 - \dfrac{2}{m}\right)}{E} = -\frac{3 \times 1{,}000 \times .4}{30 \times 10^6} = -\frac{4}{10^5}$$

The decrease in the volume is, therefore,

$$\frac{4}{10^5}\frac{\pi d^3}{6} = 0.020.9 \text{ cubic inches.}$$

Example 14.—Referring to Fig. 26, a rubber cylinder A is compressed in the steel cylinder B by a force P. Determine the pressure between the rubber and the steel if $P = 1{,}000$ lbs., $d = 2$ ins. Poisson's ratio for rubber, $1/m = .45$.

Solution.—Let p denote the compressive stresses over any cross-section of the cylinder and q the pressure over the surface of the cylinder. Neglecting extension of the steel cylinder and using formula (13), page 17,

$$0 = \frac{q}{E} - \frac{1}{mE}(p + q),$$

from which

$$q = \frac{p}{m - 1} = \frac{.45}{1 - .45} \times \frac{1{,}000 \times 4}{\pi \times 2^2} = 261 \text{ lbs. per sq. inch.}$$

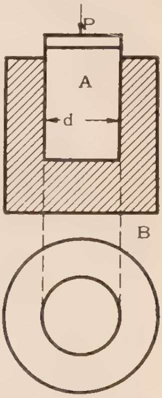

Fig. 26.

6. Vessels Subjected to Internal Pressure.—*General Consideration.*—The vessels having the form of solids of revolution and subjected to internal pressure distributed symmetrically with reference to the axis of symmetry 0-0 (Fig. 27) will be considered here. For this case the deformation consists substantially of extension, (bending of the wall can be neglected) and the tensile stresses can be considered as uniformly distributed over the thickness of the wall. Imagine a small element *mnrs* of the wall contained between meridians *mn* and *sr*, and two sections *ms* and *nr* normal to these meridians. Let

dx and dy = small dimensions of the element *mnrs*,
$P_y \cdot dx$ and $P_x \cdot dy$ = the tensile forces acting on the edges of the element,
ρ_1 and ρ_2 = the *radii of curvature* of the meridian and of the section normal to the meridian, respectively,
q = the internal pressure,
γ = weight per unit volume,
t = thickness of wall,

Other notation, see page 7.

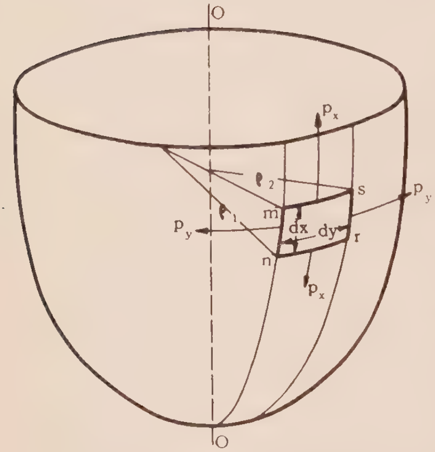

FIG. 27.—Vessel having a generated form.

Due to the curvature $1/\rho_2$, the tensile forces $P_y \cdot dx$, acting on the edges *mn* and *sr*, produce a resultant normal to the element *mnrs* and equal to

$$P_y \cdot dx \cdot \frac{dy}{\rho_2} \tag{a}$$

In the same manner it can be shown that the forces $P_x \cdot dy$ produce a resultant

$$P_x \cdot dy \cdot \frac{dx}{\rho_1} \tag{b}$$

The forces (*a*) and (*b*) balance the pressure distributed over the element *mnrs*, therefore

$$\frac{P_y}{\rho_2} dxdy + \frac{P_x}{\rho_1} dxdy = qdxdy, \tag{c}$$

from which

$$q = \frac{P_x}{\rho_1} + \frac{P_y}{\rho_2}.$$

Dividing this equation by the thickness of the wall t the following equation is obtained:

$$\frac{q}{t} = \frac{p_x}{\rho_1} + \frac{p_y}{\rho_2} \tag{15}$$

which represents the relation between the tensile stress p_x in the direction of the meridian and tensile stress p_y in the direction perpendicular to the meridian. Some applications of this equation are now to be considered.

Cylindrical Boiler with Spherical Ends Submitted to Uniform Internal Pressure (Fig. 28).—Using equation (15) page 18 and remembering that, for a cylinder, $1/\rho_1 = 0$ and $1/\rho_2 = 2/d$, it follows that $2p_y/d = q/t$, from which

$$p_y = \frac{qd}{2t}. \tag{16}$$

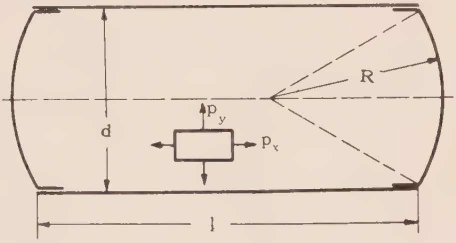

FIG. 28.—Cylindrical boiler.

In calculating p_x it has to be borne in mind that these tensile stresses, uniformly distributed over the cross-section of the cylindrical wall, are in equilibrium with the pressure distributed over the ends; therefore

$$\pi d t p_x = \frac{\pi d^2}{4} q,$$

from which

$$p_x = \frac{qd}{4t} \tag{17}$$

In calculating the tensile stresses in the spherical ends of the boiler it is observed that

$$\rho_1 = \rho_2 = R \text{ and } p_x = p_y = p$$

then from (15),

$$p = \frac{qR}{2t} \tag{18}$$

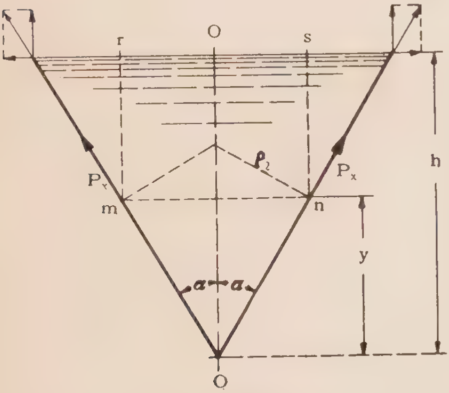

FIG. 29.—Conical tank.

Conical Tank.—A tank, conical in form, containing liquid will now be considered (Fig. 29). In this case the curvature of the meridian $1/\rho_1 = 0$, and the stress p_y, perpendicular to the meridian sections, can be calculated from equation (15). Considering section mn, distant $h - y$ from the level of the liquid the internal pressure is,

$$q = (h - y)\gamma;$$

the radius of curvature is

$$\rho_2 = \frac{y \tan \alpha}{\cos \alpha}$$

where γ denotes weight per unit volume of the liquid.

Substituting in equation (15),

$$p_y = \frac{q\rho_2}{t} = \frac{(h - y)\gamma}{t} \cdot \frac{y \tan \alpha}{\cos \alpha}.$$

The maximum value of this stress occurs when the product $(h - y) \times y$ becomes maximum. Thus, making the derivative of $(h - y)y$ equal to zero, we get

$$h - y = y \text{ or } y = \frac{h}{2},$$

and this stress is given by

$$(p_y)_{\max} = \frac{h^2\gamma \tan \alpha}{4t \cos \alpha}$$

In calculating the stress p_x at the points m, n, and noting that these stresses balance the weight of the volume $rmOns$ of the liquid, it follows that

$$2\pi y \tan \alpha t p_x \cos \alpha = \pi y^2 \tan^2 \alpha\left(h - y + \frac{y}{3}\right)\gamma,$$

from which

$$p_x = \frac{y \tan \alpha\gamma}{2t \cos \alpha}\left(h - \frac{2}{3} y\right),$$

Example 15.—Determine the increase in the volume of the cylindrical boiler, considered above (Fig. 28), produced by an internal pressure q.

Solution.—Taking $1/m = .3$, the unit elongation of the length l is

$$e_x = \frac{p_x}{E} - \frac{1}{m}\frac{p_y}{E} = \frac{qd}{4tE}\left(1 - \frac{2}{m}\right) = .1\frac{qd}{tE}$$

and the unit elongation of the diameter d is

$$e_y = \frac{p_y}{E} - \frac{1}{m}\frac{p_x}{E} = \frac{qd}{2tE}\left(1 - \frac{1}{2m}\right) = .425\frac{qd}{tE}$$

The expansion of the volume of the cylindrical part of the boiler, neglecting the extension of the spherical ends, is

$$\frac{l(1 + e_x)\pi d^2(1 + e_y)^2}{4} - \frac{\pi d^2 l}{4} = \frac{\pi d^2 l}{4}(e_x + 2e_y) =$$

$$\frac{\pi d^2 l}{4} \cdot \frac{qd}{tE}(.1 + .85) = .95\frac{\pi d^2}{4} l \cdot \frac{qd}{tE}.$$

Example 16.—Determine the internal pressure in a spherical steel boiler of radius R, if unit expansion of volume produced by this pressure is .001 and $t/d = .01$.

Solution.—From equation 18, page 19,

$$p = \frac{qR}{2t} = 25q.$$

Extension of the wall is

$$e = \frac{p}{E} - \frac{1}{m}\frac{p}{E} = .7\frac{25q}{E}.$$

The expansion per unit volume is

$$3\epsilon' = 3 \times .7 \times \frac{25q}{E}, \text{ in which}$$

q will be found from the equation

$$3 \times .7 \times \frac{25q}{E} = .001,$$

from which

$$q = \frac{.001 \times E}{3 \times .7 \times 25} = 571 \text{ lbs. per sq. inch.}$$

Example 17.—Determine the stresses in a tank represented in Fig. 30.

Solution.—Using the notation shown in Fig. 30, for any point m on the spherical part of the tank, equation (15) gives

$$\frac{p_x + p_y}{R} = \frac{\gamma x}{t} \qquad \text{(a)}$$

Noting that stresses p_x are in equilibrium with the weight of the volume *srmon* of the liquid, the second equation can be obtained as follows:

$$p_x = \frac{\gamma R}{t}\left(\frac{h - R}{2} + \frac{R}{3}\,\frac{1 - \sin^3 \alpha}{\cos^2 \alpha}\right)$$

Substituting in (a),

$$p_y = \frac{\gamma R}{t}\left(\frac{h - R}{2} + \frac{R}{3}\,\frac{\sin^3 \alpha + 3 \sin \alpha \cos^2 \alpha - 1}{\cos^2 \alpha}\right)$$

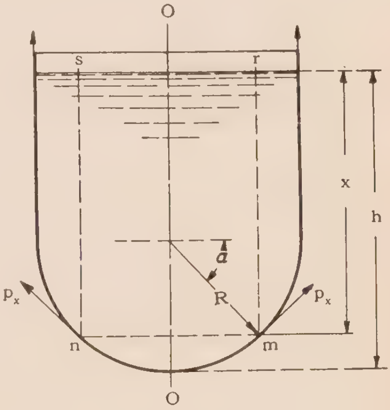

FIG. 30.

7. Compression of Balls and Rollers.—The continued widening of the field of application of ball and roller bearings makes it necessary to consider certain aspects of the theory of balls and rollers subjected to compressive forces. A general solution of the problem of pressure distribution over contact surfaces of two compressed elastic bodies was obtained by Herz.* Some of these results having a practical application will now be considered.

General Case.—Let $1/r_1$ and $1/r_1^1$ denote the principal curvatures of one body, and $1/r_2$ and $1/r_2^1$ of another body† at the point of contact, ϕ the angle between the sections containing curvatures $1/r_1$ and $1/r_2$. The *surface of contact* for the general case is an ellipse, the mi-axes of which can be calculated by the following formulae:

---

* H. Herz, *Gesammelte Werke*, Vol. 1 (Leipzig), 1895.

Further development of the theory on stresses in ball bearings, see in papers:
K. Sundberg, *Teknisk Tidskrift, afd. Mekanik,* Vol. 4, 1919.
A. Palmgren, *Engineering,* February 12, 1919.
A. Palmgren, *The Inst. of Automobile Eng. Proc.* V. XVII, p. 385, 1922–1923.
S. Fuchs, *Physikalische Zeitschr.* p. 213, 1921.
See also F. Heerwagen, *Zeitschr. d. Ver. D. Ing.* Vol. 45, p. 1701, 1901.

† The curvatures of the body consider as positive if the corresponding center of curvature is within this body.

$$a = \alpha\sqrt[3]{\frac{P\delta}{H}} \qquad (19)$$

$$b = \beta\sqrt[3]{\frac{P\delta}{H}}$$

where P = compressive force,

$$H = \frac{4}{3}\,\frac{E}{1 - \left(\frac{1}{m}\right)^2}$$

$$\delta = \frac{4}{\frac{1}{r_1} + \frac{1}{r_1{}^1} + \frac{1}{r_2} + \frac{1}{r_2{}^1}}$$

The constants α and β are given in Table I. The angle θ in the first column of the table can be calculated as follows:

$$A = \frac{2}{\delta}$$

$$B = +\frac{1}{2}\sqrt{\left(\frac{1}{r_1} - \frac{1}{r_1{}^1}\right)^2 + \left(\frac{1}{r_2} - \frac{1}{r_2{}^1}\right)^2 + 2\left(\frac{1}{r_1} - \frac{1}{r_1{}^1}\right)\left(\frac{1}{r_2} - \frac{1}{r_2{}^1}\right)\cos 2\phi} \qquad \text{(a)}$$

Then

$$\cos\theta = \frac{B}{A}. \qquad \text{(b)}$$

TABLE I.*—CONSTANTS FOR CALCULATING SEMI-AXES OF THE ELLIPSE OF CONTACT

θ degrees	α	β	θ degrees	α	β
30	2.731	.493	65	1.378	.759
35	2.397	.530	70	1.284	.802
40	2.136	.567	75	1.202	.846
45	1.926	.604	80	1.128	.893
50	1.754	.641	85	1.061	.944
55	1.611	.678	90	1.000	1.000
60	1.486	.717			

---

* The table was taken from the paper *Friction and Carrying Capacity of Ball and Roller Bearings*, by H. L. Whittemore and S. N. Petrenko. *Technical Papers of the Bureau of Standards* #201, 1921.

The expression for the maximum stress at the center of the contact surface is, then,

$$p_{\max} = 1.5 \frac{P}{\pi ab} \tag{20}$$

where a and b are calculated from (19).

Compression of Balls.—In the case of two balls compressed by forces P, Fig. 31, the pressures are distributed over a small circle of contact mn. From general formulae (a) and (b) $\theta = 90°$ and from the table above $\alpha = \beta = 1$. Then from (19) *the radius of the circle of contact* is

$$\rho = .881\sqrt[3]{\frac{P}{E}\frac{d_1 d_2}{d_1 + d_2}}^{*} \tag{c}$$

Substituting in (20), $a = b = \rho$; the following formula for *maximum pressure at the center of the contact circle* will be obtained,

$$p_{\max} = .616\sqrt[3]{PE^2\left(\frac{d_1 + d_2}{d_1 d_2}\right)^2} \tag{d}$$

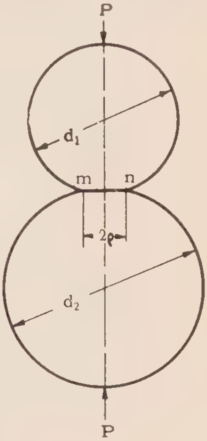

FIG. 31.—Two balls in contact.

Considering one of the diameters as indefinitely large, the following formulae are obtained:

$$\rho = .881\sqrt[3]{\frac{Pd}{E}} \tag{21}$$

$$p_{\max} = .616\sqrt[3]{\frac{PE^2}{d^2}} \tag{22}$$

These determine the compressive stress on the surface of contact of a ball of diameter d when forced against an elastic body having a plane surface. It is easy to see from (22) that $p_{\max}$ remains constant if P varies in the same ratio as d^2.

The experiments made† show that for the case of a ball and a plane surface of *hardened crucible steel* the safe limit for compressive force P is expressed by the following:

$$P_{\max} = 700d^2 \tag{23}$$

in which d is in inches and P in pounds.

---

* Here it is taken $1/m = .30$.

† Stribeck, *Zeitschr. d. Ver. Deutsch. Ing.* p. 73, 1901.
Schwinning, *Zeitschr. d. Ver. Deutsch. Ing.* p. 332, 1901.
A. Bauschlicher, *Zeitschr. d. Ver. Deutsch. Ing.* p. 1185, 1908.

For the case of a *ball in a spherical seat,* the sign of d_2 in formulae (c) and (d) must be changed and the following is obtained:

$$\rho = .881 \sqrt[3]{\frac{P}{E}\,\frac{d_1 d_2}{d_2 - d_1}}$$

$$p^{\max} = .616 \sqrt[3]{PE^2 \left(\frac{d_2 - d_1}{d_1 d_2}\right)^2}$$

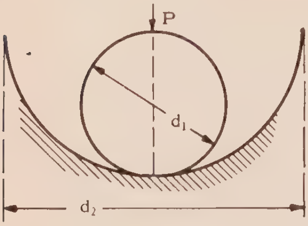

FIG. 32.—A ball and seat.

Compression of Rollers.—In the case of *rollers in compression,* Fig. 33, the contact area becomes rectangular and the width b of this strip is determined by equation*

$$b = 2.15 \sqrt{\frac{P'}{E}\,\frac{d_1 d_2}{d_1 + d_2}}. \tag{24}$$

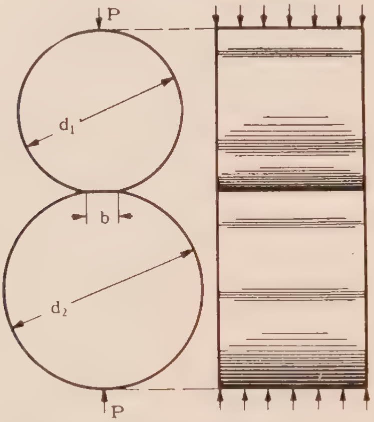

FIG. 33.—Two cylinders in contact.

Where P' denotes the compressive force per unit length of the roller. the maximum pressure at the middle of this strip is

$$p_{\max} = .591 \sqrt{P'E\,\frac{d_1 + d_2}{d_1 d_2}} \tag{25}$$

If one of the diameters be taken as infinitely large as in the case of a roller in contact with a plane surface, the following expressions are obtained:

$$b = 2.15 \sqrt{\frac{P'd}{E}} \tag{26}$$

$$p_{\max} = .591 \sqrt{\frac{P'E}{d}} \tag{27}$$

---

* A. Foeppl, Technische Mechanik, Vol. 5, p. 351.

It will be seen that the maximum stress remains constant if P' varies in the same proportion as d. The safe limit for P' for the case of steel rollers can be obtained from equation

$$P' = 150n \tag{28}$$

Example 18.—Determine the maximum pressure at the point of contact C of a single row ball bearing, shown in Fig. 34. The dimaeter of ball $d = 1.5$ in., radius of the grooves $r = 1$ in., diameter of the outer race 8 in. and compressive force $P = 5{,}000$ lbs.

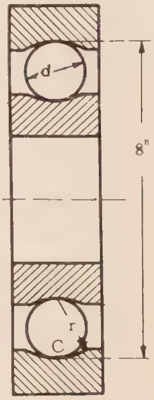

Fig. 34.

Solution.—By using equations of paragraph 7 and taking into account that $r_1 = r_1^1 = 1.5/2$ in., $r_2 = -1$ in., $r_2^1 = -4$ in.,

$$\delta = \frac{4}{\frac{2}{1.5} + \frac{2}{1.5} - \frac{1}{1} - \frac{1}{4}} = 2.823$$

$$H = \frac{4}{3} \times \frac{30 \times 10^6}{.91}$$

$$2A = 1.417$$

$$2B = \frac{1}{1} - \frac{1}{4} = .750$$

$$\cos\theta = \frac{.750}{1.417} = .529$$

$$\theta = 58^\circ$$

Then from Table I, page 22, by interpolation,

$$\alpha = 1.536,\ \beta = .701.$$

The semi-axes of the ellipsis of contact are

$$a = 1.536\sqrt[3]{\frac{P\delta}{H}} = .105 \text{ in.}$$

$$b = .701\sqrt[3]{\frac{P\delta}{H}} = .048 \text{ in.}$$

$$p_{\max} = 1.5\frac{5{,}000}{\pi ab} = 475{,}000 \text{ lbs. per sq. inch.}$$

Such high stresses can be sustained due to the fact that at the center of the circle of contact the material is compressed not only in the direction of the force P but also in a lateral direction.

CHAPTER II

TORSION

8. Shafts of Constant Circular Cross-section.—*Elastic Stage.*—When a cylindrical circular shaft is twisted by a couple the well known solution can be obtained by making the following *assumptions:* 1. Cross-sections of the shaft originally plane and perpendicular to the axis of the shaft remain so after torsion. 2. Radii of circular cross-sections remain straight lines.

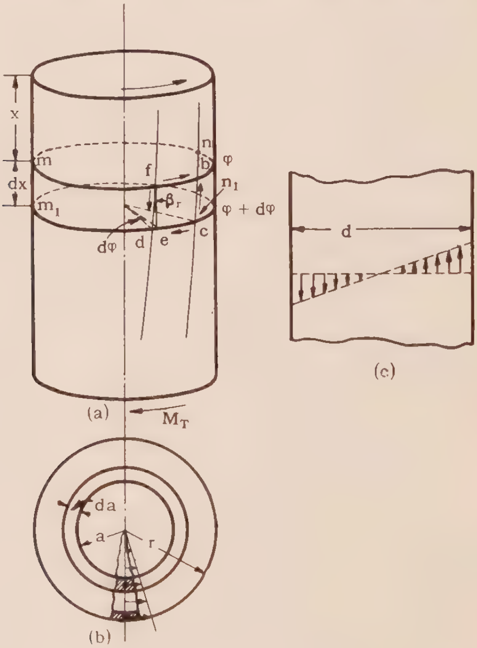

Fig. 35.—Twist of a shaft of circular cross section.

On these assumptions, torsion consists of rotation of circular cross-sections about the axis of the shaft. From the arrangement shown in Fig. 35, assume that the shaft is fixed at the upper end and that a *twisting moment* M_t is acting at the bottom.

Let:

ϕ = angle of twist.
ϕ_l = twist, in length l.
M_t = torque moment.
G = modulus of elasticity in shear.
β_a, β_r = shear at distances a and r from axis.
p_t = shearing stress.
r = radius.
d = diameter.
I_p = polar moment of inertia.
A = area of cross-section.
C = torsional rigidity of the shaft.

Let ϕ denote the angle of rotation due to twist of any cross-section mn distant x from the fixed end of the shaft; then for a section m_1n_1, distant dx from mn, the angle of rotation will be

$$\phi + d\phi.$$

It is easy to see that, due to the twist, an element $bcdf$ included between the two cross-sections mentioned above, and two straight lines fd and bc originally parallel to the axis of the shaft, will be in a state of pure shear.* The magnitude of this shear will be as follows:

$$\beta_r = \frac{ed}{dx} = r\frac{d\phi}{dx} \tag{a}$$

Now from the assumption (2) above, it follows at once that for any other element taken on the cylindrical surface of radius a, the shear will be

$$\beta_a = a\frac{d\phi}{dx}$$

and the corresponding shearing stress, from equation (12) page 16, will be

$$p_t = Ga\frac{d\phi}{dx}. \tag{b}$$

The stress is proportional to the distance a from the center of the cross-section, as shown in Fig. 35 (b).

In determining the magnitude of $d\phi/dx$ in equation (b) the condition of equilibrium will be used. Thus, the shearing stress must be of such magnitude as to cause the moment of all shearing forces distributed over any cross-section of the shaft, to equal the *torque moment*

---

* The dimension of the element in the radial direction is considered as very small one.

M_t. The shearing forces distributed over any elementary ring at radius a and of thickness da (Fig. 35) give a torque moment

$$dM_t = 2\pi a da p_t a \tag{c}$$

By varying a from 0 to r and integrating all moments such as given in (c), the equation becomes

$$M_t = \int_0^r 2\pi a da p_t a = G \frac{d\phi}{dx} I_p \tag{d}$$

in which

$$I_p = \int_0^r 2\pi a da a^2 = \frac{\pi r^4}{2}$$

and denotes the *polar moment of inertia* of the cross-section.

By integrating (*d*), the *angle of twist* ϕ_l of the shaft will be obtained:

$$\phi_l = \frac{M_t l}{G I_p}. \tag{29}$$

By using (d), the equation (b) for shearing stresses becomes

$$p_t = \frac{M_t a}{I_p}; \tag{30}$$

and *maximum shearing stress* will be

$$(p_t)_{\max} = \frac{M_t r}{I_p} = \frac{2M_t}{\pi r^3} = \frac{16M_t}{\pi d^3} \tag{31}$$

in which d denotes the diameter of the shaft.

From the consideration of equilibrium of the element *fbcd* in Fig. 35, it follows at once that stresses of the same magnitude as given by equation (30) are acting in axial sections of the shaft, as well as in cross-sections, and are distributed as shown in Fig. 35 (c). To these stresses must be attributed the longitudinal splitting during twisting of some materials such as wood.

Torsion beyond the Elastic Limit.—It will be appreciated that equations (30) and (31) have been obtained on the basis of *Hooke's law* and can only be used within the proportional limit. Beyond this limit, stress distribution depends largely on the ductility of the material. In the case of ductile materials, such as mild steel, the *torsion test curve* has a shape similar to that of the *tensile test curve* (Fig. 268, p. 479). The portion where the curve becomes parallel to the strain axis indicates that the material over the entire cross-section is in a state of yielding and that the corresponding stresses are, more or less, uniformly distributed over the cross-section. If $(p_t)_{y.p.}$

denotes the magnitude of these stresses the following equation, instead of equation (d) above, will be obtained:

$$\int_0^r (p_t)_{y.p.} 2\pi adaa = M_t \qquad \text{(e)}$$

from which

$$(p_t)_{y.p.} = \frac{3M_t}{2\pi r^3} \qquad (32)$$

The same formula must be used in calculating also the *ultimate strength for shear* of ductile materials. In this case p_t becomes the ultimate strength at shear.

Potential Energy of Twist.—It will be understood from elementary consideration that the torque moment during twisting is doing work on the shaft. Within the limits of elasticity, this work will be transformed into *potential energy of deformation*. Let the line OS (Fig. 36) represent the *elastic stage* of a torsion test curve in which twisting moments are plotted as ordinates on a base of angular deformation. The work done on the material up to any point A is represented by the area of the triangle OAB and will be equal to

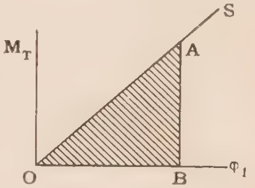

FIG. 36.—Work done during twist.

$$\frac{M_t\phi_t}{2}.$$

Substituting (29) for ϕ_t, the following expression for the *potential energy of twist* is obtained:

$$U = \frac{M_t^2 l}{2GI_p}. \qquad (33)$$

Example 19.—Determine the shaft diameter d of a machine of 200 h.p. if the speed $n = 120$ R.P.M. and the working stress = 3,000 lbs. per sq. inch.

Solution.—The torque moment is

$$M_t = \frac{12 \times 33{,}000 \times 200}{2\pi \times 120} \text{ pound inches}$$

Then from (31),

$$d = \sqrt[3]{\frac{16M_t}{\pi(p_t)_{\max}}} = \sqrt[3]{\frac{16 \times 12 \times 33{,}000 \times 200}{2\pi^2 \times 120 \times 3{,}000}} = 5.6 \text{ inches.}$$

Example 20.—Determine the horse-power transmitted by a propeller shaft if $d = 6$ ins., $n = 120$ R.P.M., $G = 12 \times 10^6$ lbs. per sq. inch, and the angle of twist, as measured between two cross-sections 25 ft. apart, is equal to $\frac{1}{15}$ of a radian.

Solution.—From the equation (29),

$$M_t = \frac{\phi_t GI_p}{l} = \frac{12 \times 10^6 \times \pi \times 6^4}{15 \times 32 \times 25 \times 12}$$

The power transmitted is

$$\frac{M_t \times 2\pi n}{12 \times 33{,}000} = \frac{12 \times 10^6 \times \pi \times 6^4 \times 2\pi \times 120}{12 \times 33{,}000 \times 15 \times 32 \times 25 \times 12} = 646 \text{ h.p.}$$

Example 21.—Determine the outer diameter D and the internal diameter d of a hollow propeller shaft transmitting 8,000 h.p. if n = 100 R.P.M., $D/d = 2$, and the working stress is equal to 4,500 lbs. per sq. inch.

Solution.—Torque moment

$$M_t = \frac{8{,}000 \times 12 \times 33{,}000}{2\pi \times 100}$$

$$I_p = \frac{\pi D^4}{32} - \frac{\pi d^4}{32} = \frac{15}{16}\frac{\pi D^4}{32}$$

Maximum stress is determined by the equation

$$(p_t)_{\max} = \frac{M_t D}{2I_p} = \frac{16}{15} \times \frac{16 M_t}{\pi D^3},$$

from which

$$D = \sqrt[3]{\frac{16}{15} \times \frac{16 \times 8{,}000 \times 12 \times 33{,}000}{2\pi \times 100 \times \pi \times 4{,}500}} = 18.2 \text{ in.}$$

Example 22.—Figure 37 shows a circular shaft AB with clamped ends submitted to the action of a torque moment M_t, applied in an intermediate cross-section mn.* Determine the angle of twist if the working stress $(p_t)_w$ is known.

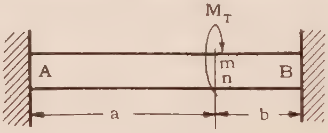

Fig. 37.

Solution.—For both parts of the shaft the angles of twist are equal, therefore the twisting moments will be inversely proportional to the lengths of these parts. If $a > b$, the greater twisting moment will be in the right part of the shaft and its magnitude is

$$\frac{M_t a}{a + b} \tag{a}$$

Substituting this for torque moment, and $(p_t)_w$ for $(p_t)_{\max}$ in equation (31), the following equation for d is obtained:

$$d = \sqrt[3]{\frac{16 a M_t}{(a + b)\pi (p_t)_w}} \tag{b}$$

Now the angle of twist can be obtained by using equation (29) page 28.

9. Helical Spring, Close Coiled.†

—Assume that a close coiled **helical spring** of circular cross-section is submitted to the action of axial forces P (Fig. 38), and that any one coil lies nearly in a plane perpendicular to the axis of the helix. The stresses over any axial section of the coil can be reduced to a shearing force P and to a torque moment PR as shown in Fig. 38. Neglecting the stresses produced by the shearing force and using formula (31) the following *equation for maximum stress* is obtained:

---

* Such a problem may be encountered in considering the twist of driver axles for electric locomotives.

† A more detailed consideration of stresses in helical springs will be given below in par. 54.

$$(p_t)_{\max} = \frac{16\,PR}{\pi d^3} \tag{34}$$

The extension δ of the spring can be obtained from the consideration of the potential energy of deformation.

On the assumptions made above, any coil may be regarded as subjected to torsion only. Then, by using equation (33), the potential energy of the spring will be

$$U = \frac{M_t^2 l}{2GI_p} = \frac{P^2R^2 \cdot 2\pi Rn}{2\,G \cdot \frac{\pi d^4}{32}} \tag{a}$$

in which n denotes the number of coils. Equating (a) to the work done by the force P in extending the spring, the following equation is obtained:

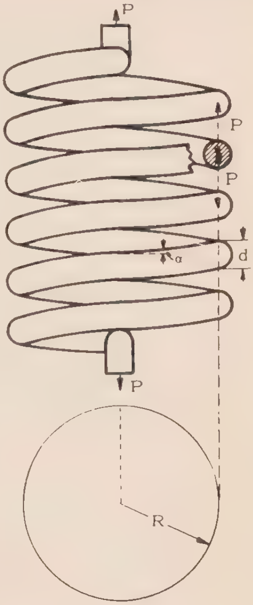

FIG. 38.—Close coiled helical spring in tension.

$$\frac{P\delta}{2} = \frac{P^2R^2 \cdot 2\pi Rn}{2G \cdot \frac{\pi d^4}{32}}$$

from which

$$\delta = \frac{64nPR^3}{Gd^4} \tag{35}$$

This formula can be used in the approximate calculation of the stiffness of a helical spring.*

Example 23.—A conical spring (Fig. 39) is submitted to the action of axial forces P. Determine the safe magnitude of P if the working stress $(p_t)_{\max} =$ 45,000 lbs. per sq. inch; the diameter of the cross-section, $d = 1$ in.; the radius of the cone at the top of the spring, $r_1 = 2$ in.; and at the bottom, $r_2 = 8$ in. Determine the extension of the spring if the number of coils $= n$ and the horizontal projection of the center line of the spring is a spiral given by the equation

---

* Experimental work on extension of helical springs: see Zacharias, *Mitteilungen über Forschungsarbeiten*, #106 (Berlin).

$$\rho = r_1 + \frac{(r_2 - r_1)\theta}{2\pi n}.$$

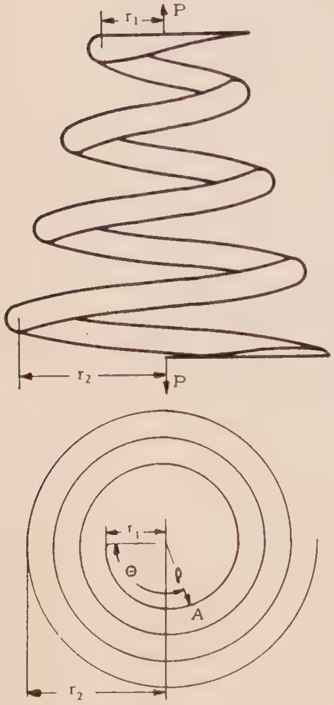

FIG. 39.

Solution.—For any point A of the spring determined by the magnitude of the angle θ, the distance from the axis of the spring is

$$\rho = r_1 + \frac{(r_2 - r_1)\theta}{2\pi n}$$

and the corresponding torque moment

$$M_t = P\left(r_1 + \frac{(r_2 - r_1)\theta}{2\pi n}\right)$$

The maximum torque moment, at $\theta = 2\pi n$, is Pr_2. Using equation (31), the safe limit for P will be determined by the equation

$$(p_t)_w = \frac{16Pr_2}{\pi d^3}$$

from which

$$P = \frac{45{,}000 \times \pi}{16 \times 8} = 1{,}100 \text{ lbs.}$$

In calculating the extension of the spring the expression for the potential energy of deformation will be used. The length of an element of the spring is

$$ds = \left[r_1 + \frac{(r_2 - r_1)\theta}{2\pi n}\right]d\theta.$$

The potential energy of deformation of this element is

$$dU = \frac{M_t^2 ds}{2GI_p} = \frac{16P^2}{G\pi d^4}\left[r_1 + \frac{(r_2 - r_1)\theta}{2\pi n}\right]^3 d\theta.$$

Now the extension of the spring δ will be determined by the equation

$$\frac{P\delta}{2} = \int_0^{2\pi n} dU = \int_0^{2\pi n} \frac{16P^2}{G\pi d^4}\left(r_1 + \frac{(r_2 - r_1)\theta}{2\pi n}\right)^3 d\theta$$

from which

$$\delta = \frac{16Pn}{Gd^4}(r_2^2 + r_1^2)(r_2 + r_1) = \frac{16P(r_2^2 + r_1^2)l}{\pi G d^4}$$

in which

$$l = 2\pi n \frac{(r_2 + r_1)}{2}$$

and denotes the length of the spring.

When $r_1 = r_2$, the result obtained is the same as that of equation (35).

10. Shafts of Non-circular Cross-section.—When non-circular shafts are subjected to twist, cross-sections originally plane become distorted and the stress distribution can not be obtained in an elementary way.* In such cases, however, the fundamental equations of elasticity must be used. Some numerical results obtained from such are given below.

Rectangular Cross-section.—It can be shown that, due to distortion of the cross-section, the maximum shear occurs at the midpoint of the faces of the bar; and at points on the corners the stress becomes zero. Let Fig. 40 represent the cross-section of the bar, then the maximum stress will occur at points *m-m* in the middle of the larger sides. *The magnitude of* $(p_t)_{\max}$ can be calculated from equation

$$(p_t)_{\max} = \frac{M_t}{\alpha bc^2} \tag{36}$$

in which α denotes a constant depending on the magnitude of the ratio b/c. A few values of this constant are given in Table II. Sufficiently accurate results can also be obtained by using the approximate relation

$$(p_t)_{\max} = \frac{M_t(3b + 1.8c)}{b^2c^2}$$

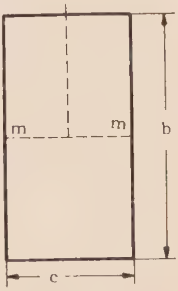

FIG. 40.—A shaft of rectangular cross section.

TABLE II.—TABLE OF CONSTANTS FOR RECTANGULAR CROSS SECTIONS

$b/c =$	1	1.5	1.75	2	2.50	3	4	10	∞
$\alpha =$	.208	.231	.239	.246	.258	.267	.282	.312	.333
$\gamma =$	.141	.196	.214	.229	.249	.263	.281	.312	.333

The angle of twist can be obtained from the equation

$$\phi_l = \frac{M_t l}{\gamma G b c^3} \tag{37}$$

in which l denotes the length of the shaft and γ a constant depending on the magnitude of the ratio b/c. Numerical values of this factor are given in Table II.

Elliptical Cross-section.—In the case of elliptical cross-sections the maximum stress occurs at the ends of the minor axis *m-m* (Fig. 41). Along the principal axes of the ellipse the shearing stresses are perpendicular to these axes and vary

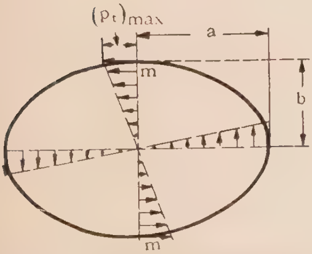

FIG. 41.—A shaft of elliptical cross section.

---

* General solution of this problem belongs to St. Venant. An account of his work will be found in Todhunter and Pearson's "History of the Theory of Elasticity," p. 312. For new literature on the subject, see paper of Th. Pöschl, *Zeitsch. f. Angew. Math.*, Vol. 1, p. 312, 1921.

corresponding to a linear law as shown in the figure. The **magnitude of** $(p_t)_{\max}$ is determined by the equation

$$(p_t)_{\max} = \frac{2M_t}{\pi ab^2} \tag{38}$$

In the case of $a = b$, this equation becomes the well known expression for circular shafts. *The angle of twist* of elliptical shafts is determined from the equation

$$\phi_l = \frac{4\pi^2 M_t l I_p}{GA^4} \tag{39}$$

in which $A = \pi ab$ is the area, and

$$I_p = \frac{\pi ab^3}{4} + \frac{\pi ba^3}{4}$$

is the polar moment of inertia of the cross-section.

Other Forms of Cross-sections.—In all the cases considered above, the *angle of twist* can be represented by the expression

$$\phi_l = \frac{M_t l}{C} \tag{40}$$

where the magnitude of C depends on the dimensions of the cross-section and is proportional to the modulus of rigidity G. The quantity C is called the *torsional rigidity* of the shaft. In the case of elliptical sections,

$$C = \frac{GA^4}{4\pi^2 I_p} \tag{41}$$

S. Venant, who gave solutions for various shapes of cross-sections, observed that formula (41) could be used as an approximate formula for all cases of *solid shafts*. In other words, that the angle of twist for a solid shaft is approximately equal in magnitude to that for an elliptical shaft of the same cross-sectional area and the same polar moment of inertia. Applying this reasoning, and taking, for instance, a square cross-section in which

$$A = a^2, \text{ then } I_p = \frac{a^4}{6}.$$

From (41),

$$C = \frac{Ga^4}{6.58} = .152Ga^4.$$

Then the same quantity, calculated from Table II, for a rectangular cross-section would be

$$C = \gamma Ga^4 = .141Ga^4,$$

or the error for the approximation would be about 7.8%. For a rectangular section, the ratio of sides being equal to 2, the same approximate formula gives an error equal to 6.1%. For cross-sections such as I beams, the same approximate method can be applied in calculating the angles of twist. A more accurate solution of the same problem will be shown below.*

11. Torsion of Circular Shafts of Variable Cross-section.—*Graphical Solution.*—A general solution of the problem shows† that in the case where the diameter is not constant, cross-sections originally plane remain so after twisting, but the radii of these sections become curved and the stresses are no longer proportional to the distance from the axis of the shaft.

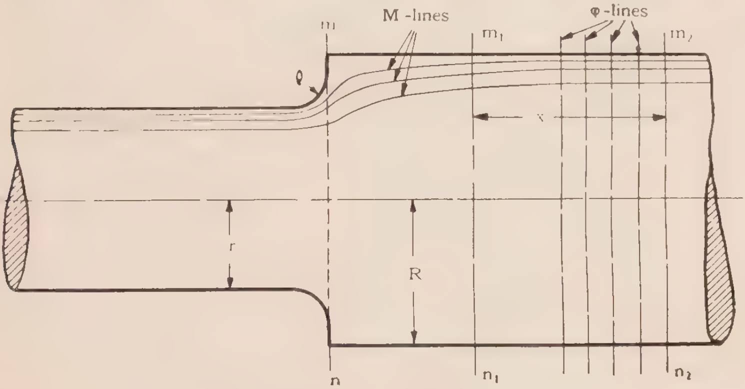

FIG. 42.—Circular shaft of variable cross section.

Solutions so far obtained for a shaft of conical form‡ and for one having the form of a paraboloid of revolution§ show that the simple formula for maximum stress obtained above for a shaft having a constant circular section, is accurate enough for the cases of variable section, provided the change in section is not too rapid. In the case of *sharp variation* of cross-section, high concentration of stresses may occur in places, special consideration of such *local stresses* in these regions becoming necessary. The case of a shaft consisting of two portions of different radii, a type of construction widely used in service, will now be considered. Let Fig. 42 represent the axial section of the shaft, r and R denoting the radii of the two sections.

---

* Experimental investigation of torsional rigidity of I beams, see A. Foeppl, *Sitzungsber. d. Bayerischen Akademie d. Wissenschaften,* p. 295, 1921.

† General solution of the problem belongs to I. H. Michell, *Proc. London Mathem. Soc.* Vol. 31 (1899). In practice the most important case is that of torsion of a shaft consisting of two cylindrical parts of different radii. This case was considered first by A. Foeppl, see *Technische Mechanik* Vol. 5, p. 177, 1907. The literature on this subject is compiled in an article by Th. Poeschl, *Zeitschr. f. Angew. Mathem. u. Mechanik,* Vol. 2, p. 137, 1922 (Berlin).

‡ See the book of A. Foeppl mentioned above.

§ A. Dinnik, *Bulletin of the Polytechnical Inst. in Novotsherkassk,* 1912, Russia.

In solving the problem an approximate method will be applied.* Consider first any section m_1n_1 at a considerable distance from the section mn where the sharp variation occurs. The stresses in the section m_1n_1 can be obtained by using formulae for the cylindrical shaft previously considered. The shearing stress at any point of the cross-section distant a from the axis of the shaft will be given by

$$p_t = \frac{(p_t)_{\max}\, a}{R} \tag{a}$$

where

$$(p_t)_{\max} = \frac{2M_t}{\pi R^3} \tag{b}$$

The direction of this stress along an axial section will be parallel to the axis of the shaft.

Imagine now a cylindrical surface of any radius a concentric with the shaft. It can be concluded from the equation (d) page 28 that the moment M_a transmitted by the part of the shaft within this surface will be

$$M_a = M_t\left(\frac{a}{R}\right)^4 \tag{c}$$

Dividing the torque moment in n equal parts and substituting in (c)

$$M_a = \frac{1}{n}\, M_t,\ M_a = \frac{2}{n}\, M_t \text{ and so on}$$

the shaft can be divided into concentric cylindrical shells transmitting equal parts of the torque moment M_t. Some corresponding lines of division in axial sections are shown in Fig. 42. In the following these lines will be called *lines of constant*, M_a or *M-lines*. Let ΔM denote the torque moment transmitted by every cylindrical shell and Δa the variable thickness of shells, then by differentiation of (c),

$$\Delta a = \Delta M_a \frac{R^4}{4M_t a^3} \tag{d}$$

or using (a) and (b)

$$\frac{\Delta M_a}{\Delta a} = 2\pi a^2 p_t \tag{e}$$

---

* This method was developed by F. A. Willers, *Zeitschr. f. Mathem. u. Phys.* Vol. 55, p. 225, 1907.

From these results it is seen that the system of M-lines shows how the stress distribution varies over an axial section of the shaft, namely: (1) the direction of lines coincides with the direction of stress in points of these lines; (2) the magnitude of stress is determined by the distance Δa between the consecutive M-lines, because, as it is seen from (e), the quantity $a^2 p_t$ is inversely proportional to the distance Δa between the M-lines.

The angle of twist of any cross-section $m_1 n_1$ at a considerable distance from the section mn is

$$\phi = \frac{2M_t x}{G\pi R^4} \tag{f}$$

in which x denotes the distance of $m_1 n_1$ from a reference cross-section $m_2 n_2$ of the shaft. Dividing the angle of twist ϕ in equal parts $\Delta\phi$ and tracing the corresponding cross-sections, the system of lines $\phi =$ constant will be obtained. The distances between these lines, as calculated from (f), are

$$\Delta x = \Delta\phi \frac{G\pi R^4}{2\ M_t} \tag{h}$$

Some of these lines are shown in Fig. 42. An orthogonal system of M and ϕ-lines divides the longitudinal section of the shaft into small rectangles with the ratio of sides equal to

$$\frac{\Delta a}{\Delta x} = \Delta M_a \frac{R^4}{4M_t a^3} : \Delta\phi \frac{\pi R^4 G}{2M_t} = \frac{\Delta M_a}{\Delta\phi} \frac{1}{2\pi a^3 G} \tag{g}$$

In the same manner the orthogonal system of M and ϕ-lines can be traced on the part of the shaft of radius r. Retaining for ΔM_a and $\Delta\phi$ the same values as above and denoting by a_1 the distances of M-lines from the axis of the shaft and by x_1 distances along the shaft measured from a reference section on the left hand side of shaft, the following equations will be obtained from (c), (d), and (h):

$$a_1 = \frac{ar}{R}$$

$$\Delta a_1 = \Delta M_a \frac{r^4}{4M_t a_1^3} = \Delta a \frac{r}{R}$$

$$\Delta x_1 = \Delta\phi \frac{G\pi r^4}{2M_t} = \Delta x \frac{r^4}{R^4}$$

The longitudinal section of the left part of the shaft will be divided into small rectangles with the ratio of sides equal to

$$\frac{\Delta a_1}{\Delta x_1} = \frac{\Delta M_a}{\Delta\phi} \frac{1}{2\pi a_1^3 G}$$

Near the cross-section *mn*, the *M* and ϕ-lines become curvilinear, but remain orthogonal and retain the properties stated above;* which properties may be summed:

1. The tangent to the curved *M*-line at any point gives the direction of the stress p_t at this point.

2. The distance between two consecutive *M*-lines is inversely proportional to a^2p_t, where a, as before, denotes the distance of the point considered from the axis of the shaft.

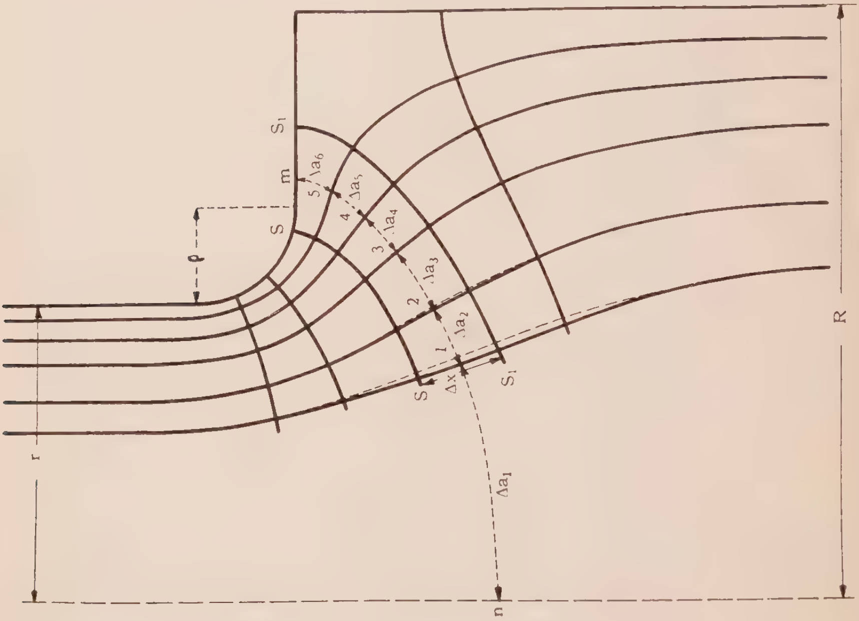

Fig. 43.

3. All points on the same ϕ-line move through the same angle during twist.

4. An orthogonal system of *M* and ϕ-lines divides the axial section of the shaft in curvilinear rectangles having the side-ratio given by (g).

By using this data a method for tracing the *M* and ϕ-lines near the cross-section *mn* is devised. In the first place the straight *M* lines in both cylindrical parts of the shaft must be drawn as explained above. Then the corresponding rectilinear parts of the *M*-lines must be drawn properly connected by continuous curves. In such manner a first approximation for M-lines is obtained. It may be very approximate, but by using it together with equation (g) further corrections can be obtained as follows: Orthogonal to the M-lines, obtained as explained above, the two curves ss and s_1s_1 and the middle curve mn between them must be traced as shown in Fig. 43. Now proceeding along mn the torque moment M_a corresponding to any radial distance a can be calculated by using equation (g). This equation gives

---

* See paper by F. A. Willers, mentioned above.

$$\Delta M_a = 2\pi a^3 G \Delta\phi \frac{\Delta a}{\Delta x} \tag{k}$$

The quantities Δa and Δx represent distances between the middle points of opposite sides of the curvilinear rectangles bounded by ss, s_1s_1, and the M-lines. These quantities are to be taken from the drawing as shown in Fig. 43. Along the mn line $\Delta\phi$ remains constant: a represents the distances from the axis of the shaft.

In the table below all these quantities for points 1, . . . 6, in Fig. 43 are given. The units for the measurements may be taken arbitrarily. In the case under consideration the unit length in measuring a was taken equal to $\frac{5}{16}$ inch. In measuring Δa and Δx the unit length was equal to $\frac{1}{100}$ inch.

	1	2	3	4	5	6
$a =$	3.98	4.91	5.90	6.50	6.92	7.13
$\Delta a =$	127.	32.	37.	25.	23.	21.
$\Delta x =$	45.0	44.0	44.0	48.0	52.5	55.0
$a^3 =$	63.0	118.	205.	275.	331.	362.
$a^3/\Delta x =$	1.40	2.68	4.66	5.72	6.30	6.58

From (k),

$$M_a = c \int_0^a \frac{a^3}{\Delta x}\, da$$

in which c is a constant.

In Fig. 44 the quantity $a^3/\Delta x$ is represented graphically as a function of distance measured along the mn curve. Then the increasing of M_a along the mn curve can be obtained graphically as the integral of the curve $a^3/\Delta x$.

This is shown drawn in Fig. 44 as follows: The $a^3/\Delta x$ curve is replaced by the line 1, 2, 3, 4, 5, 6, 7 in such a manner that the cross-hatched areas on both sides of verticals 1-2, 3-4 and 5-6 are equal. Considering 1-2, 3-4 and 5-6 as forces and taking arbitrary length H, as pole-distance, the funicular polygon $obcde$ was obtained. It is easy to see that the sides of this polygon must be tangent to the integral curve of the $a^3/\Delta x$ curve at points e, g, f, o. Now the integral curve desired can be traced through these points. The end ordinate *ek* of the curve obtained represents, to some scale, the complete torque moment M_t. Dividing this ordinate in parts, as shown in Fig. 44, it is easy to locate on the integral curve the points corresponding to $.8M_t$, $.6M_t$, $.4M_t$, $.2M_t$ and $.1M_t$. The abscissae of these points give the second approximation for the distances Δa_1, . . . Δa_6.

In Fig. 43 the first approximation for the M-lines is shown with dotted lines and the second approximation with full lines. It is seen that in the second approximation only the distances Δa_2 and Δa_3 are somewhat changed. Performing similar calculations as described above for a number of ϕ curves, enough points can be obtained for tracing the second approximation of M-lines. Further approximation, if necessary, can be obtained by proceeding with the second approximation in the same manner as explained above. The diminishing of distances Δa near the fillets indicates at once the concentration of stresses in this portion of the shaft. A first approximation for these local stresses near the fillet can be obtained by measuring distances Δa and using equation (e). Further approximations can be calculated numerically.*

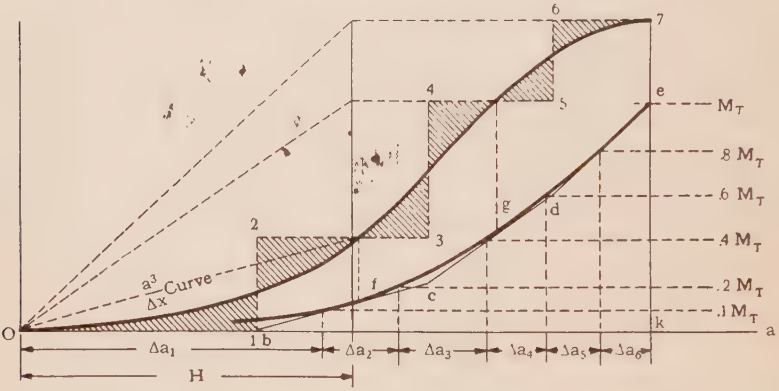

FIG. 44.

Numerical Results.—Some results obtained in this manner and having a practical application are given below. The maximum shearing stress $(p_t)_{\max}$ in the region of the *fillet*, Fig. 42, is a function of the two quantities: r/R and ρ/r in which ρ denotes the radius of the fillet. The curve in Fig. 45 represents $(p_t)_{\max}$ calculated for $r/R = 3/4$ and for ρ/r varying in the limits $0.05 - 0.25$. The stress

---

* The method of calculation is shown in the paper of Willers mentioned above.

$(p_t)_0$ calculated for the cylindrical shaft of radius r by using equation (31) is given in the same figure. It is easy to see that stress concentration increases with the decrease of ρ/r. For $\rho/r = .25$, $(p_t)_{\max}: (p_t)_0 = 1.25$; and for $\rho/r = 0.05$, the same ratio is equal to approximately 2. The theoretical investigation shows that by further diminishing of ρ/r, $(p_t)_{\max}$ increases in proportion $1/\sqrt[3]{\rho}$; and if $\rho = 0$, it becomes theoretically equal to infinity. The curve in Fig. 46 represents $(p_t)_{\max}$ as a function of $\frac{R-r}{r}$. Ratio ρ/r is taken here equal to .10. It is seen that the stress concentration increases with the increasing of $\frac{R-r}{r}$. For $\frac{R-r}{r} = .8$, the coefficient of concentration is about 1.75. For $\frac{R-r}{r} = .2$, the same coefficient is about 1.50.

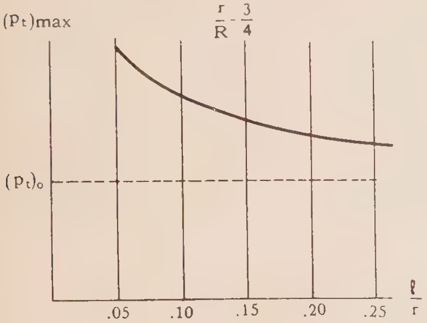

FIG. 45.—Stress concentration produced by fillets for the case $\frac{r}{R} = \frac{3}{4}$.

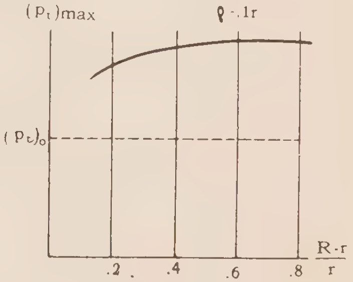

FIG. 46.—Stress concentration produced by fillets for the case $\frac{\rho}{r} = .1$.

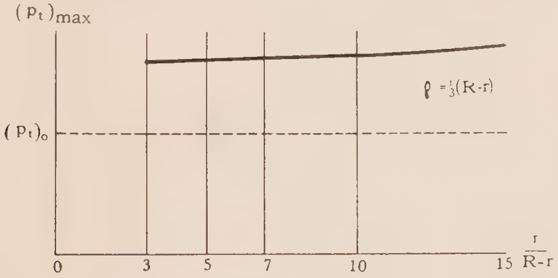

FIG. 47.—Stress concentration produced by fillets for the case $\rho = \frac{1}{3}(R - r)$.

In Fig. 47 values of $(p_t)_{\max}$ are given for $\rho = \frac{1}{3}(R - r)$. It is seen that if $\frac{\rho}{R - r}$ is constant, only small variations of ratio $\frac{(p_t)_{\max}}{(p_t)_0}$ take place.

In Fig. 48 the coefficients of stress concentration produced by a *groove* of semi-circular cross-section (Fig. 49) are given. $(p_t)_{\max}$ occurs in points a. This stress increases with decreasing of the ratio R/ρ.

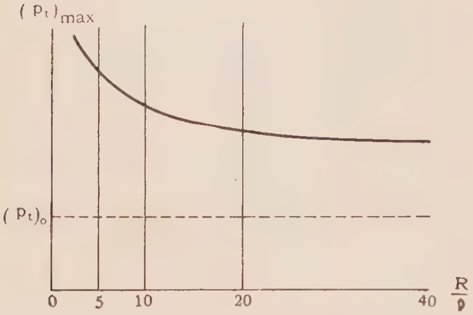

FIG. 48.—Stress concentration produced by a groove of semi-circular cross section.

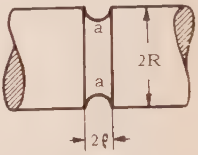

FIG. 49.—A groove of a semi-circular cross section.

12. Hydrodynamical Analogy.

General Consideration.—The torsion problem of cylindrical bars is mathematically identical to that of the motion of a *frictionless fluid* moving with uniform angular velocity inside a cylindrical shell having the same cross-section as the bar. The velocity of the circulating fluid at any point is taken as representing the shearing stress at that point of the cross-section of the bar when twisted. By using this analogy, certain conclusions on the stress-distribution after twisting can be easily obtained.

In the case of a circular cross-section, the velocity of the fluid moving with uniform angular velocity will be proportional to the distance from the center of the circle. This is in complete agreement with the stress-distribution for a circular shaft. In the case of an elliptical cross-section, the velocities of the circulating fluid at points on the minor axis must be greater than those at corresponding points on the major axis. This follows at once if the fact be taken into consideration that the quantities of fluid passing axial sections of the elliptical shell in unit time must be equal. The region of greater velocities for the case of the fluid will correspond to the region of the greater stresses in the case of the twisted elliptical shaft.

Analogous conclusions can be made in the case of a rectangular cross-section, in which maximum stresses must be expected in the middle points of the larger sides (Fig. 40). At a corner of the section the velocity of the circulating fluid becomes equal to zero. This indicates that, when twisted, the tangential stresses at the corners of rectangular bars become equal to zero.

*Longitudinal Holes and Grooves.**—The result of boring a small hole in a shaft of circular section (Fig. 50) will be to modify the velocity system in that neighborhood in the same way as a solid cylinder changes the velocities in the stream flowing past it. The velocities at the front and rear points m and n are reduced to zero, while those at the side points m_1 and n_1 are doubled. A hole of this kind therefore doubles the maximum stress in the portion of the shaft where it is located. If there is a *semi-circular groove* on the surface parallel to the length of the shaft (Fig. 50) the effect will be the same, in that the shear in the neighborhood of the point n may be nearly twice the shearing stress calculated for the points on the surface of a shaft without the groove.

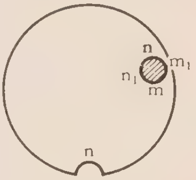

FIG. 50.—Stress concentration produced by circular holes and grooves.

In the case of a *hole of elliptical cross-section* or of a *groove of semi-elliptical cross-section,* the same *hydrodynamical analogy* can be used. If v denotes the velocity of the stream, then the velocity at points m-m is zero (Fig. 51), while at points n-n it is equal to

$$v\left(1 + \frac{a}{b}\right) \tag{a}$$

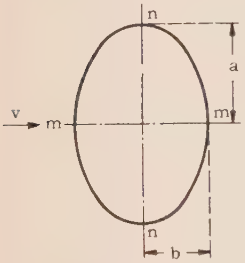

FIG. 51.—Elliptical hole.

It is seen that the maximum stress produced in this case depends on the magnitude of the ratio a/b. The weakening effect of an elliptical hole will be greater when the major axis of the ellipse extends in a radial direction than when this axis runs circumferentially in direction. The same equation (a) can be used also in the case of a semi-elliptical groove on the surface parallel to the axis of the shaft.

In the case of a *keyway* with sharp corners (Fig. 52), the velocity of the fluid at the corner projecting outwards (points m-m) vanishes and therefore the shearing stress in the corresponding torsion problem will be equal to zero at such corners. At points n-n, vertices of reentrant angles, the velocity of the circulating fluid becomes theoretically infinite. In the corresponding torsion problem the shearing stresses become also infinite at points *n-n*, i.e., a small torque moment will produce permanent set at these points. This concentration of stress can be decreased by rounding the corners *n-n*.

---

* Larmour, *Phil. Mag.* Vol. 33, p. 76, 1892.

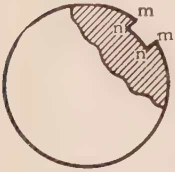

FIG. 52.—Stress concentration produced by keyways.

From the experiments made,* by using the membrane-method, (explained, paragraph 13, page 44) the coefficients k of stress concentration, given in Table III, were obtained. The dimensions of the shaft were: outside diameter of shaft 10 in.; inside diameter 5.8 in.; depth of keyway 1.0 in.; width of keyway 2.5 in.; radius of fillet in corner of keyway, in inches = ρ. The maximum stress at the rounded corner will be obtained by multiplying the maximum stress in a similar shaft without keyway by the corresponding coefficient of stress concentration.

TABLE III.—STRESS CONCENTRATION CONSTANTS FOR KEYWAYS

ρ inches............	.1	.2	.3	.4	.5	.6	.7
k.................	5.4	3.4	2.7	2.3	2.1	2.0	1.9

In all the cases considered above, the high stresses obtained were of a "local" character. They decreased rapidly with increase of distance from the overstressed points.

In a static test of such shafts, the *weakening effect* of grooves and cavities may remain unnoticed provided the material of the shaft is ductile enough. Different results, however, may be expected, for dynamic conditions, when the twisting moment, due to vibrations, passes through a large number of cycles per second. Under such conditions the fatigue of material at these *overstressed* portions of the shaft may take place, and as a result a gradual development of *cracks* may begin,† which will ultimately lead to failure.

13. Membrane Analogy.—*General Consideration.*—Let a *homogeneous membrane* with outlines similar to the cross section of the torsional member, be stretched at the edges with a uniform tension of p pounds per unit length. If the membrane be subjected to a uniform pressure of amount q per unit of area, it will undergo a small deflection, and if

---

* See "The Mechanical Properties of Fluids—A Collective Work," p. 245, 1924, D. Van Nostrand Co.

† Some experimental work in this field was done at the National Physical Laboratory, Middlesex, England.

$$\frac{q}{p} = 2G\frac{d\phi}{dx}, \tag{a}$$

the equation of equilibrium of the membrane will coincide with that of the torsion problem.* This makes it possible to study the stress-distribution of shear over the cross-section, in an experimental manner.

If the curved surface of the deflected membrane be represented by its *contour-lines* the following relations of these lines to the stress distribution due to twist can be stated:

1. The tangent to any contour-line at any point of the membrane gives the direction of the shearing stress at the corresponding point in the cross-section of the twisted bar.

2. The slope of the surface of the membrane with respect to the plane of its edges at any point gives the magnitude of shearing stress at the corresponding point in the twisted bar.

3. Twice the volume included between the surface of the deflected membrane and the plane of its outline is equal to the torque moment of the twisted bar.

On the basis of these statements, certain conclusions regarding the stress-distribution during torsion can be easily obtained. Taking for instance, a rectangular cross-section, the corresponding surface of the deflected membrane is represented by its contour-lines in Fig. 53.

1. It is easy to see that the slope of the membrane at any point on section *om* will be greater than that at a point on the same contour line in section *on*. This indicates that at twist the shearing stresses at points on the axis *om* will be greater than that at corresponding points on the axis *on*.

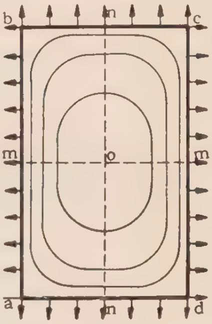

Fig. 53.—Membrane analogy for a rectangular cross section.

2. The maximum stress, corresponding to maximum slope will act at points *m-m*.

3. At the corners *a*, *b*, *c*, *d*, where the surface of the membrane coincides with the plane of the contour *abcd*, the slope of this surface becomes equal to zero. This indicates that at these points the shearing stress is equal to zero.

---

* This analogy was developed by L. Prandtl, see *Phys. Zeitschr.* p. 758 (1903). *Jahresberichte d. Deutsch. Math. Ver.* Vol. 13, p. 31, 1904. See also author's paper *Proc. London Math. Soc.*, Ser. 2., Vol. 20, p. 389, 1921.

In his experiments, L. Prandtl used, instead of a membrane, a soap film, and measured the slope of the surface by an optical method.*

Narrow Rectangular Cross-section.—By using the membrane analogy the stress-distribution for this case can be easily obtained. Neglecting the effect of the short sides of the rectangle it can be assumed that the sectional outline of the surface of the uniformly loaded membrane is parabolic (Fig. 54). By this assumption the maximum deflection of the membrane can be calculated from the known equation for a uniformly loaded *flexible cord:*

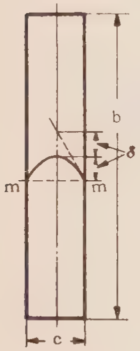

FIG. 54.—Membrane analogy for a narrow rectangular cross section.

$$\delta = \frac{qc^2}{8p}. \tag{b}$$

From (a) and (b),

$$\delta = \frac{c^2}{4} G \frac{d\phi}{dx} \tag{c}$$

The volume of the parabolic cylinder formed by deflection surface of the membrane will be

$$V = \frac{2}{3} \delta cb = \frac{bc^3 G}{6} \frac{d\phi}{dx} \tag{d}$$

The slope at points m-m for a parabola is

$$\frac{4\delta}{c} = cG \frac{d\phi}{dx} \tag{e}$$

Now, by using the membrane analogy, the following *formulae for torque moment and maximum stress* will be obtained:

$$M_t = 2V = \frac{bc^3}{3} G \frac{d\phi}{dx} \tag{42}$$

$$(p_t)_{\max} = cG \frac{d\phi}{dx} = \frac{3M_t}{bc^2} \tag{43}$$

These results are in complete agreement with equations (36) and (37) page 33 where α and β of these equations equal $\frac{1}{3}$.

From the membrane analogy, it also follows that for the case of a slotted thin tube (Fig. 55), the equations (42) and (43) can be used, substituting $2\pi R$ for b in equations (42) and (43). Then

$$M_t = \frac{2}{3} \pi R c^3 G \frac{d\phi}{dx}$$

$$(p_t)_{\max} = \frac{3}{2\pi} \frac{M_t}{Rc^2} \tag{44}$$

---

* See Anthes, *Dinglers Polyt. Journal*, p. 342, 1906. Further development of this method was done by A. A. Griffith and G. T. Taylor, *London Engineering*, Vol. 104, 1917.

The same membrane analogy shows that in such cases as are represented in Fig. 56, the torsional rigidity of the bars can be calculated by dividing the cross-sections into component narrow rectangles as shown in the figure and applying to these rectangles equation (42). Summing the results obtained in this manner for these rectangles, the torsional rigidities for the complete sections of Fig. 56 can be obtained.

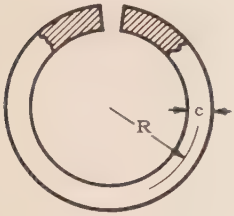

Fig. 55.—A split circular tube.

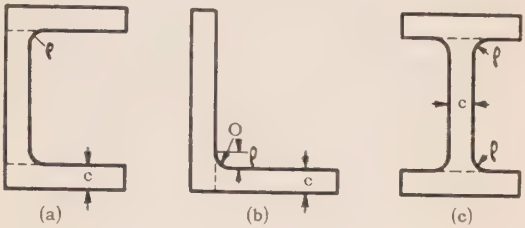

(a) (b) (c)

Fig. 56.

The maximum stress in such cases usually will occur at the re-entrant angles, such as at 0 in Fig. 56 (b). This stress can be represented by the equation*

$$(p_t)_{\max} = 1.74 \sqrt[3]{\frac{c}{\rho}} \cdot cG \frac{d\phi}{dx} \tag{45}$$

in which c/ρ is the ratio of the thickness of the section to the radius of the fillet. Comparing (45) and (43) it is seen that the quantity $1.74\sqrt[3]{\frac{c}{\rho}}$ represents in this case the *coefficient of stress concentration.*

Tubular Sections.†—In applying the membrane analogy to the cases of tubular sections it is only necessary to imagine that the outer and inner boundaries of the section are located in different horizontal planes and that the membrane connects the boundaries as at *n-m*. The planes *mm* and *nn* are considered as rigid (Fig. 57). If the thickness of the tube is small the curvature of the membrane can be neglected and the slope of its surface assumed constant over the thickness of the wall. In this case the shearing

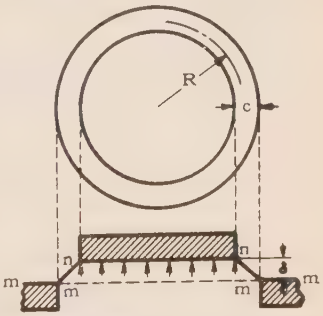

Fig. 57.—Membrane analogy for the case of a circular tube.

---

* See E. Trefftz, *Zeitschr. f. Angew. Math. u. Mech.*, Vol. 2, p. 263, 1922.

† R. Bredt, *Zeitschr. d. Ver. Deutsch. Ing.*, p. 815, 1896.
H. Lorenz, *Technische Elasticitäts-lehre*, p. 98, 1913.
J. Prescott, *Phil. Mag.*, Vol. 60, 1920.

stress becomes constant over the cross-section of the tube and is given by the equation

$$p_t = \frac{\delta}{c} \tag{f}$$

in which c = thickness of the wall, and δ = the difference in the levels of the two contours. The volume included between the planes m-m, n-n, and the surface of the membrane is

$$V = \pi R^2\delta$$

By using equation (f), the following equation for calculating torque moment is obtained:

$$M_t = 2V = 2\pi cR^2p_t$$

from which

$$p_t = \frac{M_t}{2\pi cR^2}.$$

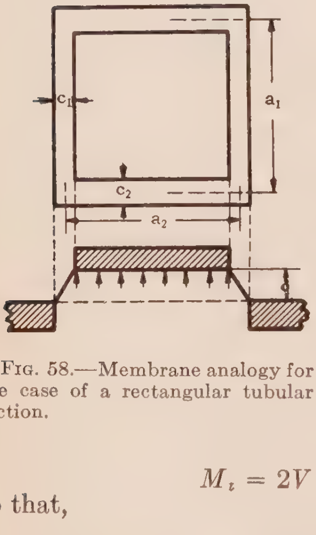

Fig. 58.—Membrane analogy for the case of a rectangular tubular section.

Comparing this with equation (44) it can be concluded that a longitudinal slot in a thin circular tube produces increase of stress in the ratio $3R/c$.

The same method can be used in the case of a tube of rectangular section (Fig. 58). In this case shearing stresses for thicknesses c_1 and c_2 of the wall will become

$$p_t' = \frac{\delta}{c_1}, \quad p_t'' = \frac{\delta}{c_2};$$

so that

$$p_t' : p_t'' = c_2 : c_1.$$

The magnitude of the torque moment will be

$$M_t = 2V = 2a_1a_2\delta = 2a_1a_2c_1p_t';$$

so that,

$$p_t' = p_t''\frac{c_2}{c_1} = \frac{M_t}{2a_1a_2c_1} \tag{46}$$

In calculating the angle of twist the expression for the potential energy of deformation can be applied. The potential energy at shear per unit volume is $p_t^2/2G$; therefore, the potential energy of the twisted rectangular tube will be

$$U = \frac{p_t'^2}{G}a_1c_1l + \frac{p_t''^2}{G}a_2c_2l = \frac{M_t^2l}{4G}\left(\frac{1}{a_1a_2^2c_1} + \frac{1}{a_1^2a_2c_2}\right)$$

in which l = the length of the tube.

The angle of twist will be determined by the equation

$$\frac{M_t\phi_l}{2} = U$$

from which

$$\phi_l = \frac{M_t l}{2G}\left(\frac{1}{a_1 a_2^2 c_1} + \frac{1}{a_1^2 a_2 c_2}\right) \tag{47}$$

The examples given above emphasize the importance of the hydrodynamical and membrane analogies in the solution of technical problems of twist. Their use enables us to obtain a picture of stress distribution in such regions where analysis alone would be impossible.

CHAPTER III

STRESSES IN BEAMS

14. Pure Bending.—*Simplest Case.*—A prismatical bar under the action of equal and opposite couples at its ends is said to undergo *pure bending* (Fig. 59). Considering the simplest case, where the bar has a longitudinal plane of symmetry and the external couples are acting in this plane, it is easy to see that bending will take place in this same plane. The solution of the problem for stress distribution and deflection of the bar can be obtained on the assumption that transverse sections of the bar originally plane, after bending, remain plane and normal to the *longitudinal fibres*. Thus the cross-sections *mm* and *rr* become, after bending, inclined one to the other. The longitudinal fibres on the convex side suffer extension and on the concave side—compression. The line *nn* represents the layer of fibres which does not undergo deformation at bending. This layer is called the *neutral surface* and its intersection with any cross-section is called the *neutral axis.*

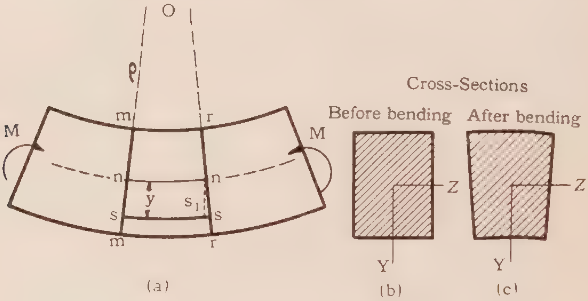

FIG. 59.—Pure bending.

Let:

l = length of beam.

b = width of rectangular beam.

h = depth of beam.

ρ = radius of curvature of beam.

I = moment of inertia of cross section about the neutral axis.
S = section modulus.
y = distance of elementary area from neutral axis.
E = modulus of elasticity.
$\frac{1}{m}$ = Poisson's ratio.
p = normal stress (tension or compression).
p_t = shearing stress.
e = unit elongation.
M = bending moment.
Q = shearing force.
q = uniformly distributed load per unit length.

Drawing ns_1 parallel to ns, (Fig. 59) the elongation ss_1 of any fibre ss, distant y from the neutral surface, is obtained. From the similarity of triangles nss_1 and onn an expression for the unit elongation of the fibre ss can be written as follows:

$$e = \frac{ss_1}{nn} = \frac{y}{\rho} \tag{a}$$

in which ρ denotes the *radius of curvature* of the bent bar.

The strain in the fibres in a longitudinal direction is accompanied by a *lateral deformation*. Due to this, the shape of all cross-sections undergoes some change. For instance, a rectangular cross-section such as Fig. 59 (b) assumes, after bending, the form shown in Fig. 59 (c). From experiments made it has been shown that the lateral expansion and contraction have the same ratio to the longitudinal strain of the fibres as in the case of simple tension. Therefore the stresses can be calculated, from (a), as follows:

$$p = \frac{Ey}{\rho} \tag{b}$$

The position of the neutral surface and the radius of curvature can be calculated from the condition that the stresses distributed over any cross-section of the bar must give rise to a *resisting couple* balancing the external couple M.

Let dA denote the elementary area of a cross-section distant y from the neutral axis, then from the condition mentioned above,

$$\int \frac{Ey}{\rho}\, dA = 0 \tag{c}$$

$$\int \frac{Ey^2}{\rho}\, dA = M \tag{d}$$

It follows at once from (c) that the neutral axis passes through the *center of gravity* of the section. From (d) the following equation for the curvature is obtained:

$$\frac{1}{\rho} = \frac{M}{EI} \tag{48}$$

In this expression, $I = \int y^2 dA$ represents the *moment of inertia* of the cross-sectional area about the neutral axis.

Substituting equation (48) in (b), the following equation for stresses is obtained:

$$p = \frac{My}{I} \tag{49}$$

The extreme values of p occur at points farthest removed from the neutral axis. When these points are equally distant from the neutral axis, and h denotes the height of the cross-section, the following extreme intensities of tensile and compressive stresses can be obtained:

$$p_{\text{tensile}} = p_{\text{comp.}} = \frac{Mh}{2I} = \frac{M}{S} \tag{50}$$

where

$$S = \frac{2I}{h} \tag{51}$$

is called the *section modulus.*

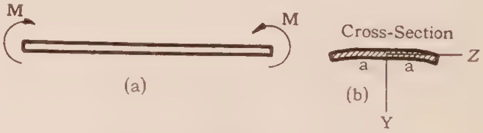

FIG. 60.—Bending of thin strip.

Bending of Thin Strips.—In the case of bending of a thin strip (Fig. 60) the lateral strain takes place only near the edges (Fig. 60 (b)).

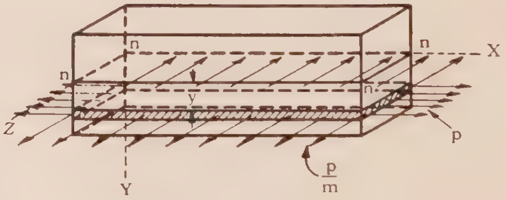

FIG. 61.—Combined stress in a thin strip due to bending.

The middle part of the strip (such as shown by *a-a* in the cross-section view Fig. 60 (b)) becomes bent into a cylindrical form the axis of which is parallel to the Z axis. The state of stress of any longitudinal fibre distant y from the neutral axis will be, due to the prevention of lateral contraction, as shown in Fig. 61. The equation (b) page 51 will then be modified (see equation (10a) page 12, and discussion) such that

$$p = \frac{Ey}{\left(1 - \frac{1}{m^2}\right)\rho},$$

i.e., the rigidity of the strip, due to the deflection into a cylindrical surface, increases in the ratio

$$\frac{1}{1 - \frac{1}{m^2}}.$$

This correction must be taken into consideration when calculating the modulus of elasticity from experiments on the bending of strips.*

General Case.—All the results obtained above for the case of a symmetrical beam hold also for unsymmetrical cross-sections. It is only necessary that the plane of external couples M (Fig. 59) contains one of the two *principal axes of inertia* Y and Z of the cross-section. These two planes XY and XZ will, in all future considerations, be called *principal planes of flexure;* the corresponding quantities EI_1 and EI_2 will be called *principal flexural rigidities* of the beam. When the plane of the couples is inclined to the principal planes of the beam, the couples can be resolved into component couples acting in the principal planes. The deflection and stresses produced by these components can be obtained as explained above. By adding these deflections vectorially, the pure bending problem for a general case may be solved.

Potential Energy Due to Pure Bending.—The couples M (Fig. 59) produce work during bending, which will be transformed into potential energy. Let U be the amount of this stored energy in the bent beam and denoting by θ the angle of rotation of one end of the beam in relation to the other, then the following equation for the work done by the couples is obtained:

$$U = \frac{M\theta}{2}.$$

If l denotes the length of the beam, then

$$\theta = \frac{l}{\rho} = \frac{Ml}{EI}$$

---

* See author's paper in *Mechanical Engineering*, p. 259, 1923.

and the expression for the potential energy produced by bending will be

$$U = \frac{M^2 l}{2EI} \tag{52}$$

Bending beyond the Elastic Limit.—If bending is continued beyond the proportional limit, the stresses in the longitudinal fibres will no longer be proportional to the longitudinal strains and the distribution of stress will not be as given by equation (49). Experimental data so far obtained* shows, however, that in bending beyond the elastic limit, the assumption that plane sections remain plane is approximately true. Therefore the strains of longitudinal fibres will be proportional to the distances from the neutral axis and the normal stresses will vary from the neutral axis to the extreme fibres as in the *stress-strain diagram* for direct stress. If these diagrams can be expressed analytically the position of the neutral axis and the bending moment corresponding to a given value of curvature $1/\rho$ can be calculated from equations (c) and (d) page 51. The simplest case will be that of a rectangular beam, the material of which has the same form of diagram for tension and compression. For such, the neutral axis will continue to pass through the centre of gravity of the cross-section, the distribution of tension and compression being symmetrical, but the intensity of stress will not be proportional to the distance from the neutral surface (Fig. 62). For a given magnitude of curvature, i.e., for a given extreme extension and compression, equal to $h/2\rho$, the corresponding maximum tension and compression can be easily found from tensile and compressive test diagrams.† These diagrams give the curve *ros* of stress-distribution over the cross-section *mn*. The moment of the areas *mro* and *osn* about the neutral axis multiplied by the width b of the cross-section gives the magnitude of the corresponding bending moment. By repeating this calculation for different values of curvature, the

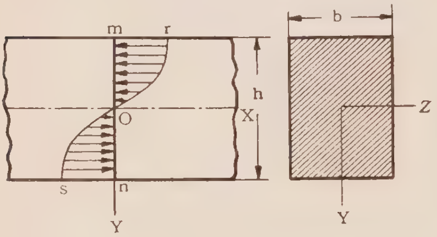

FIG. 62.—Stress distribution beyond proportional limit.

---

* See Bach, *Elasticität und Festigkeit*, p. 224, 1905.
H. Herbert, *Diss. Göttingen*, 1909.

† It is assumed that the diagrams of tension and compression, similar to Fig. 271 and Fig. 280, for the beam material are available.

relation between $1/\rho$ and M can be established, which must be taken instead of equation 48, in calculating the deflection of a beam stressed beyond the proportional limit.

Example 24.—Determine the maximum stress and deflection in a locomotive axle if the material be steel and the following conditions be given (Fig. 63):

l = length between supports = 59 in.
L = distance between center lines of springs = 86 in.
d = diameter of axle at end of journal = 10 in.
W = spring borne load per journal = 26,000 lbs.

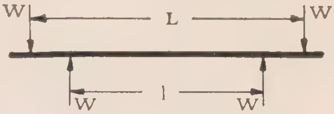

FIG. 63.

Solution.—The transfer of weight from one journal to another under dynamic conditions is neglected. The reaction between the wheel and rail is considered as a load concentrated at the middle of the rim. If the bending moment produced in the axle be M, then

$$M = \frac{W}{2}(L - l) = \left(26{,}000 \times 13.5\right) \text{ lbs. ins.}$$

The maximum stress $p_{\max}$ then becomes

$$p_{\max} = \frac{M}{S} = \frac{32W(L - l)}{2\pi d^3} = \frac{32 \times 26{,}000 \times 13.5}{\pi \times 10^3} = 3{,}580 \text{ lbs. per sq. inch.}$$

The deflection of the axle bent to a slight circular arc $= \delta = l^2/8\rho =$

$$\frac{l^2}{8}\frac{M}{EI} = \frac{59^2 \times 26{,}000 \times 13.5 \times 64}{8 \times 30 \times 10^6 \times \pi \times 10^4} = .0104 \text{ in.}$$

Example 25.—Determine the maximum stress produced in a steel wire of diameter $d = \frac{1}{32}$ in. when coiled round a pulley of diameter $D = 20$ in.

Solution.—The maximum elongation due to bending is

$$e = \frac{d}{D} = \frac{1}{32 \times 20}$$

and the corresponding tensile stress becomes

$$p = eE = \frac{30 \times 10^6}{32 \times 20} = 47{,}000 \text{ lbs. per sq. inch.}$$

Example 26.—A steel rule having a cross-section $\frac{1}{32}$ in. × 1 in. and a length $l = 10$ in. is bent by couples at the ends into a circular arc of 60°. Determine the maximum stress and deflection.

Solution.—The radius of curvature ρ is determined from the equation, $l = \frac{1}{6}2\pi\rho$, from which

$$\rho = \frac{3l}{\pi} = 9.55 \text{ in.}$$

and the maximum stress will be given by

$$p_{\max} = \frac{\frac{1}{32}E}{2\rho} = \frac{30 \times 10^6}{32 \times 2 \times 9.55} = 49{,}000 \text{ lbs. per sq. inch.}$$

The deflection calculated as for a circular arc will become

$$\delta = \rho(1 - \cos 30°) = .134\rho = 1.28 \text{ in.}$$

Example 27.—Determine the width x of a cast iron beam having the section as shown in Fig. 64, such that the maximum tensile stress will be one-third of the maximum compression stress.

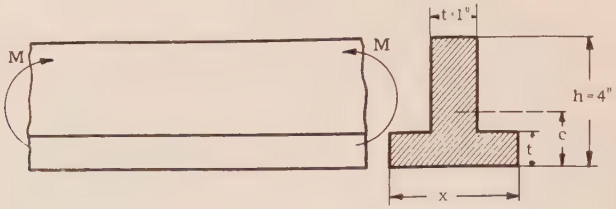

FIG. 64.

Solution.—In order to satisfy the conditions, it is necessary for the beam to have dimensions such that the distance of the center of gravity from the extreme bottom edge will satisfy the equation

$$c = \tfrac{1}{4}h. \tag{a}$$

Now, referring to Fig. 64, the position of the center of gravity is calculated by the equation

$$c = \frac{th \cdot \dfrac{h}{2} + (x - t)\dfrac{t^2}{2}}{th + (x - t)t} \tag{b}$$

therefore from (a) and (b),

$$x = t + \frac{h^2}{h - 2t} = 1 + \frac{16}{4 - 2} = 9 \text{ in.}$$

Example 28.—Determine the curvature produced in a freely supported beam of rectangular cross-section by non-uniform heating over the depth h of the cross-section. The temperature at any point distant y from the bottom of the cross-section of the beam being given by the equation $t = t_0 + (t_1 - t_0)y/h$, where $t_0 - t_1 = 45°$C. and the coefficient of expansion $\alpha_s = 125 \times 10^{-7}$. What stresses will be produced if the ends of the beam are clamped?

Solution.—The difference between the unit elongation in the top and bottom fibres of the cross-section is $\alpha(t_0 - t_1)$. Therefore the curvature due to non-uniform temperature distribution can be determined from the equation $\alpha(t_0 - t_1) = h/\rho$. The maximum stress in the case of clamped ends,

$$p_{\max} = \frac{h}{2\rho}E = \frac{\alpha(t_0 - t_1)E}{2} = \frac{125 \times 45 \times 3}{2} = 8{,}450 \text{ lbs. per sq. inch.}$$

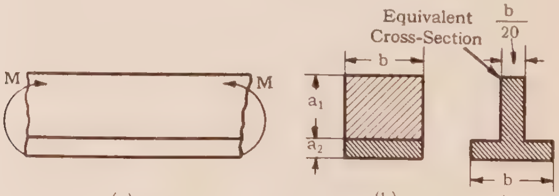

(a) (b) (c)

FIG. 65.

Example 29.—Figure 65 (a), (b) shows a rectangular beam of wood reinforced by a steel plate, and submitted to pure bending. Determine the ratio of maximum tensile stress in steel to maximum compression stress in wood if $a_1 : a_2 = 10$ and $E_s : E_w = 20$.

Solution.—Due to the fact that the modulus of elasticity of wood is $\frac{1}{20}$ as great as that of steel, the wooden part of the beam in bending can be replaced by its equivalent in steel as shown in Fig. 65 (c). It is necessary only to take the width of the equivalent steel part $\frac{1}{20}$ as great as that of wood. In such a manner the problem is reduced to the consideration of bending of a steel beam of cross-section as shown in Fig. 65 (c).

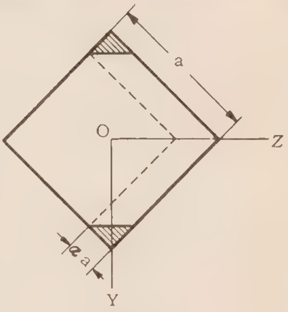

FIG. 66.

Example 30.—If the neutral axis of the cross-section shown in Fig. 66 is OZ, the section modulus can be increased by cutting out the corners as shown in the figure. Determine the magnitude of shaded areas so that the section modulus will have a maximum value.

Solution.—Let $1 : (1 - \alpha)$ denote the ratio of reduction in depth of the cross-section. Then

$$I = \frac{a^4(1-\alpha)^4}{12} + \frac{\alpha a\sqrt{2}(1-\alpha)^3(a\sqrt{2})^3}{12} = \frac{a^4(1-\alpha)^3}{12}(1+3\alpha).$$

The corresponding section modulus

$$S = \frac{a^4(1-\alpha)^3(1+3\alpha)\sqrt{2}}{12\,a(1-\alpha)}$$

From the equation $dS/d\alpha = 0$, it will be found $\alpha = \frac{1}{9}$. The corresponding section modulus will be about 5% larger than that for the square cross-section.

Example 31.—Determine analytically and graphically the relation between the bending moment M and maximum strain, in a beam of rectangular cross-section, the material of which does not follow Hooke's law. Assume the stress-strain diagrams for tension and compression have the same form, which is represented analytically by the equation

$$p = 15 \times 10^6 \times e - \frac{15 \times 10^9 \times e^2}{2}$$

where e is an extension less than 1/1,000.

Solution.—In this case the neutral axis goes through the center of gravity of the cross-section (Fig. 62). Let e_0 denote unit elongation and unit compression in most remote fibres. Then the stress at any point, distant y from the neutral axis, will be

$$p = 15 \times 10^6 e_0 \frac{2y}{h} - \frac{15 \times 10^9}{2}\frac{4y^2}{h^2}e_0^2 \qquad \text{(a)}$$

The equation for determining e_0 will be

$$2\int_0^{h/2} pbydy = 2b\left\{15 \times 10^6\, e_0 \frac{h^2}{12} - \frac{15 \times 10^9}{2} \times \frac{h^2}{16}e_0^2\right\} = M$$

from which

$$e_0^2 - \frac{8}{3}\frac{e_0}{10^3} + \frac{M \times 16}{bh^2 15 \times 10^9} = 0 \qquad \text{(b)}$$

For all values of $e_0 < .001$ the corresponding bending moment can be easily obtained from (b) and the corresponding stress from (a). If e_0 is very small, the first term of the equation (b) can be neglected. Then

$$e_0 = \frac{M \times 6}{bh^2 \times 15 \times 10^6}$$

It will be seen that this coincides with the usual equation (50) page 52 for a material following Hooke's law and having

$$E = 15 \times 10^6 \text{ lbs. per sq. inch.}$$

In the graphical solution, the stress distribution corresponding to a given maximum stress value must be obtained from the tensile test diagram such as *sor* (Fig. 62). The corresponding bending moment will then be obtained by constructing a *funicular polygon* for stress distribution given by areas *mor* and *son*.

Example 32.—Assuming the hypothesis that cross-sections during bending remain plane, determine the deflection and calculate the stresses produced in a freely supported bar of a rectangular cross-section (Fig. 67) built up from *nickel steel* as at *s* and *monel metal* as at *m*, when uniformly heated. The thicknesses of both materials can be taken as equal. What additional stresses will be produced by clamping the ends of the bar?

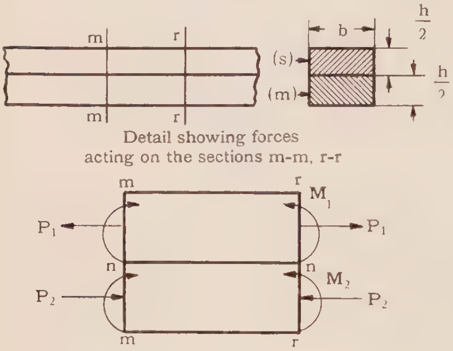

FIG. 67.

Solution.—The coefficient of expansion of monel metal is greater than that for steel, therefore when heated the beam will deflect convex downwards. The internal stresses over the cross-section of the steel can be reduced to a tensile force P_1 and to a couple M_1. In the same manner for the monel metal, the internal stresses can be reduced to a compressive force P_2 and to a couple M_2. The stresses over any cross-section of the beam must be in equilibrium; therefore, let

$$P = P_1 = P_2$$

then

$$\frac{Ph}{2} = M_1 + M_2 \tag{a}$$

Let

ρ = radius of curvature of beam,
t = temperature.
α = coefficient of expansion.
E_sI_s = the flexural rigidity of steel,
E_mI_m = the flexural rigidity of monel metal.
Other notation as in Fig. 67.

Then

$$M_1 = \frac{E_sI_s}{\rho}$$

$$M_2 = \frac{E_mI_m}{\rho}$$

$$\frac{Ph}{2} = \frac{E_sI_s}{\rho} + \frac{E_mI_m}{\rho} \tag{b}$$

The curvature $1/\rho$ will be determined from the condition that on the bearing surface n-n, the unit elongation of monel and steel must be the same; therefore,

$$\alpha_s t + \frac{2P_1}{E_s hb} + \frac{h}{4\rho} = \alpha_m t - \frac{2P_2}{E_m hb} - \frac{h}{4\rho}$$

$$\frac{2P}{hb}\left\{\frac{1}{E_s} + \frac{1}{E_m}\right\} = (\alpha_m - \alpha_s)t - \frac{h}{2\rho},$$

or using (b)

$$\frac{4}{h^2 b}\frac{1}{\rho}(E_s I_s + E_m I_m)\left(\frac{1}{E_s} + \frac{1}{E_m}\right) = (\alpha_m - \alpha_s)t - \frac{h}{2\rho} \qquad (c)$$

Now

$$I_s = I_m = \frac{bh^3}{96}$$

and

$$E_s = 1.15 E_m$$

Substituting in (c),

$$\frac{4.02}{24}\frac{h}{\rho} + \frac{h}{2\rho} = (\alpha_m - \alpha_s)t$$

$$\frac{1}{\rho} = 1.5\frac{(\alpha_m - \alpha_s)t}{h}.$$

In the case of clamped ends this curvature will be annihilated by the end couples, the magnitude of which can be calculated as explained in the solution of example (29) page 56.

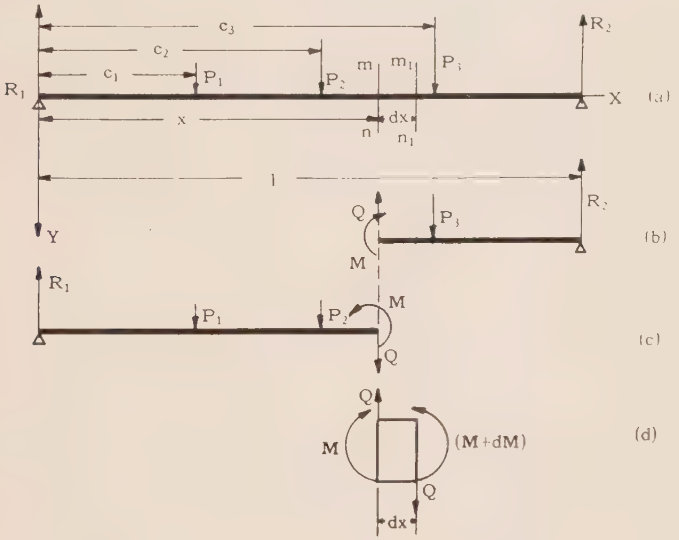

FIG. 68.—Graphical representation of bending moment and shearing force.

15. Bending Moment and Shearing Force.—A beam carrying a number of *transverse loads in* one of its *principal planes* will now be considered. Assuming the beam is *simply supported* (Fig. 68), the reactions R_1 and R_2 can be easily calculated from the known equations of statics. In studying the stresses acting across any section mn, it is supposed that the left part of the beam has been removed and the equilibrium of the right part of the beam (Fig. 68 (b)) alone has to be considered. These stresses must be *statically equivalent* to the system of forces acting on the left part of the beam and can be reduced to a transverse force

$$Q = R_1 - P_1 - P_2 \tag{a}$$

and to a couple

$$M = R_1x - P_1(x - c_1) - P_2(x - c_2) \tag{b}$$

Considering in the same manner the left part of the beam, (Fig. 68 (c)), the transverse force Q and the couple M of the same magnitude but opposite in direction will be obtained.

An element of the beam contained between two cross-sections mn and m_1n_1, distant dx apart, will be subjected to forces represented in Fig. 68 (d). It is seen that the couples M produce bending of the element and the forces Q produce shear.

The force Q equal to the algebraic sum of the vertical forces on either side of the section mn is called the *shearing force* on this section.

The couple M equal to the algebraic sum of the moments of the vertical forces on either side of the section mn is called the *bending moment* on this section.

The directions of M and Q shown in Fig. 68 (d) will be considered in the future as positive. From the equilibrium of the element between the sections mn and m_1n_1 it follows at once that

$$\frac{dM}{dx} = Q \tag{53}$$

i.e., the shearing force at any cross-section can be obtained as the derivative of the bending moment acting on this section. Usually both shearing force and bending moment vary in magnitude along the axis of a loaded beam. This variation may be presented graphically by curves extending over the length of the beam, the ordinates of one of such curves representing to scale the bending moments and of the other the shearing forces. These are called *diagrams of bending moment and of shearing force*, respectively. Some diagrams of this kind will be considered in examples below.

Example 33.—Construct diagrams of bending moment and shearing force for the six cases given in Fig. 69. M and Q denote diagrams of bending moment and shearing force respectively.

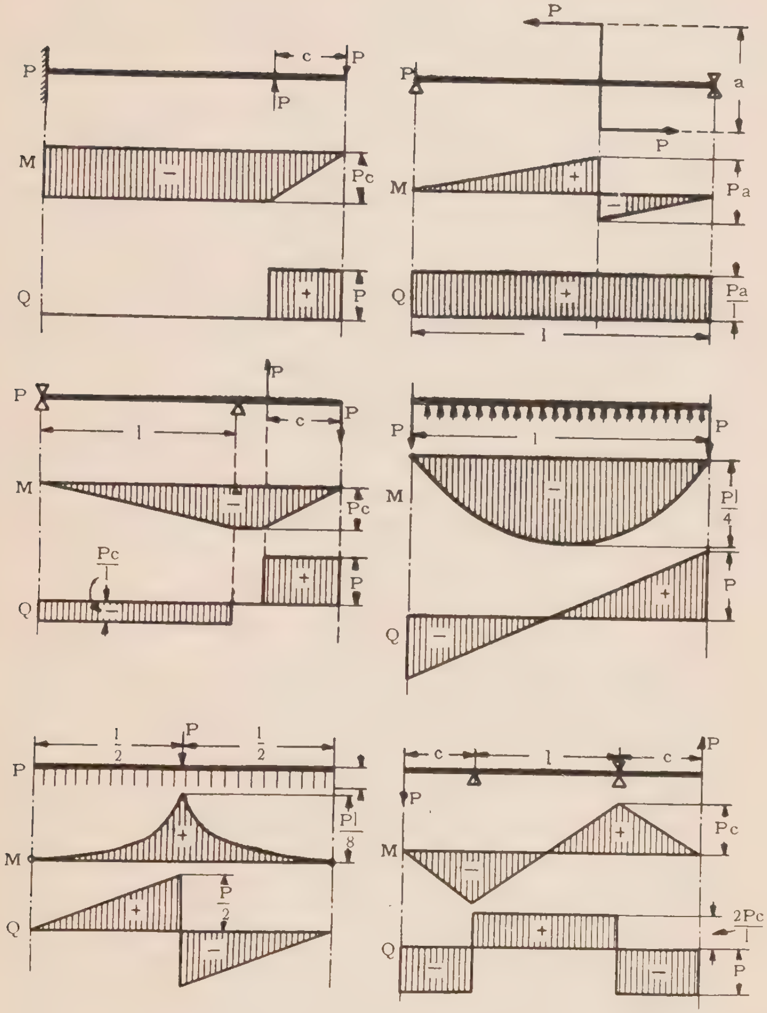
P
c
P
P
M
−
Pc
Q
+
P
P
P
P
a
P
M
+
−
Pa
Q
+
Pa/l
l
P
P
l
c
P
M
−
Pc
Pc/l
Q
−
+
P
P
l
P
M
−
Pl/4
Q
−
+
P
l/2
P
l/2
P
Pl/8
M
+
Q
+
P/2
−
c
l
c
P
P
M
−
+
Pc
Q
−
+
−
2Pc/l
P

Fig. 69.

16. Normal Stresses.—The normal stresses acting over any cross-section of a beam are due to the bending moment on this section and can be calculated by using equation (49) page 52, obtained above for the case of pure bending. The results obtained in such a manner agree with those obtained from the exact theory of bending,[*] provided the cross-section under consideration is at a considerable distance from the points of application of the loads, for example, not closer than the depth of the largest cross-sectional dimension. It is well to note that for the portions of the beam in close proximity to the loads, a more complicated stress distribution occurs. To demonstrate this fact, the case of a beam of narrow rectangular cross-section will now be considered. Near to the point of application of a concentrated load W (Fig. 70), *local stresses* will be produced. The exact solution[†] of this problem shows that these stresses at any point A are simple compression in a radial direction, the magnitude of which is determined by the equation

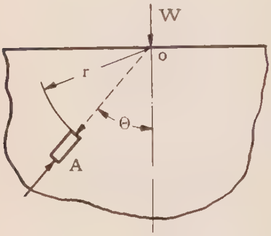

FIG. 70.—Local stresses in the region of a concentrated load.

$$p_r = \frac{2W}{\pi t}\frac{\cos\theta}{r}$$

in which

t = width of the beam,
r = the distance from the point 0,
θ = the angle shown in the figure.

These stresses must be combined with stresses calculated from equation (49),[‡] page 52.

In the case of a uniformly loaded beam (Fig. 71), the normal stresses over any cross-section mn at a considerable distance from the ends are given by the equation[§]

$$p = \frac{qx(l-x)y}{2I} - \frac{q}{2I}\left(\frac{h^2y}{10} - \frac{2}{3}y^3\right).$$

---

[*] An exact solution of this elasticity problem belongs to Saint-Venant, *Journal de Math.* (Liouville), 1856. An account of St. Venant's famous work will be found in Todhunter and Pearson's "History of the Theory of Elasticity."

[†] This solution was obtained by Flamant, "*Annales des Ponts et Chaussées,*" 1893 (Paris).

[‡] See L. N. G. Filon, *Phil. Trans.* Vol. 201, A, 1903.

[§] This result was obtained by A. Mesnager; *Annales des Ponts et Chaussées*, p. 161, II, 1901.

The first term on the right side of this equation represents the normal stresses as obtained from the equation (49). The second term represents the correction necessary to the usual formula. It is easy to see that this correction for the middle part of the beam is small in comparison with the first term, provided that the depth h of the beam is small in comparison with the length l of the beam. The discrepancy between the usual formula and the exact solution is due to the pressure between the longitudinal fibres produced by the load q. These pressures, which are neglected in an elementary consideration, decrease from the upper edge of the beam to the bottom and can be obtained from the equation

$$p_y = -\frac{q}{2t}\left(1 - \frac{3y}{h} + \frac{4y^3}{h^3}\right).$$

If $y = -h/2$, $p_y = -q/t$; if $y = +h/2$, $p_y = 0$.

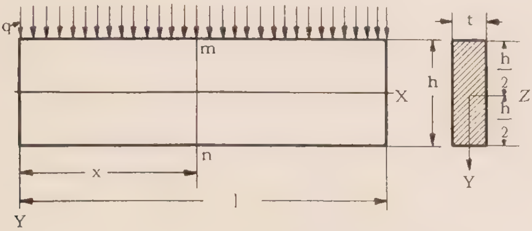

FIG. 71.—Special case of uniform load.

It will therefore be apparent that, while in general the elementary equations can be applied, in exceptional cases such as mentioned above, the stress distribution becomes more complicated and the real picture of this distribution can only be obtained by the application of the *general equations of the theory of elasticity*.

17. Shearing Stresses.—The shearing stresses acting over any cross-section of a beam are due to the shearing force on this section. General theory of distribution of these stresses belongs to Saint Venant.*

In the case of a rectangular cross-section (Fig. 72) an approximate solution can be easily obtained on the assumption that shearing stresses are parallel to the shearing force Q and constant along any line *ss* parallel to the neutral axis.† The vertical shearing stresses at points on the line *s-s* of the cross-section are accompanied by horizontal shearing stresses of the same magnitude distributed uniformly over the plane *cd* parallel to the neutral surface. The latter shearing stresses can be obtained from the equation of equilibrium of the element *abdc* cut out from the beam by two cross-sections *mn* and m_1n_1 and by the plane *cd*. Resolving all forces acting on the element in the *X* direction, the following equation is obtained:

---

* See footnote page 62.

† First consideration of shearing stresses at bending belongs to the Russian engineer, Jouravski. For the French translation of his paper see "*Annales des Ponts et Chaussées,*" 1856.

$$-\int_c^{h/2}\frac{MydA}{I} - p_t b dx + \int_c^{h/2}\frac{(M + dM)ydA}{I} = 0$$

from which the shearing stress at distance *c* from neutral axis is

$$p_t = \frac{dM}{dx}\frac{1}{bI}\int_c^{h/2} ydA = \frac{Q}{bI}\int_c^{h/2} ydA \tag{54}$$

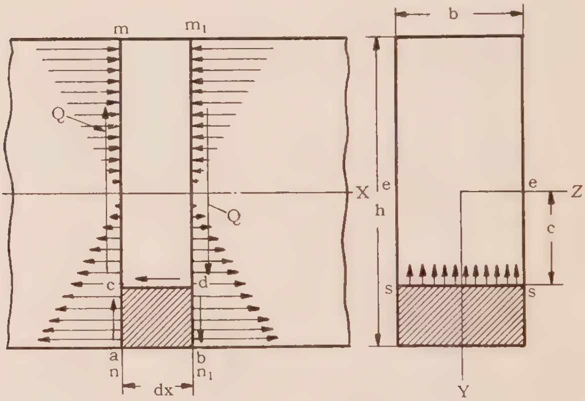

Fig. 72.—Distribution of shearing stresses due to bending.

It may be noted that the integral on the right side of the equation represents the moment of the part of the cross-section below the line *ss* about the neutral axis *OZ*, or in the case of a rectangular section,

$$\int_c^{h/2} ydA = \frac{b}{2}\left(\frac{h^2}{4} - c^2\right) \tag{c}$$

i.e., the shearing stresses vary according to a parabolic law and the maximum shearing stress occurs at points on the neutral axis.

Substituting (c) in (54),

$$(p_t)_{\max} = \frac{3}{2}\frac{Q}{bh} \tag{55}$$

i.e., the maximum of p_t is 50% greater than the average shearing stress as obtained by dividing the shearing force Q, by the area of the cross-section.

The exact solution of the problem shows that shearing stresses are not constant over the width of the cross-section. The maximum value of these stresses takes place in points *e-e* at the ends of the neutral axis and can be calculated from the equation

$$(p_t)_{\max} = \alpha \left(\frac{3}{2}\frac{Q}{bh}\right)$$

in which α is a constant depending on the magnitude of the ratio b/h. Several values of this constant are given in Table IV.* It is seen that in the case of a narrow rectangle, equation (54) has a high accuracy.

TABLE IV.—MAX. SHEARING STRESS CONSTANTS FOR RECTANGULAR SECTION

b/h = ...	½	1	2	4
α = ...	1.033	1.126	1.396	1.988

Equation (54) is used also for approximate calculations of the shearing stresses on other forms of cross-sections. Applying it for instance to the case of a circular cross-section, the equation for maximum shearing stress will be

$$(p_t)_{\max} = \frac{4}{3}\frac{Q}{\pi r^2}$$

where r denotes the radius of the cross-section.

The exact solution for this case shows that the maximum shearing stress takes place at the center of the circle and is determined by the equation†

$$(p_t)_{\max} = 1.38\frac{Q}{\pi r^2}$$

thus showing that the approximate equation is accurate enough for practical applications.

From equation (54), therefore, it can be concluded that the shearing stresses can assume importance only in cases where the cross-sections have the form of a very narrow rectangle or an *I* section with a thin web. For cross-sections where the width is large, the shearing stresses become usually small and should be taken into consideration only in the case of such materials as wood which sustains comparatively large tensile and compressive stresses and is very weak in resisting shearing stresses along the fibres.

---

* The table is taken from the author's paper, see *London Math. Soc. Proc.* Ser. 2, Vol. 20, p. 404.

† Poisson's ratio is taken equal to .30.

Solutions obtained above for the distribution of shearing stresses give the true picture of this distribution only for cross-sections at considerable distance from points of application of loads. Near these points the stress distribution is more complicated. In Fig. 73 the distribution of shearing stresses over the cross-section *mn* of a beam of very narrow rectangular cross-section, for different values of the distance 2*b* between the loads, is graphically represented.* It is seen that when this distance is small in comparison with the height of the beam, the stress distribution does not follow the parabolic law obtained above.

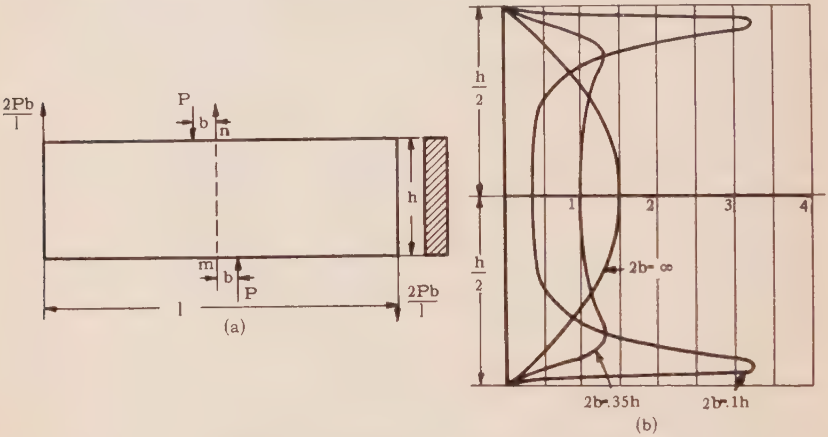

Fig. 73.—Distribution of shearing stresses near to a concentrated load.

Example 34.—Determine the shearing stress at the neutral axis of a girder, the web of which is $\frac{3}{4}$ in. thick and 50 in. high, the flanges consisting of two pairs of angles 6 in. × 6 in. × $\frac{1}{2}$ in. when the total shearing force on the section is 150,000 lbs. Determine also the shearing stresses in the rivets attaching the web to the flanges if the diameter of these rivets is 1 in. and the pitch $a = 4$ in.

Solution.—Substituting in equation (54) page 64, $Q = 150{,}000$ lbs., $b = \frac{3}{4}$ in.

$$I = \frac{3}{4} \times \frac{50^3}{12} + 4(19.9 + 5.75 \times 23.3^2) = 7{,}810 + 12{,}590 = 20{,}400 \text{ in.}^4$$

$$\int_0^{h/2} y\,dA = \frac{3}{4} \times \frac{25 \times 25}{2} + 2 \times 5.75 \times 23.3 = 234 + 268 = 502 \text{ in.}^3.$$

$$p_t = \frac{150{,}000 \times 502}{\frac{3}{4} \times 20{,}400} = 4{,}920 \text{ lbs. per sq. in.}$$

---

* This solution was obtained by L. N. G. Filon, *Phil. Trans.*, Vol. 201-A, p. 126, 1903.

By using the same method as in obtaining equation (54), page 64, the shearing force on each rivet will be

$$P = \frac{Q \times T \times a}{I} = \frac{150{,}000 \times 268 \times 4}{20{,}400} = 7{,}900 \text{ lbs.}$$

where T is the moment of the area of the cross-section of the flange-angles about the neutral axis. Since the rivets are in double shear the magnitude of the shearing stress in rivets will be given by

$$\frac{P}{2 \times \frac{\pi d^2}{4}} = \frac{7{,}900 \times 2}{3.14} = 5{,}030 \text{ lbs. per sq. inch.}$$

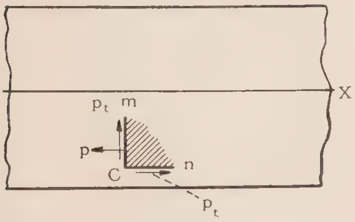

FIG. 74.—Normal and shearing stresses due to bending.

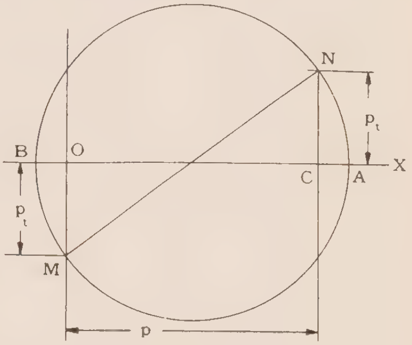

FIG. 75.—Mohr circle for stresses during bending.

18. Principal Stresses in Beams.—In considering the state of stress at any point C of a beam (Fig. 74), the normal and the tangential stresses across the elementary areas, Cm and Cn, can be calculated by using equations (49) page 52 and (54) page 64. When p and p_t are determined, the maximum normal and shearing stress at point C can easily be obtained by using *Mohr's circle* (par. 4, page 13). Taking as co-ordinates the stresses over any two perpendicular elementary areas, such as mentioned above, the diameter MN of the *Mohr circle* will be obtained (Fig. 75). If the circle be drawn for these conditions, then the points A and B on the X axis, representing the maximum tension and maximum compression, will be obtained. It is easy to see that

$$AO + OB = MN = \sqrt{p^2 + 4p_t^2}$$

and that;

$$AO - OB = OC = p$$

therefore, from fundamentals of Mohr circle,

$$p_{\max} = AO = \frac{p}{2} + \frac{1}{2}\sqrt{p^2 + 4p_t^2} \tag{56}$$

$$p_{\min} = -OB = \frac{p}{2} - \frac{1}{2}\sqrt{p^2 + 4p_t^2} \tag{57}$$

The stresses $p_{\max}$ and $p_{\min}$ are the *principal stresses* produced in the point C of the beam, due to bending. The *maximum tangential stress*, given by the radius of the circle, will then be

$$(p_t)_{\max} = \tfrac{1}{2}MN = \tfrac{1}{2}\sqrt{p^2 + 4p_t^2} \qquad (58)$$

19. Beams of Variable Cross-section.—*Bending of a Wedge.*—In all previous considerations of beams the prismatical form has been assumed. The fundamental equations for calculating the stresses, obtained on this assumption, are applied often also in cases of beams of variable cross-section. In order to give some idea on the accuracy of this kind of calculation, the case of bending of a cantilever having the form of a wedge (Fig. 76) will now be considered. From the exact solution of this problem* it follows that in any point A of the beam, a simple radial stress of magnitude

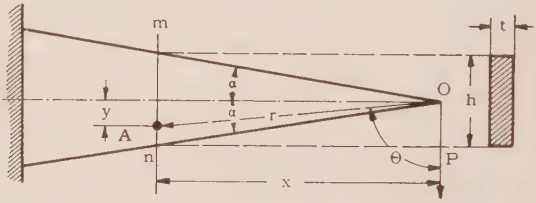

FIG. 76.—Bending of a wedge.

$$p_r = k\frac{P\cos\theta}{rt} \qquad (a)$$

will be produced, where:

r = the distance of the point A and O,
t = the thickness of the wedge,
θ = the angle between the radius AO and the direction of the force,
$k = -\dfrac{2}{2\alpha - \sin 2\alpha}$, a constant to be determined from the equation

of equilibrium, $\displaystyle\int_{\frac{\pi}{2}-\alpha}^{\frac{\pi}{2}+\alpha} tp_r\, r\cos\theta d\theta + P = 0$

From equation (a) the stress distribution over any cross-section mn of the beam can be obtained. The normal and tangential components of these stresses will be

$$p = -\frac{2My\sin^4\theta}{tx^3(2\alpha - \sin 2\alpha)} = -\frac{My}{I}\cdot\frac{4}{3}\frac{\tan^3\alpha\sin^4\theta}{2\alpha - \sin 2\alpha}$$

---

* See J. H. Michell, *Proceedings of the London Math. Soc.*, Vol. 34, 1902.

and

$$p_t = \frac{2Py^2 \sin^4 \theta}{tx^3(2\alpha - \sin 2\alpha)} = \frac{P}{A} \frac{16y^2}{h^2} \frac{\tan^3 \alpha \sin^4 \theta}{2\alpha - \sin 2\alpha}$$

in which $I = th^3/12$, A (area) $= th$ and $M = Px$

At $\theta = \pi/2$, the normal and shearing stresses become equal to zero while the maximum normal and shearing stress will occur at $\theta = \frac{\pi}{2} + \alpha$. They can be calculated from equations

$$(p)_{\max} = \beta \frac{Mh}{2I}$$

$$(p_t)_{\max} = \gamma \frac{P}{A}$$

in which

$$\beta = \frac{4}{3} \frac{\tan^3 \alpha \cos^4 \alpha}{2\alpha - \sin 2\alpha}; \gamma = 4 \frac{\tan^3 \alpha \cos^4 \alpha}{2\alpha - \sin 2\alpha}$$

Several values of constants β and γ are given in Table V.

TABLE V.—MAXIMUM NORMAL AND SHEARING STRESS CONSTANTS FOR WEDGE

α = ...	5°	10°	15°	20°
β = ...	1.00	.97	.947	.906
γ = ...	3	2.91	2.84	2.72

It is seen that the maximum normal stress is approximately the same as that obtained from the equation (50) page 52, provided that α is a small angle. With increasing value of α the error of equation (50) increases and for $\alpha = 20°$ the difference between the exact solution and the value given by equation (50) may be as much as 10%. The maximum shearing stress is about three times greater than the average shearing stress P/A and occurs at points most remote from the neutral axis, which latter fact it is important to note is in direct opposition to the results obtained from equation (54) for prismatical bars. Taking into account the fact that in many cases the tangential stresses can be neglected and only normal stresses considered, it can be concluded from the consideration given above, that formula (50) given for prismatical bars can be used with sufficient accuracy also in cases of bars of variable cross-section, provided this variation is not too rapid.

Effect of Holes and Grooves.—In cases of *sharp variation* of cross-sections as produced, for instance, by grooves or holes, the usual formula (50) does not give satisfactory results, and additional considerations of stress concentration is of practical importance. In these considerations, solutions previously given for tension of bars of variable cross-section can be used (§2 page 8). For instance, it can be concluded at once that in the case of a pin, shown in Fig. 77, a circular hole of a small diameter at A produces very high stress-concentration and that the coefficient of concentration is about equal to 3 (§2, page 8). For a fillet also a high stress concentration must be expected, the magnitude of which will depend on the radius ρ of the fillet. The danger of this stress concentration in the case of stress reversal was explained before (paragraph 2).*

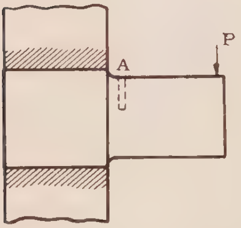

Fig. 77.—Stress concentration due to hole and fillet.

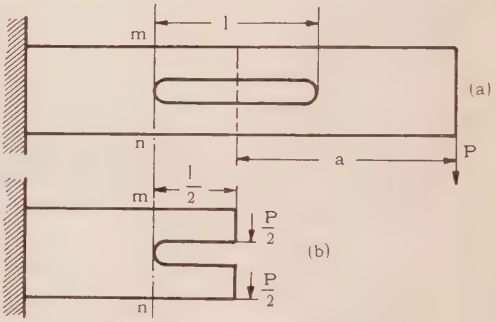

Fig. 78.—Beam with elongated hole.

In the case of elongated holes located at the neutral surface (Fig. 78) additional bending, shown in Fig. 78 (b), must be taken into account. The maximum normal stresses at m and n will be given by the equation

$$P_{\max} = \frac{Pa}{S} + \frac{Pl}{4S_1}$$

in which S denotes the section modulus of the entire section of the beam and S_1, the section modulus for upper and lower parts of the beam separated by the hole, as shown in Fig. 78 (b).

---

* See also Part II, par. 123.

CHAPTER IV

DEFLECTION OF BEAMS

20. Deflection Due to Bending Moment.*—*General Equation.*—The deflection of beams produced by a bending moment can be determined from the equation (48) page 52. Taking into account that the deflection is very small in comparison with the span, the known approximate equation given in (a) for the curvature can be used:

$$\frac{1}{\rho} = \pm\frac{d^2y}{dx^2} \tag{a}$$

Considering the curvature as positive if convex downwards and taking the directions of axes as shown in Fig. 68, the minus sign in (a) must be used and the differential equation for the deflection curve will become, from (a) and (48),

$$EI\frac{d^2y}{dx^2} = -M. \tag{59}$$

A solution of this equation in the case of transverse loading can be obtained very easily because M will be a function of x only.

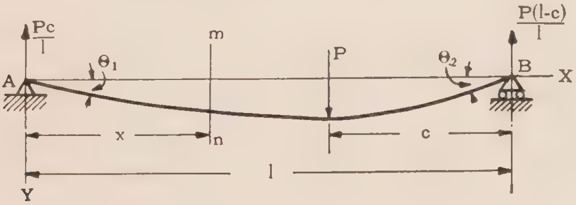

FIG. 79.

Simply Supported Beam.—Take for instance the case of a beam simply supported and having a single concentrated load as in Fig. 79. Equation (59) for the left side of the beam $x < (l - c)$, will be

$$EI\frac{d^2y}{dx^2} = -\frac{Pc}{l}x \tag{b}$$

The same equation for the right side $x > (l - c)$, will be

$$EI\frac{d^2y}{dx^2} = -\frac{Pc}{l}x + P(x + c - l) \tag{c}$$

---

* Notation in this chapter is same as in Chapter III.

By integrating (b), the following is obtained:

$$EI\frac{dy}{dx} = -\frac{Pcx^2}{2l} + C_1, \tag{d}$$

$$EIy = -\frac{Pcx^3}{6l} + C_1x + C_2, \tag{e}$$

where C_1 and C_2 denote arbitrary constants which will be determined later from the conditions at the ends.

Performing now the integration of (c) we will have

$$EI\frac{dy}{dx} = -\frac{Pcx^2}{2l} + \frac{P(x + c - l)^2}{2} + C_3 \tag{f}$$

$$EIy = -\frac{Pcx^3}{6l} + \frac{P(x + c - l)^3}{6} + C_3x + C_4 \tag{g}$$

It follows from conditions of continuity at the point of application of the load P, that the right sides of equations (d) and (e) must be equal to those of (f) and (g) respectively, provided that $x = l - c$. From this follows

$$C_1 = C_3 \text{ and } C_2 = C_4 \tag{h}$$

Two further equations for determining the arbitrary constants will be obtained from the conditions at the ends of the beam. Remembering that the deflection at the left end ($x = 0$) of the beam is zero, it follows from (e) and (h) that

$$C_2 = C_4 = 0 \tag{i}$$

In the same manner from the condition at the right end, by using equation (g) and substituting l for x and zero for y, we get

$$C_3 = \frac{Pc(l^2 - c^2)}{6l} \tag{j}$$

Substituting the values of the arbitrary constants in equations (d), (e), (f), and (g) the following is obtained: For the left side of the beam,

$$EI\frac{dy}{dx} = \frac{Pc}{6l}(-3x^2 + l^2 - c^2) \tag{60}$$

$$EIy = \frac{Pc}{6l}(-x^3 + l^2x - c^2x). \tag{61}$$

For the right side,

$$EI\frac{dy}{dx} = -\frac{Pcx^2}{2l} + \frac{P(x + c - l)^2}{2} + \frac{Pc(l^2 - c^2)}{6l} \tag{62}$$

$$EIy = -\frac{Pcx^3}{6l} + \frac{P(x + c - l)^3}{6} + \frac{Pcx(l^2 - c^2)}{6l}. \tag{63}$$

By using (60) and (62) the slope of the deflection curve at every point can be calculated. The rotation of the left end of the beam denoted by the angle θ_1 will be

$$\theta_1 = \left(\frac{dy}{dx}\right)_{x=0} = \frac{Pc(l^2 - c^2)}{6lEI} \tag{64}$$

In the same manner, the angle θ_2 at the right end, from (62), becomes

$$\theta_2 = -\left(\frac{dy}{dx}\right)_{x=l} = \frac{Pc(l - c)(2l - c)}{6lEI} \tag{65}$$

By using (61) and (63) the deflection at any point of the beam can easily be obtained. If x be taken as equal to $(l - c)$ and be substituted in (61), the deflection at the point of application of the load will be obtained:

$$(y)_{x=l-c} = \frac{Pc^2(l - c)^2}{3lEI} \tag{66}$$

If $c < (l - c)$, the maximum deflection will be to the left of the load and the position of the point of maximum deflection will be obtained by putting the slope (60) equal to zero; then

$$x = \sqrt{\tfrac{1}{3}(l^2 - c^2)} \tag{k}$$

Substituting this in (61),

$$y_{\max} = \frac{Pc(l^2 - c^2)^{3/2}}{9\sqrt{3}EIl}$$

In order to obtain the deflection at the middle it is necessary only to substitute in (61) $x = l/2$; then

$$(y)_{x=l/2} = \frac{Pc}{48EI}(3l^2 - 4c^2) \tag{67}$$

It is seen from (k) that the point of maximum deflection is always very near to the middle of the beam. In the limiting case, when $c = 0$, this distance is equal to $l/\sqrt{3} - l/2 = .077l$. Due to this fact, the deflection at the middle is a close approximation to the maximum deflection. In the most unfavorable case ($c = 0$), the difference between these two deflections is only 2.5%. The same conclusion can also be made for the case where several transverse forces having the same direction are acting on the beam.

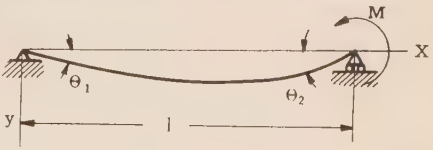

FIG. 80.

Assuming that the distance c approaches zero and at the same time the load increases so that the product Pc remains constant, then approaching the limit $c = 0$, we will have the case of bending of a beam by a couple $M = Pc$ (Fig. 80). Substituting in (61) $c = 0$

and $Pc = M$, the following equation for the deflection curve will be obtained for this case:

$$y = \frac{Mx(l^2 - x^2)}{6EIl} \tag{68}$$

In the same manner, by using (64) and (65) the following values for the angles at the ends will be obtained:

$$\theta_1 = \frac{Ml}{6EI} \qquad \theta_2 = \frac{Ml}{3EI} \tag{69}$$

By using this analysis in conjunction with the principle of superposition described in the next paragraph, the case for couples acting on both ends of the beam can easily be considered.

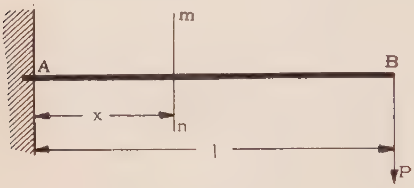

Fig. 81.

Cantilever Beam.—The equation (59) in this case (Fig. 81) will be

$$EI\frac{d^2y}{dx^2} = P(l - x)$$

By integration, this becomes

$$EI\frac{dy}{dx} = Px\left(l - \frac{x}{2}\right) + C_1$$

$$EIy = Px^2\left(\frac{l}{2} - \frac{x}{6}\right) + C_1x + C_2$$

From the condition that at the left end of the beam the slope and the deflection are equal to zero, it follows that

$$C_1 = 0 \text{ and } C_2 = 0$$

Therefore

$$EI\frac{dy}{dx} = Px\left(l - \frac{x}{2}\right)$$

$$EIy = Px^2\left(\frac{l}{2} - \frac{x}{6}\right)$$

The slope and the deflection at the right end of the cantilever will be

$$\left(\frac{dy}{dx}\right)_{x=l} = \frac{Pl^2}{2EI} \tag{70}$$

$$(y)_{x=l} = \frac{Pl^3}{3EI} \tag{71}$$

So far only the very simple cases of loading have been considered. When several loads are acting on a beam the solution of the problem will require the determination of certain arbitrary constants, the number of which will increase with the number of external loads. The use of purely analytical methods for such problems is very cumbersome and tedious. This can be avoided by applying the graphical analysis in conjunction with the principle of superposition. Not only by the use of such methods are these complicated expressions rendered unnecessary, but due to the fact that it is essential to make certain sketches of the particular loading, a clearer mental picture is obtained than by the use of pure mathematical analysis alone. In the next two paragraphs we will come to a consideration of these methods.

Example 35.—Two planks of different thicknesses h_1 and h_2, freely superimposed, support a uniformly distributed load as shown in Fig. 82. Determine the ratio of the maximum stresses occurring in each.

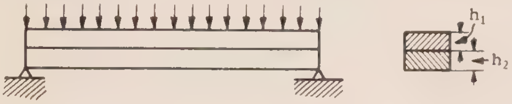

FIG. 82.

Solution.—From the fact that both planks have, during deflection, the same curvature, it follows at once that the bending moments of the planks are in the same ratio as the moments of inertia of their cross-sections, i.e., in the ratio $h_1^3 : h_2^3$. The section moduli will be in the ratio $h_1^2 : h_2^2$. Therefore, the maximum stresses in the two planks will be in the ratio $h_1 : h_2$.

Example 36.—Determine the maximum bending moment for a simply supported beam carrying an unequally distributed load W represented in Fig. 83 by the triangle ACB.

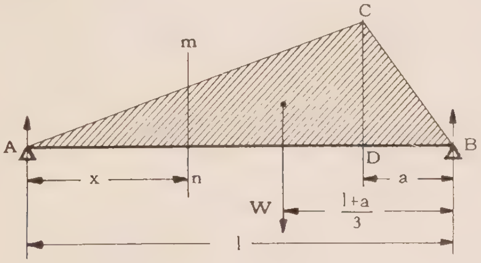

FIG. 83.

Solution.—Assuming the load concentrated at the center of gravity of the triangle ACB, the distance of this load from the end B is $\frac{l+a}{3}$. The reaction at the support A will be

$$A = \frac{W(l+a)}{3l}$$

Let a be less than $l/2$, then the maximum bending moment will be in the part AD of the beam. At any cross-section mn of this part the bending moment is,

$$M = Ax - \frac{Wx^2}{l(l-a)}\frac{x}{3} = \frac{Wx}{3l(l-a)}(l^2 - a^2 - x^2) \tag{p}$$

From the equation $dM/dx = 0$, the distance of the maximum bending moment from A will then be given by

$$d = \sqrt{\frac{l^2 - a^2}{3}}$$

Substituting this, instead of x, in equation (p),

$$M_{\max} = \frac{2W}{9\sqrt{3}}\left(1 + \frac{a}{l}\right)\sqrt{l^2 - a^2}.$$

Example 37.—A steel bar AB has such an initial curvature that after being straightened by the forces P (Fig. 84) a uniformly distributed pressure is produced along the length of the rigid plane surface MN. Determine the forces P necessary to straighten the bar and the maximum stress produced in it if $l = 20$ in., $\delta = .1$ in. and the cross-section of the bar is a square having 1 in. sides.

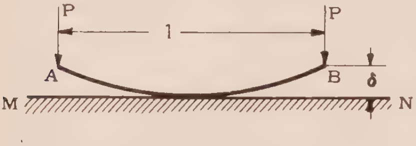

FIG. 84.

Solution.—In order to obtain a uniformly distributed pressure, the initial curvature of the bar must be the same as the deflection curve of a simply supported beam carrying a uniformly distributed load of intensity $2P/l$.

Then, by using the known equations, we have

$$M_{\max} = \frac{2P}{l}\cdot\frac{l^2}{8} = \frac{Pl}{4} \tag{a}$$

$$\delta = \frac{5}{384}\,\frac{2P}{l}\cdot\frac{l^4}{EI} \tag{b}$$

The maximum stress will be

$$p_{\max} = \frac{M_{\max}}{S} = \frac{M_{\max}h}{2I} = \frac{Plh}{8I} \tag{c}$$

Now from (b),

$$\frac{Pl}{8I} = \frac{24E\delta}{5l^2}$$

Substituting in (c),

$$p_{\max} = \frac{24E\delta h}{5l^2} = \frac{24 \times 30 \times 10^6 \times .1 \times 1}{5 \times 20^2} = 36{,}000 \text{ lbs. per sq. inch}$$

and from (c),

$$P = \frac{8Ip_{\max.}}{lh} = \frac{8 \times 36{,}000}{12 \times 20 \times 1} = 1{,}200 \text{ lbs.}$$

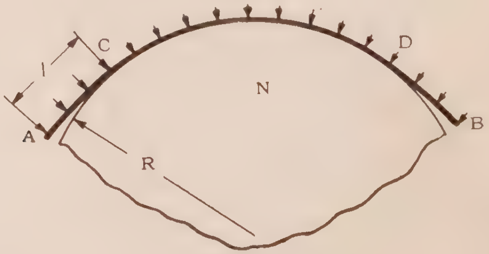

FIG. 85.

Example 38.—A circular disc N of radius R (Fig. 85) produces on a thin steel strip AB of thickness h a uniformly distributed attraction in a radial direction equal to q lbs. per sq. inch. Determine the length l of the unsupported part AC of the strip and the maximum stress in it if $h = .01$ inch, $R = 3$ in., and $q = 15$ lbs. per sq. inch.

Solution.—The length of the unsupported part of the strip will be determined from the condition that at point C, the curvature produced by the uniformly distributed load q must be equal to $1/R$. Therefore

$$\frac{ql^2}{2} = \frac{EI}{R}$$

from which

$$l = \sqrt{\frac{2EI}{qR}} = \sqrt{\frac{2 \times 30 \times 10^6 \times (.01)^3}{12 \times 15 \times 3}} = \frac{1}{3}\text{ in.}$$

The maximum stress is determined from the equation

$$p_{\max} = \frac{Eh}{2R} = \frac{30 \times 10^6 \times .01}{2 \times 3} = 50{,}000 \text{ lbs. per sq. inch.}$$

21. Principle of Superposition for Simple Bending.—*General Consideration.*—It can be shown easily that when several transverse loads act on a beam the deflection at any point can be obtained by superimposing the deflections produced at this point by each of the single loads. Taking for instance the case represented in Fig. 68 page 59, the equation (59) page 71 for any cross-section (mn) will become

$$EI\frac{d^2y}{dx^2} = -\frac{P_1c_1}{l}(l - x) - \frac{P_2c_2}{l}(l - x) - \frac{P_3(l - c_3)x}{l} \qquad \text{(a)}$$

This equation can be considered as the sum of the following equations:

$$\begin{aligned} EI\frac{d^2y_1}{dx^2} &= -\frac{P_1\,c_1(l - x)}{l} \\ EI\frac{d^2y_2}{dx^2} &= -\frac{P_2c_2(l - x)}{l} \\ EI\frac{d^2y_3}{dx^2} &= -\frac{P_3(l - c_3)x}{l} \end{aligned} \qquad \text{(b)}$$

in which y_1, y_2, and y_3 denote the deflections produced by the forces P_1, P_2, and P_3, respectively. The solution of (a) will be represented by the sum of the solutions of equations (b). It will therefore be seen that the superimposing of the deflection produced by a system of forces P_1, P_2, etc. acting on a beam gives the same result as the summation of the deflections for each of the individual loads. This principle known as that of superposition is, therefore, justified for the case of transverse loading.

Applying this principle and using the equations obtained above for a single load, the solutions for the more complicated cases of bending can easily be obtained.

Uniformly Distributed Load.—Consider, for instance, the case of a beam with a uniformly distributed load (Fig. 86). Let q denote the load per unit length. Then the deflection at the middle of the beam produced by any element qdc by using equation (67) page 73 will be

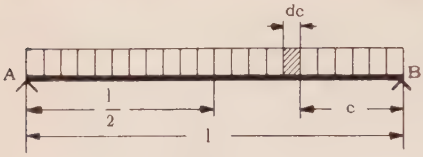

Fig. 86.

$$dy = \frac{qcdc}{48EI}(3l^2 - 4c^2).$$

Summing the effects of all such elements of loading on the right half of the beam and doubling this for the complete beam, the deflection at the middle produced by the uniform load will be obtained as follows:

$$\delta = (y)_{x=l/2} = 2\int_0^{l/2} \frac{qc}{48EI}(3l^2 - 4c^2)dc = \frac{5}{384}\frac{ql^4}{EI} \tag{72}$$

In order to obtain the slope of the deflection curve at the left end of the beam the equation (64) page 73 will be used. The rotation of the left end of the beam, produced by an element qdc of the load, will be

$$\frac{qcdc(l^2 - c^2)}{6lEI}$$

and the slope at the supports produced by the entire distributed load will then be

$$\left(\frac{dy}{dx}\right)_{x=0} = \int_0^l \frac{qcdc(l^2 - c^2)}{6lEI} = \frac{ql^3}{24EI} \tag{73}$$

If a uniform loading be distributed only along a part of the span (Fig. 87), the same method can be used. Equation (67) is obtained on the assumption that $c < l/2$. Using this equation in the case under consideration the load must be divided by the middle section (mn) in two parts. The load on the right side will produce at the middle the deflection

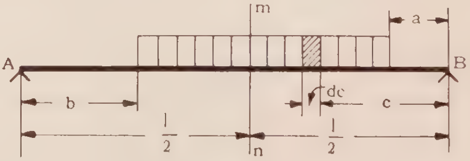

Fig. 87.

$$\int_a^{l/2} \frac{qc}{48EI}(3l^2 - 4c^2)dc = \frac{ql^4}{48EI}\left(\frac{5}{16} - \frac{3}{2}\frac{a^2}{l^2} + \frac{a^4}{l^4}\right)$$

For the left part of the beam this will become,

$$\int_b^{l/2} \frac{qc}{48EI}(3l^2 - 4c^2)dc = \frac{ql^4}{48EI}\left(\frac{5}{16} - \frac{3}{2}\frac{b^2}{l^2} + \frac{b^4}{l^4}\right)$$

giving the complete deflection as

$$(y)_{x=l/2} = \frac{ql^4}{48EI}\left(\frac{5}{8} - \frac{3}{2}\frac{a^2 + b^2}{l^2} + \frac{a^4 + b^4}{l^4}\right) \tag{c}$$

This is the general equation for deflection for a distributed load. If $a = b = 0$, the equation (c) becomes (72) for a uniformly distributed load over the entire span.

Example 39.—Determine: the stress and deflection at the middle of the I beam shown in Fig. 88, also the angles of rotation of the ends when the beam is subjected to hydrostatic pressure; where $l = 12$ ft., $d = 3$ ft., $h = 8$ in., the moment of inertia of the cross-section about neutral axis, $I = 56.9$ in.^{4}, γ = wt. per unit vol.

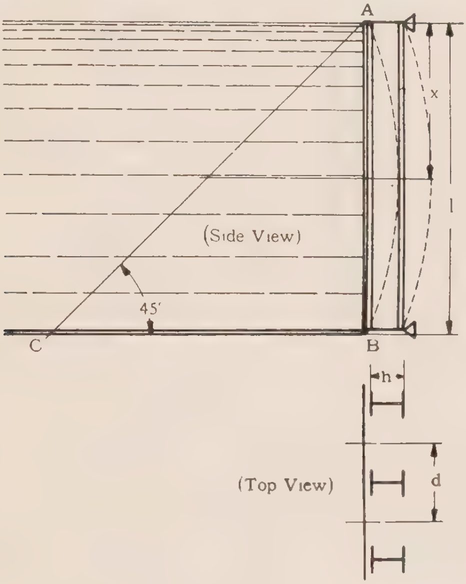

FIG. 88.

Solution.—The complete load, represented by the triangular prism ABC, is

$$W = \frac{l^2d}{2}\gamma = \frac{12^2 \times 3}{2} \times 62.4 = 13{,}470 \text{ lbs.}$$

The reactions are: $A = W/3 = 4{,}490$ lbs., $B = 2/3W = 8{,}980$ lbs.

The bending moment at any cross-section will therefore be

$$M = \frac{Wx}{3} - \frac{Wx^2}{l^2}\cdot\frac{x}{3} \tag{a}$$

Maximum bending moment will be at $x = l/\sqrt{3}$.
Substituting in (a),

$$M_{\max} = \frac{Wl}{3\sqrt{3}}\left(1 - \frac{1}{3}\right) = \frac{2Wl}{9\sqrt{3}} = 20{,}700 \times 12 \text{ lbs. in.},$$

$$p_{\max} = \frac{20{,}700 \times 12 \times 4}{56.9} = 17{,}500 \text{ lbs. per sq. inch}$$

Deflection at the middle will be

$$\delta = \frac{5}{384}\frac{Wl^3}{EI} = \frac{5}{384} \times \frac{13{,}470 \times 144^3}{30 \times 10^6 \times 56.9} = .31 \text{ in.}$$

Example 40.—Determine the necessary section modulus of an I beam shown in Fig. 89 if $q = 500$ lbs. per foot and working stress $p_w = 16{,}000$ lbs. per sq. inch. What will be the deflection at the middle of the beam?

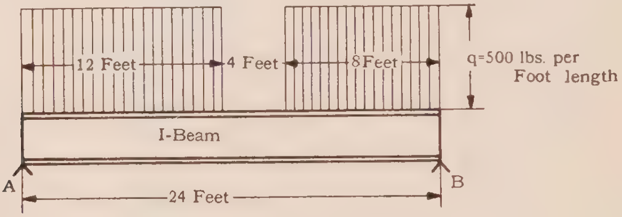

FIG. 89.

Solution.—The reaction at A is

$$A = \frac{6{,}000 \times 18 + 4{,}000 \times 4}{24} = 5{,}167 \text{ lbs.}$$

$M_{\max}$ will be distant $5{,}167/500 = 10.33$ ft. from the end A, the magnitude being given by

$$M_{\max} = 5{,}167 \times 10.33 - \frac{500 \times (10.33)^2}{2} = 53{,}400 - 26{,}700 = 26{,}700 \text{ lb. feet.}$$

Taking an I beam 9 in. deep, $I = 91.4$ in.^{4}
The deflection at the middle produced by the load on the left half of the beam will be

$$\delta_1 = \frac{1}{2} \times \frac{5}{384}\frac{ql^4}{EI}$$

The deflection at the middle produced by the load on the right half of the beam, by using equation (67), is

$$\delta_2 = \int_0^{l/3} \frac{qcdc}{48EI}(3l^2 - 4c^2) = \frac{25}{48 \times 162}\frac{ql^4}{EI}$$

The complete deflection will then be

$$\delta = \delta_1 + \delta_2 = \left(\frac{1}{2} \times \frac{5}{384} + \frac{25}{48 \times 162}\right)\frac{ql^4}{EI} = 1.02 \text{ in.}$$

Example 41.—Determine the deflection at the end B of a cantilever beam carrying a uniformly distributed load (q lbs. per unit length) over the left half of the span (Fig. 90 (a)).

Solution.—The deflection at B produced by the element qdc of the load (Fig. 90 (b)) can be obtained by using the equations (70) and (71) for a cantilever beam with a single load at the end. This deflection consists of two parts as follows:

$$\delta_1 = \frac{qdc \cdot c^3}{3EI}; \qquad \delta_2 = \frac{qdc \cdot c^2}{2EI}(l - c).$$

The deflection in the case shown in Fig. 90 (a) will be

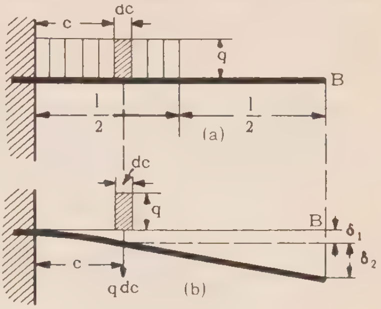

FIG. 90.

$$\delta = \int_0^{l/2} (\delta_1 + \delta_2) = \frac{7}{384}\frac{ql^4}{EI}.$$

If the same load will be distributed along the right half of the beam, the deflection will be,

$$\delta = \int_{l/2}^{l} (\delta_1 + \delta_2) = \frac{41}{384} \cdot \frac{ql^4}{EI}.$$

Example 42.—A beam of the length $l + c_1 + c_2$ is placed on supports l apart and overhanging them by lengths c_1 and c_2. Determine the deflections at the end C and at the midpoint between the supports produced by concentrated loads shown in Fig. 91.

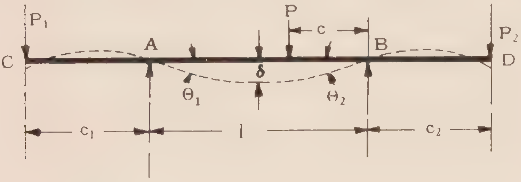

FIG. 91.

Solution.—Part of the beam between sections A and B will be in the same condition as a beam loaded by the force P and by the couples P_1c_1 and P_2c_2 at the supports A and B. By using equations (67) and (68) pages 73 and 74 and the principle of superposition the deflection at the middle will be

$$\delta = \frac{Pc}{48EI}(3l^2 - 4c^2) - \frac{P_1c_1l^2}{16EI} - \frac{P_2c_2l^2}{16EI}.$$

The slope at the support A will be obtained by using equations (64), (65), and (69) pages 73 and 74.

$$\theta_1 = \frac{Pc(l^2 - c^2)}{6lEI} - \frac{P_1c_1l}{3EI} - \frac{P_2c_2l}{6EI}.$$

Now by using the equation (71), page 74, the deflection at the end C will be

$$\frac{P_1c_1^3}{3EI} - c_1\theta_1.$$

22. Graphical Determination of Deflections.—If the effect of shearing force is neglected, the deflection of a beam can be determined by the integration of the equation (59) page 71. This deflection can also be obtained graphically if the fact be taken into consideration that equation (59) coincides with the equation of a funicular curve constructed for a properly chosen loading. It is proposed to develop here the method of performing this operation. Let a simply supported beam AB Fig. 92 be loaded by a distributed load represented by the curve uw. The corresponding polygon of forces is shown in Fig. 92 (b) and the corresponding funicular curve, constructed in the usual manner, is shown in Fig. 92 (c). The slope of this curve at any point t will be determined by the corresponding ray Oc, of the polygon (b); therefore

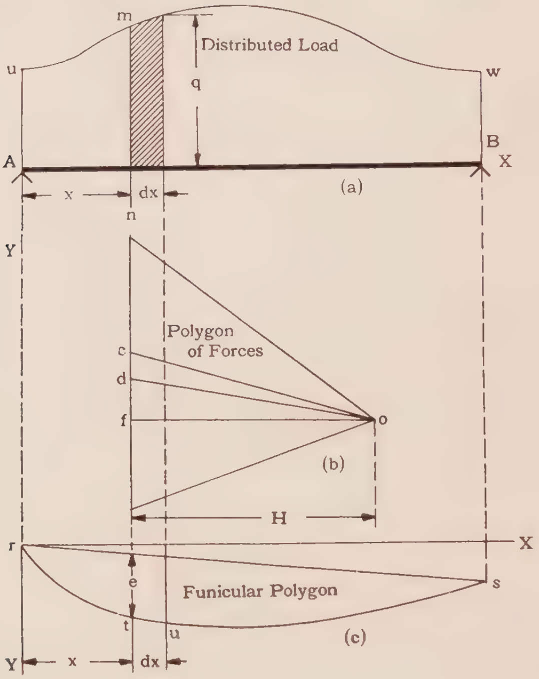

Fig. 92.

$$\frac{dy}{dx} = \frac{fc}{fo} \tag{a}$$

For a point u, an infinitely small distance away on the same curve, the slope will be

$$\frac{dy}{dx} + \frac{d^2y}{dx^2}dx = \frac{fd}{fo} \tag{b}$$

Subtracting (a) from (b) and taking into account that $fc - fd = dc = qdx$, and $fo = H$, where H denotes the pole distance, the following equation of the funicular curve will be obtained:

$$H\frac{d^2y}{dx^2} = -q \tag{c}$$

This equation completely coincides with the equation (59) page 71 if only

$$q = M \text{ and } H = EI.$$

From this it is seen that the deflection curve can be obtained graphically as a funicular line for an *imaginary loading*. It is necessary only to take the intensity of the imaginary loading at every section of the beam equal to the bending moment on this section and take the pole-distance equal to the flexural rigidity of the beam. It is important to note that the intensity of an imaginary loading, equal to M, has the dimension of *force* × *length*, therefore the imaginary forces of the polygon (*b*) have the dimension *force* × *length*². The pole-distance, $H = EI$, has the same dimension. The deflections of the beam will be given by the vertical distances between the closing line rs (Fig. 92 (c)) and the curve rts, measured to the same scale as the span of the beam. In order to obtain deflections to a larger scale, say n times larger, it is necessary only to diminish in the same proportion the pole distance, i.e., to put $H = 1/nEI$. Usually this method of adopting a diminished pole distance is always used because otherwise, the deflections obtained will be so small that it will be difficult to measure them with sufficient accuracy.

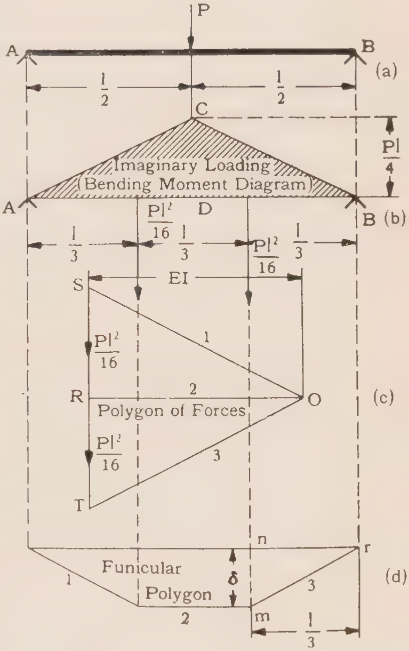

FIG. 93.

A simple case in applying these principles will now be considered. Take, for instance, the case of a beam simply supported with a concentrated load at the middle, Fig. 93 (a). In order to obtain the deflection at the middle graphically, imagine the beam carrying a non-uniform loading, represented by the triangle ACB, i.e., by a load having the same intensity as that of the bending moment for the case under consideration. Dividing the load into two parts, the corresponding polygon of forces will be as shown in (c). In Fig. 93 (d) the three tangents to the funicular curve are given, and the deflection δ at the middle is obtained. From the similarity of the triangles mnr and TRO it follows that

$$\delta : \frac{Pl^2}{16} = \frac{l}{3} : EI,$$

or

$$\delta = \frac{Pl^3}{48EI}$$

If this deflection be drawn to scale it will then be necessary to take EI/n instead of EI, and due to this the deflection δ will be obtained to a scale n times larger than that used for the span. This method requires, therefore, a certain amount of accurate drawing in order that a correct solution may be had. In the next paragraph we come to a method where no scale drawings are required.

23. Grapho-analytical Method of Calculating Deflections.—*General.*—By considering the deflection curve as a funicular curve for an imaginary loading, a very simple method for calculating deflections can be derived. It has been shown that, provided the loading is represented by the diagram of bending moment and the pole distance H is taken equal to EI, the depth e (Fig. 92 (c)) will then represent the deflection at section mn. Now from a general property of the funicular polygons it follows that the length e multiplied by the pole distance H is equal to the bending moment produced by the imaginary loading. Therefore the deflection of the beam at any section will be given by the equation

$$y = \frac{M'}{EI} \tag{74}$$

in which M' denotes the bending moment at the section under consideration, produced by the imaginary loading. Using the equation (53) page 60, the following equation for calculating the slope of the deflection curve will be obtained:

$$\frac{dy}{dx} = \frac{1}{EI}\frac{d(M')}{dx} = \frac{Q'}{EI} \tag{75}$$

in which Q' denotes the shearing force produced by imaginary loading.

Since the magnitude of the shearing force at each support is equal to the reaction of the support, it follows that the angle of rotation of the ends of a beam simply supported will be obtained by dividing the reactions at the supports due to the imaginary loading by the flexural rigidity EI of the beam. Some applications of this method will now be considered.

Simply Supported Beam with a Concentrated Load at the Middle.—For this case the corresponding imaginary loading is shown in Fig. 94 (b). The reactions at the supports will be equal to $Pl^2/16$; therefore

$$\theta_1 = \theta_2 = \frac{Pl^2}{16EI}$$

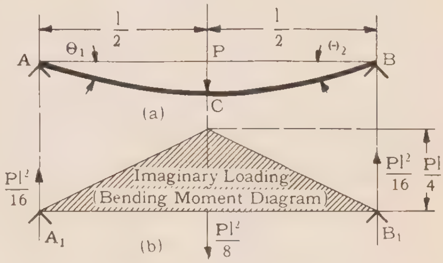

FIG. 94.

The bending moment produced by the imaginary loading at the cross-section C, found by taking moments about this point, will become

$$\frac{Pl^2}{16} \cdot \frac{l}{3} = \frac{Pl^3}{48}$$

Therefore the deflection at C will be

$$\delta = \frac{Pl^3}{48EI}$$

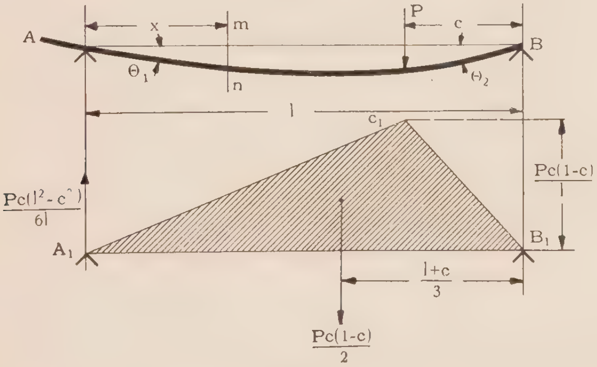

FIG. 95.

Simply Supported Beam with Non-central Load.—The corresponding imaginary loading in this case as shown in Fig. 95 will be

$$\frac{Pc(l-c)}{l} \cdot \frac{l}{2}$$

Assuming this load as acting at the center of gravity of the triangle $A_1B_1C_1$, the reactions on the supports will be

$$\frac{Pc(l-c)(l+c)}{6l} \text{ and } \frac{Pc(l-c)(2l-c)}{6l}$$

Therefore

$$\theta_1 = \frac{Pc(l^2-c^2)}{6lEI};\ \theta_2 = \frac{Pc(l-c)(2l-c)}{6lEI}$$

These coincide with the values given by equations (64) and (65) page 73. In order to obtain the deflection at any cross-section *mn* of the beam, the bending moment produced at this section by the imaginary loading must be calculated. The magnitude of this moment is

$$\frac{Pc(l^2-c^2)}{6l}x - \frac{Pcx^2}{2l}\cdot\frac{x}{3} = \frac{Pcx}{6l}(l^2-c^2-x^2)$$

Therefore the deflection curve for the left part of the beam will be

$$y = \frac{Pcx}{6lEI}(l^2-c^2-x^2)$$

which coincides with equation (61) page 72 obtained before by an analytical method.

Cantilever Beam.—In the case of a cantilever beam loaded at the end (Fig. 96), the imaginary load will be as shown in (b). The question of supporting the imaginary beam, which is fundamental in such analysis was not previously discussed but will now be considered. The determining of the conditions at the supports for the imaginary beam is equivalent to determining the arbitrary constants in analytical considerations of the deflection curve. The support for the imaginary beam must be so taken as to satisfy the conditions at the ends of the real beam. In the case of a simply supported beam the condition at the ends will be satisfied provided the imaginary beam be also taken as simply supported. The bending moments at the supports produced by the imaginary loading, becomes in such a case equal to zero, corresponding to zero deflection at the ends of the real beam.

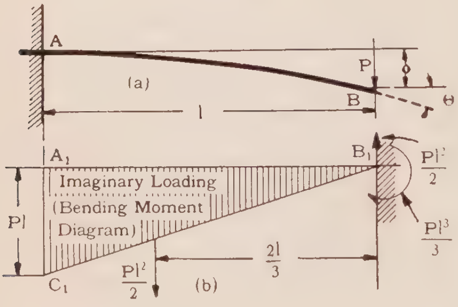

FIG. 96.

In the case of a cantilever beam Fig. 96 (a) the deflection and the slope at the end A are equal to zero, therefore the conditions for the imaginary beam A_1B_1 must be so chosen that the shearing force and the bending moment at the end A_1 be equal to zero, i.e., the end A_1 must be free. At the end B of the real beam the deflection and the slope are not zero, therefore at the end B_1 of the imaginary beam a shearing force and a bending moment must act. This end must be considered as built in. These conditions are satisfied by the arrangement shown in Fig. 96 (b).

Assuming the imaginary load concentrated at the center of gravity of the triangle $A_1B_1C_1$ the reaction at B_1 will be equal to $Pl^2/2$ and the bending moment equal to $Pl^3/3$; therefore, for the real beam (a) the slope and the deflection will be

$$\theta = \frac{Pl^2}{2EI} \text{ and } \delta = \frac{Pl^3}{3EI}$$

Beam with Overhanging Ends.—In the case of a beam with one overhanging end (Fig. 97, (a)), the imaginary loading will be represented by the area of the triangle $A_1D_1C_1 = \frac{1}{2}Pc(l + c)$. In determining the condition of supporting the imaginary beam it is necessary to remember that at the end A of the real beam the deflection is zero while the slope is not zero. At the end C neither the deflection nor the slope have zero values. Therefore, at the end A_1 of the imaginary beam a shearing force must act and at the end C_1 both a shearing force and bending moment must act. The force at A_1 will be determined from the condition that at B_1 the bending moment must be equal to zero because the deflection of the real beam at B is equal to zero.

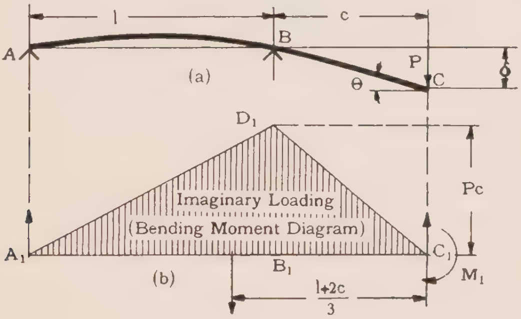

FIG. 97.

In this manner the equation

$$A_1 l = \frac{Pcl}{2} \cdot \frac{l}{3}$$

is obtained, from which $A_1 = Pcl/6$.

The reaction C_1 and the bending moment M_1 at the end C_1 can be obtained from the equations of statics:

$$C_1 = \frac{Pc(l + c)}{2} - A_1 = \frac{Pc}{2}\left(\frac{2}{3}\,l + c\right)$$

$$M_1 = \frac{Pc(l + c)}{2} \cdot \frac{l + 2c}{3} - A_1(l + c) = \frac{Pc^2(l + c)}{3}.$$

Therefore, the slope and deflection at the end C of the real beam will be

$$\theta = \frac{Pc}{2EI}\left(\frac{2}{3}\,l + c\right),$$

$$\delta = \frac{Pc^2(l + c)}{3EI}.$$

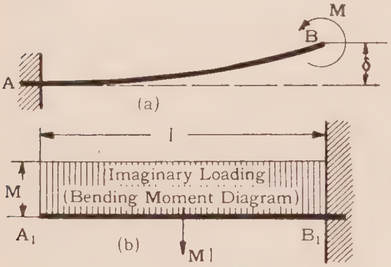

FIG. 98.

Example 43.—Determine the deflection at the end B of a cantilever beam AB produced by a couple M (Fig. 98).

Solution.—The corresponding imaginary loading is shown in (b). Assuming the imaginary beam has a built-in end at B_1, the bending moment at this end will be equal to $Ml^2/2$; therefore, the deflection of the real beam will be

$$\delta = \frac{Ml^2}{2EI}.$$

Example 44.—Determine the angles θ and the deflection at the middle of the beam AB symmetrically loaded by concentrated forces P (Fig. 99).

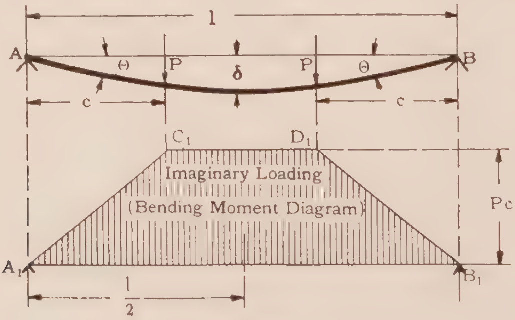

FIG. 99.

Solution.—The corresponding imaginary loading is given by the area of the trapezium $A_1C_1D_1B_1 = Pc(l - c)$. Assuming the imaginary beam simply supported at A_1 and B_1, the reactions at these points will be equal to $Pc(l - c)/2$; therefore

$$\theta = \frac{Pc(l - c)}{2EI}.$$

The bending moment at the middle of the imaginary beam is

$$\frac{Pc(l - c)}{2} \cdot \frac{l}{2} - \frac{Pcl}{2} \cdot \frac{l}{4} + \frac{Pc^2}{2}\left(\frac{l}{2} - \frac{c}{3}\right) = \frac{Pc}{4}\left(\frac{l^2}{2} - \frac{2}{3}c^2\right);$$

therefore the deflection at the middle of the real beam is

$$\delta = \frac{Pc}{4EI}\left(\frac{l^2}{2} - \frac{2}{3}c^2\right).$$

Example 45.—Determine the angles θ_1 and θ_2 and the deflection at any cross-section mn of a beam AB simply supported at the ends and bent by a couple Pc, Fig. 100.

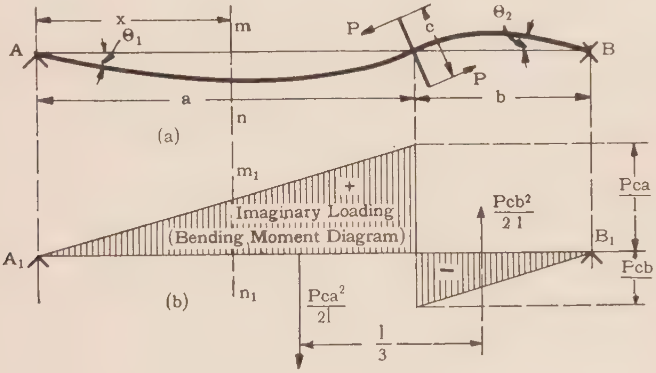

FIG. 100.

Solution.—The corresponding imaginary loading is shown in (b). The reactions at A_1 and B_1 will be

$$A_1 = \frac{1}{l}\left[\frac{Pca^2}{2l}\left(b + \frac{a}{3}\right) - \frac{Pcb^2}{2l} \cdot \frac{2}{3}b\right]$$

$$B_1 = \frac{1}{l}\left[\frac{Pca^2}{2l} \cdot \frac{2a}{3} - \frac{Pcb^2}{2l}\left(a + \frac{b}{3}\right)\right];$$

therefore

$$\theta_1 = \frac{Pc}{2l^2EI}\left[a^2\left(b + \frac{a}{3}\right) - \frac{2}{3}b^3\right]$$

$$\theta_2 = \frac{Pc}{2l^2EI}\left[\frac{2}{3}a^3 - b^2\left(a + \frac{b}{3}\right)\right].$$

If $a = b = l/2$,

$$\theta_1 = \theta_2 = \frac{Pcl}{24EI}.$$

The bending moment at m_1n_1 is]

$$A_1x - \frac{Pca^2}{2l} \cdot \frac{x^2}{a^2} \cdot \frac{x}{3} = \frac{Pcx}{2l^2}\left[a^2\left(b + \frac{a}{3}\right) - \frac{2}{3}b^3\right] - \frac{Pcx^3}{6l}.$$

Therefore the deflection curve for the left part of the real beam is

$$y = \frac{Pcx}{2l^2EI}\left[a^2\left(b + \frac{a}{3}\right) - \frac{2}{3}b^3\right] - \frac{Pcx^3}{6lEI}.$$

Example 46.—Determine the angles of rotation of the ends of a simply supported beam loaded uniformly.

Solution.—The imaginary loading in this case will be a parabola with the maximum ordinate equal to $ql^2/8$. The amount of imaginary loading will be

$$\frac{2}{3}\frac{ql^2}{8}\cdot l = \frac{ql^3}{12}.$$

The corresponding reactions are $ql^3/24$.
Therefore the angles of rotation at the ends will be

$$\theta_1 = \theta_2 = \frac{ql^3}{24EI}$$

24. Deflection of Beams of Variable Cross-section.—*Analytical Method.*—In determining the deflection of beams of variable cross-section, equation (59) page 71, obtained for prismatical bars, can be used with sufficient accuracy. Taking the equation in the form

$$\frac{d^2y}{dx^2} = -\frac{M}{EI}, \tag{a}$$

the deflection can easily be obtained, provided I is a known function of x. Taking the case of a cantilever beam of rectangular cross-section having constant width b and variable depth h, let a load P concentrated at the end act as shown in Fig. 101. Assume that the variation of h is such that the maximum normal stress remains constant along the cantilever, i.e.,

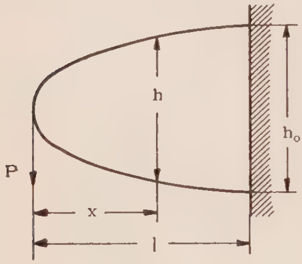

FIG. 101.

$$\frac{M}{S} = \frac{6Px}{bh^2} = \frac{6Pl}{bh_0^2}.$$

Then $h = h_0\sqrt{x/l}$ and

$$I = \frac{bh_0^3}{12}\left(\frac{x}{l}\right)^{3/2}.$$

Equation (a) will be

$$\frac{d^2y}{dx^2} = \frac{12Pl^{3/2}x^{-1/2}}{Ebh_0^3}$$

from which we have

$$\frac{dy}{dx} = \frac{24Pl^{3/2}x^{1/2}}{Ebh_0^3} + C \tag{b}$$

From the condition at the built-in end we know,

$$\left(\frac{dy}{dx}\right)_{x=l} = 0;$$

therefore

$$C = -\frac{24Pl^2}{Ebh_0^3}.$$

Substituting in (b) and integrating,

$$y = \frac{16Pl^{3/2}x^{3/2}}{Ebh_0^3} - \frac{24Pl^2x}{Ebh_0^3} + C_1.$$

From the condition at the built-in end, we again know $(y)_{x=l} = 0$; therefore

$$C_1 = \frac{8Pl^3}{Ebh_0^3}.$$

Inserting the values of these constants, the equation of the deflection curve becomes

$$y = \frac{16Pl^{3/2}x^{3/2}}{Ebh_0^3} - \frac{24Pl^2x}{Ebh_0^3} + \frac{8Pl^3}{Ebh_0^3} \qquad \text{(c)}$$

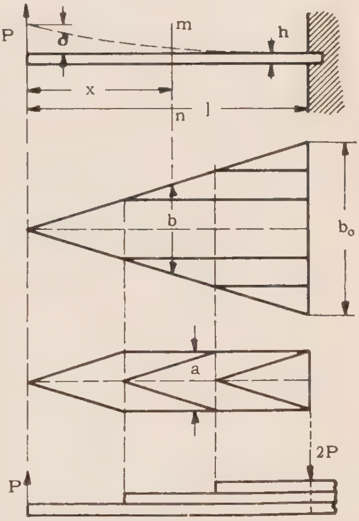

FIG. 102.

from which the deflection at the end is obtained as follows:

$$(y)_{x=0} = \frac{8Pl^3}{Ebh_0^3} = \frac{2}{3}\frac{Pl^3}{EI_0} \qquad (76)$$

It will be observed that the deflection is twice as large as that of a prismatical bar having constant flexural rigidity EI_0, subjected to the same magnitude of maximum normal stress.

As a second example, consider a cantilever of rectangular cross-section having constant depth h and variable width b (Fig. 102). Due to the fact that the section modulus of the beam increases with x in the same proportion as the bending moment, the maximum stress remains constant along the beam. Therefore, the deflection curve will be an arc of a circle, the radius ρ of which will be determined from the equation

$$p_{\max} = \frac{hE}{2\rho}. \qquad \text{(d)}$$

The deflection at the end for a circular curve is

$$\delta = \frac{l^2}{2\rho}, \tag{e}$$

or using (d),

$$\delta = \frac{p_{\max} l^2}{hE} \tag{77}$$

It is seen from equation (77) that for a constant value of $p_{\max}/E$ the deflection is proportional to l^2 and inversely proportional to h.

The results obtained can be applied to a leaf type spring for the approximate determination of the stresses and deflection. It is only necessary to imagine the triangular plate under consideration divided into strips arranged as shown in Fig. 102. The initial curvature and the friction between the strips can be neglected for an approximate solution* and equation (77) can then be considered as sufficiently accurate.

Graphical Method.—In using a graphical method, the deflection curve can be obtained exactly in the same way as explained above for prismatical beams. It is only necessary to bear in mind that the curvature of the deflection line at any cross-section is equal to the ratio M/EI (equation (a) page 90). From this it is clear that an increase in the flexural rigidity for a given section will have the same effect on the deflection as a decrease (in the same ratio) of the bending moment at that section. It can be concluded from this that the problem on the deflection of beams of variable cross-section can be reduced to that of beams of constant cross-section. For example, the deflection of a shaft (Fig. 103) having two different cross-sections with the moments of inertia I_0 and I_1, and loaded by P, can be reduced to that for a cylindrical shaft having moment of inertia I_0.

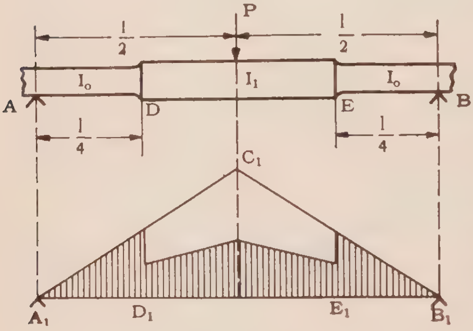

Fig. 103.

---

* The problem is discussed more in detail in the following papers:

A. Castigliano, "Theorie des Biegungs—und Torsions—Federn," Wien, 1888.

Loewe, *Automobiltechnische Bibliothek*, Vol. VI (Berlin), 1918.

Y. Tanaka, *Zeitschr. f. Angew. Math. u. Mech.* Vol. 2, p. 26, 1922.

D. Landau and Percy L. Parr, *Journal of Franklin Institute*, 1918–1919.

It is only necessary, instead of a triangular imaginary loading $A_1C_1B_1$, to take the imaginary loading represented by the shaded area in Fig. 103. This area is obtained by reducing ordinates of the diagram along the distance DE in the ratio I_0/I_1.

The same method can be used also in cases where the cross-section of the beam varies continuously.

Grapho-analytical Method.—Provided that the imaginary loading has been obtained by the transformation of the diagram of bending moment as explained above, further determination of deflections can be made analytically. The magnitude of the deflections and slope at any cross-section of the beam will be obtained as equal to the bending moment and shearing force of the imaginary loading divided by EI.

This method already has been fully explained in paragraph 22, page 82 and no further explanation seems necessary here.

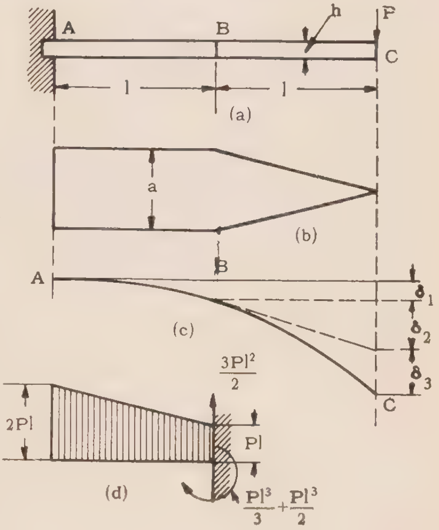

FIG. 104.

Example 47.—A steel plate having a form shown in Fig. 104 is built in at one end and loaded by a force P at the other. Determine the deflection at the end if $2l$ = the length, a = width, h = the thickness of the plate, and P = the load at the end.

Solution.—The deflection will consist of three parts, Fig. 104 (c); (1) δ_1 = deflection at B, (2) δ_2 = deflection at C due to the slope at B, and (3) δ_3 = deflection due to bending of the part BC of the plate.

By using the grapho-analytical method (Fig. 104 (d)), it is seen that

$$\delta_1 = \frac{Pl^3}{3EI} + \frac{Pl^3}{2EI}, \qquad \delta_2 = \frac{3}{2}\frac{Pl^3}{EI}.$$

The deflection δ_3 will be obtained from the equation (e):

$$\delta_3 = \frac{l^2}{2\rho} = \frac{Pl^3}{2EI}$$

and the complete deflection is given by

$$\delta = \delta_1 + \delta_2 + \delta_3.$$

Example 48.—Determine the width d of a carriage spring, Fig. 102, page 91, and its deflection if $2P$ = 12,000 lbs., $h = \frac{1}{2}$ in., $2l$ = 48 in., $p_{\max}$ = 70,000 lbs. per sq. inch, and the number of plates $n = 10$.

Solution.—The equation for the maximum stress is

$$p_{\max} = \frac{6Pl}{ndh^2}$$

from which

$$d = \frac{6Pl}{np_{\max}h^2} = \frac{6 \times 6{,}000 \times 24 \times 4}{10 \times 70{,}000} = 4.93 \text{ in.}$$

The deflection is determined from the equation (77):

$$\delta = \frac{70{,}000 \times 24^2}{\frac{1}{2} \times 30 \times 10^6} = 2.69 \text{ in.}$$

Example 49.—Compare the deflection at the middle, and the angles of rotation of the ends, of a shaft shown in Fig. 103, page 92, with those of a shaft of the same length but having a constant cross-section the moment of inertia of which is equal to I_0. Take $I_1 : I_0 = 2$.

Solution.—Due to greater flexural rigidity at the middle, the angles of rotation at the ends of the shaft shown in Fig. 103 will be less than those of the cylindrical shaft, in the same ratio that the shaded area of the triangle $A_1C_1B_1$ bears to the total area of the triangle $A_1C_1B_1$, which total area corresponds to the cylindrical shaft. This becomes, for the values given, $\frac{5}{8} : 1$.

The deflections at the middle for the two types of shafts will have the same ratio one to another as that of the bending moments produced by the shaded area in one case and by the area of the triangle $A_1C_1B_1$ in the other. It is easy to show that this will be $\frac{9}{16} : 1$.

25. Deflection Due to Shearing Force.—*General Equation.*—It has been shown in paragraph 17 page 63 that the shearing stress over the neutral surface of a beam can be represented by equation

$$p_t = m\frac{Q}{A}$$

in which A denotes the area of the cross-section and m a numerical factor, the magnitude of which depends on the shape of the cross-section. The approximate solutions previously discussed give, for instance, $m = \frac{3}{2}$ for a rectangle and $m = \frac{4}{3}$ for a circular cross-section.

The corresponding shear will be

$$\beta = m\frac{Q}{AG} \tag{a}$$

If Q varies along the length of the beam, the shear also will vary; in this manner an additional curvature due to this shear will be produced. This additional curvature will be

$$-\frac{d\beta}{dx} = -\frac{m}{AG}\frac{dQ}{dx} = -\frac{m}{AG}\frac{d^2M}{dx^2} \tag{b}$$

The minus sign in (b) is taken due to the fact that positive values of $d\beta/dx$ correspond to a curvature convex upwards. Adding this to the curvature M/EI produced by the bending moment, the following equation for the complete deflection of the beam will be obtained:

$$EI\frac{d^2y}{dx^2} = -M + m\frac{EI}{AG}\frac{d^2M}{dx^2} \tag{78}$$

This equation, instead of equation (59) page 71, must be used in all cases for determining deflection where the effect of the shearing force is not negligible in comparison with that of bending moment.

Distributed Load.—In the case of a uniformly distributed load (Fig. 105), the bending moment is

$$M = \frac{ql}{2}x - \frac{qx^2}{2}$$

The additional term on the right side of the equation (78), representing the effect of shearing forces, will be

$$-m\frac{EI}{AG}q \tag{a}$$

This must be considered as an additional imaginary loading in using the grapho-analytical method. Therefore the additional deflection produced by shear will be equal to the bending moment of the imaginary loading, shown in Fig. 105 (b), divided by EI. For the middle of the beam this additional deflection will be

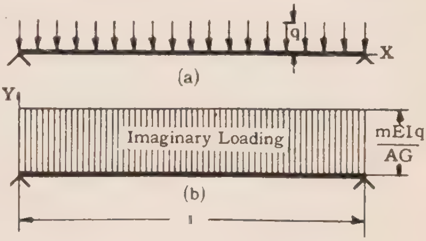

FIG. 105.

$$\frac{M'}{EI} = \frac{mql^2}{8AG}$$

Adding this to the known deflection produced by the bending moment, the following expression for the complete deflection at the middle will be obtained:

$$\delta = \frac{5}{384}\frac{ql^4}{EI} + \frac{mql^2}{8AG};$$

or

$$\delta = \frac{5}{384}\frac{ql^4}{EI}\left(1 + \frac{48m}{5} \times \frac{i^2}{l^2} \times \frac{E}{G}\right)$$

in which $i = \sqrt{I/A}$ denotes the radius of gyration of the cross section.

For a rectangular cross-section $i^2 = \frac{1}{12}h^2$,

$$m = 1.5.$$

Putting

$$\frac{E}{G} = 2\left(1 + \frac{1}{m}\right) = 2.6,$$

$$\delta = \frac{5}{384}\frac{ql^4}{EI}\left(1 + \frac{15.6}{5}\frac{h^2}{l^2}\right).$$

For $l:h = 10$ the effect of the shearing stress is about 3%. With decrease of the ratio l/h this effect of shearing forces on the deflection increases.

For I-beams the factor m is larger than 2 and the effect of shearing forces in the case of short beams of this type can be comparatively great. For instance, take $h = 24$ in., $A = 31.0$ sq. ins., $I = 2{,}810$ in.^{4} the thickness of the web $t = .625$ inches, $l = 24 \times 6$ in. Then $i^2 = 90.8$ sq. ins., and

$$m = \frac{A\int_0^{h/2} ydA}{It} = \frac{31.0 \times 137}{2{,}810 \times .625} = 2.42$$

which means that the additional deflection will become

$$\frac{5}{384}\frac{ql^4}{EI} \times \frac{48}{5} \times 2.42 \times \frac{90.8}{144^2} \times 2.6 = .265 \times \frac{5ql^4}{384\,EI}.$$

The additional deflection due to shear in this case is equal to 26.5% of the deflection produced by the bending moment, and must therefore be considered.

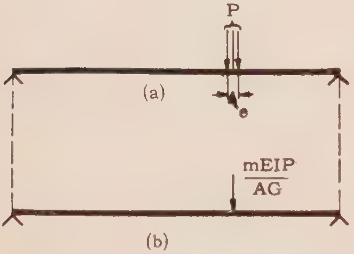

FIG. 106.

Concentrated Load.—A concentrated force P can be considered as the limiting case of a load distributed over a very short part e of the beam Fig. 106. The amount of the corresponding imaginary loading, represented by the second term on the right side of the equation (78) will be

$$m\frac{EI}{AG}\int_0^e \frac{d^2M}{dx^2}dx = m\frac{EI}{AG}\int_0^e \frac{dQ}{dx}dx = m\frac{EI}{AG}\left| Q \right|_0^e = \frac{mEI}{AG}P \qquad \text{(b)}$$

The bending moment, due to this imaginary concentrated load (Fig. 106, (b), divided by EI gives the additional deflection produced by shear. Take, for instance, a central loading of a beam on two supports. The bending moment at the middle produced by the load (b) is

$$M' = \frac{mEI}{AG}\frac{Pl}{4}$$

Therefore the additional deflection is

$$\frac{M'}{EI}=\frac{mPl}{4AG}$$

and the equation for complete deflection will become

$$\delta=\frac{Pl^3}{48EI}+\frac{mPl}{4AG}=\frac{Pl^3}{48EI}\left(1+\frac{12mi^2}{l^2}\frac{E}{G}\right)$$

Take for instance a rectangular cross-section,

$$\frac{i^2}{l^2}=\frac{1}{12}\frac{h^2}{l^2};\quad m=1.5.$$

Then the increase of deflection in % is $390h^2/l^2$. For $h/l=.1$, the effect of shearing force will be about 4%.

CHAPTER V

STATICALLY INDETERMINATE CASES OF BENDING

26. General Considerations.—Three types of supports for beams used in practice are shown in Fig. 107. In the case of a beam with one built-in end (a) it is necessary to know three *elements* for the complete determination of the *reaction,* namely: (1) magnitude of the reaction, (2) its direction, and (3) its point of application. In the case of a pin (b) there are two unknown elements: (1) the magnitude of the reaction, and (2) its direction. Neglecting friction, the reaction must always go through the center of the pin. In the case of a pin on rollers only the magnitude of the reaction is unknown since the direction will be perpendicular to the plane of rolling.

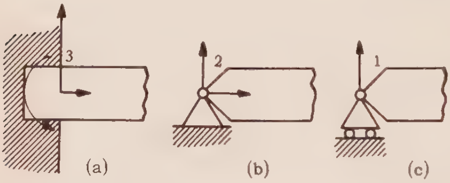

Fig. 107.—Various kinds of fastening ends.

Assuming that all the forces acting on a beam are in the same plane, it will be possible to write down only three equations of statics for determination of the reactions. If there be three unknown *reactive elements* these can be calculated from the equations of statics, i.e., the problem will be *statically determinate.* A beam simply supported (Fig. 79, page 71) and a cantilever beam represent statically determinate cases. If the number of reactive elements be more than three, the number of equations of statics will be less than the number of unknown quantities and the problem becomes *statically indeterminate.* It is usual to say that a beam has one, two, or three *superfluous reactive elements* if the general number of reactive elements is equal to $3 + 1 = 4$, $3 + 2 = 5$, $3 + 3 = 6$ and so on respectively. For instance, the beam with one end built in and the other simply supported, represented in Fig. 109, has only one superfluous element, and the beam with both ends built in will have, generally speaking, three superfluous reactive elements.

It is easy to show that in the case of transverse loading of a beam, the longitudinal reactions usually can be neglected without any substantial error. Take, for instance, a beam, the ends of which are attached by pins to fixed supports, Fig. 108. It is seen at once that a vertical loading produces not only vertical reactions A and B but also two equal and opposite horizontal reactions S. The number of equations of statics in this case is insufficient for calculating the forces S. The additional equation necessary is found from the consideration of deformations of the beam. It is clear that during deflection the axis of the beam undergoes a longitudinal extension equal to the difference between the length of the curved central line and the distance between the support. Assuming as an approximation that the deflection curve is a parabola with maximum ordinate equal to δ, then the elongation will be $\frac{8}{3}\delta^2/l$; the corresponding unit elongation will be $\frac{8}{3}\delta^2/l^2$, and the corresponding axial tensile stress will be

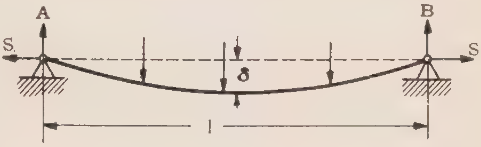

FIG. 108.—Beam with fixed pins at the ends.

$$p = \frac{\frac{8}{3}\delta^2}{l^2} \times E. \qquad (a)$$

Usually the deflection is a very small quantity and the stress (a) can be neglected. Take, for instance, $\delta/l = .001$ and $E = 30 \times 10^6$ lbs. per sq. inch, then,

$$p = \tfrac{8}{3}10^{-6} \times 30 \times 10^6 = 80 \text{ lbs. per sq. inch.}$$

It is clear that, in such cases, the longitudinal reactions S can be neglected and only the reactions A and B need to be taken into consideration. This assumption does not infer that the longitudinal forces can always be neglected; and in the bending of flexible bars and thin strips, which are considered later, it will be shown that these longitudinal forces S may have a practical importance.

27. Beam: One End Built in, the Other Simply Supported.—Consider first the case with one concentrated force P. In the solution of statically indeterminate problems, the superfluous fastenings of the beam will be removed and the deflection of the beam for statically determinate conditions will be considered. The effect of superfluous reactive elements will then be studied separately. In this manner the problem will be reduced to two or more statically determinate cases and by combining these, the solution of the problem will be obtained without the employment of complicated expressions. For the special case under review it is easy to see that the bending of the beam represented in Fig. 109 (a) can be obtained by a combination of cases (b) and (c). It is necessary to determine only such a magnitude of M_a that

$$\theta_1 = \theta_1'. \tag{b}$$

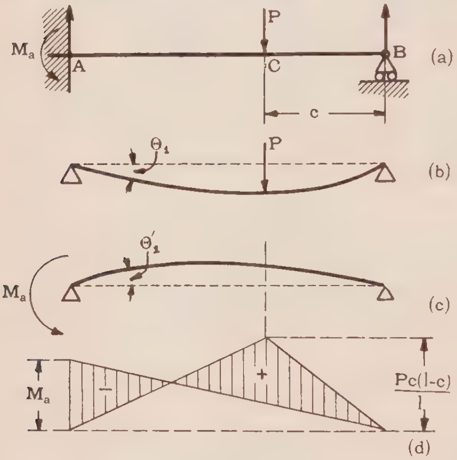

FIG. 109.—Beam: One end built in, the other simply supported.

Thus, the rotation of the left end of the beam, due to the force P, will be annihilated by M_a, and the condition of the built-in end with zero slope will be satisfied. For obtaining M_a, it is necessary only to substitute in (b) the known equations (64) and (69) for θ_1 and θ_1'. Then

$$\frac{Pc(l^2 - c^2)}{6lEI} = \frac{M_a l}{3EI}$$

from which

$$M_a = \frac{Pc(l^2 - c^2)}{2l^2} \tag{79}$$

Now the diagram of bending moment can be obtained by the diagrams for combining the cases (b) and (c) as shown in Fig. 109 (d). The maximum bending moment will be found by comparing the absolute values of the moments at A and at C.

The deflection curve can also be obtained by combining the deflections in cases (b) and (c). The equations of the deflection curves for both these cases have already been given in (61), (63), and (68).

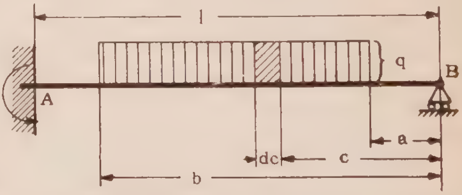

FIG. 110.—Beam with a built-in end, uniformly loaded along the length $b - a$.

Having a solution for this single concentrated load and using the principle of superposition, the problem can be solved for other types of transverse loading by simply extending the above theory. Take, for instance, the case represented in Fig. 110, the moment at the support A, produced by any element qdc of the load, will be obtained from (79) as follows:

$$dM_a = \frac{qcdc(l^2 - c^2)}{2l^2}$$

from which

$$M_a = \int_a^b \frac{qcdc(l^2 - c^2)}{2l^2} = \frac{q}{2l^2}\left(\frac{l^2(b^2 - a^2)}{2} - \frac{b^4 - a^4}{4}\right).$$

If the load be distributed along the entire length of the beam, then $a = 0$ and $b = l$, giving the known equation for a uniformly loaded beam:

$$M_a = \frac{ql^2}{8}$$

The deflection at the middle will be obtained by combining the deflection due to the uniform loading and that due to the couple M_a, i.e.,

$$\delta = \frac{5}{384}\frac{ql^4}{EI} - \frac{M_a l^2}{16EI} = \frac{ql^4}{192EI} \tag{80}$$

Example 50.—Determine the deflection of the end C of the beam ABC shown in Fig. 111 (a).

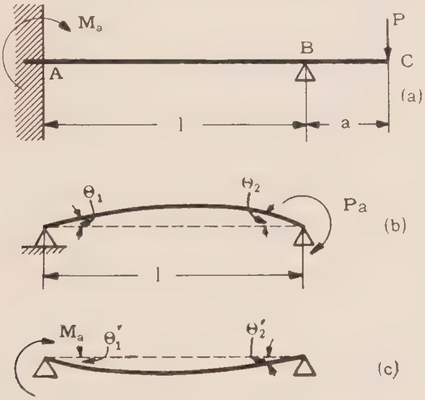

FIG. 111.

Solution.—Combining the cases (b) and (c), the superfluous element, couple M_a, will be found from the equation $\theta_1 = \theta_1'$, or $Pal/6EI = M_al/3EI$, i.e., $M_a = Pa/2$.

The deflection at C will be

$$\delta = \frac{Pa^3}{3EI} + a(\theta_2 - \theta_2') = \frac{Pa^3}{3EI} + a\left(\frac{Pal}{3EI} - \frac{Pal}{12EI}\right) = \frac{Pa^3}{3EI} + \frac{Pa^2l}{4EI}.$$

The first term on the right side represents the deflection of a cantilever and the second represents the deflection due to rotation of the section B.

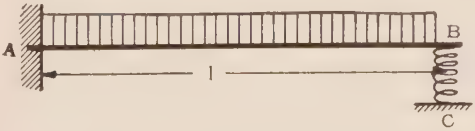

FIG. 112.

Example 51.—Determine the deflection (Fig. 112) at the end B of a uniformly loaded beam AB, the end A of which is built in, the end B being supported by the spring BC, if the dimensions of the beam and the flexibility of the spring are known.

Solution.—Let δ denote the deflection at B, X denote the pressure on the spring and k the compression of the spring produced by a unit force. Then

$$\delta = \frac{ql^4}{8EI} - \frac{Xl^3}{3EI} = kX$$

$$X = \frac{3}{8}ql\frac{1}{1 + \frac{3EIk}{l^3}} \tag{81}$$

For $k = 0$, the expression becomes that for a beam with a rigid support at B.

Example 52.—Determine the pressure of the beam AB on the support B (Fig. 113) due to non-uniform heating of the beam, provided that the temperature varies from t_0 at the bottom to t at the top of the beam according to a linear law.

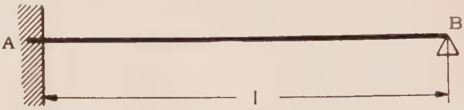

Fig. 113.

The dimensions, elastic property of the material, and coefficient of expansion due to heating are known.

Solution.—Removing the support at B, then, due to the non-uniform heating, the deflection curve of the beam will become an arc of a circle. The radius of this circle will be determined by the equation

$$\frac{1}{\rho} = \frac{\alpha(t - t_0)}{h}$$

in which h = depth of the beam, and α = coefficient of expansion.
The corresponding deflection at B can be found as for an arc of a circle and is

$$\delta = \frac{l^2}{2\rho} = \frac{l^2\alpha(t - t_0)}{2h}.$$

Now this deflection must be annihilated by the reaction of the support B. Let X denote this reaction, then

$$\frac{Xl^3}{3EI} = \frac{l^2\alpha(t - t_0)}{2h},$$

or

$$X = \frac{3EI}{2hl}\alpha(t - t_0) \tag{82}$$

28. Beam with Built-in Ends.—By using the same method as before, the solution of problems involving two superfluous reactive elements M_a and M_b (Fig. 114, (a)) can be obtained. This is accomplished by combining the solutions of the two statically determinate problems shown in (b) and (c). It is easy to see that the conditions at the end of the given beam will be satisfied, if only

$$\theta_1 = \theta_1', \quad \theta_2 = \theta_2'. \tag{a}$$

From these equations the statically indeterminate couples M_a and M_b will be obtained. By using equations (64) and (69), equations (a) can be represented as follows:

$$\frac{Pc(l^2 - c^2)}{6lEI} = \frac{M_a l}{3EI} + \frac{M_b l}{6EI};$$
$$\frac{Pc(l - c)(2l - c)}{6lEI} = \frac{M_a l}{6EI} + \frac{M_b l}{3EI}$$

from which

$$M_a = \frac{Pc^2(l - c)}{l^2}, \quad M_b = \frac{Pc(l - c)^2}{l^2} \tag{83}$$

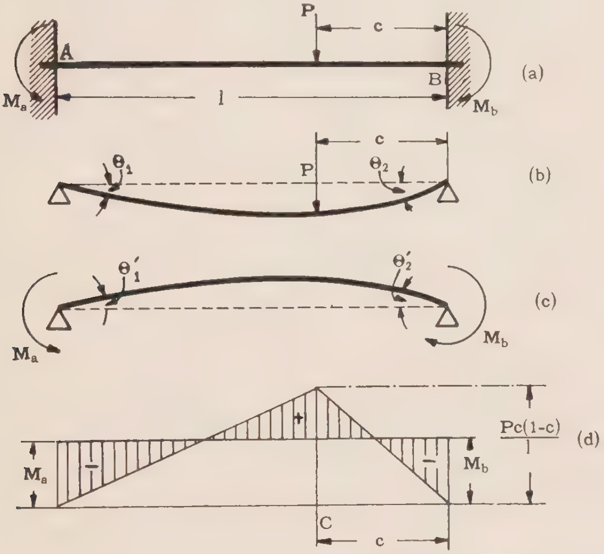

FIG. 114.—Beam with built-in ends.

By combining the diagrams of bending moments for the cases (b) and (c), the diagram shown in Fig. 114 (d) is obtained. In calculating the maximum stresses, the magnitude of the bending moment at C must be compared to that occurring at the nearest support. From (83) it is seen that the maximum value of M_b will be obtained when

$$l - c = \tfrac{2}{3}l.$$

This maximum is equal to $4Pl/27$. The maximum value of bending moment at C takes place when $c = l/2$. This maximum bending moment is equal to $Pl/8$. Having the solution for a single concentrated load P and using the principle of superposition, any other type of transverse loading can be considered easily. Take, for instance, the case represented in Fig. 115. The elementary loading on the length dc will be

$$\frac{q_0 c\,dc}{l}$$

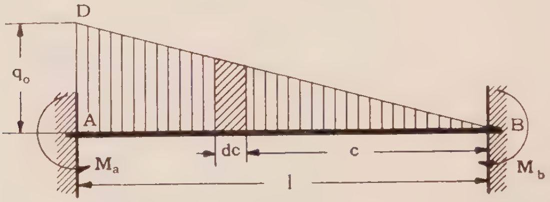

FIG. 115.—Built-in ends, triangular loading.

and the couples acting at the ends, produced by this elementary loading, as obtained from equations (83), are

$$dM_a = \frac{q_0 c^3 (l - c)dc}{l^3}, \quad dM_b = \frac{q_0 c^2 (l - c)^2 dc}{l^3};$$

therefore

$$M_a = \int_0^l \frac{q_0 c^3 (l - c)dc}{l^3} = \frac{q_0 l^2}{20}, \quad M_b = \int_0^l \frac{q_0 c^2 (l - c)^2 dc}{l^3} = \frac{q_0 l^2}{30}.$$

Now the bending moment and deflection at any point can be obtained by combining the deflection produced by the loading with that produced by these couples. It will be apparent therefore that many involved problems on beams can be split up into simple ones and solved in an easy manner by this grapho-analytical method.

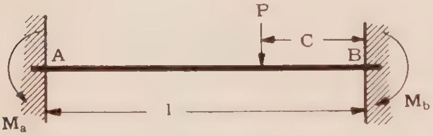

FIG. 116.

Example 53.—Determine the effect of a small vertical displacement δ of the built-in end A of the beam AB (Fig. 116).

Solution.—Remove the support A then the deflection δ_1 at A and the slope θ_1 at this point will be found as for a cantilever built-in at B and loaded by P, i.e.,

$$\delta_1 = \frac{Pc^3}{3EI} + \frac{Pc^2}{2EI}(l - c)$$

$$\theta_1 = \frac{Pc^2}{2EI}$$

Applying at A a reactive force X in the direction upwards and a reactive couple Y in the same direction as M_a, of such magnitude as to annihilate the slope θ_1 and to make the deflection equal to δ, the equations for determining the unknown quantities X and Y will become

$$\frac{Xl^2}{2EI} - \frac{Yl}{EI} = \frac{Pc^2}{2EI}$$

and

$$\frac{Xl^3}{3EI} - \frac{Yl^2}{2EI} = \delta_1 - \delta$$

Example 54.—Determine the bending moments at the ends of a beam AB (Fig. 117) having built-in ends and being centrally loaded. Take $I_1/I_0 = 2$.

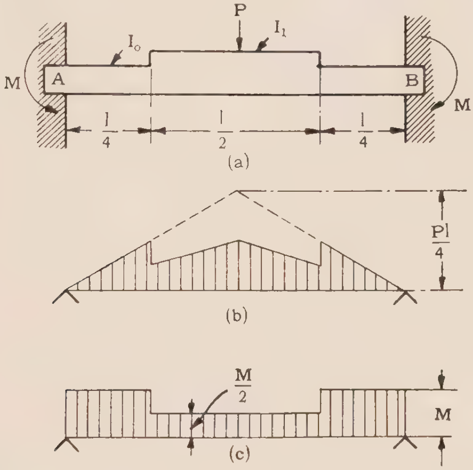

FIG. 117.

Solution.—A solution is obtained by combining the two simple cases shown in (b) and (c). It is clear that the conditions at the built-in ends of the given beam AB will be satisfied if the slope at the end will be equal to zero, i.e., if the reactions of the imaginary loading for (b) and (c) be equal. Therefore the equation for calculating M will be

$$\frac{Pl}{4}\cdot\frac{l}{2} - \frac{3}{8}\,\frac{Pl}{4}\,\frac{l}{2} = Ml - \frac{Ml}{4}$$

from which

$$M = \tfrac{5}{48}Pl$$

29. Frames.—*Symmetrical Case.*—The method used above for the cases of statically indeterminate beams can be applied also in the consideration of frames. Take, for instance, the simplest case of a symmetrical and symmetrically loaded rectangular frame shown in Fig.

118. The sides of the frame are prismatical bars rigidly connected to each other at the corners A, B, C, D. The deflection of these sides produced by the central forces P is shown in the figure by dotted lines. Let EI denote the flexural rigidity of the horizontal bars and EI_1 that of the vertical bars. Other notations are as shown in Fig. 118. In this case, due to symmetry, there will only be one superfluous element, namely, the bending moment M at the corners of the frame. By cutting the frame at the corners and applying couples M, the problem will be reduced to the consideration of bending of two simply supported bars, AB and AC. The equation for determining the superfluous couple M will be obtained from the condition that the angles of rotation θ_1 and θ_1' at the corner A must be equal. Determining these angles by using the grapho-analytical method (paragraph 23, page 84), the equation will be (see Fig. 118, (b))

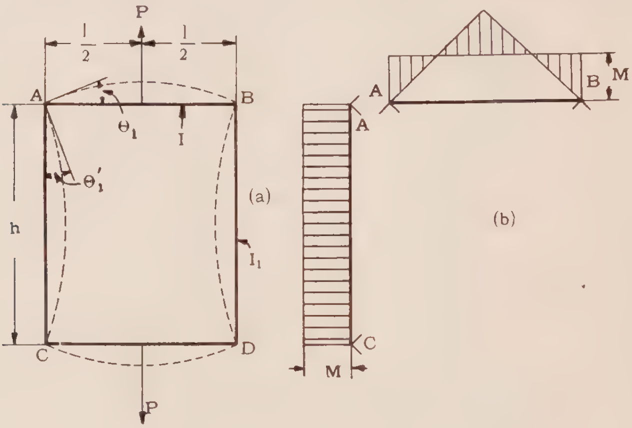

Fig. 118.—Symmetrical loading of a rectangular frame.

$$\frac{Pl^2}{16EI} - \frac{Ml}{2EI} = \frac{Mh}{2EI_1}$$

from which

$$M = \frac{Pl}{8} \frac{1}{1 + \frac{h}{l}\frac{I}{I_1}} \tag{a}$$

If I/I_1 be a small quantity, i.e., if the vertical bars are very rigid in comparison with the horizontal bars, the magnitude of M, obtained from (a), will be about the same as for the case of a beam with built-in ends. If I/I_1 be very large, the horizontal bars will have about the same end conditions as a beam with simply supported ends. The diagrams of bending moment for the horizontal and vertical bars are represented in Fig. 118, by the shaded areas.

For an example of a frame with two superfluous elements, we shall consider the case shown in Fig. 119. In this case the bending moments M and M_1 at A and C are taken as superfluous elements. One of the equations for determining the superfluous elements will be obtained from the condition $\theta_1 = \theta_1'$ (notations are as shown in Fig. 119). Another equation will be found from the condition that the end C of the vertical bar AC is a built-in end. By using the known equations (64) and (69) for rotation of ends, the following will be obtained:

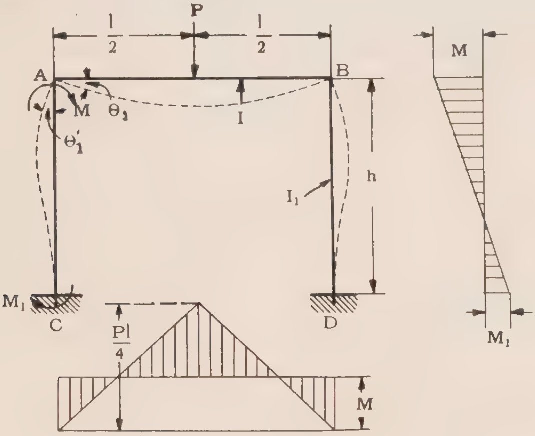

Fig. 119.—Symmetrical loading.

$$\theta_1 = \frac{Pl^2}{16EI} - \frac{Ml}{2EI},$$

$$\theta_1' = \frac{Mh}{3EI_1} - \frac{M_1h}{6EI_1}.$$

From the condition at the corner A, we will have $\theta_1 = \theta_1'$, or

$$\frac{Pl^2}{16EI} - \frac{Ml}{2EI} = \frac{Mh}{3EI_1} - \frac{M_1h}{6EI_1}. \tag{b}$$

The second equation will be obtained from the condition at the built-in end C as follows:

$$\frac{Mh}{6EI_1} - \frac{M_1h}{3EI_1} = 0 \tag{c}$$

from which

$$M_1 = \tfrac{1}{2}M. \tag{d}$$

Substituting in (b), the magnitude of M will be obtained. The corresponding diagrams of bending moments are shown in the figure by shaded areas.

Unsymmetrical Case.—It is easy to see that an unsymmetrical case shown in Fig. 120 (a) can be solved by combining the case (b) and (c). The case shown in (b) is a symmetrical one and can be considered exactly in the same manner as previously explained. From the consideration of the case shown in (c), it can be concluded that the *point of inflection* O of the horizontal bar AB will be situated at the middle of the bar. The magnitude X of the shearing force at the middle cross-section will be found from the condition that the vertical deflection of O is equal to zero, Fig. 120 (d). This deflection consists of two parts, deflection δ_1 calculated for O being the free end of the cantilever OB, and the deflection δ_2 due to rotation of the end B of the vertical bar BC. By using the known equations for a cantilever, (paragraph 20, page 74) and by using notations from the figure, the following equations will be obtained:

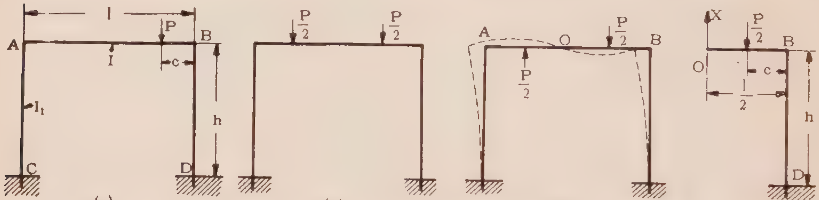

(a) (b) (c) (d)

FIG. 120.—Unsymmetrical loading of a frame.

$$\delta_1 = \frac{P}{2}\frac{c^3}{3EI} + \frac{P}{2}\frac{c^2}{2EI}\left(\frac{l}{2} - c\right) - \frac{X\left(\frac{l}{2}\right)^3}{3EI},$$

$$\delta_2 = \left(\frac{P}{2}c - X\frac{l}{2}\right)\frac{h}{EI_1}\cdot\frac{l}{2}.$$

Substituting this in the equation $\delta_1 + \delta_2 = 0$, the magnitude X of the shearing force will be obtained. Having determined X, the bending moment at every cross-section of the frame (c) can easily be calculated. Combining this with the bending moments for the symmetrical case (b), the solution of the problem (a) will be obtained. If solution for the case of one concentrated force is found, any other kind of loading on the side AB can be considered by using the principle of superposition. The method shown here of reducing the problem to two simple cases (b) and (c) can be used in many other cases as a means of obtaining a simple solution.

Example 55.—A tank of rectangular cross-section $a \times b$ (Fig. 121), having thin walls, is submitted to internal hydrostatic pressure q lbs. per sq. inch. The walls of the tank are strengthened by the rigid frames. Determine the maximum bending moment in the frame.

Solution.—From the condition of symmetry it can be concluded that the bending moments at all corners of the frame are equal. The magnitude M of this moment will be found from the condition that the rotation of the end A of the bar AB must be equal to the rotation of the end A of the bar AC, Fig. 121 (b). Determining the angles of rotation by using the grapho-analytical method (paragraph 23) and notations from the figure, the equation for calculating M will be

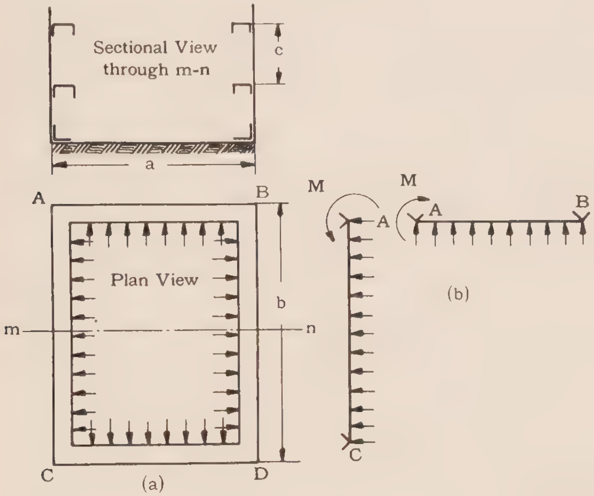

Fig. 121.

$$\frac{qa^3}{24EI} - \frac{Ma}{2EI} = \frac{Mb}{2EI} - \frac{qb^3}{24EI}$$

from which

$$M = \frac{q(a^3 + b^3)}{12(a + b)}.$$

If $a = b$,

$$M = \frac{qa^2}{12},$$

i.e., the bending moment in this case becomes the same as that for a beam with built-in ends.

Example 56.—A square frame $ABCD$ is pressed onto a circular shaft of diameter d. Determine the pressure X between the frame and the shaft if the difference between the diameter d of the shaft and inside dimension of the frame is $d/1{,}000$.

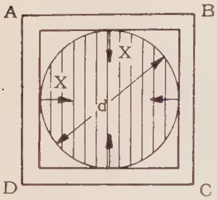

FIG. 122.

Solution.—From the condition of symmetry it can be concluded that the bars of the frame do not undergo rotation at the end. Using the known formula of deflection for a beam with built-in ends (paragraph 28) the equation for calculating the pressure will be

$$2 \times \frac{Xd^3}{192EI} = \frac{1}{1{,}000}d$$

from which

$$X = \frac{.096EI}{d^2}.$$

Example 57.—A rectangular frame $ACDB$ (Fig. 123) made from a bar of circular cross-section is built in at A and B and loaded at the middle of the side DC by a load P perpendicular to the plane of the frame. Determine the deflection at the point of application of the load. Notations are as shown in the figure.

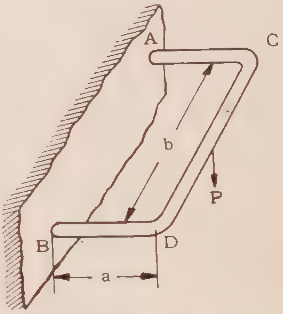

FIG. 123.

Solution.—Let M denote the bending moment at the ends of the bar DC. The magnitude of M will be found from the condition that the angles of twist of the parts BD and CA are equal to the angles of rotation of the ends of the bar DC, i.e.,

$$\frac{Ma}{I_pG} = \frac{Pb^2}{16EI} - \frac{Mb}{2EI}$$

from which

$$M = \frac{Pb}{8} \frac{1}{1 + \frac{Ea}{Gb}}.$$

The deflection will be

$$\delta = \frac{P}{2}\frac{a^3}{3EI} + \frac{Pb^3}{48EI} - \frac{Mb^2}{8EI}.$$

The first term on the right side represents the deflections of the cantilever AC and BD. The two remaining terms represent the deflection of the beam DC.

30. Beams on Three Supports.—In the case of a beam on three supports (Fig. 124, (a)), there will be one superfluous reactive element. Let the reaction of the intermediate support C be this element. Then the solution of the case (a) will be obtained by combining cases represented in (b) and (c). The intermediate reaction X will be obtained from the condition that the deflection at C is equal to zero, i.e. $\delta_1 = \delta_2$, or by using equations (61) and (66),

$$\frac{Pcl_1[(l_1 + l_2)^2 - l_1^2 - c^2]}{6(l_1 + l_2)EI} = \frac{Xl_1^2l_2^2}{3(l_1 + l_2)EI}$$

from which

$$X = \frac{Pc[(l_1 + l_2)^2 - l_1^2 - c^2]}{2l_1l_2^2} \tag{84}$$

If P will act on the left span of the beam, the same formula can be used, but in this case it is necessary to measure the distance c from the support A and to interchange l_1 and l_2.

For $l_1 = l_2 = l$,

$$X = \frac{Pc(3l^2 - c^2)}{2l^3} \tag{85}$$

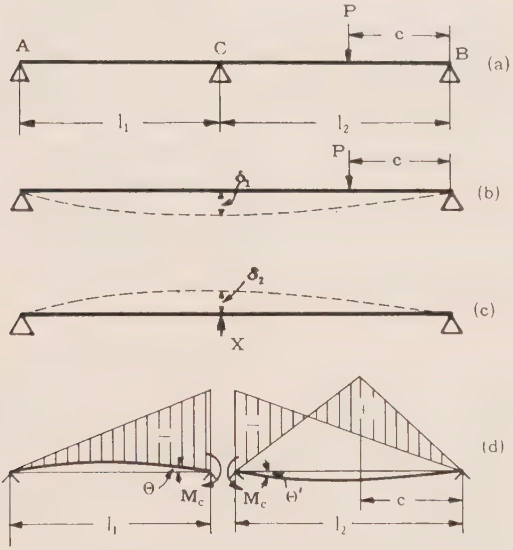

Fig. 124.—Beam on three supports.

If the solution for a single load P is obtained, any other loading can easily be considered by using the principle of superposition.

The same problem can be solved in another manner. Imagine the beam cut into two parts by a cross-section through C (Fig. 124 (d)), and let M_c denote the magnitude of the bending moment of the given beam at the cross-section. In such manner the problem is reduced to the consideration of two simply supported beams shown in (d). The magnitude of M_c will be determined from the condition $\theta = \theta'$, or using the known equations (64) and (69) for angles of rotation,

$$\frac{M_cl_1}{3EI} = \frac{Pc(l_2^2 - c^2)}{6l_2EI} - \frac{M_cl_2}{3EI}$$

from which

$$M_c = \frac{Pc(l_2^2 - c^2)}{2l_2(l_1 + l_2)}. \tag{86}$$

The diagram of bending moment is represented in Fig. 124 (d) by the shaded area.

31. Continuous Beams.—In the case of a continuous beam on many supports, Fig. 125 (a) one support is usually an immovable pin while the other supports are pins on rollers. In this arrangement every intermediate support has only one unknown element; the magnitude of the vertical reaction; therefore the number of superfluous reactive elements is equal to the number of intermediate supports. For instance, in the case shown in Fig. 125 (a) the number of superfluous elements is equal to five. Both methods shown in the previous paragraph can also be used here. But if the number of supports is large, the second method, in which the bending moments on the supports are taken as superfluous elements, is by far the simpler method.

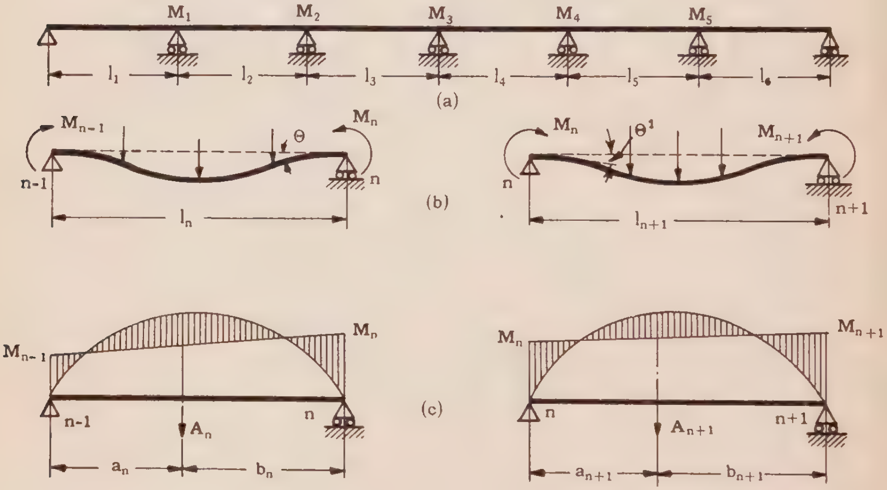

FIG. 125.—Continuous beam.

Let Fig. 125 (b) represent two adjacent spans of a continuous beam cut out by the sections on the supports. It is easy to see that if the bending moments on the supports are known the problem on bending of the continuous beam will be reduced to that of calculating simply supported beams. In this case the number of beams is equal to the number of spans in the continuous beam. For calculating the bending moments at the supports, the conditions of continuity of the deflection curve at the supports can be used. It will be assumed that the bending moments at the supports are positive as shown in Fig. 125 (b) and that the angles of rotation of the ends are positive if the rotation has the same direction as the corresponding couple. Under these conditions the angles θ and θ' as shown in Fig. 125 both will be positive and the condition of continuity at any support n will be

$$\theta = -\theta' \tag{a}$$

General expressions for these angles can be obtained by using the grapho-analytical method. Let A_n denote the area of the imaginary loading on the span n, corresponding to the real load, and let a_n and b_n determine the position of the center of gravity of this loading, Fig. 125 (c). An analogous notation will be used also for $n + 1$ span. Then, taking the rotation of ends by the real loading and by the couples at the supports into consideration, equation (a) will be represented in the following form:

$$\frac{A_n a_n}{l_n EI} + \frac{M_n l_n}{3EI} + \frac{M_{n-1} l_n}{6EI} = -\left(\frac{A_{n+1} b_{n+1}}{l_{n+1} EI} + \frac{M_n l_{n+1}}{3EI} + \frac{M_{n+1} l_{n+1}}{6EI}\right),$$

or

$$M_{n-1} l_n + 2M_n(l_n + l_{n+1}) + M_{n+1} l_{n+1} = -\frac{6A_n a_n}{l_n} - \frac{6A_{n+1} b_{n+1}}{l_{n+1}}. \tag{87}$$

This is the known *equation of three moments* which can be used in the consideration of beams on many supports. It is clear that the number of these equations is equal to the number of intermediate supports and the bending moments at the supports can be calculated without difficulty, if the ends of the continuous beam are simply supported. If one or both ends are built in, then additional equations will be necessary expressing the condition that no rotation occurs at the built-in end.

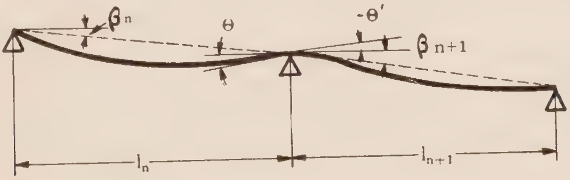

FIG. 126.—Continuous beam, the supports of which are not on the same level.

The general equation of continuity (a) can be used also for those cases where, by mis-alignment, the supports are either not situated on the same level, or have been, due to the bending, subjected to vertical displacements (Fig. 126). Let β_n and β_{n+1} denote the angles of inclination to the horizontal of the straight lines connecting the points of support in the nth and $n + 1$th spans. Remembering that while using the grapho-analytical method the angles of rotation are measured from the line connecting the centers of pins; it can be concluded from Fig. 126 that

$$\theta = \frac{A_n a_n}{l_n EI} + \frac{M_n l_n}{3EI} + \frac{M_{n-1} l_n}{6EI} - \beta_n.$$

Exactly in the same manner,

$$\theta' = \frac{A_{n+1} b_{n+1}}{l_{n+1} EI} + \frac{M_n l_{n+1}}{3EI} + \frac{M_{n+1} l_{n+1}}{6EI} + \beta_{n+1}.$$

Substituting in (a),

$$M_{n-1} l_n + 2M_n(l_n + l_{n+1}) + M_{n+1} l_{n+1} = -\frac{6A_n a_n}{l_n} - \frac{6A_{n+1} b_{n+1}}{l_{n+1}} + 6EI(\beta_n - \beta_{n+1}) \quad (88)$$

If h_{n-1}, h_n, and h_{n+1} denote the vertical distances of the supports $n - 1$, n, and $n + 1$ in a downward direction from a horizontal reference line, the following expressions for β_n and β_{n+1} must be substituted in (88) to obtain a final solution:

$$\beta_n = \frac{h_n - h_{n-1}}{l_n}; \beta_{n+1} = \frac{h_{n+1} - h_n}{l_{n+1}} \quad (89)$$

If h_{n-1}, h_n, . . . are known, the bending moments at the supports easily can be calculated from equations (88).

Example 58.—Construct the diagram of bending moments and shearing forces for the continuous beam shown in Fig. 127 if $P = ql$, $c = l/4$.

Solution.—In this case the imaginary loading for the first span will be represented by a parabolic segment the area of which is

$$A_1 = \frac{2}{3} l \cdot \frac{ql^2}{8} = \frac{ql^3}{12},$$

Distances of the center of gravity of this area

$$a_1 = b_1 = \frac{l}{2}.$$

For the 2nd span $A_2 = 0$.
For the third span, $A_3 = Pc(l - c)/2$, $b_3 = \frac{1}{3}(l + c)$.

Substituting this in equation (87) page 113, the equations for determining the bending moments M_1 and M_2 will be

$$4M_1 l + M_2 l = -\frac{ql^3}{4},$$

$$M_1 l + 4M_2 l = -\frac{Pc(l^2 - c^2)}{l}$$

from which

$$M_1 = -\frac{ql^2}{15} + \frac{Pc(l^2 - c^2)}{15l^2} = -\frac{49}{960}ql^2,$$
$$M_2 = \frac{ql^2}{60} - \frac{4}{15}\frac{Pc(l^2 - c^2)}{l^2} = -\frac{44}{960}ql^2$$

The diagram of bending moment obtained will be as shown in Fig. 127 (b). To obtain the diagrams of shearing force it will be necessary to evaluate the reactions at the supports produced by the separate spans. Reasoning in this way it becomes evident that the pressures on the supports 0 and 1 produced by the first span of the beam will be

$$\frac{ql}{2} + \frac{M_1}{l} = .449ql \text{ and } \frac{ql}{2} - \frac{M_1}{l} = .551ql,$$

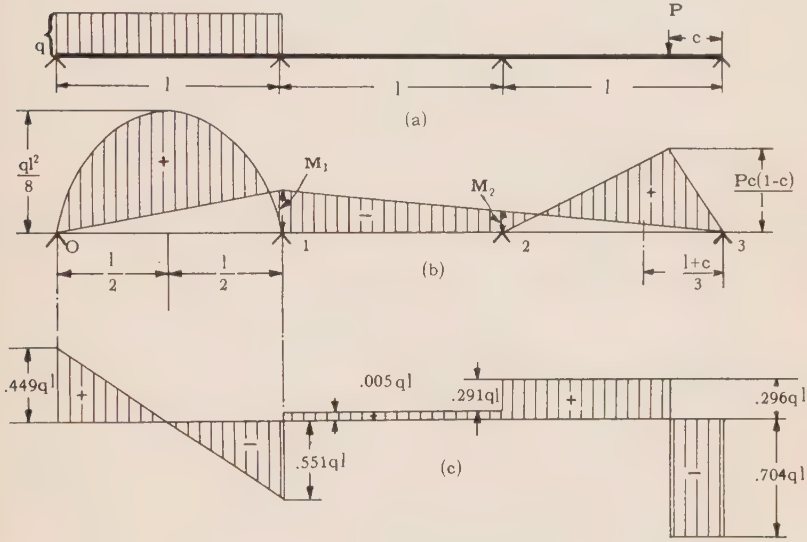

FIG. 127.

while on the supports 1 and 2 by the second span of the beam it will be

$$\frac{M_2 - M_1}{l} = .005ql \text{ and } \frac{M_1 - M_2}{l} = -.005ql,$$

and on the supports 2 and 3 produced by the third span it will be

$$\frac{Pc}{l} - \frac{M_2}{l} = .296ql \text{ and } \frac{P(l-c)}{l} + \frac{M_2}{l} = .704ql.$$

From this, the corresponding diagram of shearing force is obtained as shown in Fig. 127 (c).

Example 59.—Determine the diagram of bending moment for the case shown in Fig. 128.

Solution.—Equation (87) page 113 for this case will become

$$M_0l + 4M_1l + M_2l = 0 \tag{a}$$

Now, from the condition at the support 2,

$$M_2 = -Pc \tag{b}$$

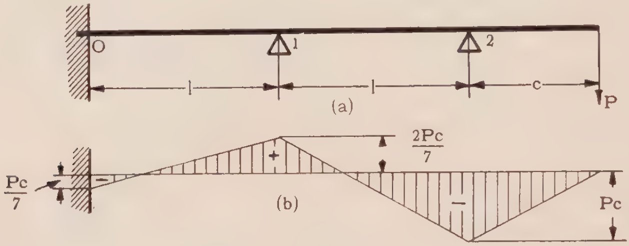

Fig. 128.

while from the condition at the built-in end, we have

$$\frac{M_0l}{3EI} + \frac{M_1l}{6EI} = 0. \tag{c}$$

From (a), (b), and (c),

$$M_0 = -\tfrac{1}{7}Pc,\ M_1 = \tfrac{2}{7}Pc,\ M_2 = -Pc.$$

The diagram of bending moments derived from this data will be as shown in Fig. 128 (b).

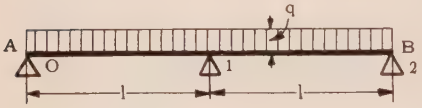

Fig. 129.

Example 60.—Consider the effect on the maximum stress in the continuous beam AB (Fig. 129) of a small downward displacement Δ at the middle support

Solution.—Equation (88) for this case will become

$$4M_1l = -\frac{ql^3}{2} + 6EI\frac{2\Delta}{l},$$

$$M_1 = -\frac{ql^2}{8}\left(1 - \frac{24EI\Delta}{ql^4}\right) = -\frac{ql^2}{8}\left(1 - \frac{5}{16}\frac{\Delta}{\delta}\right)$$

in which

$$\delta = \frac{5}{384}\frac{ql^4}{EI}$$

is the deflection of a simply supported beam of the length l. It is clear that the effect on the maximum bending moment due to the displacement of the middle support increases with an increase in the rigidity of the beam. For a very rigid beam, δ is very small and the slightest displacement Δ of the support may produce a large effect on the magnitude of the maximum bending moment. This fact must be given due consideration in design, and the application of the theory is only justifiable when precautions have been taken to ensure alignment.

32. Potential Energy of Deformation.—Another method for solving statically indeterminate problems, which is based on the consideration of the potential energy of deformation, will now be discussed. It has been shown (when considering the simplest problems in the twist of circular shafts and pure bending of prismatical rods) that the potential energy of deformation can be represented as a homogeneous function, of the second order, of external forces or of displacements. See equations (33) and (52). Assuming that the material follows Hooke's law and that the structure is such that the principle of super position can be applied,* the same conclusion can be obtained for the most general case. Take, for instance, the general case of deformation in one plane and assume that an elastic structure simply supported at A and B is submitted to the action of external forces P_1, P_2, P_3 . . . (Fig. 130). Let δ_1, δ_2, δ_3 . . . denote the displacements of the points of applications of the forces each in a direction corresponding to the force. Assuming that the forces are increasing slowly, so that any dynamical effect can be neglected, the work done by these forces during deformation, within the limits of elasticity, will be equal to the potential energy of deformation stored in the deformed structure. The amount of the energy does not depend on the order in which the forces are applied and is completely determined by the final magnitudes of these forces. Assume that all forces P_1, P_2, P_3 . . . are increasing simultaneously in such a manner that their respective ratios remain always constant. Since the relation between any of these forces and the corresponding displacement can be represented by a straight line OA as shown in Fig. 131, the work done by the force during

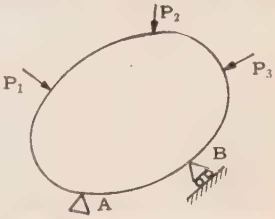

Fig. 130. Elastic structure submitted to the action of external forces.

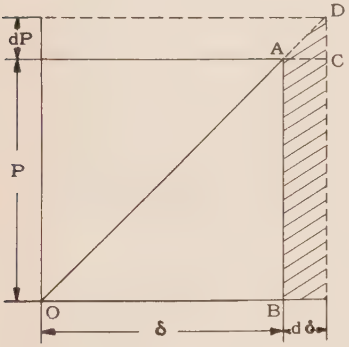

Fig. 131.—Diagram of potential energy.

---

* Such systems as considered in example 10, page 7, are excluded from this consideration because the displacement in that case is not proportional to the force and the principle of superposition can not be applied.

deformation will be represented by the triangle $OAB = P\delta/2$. It follows, therefore, that the potential energy stored in the structure during the action of forces P_1, P_2, P_3, will be

$$U = \frac{P_1\delta_1}{2} + \frac{P_2\delta_2}{2} + \cdots \tag{90}$$

On the assumptions made above, δ_1, δ_2, δ_3 . . are linear functions of forces P_1, P_2, P_3, . . . Substituting these functions in (90), a general expression for the potential energy will be obtained in the form of a homogeneous function of the second order of external forces. If the forces be represented as linear functions of displacements and these functions be substituted in (90), the expression for the potential energy in the form of a homogeneous function of the second order of displacements will be obtained. Both forms of the potential energy have important practical applications.

In the considerations above, the reactions at the supports A and B were not taken into account. These reactions easily can be obtained from the equations of statics if the forces P_1, P_2, P_3, . . . are known. The work done by the reactions during the deformation will be equal to zero due to the fact that the displacement at A is zero and the displacement at B is perpendicular to the reaction, friction at the support being neglected.

In cases of statically indeterminate systems it will be assumed that the *redundant fastenings* at the supports are removed and the corresponding *redundant reactive elements* X, Y, . . . are applied as external forces. In this case the expression (90) of the potential energy will include not only the terms containing the given forces P_1, P_2, P_3 but also terms due to the unknown reactive elements X, Y, . . .

The term "force" will be used in the future in its *generalized meaning* sometimes denoting certain groups of forces. For instance, two equal and opposite forces acting along the same line (Fig. 132, (a)), a couple and the corresponding reactions (Fig. 132 (b)), or two equal and opposite couples as shown in Fig. 132 (c), can be denoted by one letter and considered as generalized forces. The corresponding displacements should be so chosen as to make the product of the force by

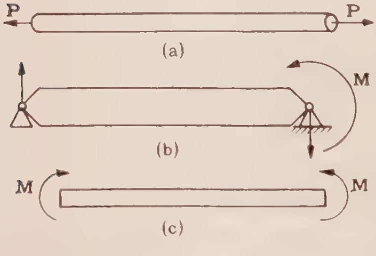

Fig. 132.—Different types of generalized forces.

half of the corresponding displacement equal to the work done. The corresponding displacement for the case (a) will be the extension of the bar; for the case (b), the rotation of the end of the beam; and for the case (c), the rotation of one end of the rod with respect to the other end.

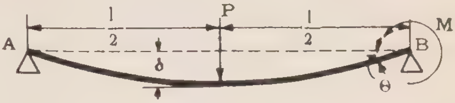

FIG. 133.—Bending by a force and a couple.

Take, for instance, the case represented in Fig. 133. In calculating the potential energy, the force P and the *generalized force* M must be taken into consideration. The corresponding displacements are the deflection δ and the angle of rotation θ. By using the known equations we have

$$\delta = \frac{Pl^3}{48EI} + \frac{Ml^2}{16EI} \tag{a}$$

$$\theta = \frac{Pl^2}{16EI} + \frac{Ml}{3EI} \tag{b}$$

Substituting in (90),

$$U = \frac{P}{2}\left(\frac{Pl^3}{48EI} + \frac{Ml^2}{16EI}\right) + \frac{M}{2}\left(\frac{Pl^2}{16EI} + \frac{Ml}{3EI}\right) = \frac{1}{EI}\left(\frac{P^2l^3}{96} + \frac{M^2l}{6} + \frac{MPl^2}{16}\right) \tag{c}$$

i.e., the potential energy is a homogeneous function of the second order of the external forces P and M. Determining P and M from equations (a) and (b), and substituting them in (c), an expression for the potential energy as a function of displacements δ and θ will be obtained. Application of a general expression for potential energy will now be considered.

33. Theorem of Castigliano.—*General.*—Castigliano showed* that in all cases when the potential energy of deformation of any elastic system is represented by a homogeneous function of second order of external forces, partial derivative of potential energy with respect to any external force gives the displacement corresponding to this force. Taking, for instance, expressions (a), (b), and (c) of the previous paragraph, it is easy to show that

$$\frac{\partial U}{\partial P} = \frac{Pl^3}{48EI} + \frac{Ml^2}{16EI} = \delta,$$

$$\frac{\partial U}{\partial M} = \frac{Ml}{3EI} + \frac{Pl^2}{16EI} = \theta$$

which is in agreement with the statement above, of Castigliano.

---

* "Nuova Teoria Intorno dell' Equilibrio dei Sistemi Elastici" Torino, Atti della Academia delle scienze, 1875, and "Theorie de l'équilibre des systèmes élastiques," Turin, 1879.

Single Force.—In the case of a single external force the proof of Castigliano's theorem can be obtained at once from the Fig. 131. It is easy to see that if the displacement δ obtains an infinitely small increase $d\delta$ the corresponding increase of the potential energy, represented by the shadowed area, will be

$$dU = Pd\delta \tag{a}$$

from which

$$\frac{dU}{d\delta} = P \tag{91}$$

i.e., if the potential energy is represented as a function of displacements, the derivative of this expression with respect to the displacement gives the corresponding force. The applications of this statement in solution of practical problems will be shown below.

Now considering the infinitely small triangle ADC (Fig. 131) similar to the triangle OAB, it is seen that

$$\frac{d\delta}{dP} = \frac{\delta}{P}, \quad \text{or} \quad d\delta = \frac{\delta \cdot dP}{P} \tag{b}$$

Substituting this in (a) the statement of Castigliano will be obtained:

$$\frac{dU}{dP} = \delta \tag{92}$$

It is of importance to note here that in developing equation (91) it was not necessary to make any assumption on the form of the function representing potential energy of the system. It holds in cases where the relation between P and δ is not linear and the potential energy is no longer a function of the second order. In developing (92) the linear relation (b) between the force and the corresponding displacement was assumed. The equation obtained on this assumption gives true results only in cases where the expression for the potential energy is a homogeneous function of the second degree.

General Case.—A general case represented in Fig. 130 is now to be considered. Assume that the potential energy of deformation is represented as a function of the forces $P_1, P_2, \ldots$ so that,

$$U = \phi(P_1, P_2 \ldots)$$

If a small increase dP_n will be given to any external force P_n the potential energy will increase also and the new amount of it will be,

$$U + \frac{\partial U}{\partial P_n} dP_n \tag{f}$$

But the magnitude of the potential energy does not depend on the order in which the forces are applied to the elastic structure. It can be assumed, for instance, that an infinitely small load dP_n was applied first and afterwards forces $P_1, P_2 \ldots P_n \ldots$ The load dP_n will produce only an infinitely small displacement; so the corresponding work done will be a small quantity of the second order and can be neglected. Applying now forces $P_1, P_2, \ldots P_n \ldots$ it must be noticed that their effect will not be modified by the load dP_n previously applied* and the work done by these forces will be equal to U, as before. But during the application of these forces the load dP_n, previously applied, will produce the work,

$$dP_n\delta_n$$

So that the complete expression for the potential energy will be,

$$U + dP_n\delta_n \tag{g}$$

Comparing this with (f)

$$\frac{\partial U}{\partial P_n} = \delta_n \tag{93}$$

which represents a general proof of the theorem of Castigliano.

It was assumed in this consideration that every force P can obtain an arbitrary increase dP without changing any of the other external forces, otherwise it was assumed that forces $P_1, P_2, \ldots P_n, \ldots$ are independent of each other. The reactive forces necessary for equilibrium are excluded from this consideration, as explained in the previous paragraph.

Example 61.—Determine the deflection and the slope (Fig. 134) at the end A of the cantilever AB, produced by the force P and the couple M_a.

Solution.—The bending moment at any cross-section mn is $M = -Px - M_a$

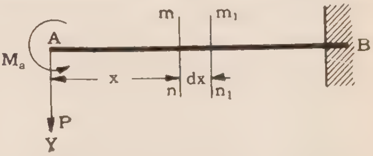

Fig. 134.

The potential energy of an element of the beam, included between cross-sections mn and m_1n_1, from (52) will be

$$\frac{M^2dx}{2EI}$$

The complete expression for the potential energy of the beam will be

$$U = \int_0^l \frac{M^2dx}{2EI},$$

The deflection at A will be obtained as follows:

$$\delta = \frac{\partial U}{\partial P} = \int_0^l \frac{M\frac{\partial M}{\partial P}}{EI}dx = \frac{1}{EI}\int_0^l (Px + M_a)x\,dx = \frac{Pl^3}{3EI} + \frac{M_al^2}{2EI}.$$

---

* It follows from the principle of superposition.

The slope at A will be

$$\theta = \frac{\partial U}{\partial M_a} = \int_0^l \frac{M \dfrac{\partial M}{\partial M_a}}{EI} dx = \frac{1}{EI}\int_0^l (Px + M_a)dx = \frac{Pl^2}{2EI} + \frac{M_a l}{EI}.$$

Example 62.—Determine the deflection at the middle of a uniformly loaded beam with simply supported ends (Fig. 135).

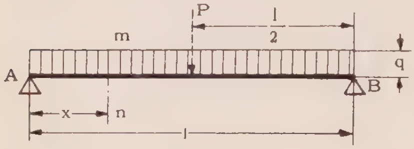

FIG. 135.

Solution.—In order to obtain deflection, by using Castigliano theorem, at a point in which no external concentrated force is applied, the following method can be used: It is necessary to apply in this point an additional imaginary force P and to calculate the derivative $\partial U/\partial P$. The magnitude of this derivative for $P = 0$ gives the deflection desired. In the case represented in Fig. 135, the bending moment at any cross-section on the left from P is

$$M = \left(\frac{ql}{2} + \frac{P}{2}\right)x - \frac{qx^2}{2}$$

The potential energy of bending will be

$$U = 2\int_0^{l/2} \frac{M^2 dx}{2EI}$$

The deflection at the middle

$$\delta = \left(\frac{\partial U}{\partial P}\right)_{P=0} = \frac{2}{EI}\int_0^{l/2} (\mathrm{M})_{P=0} \frac{\partial M}{\partial P} dx = \frac{2}{EI}\int_0^{l/2} \left(\frac{qlx}{2} - \frac{qx^2}{2}\right)\frac{x}{2} dx = \frac{5}{384}\frac{ql^4}{EI}.$$

For determining the angle of rotation θ of the end A of the beam (Fig. 135) a couple M_a must be added. Then, by using Castigliano theorem,

$$\theta = \left(\frac{\partial U}{\partial M_a}\right)_{M_a=0}.$$

Exceptional Case.—Let us consider again the exceptional case given in example (10) page 7. The tensile force in bars of this system is

$$S = \tfrac{1}{2}\sqrt[3]{P^2 EA} \tag{c}$$

The displacement of the point of application of the force P is

$$\delta = l\sqrt[3]{\frac{P}{EA}} \tag{d}$$

and the potential energy of extension is equal to

$$U = 2\cdot\frac{S}{2}\cdot\frac{Sl}{EA} = \frac{Pl}{4}\sqrt[3]{\frac{P}{EA}} = \frac{P\delta}{4} \tag{e}$$

Due to the fact that the displacement δ is no longer proportional to the force, the potential energy cannot be a second degree function of the external forces and equation (92) will therefore not give the true value of the displacement. It is also seen from (e) that the potential energy is no longer equal to half the product of force and corresponding displacement, but will be represented by the shaded area of Fig. 136, in which the curve OMA represents equation (d). It follows from (e) that this shaded area is equal to half of the triangle OAB. Determining P from (d) and substituting in (e), the expression for the potential energy will be obtained in the following form:

$$U = \frac{AE\delta^4}{4l^3} \tag{f}$$

In this case potential energy is no longer a function of the second order of the displacement; nevertheless equation (91) gives a correct value for the force, because from (g) and (d),

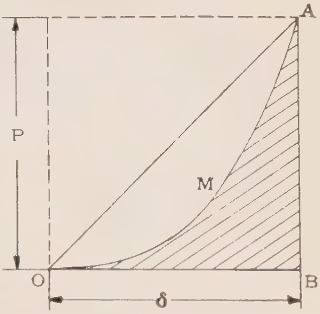

FIG. 136.—Diagram of the potential energy.

$$\frac{dU}{d\delta} = \frac{AE\delta^3}{l^3} = P. \tag{g}$$

This will serve to show that there are cases where the potential energy is no longer a function of the second order of the force and that in such cases the Castigliano theorem cannot be applied. Nevertheless, equation (91) always holds and can be applied in the solution of these problems.

34. Theorem of Least Work.—This theorem follows at once from the theorem of Castigliano and is very useful in analyzing structures with superfluous reactive elements. In considering such structures it will always be assumed that the superfluous fastenings are removed and that corresponding superfluous reactive elements X, Y, Z, . . . are applied to the structure. If the superfluous fastenings are such that there are no displacements corresponding to the forces X, Y, Z, then from Castigliano's theorem it follows that

$$\frac{\partial U}{\partial X} = 0; \quad \frac{\partial U}{\partial Y} = 0; \quad \frac{\partial U}{\partial Z} = 0. \tag{a}$$

The number of these equations is equal to the number of superfluous reactive elements; all these unknown quantities can be found from equations (a).

It is easy to show that the second derivative of U with respect to any external force always will be positive.* Therefore, the previous equations (a) represent conditions of minimum U. It follows, therefore, that the magnitudes of the superfluous reactive elements are such as to reduce the potential energy of the system to a minimum value.

---

* Due to the fact that the function $U = aX^2 + bY^2 + cZ^2 + dXY + eXZ + \dots$ must be positive for all values of $X, Y, Z \dots$, the coefficients $a, b, c, \dots$ for $X^2, Y^2, Z^2 \dots$ must be positive; therefore, the second derivatives of U with respect to $X, Y, Z \dots$ must be positive.

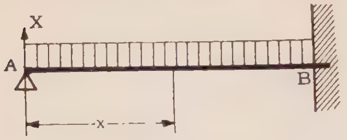

FIG. 137.—Beam with a built in end.

Take, for instance, a beam represented in Fig. 137, and consider the support A as a superfluous fastening. Then on removing this support and applying an unknown reaction X, a statically determinate cantilever beam will be obtained. The bending moment at any cross-section is given by $M = Xx - qx^2/2$ and the potential energy by

$$U = \int_0^l \frac{M^2dx}{2EI}.$$

The unknown reaction X will then be found from the equation

$$\frac{\partial U}{\partial X} = \frac{1}{EI}\int_0^l M\frac{\partial M}{\partial X}dx = \frac{1}{EI}\int_0^l \left(Xx - \frac{qx^2}{2}\right)xdx = \frac{1}{EI}\left(\frac{Xl^3}{3} - \frac{ql^4}{8}\right) = 0$$

from which

$$X = \tfrac{3}{8}ql.$$

The same method can be used for determining the superfluous internal forces in a structure. Take, for instance, a frame (Fig. 138 (a)), submitted to the action of forces $P_1, P_2, \ldots$ The stresses acting on any cross-section mn of the frame can be reduced to a longitudinal force S; shearing force Q, and bending moment M as shown in (b). The magnitude of these forces cannot be found from the equations of statics. They are *statically indeterminate* and, consequently, the *principle of least work* can be used for their evaluation. Considering S, Q, and M as *generalized forces* it can be concluded from the condition of continuity at the section mn that there will be no displacements corresponding to these forces, because due to continuity of the frame, there will be no motion of section a relative to b. Therefore,

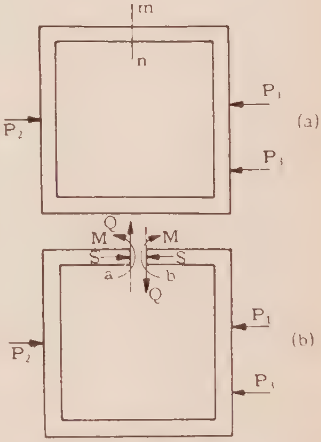

FIG. 138.—General case of a frame.

$$\frac{\partial U}{\partial S} = 0, \quad \frac{\partial U}{\partial Q} = 0, \quad \frac{\partial U}{\partial M} = 0.$$

These three equations can be used for determining S, Q, and M. The magnitude of these statically indeterminite forces is such as to reduce the potential energy of the deformed frame to a minimum.

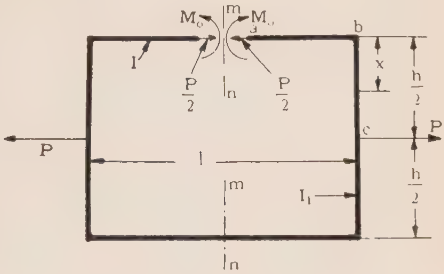

FIG. 139.

Example 63.—Consider the bending of the symmetrical frame shown in Fig. 139.

Solution.—Because of symmetry of the figure, it can be concluded that there will be no shearing force in the middle cross-section mn and that the longitudinal force will be equal to $P/2$. The single statically indeterminate element will be the bending moment M_0 at this cross-section. For determining this moment the principle of least work will be used. The potential energy* will be four times the energy stored in one quadrant abc of the frame and will be (notations as shown in Fig. 139)

$$U = 4\left(\frac{M_0{}^2 l}{4EI} + \int_0^{h/2} \frac{\left(M_0 - \frac{Px}{2}\right)^2 dx}{2EI_1}\right)$$

Substituting in the equation

$$\frac{\partial U}{\partial M_0} = 0,$$

it follows that

$$\frac{M_0 l}{2EI} + \frac{M_0 h}{2EI_1} - \frac{Ph^2}{16EI_1} = 0$$

from which

$$M_0 = \frac{Ph}{8}\,\frac{1}{1 + \frac{l}{h}\frac{I_1}{I}}$$

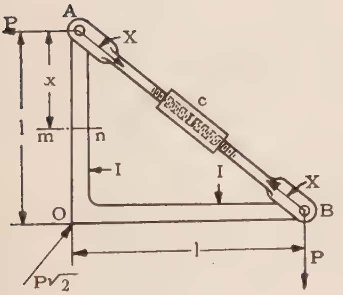

FIG. 140.

Example 64.—Determine the tensile force in the string AB (Fig. 140) of the structure OAB, produced by the forces P. What variation will be produced in this force by one turn of the nut C, if the dimensions of the structure and the pitch of the screw thread be known.

Solution.—Let X = tensile force in the string AB, A_1 = area of the cross-section of the arms OA and OB, A = area of the cross-section of the string AB. The bending moment at any cross-section mn will be

$$M = \left(P - \frac{X\sqrt{2}}{2}\right)x.$$

The potential energy stored by bending of the bars OA and OB will be

---

* Potential energy of tension is neglected in comparison with the potential energy of bending.

$$U_1 = 2\int_0^l \frac{\left(P - \frac{X\sqrt{2}}{2}\right)^2 x^2dx}{2EI}$$

The energy stored by tension in AB will be

$$U_2 = \frac{l\sqrt{2}X^2}{2EA}$$

and the energy of compression in OA and OB will be

$$U_3 = \frac{2X^2l}{4EA_1}$$

Substituting this in the equation,

$$\frac{\partial U}{\partial X} = \frac{\partial(U_1 + U_2 + U_3)}{\partial X} = 0 \tag{a}$$

The following equation will be obtained:

$$\frac{Xl^3}{3EI} + \frac{Xl\sqrt{2}}{AE} + \frac{Xl}{EA_1} = \frac{Pl^3\sqrt{2}}{3EI} \tag{b}$$

from which X can be calculated. If h denotes the pitch of the screw, C, the displacement corresponding to the forces X produced by one turn of the nut, will be equal to $2h$. This quantity, instead of zero, must be now inserted in the right side of equation (a).

35. Reciprocal Theorem.*—This important theorem is very useful in considering statically indeterminate structures submitted to the action of moving load. In using this theorem two different states of stress of the same structure are to be compared. The statement of the theorem is as follows: The work done by the forces of the first state of stress on the corresponding displacements of the second state is equal to the work done by the forces of the second state on the corresponding displacements of the first. Let an elastic structure be submitted

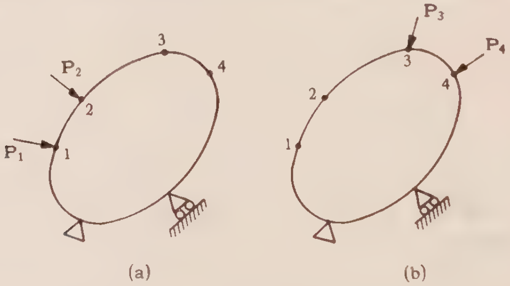

Fig. 141.—Two states of stress.

---

* Particular case of this theorem was obtained by C. Maxwell, see *Phil. Mag.* Vol. 27, p. 294, 1864. For a general proof of the theorem, see Lord Rayleigh, *Scientific Papers* Vol. I, p. 179.

(Fig. 141), in the first case, to the action of forces P_1 and P_2 and in the second case to the action of P_3 and P_4. The supports are such that the reactions can be determined from the equations of statics.* Let $\delta_1, \ . \ . \ . \ \delta_4$ denote the displacements of points 1, . . . 4 corresponding to the forces $P_1, \ . \ . \ . \ P_4$ in the first state of stress (Fig. 141 (a)), and let $\delta_1{}^1, \ . \ . \ . \ \delta_4{}^1$ denote the displacements in the same directions for the second state of stress. Then the *reciprocal theorem* gives

$$P_1\delta_1{}^1 + P_2\delta_2{}^1 = P_3\delta_3 + P_4\delta_4 \tag{94}$$

In order to prove this statement consider the potential energy of the elastic structure when all forces P_1, P_2, P_3 and P_4 are acting. Assume first that forces P_1 and P_2 are applied first, the corresponding potential energy will then be

$$\frac{P_1\delta_1}{2} + \frac{P_2\delta_2}{2} \tag{a}$$

Now, in addition apply forces P_3 and P_4, the work done by these forces will be

$$\frac{P_3\delta_3{}^1}{2} + \frac{P_4\delta_4{}^1}{2} \tag{b}$$

During the application of the forces P_3 and P_4, the forces P_1 and P_2, previously applied, will perform the displacements $\delta_1{}^1$ and $\delta_2{}^1$ and will produce the work

$$P_1\delta_1{}^1 + P_2\delta_2{}^1 \tag{c}$$

So that the complete expression for the potential energy after application of all the forces will be obtained by summing (a), (b), and (c):

$$U = \frac{P_1\delta_1}{2} + \frac{P_2\delta_2}{2} + \frac{P_3\delta_3{}^1}{2} + \frac{P_4\delta_4{}^1}{2} + P_1\delta_1{}^1 + P_2\delta_2{}^1 \tag{d}$$

Repeating the same reasoning but putting first forces P_3 and P_4 and afterwards P_1 and P_2 the following expression for the energy will be obtained:

$$U = \frac{P_3\delta_3{}^1}{2} + \frac{P_4\delta_4{}^1}{2} + \frac{P_1\delta_1}{2} + \frac{P_2\delta_2}{2} + P_3\delta_3 + P_4\delta_4 \tag{e}$$

On the basis that the value of the potential energy does not depend on the order in which the forces were applied but only on the final magnitude of these forces, then the expressions (d) and (e) will be equal, from which the general equation (94) given above, will be obtained.

---

* In the case of statically indeterminate systems it is assumed that superfluous fastenings are removed and the corresponding superfluous reactive elements X, Y, . . . are applied to the structure.

In a particular case, when in the first state of stress, only a single force P_1 is acting; and in the second state, a force P_2 is acting, in which case equation (94) becomes

$$P_1\delta_1{}^1 = P_2\delta_2 \tag{94a}$$

and if $P_1 = P_2$, it follows that $\delta_1{}^1 = \delta_2$. The application of this theorem in the solution of statically indeterminate problems will now be shown for a simple problem represented in Fig. 142. Let us consider the *real condition* of the beam, shown in Fig. 142 (a), as the first state of stress. The reaction X at the support A is taken as the superfluous element. For the second state of stress, the *fictitious state* shown in Fig. 142 (b) is considered. The superfluous support is removed and instead of the unknown reaction X a force equal to unity, acting in a downward direction, is taken. This second state of stress is a very simple one and its deflection curve can be found without any difficulty. Let δ denote the deflection at the end A, and y denote the deflection at the point of application of the force P. The work done by the forces of the state (a) on the corresponding displacement for the state (b) is $Py - X\delta$. The work of the force unity, of the second state on the corresponding displacement of the first state is equal to zero because the displacement of the point A in the first state is equal to zero. Due to the fact that the displacements at the built in end are equal to zero, it is not necessary to consider the reactions at this end, for the corresponding work is always equal to zero. The reciprocal theorem gives $Py - X\delta = 0$ from which $X = Py/\delta$. It is seen that in the case of a moving load P, the reaction X changes in proportion to y, i.e., the deflection curve of the state (b) gives a complete picture of the manner in which X varies, due to the motion of P. This curve is called the *line of influence* of the reaction X.

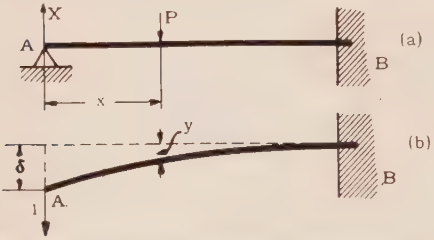

FIG. 142.—Line of influence of the reaction X.

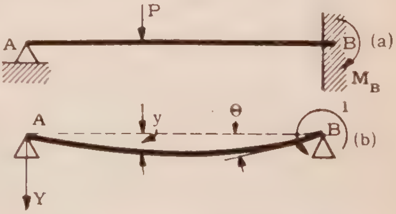

FIG. 143.—Line of influence of the couple M_b.

If instead of the reaction at the support A, the reactive couple M_b at B be considered as the superfluous reactive element, the two states of stress shown in Fig. 143 must be compared. The case (a) represents the real conditions of the beam. The case (b) is the fictitious state of stress in which the superfluous fastening at B is removed, and, instead of the unknown reactive couple M_b a couple equal to unity has been applied. This second state of stress is a simple one. The deflection y and rotation θ can easily be obtained. Applying the reciprocal theorem we have

$$Py - M_b\theta = 0$$

from which

$$M_b = \frac{Py}{\theta}.$$

Again, the deflection curve for the fictitious state of stress represents the *line of influence* for the superfluous reactive element M_b.

36. Deflection Curve Represented by a Trigonometrical Series.—By making use of the expression for the potential energy of deformation, the deflection curve in the form of a trigonometrical series for a simply supported beam can be obtained. It will be shown that this method of analysis is very useful in solving problems on the bending of beams when transverse and longitudinal forces are acting simultaneously (see Chapter VII).

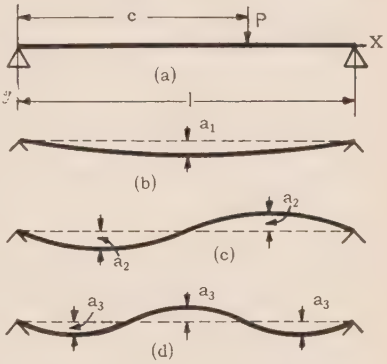

FIG. 144.—Deflection curve represented by a trigonometrical series.

We shall first consider the case of a single force P (Fig. 144), because from this single consideration every other case of loading can be obtained easily by using the principle of superposition. The deflection curve for this case can be represented by the following series:

$$y = a_1 \sin \frac{\pi x}{l} + a_2 \sin \frac{2\pi x}{l} + a_3 \sin \frac{3\pi x}{l} + \cdot \cdot \cdot \qquad \text{(a)}$$

Geometrically this means that the deflection curve can be obtained by superimposing simple sinusoidal curves such as shown in (b), (c), (d), and so on. The first of these curves represents the first term in (a); the second curve, the second term and so on. The coefficients a_1, a_2, a_3 of the series give the maximum ordinates of these sine curves; and the numerical factors 1, 2, 3, etc., the number of waves.

It can be shown analytically that by increasing the number of terms in the series (a) the deflection curve can be represented to any desired degree of accuracy. It is seen from equation (52) that the potential energy of a bent beam is

$$U = \int_o^l \frac{M^2 dx}{2EI},$$

and since

$$M = -EI\frac{d^2y}{dx^2}$$

then

$$U = \frac{EI}{2}\int_o^l \left(\frac{d^2y}{dx^2}\right)^2 dx \tag{95}$$

In order to obtain U as a function of the quantities $a_1, a_2, \ldots$ it is necessary to differentiate the series (a) twice and to substitute the second derivative, obtained in this manner, in the equation (95). The expression for the square of this derivative will contain terms of two kinds, such as

$$\frac{n^4\pi^4}{l^4}a_n^2 \sin^2\frac{n\pi x}{l} \text{ and } 2a_n a_m \frac{n^2m^2\pi^4}{l^4}\sin\frac{n\pi x}{l}\cdot\sin\frac{m\pi x}{l}.$$

It can be shown that

$$\int_o^l \sin^2\frac{n\pi x}{l}dx = l/2,$$

and

$$\int_o^l \sin\frac{n\pi x}{l}\sin\frac{m\pi x}{l}dx = 0.$$

Then equation (95), after integration, becomes

$$U = \frac{EI\pi^4}{4l^3}\left(1^4a_1^2 + 2^4a_2^2 + 3^4a_3^2 + \ldots\right) = \frac{EI\pi^4}{4l^3}\sum_{n=1}^{n=\infty} n^4a_n^2 \tag{96}$$

By using this equation, the coefficients in the series (a) can now be determined. It is known that if an elastic system undergoes a small displacement from the position of equilibrium, then the corresponding increase in the potential energy is equal to the work done by the external forces during such a displacement. By using series (a) for the deflection curve, the small displacements can be obtained by changing the coefficients $a_1, a_2, a_3, \ldots$ Assume that any coefficient a_n obtains an increase da_n, i.e., in the series (a) instead of the term $a_n \sin n\pi x/l$ we will have the term $(a_n + da_n)\sin n\pi x/l$, the other members remaining constant. It is seen that the increase da_n in the coefficient a_n means the superimposing on the deflection curve of an additional very small deflection given by the sine curve $da_n \sin n\pi x/l$. During this additional deflection, the point of application of the force P, distant c from the origin of coordinates, undergoes a vertical displacement equal to $da_n \sin n\pi c/l$, and the force P will perform work given by

$$da_n \sin \frac{n\pi c}{l} \cdot P. \tag{b}$$

Consider now the increase in the potential energy (equation 96). The energy is represented as a function of $a_1, a_2, a_3, \ldots$ and an increase of this function corresponding to the increase da_n of any coefficient a_n is

$$\partial U = \frac{\partial U}{\partial a_n} da_n = \frac{EI\pi^4}{2l^3} n^4 a_n da_n \tag{c}$$

This must be equal to the work done by equation (b); therefore

$$\frac{EI\pi^4}{2l^3} n^4 a_n = P \sin \frac{n\pi c}{l},$$

or

$$a_n = \frac{2Pl^3 \sin \frac{n\pi c}{l}}{EI\,\pi^4 n^4}$$

Substituting this in (a), the following expression is obtained for the deflection curve:

$$y = \frac{2Pl^3}{EI\pi^4}\left(\frac{\sin \frac{\pi c}{l} \sin \frac{\pi x}{l}}{1^4} + \frac{\sin \frac{2\pi c}{l} \sin \frac{2\pi x}{l}}{2^4} + \frac{\sin \frac{3\pi c}{l} \sin \frac{3\pi x}{l}}{3^4}\right) \tag{97}$$

from which the deflection at any point easily can be obtained. In order to obtain the deflection at the middle, when the load is also acting there, it is only necessary to put $c = x = l/2$ which gives

$$(y)_{x=l/2} = \frac{2Pl^3}{EI\pi^4}\left(\frac{1}{1^4} + \frac{1}{3^4} + \frac{1}{5^4} \cdots\right) \tag{98}$$

It is seen that by taking only the first member of the series, the deflection is obtained with an accuracy of about 1½%.

If instead of a single concentrated load a uniformly distributed load is acting on the beam, the deflection curve can be obtained from (97) by using the principle of superposition. Substituting in (97) qdc instead of P and integrating the equation between the limits $c = 0$ and $c = l$ we have

$$y = \frac{4ql^4}{EI\pi^5}\left(\frac{\sin \frac{\pi x}{l}}{1^5} + \frac{\sin \frac{3\pi x}{l}}{3^5} + \frac{\sin \frac{5\pi x}{l}}{5^5} + \cdots\right)$$

giving the deflection at the middle ($x = l/2$);

$$(y)_{x=l/2} = \frac{4ql^4}{EI\pi^5}\left(1 - \frac{1}{3^5} + \frac{1}{5^5} \cdot \cdot \cdot \right)$$

If only the first term of the series be taken, then the error in the deflection at the middle will be about ¼%.

This method of expressing deflection curves by means of a trigonometrical series is very useful and it will be used afterwards in studying the bending of beams submitted simultaneously to transverse and longitudinal forces.

CHAPTER VI

BENDING OF BARS ON ELASTIC FOUNDATION

37. General Equation of Deflection Curve.—Assume that a prismatic bar AB, loaded by a distributed load q (Fig. 145), is supported along its entire length by a continuous elastic foundation, such that when the bar is deflected the intensity of the continuously distributed reaction at every section is proportional to the deflection at that section. Under such conditions the reaction per unit length of the bar can be represented by the expression ky in which k, called the *modulus of the foundation*, denotes the reaction per unit length, provided the deflexion is equal to unity. The simple assumption that the continuous reaction of the foundation is proportional to the deflection, is a good approximation in many practical cases. For instance in the case of railway tracks, the solution obtained on this basis is in good agreement with actual conditions.

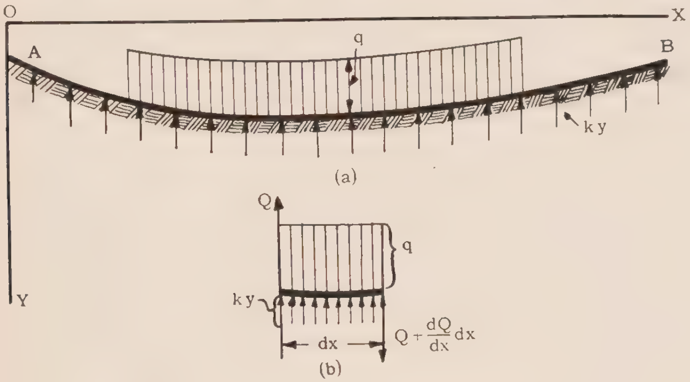

FIG. 145.—Bar on an elastic foundation.

In studying the deflection curve of the bar the differential equation (59) will be used. Differentiating this equation twice and using equation (53) we have

$$EI\frac{d^4y}{dx^4} = -\frac{d^2M}{dx^2} = -\frac{dQ}{dx}. \qquad \text{(a)}$$

An expression for the derivation dQ/dx of the shearing force with respect to x can be obtained from the consideration of equilibrium of an infinitely small element of the beam, Fig. 145 (b). Considering the vertical forces acting on this element, the equation of equilibrium of this element will be*

$$qdx + \left(Q + \frac{dQ}{dx}dx\right) - Q - kydx = 0,$$

or

$$\frac{dQ}{dx} = ky - q.$$

Substituting this in (a), we have

$$EI\frac{d^4y}{dx^4} = q - ky \tag{99}$$

This is the general equation for the deflection curve of a bar supported on an elastic foundation.

Along the unloaded part of the bar, $q = 0$. The differential equation (99) then becomes

$$EI\frac{d^4y}{dx^4} = -ky. \tag{100}$$

If we denote

$$\sqrt[4]{\frac{k}{4EI}} = \beta, \tag{101}$$

A general solution of (100) will be represented as follows:

$$y = e^{\beta x}(A \cos \beta x + B \sin \beta x) + e^{-\beta x}(C \cos \beta x + D \sin \beta x) \tag{b}$$

This statement can easily be verified by substituting (b) in equation (100). In particular cases the arbitrary constants A, B, C, and D of the solution must be determined from the conditions existing at the ends of the bar.

The general case for a distributed load equation (99) will be solved in a similar manner. It is only necessary to add to the solution given by (b) the particular solution of equation (99). We will now come to a consideration of some special problems involving the application of this theory.

38. Infinitely Long Bar. -*Single Concentrated Load.*—Taking the origin of coordinates at the point of application of the force (Fig. 146), then from conditions of symmetry, only that part of the bar to the right of the load need be considered.

---

* In consideration of this element the direction of positive shearing force Q is taken as was explained before (paragraph 15); q is considered as positive if it has a downward direction.

In applying the general equation (b) page 134, to the solution of this case, the arbitrary constants must first be found. To arrive at this solution it is natural to assume that at points infinitely distant from the force P the deflection and the curvature are equal to zero. Due to the fact that the function $e^{\beta x}$ continues to increase with increase of x, it follows that the arbitrary constants A and B must be zero in order to satisfy the conditions at the end $x = \infty$. Assuming in equation (b) that

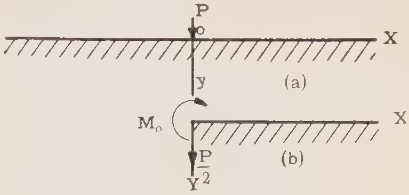

Fig. 146.—Infinitely long bar on an elastic foundation.

$$A = B = 0,$$

the deflection curve for the right part of the bar becomes

$$y = e^{-\beta x}(C \cos \beta x + D \sin \beta x) \qquad \text{(a)}$$

The two remaining arbitrary constants C and D must be found from the conditions at the origin, i.e., at the point 0. At this point the deflection curve must have zero slope; therefore

$$\left(\frac{dy}{dx}\right)_{x=0} = 0,$$

or, substituting (a),

$$-\beta[e^{-\beta x}(C \cos \beta x + D \sin \beta x + C \sin \beta x - D \cos \beta x)]_{x=0} = -\beta(C - D) = 0$$

from which

$$C = D.$$

The equation (a) therefore becomes

$$y = Ce^{-\beta x}(\cos \beta x + \sin \beta x) \qquad \text{(b)}$$

which is fundamental for this condition of loading.

The consecutive derivatives of this equation give:

$$\frac{dy}{dx} = -2\beta Ce^{-\beta x} \sin \beta x$$

$$\frac{d^2y}{dx^2} = 2\beta^2 Ce^{-\beta x} (\sin \beta x - \cos \beta x) \qquad \text{(c)}$$

$$\frac{d^3y}{dx^3} = 4\beta^3 Ce^{-\beta x} \cos \beta x. \qquad \text{(d)}$$

The constant C will be determined from the condition that at $x = 0$ the shearing force for the right part of the bar (Fig. 146, (b)) is given by

$$Q = \left(-EI\frac{d^3y}{dx^3}\right)_{x=0} = -\frac{P}{2},$$

or, using (d),

$$EI4\beta^3C = \frac{P}{2}$$

from which

$$C = \frac{P}{8\beta^3EI}.$$

Substituting this in (b) and (c), the following general expressions are obtained for the deflection and bending moment curves:

$$y = \frac{P}{8\beta^3EI}e^{-\beta x}(\cos\beta x + \sin\beta x) \tag{102}$$

$$M = -EI\frac{d^2y}{dx^2} = -\frac{P}{4\beta}e^{-\beta x}(\sin\beta x - \cos\beta x) \tag{103}$$

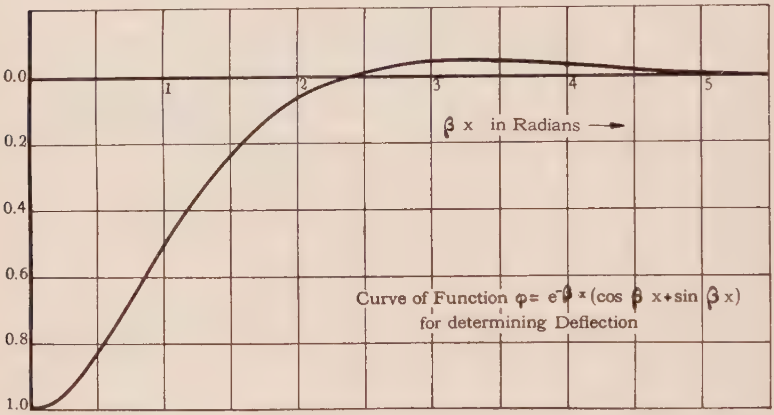

Fig. 147.

Both the expressions (102) and (103) have, when plotted, a wave form with gradually reduced amplitude. The length of this wave will be given by

$$L = \frac{2\pi}{\beta} = 2\pi\sqrt[4]{\frac{4EI}{k}} \tag{104}$$

In order to simplify the determination of the deflection, the bending moment, and the shearing force, Table VI is given,* in which the following notations are used:

$$\begin{aligned} \phi &= e^{-\beta x}(\cos\beta x + \sin\beta x) \\ \psi &= e^{-\beta x}(\sin\beta x - \cos\beta x) \\ \theta &= e^{-\beta x}\cos\beta x \end{aligned} \tag{e}$$

---

* The Table VI is taken from the book "Die Berechnung des Eisenbahn Oberbaues," by Zimmermann (Berlin), 1888.

In Figs. 147 and 148 the functions ϕ and ψ are shown graphically. The maximum deflection and maximum bending moment occur at the origin and are respectively equal to

$$\delta = (y)_{x=0} = \frac{P}{8\beta^3 EI} = \frac{P\beta}{2k} \tag{105}$$

$$M_0 = (M)_{x=0} = \frac{P}{4\beta} \tag{106}$$

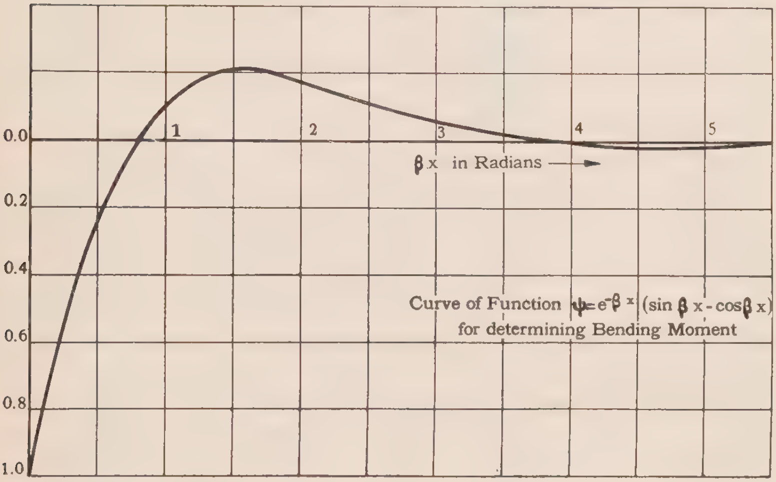

FIG. 148.

By applying this theory together with the principle of superposition, the deflection produced in an infinitely long bar for any other type of loading can easily be obtained without the recourse to long and complicated expressions. The effect produced by concentrated loads can thus be obtained directly by using Table VI or the curves of Figs. 147 and 148. Such an application will be considered later for the case of a railway track.

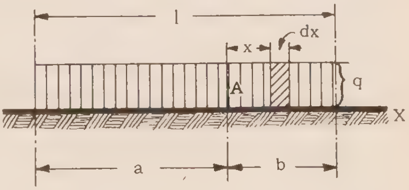

FIG. 149.

Distributed Load.—The application of this theory to the case of a distributed load will now be considered. Let a uniform loading be distributed over a length l of an infinitely long bar (Fig. 149). Consider any point A, and let a and b represent the distances from this point to the ends of the loaded part of the bar. The deflection at

TABLE VI.—CONSTANTS FOR CALCULATING DEFLECTION, BENDING MOMENT AND SHEARING FORCE IN A BAR ON ELASTIC FOUNDATION

βx	ϕ	ψ	θ
.0	1.0000	−1.0000	1.0000
.1	.9907	− .8100	.9003
.2	.9651	− .6398	.8024
.3	.9267	− .4888	.7077
.4	.8784	− .3564	.6174
.5	.8231	− .2415	.5323
.6	.7628	− .1431	.4530
.7	.6997	− .0599	.3798
.8	.6354	+ .0093	.3131
.9	.5712	.0657	.2527
1.0	.5083	.1108	.1988
1.1	.4476	.1457	.1510
1.2	.3899	.1716	.1091
1.3	.3355	.1897	.0729
1.4	.2849	.2011	.0419
1.5	.2384	.2068	.0158
1.6	.1959	.2077	− .0059
1.7	.1576	.2047	− .0235
1.8	.1234	.1985	− .0376
1.9	.0932	.1899	− .0484
2.0	.0667	.1794	− .0563
2.1	.0439	.1675	− .0618
2.2	.0244	.1548	− .0652
2.3	.0080	.1416	− .0668
2.4	− .0056	.1282	− .0669
2.5	− .0166	.1149	− .0658
2.6	− .0254	.1019	− .0636
2.7	− .0320	.0895	− .0608
2.8	− .0369	.0777	− .0573
2.9	− .0403	.0666	− .0534
3.0	− .0423	.0563	− .0493
3.1	− .0431	.0469	− .0450
3.2	− .0431	.0383	− .0407
3.3	− .0422	.0306	− .0364
3.4	− .0408	.0237	− .0323
3.5	− .0389	.0177	− .0283
3.6	− .0366	.0124	− .0245
3.7	− .0341	.0079	− .0210
3.8	− .0314	.0040	− .0177
3.9	− .0286	.0008	− .0147
4.0	− .0258	− .0019	− .0120
4.1	− .0231	− .0040	− .0095
4.2	− .0204	− .0057	− .0074
4.3	− .0179	− .0070	− .0054
4.4	− .0155	− .0079	− .0038
4.5	− .0132	− .0085	− .0023
4.6	− .0111	− .0089	− .0011
4.7	− .0092	− .0090	− .0001
4.8	− .0075	− .0089	+ .0007
4.9	− .0059	− .0087	.0014
5.0	− .0046	− .0084	.0019
5.1	− .0033	− .0080	.0023
5.2	− .0023	− .0075	.0026
5.3	− .0014	− .0069	.0028
5.4	− .0006	− .0064	.0029
5.5	.0	− .0058	.0029
5.6	+ .0005	− .0052	.0029
5.7	.0010	− .0046	.0028
5.8	.0013	− .0041	.0027
5.9	.0015	− .0036	.0026
6.0	.0017	− .0031	.0024
6.1	.0018	− .0026	.0022
6.2	.0019	− .0022	.0020
6.3	.0019	− .0018	.0018
6.4	.0018	− .0015	.0017
6.5	.0018	− .0012	.0015
6.6	.0017	− .0009	.0013
6.7	.0016	− .0006	.0011
6.8	.0015	− .0004	.0010
6.9	.0014	− .0002	.0008
7.0	.0013	− .0001	.0007

A, produced by an element qdx of the load, will be obtained by substituting qdx for P in equation (102). This gives

$$\frac{qdx}{8\beta^3EI}e^{-\beta x}(\cos\beta x + \sin\beta x).$$

The deflection produced at A by the loading distributed over the length l will then become:

$$y = \int_0^b \frac{qdx}{8\beta^3EI}e^{-\beta x}(\cos\beta x + \sin\beta x) + \int_0^a \frac{qdx}{8\beta^3EI} e^{-\beta x}(\cos\beta x + \sin\beta x) = \frac{q}{2k}(2 - e^{-\beta b}\cos\beta l - e^{-\beta a}\cos\beta a) \qquad \text{(f)}$$

If a and b are comparatively large,* the values $e^{-\beta b}$ and $e^{-\beta a}$ will be relatively small and the deflection will be approximately equal to q/k, i.e., at points remote from the ends of the loaded part of the bar, the bending of the bar can be neglected and it can be assumed that the uniform loading q is directly transmitted to the elastic foundation. By taking the point A at the end of the loaded part of the bar we will have $a = 0$, $b = l$, $e^{-\beta a}\cos\beta a = 1$, $e^{-\beta b}\cos\beta b = 0$, and $y = q/2k$, i.e., the deflection now has only one-half of the value obtained above.

Considering another extreme case where the length of the loaded part of the bar is very short, and taking the point A at the middle, we have

$$\beta a = \beta b = \frac{\beta l}{2}.$$

Taking this in conjunction with the approximation

$$e^{-\frac{\beta l}{2}}\cos\frac{\beta l}{2} = 1 - \frac{\beta l}{2},$$

and substituting in (f), we get

$$y = \frac{q}{k}\left(1 - e^{-\frac{\beta l}{2}}\cos\frac{\beta l}{2}\right) = q\frac{\beta l}{2k}.$$

This is in agreement with equation (105) obtained previously for the case of the concentrated load.

Combination of Force and Couple Acting at the End of a Long Bar.—Following the same reasoning as in the previous case, it can be concluded that the general solution for an infinitely long bar shown in Fig. 150 must be of the form

---

* For instance, if they are of the same order as the wave length L, given by the equation (104).

$$y = e^{-\beta x}(C \cos \beta x + D \sin \beta x). \tag{g}$$

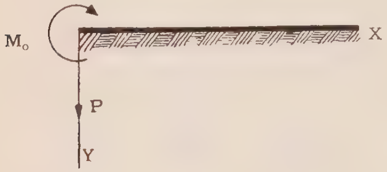

Fig. 150.

The conditions at the origin, i.e., under the load P, for determining arbitrary constants C and D are:

$$EI\left(\frac{d^2y}{dx^2}\right)_{x=0} = -M_0$$

$$EI\left(\frac{d^3y}{dx^3}\right)_{x=0} = -Q = P.$$

Determining C and D from these equations in a similar manner as indicated in the previous paragraph and substituting in (g), the following expression for the deflection curve will be obtained:

$$y = \frac{e^{-\beta x}}{2\beta^3 EI}[P \cos \beta x - \beta M_0 (\cos \beta x - \sin \beta x)]. \tag{107}$$

The deflection at the end will be

$$\delta = (y)_{x=0} = \frac{1}{2\beta^3 EI}(P - \beta M_0) \tag{108}$$

By differentiating equation (107), the expression for the slope will be obtained. At the end ($x = 0$) this will become

$$\left(\frac{dy}{dx}\right)_{x=0} = -\frac{1}{2\beta^2 EI}(P - 2\beta M_0) \tag{109}$$

By using these equations in conjunction with the principle of superposition, more complicated problems can be solved.

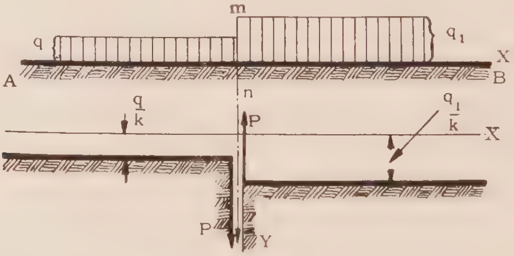

Fig. 151.

Example 65.—A prismatical bar AB of great length (Fig. 151) is supported by an elastic foundation. Determine the bending due to an abrupt change in the intensity of the uniformly distributed load.

Solution.—Imagine the bar cut into two parts by the cross-section mn. The displacement due to the compression of the foundation will become equal to q/k on the left of section mn, and q_1/k on the right. Now, in order to satisfy the condition of continuity of the deflection curve, forces P must be applied as shown in the figure. By using equation (108), in which, for our case, M_0 must be made equal to zero and observing that the sum of deflections produced by forces P must annihilate the difference in compression of foundation, the following equation for determining P will be obtained:

$$2 \cdot \frac{P}{2\beta^3 EI} = \frac{q_1}{k} - \frac{q}{k}.$$

Having determined the magnitude of P, the deflection curve can be obtained by combining the constant compression q_1/k (for the right side of the bar) and q/k (for the left side) with the deflection produced by forces P as given by equation (107).

In such manner we have:

$$y = \frac{q_1}{k} - \frac{P}{2\beta^3 EI} e^{-\beta x} \cos \beta x \qquad \text{for } x > 0$$

$$y = \frac{q}{k} + \frac{P}{2\beta^3 EI} e^{\beta x} \cos \beta x \qquad \text{for } x < 0$$

39. Stresses in Railroad Track.—The following method of analyzing stresses in rails is based upon the assumption that there is a continuous elastic support under the rail. This assumption is a good approximation* since the distance between the ties is small in comparison to the wave length L of the deflection curve given by equation (104). In order to obtain the magnitude k of the modulus of foundation, the load required to depress one tie† one unit must be divided by the tie spacing. Suppose for instance, that the tie is depressed .3 inch under a load of 10,000 pounds and that the tie spacing is 22 inches, then

$$k = \frac{10{,}000}{.3 \times 22} = 1{,}500 \text{ lbs. per sq. inch.}$$

Consider first the case of a single wheel load P, then, for maximum deflection and maximum bending moment, equations (105) and (106) can be used. The maximum stress due to the bending of the rail will be

$$p_{\max} = \frac{M_{\max}}{S} = \frac{P}{4\beta S} = \frac{P}{4S}\sqrt[4]{\frac{4EI}{k}} \qquad \text{(a)}$$

where S denotes the section modulus of the rail.

In order to compare stresses in rails the cross-sections of which are geometrically similar, equation (a) may be represented in the following form:

$$p_{\max} = \frac{P}{A} \cdot \frac{A\sqrt[4]{I}}{4S} \cdot \sqrt[4]{\frac{4E}{k}} \qquad (110)$$

---

* See author's paper on *Strength of Rails*—Transactions of the Institute of Way of Communications (1915), Petersburg, Russia.

† It is assumed that the tie is symmetrically loaded by two loads corresponding to the rail pressures.

in which A = area of the cross-section of the rail. Since the second factor on the right side of equation (110) remains constant for geometrically similar cross-sections and since the third factor does not depend on the dimensions of the rail, the maximum stress is therefore inversely proportional to the area of the cross-section, i.e., inversely proportional to the weight of the rail per unit length.

The maximum pressure $R_{\max}$ on a tie is obtained by multiplying the maximum depression by the tie spacing and by the modulus of foundation. By using equation (105),

$$R_{\max} = \frac{P\beta}{2k} \cdot l \cdot k = \frac{P\beta l}{2} = \frac{P}{2}\sqrt[4]{\frac{kl^4}{4EI}}$$

It is seen from this that the pressure on the tie depends principally on the tie spacing.

In the case where several loads act on the rail, the principle of superposition may be used; and for the purpose of illustrating the method of calculation a numerical example will be discussed. Consider a 100-lb. rail section with $I = 44$ in.^{4} and with such a tie spacing that $k = 1{,}500$ lbs. per sq. inch, then from equation (101),

$$\beta = \sqrt[4]{\frac{k}{4EI}} = \sqrt[4]{\frac{1{,}500}{4 \times 30 \times 10^6 \times 44}} = \frac{1}{43.3}\ \text{in.}^{-1}$$

and from equation (104),

$$L = \frac{2\pi}{\beta} = 272 \text{ in.}$$

Taking a system of four equal loads, 66 inches apart, and fixing the origin of coordinates at the point of contact of the first wheel, the values of βx for other wheels will be as given in Table A.

TABLE A.—FOR CALCULATING DEFLECTIONS AND BENDING MOMENTS IN THE RAIL

Loads.	1	2	3	4
βx = ...	0	1.52	3.05	4.57
ψ = ...	−1	.207	.051	− .008
ϕ = ...	1	.230	− .042	− .012

The corresponding values of functions ϕ and ψ (Eq. e, p. 136), taken from the numerical Table VI of the previous paragraph are also given. Now, superimposing the effects of all the loads acting on the rail, the bending moment under the first wheel will be

$$M_1 = \frac{P}{4\beta}(1 - .207 - .051 + .008) = .75\frac{P}{4\beta},$$

i.e., the bending moment is 25% less than that produced by a single load P.

For the point of contact of the second wheel,

$$M_2 = \frac{P}{4\beta}[1 - (2 \times .207) - .051] = .535\,\frac{P}{4\beta}.$$

The deflection at the point of contact of the first wheel will be

$$\delta_1 = \frac{P\beta}{2k}(1 + .230 - .042 - .012) = 1.18\frac{P\beta}{2k}.$$

In the same manner the deflections at other points can easily be obtained.

It is seen that this analysis is easily applied for determining the effect of a combination of loads having any arrangement and any spacing.

The analysis is based on the assumption that the rail support is capable of developing negative reactions. Since there is play between the rail and the spikes, there will be little resistance to the upward movement of the rail which will tend to increase the bending moment in the rail under the first and the last wheels.

Other elements enter into the problem and these may effect the accuracy of the analysis. Nevertheless, in general, the theory of the deflection of the rail, produced by static loading, is in good agreement with the experiments made.*

40. Deformation of a Cylindrical Tube Symmetrical about the Axis.—The analysis given for a bar on elastic foundation can be used also in considering the deformation of a circular tube symmetrical about the axis. Assume, for instance, that a circular tube is submitted to the action of forces acting in a radial direction and uniformly distributed around a circle mn (Fig. 152). Due to symmetry it is sufficient

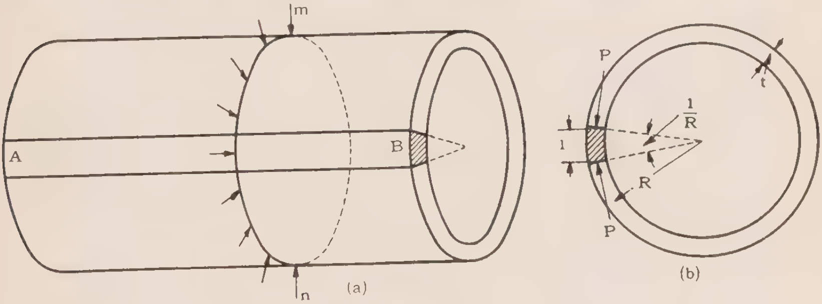

FIG. 152.

---

* See *Progress Report of the Special Committee on Stresses in Railroad Track.* Bulletin of the American Railway Engineering Association, March, 1918.

to consider only one longitudinal element AB of the tube, the width of the element being taken equal to unity. The forces mentioned above will produce deflection of the element AB in a radial direction. Let y denote the radial displacement at any cross-section of this element. The corresponding unit compression in a circumferential direction is y/R, where R denotes the middle radius of the tube. The compressive forces per unit length of the element AB will be (Fig. 152 (b)):

$$P = \frac{Ey}{R} \cdot t \tag{a}$$

where t = the thickness of the tube.

The resultant of the forces P, having a radial direction, is equal to

$$P \cdot \frac{1}{R} = \frac{Et}{R^2} \cdot y \tag{b}$$

This force, opposing the deflection of the element AB, is proportional to the deflection; therefore the conditions are the same as in the case of a bar supported on elastic foundation. From (b) it can be concluded that the modulus of foundation in this case is

$$k = \frac{Et}{R^2}.$$

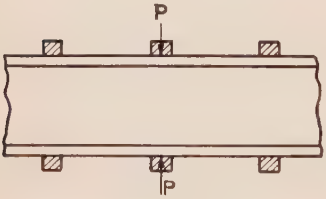

FIG. 153.

Consider, for instance, bending produced in a circular tube by shrinking reinforcing rings onto the tube (Fig. 153). Assuming that the width of the ring is very small, the equations obtained for a single concentrated load (page 136) can be used. Let P denote the compressive force acting on the tube per unit length of the circumference, then the deflection of the wall of the tube in a radial direction from equation (105) will be

$$\delta = \frac{P\beta}{2k} \tag{c}$$

in which

$$k = \frac{Et}{R^2}.$$

In calculating β it is necessary to take into consideration the fact that the cross-section of the longitudinal element AB will not be distorted during bending; therefore the extension and compression of the longitudinal fibres will not be accompanied by lateral contraction and expansion. In such cases,

$$\frac{E}{1-\frac{1}{m^2}}$$

instead of E must be used as explained in the consideration of pure bending (paragraph 14). Instead of (101), the following equation will be obtained:

$$\beta = \sqrt[4]{\frac{k\left(1-\frac{1}{m^2}\right)}{4EI}} = \sqrt[4]{\frac{3\left(1-\frac{1}{m^2}\right)}{R^2t^2}} \tag{111}$$

Therefore, from (c),

$$\delta = \frac{PR^2}{2Et}\sqrt[4]{\frac{3\left(1-\frac{1}{m^2}\right)}{R^2t^2}} = \frac{PR}{2Et}\sqrt{\frac{R}{t}}\sqrt[4]{3 \times .91} = .643\frac{P}{E}\left(\frac{R}{t}\right)^{3/2}.$$

The radial extension of the ring produced by the forces P is

$$\delta_1 = \frac{PR^2}{EA}$$

in which A = the area of the cross-section of the ring.

If Δ denotes the initial difference between the external radius of the tube and the internal radius of the ring the following equation for determining P will be obtained

$$\delta + \delta_1 = \Delta$$

or

$$.643\frac{P}{E}\left(\frac{R}{t}\right)^{3/2} + \frac{PR^2}{EA} = \Delta \tag{112}$$

Substituting P in equation (106) the maximum bending moment produced in the wall of the tube will be obtained. In this consideration it has been assumed that a single ring acts on the tube. If several rings are used, the bending in the tube and the corresponding stresses can easily be obtained by applying the principle of superposition explained in paragraph 39.

The same method can be applied also in those cases where a cylindrical tube with reinforcing rings is submitted to either a uniform internal or a uniform external hydrostatic pressure. For instance, in considering stresses in the hull of a submarine having a circular cross-section (Fig. 154), the pressure on the strengthening rings will be found

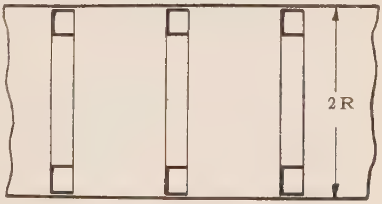

Fig. 154.

from the equation (112). It is necessary only to put $\Delta = \frac{qR^2}{Et}$, where q denotes the uniform hydrostatic pressure and t, the thickness of the wall. Taking, for instance, the strengthening rings as very rigid and neglecting in equation (112) the second term on the left side, we have

$$.643\frac{P}{E}\left(\frac{R}{t}\right)^{3/2} = \frac{qR^2}{Et},$$

or

$$P = \frac{1}{.643}q\sqrt{Rt}.$$

The corresponding maximum bending stress will be

$$p_{\max} = \left(\frac{6M}{t^2}\right)_{\max} = \frac{6P}{4\beta t^2} = \frac{3}{2} \times \frac{1}{.643}q\sqrt{Rt}\frac{1}{t^2}\sqrt[4]{\frac{R^2t^2}{3\left(1 - \frac{1}{m^2}\right)}} = \frac{1.82qR}{t},$$

i.e., the maximum bending stress is 82% higher than the uniform compressive stress $\frac{qR}{t}$ produced in a cylindrical tube without reinforcing rings.*

The problem on the shrink fit pressure between the shaft and the hub, when the latter consists of two parts of different thicknesses, also can be solved by using the theory of bending of a bar on elastic foundation. It is necessary only to divide the hub into two cylindrical parts of different thicknesses and find out the pressures and the compressions of the shaft for both these parts separately. Afterwards, on the section of the hub separating these two parts, shearing forces and moments must be applied so as to satisfy the condition of continuity. See Example (65) page 140.

41. Thermal Stresses in Hollow Cylinders Due to Non-uniform Heating along the Axis of the Cylinder.—The problem of the distribution of thermal stresses in cylindrical shells is of practical interest when applied to the design of turbines, Diesel engine cylinders, and many other similar structures. For calculating these stresses, the temperature distribution in the cylinder wall must be known. The few experimental investigations which have been made in this direction indicate that both the temperature gradient lengthwise of the cylinder and the temperature gradient in a radial direction should be considered. The effect of the temperature gradient in an axial direction will here be discussed.

---

* For a detailed consideration of this problem, see K. v. Sanden's paper: *Ueber das Festigkeitsproblem querversteifter Hohlzylinder unter allseitig gleichmässigem Aussendruck*, in *Werft and Reederei*, p. 189, 1920. Also a bibliography on the subject is given there.

If the temperature distribution is symmetrical relative to the axis, a symmetrical distribution of stress is also obtained, and in calculating these stresses it is, as before, only necessary to consider an elementary strip AB of unit breadth cut from the cylinder wall (Fig. 152). Let T_0 denote the initial uniform temperature of the cylinder and T the temperature after heating, which is constant in both radial and circumferential directions, but is variable along the axis of the cylinder. As before, let y denote the radial displacement, p_θ the compressive stress in the wall in a circumferential direction and α the coefficient of linear expansion. Then the unit compression in a circumferential direction will be the elastic compression minus the thermal expansion,

$$e_\theta = \frac{y}{R} = \frac{p_\theta}{E} - \alpha(T - T_0)$$

from which

$$p_\theta = \frac{yE}{R} + \alpha E(T - T_0).$$

In a circumferential direction, the compressive force per unit length of the longitudinal element will be

$$tp_\theta = \frac{yEt}{R} + \alpha Et(T - T_0).$$

The corresponding radial reaction opposing the deflection of the element AB is

$$tp_\theta\frac{1}{R} = \frac{yEt}{R^2} + \frac{\alpha Et}{R}(T - T_0).$$

The right hand side of the equation represents the distributed forces acting on the element AB, $\alpha Et/R(T - T_0)$ being equivalent to q in equation (99). Therefore, the differential equation for this case will be the same as for a beam supported on a continuous elastic foundation and loaded by a distributed loading of intensity $\alpha Et/R(T - T_0)$. In this way we obtain

$$\frac{EI}{1 - \frac{1}{m^2}}\frac{d^4y}{dx^4} = -\left[\frac{yEt}{R^2} + \frac{\alpha Et}{R}(T - T_0)\right]. \tag{113}$$

On the particular solution of this equation the general solution of the homogeneous differential equation

$$\frac{EI}{1 - \frac{1}{m^2}}\frac{d^4y}{dx^4} = -\frac{Ety}{R^2} \tag{114}$$

must be superimposed and the constants of integration determined in such a manner as to satisfy the conditions at the ends of the cylinder.

The following simple case will now be considered. The part of the cylinder on the right side of the cross-section *mn* (Fig. 155) is maintained at constant temperature (T_0), while on the left side there is a linear decrease in temperature as represented by the equation (notations shown in Fig. 155).

$$T = T_0 - \frac{(T_0 - T_1)x}{a}$$

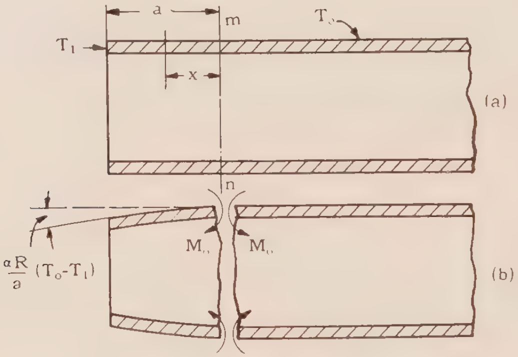

FIG. 155.

For this case the particular solution of equation (113) page 147, will be

$$y = \frac{\alpha R(T_0 - T_1)x}{a}.$$

If we consider only this particular solution, we obtain the displacements shown in Fig. 155 (b), which gives a case equivalent to that of two abutting bars on an elastic foundation but out of line by an angle

$$\frac{\alpha R(T_0 - T_1)}{a}.$$

This particular solution represents the condition of the cylinder if no bending forces act on a longitudinal element. The general solution of equation (114) represents the effect of the bending moment and must be superimposed on the particular solution in such a way as to satisfy the condition of continuity at the section *mn* and the conditions at the ends of the cylinder.

To simplify the problem, assume first that the cross-section *mn* is far enough from the ends so that the equations for an infinitely long bar can be used with good approximation. Then, the general solution merely represents a bending moment sufficient to rotate each of the ends through an angle

$$\frac{\alpha R(T_0 - T_1)}{2a},$$

thus satisfying the condition of continuity of the bar. Using equation (109) page 140 and putting

$$\frac{E}{1 - \frac{1}{m^2}}$$

instead of E it follows:

$$\frac{M_0\left(1 - \frac{1}{m^2}\right)}{\beta EI} = \frac{\alpha R(T_0 - T_1)}{2a},$$

$$p_{\max} = \frac{6M_0}{t^2} = \frac{3\alpha R\beta EI}{t^2\left(1 - \frac{1}{m^2}\right)a}(T_0 - T_1),$$

or putting $I = t^3/12$,

$$\beta = \sqrt[4]{\frac{3\left(1 - \frac{1}{m^2}\right)}{R^2t^2}}, \qquad \text{See Equation (111)}$$

$$p_{\max} = \frac{tE}{4\left(1 - \frac{1}{m^2}\right)}\sqrt[4]{\frac{3\left(1 - \frac{1}{m^2}\right)}{R^2t^2}}\,\frac{\alpha R}{a}(T_0 - T_1).$$

Assuming that $1/m^2 = .09$,

$$p_{\max} = .353\frac{E\alpha}{a}\sqrt{Rt}(T_0 - T_1).$$

For a numerical example, take a cast iron cylinder having the following dimensions: $R = 9\frac{11}{16}$ in., $t = 1\frac{3}{8}$ in., $a = 4\frac{1}{4}$ in., $\alpha = 101 \times 10^{-7}$, $E = 14 \times 10^6$ lbs. per sq. inch., $T_0 - T_1 = 180$°C.

This gives

$$p_{\max} = 7{,}720 \text{ lbs. per sq. inch.}$$

Now consider the error due to the assumption that the distance a is large.

From the equation (107) page 140 it follows that the deflection produced by the moment M_0 (Fig. 155) to the left of mn is*

$$y = \frac{M_0\left(1 - \frac{1}{m^2}\right)}{2\beta^2 EI} e^{-\beta x} (\cos \beta x - \sin \beta x).$$

By successive differentiation we have

$$\frac{dy}{dx} = -\frac{M_0\left(1 - \frac{1}{m^2}\right)}{\beta EI} e^{-\beta x} \cos \beta x,$$

$$\frac{d^2y}{dx^2} = \frac{M_0\left(1 - \frac{1}{m^2}\right)}{EI} e^{-\beta x} (\cos \beta x + \sin \beta x),$$

and

$$\frac{d^3y}{dx^3} = -\frac{2M_0\beta\left(1 - \frac{1}{m^2}\right)}{EI} e^{-\beta x} \sin \beta x.$$

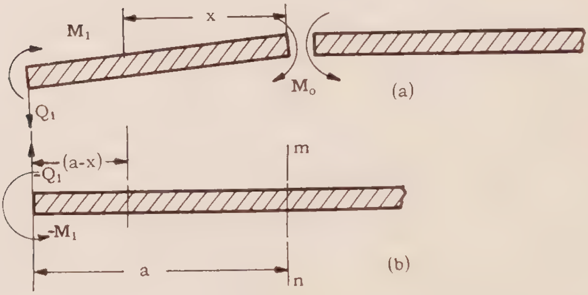

FIG. 156.

The bending moment and shearing force produced by M_0 at distance x from mn (Fig. 155) will be

$$M = -\frac{EI}{1 - \frac{1}{m^2}} \frac{d^2y}{dx^2} = -M_0 e^{-\beta x} (\cos \beta x + \sin \beta x),$$

$$Q = -\frac{EI}{1 - \frac{1}{m^2}} \frac{d^3y}{dx^3} = 2M_0 \beta e^{-\beta x} \sin \beta x,$$

---

* The sign is changed in accordance with the change of the direction of the moment.

or, by using notations of the paragraph 38, page 136 (equation e), and Table VI,

$$M = -M_0\phi,$$
$$Q = M_0\beta(\phi + \psi).$$

The bending moment M_1 and the shearing force Q_1 at the end of the cylinder will be

$$M_1 = -M_0(\phi)_{x=a} \tag{a}$$
$$Q_1 = M_0\beta(\phi + \psi)_{x=a}. \tag{b}$$

The couple M_1 and the shearing force Q_1 are shown in Fig. 156 (a).

In order to obtain the end of the cylinder free from stresses, the forces $(-Q_1, -M_1)$ shown in Fig. 156 (b) must be superimposed on forces shown in Fig. 156 (a). The deflection produced by the forces of Fig. 156 (b), by using equation (107) page 140, is

$$y = \frac{e^{-\beta(a-x)}\left(1 - \frac{1}{m^2}\right)}{2\beta^3 EI}\left\{-Q_1 \cos\beta(a - x) + \beta M_1\left[(\cos\beta(x - a) - \sin\beta(x - a)\right]\right\}.$$

The corresponding bending moment will be

$$M = \frac{Q_1}{\beta}e^{-\beta(a-x)}\sin\beta(a - x) - M_1 e^{-\beta(a-x)}\left[\cos\beta(a - x) + \sin\beta(a - x)\right],$$

or by using notation of paragraph 38, equation (e),

$$M = \frac{Q_1}{2\beta}(\phi + \psi)_{a-x} - M_1(\phi)_{a-x}.$$

At the cross-section mn this expression becomes,

$$M = \frac{Q_1}{2\beta}(\phi + \psi)_{x=a} - M_1(\phi)_{x=a},$$

or, using (a) and (b),

$$M = \frac{M_0}{2}(\phi + \psi)^2_{x=a} + M_0(\phi)^2_{x=a}. \tag{c}$$

This gives the correction necessary to be applied to the bending moment obtained above, on the assumption that the distance a is very large.

Taking the numerical example considered above,

$$\beta = \sqrt[4]{\frac{3\left(1 - \frac{1}{m^2}\right)}{R^2t^2}} = \frac{1.285}{\sqrt{Rt}} = \frac{1}{2.84}\ (\text{in.})^{-1}$$

Therefore,

$$\beta a = \frac{4.25}{2.84} = 1.50.$$

Now from the numerical Table VI of paragraph 38 (page 138),

$$\phi(1.50) = .238,$$
$$\psi(1.50) = .207.$$

The correction given by (c) will therefore become

$$M = \frac{M_0}{2}(.238 + .207)^2 + M_0(.238)^2 = .156M_0 \qquad \text{(d)}$$

Due to the fact that in this consideration the bending moment was considered as positive when the corresponding curvature was convex towards the axis of the cylinder, the correction (d) obtained above must be subtracted from the moment M_0 obtained on the assumption that a is very large. Therefore, the maximum bending moment calculated above must be diminished in the ratio

$1 - .156 = .844$, i.e., $p_{\text{Max}} = 7{,}720 \times .844 = 6{,}510$ lbs. per sq. inch.

From this it will be seen that the correction necessary to establish the conditions of free ends is about 16% for the case considered, a value which is by no means negligible. Furthermore it should be noted that the method developed above can be used also for those cases where the conditions existing at the ends of the cylinder are other than in the example considered.

CHAPTER VII

DIRECT AND BENDING STRESSES

42. Eccentric Longitudinal Loads.—*Case of a Short Strut.*—Assume that a prismatical bar AB is submitted to the action of a compressive force S (Fig. 157 (a)) the line of action of which is parallel to the axis of the bar and intersects a principal axis Y of the cross-section at a distance e from the centroid of the section. Bending will then take place in the XY plane. If the strut is short, the deflection due to this bending can be neglected in comparison with the eccentricity e, and it can be assumed that the bending moment along the bar is constant and equal to Se. The intensity of the compressive stress at any point in a cross-section will be the algebraic sum of the uniform stress S/A and of the stress Sey/I produced by the bending, i.e.,

$$p = \frac{S}{A} + \frac{Sey}{I}.$$

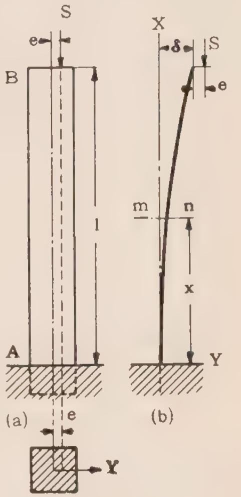

FIG. 157.—Eccentric longitudinal load.

The deflection at the end will be obtained by using the grapho-analytical method (Example 43, page 88) as follows:

$$\delta = \frac{Sel^2}{2EI} \qquad (115)$$

Case of a Long Strut.

Let

e = eccentricity

i = radius of gyration

S = longitudinal force

$k^2 = \dfrac{S}{EI}$

S_{cr} = critical load

$\alpha^2 = \dfrac{S}{S_{cr}}$

$p_{cr} = \frac{S_{cr}}{A}$ = critical compressive stress

$u = \frac{l}{2}\sqrt{\frac{S}{EI}}$

βl = reduced length

β = reduction coefficient

T = work done by external forces during deformation

If the strut is not short, deflections of the central axis can no longer be neglected in comparison with e; and the bending moment varies along the axis of the strut. The maximum stress will depend not only on the eccentricity e of the load but also on the deflection δ of the strut. The bending moment at any cross-section mn (Fig. 157 (b)) of the strut after bending will be $S(\delta + e - y)$, and the equation of the deflection curve can be written:

$$EI\frac{d^2y}{dx^2} = S(\delta + e - y). \tag{a}$$

If we denote

$$\frac{S}{EI} = k^2, \tag{116}$$

the general solution of (a) will be obtained in the following form:

$$y = C_1 \sin kx + C_2 \cos kx + \delta + e \tag{b}$$

From the conditions at the built in end it follows: $(y)_{x=0} = 0$

$$\left(\frac{dy}{dx}\right)_{x=0} = 0$$

Therefore, the arbitrary constants in (b) will be

$$C_1 = 0,\ C_2 = -(\delta + e);$$

and the equation of the deflection curve becomes

$$y = (\delta + e)(1 - \cos kx). \tag{c}$$

At the end B the deflection is equal to δ; therefore, from (c),

$$\delta = (\delta + e)(1 - \cos kl),$$

or

$$\delta = \frac{e(1 - \cos kl)}{\cos kl}. \tag{117}$$

Substituting in (c),

$$y = \frac{e(1 - \cos kx)}{\cos kl} \tag{118}$$

It is easy to see that the deflection δ is no longer a linear function of S and, with increase of load, will not increase in the same proportion.

In the case of a short strut the quantity kl is small and it is sufficiently accurate to assume that

$$\cos kl = 1 - \frac{k^2l^2}{2}$$

Therefore, in this case, equation (117) gives

$$\delta = \frac{ek^2l^2}{2\left(1 - \frac{k^2l^2}{2}\right)} = \frac{eSl^2}{2EI\left(1 - \frac{k^2l^2}{2}\right)}.$$

Neglecting the small quantity $k^2l^2/2$ in the denominator, the equation above will reduce to that for a short strut equation (115) previously discussed.

With increase in the load S, k increases; therefore the deflection also increases, but more rapidly than S. A series of values of this deflection are given in Table VII. It is seen from the table that deflections increase very rapidly if the quantity kl approaches the value $\pi/2$. When $kl = \pi/2$, we have

$$S = EIk^2 = \frac{EI\pi^2}{4l^2}, \tag{119}$$

and the deflection equation (117) becomes, theoretically speaking, infinitely large. This means that a compressive force of such a magnitude will produce a large deflection and that deformations beyond the elastic limit may be expected. This magnitude of the load is called the *critical load*, and will be denoted by S_{cr}.

TABLE VII.—DEFLECTIONS PRODUCED BY AN ECCENTRIC LONGITUDINAL LOAD

$kl =$	.1	.5	1.0	1.5	$\frac{1}{2}\pi$
$\delta =$	$.005e$	$.139e$	$.851e$	$13.1e$	∞
Approx. $\delta =$	$.005e$	$.139e$	$.840e$	$12.8e$	∞
$\sec kl =$	1.005	1.140	1.867	13.2	∞

The deflection δ depends principally on the magnitude of the ratio $S:S_{cr}$ and can be represented with a good approximation in the following form:

$$\delta = \frac{Sel^2}{2EI} \cdot \frac{1}{1 - \frac{S}{S_{cr}}}.$$

The first factor on the right side represents the deflection calculated from the cantilever formula (115), i.e., neglecting the effect of deflections on the magnitude of the bending moment. The second factor is due to the effect of the deflection on the bending moment.

Denoting

$$\delta_0 = \frac{Sel^2}{2EI} \quad \text{and} \quad \alpha^2 = \frac{S}{S_{cr}} \tag{120}$$

we have

$$\delta = \frac{\delta_0}{1 - \alpha^2}. \tag{121}$$

Some numerical results obtained from this equation are given in the third line of Table VII. It is seen that the approximate equation (121) gives sufficient accuracy and can be used in practical applications.

The maximum bending moment during bending of the strut will be at the built-in end and can be represented as follows:

$$M_{\max} = S(e + \delta) = S\left(e + \frac{e(1 - \cos kl)}{\cos kl}\right) = Se \cdot \sec kl \tag{122}$$

A series of values of sec kl is given in the Table VII. It is seen that $M_{\max}$ increases without limit when S approaches S_{cr}.

43. Struts with Lateral Loads.—*General.*—When a prismatic bar is subjected to the action of axial and transverse forces, the stress intensity at any cross-section will be the algebraic sum of the direct tensile or compressive stress and the direct stress produced by bending. The latter stresses are the algebraic sum of the bending stress produced by the lateral forces and those produced by the longitudinal forces. The bending moments due to the longitudinal forces depend on the deflections; therefore the complete solution of the problem can only be obtained from the consideration of the deflection curve of the bar. Some simple problems of this kind will now be considered.*

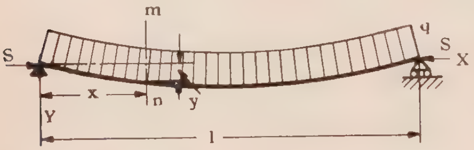

FIG. 158.—Strut with uniformly distributed lateral load.

Strut with Uniformly Distributed Lateral Load.—It is seen from Fig. 158 that for a strut having a uniform lateral load, the bending moment at any cross-section mn is

$$M = ql\frac{x}{2} - q\frac{x^2}{2} + Sy.$$

The differential equation of the deflection curve will be

$$EI\frac{d^2y}{dx^2} = -q\frac{l}{2}x + q\frac{x^2}{2} - Sy. \tag{a}$$

---

* Several problems of this kind were considered by A. P. Van der Fleet, *Bulletin of the Society of Engineers of Ways of Communication*, 1900–1903 (Petersburg). See also paper by A. Morley, *Phil. Mag.*, June, 1908.

Using the notation in equation (116),

$$\frac{S}{EI} = k^2. \tag{b}$$

A general solution of (a) will be

$$y = A \sin kx + B \cos kx + \frac{1}{S}\left(-q\frac{lx}{2} + q\frac{x^2}{2}\right) - \frac{qEI}{S^2}. \tag{c}$$

From the conditions at the ends,

$$(y)_{x=0} = 0 \text{ and } (y)_{x=l} = 0.$$

We have

$$A = \frac{qEI}{S^2} \cdot \frac{1 - \cos kl}{\sin kl} \quad \text{and} \quad B = \frac{qEI}{S^2}.$$

Substituting in (c),

$$y = \frac{qEI}{S^2} \cdot \frac{1 - \cos kl}{\sin kl} \cdot \sin kx - \frac{qEI}{S^2}(1 - \cos kx) - \frac{qx}{2S}(l - x) \tag{d}$$

By using the notation

$$\frac{kl}{2} = \frac{l}{2}\sqrt{\frac{S}{EI}} = u, \tag{123}$$

equation (d) of the deflection curve can be represented in the following form:

$$y = \frac{qEI}{S^2}\left[\frac{\cos\left(1 - \frac{2x}{l}\right)u}{\cos u} - 1\right] - \frac{qx}{2S}(l - x). \tag{e}$$

By putting $x = l/2$, the deflection at the middle will be:

$$\delta = (y)_{x=\frac{l}{2}} = \frac{qEI}{S^2}\left(\frac{1}{\cos u} - 1 - \frac{l^2S}{8EI}\right)$$

or, by using notation (b),

$$\delta = \frac{q}{Sk^2}\left(\sec u - 1 - \frac{1}{2}u^2\right). \tag{f}$$

In order to compare this deflection with the known deflection produced by transverse forces alone, equation (f) can be represented in the following form:

$$\delta = \frac{5}{384}\frac{ql^4}{EI}\frac{\sec u - 1 - \frac{1}{2}u^2}{\frac{5}{24}u^4}. \tag{124}$$

The trigonometrical factor on the right side of (124) represents the effect of the longitudinal compression on the deflection produced by the transverse loading alone. The magnitude of this factor depends on the magnitude of u. If u is a very small quantity, it can be assumed that

$$\sec u = 1 + \tfrac{1}{2}u^2 + \tfrac{5}{24}u^4.$$

Substituting in (124), the trigonometrical factor becomes equal to unity and the known equation for the deflection produced by lateral forces alone will be obtained. Another extreme case will be obtained when u approaches the value $\pi/2$. The compressive force as seen from equation (123) p. 157 approaches the critical value given by

$$S_{cr} = \frac{EI\pi^2}{l^2}. \tag{125}$$

In this case the trigonometrical factor in equation (124) becomes infinitely large. Here large deflections and deformations beyond the elastic limit will be produced by a very small lateral loading. This case will be discussed later in considering column theories. In design problems the approximate equation (121) can be used for calculating the maximum deflection at the middle, instead of the exact solution (124). In using eq. 121 as before, δ_0 denotes the deflection produced by the lateral loading only and $\alpha^2 = S/S_{cr}$, where S_{cr} is now determined by the equation (125). If α^2 is a small quantity, the effect of the longitudinal force on the deflection will be small and can be neglected.

The magnitude of the bending moment at any cross-section will be obtained by substituting the expression (e) for the deflection curve in the known equation $M = -EId^2y/dx^2$. Performing the differentiation, the bending moment at the middle becomes

$$M_{\max} = -EI\left(\frac{d^2y}{dx^2}\right)_{x=l/2} = \frac{EIq}{S}\,\frac{1-\cos u}{\cos u},$$

or by using equation (123) p. 157,

$$M_{\max} = \frac{ql^2}{8}\,\frac{2(1-\cos u)}{u^2\cos u}. \tag{126}$$

If the approximate equation (121) for the deflection at the middle be used, the following approximate expression for the maximum bending moment will be obtained:

$$M_{\max} = \frac{ql^2}{8} + S\delta = \frac{ql^2}{8} + \frac{S\delta_0}{1-\alpha^2} = \frac{ql^2}{8}\left(1 + \frac{1.028\alpha^2}{1-\alpha^2}\right). \tag{127}$$

This equation always gives sufficient accuracy for practical applications.

Strut with Uniform Lateral Load and with Built-in Ends.—If the ends of the strut are built-in, the deflection curve can be obtained in the same manner as in the previous case. It will now have the following form:

$$y = \frac{q}{Sk^2}\,\frac{u}{\tan u}\left(\frac{\cos u\left(1-\frac{2x}{l}\right)}{\cos u} - 1\right) - \frac{q}{2S}\,x(l-x). \tag{128}$$

The deflection at the middle will be

$$\delta = (y)_{x=l/2} = \frac{q}{Sk^2}\,\frac{u(1 - \cos u)}{\sin u} - \frac{ql^2}{8S},$$

or

$$\delta = \frac{ql^4}{384EI}\,\frac{24}{u^4}\left(\frac{u(1 - \cos u)}{\sin u} - \frac{1}{2}\,u^2\right) \tag{129}$$

Here, again, the first factor represents the deflection produced by lateral loading alone. It is seen that the deflection (129) increases very quickly when u approaches the value π. The compressive force S will then approach its critical value

$$S_{cr} = \frac{4EI\pi^2}{l^2}. \tag{130}$$

The bending moments at the built-in ends will be

$$M_a = M_b = -\frac{ql^2}{12}\,\frac{\tan u - u}{\frac{1}{3}\,u^2 \tan u} \tag{131}$$

For the middle we have

$$(M)_{x=l/2} = \frac{ql^2}{24}\,\frac{6\left(\frac{u}{\sin u} - 1\right)}{u^2}. \tag{132}$$

The first factor in these equations represents the known bending moments produced by lateral loading acting alone.

44. Tie-rod with Lateral Loading.—The analysis considered in the previous paragraph can also be used in the case of tensile longitudinal forces S; it is only necessary to change the sign of S and therefore to put, as seen from equation (123), $u\sqrt{-1} = ui$ instead of u in all formulae previously obtained. Remembering that

$$\sin xi = i \sinh x \quad \text{and} \quad \cos xi = \cosh x,$$

where $\sinh x$ and $\cosh x$ denote hyperbolic functions,* the following equations for a tie-rod with a uniform lateral load can be obtained from the equations of the previous paragraph:

In the case of simply supported ends the deflection at the middle, from equation 124, will be

$$\delta = \frac{5}{384}\,\frac{ql^4}{EI}\,\phi_1(u) \tag{133}$$

where function $\phi_1(u)$ is

$$\phi_1(u) = \frac{\operatorname{sech} u - 1 + \frac{1}{2}u^2}{\frac{5}{24}u^4}$$

---

* For complete tables of these functions see, W. Ligowski, *Tafeln der Hyperbelfunctionen* (Berlin), also the book of the same author, "Taschenbuch der Mathematik, 1893.

The maximum bending moment, at the middle, from equation (126) becomes

$$M_{\max} = \frac{ql^2}{8}\psi_1(u) \tag{134}$$

where function $\psi_1(u)$ is

$$\psi_1(u) = \frac{2(\cosh u - 1)}{u^2 \cosh u}$$

In the case of built-in ends, the deflection at the middle, from equation (129), will be

$$\delta = \frac{ql^4}{384EI}\phi_2(u) \tag{135}$$

where

$$\phi_2(u) = \frac{24}{u^4}\left(\frac{u(1 - \cosh u)}{\sinh u} + \frac{1}{2}u^2\right).$$

Also, the bending moments at the ends will become, from equation (131),

$$M_a = M_b = -\frac{ql^2}{12}\psi_2(u) \tag{136}$$

where

$$\psi_2(u) = \frac{3}{u^2}\,\frac{u - \tanh u}{\tanh u}.$$

The bending moment at the middle, from equation (132),

$$(M)_{x=l/2} = \frac{ql^2}{24}\psi_3(u) \tag{137}$$

where

$$\psi_3(u) = \frac{6}{u^2}\left(1 - \frac{u}{\sinh u}\right).$$

In order to simplify calculations of deflections and of bending moments in the case of a laterally loaded tie-rod some numerical values of functions ϕ_1, ϕ_2, ψ_1, ψ_2, and ψ_3 are given in Table VIII.

All these functions are equal to unity at $u = 0$, i.e., when only a transverse loading is acting. With increase in the longitudinal tensile force these functions decrease, i.e., the longitudinal tensile forces diminish the deflection and the maximum bending moments in the laterally loaded tie-rods.

Some applications of the values in Table VIII will be given later when the bending of thin plates (see page 260), is considered.

TABLE VIII.—DEFLECTIONS AND MAXIMUM BENDING MOMENT CONSTANTS IN LATERALLY LOADED TIE-RODS

u	ϕ_1	ϕ_2	ψ_1	ψ_2	ψ_3	u	ϕ_1	ϕ_2	ψ_1	ψ_2	ψ_3
0	1.000	1.000	1.000	1.000	1.000	6.5	.054	.197	.047	.391	.139
.5	.908	.976	.905	.984	.972	7.0	.047	.175	.041	.367	.121
1.0	.711	.909	.704	.939	.894	7.5	.041	.156	.036	.347	.106
1.5	.532	.817	.511	.876	.788	8.0	.036	.141	.031	.328	.093
2.0	.380	.715	.367	.806	.673	8.5	.032	.127	.028	.311	.083
2.5	.281	.617	.268	.736	.563	9.0	.029	.115	.025	.296	.074
3.0	.213	.529	.200	.672	.467	9.5	.026	.105	.022	.283	.066
3.5	.166	.453	.153	.614	.386	10.0	.024	.096	.020	.270	.060
4.0	.132	.388	.120	.563	.320	10.5	.021	.088	.018	.259	.054
4.5	.107	.335	.097	.519	.267	11.0	.020	.081	.017	.248	.050
5.0	.088	.291	.079	.480	.224	11.5	.018	.075	.015	.238	.045
5.5	.074	.254	.066	.446	.189	12.0	.016	.069	.014	.229	.042
6.0	.063	.223	.055	.417	.162						

45. Application of Trigonometrical Series.*—Problems on bending of struts and tie-rods with lateral loads can be solved by using the expression of the deflection curve in the form of a trigonometrical series.

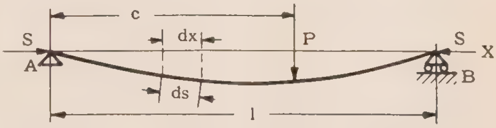

FIG. 159.—Compressed member with single lateral force.

In the case of a strut with simply supported ends the deflection curve can be represented in the following form (page 129):

$$y = a_1 \sin \frac{\pi x}{l} + a_2 \sin \frac{2\pi x}{l} + a_3 \sin \frac{3\pi x}{l} + \cdots \qquad \text{(a)}$$

It was shown (see Eq. 96, p. 130) that the potential energy of bending in this case will be:

$$U = \frac{EI\pi^4}{4l^3} \sum_{n=1}^{\infty} n^4 a_n^2 \qquad \text{(b)}$$

The coefficients a_1, a_2, a_3, . . . in (a) will be found by using *the principle of virtual displacements.* The increase of the potential energy of deformation of the strut during any small displacement from the position of equilibrium must be equal to the work done by external forces during this displacement. Assume, for instance, that any coefficient a_n in (a) undergoes a small increase da_n. This means that the deflection curve (a) obtains an additional deflection

---

* See author's paper, Application of General Coordinates in Solution of Problems on Bending of Bars and Plates, *Bulletin of the Polytechnical Institute in Kiev*, 1908 (Russian). See also author's paper in *Annales des Travaux Publics de Belgique*, p. 263, 1914. The same problem: see H. M. Westergaard, *Proc.* of Amer. Soc. Civ. Eng., vol. 47, pp. 455–533.

$$dy = da_n \sin \frac{n\pi x}{l}. \tag{c}$$

The corresponding increase of the potential energy will be, from (b),

$$\frac{\partial U}{\partial a_n} da_n = \frac{EI\pi^4}{2l^3} n^4 a_n da_n. \tag{d}$$

The displacement of the point of application of the force P corresponding to this deflection, from (c), is $(dy)_{x=c} = da_n \sin n\pi c/l$, and the corresponding work of P will be $Pda_n \sin n\pi c/l$. (e)

In order to find out the work done by the longitudinal forces S during the displacement (c), the difference λ between the length of the curved central line of the strut and the distance AB between the centers of the supports A and B will now be considered. In the case of a rather flat curve the difference between the length of any element ds and the corresponding projection dx can be taken as follows:

$$ds - dx = \frac{1}{2}\left(\frac{dy}{dx}\right)^2 dx.$$

Therefore,

$$\lambda = \frac{1}{2}\int_0^l \left(\frac{dy}{dx}\right)^2 dx. \tag{138}$$

Substituting, from (a), the value of y and integrating we have

$$\lambda = \frac{\pi^2}{4l}\sum_{n=1}^{\infty} n^2 a_n^2.$$

The small variation of λ during the displacement (c) will be

$$\frac{\partial \lambda}{\partial a_n} da_n = \frac{\pi^2}{2l} n^2 a_n da_n$$

and the corresponding work of the longitudinal forces is

$$\frac{S\pi^2}{2l} n^2 a_n da_n. \tag{f}$$

Now in line with our previous statement, by using (d), (e), and (f), the equation for determining a_n will be

$$\frac{EI\pi^4}{2l^3} n^4 a_n da_n = Pda_n \sin \frac{n\pi c}{l} + \frac{S\pi^2}{2l} n^2 a_n da_n$$

from which

$$a_n = \frac{2Pl^3}{EI\pi^4} \cdot \frac{\sin \frac{n\pi c}{l}}{n^4 - n^2 \frac{Sl^2}{EI\pi^2}}.$$

Remembering that $EI\pi^2/l^2$ is the critical value of compressive force in the case of a strut with simply supported ends, and denoting as before $S/S_{cr} = \alpha^2$, we have

$$a_n = \frac{2Pl^3}{EI\pi^4} \cdot \frac{\sin \frac{n\pi c}{l}}{n^4 - \alpha^2 n^2}.$$

Substituting in (a),

$$y = \frac{2Pl^3}{EI\pi^4}\left(\frac{\sin \frac{\pi c}{l} \sin \frac{\pi x}{l}}{1 - \alpha^2} + \frac{\sin \frac{2\pi c}{l} \sin \frac{2\pi x}{l}}{2^4 - 2^2\alpha^2} + \cdots \right) \tag{139}$$

Comparing this with equation (97) page 131, obtained for the case of a lateral force P only, it is seen that due to the action of the longitudinal compressive forces S, the deflection of the strut will be increased. Due to the fact that the first term of equation (139) represents a good approximation, it can be concluded that the increase of the deflection produced by the longitudinal forces will be approximately in the ratio* $1 : (1 - \alpha^2)$. This conclusion will be obtained also in the case where several concentrated lateral loads having the same direction, or a lateral distributed load are acting on the strut. In these cases equation (121) can be used for calculating the maximum deflection. If this deflection is known, the bending moment produced by the longitudinal forces can easily be calculated.

If, instead of compression forces, longitudinal tensile forces S are acting, the same method of consideration as given above can be used. In order to obtain a general expression for the deflection curve, it is necessary only to change α^2 to $-\alpha^2$ in equation (139).

If several lateral forces of the same direction are acting on the tie, an approximate equation for calculating the maximum deflection will be

$$\delta = \frac{\delta_0}{1 + \alpha^2}. \tag{140}$$

In the case of longitudinal tensile forces, α^2 can be larger than unit; and the accuracy of the approximate equation (140) decreases with increase in α^2. Taking, for instance, a uniformly distributed lateral load, the error of (140) at $\alpha^2 = 1$ will be about .3% only. At $\alpha^2 = 2$, the error is .7%, and at $\alpha^2 = 10$ the error is 1.7%. In the case of built-in ends the approximate equation for calculating the deflection at the middle will be

---

* It was used above. (See Equation (121), p. 156.)

$$\delta = \frac{\delta_0}{1 \mp \frac{\alpha^2}{4}}. \tag{141}$$

In this case the minus and plus signs correspond to compression and tension respectively, and $\alpha^2 = Sl^2/EI\pi^2$.

The applications of these approximate equations will be shown later in considering the deflection of thin rectangular plates.

46. Column Theory.—*General.*—In considering the bending and compression of struts (paragraphs 42 and 43), the limiting values of the compressive force were obtained, beyond which sidewise buckling could occur. Euler* was the first to develop these critical values; and the results are of great importance in our consideration. They show that the critical load depends on the method of fastening the ends of the column. Below is given such relations for four distinct types of fastening:

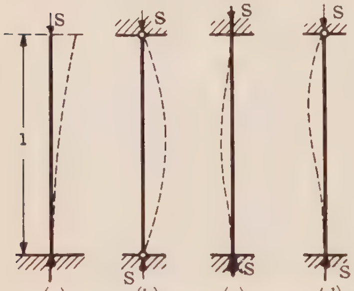

FIG. 160.—Columns with different end conditions.

1. Long Pillar (Fig. 160 (a)) having one end built in and another free:

$$S_{cr} = \frac{\pi^2 EI}{4l^2}. \tag{142}$$

2. Long Strut (Fig. 160 (b)) having both ends hinged, assumed frictionless:

$$S_{cr} = \frac{\pi^2 EI}{l^2}. \tag{143}$$

3. Strut (Fig. 160 (c)) having both ends built in:

$$S_{cr} = \frac{4\pi^2 EI}{l^2}. \tag{144}$$

4. Strut (Fig. 160 (d)) having one end built in and another on a frictionless hinge:

$$S_{cr} = \frac{2.047\pi^2 EI}{l^2}. \tag{145}$$

---

* *Histoire de l'Academie*, vol. 13, 1757 (Berlin).

From these equations the critical load can be determined for these conditions of loading. Experiment and theory show that, when the compressive force in the strut approaches the critical value,* as above, *buckling* of the strut begins and deflection increases so rapidly with the increase of load that the load equal to the critical value is usually sufficient to produce complete failure of the structure. It therefore follows that this critical load must be considered as the criterion of strength for columns and struts. It is seen from the equations above that this strength does not depend on the ultimate strength of the material but only on the dimensions of the structure and on the elastic property of the material. Furthermore, in the cases of long and thin bars a sidewise buckling may occur at the stresses far below the proportional limit of the material, and even below the stress considered as permissible for simple tension. Due to this fact the problem on the *sidewise buckling of compression members* and on *their elastic stability* becomes of great practical importance especially in modern steel structures where materials of high strength are used and where transverse dimensions of the members are likely to become small in comparison with the length. Some advanced theory of this subject will be developed later. (See Par. 47.) At present the simplest formulae given above for determining these critical loads will be discussed in more detail.

Limitation of the Use of Euler's Formulae.—The equations given above for determining the critical loads are of the form

$$S_{cr} = \frac{\pi^2 EI}{(\beta l)^2} \tag{a}$$

in which β denotes a numerical factor depending on the manner of fastening the ends of the strut.

Comparing (a) with equation (143) it is seen that the determination of the critical load for different manners of end fastening can be reduced to the determination of the critical load for a strut with hinged ends. It is only necessary to take, instead of the real length l, a *reduced length* βl, depending on the manner of fastening the ends. For cases represented in Fig. 160, the values of the *reduction coefficient* β are respectively: $\beta = 2$, $\beta = 1$, $\beta = .5$, $\beta = .699$. Some additional values of this coefficient will be given later.

Coming now to the *fundamental* case of a strut with hinged ends, the *critical compressive stress* will be, from equation (143),

$$p_{cr} = \frac{S_{cr}}{A} = \frac{\pi^2 E i^2}{l^2} \tag{146}$$

---

* Limitations of application of these equations will be discussed later.

where A denotes the area of the cross section and i, its radius of gyration. If the strut is free to deflect in all directions, buckling is likely to occur in that direction having the smallest *flexural rigidity;* so in equation (146) the smallest value for i must be substituted.

It is seen that for a given material the magnitude of p depends only on the ratio i/l, and the strength of the strut can be increased without changing its cross sectional area, only by increasing i/l. This can be accomplished by distributing the material as far as possible from the principal axes of the cross-section. This means that, for a compression member, tubular and built up sections (Fig. 161) are more economical than solid sections. By diminishing the thickness of such sections and increasing their transverse dimensions their stability can be increased without increasing the quantity of material, but there is a limit for the wall thickness, below which the section itself becomes unstable and, instead of a buckling of the strut as a whole, a corrugation of the wall of the tube may occur.[*]

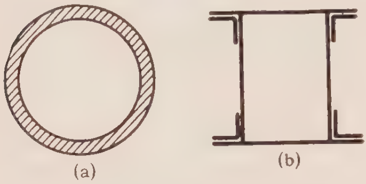

Tubular section

Built-up section

FIG. 161.

In developing equation (146) for the critical stress it was assumed that the material follows Hooke's law. It must be well understood, therefore, that this equation only gives satisfactory results in those cases where p_{cr}, calculated from the equation, is less than the limit of proportionality of the material. Beyond this limit, deformations increase more rapidly than the stresses and the true critical stress will be less than shown by equation (146). The limiting value of the ratio i/l, for which the Euler's formula can be used, depends on the magnitude of the proportional limit of the material. Taking, for instance, structural steel with $E = 30 \times 10^6$ lbs. per sq. in. and a proportional limit $p = 30{,}000$ lbs. per sq. in., then, from (146), $l/i = 100$. For $l/i > 100$, Euler's formulae give true values for critical stress. For $l/i < 100$, the values of p_{cr}, calculated from (146) will be greater than the true critical stress. It is clear that by using structural steel having a higher proportional limit the limits of applicability of Euler's formula can be enlarged. A graphical representation showing how p_{cr} varies with l/i is given for steel by the curve *CBD* in Fig. 162.

---

[*] This phenomenon is of a great practical interest for structural engineering but it can not be considered here in detail. Some data, important for rectangular tube design, will be given later. (See page 294.) The problem on the stability of compressed thin cylindrical tubes was considered by R. V. Southwell, See *Phil. Trans. Roy. Soc.*, Ser. A, Vol. 213, p. 187, 1913. See also author's papers: (1) Einige Stabilitäts Probleme der Elasticitätstheorie, *Z. f. Math. u. Phys.*, Vol. 58, p. 337, 1910; (2) *Bulletin of the Electr. Inst.* (Petersburg), Vol. XI, 1914.

Empirical Formulae.—Beyond the proportional limit Euler's formulae can not be applied and the true values of critical stress must be determined from experiments.* From a series of very elaborate experiments with solid struts having hinged-ends, Tetmayer showed† that for structural steel the critical stress in lbs. per sq. in. can be represented by a straight line formula (see Fig. 162) which can be approximately stated as follows:

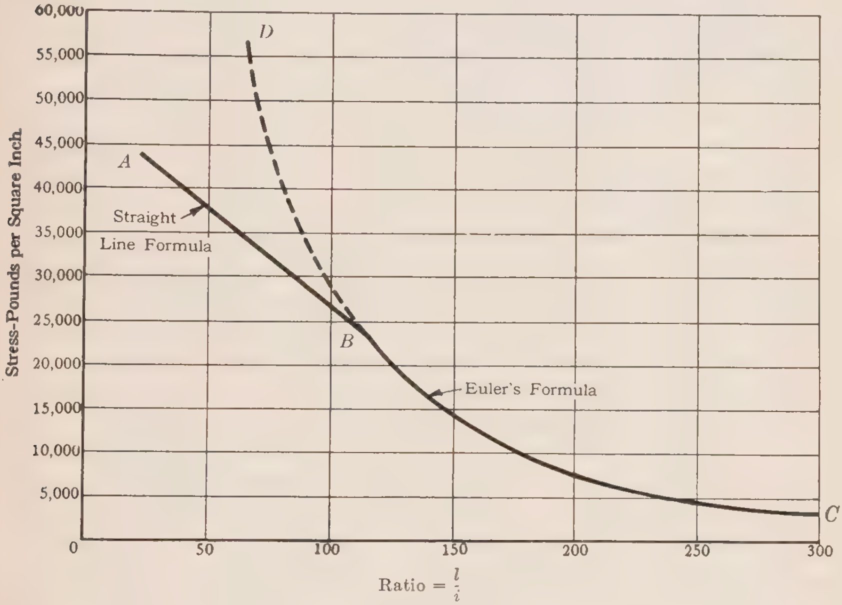

Fig. 162.—Curve representing variation of critical stress with $\frac{l}{i}$ for structural steel.

$$p_{cr} = 48{,}000 - 210\frac{l}{i} \qquad (147)$$

---

* For simplest cross-sections such as a rectangle, for instance, analysis can be used also in obtaining the critical stress beyond the elastic limit. In such cases the theory of bending of beams beyond the elastic limit must be used (Par. 14). Important work in this direction was done by Th. Kármán. See *Untersuchungen über Knickfestigkeit*, Dissertation, Göttingen, 1909.

† See Tetmayer's work, *Die Gesetze der Knikungs und Zusammengesetzten Druckfestigkeit*, 3d. Ed., 1903. See also an extensive analysis of experimental results made by J. M. Moncrieff, Proc. Amer. Soc. Civ. Eng. Vol. 45.

The straight line formula for mild steel, used in this country is*

$$p_{cr} = 52{,}500 - 220\frac{l}{i},$$

which does not differ much from Tetmayer's formula.

For cast iron, Tetmayer's experiments give,

$$p_{cr} = 110{,}000 - 1{,}700\frac{l}{i} + 7.5\left(\frac{l}{i}\right)^2 \tag{148}$$

Rankin Formula for Columns.—In this country and in England the Gordon-Rankin formula is used widely for determining the critical stress. This formula has the following form:

$$p_{cr} = \frac{p'}{1 + \gamma\left(\frac{l}{i}\right)^2} \tag{149}$$

in which p' denotes the critical stress for compression of short bars and γ a constant depending on the material. For solid bars of structural steel the following values for p' and γ are sometimes taken: $p' = 46,$ 000 lb. per sq. in. and $\gamma = 1/7{,}500$.

Choice of a Formula.—For structural steel, if the ratio l/i exceeds 110, Euler's formulae may be used to give critical stress and a factor of safety of about 4 may be used to determine the working stress. For shorter struts the straight line formula or Rankine formula may be used with factors of safety of about 4. Actual struts usually deviate from the conditions of the ideal cases of Fig. 160; and a choice of the proper factor of safety depends in large measure on the judgment and feeling of the engineer. Take, for instance, the question of fastening the ends. The ideal conditions of *fixed* and *hinged* ends are never completely fulfilled in an actual structure. It is difficult to approximate to a built in end because the ends of the strut are usually attached

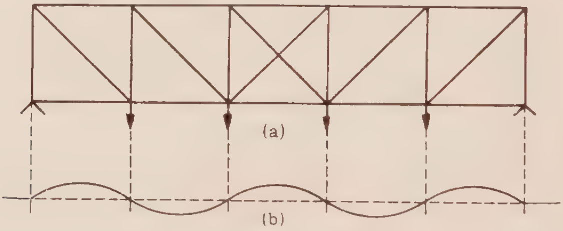

Fig. 163.—Buckled compressed chord.

---

* See "Applied Mechanics," by Fuller and Johnson, p. 361, 1919.

to more or less elastic parts of the structure and a small displacement at the ends may effect in large measure the magnitude of the critical load. The ends attached to a structure by some form of pin-joint will approximate more or less to the *hinged* condition. The same condition takes place in the upper chord compression members of a bridge (Fig. 163). The compressed chord may buckle in a wave curve shown in Fig. 163 (b), and in such cases points of inflection can be considered as ideal pins. It is otherwise with the compression members of a square frame (Fig. 164). It is easy to see that the horizontal bars of the frame will resist the buckling of the compressed members. The strength conditions of the strut for this case will be intermediate between the two ideal cases: *hinged* ends and *fixed* ends. Analysis made on the assumption that all members of the frame have the same section give for the critical load, in this case, $S_{cr} = 16.5EI/l^2$.

Another point to be noted is that the effect of the manner of fastening ends on the magnitude of the critical loads is high only in those cases where buckling may occur within elastic limit and therefore Euler's formula can be used. For comparatively short struts, where the straight line empirical formula is used for calculating critical loads, the difference in the critical load, due to the different manner of attachment, is not so great.

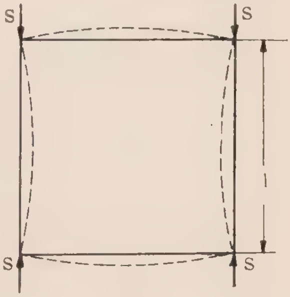

FIG. 164.—Buckled frame.

The column theory so far considered assumes compression of solid members of constant cross-section. More complicated problems on buckling of laticed members and of members of variable sections will be considered below, by using, for determining the critical loads, an approximate method based on the consideration of the energy of the system.

47. Energy Method.*—*General.*—The Euler's formulae given above were obtained by solving the corresponding differential equations of the deflection curve for a compression member. In the simplest cases this solution gives no difficulty, but there are many practically important problems where this equation becomes complicated, and it is not easy in such cases to obtain an exact value for the critical load. An approximate method is then valuable and the one described below can be used with sufficient accuracy. The method is based on the consideration of the elastic stability of the compression member. As a simpler example, a pillar built in at the bottom and free at the top (Fig. 160 (a)) will be considered. It is clear that the straight compressed form of equilibrium of the bar remains stable as long as the compressive force S is small; and if any lateral force be applied and a deflection, shown in the figure by the dotted line, be produced, this deflection will disappear as soon as the lateral force is removed. By gradually increasing the load S, a limit can be reached, when the straight form of equilibrium becomes *unstable* and a *lateral buckling* of the bar begins. This critical value of the load can be found by comparing the energy of the system for two cases: (1) when the bar is simply *compressed*, and (2) when it is *compressed and bent*. It is clear that if the bar is bent its potential energy of deformation is larger than that of the straight compressed form, because the energy U of bending must be added to the energy of compression. Another point which it is necessary to consider is that of the work done by the vertical load S during bending. It is easy to see that the deflection of the bar is accompanied by a lowering of the point of application of the load S; therefore this load produces some positive work T. Now, if this work T is less than the potential energy U of bending, the deflection of the bar is connected with an increase of energy; therefore it is necessary to apply some additional lateral force to produce bending. In such case the straight form of equilibrium is stable. On the other hand when $T > U$, the deflection of the bar will be accompanied by the diminishing of the energy of the system and the bending will proceed without application of any lateral force, i.e., the straight form of equilibrium is unstable. The critical value of the compressive force will be found from the equation,

---

* See author's papers "On the Stability of Elastic Systems," *Bulletin of the Polytechnical Inst. in Kiev*, 1910. Sur la Stabilité des Sistèmes Élastiques, *Annales des Ponts et Chaussées*, 1913 (Paris).

$$T = U \tag{150}$$

In order to obtain from this equation the magnitude of the critical load, expressions for T and U are necessary.

It follows from equation (c) page 154, that the deflection curve of the bar, when under the action of a central compressive force equal to the critical load ($k = \pi/2l$), is,

$$y = \delta\left(1 - \cos\frac{\pi x}{2l}\right) \tag{a}$$

Substituting (a) in the equation for the potential energy of bending (Eq. 95, p. 130), the following will be obtained:

$$U = \frac{1}{2}EI\int_0^l \left(\frac{d^2y}{dx^2}\right)^2 dx = \frac{\delta^2\pi^4}{64l^3}EI \tag{b}$$

The lowering of the point of application of the load during bending, from equation (138), will be,

$$\lambda = \frac{1}{2}\int_0^l \left(\frac{dy}{dx}\right)^2 dx = \frac{\delta^2\pi^2}{16l} \tag{c}$$

Therefore,

$$T = S\lambda = \frac{\delta^2\pi^2 S}{16l} \tag{d}$$

Substituting (b) and (d) in the fundamental equation (150) we will have, $S_{cr} = \frac{EI\pi^2}{4l^2}$, which coincides completely with equation (142) given above.

In this case the deflection curve (a) was known and the exact solution for the critical load was obtained from equation (150). In cases where the deflection curve is unknown, the same equation (150) can be used for obtaining an approximation of the critical load. It is necessary to take for the deflection curve a *suitable curve* satisfying the conditions at the ends of the bar, and to proceed with the equation of this curve in exactly the same manner as explained above.

In order to show what accuracy can be obtained by using this method, the previous problem will be considered again. Assume, for instance, that in the case shown in Fig. 160 (a) the deflection curve is the same as for a cantilever loaded at the end by a transverse force P, see page 74. Then, $y = Px^2/6EI(3l - x)$.

Substituting this in the expression (b) for the potential energy U of bending, and in expression (d) for the work done by the compressive force S, the following will be obtained:

$$U = \frac{EI}{2}\int_0^l \left(\frac{d^2y}{dx^2}\right)^2 dx = \frac{P^2l^3}{6EI}$$

$$T = S\lambda = \frac{S}{2}\int_0^l \left(\frac{dy}{dx}\right)^2 dx = \frac{S}{15}\frac{P^2l^5}{(EI)^2}$$

Substituting in (150), $S_{cr} = 2.5EI/l^2$. Comparing this result with the exact formula above (142) it is seen that the error arising from this approximate solution is only about 1 per cent.

Buckling of a Pillar Uniformly Loaded along the Axis.—As another example of this approximate method, the problem on buckling of a column under the action of compressive forces uniformly distributed along the axis (Fig. 165) will be considered. In an exact solution of this problem the equation is of such a type that the use of Bessel's function is necessary.* In applying the approximate method, the following equation will be taken as giving a suitable deflection curve,

$$y = \delta\left(1 - \cos\frac{\pi x}{2l}\right)$$

from which, the corresponding potential energy of bending (Eq. b) is,

$$U = \frac{\delta^2\pi^4}{64l^3}EI \qquad \text{(e)}$$

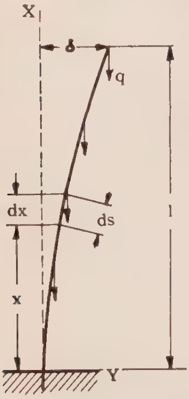

FIG. 165.—Buckling of a rod under uniformly distributed loading.

In calculating the work done by the uniform loading q, it must be noted (see Fig. 165) that due to the inclination of an element ds of the central line during bending the upper part of the loading undergoes a downward displacement equal to $ds - dx = \frac{1}{2}(dy/dx)^2dx$. The corresponding work done by this load is, $\frac{1}{2}q(l - x)(dy/dx)^2dx$. Therefore, the complete work done by the uniform loading during bending is,

$$T = \frac{1}{2}\int_0^l q(l - x)\left(\frac{dy}{dx}\right)^2 dx,$$

or, substituting (a) for y,

$$T = \frac{q\pi^2}{8}\delta^2\left(\frac{1}{4} - \frac{1}{\pi^2}\right) \qquad \text{(f)}$$

Now substituting (e) and (f) in (150) we obtain the critical load,

$$(ql)_{cr} = \frac{EI\pi^2}{1.19l^2} \qquad \text{(g)}$$

Further Approximations.—The method described above can be developed in such a manner so as to give further approximations for the critical load. The actual curve of buckling of a compression member is always that which corresponds to the *least resistance* of the member and any approximation which may be made to this curve will give for the critical load a higher value than the true critical load. It is clear also that a better approximation will be obtained if the expression for a *suitable deflection curve* will contain certain arbitrary constants which must be chosen so as to make the critical load, determined by the equation (150), a minimum.

---

* See A. E. H. Love, "Theory of Elasticity," 3rd. edition, p. 431.

Take for instance, in the example above, another deflection curve represented by,

$$y = a_1\left(1 - \cos\frac{\pi x}{2l}\right) + a_2\left(1 - \cos\frac{3\pi x}{2l}\right) \tag{h}$$

This equation satisfies the conditions at the built in end $((y)_{x=0} = 0$, $(dy/dx)_{x=0} = 0)$ and can be taken as a suitable curve in our calculations.

Substituting (h) in the expressions for the potential energy U and for the work done T we will have:

$$U = \frac{1}{2}EI\int_0^l \left(\frac{d^2y}{dx^2}\right)^2 dx = \frac{\pi^4 EI}{64l^3}(a_1^2 + 81a_2^2) \tag{k}$$

and

$$T = \frac{1}{2}\int_0^l q(l - x)\left(\frac{dy}{dx}\right)^2 dx = \frac{q\pi^2}{8}\left[a_1^2\left(\frac{1}{4} - \frac{1}{\pi^2}\right) + a_2^2\left(\frac{9}{4} - \frac{1}{\pi^2}\right) + \frac{6}{\pi^2}a_1a_2\right] \tag{m}$$

Equation (150) becomes,

$$q\int_0^l (l - x)\left(\frac{dy}{dx}\right)^2 dx = EI\int_0^l \left(\frac{d^2y}{dx^2}\right)^2 dx$$

from which

$$(ql)_{cr} = EIl\frac{\int_0^l \left(\frac{d^2y}{dx^2}\right)^2 dx}{\int_0^l (l - x)\left(\frac{dy}{dx}\right)^2 dx} \tag{n}$$

Now, as we have seen, the constants a_1 and a_2 must be so chosen that (n) will assume a minimum value. Applying the usual method for determining the minimum of a function, we have:

$$\int_0^l (l - x)\left(\frac{dy}{dx}\right)^2 dx \cdot \frac{\partial}{\partial a_1}\int_0^l \left(\frac{d^2y}{dx^2}\right)^2 dx -$$

$$- \int_0^l \left(\frac{d^2y}{dx^2}\right)^2 dx \cdot \frac{\partial}{\partial a_1}\int_0^l (l - x)\left(\frac{dy}{dx}\right)^2 dx = 0 \tag{o}$$

The same type of equation will be obtained if the derivative with respect to a_2 be taken. Now from equations (n) and (0) we have:

$$\frac{\partial}{\partial a_1}\int_0^l \left(\frac{d^2y}{dx^2}\right)^2 dx - \frac{(ql)_{cr}}{EIl}\cdot\frac{\partial}{\partial a_1}\int_0^l (l - x)\left(\frac{dy}{dx}\right)^2 dx = 0$$

or

$$\frac{\partial}{\partial a_1}\left\{\int_0^l \left(\frac{d^2y}{dx^2}\right)^2 dx - \frac{(ql)_{cr}}{EIl}\int_0^l (l - x)\left(\frac{dy}{dx}\right)^2 dx\right\} = 0$$

in the same manner,

$$\frac{\partial}{\partial a_2}\left\{\int_o^l\left(\frac{d^2y}{dx^2}\right)^2 dx - \frac{(ql)_{cr}}{EIl}\int_o^l (l - x)\left(\frac{dy}{dx}\right)^2 dx\right\} = 0$$

or substituting (k) and (m),

$$\begin{aligned}\frac{\partial}{\partial a_1}\left\{\frac{\pi^4}{32l^3}(a_1^2 + 81a_2^2) - \frac{(ql)_{cr}}{EIl}\frac{\pi^2}{4}\left[a_1^2\left(\frac{1}{4} - \frac{1}{\pi^2}\right) + \right.\right.\\ \left.\left. a_2^2\left(\frac{9}{4} - \frac{1}{\pi^2}\right) + \frac{6}{\pi^2}a_1a_2\right]\right\} = 0\end{aligned}$$

$$\begin{aligned}\frac{\partial}{\partial a_2}\left\{\frac{\pi^4}{32l^3}(a_1^2 + 81a_2^2) - \frac{(ql)_{cr}}{EIl}\frac{\pi^2}{4}\left[a_1^2\left(\frac{1}{4} - \frac{1}{\pi^2}\right) + a_2^2\right.\right.\\ \left.\left. \left(\frac{9}{4} - \frac{1}{\pi^2}\right) + \frac{6}{\pi^2}a_1a_2\right]\right\} = 0\end{aligned}$$

After differentiating,

$$\begin{aligned}\left[\frac{\pi^4}{16l^3} - \frac{(ql)_{cr}}{EIl}\frac{\pi^2}{2}\left(\frac{1}{4} - \frac{1}{\pi^2}\right)\right]a_1 - \frac{(ql)_{cr}}{EIl}\frac{3}{2}a_2 = 0\\ -\frac{(ql)_{cr}}{EIl}\frac{3}{2}a_1 + \left[\frac{81\pi^4}{16l^3} - \frac{(ql)_{cr}}{EIl}\frac{\pi^2}{2}\left(\frac{9}{4} - \frac{1}{\pi^2}\right)\right]a_2 = 0\end{aligned} \tag{p}$$

A solution of this system of two homogeneous linear equations will be $a_1 = a_2 = 0$, which shows that the straight form of equilibrium of the compressed member is a *possible form.* The possibility of buckling occurs when equations (p) may give for a_1, and a_2 solutions different from zero. The condition for this is that the determinant of the system (p) must be equal to zero, i.e.:

$$\begin{aligned}\left\{\frac{\pi^4}{16l^3} - \frac{(ql)_{cr}}{EIl}\frac{\pi^2}{2}\left(\frac{1}{4} - \frac{1}{\pi^2}\right)\right\}\left\{\frac{81\pi^4}{16l^3} - \frac{(ql)_{cr}}{EIl}\frac{\pi^2}{2}\left(\frac{9}{4} - \frac{1}{\pi^2}\right)\right\} + \\ + \left[\frac{(ql)_{cr}}{EIl}\frac{3}{2}\right]^2\Bigg\} = 0\end{aligned} \tag{p}$$

from which,

$$\begin{aligned}\left[\frac{(ql)_{cr}}{EIl}\right]^2\left[\frac{9}{4} + \frac{\pi^4}{4}\left(\frac{1}{4} - \frac{1}{\pi^2}\right)\left(\frac{9}{4} - \frac{1}{\pi^2}\right)\right] - \frac{(ql)_{cr}}{EIl}\left[\frac{81\pi^6}{32l^3}\left(\frac{1}{4} - \frac{1}{\pi^2}\right) + \right.\\ \left. + \frac{\pi^6}{32l^3}\left(\frac{9}{4} - \frac{1}{\pi^2}\right)\right] + \frac{81\pi^8}{256l^6} = 0\end{aligned} \tag{q}$$

The smaller root of this equation gives the second approximation for the critical load as follows:

$$(ql)_{cr} = \frac{\pi^2 EI}{1.25l^2} \tag{151}$$

Comparing with (g) it is seen that the error of the first approximation is about 5 per cent.

The Force Concentrated at the Intermediate Cross-section.—By applying the same approximate method, a solution of the problem on buckling of a strut loaded at the ends and in the middle (Fig. 166) can also be obtained. Let I_1 denote the moment of inertia of a section in the upper part of the strut, and I_2 the same for the lower part. Then proceeding as previously explained, the approximate value of the critical force can be represented in the following form:

$$(S_1 + S_2)_{cr} = \pi^2 \frac{EI_2}{(\beta l)^2} \tag{152}$$

The values of the coefficient β depending on the constants

$$\gamma = \frac{I_2}{I_1} \text{ and } k = \frac{S_1 + S_2}{S_1}$$

are given in Table IX.

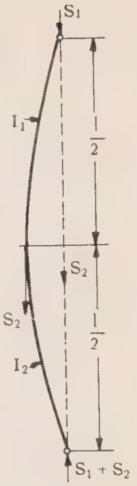

FIG. 166.—Strut with intermediate loading.

TABLE IX.—CRITICAL LOAD COEFFICIENTS (EQUATION 152)

γ \ $k =$	1.00	1.25	1.50	1.75	2.00
1.00	1.00	.95	.91	.89	.87
1.25	1.06	1.005	.97	.94	.915
1.50	1.12	1.06	1.02	.99	.96
1.75	1.18	1.11	1.07	1.04	1.005
2.00	1.24	1.16	1.12	1.08	1.05

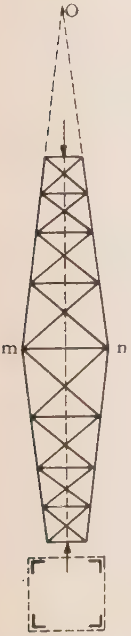

FIG. 167.—Non-uniform built-up compression member.

48. Buckling of Bars of Variable Cross-section.—The same approximate method, as explained above, can be used in the case of struts of variable cross-section. Assume that the strut represented in Fig. 167 is symmetrical about the middle cross-section *mn*. Let I_0 = moment of inertia of this cross-section. I_1 = moment of inertia of the cross-sections at the ends. The area A of the cross-section, consisting of four angles as shown in the figure, remains constant along the length of the strut. Then the moment of inertia I of any cross-section of the upper part of the member will be approximately proportional to the square of the distance from the fixed point O. The magnitude of the critical load, on the assumption of hinged ends, will be,

$$S_{cr} = m\frac{EI_o}{l^2} \tag{153}$$

The values of the coefficient m, which depend on the ratio I_1/I_0, are given in Table X.*

Table X.—Critical Load Coefficients (Equation 153)

$I_1/I_o = \ldots.$	.1	.2	.3	.4	.5	.6	7.	.8	.9	1.0
$m = \ldots\ldots$	5.40	6.38	7.07	7.62	8.08	8.51	8.90	9.25	7.57	π^2

If the strut consists of two solid cones (Fig. 168) the same equation (153) can be used. The values of m for this condition are given in Table XI.

Table XI.—Critical Load Coefficients for the Case of Fig. 168

$I_1/I_o = \ldots\ldots$	.1	.2	.3	.4	.5	.6	.7	.8	.9	1.0	2
$m = \ldots\ldots$	4.81	6.02	6.85	7.48	8.00	8.45	8.86	9.23	9.57	π^2	12.1

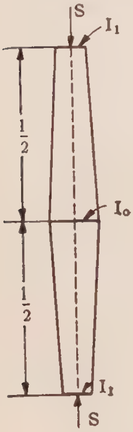

Fig. 168.—Column of variable cross-section.

It is seen from Tables X and XI that the values of critical loads depends principally on the magnitude of the ratio I_1/I_0.

49. Buckling of Latticed Struts.†—*General.*—Built up columns and latticed struts are extensively used in steel structures. Their resisting capacities are always less than those of solid columns having the same ratio l/i of length to radius of gyration, and depend on the spacing details as lattice bars, spacing plates and battens. In order to develop the theory of the buckling of latticed struts, the effect of shearing force on the magnitude of the critical load must be studied. It will be shown that this effect for the case of latticed bars is greater than for solid columns and must be taken into consideration.

The Effect of Shearing Force in Solid Struts.—In order to obtain this effect, the energy method developed in paragraph 47 will be used.

---

* This table and the following were given by A. Dinnik, *Bulletin of the Polyt. Inst. in Ekaterinoslaw* (Russia), 1914.

† See Engesser, *Zentralblat d. Bauverw.* p. 136, 1909; L. Prandtl, *Zeitschr. d. Ver. Deutsch. Ing.*, 1907. See also author's paper, *Bulletin of the Polyt. Inst. in Kiev*, 1908. These papers discuss the cause of the collapse of the Quebec Bridge.

Let AB (Fig. 169) represent a solid strut with hinged ends, buckled under the action of compressive force S. The magnitude of the bending moment and the shearing force at any cross-section mn is,

$$M = Sy;\ Q = S\frac{dy}{dx} \tag{a}$$

From our previous consideration the potential energy stored in an element of the bar will be,

$$dU = \frac{M^2dx}{2EI} + \frac{kQ^2dx}{2GA} \tag{b}$$

where A = crosssectional area
k = coefficient depending on the shape of the cross-section (Par. 17) such that
kQ/GA = the magnitude of the shear at the neutral axis.

Accordingly, the displacement of the section mn with respect to m_1n_1, due to this shear, will be $kQ/GAdx$. The second member on the right side of (b) represents the potential energy of shear stored in the element, while the first member represents the energy due to bending (Eq. 52). By using (a) and (b), the energy stored in the strut during buckling will be represented as follows:

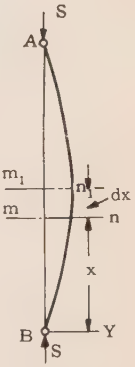

FIG. 169.—Buckled strut.

$$U = \int_0^l \frac{S^2y^2dx}{2EI} + \int_0^l \frac{kS^2}{2GA}\left(\frac{dy}{dx}\right)^2 dx \tag{c}$$

The work done by the compressive load during buckling is (see Eq. 138),

$$T = \frac{S}{2}\int_0^l \left(\frac{dy}{dx}\right)^2 dx \tag{d}$$

Assuming that the deflection curve of the buckled strut is a sine curve,

$$y = \delta \sin\frac{\pi x}{l} \tag{e}$$

and substituting (e) in (c) and (d), the following will be obtained,

$$U = \delta^2\frac{S^2l}{4EI} + \delta^2\frac{S^2l}{4GA}\,\frac{k\pi^2}{l^2} \tag{f}$$

$$T = \delta^2\frac{S\pi^2}{4l}.$$

Now, from equation (150),

$$T = U$$

$$S_{cr} = \frac{\pi^2 EI}{l^2} \frac{1}{1 + \frac{EI}{GA}\frac{k\pi^2}{l^2}} \tag{g}$$

Comparing this with Euler's formula (143) it can be concluded that, due to the action of shear, the critical load is diminished in the ratio

$$\frac{1}{1 + \frac{EI}{GA}\frac{k\pi^2}{l^2}} \tag{154}$$

Noting

$$\frac{\pi^2 EI}{l^2} = S_e : \frac{GA}{k} = S_d \tag{h}$$

equation (g) becomes,

$$S_{cr} = S_e \frac{1}{1 + \frac{S_e}{S_d}} \tag{155}$$

In the case of solid bars, S_d is very large in comparison with S_e, and the effect of the shearing force can be neglected. In the case of built up columns, especially when spacing plates or battens only are used (Fig. 171 (a)), S_d may become of the same order as S_e, in which case the effect of shearing force can no longer be neglected. This will now be considered.

The Effect of Shearing Force in Latticed Struts.—Equation (155) obtained above, can be used also for the case of latticed struts. S_e, as above, will represent the critical load obtained from Euler's formula. The magnitude of S_d will depend on the spacing details. In the case of solid struts it has a simple physical meaning. It is easy to see that the magnitude of S_d is such that

$$\frac{Q}{S_d} = \beta \tag{l}$$

represents the shear produced by the shearing force Q. It will have the same meaning also in the case of latticed struts; and for determining its magnitude the lateral displacement produced by the shearing force must be considered. This method will now be developed for particular cases of practical importance.

Consider the latticed bar shown in Fig. 170. The cross-sectional area of channels can be considered as large in comparison with cross-sectional areas of the diagonals and battens. The extension of a diagonal produced by shearing force Q will be (Fig. 170 (b)) $Qa/\sin\phi\cos\phi EA_d$ in which,

$\dfrac{Q}{\cos\phi}$ = tensile force in the diagonal

$\dfrac{a}{\sin\phi}$ = length of the diagonal

A_d = cross-sectional area of two diagonals.

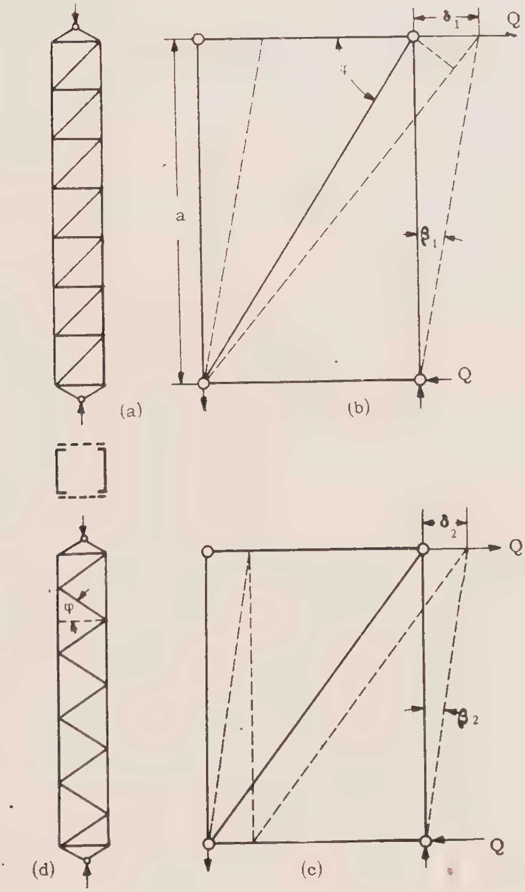

Fig. 170.—Buckling of latticed bars.

The corresponding lateral displacement is,

$$\delta_1 = \frac{Qa}{\sin\phi\cos^2\phi EA_d} \tag{k}$$

The compression of a batten and the corresponding lateral displacement (Fig. 170 (c)) is,

$$\delta_2 = \frac{Qb}{EA_p} \tag{m}$$

where

b = the length of the batten
A_p = the cross-sectional area of two battens.

From (k) and (m), the angular displacement produced by shear Q is,

$$\beta = \frac{\delta_1 + \delta_2}{a} = \frac{Q}{\sin\phi\cos^2 EA_d} + \frac{Qb}{aEA_p}.$$

Comparing this to equation (l),

$$\frac{1}{S_d} = \frac{1}{\sin\phi\cos^2 EA_d} + \frac{b}{aEA_p}$$

Substituting in (155),

$$S_{cr} = \frac{\pi^2 EI}{l^2}\,\frac{1}{1 + \dfrac{\pi^2 EI}{l^2}\left(\dfrac{1}{\sin\phi\cos^2\phi EA_d} + \dfrac{b}{aEA_p}\right)} \tag{156}$$

If the sectional areas A_d and A_p are very small in comparison with the cross-sectional area of channels (Fig. 170 (a)), the critical load (156) may be considerably lower than that obtained from Euler's formula (143).

Equation (156) can be used also in the case represented in Fig. 170 (d), it is necessary only to measure the angle ϕ as shown in the figure, and eliminate the member due to deformation of battens.

In the case of a strut where battens alone are used as in Fig. 171, in order to obtain the lateral displacement produced by the shearing force Q, the deformation of an element of the strut cut out by the sections mn and m_1n_1 must be considered. Assuming that in these sections the deflection curves of channels have points of inflection, the condition of bending will be such as shown in Fig. 171 (b). The deflection will consist of two parts: the displacement δ_1 due to bending of the batten, and the displacement δ_2 due to bending of the channels. Taking into consideration that at the ends of the batten two couples are acting equal to $Qa/2$, the angle θ of rotation of the ends of the batten will be (see Eq. 69),

$$\theta = \frac{Qa}{2}\frac{b}{3EI_2} - \frac{Qa}{2}\frac{b}{6EI_2} = \frac{Qab}{12EI_2}$$

here b = the length of the batten

EI_2 = the flexural rigidity of the batten.

The lateral displacement δ_1 produced by this bending of the batten will be

$$\delta_1 = \theta\frac{a}{2} = \frac{Qa^2b}{24EI_2} \tag{n}$$

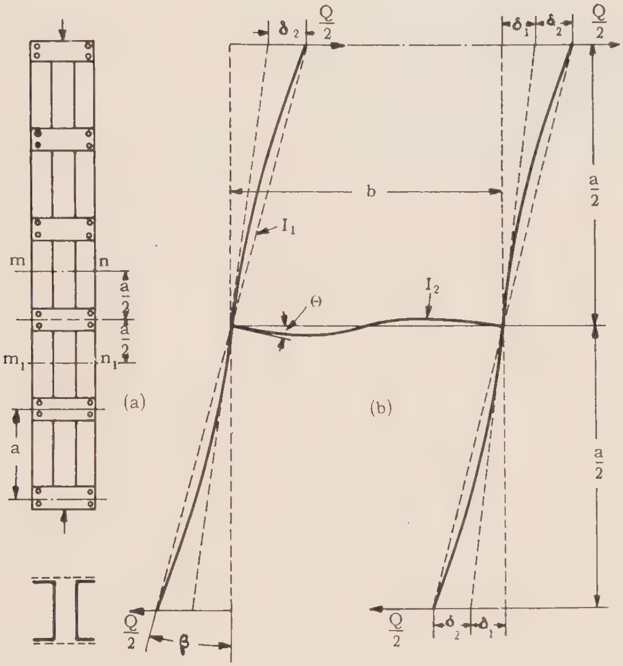

FIG. 171.—Battens in compression members.

The displacement δ_2 can be calculated from the cantilever formula

$$\delta_2 = \frac{Q}{2}\frac{\left(\frac{a}{2}\right)^3}{3EI_1} = \frac{Qa^3}{48EI_1} \tag{p}$$

The angular displacement produced by the shearing force Q will be

$$\beta = \frac{\delta_1 + \delta_2}{\frac{a}{2}} = \frac{Qab}{12EI_2} + \frac{Qa^2}{24EI_1}$$

therefore

$$\frac{1}{S_d} = \frac{ab}{12EI_2} + \frac{a^2}{24EI_1}$$

and equation (155) for determining the critical load becomes

$$S_{cr} = \frac{EI\pi^2}{l^2} \cdot \frac{1}{1 + \frac{EI\pi^2}{l^2}\left(\frac{ab}{12EI_2} + \frac{a^2}{24EI_1}\right)} \tag{157}$$

where, as before, $EI\pi^2/l^2$ represents the critical load calculated from Euler's formula. It is easy to see that when the flexural rigidity of battens is insufficient the actual critical load will be much lower than that given by Euler's formula, and in these cases the application of more accurate formula (157) becomes necessary.

CHAPTER VIII

COMBINED BENDING AND TWIST

50. Circular Shafts.—In considering twist of circular shafts (see Par. 8), it was assumed that the shafts were submitted to the action of torque moment only. In practice the shafts are usually submitted not only to twist but also to bending actions arising from the weight of the shaft itself, the weight of pulleys, and to the thrust or pull of cranks and belts.

In order to obtain the maximum stress at any cross-section of such a shaft it is necessary to consider at this section: (1) shearing stresses due to torque moment M_t, (2) normal stresses due to the bending moment M, and (3) shearing stresses due to the shearing force Q. If the shaft is not short the maximum combined stress will usually occur at the circumference of the shaft where stresses (1) and (2) attain their maximum values, and stress (3) is equal to zero. By using equations (31) page 28, and (50) page 52 these maximum values become,

$$p_t = \frac{M_t d}{2I_p} \tag{a}$$

and

$$p = \frac{Md}{2I} \tag{b}$$

where, d = the diameter of the shaft,

$I_p = \frac{\pi d^4}{32}$ = polar moment of inertia of the cross-section,

$I = \frac{\pi d^4}{64}$ = moment of inertia of the cross-section about a diameter.

Combining these stresses as explained in paragraph 18, and using equations (56) and (57) page 67, the following expressions for the maximum and minimum principal stresses are obtained:

$$p_{\max} = \tfrac{1}{2}p + \tfrac{1}{2}\sqrt{p^2 + 4p_t^2} \tag{c}$$

$$p_{\min} = \tfrac{1}{2}p - \tfrac{1}{2}\sqrt{p^2 + 4p_t^2} \tag{d}$$

Substituting in these equations the values of p and p_t given by (a) and (b) and noting that $2I/d = \pi d^3/32$, we have,

$$p_{\max} = \frac{16}{\pi d^3}\left(M + \sqrt{M^2 + M_t^2}\right) \tag{158}$$

$$p_{\min} = \frac{16}{\pi d^3}\left(M - \sqrt{M^2 + M_t^2}\right) \tag{159}$$

It is seen that the maximum principal stress (Eq. 158) has the same value as a direct bending stress, which would produce the bending moment

$$M_b = \tfrac{1}{2}\left(M + \sqrt{M^2 + M_t^2}\right).$$

It is therefore sometimes called the *equivalent bending moment.* The maximum shearing stress at the same point is,

$$(p_t)_{\max} = \frac{p_{\max} - p_{\min}}{2} = \frac{16}{\pi d^3}\sqrt{M^2 + M_t^2} \tag{160}$$

Further calculations will now depend on the particular theory of strength adapted. (See page 498.) For steel shafting *maximum shear theory* should be considered as the most satisfactory. Therefore, the diameter of the shaft must be determined in such a manner as to make the maximum shearing stress (Eq. 160) equal to the maximum shearing stress at simple tension, i.e., equal to half of the working stress p_w chosen for simple tension.

The equation for determining the diameter d, then becomes,

$$\frac{16}{\pi d^3}\sqrt{M^2 + M_t^2} = \frac{1}{2}p_w \tag{161}$$

(Further discussion of the subject given in Par. 138, page 509.)

Example 66.—A steel bar $ABCD$ (Fig. 172) of constant circular cross section, built in at the end A, is submitted to the action of the force P acting at the end D and perpendicular to the plane xy of the bar. Determine the most dangerous section and also the maximum principal stress at this section, the deflection of the end D, and the rotation of the same end about the axes parallel to X and Y axes. Take $a = b = 30$ in., $r = 15$ in., $d = 5$ in., $E = 30.10^6$ lbs. per sq. in., Poisson's ratio $1/m = .3$, and $P = 1{,}000$ lbs. Consider d as small in comparison with the lengths a, b and r.

Solution.—The part CD of the bar is in a state of simple bending; and the maximum bending moment at C is equal to Pb. The part CB of the bar is in a state of bending and also of twist. The twisting moment along CB is constant and equal to,

$$M_t' = Pb \tag{a}$$

The maximum bending moment for the same part is at B and is equal to

$$M' = Pr \tag{b}$$

The weakest section of the part BC is at B where the principal stresses, from equations (158) and (159), assume the values:

$$p_{\max} = \frac{16}{\pi d^3}\left(M' + \sqrt{M'^2 + M_t'^2}\right) \tag{c}$$

$$p_{\min} = \frac{16}{\pi d^3}\left(M' - \sqrt{M'^2 + M_t'^2}\right) \tag{d}$$

For the part AB, the torque moment is constant and equal to

$$M_t'' = Pr \tag{e}$$

while the maximum bending moment, for the same part, occurs at the section A and is equal to,

$$M'' = P(a + b) \tag{f}$$

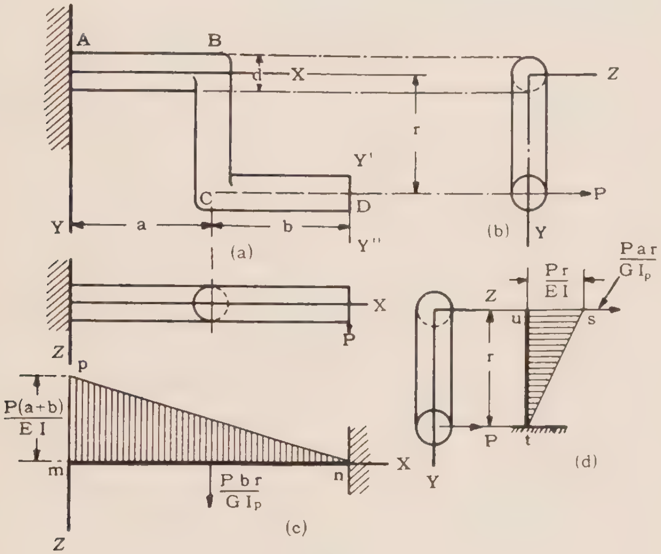

FIG. 172.

The weakest section of the part AB is therefore at the end A, where the principal stresses are:

$$p_{\max} = \frac{16}{\pi d^3}\left(M'' + \sqrt{M''^2 + M_t''^2}\right) \tag{g}$$

$$p_{\min} = \frac{16}{\pi d^3}\left(M'' - \sqrt{M''^2 + M_t''^2}\right) \tag{h}$$

Adopting the maximum shear theory, which will also be used in further calculations, the following maximum shearing stress will be obtained from equation (160) for section B of part BC:

$$(p_t)_{\max} = \frac{16}{\pi d^3}\sqrt{M'^2 + M_t'^2} = \frac{16P}{\pi d^3}\sqrt{r^2 + b^2} \tag{k}$$

and the following will be obtained for the section A of part AB:

$$(p_t)_{\max} = \frac{16}{\pi d^3}\sqrt{M''^2 + M_t''^2} = \frac{16P}{\pi d^3}\sqrt{(a + b)^2 + r^2} \tag{l}$$

Comparing (k) and (l) it can be concluded that the weakest section is at the end A, where

$$(p_t)_{\max} = \frac{16 \times 10^3}{\pi \times 5^3}\sqrt{60^2 + 15^2} = 2{,}520 \text{ lbs. per sq. in.}$$

The angle of rotation of the end D about the diameter parallel to the Y axis is due to bending of the parts AB and CD and to the twist of the part BC. The rotation due to bending will be (from Eq. 70, page 74)

$$\frac{P(a + b)^2}{2EI} = \frac{32P(a + b)^2}{E\pi d^4} \tag{m}$$

and that due to twist will be,

$$\frac{Pbr}{GI_p} = \frac{32Pbr}{G\pi d^4} \tag{n}$$

Adding (m) and (n) we have the angle of rotation for the end D about the axis $Y' - Y''$ parallel to Y equal to,

$$\frac{32P(a + b)^2}{E\pi d^4} + \frac{32Pbr}{G\pi d^4} \tag{p}$$

The angle of rotation of the same section about the axis parallel to X axis is due to bending of the part CB and to twist of the part AB and can be written down as follows:

$$\frac{32Pr^2}{E\pi d^4} + \frac{32Pra}{G\pi d^4} \tag{q}$$

It must be noted that the angle given by equation (p) can easily be obtained by using the grapho-analytical method. (See Fig. 172 (c).) The angle due to bending will be obtained as the reaction at the end n, produced by a continuous imaginary loading given by the triangle mnp. The angular displacement of the part CD with respect to the part AB, equal to the twist of the part BC, is equal to Pbr/GI_p.

It is represented in Fig. 172 (c) by an imaginary concentrated force. The corresponding reaction at the end n gives the second term in equation (p).

In calculating the deflection at D, the same imaginary loading will be used. The bending moment at the end n produced by the triangle mnp gives,

$$M = \frac{P(a + b)^3}{3EI} \tag{r}$$

This is the deflection produced by the bending of the parts AB and CD.

The bending moment at the end n, produced by the imaginary concentrated load is equal to,

$$M_1 = \frac{Pb^2r}{GI_p} \tag{s}$$

This represents the deflection at the end D, due to the twist of the part BC of the bar.

So far, angular changes in the planes parallel to XZ plane were considered. The angular changes in planes parallel to the YZ plane are due to twist of the part AB and to bending of the part BC. This can be represented by the imaginary loading of the beam ut in Fig. 172 (d). The corresponding deflection at the end

D of the bar will be given by the bending moment at the end t, produced by the triangle ust, together with the bending moment produced by the concentrated load Par/GI_p. In this manner we have

$$M_2 = \frac{Pr^3}{3EI} + \frac{Par^2}{GI_p} \tag{t}$$

Adding (r), (s), and (t) we have for the complete deflection of the end D of the bar:

$$\delta = \frac{P(a+b)^3}{3EI} + \frac{Pb^2r}{GI_p} + \frac{Pr^3}{3EI} + \frac{Par^2}{GI_p} \tag{u}$$

Example 67.—Determine the deflection at the middle O (Fig. 173), produced in a throw by a force P acting perpendicular to it. The calculations must be made for two different conditions: (1) that the ends are simply supported, (2) that the ends are built in.

The lengths of the parts of the throw are taken as shown in the figure and the transverse dimensions of these parts are considered small in comparison with the lengths. The dimensions are as follows:

a = length of the journal.
e = length of the pin.
r = radius of the throw.
d = diameter of the journal and of the pin.
h = width of the web.
c = thickness of the web.

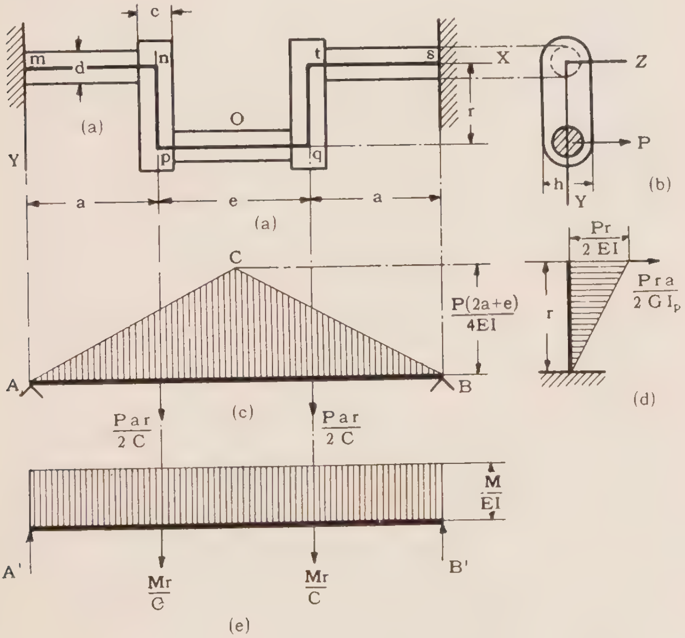

FIG. 173.

Solution.—Assuming that the ends m and s are simply supported (Fig. 173) and using the grapho-analytical method as before, the imaginary loading corresponding to the angular changes in planes parallel to the XZ plane will be as in Fig. 173 (c). The triangle ACB corresponds to bending of parts mn, pq, and ts. The concentrated imaginary loads $Par/2C$ represent the angles of twist of the webs.* The angles of rotation of the ends m and s about the diameter parallel to the Y axis, from Fig. 173 (c), are,

$$\frac{P(2a+e)^2}{16EI}+\frac{Par}{2C} \tag{a}$$

The deflection at the middle O, from Fig. 173 (c), is,

$$\frac{P(2a+e)^3}{48EI}+\frac{Pa^2r}{2C} \tag{b}$$

In order to obtain the complete deflection at O, the angular changes in the plane parallel to YZ plane must be considered. The corresponding imaginary loading is given in Fig. 173 (d). The triangular loading corresponds to the bending of the web, and the concentrated load $Pra/2GI_p$ represents the twist of a journal. The deflection at O, corresponding to the loading of Fig. 173 (d), will be,

$$\frac{Pr^3}{6EI}+\frac{Pr^2a}{2GI_p} \tag{c}$$

Adding (b) and (c), the complete deflection at O for the case of simply supported ends becomes,

$$\delta=\frac{P(2a+e)^3}{48EI}+\frac{Pa^2r}{2C}+\frac{Pr^3}{6EI}+\frac{Pr^2a}{2GI_p} \tag{d}$$

In order to obtain a solution for clamped ends, two equal and opposite couples M at the ends m and s must be applied in the plane XZ. The magnitude and direction of the couples M must be such as to annihilate the rotation of the ends given by equation (a). The corresponding imaginary loading is given in Fig. 173 (e). The angles produced by the couples M are,

$$\frac{M(2a+e)}{2EI}+\frac{Mr}{C} \tag{f}$$

Comparing (a) and (f),

$$\frac{M(2a+e)}{2EI}+\frac{Mr}{C}=\frac{P(2a+e)^2}{16EI}+\frac{Par}{2C} \tag{g}$$

From which M can be easily obtained.

The deflection produced by the couples M is, from Fig. 173 (e)

$$\frac{M(2a+e)^2}{8EI}+\frac{Mra}{C} \tag{k}$$

This deflection must be subtracted from (d) in order for us to obtain the deflection at the middle O for the case of clamped ends.

51. Single Throw Crankshaft.—*General.*—As a practical example where bending and twist are acting simultaneously, a problem on stresses and deformation of crankshafts will now be considered Fig. 174. The analysis will first be made of the deformations of a single crank due to various forces and moments.

---

* Torsional rigidity C can be obtained for a rectangular section from equation 37, page 33.

The assumptions made to simplify the problem are: (1) that the crankshaft is simply supported at the middle cross sections of the journals, and (2) the throw is considered as a bar *mnpqst* whose cross sectional dimension is small in comparison with the lengths r, e, and f. The calculations made on these assumptions are in good accord with the results obtained* on the basis of a more detailed consideration of the deformation of a single throw, where, as is usually the case, the dimensions of the cross section are not small in comparison with the lengths. The principal symbols are: (See Fig. 174).

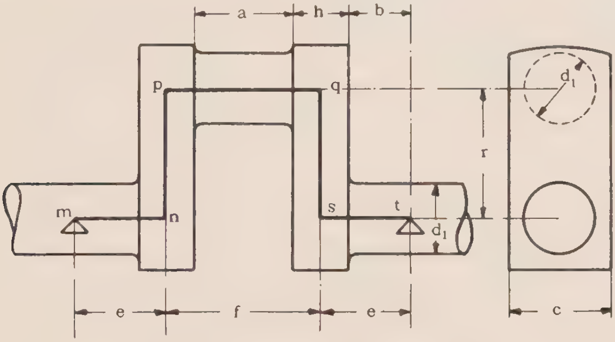

FIG. 174.—Single throw crankshaft.

$C_1 = \frac{\pi d_1^4}{32} G$ = torsional rigidity of the journal and the crank pin.

C_2 = torsional rigidity of the web with respect to twist around q-s axis. The cross section is rectangular with sides h and c, whence (Eq. 37, page 33) $C_2 = \beta c h^3 G$.

$B_1 = EI_1 = \frac{\pi d_1^4}{64} E$ = flexural rigidity of the journal and the crank pin.

$B_2 = EI_2 = \frac{hc^3}{12} E$ = flexural rigidity of the web against bending in the plane through q-s, perpendicular to the plane of Fig. 174.

$B_3 = EI_3 = \frac{ch^3}{12} E$ = flexural rigidity of the web against bending in the plane of the throw.

The axes of coordinates are chosen as shown in Fig. 175. The XY plane coincides with that of the throw and the Z axis is so directed that rotation of a right hand screw from Y to Z would produce motion in the positive direction of the X axis.*

---

* See author's paper in Trans. Amer. Soc. Mech. Eng., Vol. 44, p. 653.

The external forces acting on the throw are: (Fig. 175)

1. The thrust of the connecting rod on the crankpin, which acts in a plane perpendicular to the X axis, can be resolved into two components, P and S, parallel to the Y and Z axes, respectively.

2. The centrifugal forces due to the web and crankpin, represented by two equal forces Q, parallel to the Y axis.

3. The couple at the end which is usually resolved into three components, namely:

m, the bending moment in the plane of the throw;

M, the bending moment in the plane perpendicular to the plane of the throw; and

M_t, the twisting moment.

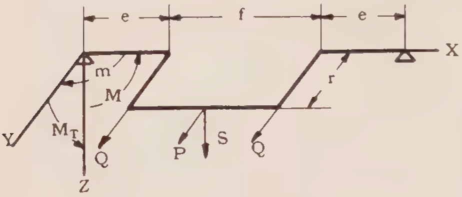

FIG. 175.—Arrangement of axis.

The positive direction of moments is shown in the figure by arrows.

The effects due to these different groups of forces will now be analyzed separately and the combined effect will be obtained by the method of superposition. In this manner formulae necessary for the study of multi-throw crankshafts will be obtained.

Bending in the Plane of the Throw.—Referring to Fig. 176 (a), consider the bending of the throw produced by the forces P, Q, and by a couple m acting at the left support in the XY plane. In order to make further development clear, the following rule of signs for couples and rotation of ends is adopted. The relation between the positive sense of the moment m and the positive direction of the Z axis is the same as that between rotation and translation of a righthand screw. The same rule is used in determining the sign of the angle of rotation of any cross-section of the journal. In accordance with this, the angle ϕ_1 (Fig. 176 (a)), representing the rotation of the left end is positive, and the angle ϕ_2 is negative. The reactions A and B at the supports are obtained as follows:

$$A = \frac{P}{2} + Q - \frac{m}{2e + f}, \quad B = \frac{P}{2} + Q + \frac{m}{2e + f}$$

The diagrams of bending moment for journals and crankpin obtained as for a simply supported beam are given separately for different groups of forces in Fig. 176 (b), (c), (d). The webs of the crankshaft are subjected to direct tension equal to the reactions A and B respectively and also to pure bending. The bending moments for the right and for the left web are Ae and Be respectively. It is seen now that the stresses produced in the elements of the crankshaft can easily be obtained by using the simple formulae for bending and direct stresses.

---

* This direction will be used further in considering bending and torsion of a multi-throw crankshaft.

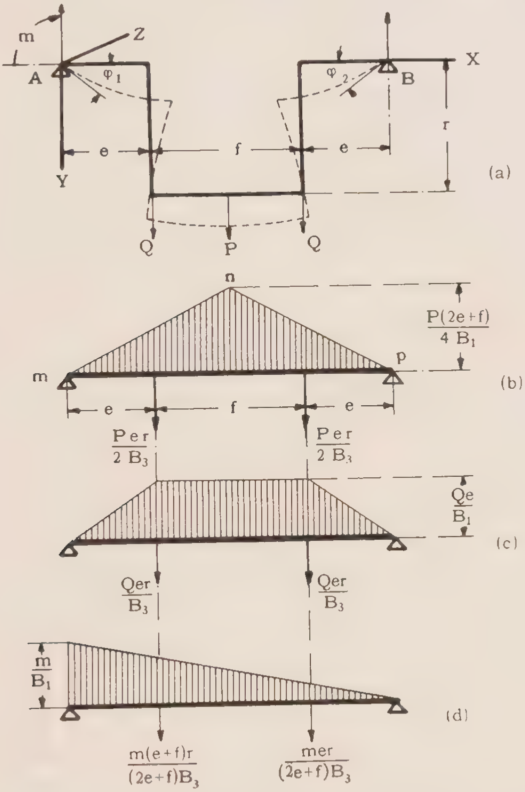

FIG. 176.—Bending in the plane of the throw.

In discussing deformation the grapho-analytical method (par. 23 page 84) will be used. In applying this method the assumption must be made that the beam is submitted to the action of a continuously distributed load the value of whose intensity at each cross-section is numerically equal to M/B, where M denotes the bending moment at the given cross section and B the flexural rigidity at the same section. The reactions at the supports, calculated for this imaginary loading, give the numerical value of the angles of rotation of the terminal cross-section of the beam. In the case of the crankshaft, this imaginary loading gives the angular changes due to the bending of the journals and crankpin. In order to take account of the deformation due to the webs, two additional concentrated forces (see Fig. 176, (b), (c), (d) numerically equal to the angular deformation of the webs must be added.*

The angles ϕ_1, ϕ_2, of rotation at the supports of the throw will be calculated in their component parts (ϕ_1', ϕ_2'), (ϕ_1'', ϕ_2''), (ϕ_1''', ϕ_2''') due respectively to the forces P, Q, and the moment m.

In the case of bending by the force P, the distributed imaginary load is represented by the triangle mnp (Fig. 176 (b)), and the additional concentrated imaginary load at each web is $Per/2B_3$. This quantity is readily obtained. Since the webs are each uniformly bent into circular arcs by the couples $Pe/2$, the curvature, $1/\rho$, from the formula $1/\rho = M/EI$, is equal to $Pe/2B_3$, and the angular deformation is $Per/2B_3$. Then,

$$\phi_1' = -\phi_2' = P\left[\frac{(2e+f)^2}{16B_1} + \frac{er}{2B_3}\right].$$

The centrifugal forces Q give, by the same rule, the continuous loading and concentrated forces as shown in Fig. 176 (c). Hence,

$$\phi_1'' = -\phi_2'' = Q\left(\frac{e(e+f)}{2B_1} + \frac{er}{B_3}\right)$$

Similarly, the moment m, Fig. 176 (d), gives:

$$\phi_1''' = m\left\{\frac{2e+f}{3B_1} + \frac{e^2r}{(2e+f)^2B_3} + \frac{(e+f)^2r)}{(2e+f)^2B_3}\right\}$$

$$\phi_2''' = -m\left\{\frac{2e+f}{6B_1} + \frac{2e(e+f)r}{(2e+f)^2B_3}\right\}$$

The sum of the effects of all the forces shown in Fig. 176 (a), then, is:

$$\phi_1 = m\alpha_1 + Pt_1 + Qt_2 \tag{162}$$

$$\phi_2 = -m\alpha_2 - Pt_1 - Qt_2 \tag{163}$$

where

$$\alpha_1 = \frac{2e+f}{3B_1} + \frac{e^2r}{(2e+f)^2B_3} + \frac{(e+f)^2r}{(2e+f)^2B_3} \tag{164}$$

$$\alpha_2 = \frac{2e+f}{6B_1} + \frac{2e(e+f)r}{(2e+f)^2B_3} \tag{165}$$

$$t_1 = \frac{(2e+f)^2}{16B_1} + \frac{er}{2B_3} \tag{166}$$

$$t_2 = \frac{e(e+f)}{2B_1} + \frac{er}{B_3} \tag{167}$$

---

* See example 66.

Bending in the Plane Perpendicular to the Plane of the Throw.—The bending of the throw (Fig. 177 (a)) by the force S, parallel to the Z axis, and a couple M, acting in the XZ plane, is now to be considered. A moment $Sr/2$ about the X axis is applied at each support to prevent rotation under the action of the force S.

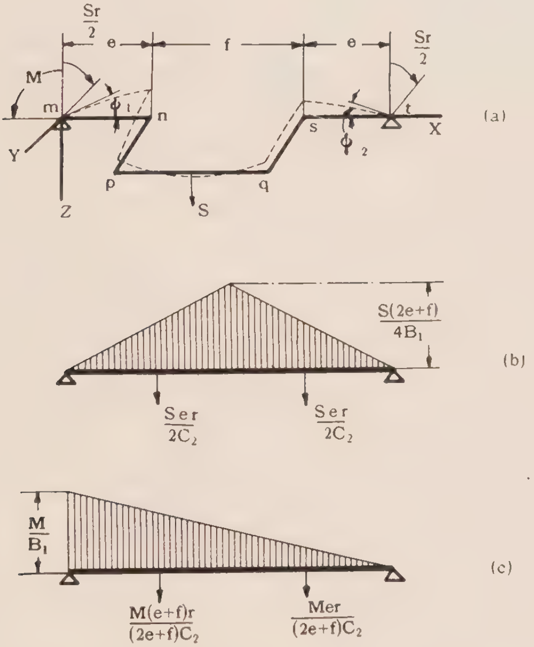

FIG. 177.—Bending of crank by forces perpendicular to throw.

By the same method as above, the angles of rotation produced by the force S (imaginary loading given in Fig. 177 (b)) are,

$$\psi_1' = -\psi_2' = -S\left[\frac{(2e+f)^2}{16B_1} + \frac{er}{2C_2}\right] \qquad \text{(a)}$$

The case of M is more complicated. The angles of rotation of the ends are affected not only by the angular deformation of different parts of the throw in the plane of M, but also by the deflection of the webs and the twist of the crankpin. The former can be calculated by the grapho-analytical method as above (loading as in Fig. 177 (c)). These angles are:

$$\psi_1'' = M\left(\frac{2e+f}{3B_1} + \frac{e^2r}{(2e+f)^2C_2} + \frac{(e+f)^2r}{(2e+f)^2C_2}\right) \qquad \text{(b)}$$

$$\psi_2'' = -M\left(\frac{2e+f}{6B_1} + \frac{2e(e+f)r}{(2e+f)^2C_2}\right)$$

The rotation of the ends due to the bending of the webs and to the twist of the crankpin can be taken from Fig. 178 (a), where the corresponding distortion of the crankshaft is shown diagrammatically in an exaggerated manner. It is seen that these angles are each equal to

$$\frac{\delta}{(2e+f)},$$

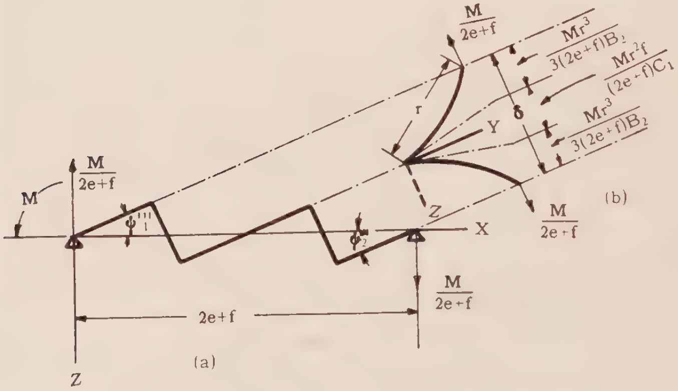

Fig. 178.—Bending of crank by couple perpendicular to throw.

where δ is the displacement shown in Fig. 178 (b). This displacement consists of twice the deflection of the web and the displacement due to the twist of the crankpin. The deflection of the web considered as a cantilever is

$$\frac{M}{2e+f}\cdot\frac{r^3}{3B_2}.$$

The displacement due to the twist is obtained by multiplying the angle of twist by the length r and equals to

$$\frac{Mfr^2}{(2e+f)C_1}.$$

In this way

$$\delta = M\left(\frac{2r^3}{3(2e+f)B_2} + \frac{fr^2}{(2e+f)C_1}\right)$$

and

$$\psi_1''' = \psi_2''' = \frac{\delta}{2e+f} = M\left(\frac{2r^3}{3(2e+f)^2B_2} + \frac{fr^2}{(2e+f)^2C_1}\right) \qquad \text{(c)}$$

The complete angles of rotation, equal to the sum of (a), (b), and (c), are:

$$\psi_1 = \beta_1 M - uS \qquad (168)$$

$$\psi_2 = -\beta_2 M + uS \qquad (169)$$

where

$$\beta_1 = \frac{2e+f}{3B_1} + \frac{e^2r}{(2e+f)^2C_2} + \frac{(e+f)^2r}{(2e+f)^2C_2} + \frac{2r^3}{3(2e+f)^2B_2} + \frac{fr^2}{(2e+f)^2C_1} \qquad (170)$$

$$\beta_2 = \frac{2e+f}{6B_1} + \frac{2e(e+f)r}{(2e+f)^2C_2} - \frac{2r^3}{3(2e+f)^2B_2} - \frac{fr^2}{(2e+f)^2C_1} \qquad (171)$$

$$u = \frac{(2e+f)^2}{16B_1} + \frac{er}{2C_2} \qquad (172)$$

These, then, are the angles of rotation of the terminal cross-sections about axes parallel to the Y axis, produced by the forces and moments given in Fig. 177 (a). As to rotation about the Z axis produced by these forces, conclusions can at once be drawn from a comparison of the cases represented in Figs. 176 and 177 and the use of the reciprocal theorem (Par. 35, page 126). It is easy to see that the forces of Fig. 176, i.e., those in the plane XY of the throw, produce displacements in the XY plane only. Reciprocally, then, the forces in the XZ plane will not produce displacements in the XY plane and therefore there will be no rotation produced by them about the Z axis. The rotation about the X axis produced by the forces of Fig. 177 (a) will be considered below.

Twist of Simply Supported Throw.—Figure 179 is a diagrammatic representation of a throw twisted by the moments M_t applied at the middle cross-sections of the journals. As before, the dotted lines represent the deformed crankshaft. The total twist consists of the sum of the deformations of the portions e of the journals, of the crankpin, and of the two webs. Now if θ_1 and θ_2 are angles of twist of the journal and the crankpin, respectively,

$$\theta_1 = \frac{M_te}{C_1}; \quad \theta_2 = \frac{M_tf}{C_1}.$$

Further, the bending of each web produces the angular displacement θ_3 equal to the angle between the tangents to the curve of flexure at its ends. The bending moment is equal to the twisting moment M_t. Since the moment at each cross-section is constant, the curve of flexure of the web is a circle. Considering it as a beam of length r,

$$\theta_3 = \frac{M_t r}{B_2}$$

The total relative angular displacement θ, measured at the middle sections of the journals, will then be,

$$\theta = 2\theta_1 + \theta_2 + 2\theta_3 = M_t w \tag{173}$$

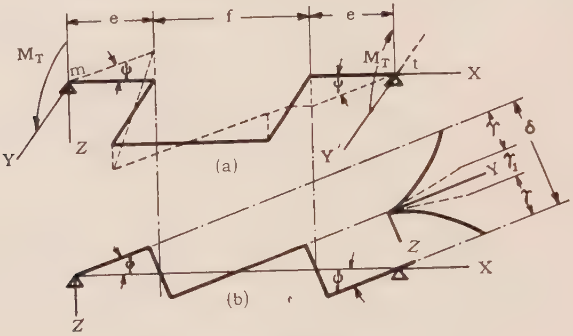

Fig. 179.—Twisting of crank.

where,

$$w = \frac{2e + f}{C_1} + \frac{2r}{B_2} \tag{173a}$$

The couples M_t produce not only the twist θ but also the rotation ψ of the terminal cross-sections about the Y and Y′axes. This rotation, due to the bending of webs and the twist of the crankpin (Fig. 179 (b)), is calculated as in (c) page 195. Then,

$$\psi = \frac{\delta}{2e + f}.$$

The flexure of the web produces a deflection,

$$\gamma = \frac{M_t r^2}{2B_2}$$

and the displacement due to the twist of the crankpin is

$$\gamma_1 = \theta_2 r = \frac{M_t f r}{C_1}$$

Then

$$\delta = 2\gamma + \gamma_1 = M_t\left(\frac{r^2}{B_2} + \frac{fr}{C_1}\right)$$

and

$$\psi = M_t s \tag{174}$$

where

$$s = \frac{1}{2e + f}\left(\frac{r^2}{B_2} + \frac{fr}{C_1}\right) \tag{175}$$

Now, the twist of the throw produced by the forces of Fig. 177 (a) can easily be found; denoting this twist by θ_0, and applying the reciprocal theorem to the cases of Figs. 177 (a) and 179 (a), it is found that

$$M\psi = M_t\theta_0$$

or, employing (174) and (175),

$$\theta_0 = \frac{M\psi}{M_t} = Ms \tag{176}$$

This twist is in the direction of the twisting couples M_t of Fig. 179 (a). When there are two bending moments, M_1 and M_2, one at each support, the corresponding twist is obtained in the same manner and will be equal to,

$$\theta_0 = (M_1 + M_2)s \tag{176a}$$

If, in the case of Fig. 177 (a), M be made equal to zero and in Fig. 179 (a) the moment $M_t + (Sr/2)$ be substituted for M_t, the combination of these two cases gives that shown in Fig. 180. In the further development of the subject the values of the angles ψ_1 and ψ_2, Fig. 180, are necessary. Using Equations (168), (169), and (174),

$$\psi_1 = \left(M_t + \frac{Sr}{2}\right)s - uS$$

$$\psi_2 = \left(M_t + \frac{Sr}{2}\right)s + uS$$

By using (172) and (175) these equations can be written as follows:

$$\psi_1 = M_t s - Sv_1 \tag{177}$$

$$\psi_2 = M_t s + Sv_2 \tag{178}$$

where

$$v_1 = u - \frac{rs}{2} = \frac{(2e + f)^2}{16B_1} + \frac{er}{2C_2} - \frac{r}{2(2e + f)}\left(\frac{r^2}{B_2} + \frac{fr}{C_1}\right) \tag{179}$$

$$v_2 = u + \frac{rs}{2} = \frac{(2e + f)^2}{16B_1} + \frac{er}{2C_2} + \frac{r}{2(2e + f)}\left(\frac{r^2}{B_2} + \frac{fr}{C_1}\right) \tag{180}$$

Twist of Throw Clamped at Middle Cross-section of Journals.—The solution of this problem will be found by superimposing the solution of the case shown in Fig. 181 on that shown in Fig. 179 (a). The couples M of Fig. 181 must be chosen in such a manner as to annihilate the angles of rotation ψ produced by the twisting moments M_t, (Fig. 179 (a)). In this way we obtain the equation

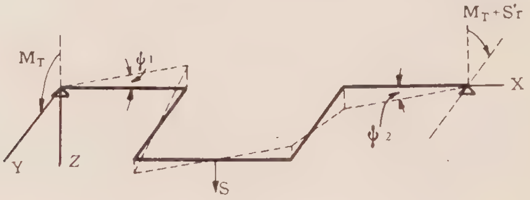

FIG. 180.—Twisting and bending of crank.

$$\psi = \psi' \qquad \text{(d)}$$

The angle ψ is given by equations (174) and (175). The angle ψ' is calculated by using equations (168) and (169) of the case shown in Fig. 177 (a). It is necessary only to put $S = 0$ in these equations and to take into account the fact that in Fig. 181 there are two terminal couples M acting in the same direction. Then,

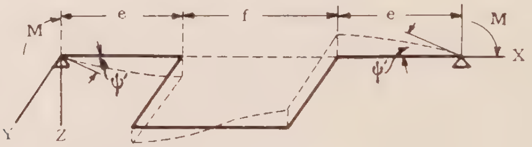

FIG. 181.—Crank having clamped ends.

$$\psi' = (\beta_1 - \beta_2)M \qquad \text{(e)}$$

where β_1 and β_2 are given by equations (170) and (171). Substituting (e) and (174) in equation (d),

$$M = \frac{M_t s}{\beta_1 - \beta_2} \qquad (181)$$

The angle of twist θ_1 for this case will be,

$$\theta_1 = \theta - 2\theta_0 \qquad \text{(f)}$$

where θ is the twist of the throw simply supported (Eq. 173), and θ_0 (Eq. 176) is the decrease of twist due to the bending moment M.

The quotient θ_1/θ gives the ratio in which the torsional flexibility of the throw decreases as a result of constraint.

Substituting equation (181) in (176) and using (173), there will be obtained from (f),

$$\frac{\theta_1}{\theta} = 1 - \frac{2\theta_0}{\theta} = 1 - \frac{2s^2}{(\beta_1 - \beta_2)w} \tag{182}$$

where β_1, β_2, s, and, w are given by equations (170), (171), (175) and (173a).

Numerical Example.—Referring to Fig. 174, let $d_1 = 10.25$ in., $a = 13$ in., $r = 11$ in., $b = 6.5$ in., $h = 5.5$ in., $c = 14$ in., whence $e = 9.25$ in., and $f = 18.5$ in. From notation page 189 we get,

$$B_1 = \pi \cdot \frac{10.25^4 E}{64} = 542E; \quad B_2 = \frac{5.5 \times 14^3 E}{12} = 1{,}258E$$

$$C_1 = \pi \cdot \frac{10.25^4 G}{32} = 1{,}085G; \; C_2 = \frac{14^3 \times 5.5^3 G}{3.6(14^2 + 5.5^2)} = 562G^*$$

Taking $E/G = 2.6$ and substituting this value in, (182),

$$\frac{\theta_1}{\theta} = 1 - \frac{0.005{,}8}{0.040{,}8} = 1 - 0.142.$$

Therefore the torsional flexibility, as compared with the case of no constraint, is decreased by 14.2 per cent.

52. The Multi-throw Crankshaft.—*General Case.*—Consider now the crankshaft with many throws (Fig. 182 shows only a portion of this shaft). Assume it to be simply supported at the middle cross-sections of the journals and number these supports in order 1, 2, 3 . . . Then the throw lying between supports $i - 1$ and i will be the $i - 1$th throw, and all forces acting on it will have this subscript. When the twisting and bending moments at every support are known it is easy to calculate the deformations of any throw from the foregoing equations. The twisting moment at any support can be calculated without difficulty from the equations of statics. For calculating the bending moments, the condition of continuity of the elastic curve at the supports must be taken into consideration. In Fig. 182 two consecutive throws cut out of a multi-throw crankshaft and having supports $i - 1$, i, and $i + 1$, are represented. The bending moment at the support i is resolved into two components, namely, the components m_i^l and M_i^l when the throw on the left of the support i is considered;

---

* The exact formula for torsional rigidity gives $C_2 = \beta c h^3 G = .250 \times 14 \times 5.5^3 G = 580G$. This differs somewhat from the result given above, but the difference is small and does not affect substantially the conclusion made.

and into the components m_i^r and M_i^r for the throw on the right of the support i*.

As before, m denotes the bending moment in the plane of the throw considered, and M the bending moment in the plane perpendicular to the plane of the throw. The positive directions of these moments are shown in Fig. 182 (a). The representation of the same moments by vectors is given in Fig. 182 (b). As m_i^l and M_i^l on the one side, and m_i^r and M_i^r on the other represent the same bending moment, the resultant of m_i^l and M_i^l must be equal and opposite to the resultant of m_i^r and M_i^r as shown in Fig. 182 (b). Therefore, denoting by γ_i the angle between the consecutive throws at i and resolving the couples in the directions y_{i-1} and z_{i-1},

$$\left.\begin{aligned} M_i^l + M_i^r \cos \gamma_i - m_i^r \sin \gamma_i &= 0 \\ m_i^l + M_i^r \sin \gamma_i + m_i^r \cos \gamma_i &= 0 \end{aligned}\right\} \tag{183}$$

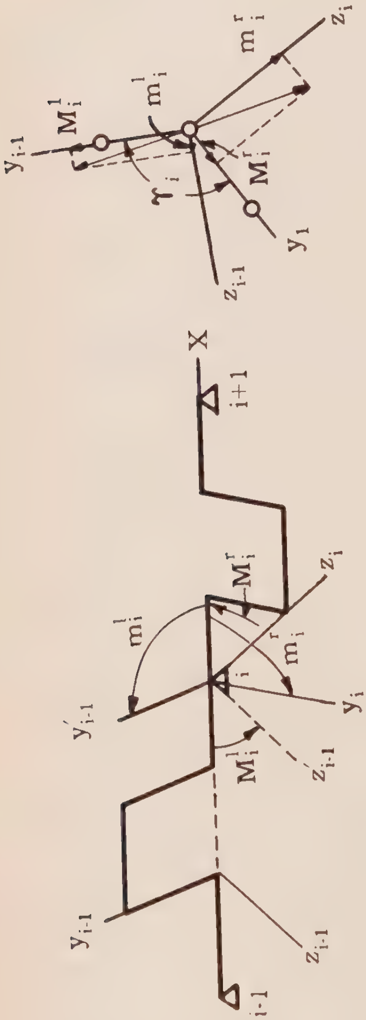

FIG. 182.—Multi-throw crankshaft.

Two more equations are obtained from the conditions of continuity. Consider the throw on the left of the support i. The positive directions of all the forces and couples acting on this throw are shown in Fig. 183. Denote by ϕ_i^l and ψ_i^l the angles of rotation of the cross-section at the support i about the axes z'_{i-1} and y'_{i-1}, respectively. The same rule holds for the signs of the angles as before.

Using Equations (162) and (163) and taking into account the directions of the couples m^r_{i-1} and m_i^l and of the forces Q_{i-1} and P_{i-1},

$$\phi_i^l = m_i^l \alpha_1 - m^r_{i-1} \alpha_2 - P_{i-1} t_1 - Q_{i-1} t_2 \tag{184}$$

---

* The letters l and r, in the superior position, $m_i^l m_i^r$, indicate that the moment is acting on the left throw or the right throw from the support i.

where α_1, α_2, t_1 and t_2 are given by equations (164), (165), (166), and (167). In the same manner, by using equations (168), (169), (177), and (178),

$$\psi_i^l = M_i^l\beta_1 - M^r{}_{i-1}\beta_2 + (M_t)_{i-1}s + S_{i-1}v_2 \tag{185}$$

where β_1, β_2, s, and v_2 are given by equations (170), (171), (175) and (180).

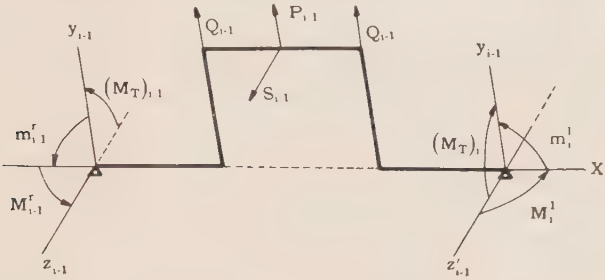

FIG. 183.—Element of multi-throw crankshaft.

Considering now the throw on the right of the support i and denoting by ϕ_i^r and ψ_i^r the angles of rotation of the cross-section at i about the Z_i and Y_i axes of this throw, the following equations are obtained in the same manner as above:

$$\left.\begin{aligned}\phi_i^r &= m_i^r\alpha_1 - m^l{}_{i+1}\alpha_2 + P_it_1 + Q_1t_2\\ \psi_i^r &= M_i^r\beta_1 - M^l{}_{i+1}\beta_2 + (M_t)_is - S_iv_1\end{aligned}\right\} \tag{186}$$

Here $(M_t)_i = (M_t)_{i-1} + S_{i-1}r$ represents the twisting moment at the support i, and the coefficient v_1 is given by equation (179). The small angles of rotation calculated from (184), (185), and (186) can be represented by vectors whose directions coincide with the directions of the corresponding axes of rotation* and whose magnitudes are proportional to the corresponding angles of rotation (Fig. 184). Now as ϕ_i^l and ψ_i^l on one side and ϕ_i^r and ψ_i^r on the other represent the rotations of the same cross-section of the journal at the support i, the resultant rotation of ϕ_i^l and ψ_i^l must be equal to that of the rotations ϕ_i^r and ψ_i^r as shown in Fig. 184. From this figure:

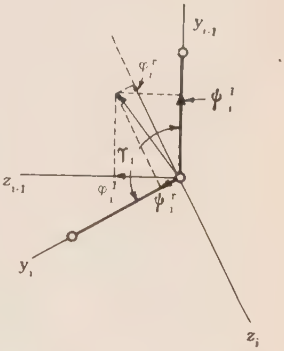

FIG. 184.—Condition of continuity at support.

---

* There exists between the positive direction of the axis of rotation and the direction of rotation the same relation as between rotation and translation in a right-hand screw.

$$\left.\begin{aligned}\phi_i{}^l &= \phi_i{}^r \cos\gamma_i + \psi_i{}^r \sin\gamma_i \\ \psi_i{}^l &= -\phi_i{}^r \sin\gamma_i + \psi_i{}^r \cos\gamma_i\end{aligned}\right\} \tag{187}$$

These equations together with those of (183) give a system of four equations for the support i. Analogous equations can be written for all the intermediate supports. In this manner are obtained a number of equations equal to the number of unknown quantities $m_i{}^l$, $m_i{}^r$, $M_i{}^l$, $M_i{}^r$, where $i = 1, 2, 3, \quad . \quad . \quad . \quad n$, and n is the number of supports.

When equations (184), (185), and (186) are substituted in (187), those of the latter number take the following form:

$$\begin{aligned} &m_i{}^l\alpha_1 - m^r{}_{i-1}\alpha_2 - P_{i-1}t_1 - Q_{i-1}t_2 = (m_i{}^r\alpha_1 - m^l{}_{i+1}\alpha_2 + P_it_1 \\ &\qquad + Q_it_2)\cos\gamma_i + [M_i{}^r\beta_1 - M^l{}_{i+1}\beta_2 - S_iv_1 + (M_t)_is]\sin\gamma_i \\ &M_i{}^l\beta_1 - M^r{}_{i-1}\beta_2 + (M_t)_{i-1}s + S_{i-1}v_2 = [M_i{}^r\beta_1 - M^l{}_{i+1}\beta_2 \\ &\qquad - S_iv_1 + (M_t)_is]\ \cos\ \gamma_i - [m_i{}^r\alpha_1 - m^l{}_{i+1}\alpha_2 + P_it_1 + Q_it_2]\ \sin\ \gamma_i \end{aligned} \tag{188}$$

Now, equations of the type of (183) give:

$$\left.\begin{aligned} &m_i{}^l = -\frac{M_i{}^r + M_i{}^l\cos\gamma_i}{\sin\gamma_i};\ m_i{}^r = \frac{M_i{}^l + M_i{}^r\cos\gamma_i}{\sin\gamma_i} \\ &m^r{}_{i-1} = \frac{M^l{}_{i-1} + M^r{}_{i-1}\ \cos\ \gamma_{i-1}}{\sin\gamma_{i-1}}; \\ &\qquad\qquad\qquad m^l{}_{i+1} = -\frac{M^r{}_{i+1} + M^l{}_{i+1}\cos\gamma_{i+1}}{\sin\gamma_{i+1}} \end{aligned}\right\} \tag{189}$$

Substituting these values in (188):

$$\left.\begin{aligned} &-\frac{\alpha_2}{\sin\gamma_{i-1}}M^l{}_{i-1} - \alpha_2\cot\gamma_{i-1}M^r{}_{i-1} - 2\alpha_1\cot\gamma_iM_i{}^l \\ &-\left\{\frac{\alpha_1}{\sin\gamma_i} + \frac{\alpha_1\cos^2\gamma_i}{\sin\gamma_i} + \beta_1\sin\gamma_i\right\}M_i{}^r + \left\{\beta_2\sin\gamma_i\right. \\ &\left.-\alpha_2\frac{\cos\gamma_i\cos\gamma_{i+1}}{\sin\gamma_{i+1}}\right\}M^l{}_{i+1} - \alpha_2\frac{\cos\gamma_iM^r{}_{i+1}}{\sin\gamma_{i+1}} = P_{i-1}t_1 \\ &+ Q_{i-1}t_2 + (P_it_1 + Q_it_2)\cos\gamma_i - S_iv_1\sin\gamma_i + (M_t)_is\sin\gamma_i. \\ &- M^r{}_{i-1}\beta_2 + (\alpha_1 + \beta_1)M_i{}^l + (\alpha_1 - \beta_1)\cos\gamma_iM_i{}^r \\ &+\left\{\beta_2\cos\gamma_i + \alpha_2\frac{\sin\gamma_i\cos\gamma_{i+1}}{\sin\gamma_{i+1}}\right\}M^l{}_{i+1} + \alpha_2\frac{\sin\gamma_i}{\sin\gamma_{i+1}}M^r{}_{i+1} \\ &= (-M_t)_{i-1}s + (M_t)_is\cos\gamma_i - S_{i-1}v_2 - S_iv_1\cos\gamma_i - \\ &\qquad\qquad\qquad (P_it_1\ +\ Q_it_2)\sin\gamma_i \end{aligned}\right\} \tag{190}$$

These equations play the same role in calculating multi-throw crankshafts as the well-known equations of three moments of Clapeyron for the calculation of continuous beams. (See Eq. 87, page 113.)

Special Cases of Equations (190).—When $\gamma_2 = \gamma_3 = \gamma$, Equations (190) take the following simplified form:

$$\left.\begin{aligned}
&-\frac{\alpha_2}{\sin\gamma}M^l{}_{i-1} - \alpha_2 \cot \gamma M^r{}_{i-1} - 2\alpha_1 \cot \gamma M_i{}^l \\
&-\Bigg\{\frac{\alpha_1}{\sin\gamma} + \alpha_1 \cos\gamma \cot\gamma + \beta_1 \sin\gamma\Bigg\} M_i{}^r + (\beta_2 \sin\gamma \\
&- \alpha_2 \cos\gamma \cot\gamma)M^l{}_{i+1} - \alpha_2 \cot\gamma M^r{}_{i+1} = P_{i-1}t_1 + Q_{i-1}t_2 \\
&+ (P_it_1 + Q_it_2)\cos\gamma - S_iv_1 \sin\gamma + (M_t)_is \sin\gamma. \\
&-M^r{}_{i-1}\beta_2 + (\alpha_1 + \beta_1)M_i{}^l + (\alpha_1 - \beta_1)\cos\gamma M_i{}^r \\
&+ (\beta_2 + \alpha_2)\cos\gamma M^l{}_{i+1} + \alpha_2 M^r{}_{i+1} = -(M_t)_{i-1}s + \\
&(M_t)_is \cos\gamma - S_{i-1}v_2 - S_iv_1 \cos\gamma - (P_it_1 + Q_it_2)\sin\gamma
\end{aligned}\right\} \quad (191)$$

Equations (191) take the form of (192) given here, when the crankshaft is subjected to twisting only. Substituting therein $P_{i-1} = P_i = Q_{i-1} = Q_i = S_{i-1} = S_i = 0$, and putting $(M_t)_{i-1} = (M_t)_i = M_t$

$$\left.\begin{aligned}
&-\frac{\alpha_2}{\sin\gamma}M^l{}_{i-1} - \alpha_2 \cot\gamma M^r{}_{i-1} - 2\alpha_1 \cot\gamma M_i{}^l \\
&\quad-\left(\frac{\alpha_1}{\sin\gamma} + \alpha_1 \cos\gamma \cot\gamma + \beta_1 \sin\gamma\right)M_i{}^r + (\beta_2 \sin\gamma \\
&\quad- \alpha_2 \cos\gamma \cot\gamma)M^l{}_{i+1} - \alpha_2 \cot\gamma M^r{}_{i+1} = M_ts \sin\gamma. \\
&-\beta_2M^r{}_{i-1} + (\alpha_1 + \beta_1)M_i{}^l + (\alpha_1 - \beta_1)\cos\gamma M_i{}^r \\
&\quad+ (\alpha_2 + \beta_2)\cos\gamma M^l{}_{i+1} + \alpha_2M^r{}_{i+1} = M_ts(\cos\gamma - 1)
\end{aligned}\right\} \quad (192)$$

53. Application of Equations to the Three-throw Crankshaft.—*General.*—In the case of the three-throw crankshaft,

$$\gamma_2 = \gamma_3 = \gamma = 120°, \ \sin\gamma = \frac{1}{2}\sqrt{3}, \ \cos\gamma = -\frac{1}{2}, \ \cot\gamma = -\frac{1}{\sqrt{3}}$$

Since the shaft is assumed to be simply supported, the bending moments at the terminal cross-sections are equal to zero, i.e.,

$$M_1{}^l = M_1{}^r = M_4{}^l = M_4{}^r = 0.$$

Under these assumptions equations (191) for the two intermediate supports become:

$$\left.\begin{aligned}
&(\alpha_1+\beta_1)M_2{}^l-\frac{1}{2}(\alpha_1-\beta_1)M_2{}^r-\frac{1}{2}(\alpha_2+\beta_2)M_3{}^l+\alpha_2M_3{}^r\\
&\qquad=-(M_t)_1s-\frac{1}{2}(M_t)_2s-S_1v_2+\frac{1}{2}S_2v_1\\
&\qquad\qquad-\frac{\sqrt{3}}{2}(P_2t_1+Q_2t_2)\\
&\alpha_1M_2{}^l-\left(\frac{5}{4}\alpha_1+\frac{3}{4}\beta_1\right)M_2{}^r+\left(\frac{3}{4}\beta_2-\frac{1}{4}\alpha_2\right)M_3{}^l+\frac{1}{2}\alpha_2M_3{}^r\\
&\qquad=\frac{3}{4}(M_t)_2s+\frac{\sqrt{3}}{2}\Big[(P_1t_1+Q_1t_2)-\\
&\qquad\qquad\frac{1}{2}(P_2t_1+Q_2t_2)\Big]-\frac{3}{4}v_1S_2\\
&-\beta_2M_2{}^r+(\alpha_1+\beta_1)M_3{}^l-\frac{1}{2}(\alpha_1-\beta_1)M_3{}^r=-(M_t)_2s-\\
&\qquad\frac{1}{2}(M_t)_3s-S_2v_2+\frac{1}{2}S_3v_1-\frac{\sqrt{3}}{2}(P_3t_1+Q_3t_2)\\
&-\alpha_2M_2{}^l+\frac{1}{2}\alpha_2M_2{}^r+\alpha_1M_3{}^l-\left(\frac{5}{4}\alpha_1+\frac{3}{4}\beta_1\right)M_3{}^r=\frac{3}{4}(M_t)_3s\\
&\qquad+\frac{\sqrt{3}}{2}\Big[P_2t_1+Q_2t_2-\frac{1}{2}(P_3t_1+Q_3t_2)\Big]-\frac{3}{4}S_3v_1
\end{aligned}\right\}\quad(193)$$

Crankshaft Subject to Twist by the Couples M_t Acting at the Ends.—Equations (193), written for the two intermediate supports, then reduce to:

$$\left.\begin{aligned}
&(\alpha_1+\beta_1)M_2{}^l-\frac{1}{2}(\alpha_1-\beta_1)M_2{}^r-\frac{1}{2}(\alpha_2+\beta_2)M_3{}^l+\alpha_2M_3{}^r\\
&\qquad=-\frac{3}{2}M_ts.\\
&\alpha_1M_2{}^l-\left(\frac{5}{4}\alpha_1+\frac{3}{4}\beta_1\right)M_2{}^r+\left(\frac{3}{4}\beta_2-\frac{1}{4}\alpha_2\right)M_3{}^l\\
&\qquad+\frac{1}{2}\alpha_2M_3{}^r=\frac{3}{4}M_ts.\\
&-\beta_2M_2{}^r+(\alpha_1+\beta_1)M_3{}^l-\frac{1}{2}(\alpha_1-\beta_1)M_3{}^r=-\frac{3}{2}M_ts\\
&-\alpha_2M_2{}^l+\frac{1}{2}\alpha_2M_2{}^r+\alpha_1M_3{}^l-\left(\frac{5}{4}\alpha_1+\frac{3}{4}\beta_1\right)M_3{}^r=\frac{3}{4}M_ts.
\end{aligned}\right\}\quad(194)$$

As a numerical example the three-throw crankshaft of a 900 hp. Diesel engine will be considered (Fig. 185) all dimensions of which are given in paragraph 51, page 199. From these and equations (164), (167), (170), (171), (175), (179), and (180) it is found that:

$$\left.\begin{aligned}
&\alpha_1 = 0.851\,\frac{2e+f}{B_1};\ \alpha_2 = 0.478\,\frac{2e+f}{B_1};\ s = 0.232\,\frac{2e+f}{B_1}\\
&\beta_1 = 0.864\,\frac{2e+f}{B_1};\ \beta_2 = 0.381\,\frac{2e+f}{B_1};\ v_1 = 0.408\frac{(2e+f)r}{B_1}\\
&v_2 = 0.640\,\frac{(2e+f)r}{B_1};t_1 = 0.559\frac{(2e+f)r}{B_1};t_2 = 1.013\frac{(2e+f)r}{B_1}
\end{aligned}\right\} \qquad (195)$$

Substituting these figures in equations (194):

$$\begin{aligned}
1.715M_2^l + 0.0065M_2^r - 0.429M_3^l + 0.478M_3^r &= -0.348M_t\\
0.851M_2^l - 1.712M_2^r + 0.1663M_3^l + 0.239M_3^r &= 0.174M_t\\
- 0.381M_2^r + 1.715M_3^l + 0.0065M_3^r &= -0.348M_t\\
- 0.478M_2^l + 0.239M_2^r + 0.851M_3^l - 1.712M_3^r &= 0.174M_t
\end{aligned}$$

from which,

$$M_2^l = -0.210M_t;\quad M_2^r = -0.260M_t;\quad M_3^l = -0.260M_t;\quad M_3^r = -0.205M_t.$$

The angle of twist for any crank is now easily obtained. Equation (173) gives the twist if there is no constraint, namely $\theta = M_tw$. The diminishing of this angle, due to the effects of the bending moments M, is calculated from equation (176a), page 197.

For the first throw,

$$\theta_0' = -0.210M_ts$$

For the second throw,

$$\theta_0'' = -(0.260 + 0.260)M_ts.$$

For the third throw,

$$\theta_0''' = -0.205M_ts.$$

The decrease of torsional rigidity due to the constraint, is:

For the first throw,

$$\frac{\theta_0'}{\theta} = \frac{0.210s}{w} = 0.0305$$

i.e., about 3%. For the second throw,

$$\frac{\theta_0''}{\theta} = \frac{0.520s}{w} = 0.0775,$$

i.e. about 7.8%. For the third throw,

$$\frac{\theta_0'''}{\theta} = \frac{0.205s}{w} = 0.0301,$$

i.e. about 3%.

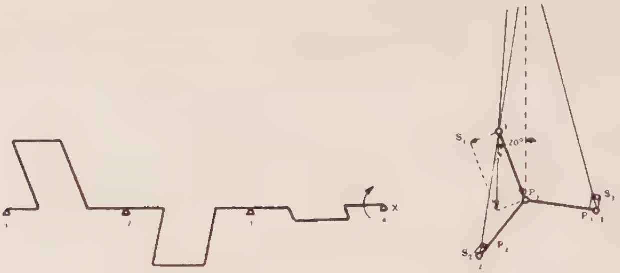

Fig. 185.—Three throw crankshaft.

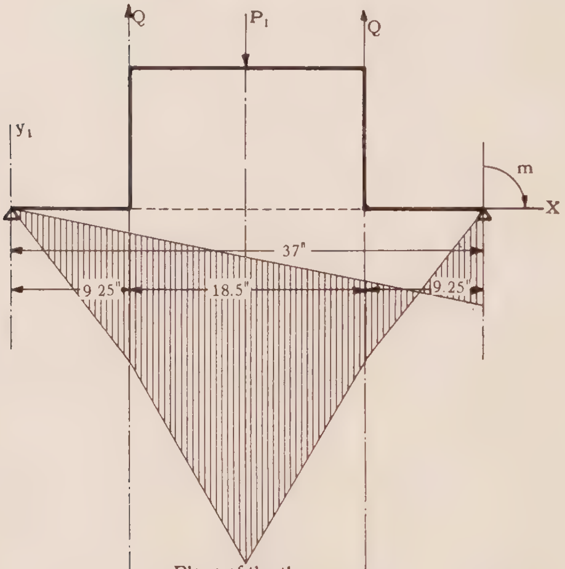

(a) Plane of the throw

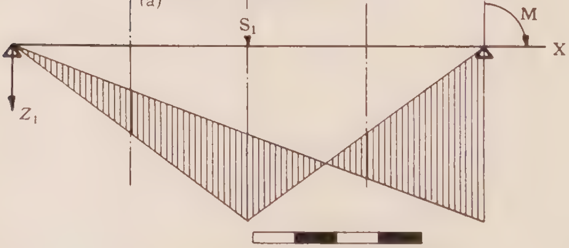

(b) Scale = 25×10^4 pound-inches

Plane perpendicular to plane of throw

Fig. 186.

In this manner the question of torsional flexibility* of the shaft considered is solved. It is seen that the effect of the constraint in the first and third throws is small. For the middle throw this effect is about half of that calculated above (Par. 51, page 199) on the assumption that the throw is clamped at the middle of the journals. Similar results may be expected for any three-throw crankshaft with $\gamma_2 = \gamma_3 =$ 120 degrees.

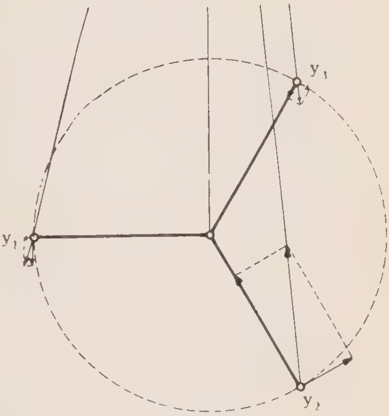

Fig. 187.

The bending and twisting of the same crankshaft due to the forces P, Q, and S acting on the crankpins may now be considered. The forces P and S are obtainable from the gas pressure and inertia force diagrams. Examining first the case given in Fig. 185, where the maximum force acts on the first throw, the values of the forces considered are as follows:

Number of crank	Angle of crank, degrees	P, pounds	S, pounds	Q, pounds
1	20	−65,000	29,400	7,700
2	140	− 9,400	− 5,830	7,700
3	260	− 4,300	11,100	7,700

Substituting in (193) the numerical values of (195) and the values of the forces given in the preceding table

$$1.715M_2^l + 0.0065M_2^r - 0.429M_3^l + 0.478M_3^r = -399 \times 10^3 \text{ lb. in.}$$

$$0.851M_2^l - 1.712M_2^r + 0.1663M_3^l + 0.239M_3^r = -206 \times 10^3 \text{ lb. in.}$$

$$-0.381M_2^r + 1.715M_3^l + 0.0065M_3^r = -96 \times 10^3 \text{ lb. in.}$$

$$-0.478M_2^l + 0.239M_2^r + 0.851M_3^l - 1.712M_3^r = 6.47 \times 10^3 \text{ lb. in.}$$

---

* This torsional rigidity of the crankshaft, as it will be seen later in chapter XI on dynamics, must be known in studying torsional vibrations.

from which,

$$M_2{}^l = -258 \times 10^3 \text{ lb. in.} \qquad M_2{}^r = -7.15 \times 10^3 \text{ lb. in.}$$
$$M_3{}^l = -54.5 \times 10^3 \text{ lb. in.} \qquad M_3{}^r = 40 \times 10^3 \text{ lb. in.}$$

These values substituted in equations (189) give:

$$m_2{}^l = -140 \times 10^3 \text{ lb. in.} \qquad m_2{}^r = -287 \times 10^3 \text{ lb. in.}$$
$$m_3{}^l = -77.5 \times 10^3 \text{ lb. in.} \qquad m_3{}^r = -86 \times 10^3 \text{ lb. in.}$$

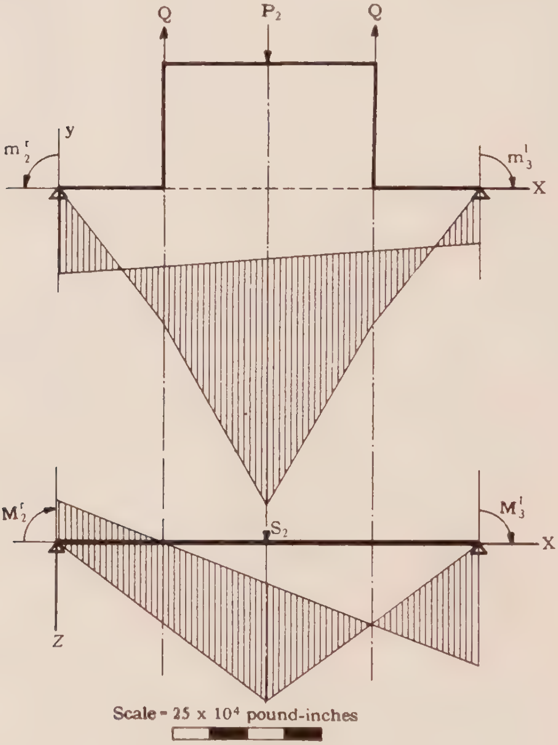

FIG. 188.

The diagrams of bending moment for the first crank, where the maximum bending moment is to be expected, are given in Fig. 186. The upper one gives the moments in the plane of the throw and the lower those in a plane perpendicular to the plane of the throw. The stress in any element of the throw may now be calculated in the usual manner.

Secondly, consider the case shown in Fig. 187, where the maximum force is acting on the second crank. The corresponding values of forces, obtained from gas pressure and inertia force diagrams, are as follows:

Number of crank	Angle of crank, degrees	P, pounds	S, pounds	Q, pounds
1	90	3,030	13,250	7,700
2	210	−70,000	30,600	7,700
3	330	− 8,100	− 5,970	7,700

Proceeding now as above, equations (193) give:

$$M_2^l = 101.5 \cdot 10^3 \text{ lb. in.} \quad M_2^r = -68.5 \cdot 10^3 \text{ lb. in.}$$
$$M_3^l = -218 \cdot 10^3 \text{ lb. in.} \quad M_3^r = -23.8 \cdot 10^3 \text{ lb. in.}$$

which values, substituted in equation (189) give:

$$m_2^l = 137 \times 10^3 \text{ lb. in.} \qquad m_2^r = 157 \times 10^3 \text{ lb. in.}$$
$$m_3^l = -98.3 \times 10^3 \text{ lb. in.} \quad m_3^r = -238 \times 10^3 \text{ lb. in.}$$

The greatest stresses are now to be expected in the second throw. The diagrams of bending moments for this throw are given in Fig. 188 from which the corresponding stresses can be calculated in the usual manner.

54. Open Coiled Helical Spring.—*Axial Load.*—In considering close coiled helical springs (Par. 9, page 31), it was assumed that the angle α, which the coils make with planes perpendicular to the axis Z of the spring (Fig. 189), is very small. Now, in open coiled springs this is not the case; and the effect of this angle on the stresses and deformation in the spring will be considered. Let OX be a tangent to the center line of the wire at any point O and the plane XY parallel to the axis Z, i.e. tangential to the cylindrical surface containing the helical center line of the wire. The moment of the force P on the normal cross section O, equal to PR, is acting in the plane containing this point and the axis Z. In the figure this moment is represented by the vector OA lying in the tangent plane XY and perpendicular to the Z axis. The relation between the positive direction of the moment PR and the direction of the vector OA is the same as between rotation and translation of a right hand screw. Resolving OA in the X and Y directions we have a torque moment,

$$M_t = OB = PR \cos \alpha \tag{a}$$

and a bending moment,

$$M = OC = PR \sin \alpha \tag{b}$$

acting on the cross section at O. The maximum principal stress will now be found, by using equation (158)

$$p_{\max} = \frac{16}{\pi d^3} PR(1 + \sin \alpha) \tag{196}$$

in which d equals the diameter of the wire.

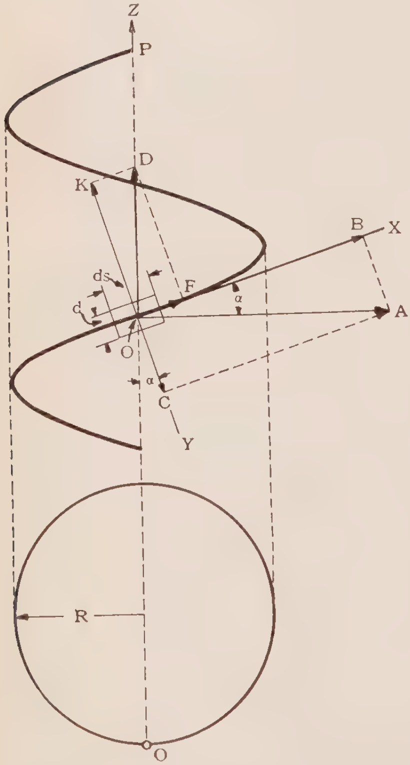

FIG. 189.—Open coiled spring under tension.

The maximum shearing stress will also be, from equation (160),

$$(p_t)_{\max} = \frac{16}{\pi d^3} PR.$$

It will be noted that this is the same as previously found for a close coiled spring (Eq. 34). The extension δ of the spring will be found from the consideration of the energy stored in the spring during deformation. The energy of deformation in an element ds of the spring, by using equations (33) and (52), is:

$$dU = \frac{M^2 ds}{2EI} + \frac{M_t{}^2 ds}{2GI_p}$$

which gives for complete energy the expression,

$$U = \left(\frac{M^2}{2EI} + \frac{M_t{}^2}{2GI_p}\right) l \tag{c}$$

where the length of n coils of the spring is denoted by,

$$l = \frac{2\pi R n}{\cos \alpha} \tag{d}$$

Now δ may be found by equating the work done to the sum of the energies due to bending and twist:

$$\frac{P\delta}{2} = l\left(\frac{M^2}{2EI} + \frac{M_t{}^2}{2GI_p}\right)$$

from which, by using (a) and (b),

$$\delta = PlR^2\left(\frac{\sin^2\alpha}{EI} + \frac{\cos^2\alpha}{GI_p}\right) = \frac{32PlR^2}{\pi d^4}\left(\frac{2\sin^2\alpha}{E} + \frac{\cos^2\alpha}{G}\right) \tag{197}$$

For $\alpha = 0$, this equation reduces to equation 35, page 31. It should be noted that equation (197) was obtained on the assumption that the wire of the spring is of circular cross section. For sections having other forms, the corresponding value of torsional rigidity C (see. Par. 10) instead of GI_p must be used.

Extension of the spring is accompanied by rotation of the ends about the Z axis. The magnitude of this rotation may easily be obtained from the consideration of angular deformations of the element ds (Fig. 189).

The angular deformation due to twist, from equation 29, is

$$\frac{M_t ds}{GI_p} \tag{e}$$

The corresponding axis of rotation is OX, therefore rotation, due to (e), about Z axis, is

$$\frac{M_t ds}{GI_p}\sin\alpha \tag{f}$$

The angular deformation due to bending will be, from equation 48,

$$\frac{M ds}{EI} \tag{g}$$

where the corresponding axis of rotation is OY.
Rotation due to (g), about the axis Z (Fig. 189) will be,

$$-\frac{M ds}{EI}\cos\alpha \tag{h}$$

hence the total rotation about Z axis, due to deformation of an element ds, is,

$$ds\left(\frac{M_t}{GI_p}\sin\alpha - \frac{M}{EI}\cos\alpha\right) \tag{k}$$

If one end of the spring be fixed the angle of rotation of the other end about the Z axis will be,

$$\phi = l\left(\frac{M_t\sin\alpha}{GI_p} - \frac{M\cos\alpha}{EI}\right) \tag{l}$$

or substituting (a) and (b) and putting $G = \dfrac{E}{2\left(1 + \frac{1}{m}\right)}$ the following result for a circular cross section will be obtained:

$$\phi = \frac{32}{\pi d^4} \frac{1}{mE} PlR \sin 2\alpha \tag{198}$$

In the case of other forms of cross-section, the corresponding value of torsional rigidity C instead of GI_p must be inserted in (l).

Axial Twist.—Let OD (Fig. 189) represent (*) the axial twisting moment M_z. Then torque moment and bending moment acting on the cross section at O will be,

$$M_t = M_z \sin \alpha \tag{m}$$
$$M = M_z \cos \alpha \tag{n}$$

The corresponding angular deformations are given by (f) and (g). It must be noted that the bending moment, represented by vector OK has an opposite direction to that of vector OC, considered before, therefore for the angle of rotation about the Z axis, equation

$$ds\left(\frac{M_t}{GI_p} \sin \alpha + \frac{M}{EI} \cos \alpha\right), \tag{p}$$

instead of equation (k), must be used. Assuming that the spring is fixed at the bottom, and using equation (m) and (n), the angle of rotation of the top end about the Z axis will be for a circular cross section:

$$\phi_1 = lM_z\left(\frac{\sin^2 \alpha}{GI_p} + \frac{\cos^2 \alpha}{EI}\right) = \frac{32lM_z}{\pi d^4}\left(\frac{\sin^2 \alpha}{G} + \frac{2 \cos^2 \alpha}{E}\right) \tag{199}$$

By using the reciprocal theorem (page 126) and remembering that the axial tensile force P produces a positive† angle of rotation (Eq. 198) about the Z axis it can be concluded that the twisting moment M_z will produce extension of the spring δ_1, which will be found from the equation, $P\delta_1 = M_z\phi$, from which, by using (198),

$$\delta_1 = \frac{32}{\pi d^4} \cdot \frac{1}{mE} M_z lR \sin 2\alpha \tag{200}$$

Axial Bending M_b.—By using the same method, as above, bending of the axis of the spring by couples M_b in the plane of the Fig. 190 (a) can be obtained. Let vector OA (Fig. 190 (b)) perpendicular to the plane of the Fig. 190 (a) represent the couple M_b acting on the cross section at O. Resolving it in two components, shown in Fig. 190 (b), we will have (1) moment,

---

* The same rule of right hand screw (p. 211) is used.

† Following the rule of right hand screw (p. 211).

$$M_1 = M_b \cos \theta \qquad \text{(r)}$$

represented by the vector OB producing bending of the wire in the plane tangent to the cylindrical surface of the radius R, and (2) moment $M_2 = M_b \sin \theta$, represented by vector OC, acting in the axial plane through O. Vector OC can be resolved into two components as was done previously with the vector OA (see Fig. 189). In this manner expressions for the torque moment* and bending moment, in the plane of coil, are obtained as follows:

$$M_t = -M_b \sin \theta \cos \alpha \qquad \text{(s)}$$

$$M = M_b \sin \theta \sin \alpha \qquad \text{(t)}$$

Assuming a circular cross section and combining (r) and (t) vectorially, the resulting bending moment will become

$$M_b\sqrt{\cos^2 \theta + \sin^2 \theta \sin^2 \alpha} \qquad \text{(u)}$$

The potential energy stored in an element $ds = Rd\theta/\cos \alpha$ of the spring by using (u) and (s) will be,

$$dU = \frac{Rd\theta}{\cos \alpha}\left[M_b{}^2\frac{(\cos^2 \theta + \sin^2 \alpha \sin^2 \theta)}{2EI} + M_b{}^2\frac{\sin^2 \theta \cos^2 \alpha}{2GI_p}\right] \qquad \text{(w)}$$

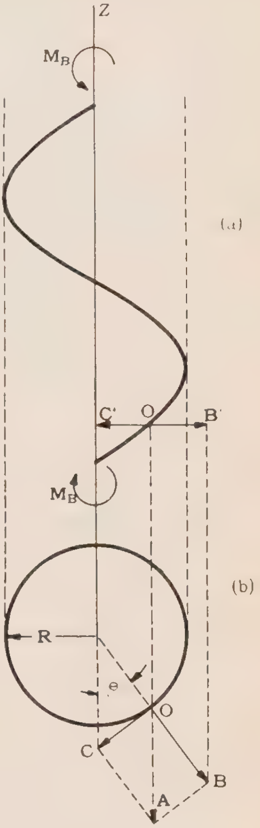

FIG. 190.—Open coiled spring under pure bending.

Integrating (w) within the limit $\theta = 0$ to $\theta = 2\pi n$, and remembering that

$$\int_0^{2\pi} \sin^2 \theta d\theta = \int_0^{2\pi} \cos^2 \theta d\theta = \pi,$$

the following expression for the potential energy of the spring will be obtained:

$$U = \frac{R\pi n}{\cos \alpha}\left[\frac{M_b{}^2(1 + \sin^2 \alpha)}{2EI} + M_b{}^2\frac{\cos^2 \alpha}{2GI_p}\right] =$$

$$= \frac{8M_b{}^2 l}{\pi d^4}\left[\frac{2(1 + \sin^2 \alpha)}{E} + \frac{\cos^2 \alpha}{G}\right]$$

---

* The direction of torque moment which we had in Fig. 189 is taken as positive.

Now the angular deflexion ψ of the upper end of the spring, if the lower end is fixed, will be found from the condition that the work done by the bending moment M_b will be equal to the energy stored in the spring, or

$$\frac{M_b\psi}{2} = \frac{8M_b{}^2l}{\pi d^4}\left[\frac{2(1 + \sin^2 \alpha)}{E} + \frac{\cos^2 \alpha}{G}\right]$$

From which,

$$\psi = \frac{16}{\pi d^4} M_b l\left[\frac{2(1 + \sin^2 \alpha)}{E} + \frac{\cos^2 \alpha}{G}\right] \tag{201}$$

Let the length of the axis of the spring be denoted by $h = l \sin \alpha$, then from (201), the curvature of this axis due to bending will be,

$$\frac{1}{\rho} = \frac{\psi}{h} = \frac{16M_b}{\pi d^4 \sin \alpha}\left[\frac{2(1 + \sin^2 \alpha)}{E} + \frac{\cos^2 \alpha}{G}\right] \tag{202}$$

and the deflection of the upper end of the spring, if the lower be fixed, will be

$$\delta = \frac{h^2}{2\rho} = \frac{\psi h}{2} = \frac{8M_b h^2}{\pi d^4 \sin \alpha}\left[\frac{2(1 + \sin^2 \alpha)}{E} + \frac{\cos^2 \alpha}{G}\right] \tag{203}$$

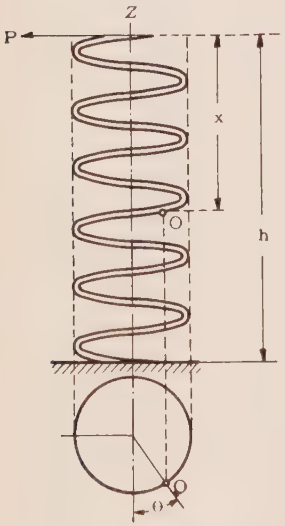

FIG. 191.—Open coiled spring bent by lateral force.

All formulae developed in this paragraph must be considered as approximations only, because R and α were treated as constants; though actually they vary during the deformation of the spring.*

Example 68.—Determine the deflection of the upper end of the spring and the stresses produced by the force P (Fig. 191).

Solution.—Comparing equation (202) with the equation (48) for the curvature of a solid bar submitted to pure bending, it is seen that instead of flexural rigidity of the bar we have in the case of a helical spring the quantity

$$\frac{\sin \alpha}{\dfrac{(1 + \sin^2 \alpha)}{2EI} + \dfrac{\cos^2 \alpha}{2GI_p}} \tag{a}$$

From this it can be concluded that for obtaining the deflection of the spring the known formula for the deflection of a cantilever can be used. It is only necessary to substitute (a) for the flexural rigidity of the cantilever. In such manner we have,†

$$\delta = \frac{Ph^3}{3 \sin \alpha}\left[\frac{1 + \sin^2 \alpha}{2EI} + \frac{\cos^2 \alpha}{2GI_p}\right] \tag{b}$$

If $\alpha = \pi/2$, this reduces to the known cantilever formula.

---

* The theory of buckling of helical springs under the action of axial compression is discussed by R. Grammel, see Z. F. Angew. Math. u. Mech. vol. 4, p. 384, 1924.

† The effect of shearing force on deflections is here neglected.

In order to find out the stresses, forces acting on the cross section of the wire at any point O (Fig. 191) will now be considered. These forces reduce to (1) the force P acting in the center of the cross section (2) the couple

$$M_b = Px \tag{c}$$

acting in the plane of the Fig. 191 and (3) the couple

$$M_z = PR \cos \theta \tag{d}$$

acting in the plane perpendicular to the axis Z. By using (m) and (s) together with (c) and (d) the following expression for the torque moment at O will now be obtained:

$$M_t = PR \cos \theta \sin \alpha - Px \sin \theta \cos \alpha \tag{e}$$

By using (n) and (t) we have for the bending moment in the plane of the coil the following expression:

$$M = PR \cos \theta \cos \alpha + Px \sin \theta \sin \alpha \tag{f}$$

Bending moment in the plane perpendicular to the plane of the coil, from (r), becomes

$$M_1 = Px \cos \theta \tag{g}$$

Combining (f) and (g) vectorially, the following expression for the complete bending moment will be obtained

$$\sqrt{M^2 + M_1^2} = P\sqrt{(R \cos \theta \cos \alpha + x \sin \theta \sin \alpha)^2 + x^2 \cos^2 \theta} \tag{h}$$

Maximum stresses will be obtained at the fixed end, where $x = h$. Two sections at this end of the spring will now be considered, namely Section $\theta = 0$ and Section $\theta = \pi/2$ (see Fig. 191). For $\theta = 0$, from (e) and (h), we have

$$M_t = PR \sin \alpha \tag{k}$$

$$\sqrt{M^2 + M_1^2} = P\sqrt{R^2 \cos^2 \alpha + h^2} \tag{l}$$

It is easy to see that in this section bending stresses are predominant.

For $\theta = \pi/2$, we have,

$$M_t = -Ph \cos \alpha \tag{m}$$

$$\sqrt{M^2 + M_1^2} = Ph \sin \alpha \tag{n}$$

For small α torque moment in this section will be much greater than bending moment. Combining shearing stresses of twist with normal stresses of bending (see Par. 50) maximum principal stress easily can be obtained.

CHAPTER IX

CURVED BARS

55. Theory of Bending.—*Pure Bending of a Curved Bar.*—A curved bar under the action of equal and opposite couples at its ends is said to undergo pure bending (Fig. 192). Considering the simplest case, when the bar has a longitudinal plane of symmetry and external couples are acting in this plane, it is easy to see that bending will take place in this same plane. The solution of the problem of stress distribution and deflection of the bar will be obtained on the assumption that transverse sections of the bar originally plane and normal to the central line remain so after bending.* Let *ab* and *cd* denote two cross-sections of the bar and $d\phi$ denote a small angle between them before bending. During bending, under the action of the couples M, the cross-section *cd* will rotate with respect to *ab*. Let $\Delta d\phi$ denote the small angle of rotation. Due to this rotation the longitudinal fibers on the convex side of the bar will be compressed and the fibers on the concave side will be extended. Let *n-n* denote the neutral surface.

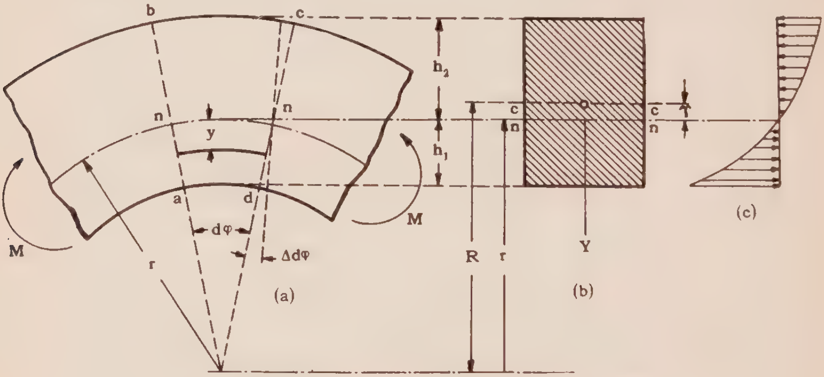

Fig. 192.—Curved bar in pure bending.

---

* This theory was developed by Winkler, *Der Civilingenieur* (1858), page 232. See also his book *Elasticität und Festigkeit* (1867), page 253.

The extension of any fiber distant* y from the neutral surface will be equal to $y\Delta d\phi$ and the corresponding unit elongation will be

$$e = \frac{y\Delta d\phi}{(r - y)d\phi} \tag{a}$$

where r denotes the radius of the neutral surface. Assuming that there is no lateral pressure between the longitudinal fibers, the stress at distance y from the neutral axis will be

$$p = \frac{Ey\Delta d\phi}{(r - y)d\phi} \tag{b}$$

It is seen that the stress distribution follows a hyperbolic law instead of a linear law, as in the case of straight bars (see Fig. 192 (c)). From the condition that stresses distributed over a cross-section are equivalent to a couple, it can be concluded that the neutral axis must be displaced from the center of gravity towards the center of curvature of the bar. It is easy to see also that, in the case of a rectangular cross-section, greater stresses will act on the concave side. In order to make the stresses in the most remote fibers (both in tension and in compression) equal, it is necessary to use cross-sections in which the center of gravity will be nearer to the concave side than it is to the convex side of the bar. Let

R = radius of curvature of the center line of a curved bar.
r = radius corresponding to neutral surface.
γ = distance of the center of gravity of cross section from neutral axis.
h = depth of the cross section.
h_1, h_2 = distances of the most remote fibers from neutral surface.
A = area of the cross section.
S = longitudinal force.
Q = shearing force.
y = distance of any element of the cross section from neutral axis.
y_1 = distance of any element of the cross section from the axis throughout the center of gravity.
v = distance of any element of the cross section from the axis through the center of curvature of the bar.
u = radial displacement in bending thin circular rings.
mA = modified area of the cross section.
s = distance measured along the axis of curved bar.
q_{cr} = critical pressure per unit length of a circular ring.

---

* y is positive towards the center of curvature.

In order to obtain the two unknown quantities r and $\Delta d\phi$ in equation (b), two equations of statics will be used. The first equation is based on the condition that the sum of all stresses over a cross-section is equal to zero. The second equation is based on the condition that the moment of these stresses about the neutral axis is equal to the moment M of the external couples. The equations are:*

$$\int p\,dA = \frac{E\Delta d\phi}{d\phi}\int\frac{y\,dA}{r-y} = 0 \tag{c}$$

$$\int py\,dA = \frac{E\Delta d\phi}{d\phi}\int\frac{y^2dA}{r-y} = M \tag{d}$$

Equation (c) will be used for determining r. The integral of equation (d) can be simplified as follows:

$$\int\frac{y^2dA}{r-y} = -\int\left(y - \frac{ry}{r-y}\right)dA = -\int y\,dA + \int\frac{ry\,dA}{r-y} \tag{e}$$

The first integral on the right side of (e) represents the moment of the cross-section about the neutral axis and the second, as seen from equation (c) is equal to zero. Therefore,

$$\int\frac{y^2dA}{r-y} = A\gamma \tag{e$_1$}$$

where γ denotes the displacement of the neutral axis from the center of gravity.

Substituting in equation (d)

$$\frac{E\Delta d\phi}{d\phi} = \frac{M}{A\gamma} \tag{204}$$

Now from equation (b)

$$p = \frac{My}{A\gamma(r-y)} \tag{f}$$

The stresses in the most remote fibers will therefore be

$$p_{\max} = \frac{Mh_1}{A\gamma(r-h_1)} \text{ and } p_{\min} = -\frac{Mh_2}{A\gamma(r+h_2)} \tag{205}$$

If r is determined from equation (c), the maximum stresses will be found from (205).

If the depth of the cross-section is small in comparison with the radius R for the central line of the bar, y can be neglected in comparison with r. Then, from equation (c), it follows that the neutral axis coincides with the center of gravity of the cross-section and, from (d), that

---

* The integral sign in these equations (c, d, e, e_1) indicates that integration is taken over the entire area of the cross-section.

$$\frac{E\Delta d\phi}{d\phi}\cdot\frac{I}{R} = M$$

or,

$$\Delta d\phi = \frac{MRd\phi}{EI} = \frac{Mds}{EI} \tag{206}$$

where ds denotes the length of the element of the central line between the sections ab and cd.

In developing equation (b), the lateral pressure between the longitudinal fibers was neglected. In the case of a narrow rectangular cross-section the exact solution,* which takes this lateral pressure into account, gives the following value of p:

$$p = \frac{4M}{N}\left(a^2 - b^2 + a^2 \log_e \frac{v}{a} + b^2 \log_e \frac{b}{v} + \frac{a^2b^2}{v^2} \log_e \frac{b}{a}\right)$$

in which,

$$N = (b^2 - a^2)^2 - 4a^2b^2 \left(\log_e \frac{b}{a}\right)^2,$$

a and b denoting the inner and outer radii of the curved bar and v denoting the distance from the center of curvature of the center line of the bar to the point for which the stress p is to be determined.

Comparative calculations show that the approximate solution is accurate enough for practical applications.

General Case.—If a curved bar be submitted to the action of any system of forces acting in its plane of symmetry, the forces at any cross-section can be reduced to a couple and a force applied at the center of gravity of the cross-section. The stresses produced by the couple can be obtained as explained above.

The force can be resolved into two components, a longitudinal force S in the direction of the tangent to the center line of the bar and a shearing force Q normal to the tangent. The longitudinal force will produce tensile or compressive stresses distributed uniformly over the cross-section and equal to S/A. Due to these stresses, the central line of the bar will undergo extension or compression and the angle $d\phi$ between two consecutive cross-sections will be changed. The magnitude of variation of the angle will be,

---

* Exact solution of this problem belongs to H. Golovin, *Bulletin of the Technological Institute* (St. Petersburg), 1881. The same problem was independently solved by L. Prandtl. See Föppl, *Technische Mechanik*, Vol. 5, p. 72, 1907.

$$\Delta d\phi = \frac{Sds}{AE} \cdot \frac{1}{R} \tag{207}$$

The transverse force Q will produce shearing stresses in the cross-section, the distribution of which can be taken the same as in the case of a straight beam (see equation 54, p. 64).

56. Particular Cases.—It has been shown in the previous paragraph that the bending stresses in curved bars can easily be calculated provided the position of neutral axis is known. In the examples which we now propose to consider, a method of determining this displacement of neutral axis with respect to the center of gravity of the cross-section is developed, from which the stress distribution can be calculated.

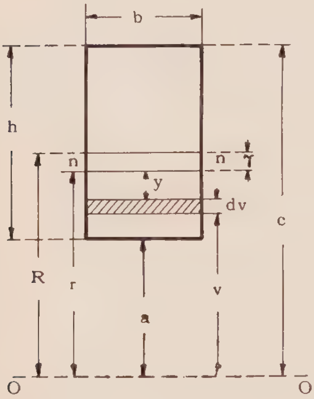

FIG. 193.—Case of rectangular section.

Rectangular Cross-section.—In order to obtain the magnitude of the radius r of the neutral surface equation

$$\int \frac{ydA}{r - y} = 0 \tag{a}$$

of the preceding paragraph, will be used. Denoting by v (Fig. 193) the distance of an element of area dA from the axis O-O through the center of the curvature, we have

$$v = r - y, \text{ and } y = r - v.$$

Substituting in (a),

$$\int \frac{(r - v)dA}{v} = 0$$

from which

$$r = \frac{A}{\displaystyle\int \frac{dA}{v}}. \tag{208}$$

In the case of a rectangular cross-section $dA = bdv$ Substituting in (208) and remembering that $A = bh$, the following equation for determining r will be obtained:

$$r = \frac{h}{\Big| \log_e v \Big|_a^c} = \frac{h}{\log_e \dfrac{c}{a}} \tag{209}$$

If the depth h of the cross-section is small in comparison with the radius R of the central line, the known series

$$\log_e \frac{c}{a} = \log_e \frac{R + \frac{1}{2}h}{R - \frac{1}{2}h} = \frac{h}{R}\left[1 + \frac{1}{3}\left(\frac{h}{2R}\right)^2 + \frac{1}{5}\left(\frac{h}{2R}\right)^4 + \cdots\right] \quad \text{(b)}$$

can be used. Then

$$\gamma = R - r = R - \frac{R}{1 + \frac{1}{3}\left(\frac{h}{2R}\right)^2 + \frac{1}{5}\left(\frac{h}{2R}\right)^4 + \cdots}$$

A first approximation will be obtained by taking only two terms in the denominator on the right side. Then,

$$\gamma = R\left[1 - \frac{1}{1 + \frac{1}{3}\left(\frac{h}{2R}\right)^2}\right] = \frac{h^2}{12R}. \tag{210}$$

By using three terms of the series (b), a second approximation,

$$\gamma = \frac{h^2}{12R}\left[1 + \frac{4}{15}\left(\frac{h}{2R}\right)^2\right] \tag{211}$$

will be obtained.

It is seen that the displacement γ of the neutral axis decreases with decrease of the ratio h/R. For small values of this ratio a linear stress distribution, instead of a hyperbolic one, can be assumed with very little error. In order to compare the values of the maximum stress obtained by assuming linear stress distribution, with that obtained on the basis of hyperbolic stress distribution, Table XII is given.

TABLE XII.—COMPARISON OF HYPERBOLIC AND LINEAR STRESS DISTRIBUTIONS

R/h	Hyperbolic stress distribution		Linear stress distribution		Error due to assuming linear stress distribution, %
	$\frac{p_{\max}}{M/AR}$	$\frac{p_{\min}}{M/AR}$	$\frac{p_{\max}}{M/AR}$	$\frac{p_{\min}}{M/AR}$	
1	9.2	− 4.4	6	− 6	35
2	14.4	−10.3	12	−12	17
3	20.2	−16.1	18	−18	10.9
4	26.2	−22.2	24	−24	9.2
10	62.0	−58.0	60	−60	3.2

For $R/h > 10$, equation (50) page 52 can always be used with sufficient accuracy.

Circular Cross-section.—Denoting by y_1 the distance of any element of area dA of the cross-section from the center of gravity (Fig. 194), and by h the diameter of the cross-section, the length of the strip will be

$$2\sqrt{\tfrac{1}{4}h^2 - y_1^2}.$$

Substituting in (208),

$$r = \frac{A}{\displaystyle\int_a^c \frac{2\sqrt{\tfrac{1}{4}h^2 - y_1^2}}{v}\,dv} = \frac{A}{\displaystyle 2\int_{-h/2}^{+h/2} \frac{\sqrt{\tfrac{1}{4}h^2 - y_1^2}}{R - y_1}\,dy_1}$$
$$= \frac{A}{2\pi\left(R - \sqrt{R^2 - \dfrac{h^2}{4}}\right)} \qquad (212)$$

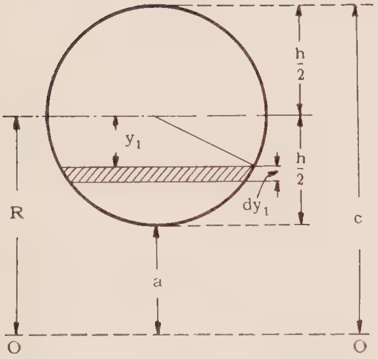

FIG. 194.—Case of circular section.

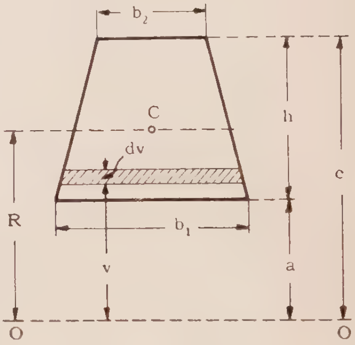

FIG. 195.—Case of trapezoidal section.

Trapezoidal Cross-section.—The length of an elemental strip distant v from the axis O-O (Fig. 195) through the center of curvature will be $b = b_2 + (b_1 - b_2)\dfrac{c - v}{c - a}$.

Substituting in equation (208),

$$r = \frac{A}{\displaystyle\int \frac{b\,dv}{v}} = \frac{A}{\dfrac{b_1 c - b_2 a}{h}\log_e \dfrac{c}{a} - (b_1 - b_2)} \qquad (213)$$

It is easy to see that by a suitable choice of the ratio b_1/b_2 the stresses $p_{\max}$ and $p_{\min}$ determined by equations (205) can be made numerically equal.

If $b_1 = b_2$, equation (213) coincides with the equation (209) obtained above for a rectangular cross-section.

$\perp$ *Cross-section.*—In this case equation (208) will be (Fig. 196)

$$r = \frac{b_1 e + b_2 f}{b_1 \int_a^d \frac{dv}{v} + b_2 \int_d^c \frac{dv}{v}} = \frac{b_1 e + b_2 f}{b_1 \log_e \frac{d}{a} + b_2 \log_e \frac{c}{d}} \qquad (214)$$

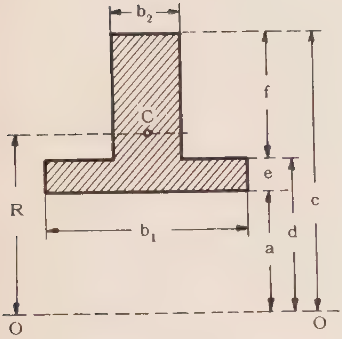

FIG. 196.—Case of $\perp$ section.

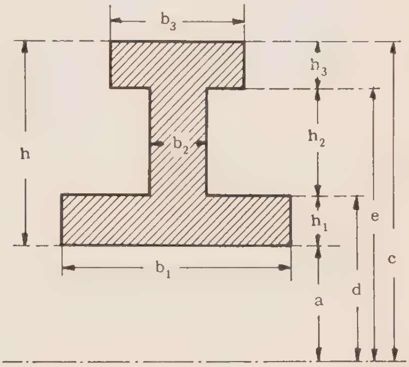

FIG. 197.—Case of I section.

I *Cross-section.*—From equation (208),

$$r = \frac{b_1 h_1 + b_2 h_2 + b_3 h_3}{b_1 \log_e \frac{d}{a} + b_2 \log_e \frac{e}{d} + b_3 \log_e \frac{c}{e}} \qquad (215)$$

Direct Determination of the Distance γ.—In previous considerations the distance γ of the neutral axis from the center of gravity of the cross-section was determined as the difference $R - r$. As h/R decreases, this difference becomes small. For sufficient accuracy in its determination, r must be calculated very accurately. In order to avoid this difficulty and to obtain γ directly, the following method can be used. Let y_1 denote distance of any element of the cross-section from the axis through the center of gravity parallel to the neutral axis, then, $y_1 = y + \gamma$ and the equation (a) becomes

$$\int \frac{(y_1 - \gamma)dA}{R - y_1} = \int \frac{y_1 dA}{R - y_1} - \gamma \int \frac{dA}{R - y_1} = 0 \qquad (c)$$

The first integral on the right side represents a *modified area* of the cross-section and can be represented as follows:

$$\int \frac{y_1 d\,A}{R - y_1} = mA \qquad (d)$$

where m denotes a constant to be determined in every particular case.

The second integral on the right side of (c) can be transformed as follows:

$$\int \frac{dA}{R - y_1} = \frac{1}{R}\int \left(1 + \frac{y_1}{R - y_1}\right) dA = \frac{1}{R}(A + mA) = \frac{A}{R}(1 + m) \quad \text{(e)}$$

Substituting (d) and (e) in (c),

$$mA - \frac{\gamma(1 + m)}{R}A = 0$$

from which

$$\gamma = R\frac{m}{1 + m} \tag{216}$$

In calculating m from equation (d), the term

$$\frac{1}{R - y_1}$$

can be expanded in the series as follows:

$$\frac{1}{R - y_1} = \frac{1}{R}\left(1 + \frac{y_1}{R} + \frac{y_1^2}{R^2} + \cdots\right)$$

Then

$$\int \frac{y_1 dA}{R - y_1} = \frac{1}{R}\int \left(1 + \frac{y_1}{R} + \frac{y_1^2}{R^2} + \cdots\right) y_1 dA$$

and

$$m = \frac{1}{AR}\int \left(1 + \frac{y_1}{R} + \frac{y_1^2}{R^2} + \cdots\right) y_1 dA \tag{217}$$

Take, for instance, a rectangular cross-section. Then

$$A = bh; \quad dA = bdy_1$$

Substituting in (217),

$$m = \frac{1}{hR}\int_{-h/2}^{+h/2}\left(1 + \frac{y_1}{R} + \frac{y_1^2}{R^2} + \cdots\right) y_1 dy_1 = \frac{1}{3}\left(\frac{h}{2R}\right)^2 + \frac{1}{5}\left(\frac{h}{2R}\right)^4 + \frac{1}{7}\left(\frac{h}{2R}\right)^6 + \cdots$$

This series converges very quickly and m can be calculated very accurately. Substituting in (216), γ will be obtained.

In the case of a circular cross-section of diameter h the same manner of calculation gives

$$m = \frac{1}{4}\left(\frac{h}{2R}\right)^2 + \frac{1}{8}\left(\frac{h}{2R}\right)^4 + \frac{5}{64}\left(\frac{h}{2R}\right)^6 + \cdots$$

Graphical Determination of γ.—If the shape of the cross-section is such that it cannot be simply expressed analytically, a graphical method of calculating m can be used. It is seen from (d) that in calculating the *modified area* every elemental area must be diminished in the ratio

$$\frac{y_1}{R - y_1}.$$

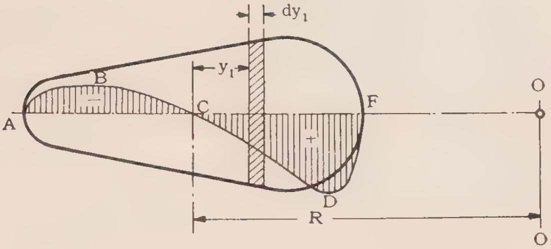

FIG. 198.—Graphical determination of neutral axis.

This can be done (Fig. 198) by retaining the width of the elemental strips unchanged and by diminishing their length in the ratio

$$\frac{y_1}{R - y_1}.$$

In such a manner the shaded area in Fig. 198 will be obtained. The difference of the areas CDF and ABC gives the modified area mA. Now m and γ can be obtained without difficulty.

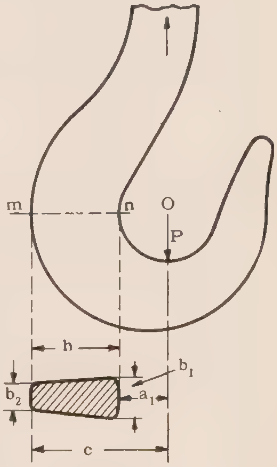

FIG. 199.

Example 69.—Determine $p_{\max}$ and $p_{\min}$ for the trapezoidal form cross-section mn of the hook represented in Fig. 199. If

$P = 4{,}500$ lbs., $b_1 = 1\frac{5}{8}$ in., $b_2 = \frac{3}{8}$ in.,
$a_1 = 1\frac{1}{4}$ in., $c = 5$ in.

Solution.—From (213),

$$r = \frac{3.750}{\dfrac{1\frac{5}{8} \times 5 - \frac{3}{8} \times 1\frac{1}{4}}{3\frac{3}{4}} \log_e \dfrac{5}{1\frac{1}{4}} - 1\frac{5}{8} + \frac{3}{8}}$$

$$= \frac{3.750}{1.580} = 2.373$$

The radius of the central line,

$$R = a_1 + \frac{b_1 + 2b_2}{b_1 + b_2}\frac{h}{3} = 2.734$$

Therefore,

$$\gamma = R - r = .361 \text{ in.}$$

$h_1 = r - a_1 = 2.373 - 1.250 = 1.123$ in.; $h_2 = c - r = 2.627$ in.
$A\gamma = 3.75 \times .361 = 1.35$; $M = P \times R = 12{,}300$ lbs. in.

The stresses produced by this bending moment, from (205) will become,

$$p_{\max} = \frac{12{,}300 \times 1.12}{1.35 \times 1.25} = 8{,}100 \text{ lbs. per sq. in.}; \; p_{\min} = -4{,}800 \text{ lbs. per sq. in.}$$

On these bending stresses a uniformly distributed tension stress $P/A = 4{,}500/3.75 = 1{,}200$ lbs. per sq. in. must be superimposed.

$$p_{\max} = 8{,}100 + 1{,}200 = 9{,}300 \text{ lbs. per sq. in.}$$
$$p_{\min} = -4{,}800 + 1{,}200 = -3{,}600 \text{ lbs. per sq. in.}$$

Example 70.—Determine the dimensions b_1 and b_3 of the I cross-section (Fig. 197) so that $p_{\max}$ and $p_{\min}$ will be numerically equal during pure bending. Given:

$h_1 = 1$ in., $h_2 = 2$ in., $h_3 = 1$ in.,
$a = 3$ in., $c = 7$ in., $b_2 = 1$ in., $b_1 + b_3 = 5$ in.

Solution.—From equations (205) it follows that the maximum compression and maximum tension will be equal if

$$\frac{h_1}{h_2} = \frac{r - h_1}{r + h_2}$$

or

$$\frac{r - a}{c - r} = \frac{a}{c}$$

from which,

$$r = \frac{2ac}{a + c} = \frac{2 \times 3 \times 7}{3 + 7} = 4.20 \text{ in.} \tag{a}$$

From equation (215),

$$r = \frac{7}{b_1 \log_e 4/3 + b_2 \log_e 6/4 + b_3 \log_e 7/6} \tag{b}$$

From (a) and (b)

$$b_1 \log_e \frac{4}{3} + b_2 \log_e \frac{6}{4} + b_3 \log_e \frac{7}{6} = \frac{7}{4.20}$$

or

$$.288 b_1 + .154 b_3 = \frac{7}{4.20} - .406 = 1.261 \tag{c}$$

Remembering that $b_3 = 5 - b_1$ and substituting this in (c), $0.134 b_1 = .491$. Therefore,

$$b_1 = \frac{.491}{.134} = 3.67 \text{ in.}; \; b_3 = 5 - b_1 = 1.33 \text{ in.}$$

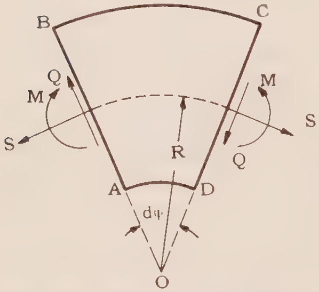

Fig. 200.—Element of curved bar

57. Deflections of Curved Bars.—*Application of Castigliano's Theorem.*—In order to obtain the deflection of a curved bar by the use of Castigliano's theorem an expression for the potential energy of deformation is required. The potential energy of deformation in the element $ABCD$ of a curved bar (Fig. 200) is equal to the work done by the external forces S, Q, M during the deformation. The couples M produce rotation of sections CD and AB with respect to each other, thus diminishing the angle $d\phi$ by the amount (see Equation 204)

$$\Delta d\phi = \frac{Md\phi}{A\gamma E} = \frac{Mds}{RA\gamma E}.$$

The corresponding energy is given by

$$dU_1 = \frac{1}{2}M\Delta d\phi = \frac{M^2ds}{2RA\gamma E}. \qquad \text{(a)}$$

When the depth of the cross-section is small in comparison to the radius R of the central line, the approximate equation (206) for the angle of rotation can be used. Then,

$$dU_1 = \frac{M^2ds}{2EI} \qquad \text{(a}_1\text{)}$$

The longitudinal forces S produce an elongation

$$\frac{Sds}{EA}$$

which increases the angle $d\phi$ an amount given by (Eq. 207)

$$\Delta_1\phi = \frac{Sds}{AER}.$$

Therefore, the work done by the forces S during their application is

$$\frac{S^2ds}{2EA}.$$

The couples M, previously applied, will now produce during the application of forces S, the negative work.*

$$-M\Delta_1\phi = -\frac{MSds}{AER}.$$

The corresponding expression for the potential energy will be,

$$dU_2 = \frac{S^2ds}{2EA} - \frac{MSds}{AER} \qquad \text{(b)}$$

Furthermore, the shearing forces Q will produce sliding of one cross-section with respect to another, equal to

$$\frac{kQds}{AG}$$

where k = numerical factor depending on the shape of the cross-section (see paragraph 17, p. 63). The corresponding potential energy will be,

$$dU_3 = \frac{kQ^2ds}{2AG} \qquad \text{(c)}$$

---

* In developing this equation the direction of forces and couples shown in Fig. 200 is considered as positive.

Adding (a), (b), and (c), the total energy of deformation of an element of the curved bar will be,

$$dU = \left(\frac{M^2}{2RA\gamma E} + \frac{S^2}{2AE} - \frac{MS}{AER} + \frac{kQ^2}{2AG}\right) ds \tag{218}$$

The complete energy of deformation for the curved bar will be*

$$U = \int_s \left(\frac{M^2}{2RA\gamma E} + \frac{S^2}{2AE} - \frac{MS}{AER} + \frac{kQ^2}{2AG}\right) ds \tag{219}$$

In many cases the effect of the longitudinal and transverse forces can be neglected and the approximate formula (a_1), instead of (a), can be used. Then,

$$U = \int_s \frac{M^2 ds}{2EI} \tag{220}$$

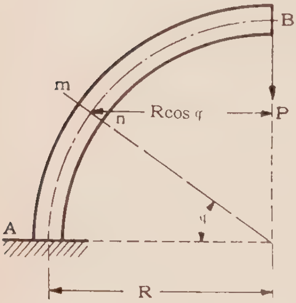

FIG. 201.

As an example of the application of Castigliano's theorem, a curved bar with a circular central line (Fig. 201) and having a rectangular cross-section clamped at the end A and loaded by a vertical load P at the end B will now be considered. For any cross-section m-n:

$$M = -PR\cos\phi, \quad S = -P\cos\phi,$$
$$Q = P\sin\phi \tag{d}$$

By using the Castigliano theorem, the deflection of the end B of the bar in the vertical direction will be,

$$\delta = \frac{\partial U}{\partial P}. \tag{e}$$

Substituting (219) for U, and using (d),

$$\delta = \frac{PR}{AE}\int_0^{\pi/2}\left[\frac{R\cos^2\phi}{\gamma} - \cos^2\phi + 2k\left(1 + \frac{1}{m}\right)\sin^2\phi\right]d\phi$$

or

$$\delta = \frac{PR}{AE}\left\{\frac{R}{\gamma}\frac{\pi}{4} + \frac{\pi}{4}\left[2k\left(1 + \frac{1}{m}\right) - 1\right]\right\} \tag{f}$$

Taking for γ the first approximation (210),

$$\delta = \frac{\pi}{4}\frac{PR}{AE}\left[\frac{12R^2}{h^2} + 2k\left(1 + \frac{1}{m}\right) - 1\right],$$

in which, for a rectangle, $k = 1.5$, $1/m$ = Poisson's ratio.

---

* The integration is taken along the axis of the curved bar.

If the first term in the bracket is large compared with the others, as is usually the case, the effect of the longitudinal and transverse forces can be neglected. The equation for the deflection will then become

$$\delta = \frac{\pi P R^3}{4EI} \tag{221}$$

Deflection Curve for a Bar with a Circular Central Line.—In order to obtain an expression for the deflection curve, the differential equation of this curve will first be obtained. Let $ABCD$ (Fig. 202) represent the central line of a circular ring after deformation and u the small radial displacements corresponding to this deformation. In order to obtain the variation of the curvature of the central line during bending, an element mn (Fig. 202, (b)) of a length $ds = Rd\phi$ will be considered. The initial curvature of this element is

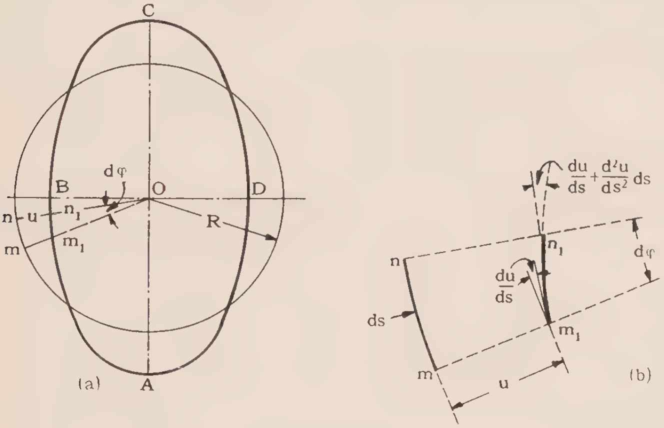

Fig. 202.

$$\frac{d\phi}{ds} = \frac{d\phi}{Rd\phi} = \frac{1}{R} \tag{a}$$

The curvature of the same element after deformation can be taken equal to the curvature of the element m_1n_1 and represented by the equation,

$$\frac{1}{\rho} = \frac{d\phi + \Delta d\phi}{ds + \Delta ds} \tag{b}$$

in which $d\phi + \Delta d\phi$ denotes the angle between the cross-sections m_1 and n_1 of the deformed bar, and $ds + \Delta ds$ the length of the element

m_1n_1. From Fig. 202 (b), by neglecting small quantities of higher order, we have:

$$\Delta d\phi = \frac{d^2u}{ds^2}\,ds, \quad \Delta ds = -\frac{dsu}{R}.$$

Substituting in (b),

$$\frac{1}{\rho} = \frac{d\phi + \dfrac{d^2u}{ds^2}\,ds}{ds\left(1 - \dfrac{u}{R}\right)}$$

or, neglecting the small quantities of higher order,

$$\frac{1}{\rho} = \frac{d\phi}{ds}\left(1 + \frac{u}{R}\right) + \frac{d^2u}{ds^2}.$$

Substituting $1/R$ for $d\phi/ds$,

$$\frac{1}{\rho} - \frac{1}{R} = \frac{u}{R^2} + \frac{d^2u}{ds^2} \tag{c}$$

The same variation in curvature can now be obtained as a function of the bending moment M. Neglecting the displacement γ of the neutral axis and using the approximate equation (206),

$$\frac{1}{\rho} - \frac{1}{R} = -\frac{\Delta d\phi}{ds} = -\frac{M}{EI}^{*} \tag{222}$$

By comparing (c) and (222) the general equation of deflection curve will be obtained:[†]

$$\frac{d^2u}{ds^2} + \frac{u}{R^2} = -\frac{M}{EI} \tag{223}$$

When R becomes infinitely large, this equation coincides with the known equation for the deflection curve of a straight bar.

In the next paragraph some applications of equation (223) will be given.

Bars with a Very Small Initial Curvature.—If a beam with a small initial curvature is bent by transverse forces only, the known equation for the deflection curve of a straight bar can be used without appreciable errors. Another result will be obtained if there are, in addition to the transversal loading, longitudinal forces acting on the

---

[*] The use of the minus sign here corresponds to the arrangement taken in Fig. 200, in which the positive bending moment produces the decrease of the curvature.

[†] This equation was established by J. Boussinesq. See *Comptes Rendues*, Vol. 97, p. 843, 1883. Various applications of this equation are given in a paper by R. Mayer in *Zeitschr. f. Math. u. Phys.*, Vol. 61, p. 246, 1913.

bar. It can be shown that a small initial curvature greatly changes the effect of these longitudinal forces on the deflection. A general expression for the deflection produced by these forces in the case of a slightly curved bar can be obtained by using a trigonometrical series.*

A beam with small initial curvature and having simply supported ends will now be considered. Let y_0 denote the very small initial deflections and y_1 the additional deflections produced by external forces, so that the complete deflection is

$$y = y_0 + y_1 \tag{a}$$

Let the initial deflection curve be represented by the series

$$y_0 = b_1 \sin \frac{\pi x}{l} + b_2 \sin \frac{2\pi x}{l} + \cdots \tag{b}$$

and the deflection produced by the load be

$$y_1 = a_1 \sin \frac{\pi x}{l} + a_2 \sin \frac{2\pi x}{l} + \cdots$$

Taking the forces shown in Fig. 159, the results obtained in paragraph 45, p. 161, can be used. It is only necessary to take instead of λ (see Eq. 138, p. 162) the quantity:

$$\lambda_1 - \lambda_0 = \frac{1}{2}\int_0^l \left[\frac{d(y_1 + y_0)}{dx}\right]^2 dx - \frac{1}{2}\int_0^l \left(\frac{dy_0}{dx}\right)^2 dx = \frac{\pi^2}{4l}\left(2\sum_{n=1}^{\infty} n^2 a_n b_n + \sum_{n=1}^{\infty} n^2 a_n{}^2\right) \tag{224}$$

According to this, the work done by the longitudinal forces S during the displacement da_n will be,

$$S\frac{\partial(\lambda_1 - \lambda_0)}{\partial a_n} da_n = S\frac{n^2\pi^2}{2l}(a_n + b_n)da_n$$

and the expression for the deflection curve will become,

$$y_1 = \frac{2Pl^3}{EI\pi^4}\left[\frac{\sin\frac{\pi c}{l}\sin\frac{\pi x}{l}}{1 - \alpha^2} + \frac{\sin\frac{2\pi c}{l}\sin\frac{2\pi x}{l}}{2^4 - 2^2\alpha^2} + \cdots\right] + \alpha^2\left(\frac{b_1 \sin\frac{\pi x}{l}}{1 - \alpha^2} + \frac{b_2 \sin\frac{2\pi x}{l}}{2^2 - \alpha^2} + \cdots\right) \tag{225}$$

Here α^2 has the same meaning, as before (see Equation 120).

---

* See Author's paper, Uber die Biegung von Stäben, die eine kleine anfängliche Krümmung haben, *Festschrift zum siebzigsten Geburtstage August Föppls*, pp. 74–81, 1923.

The expression within the first bracket on the right side represents the deflection of a straight bar, while the second bracket gives the additional deflection due to the initial curvature. Take, for instance, a bar which has an initial deflection $y_0 = b \sin \pi x/l$, i.e., maximum deflection takes place at the middle of the span and is equal to b. If longitudinal compressive forces S alone act on the bar, then the deflection at the middle produced by these forces, from (225), will be

$$a = \frac{\alpha^2 b}{1 - \alpha^2},$$

and the deflection curve will be

$$y = y_0 + y_1 = b \sin \frac{\pi x}{l} + \frac{\alpha^2 b}{1 - \alpha^2} \sin \frac{\pi x}{l} = \frac{b}{1 - \alpha^2} \sin \frac{\pi x}{l} \quad (226)$$

If instead of compression, longitudinal tensile forces are acting on the bar, it is only necessary to insert in the previous calculations $-\alpha^2$ instead of α^2. For the example considered above, the deflection will become

$$y = \frac{b}{1 + \alpha^2} \sin \frac{\pi x}{l} \quad (227)$$

The longitudinal tensile forces diminish the initial deflection. Taking, for instance, $S = S_{cr}$, we will have $\alpha^2 = 1$ and $y = \frac{1}{2} b \sin \pi x/l$. It will be seen, therefore, that tensile forces equal to the critical load diminish to half the initial deflection.

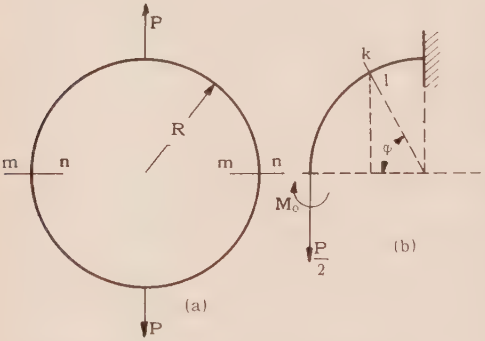

FIG. 203.—Circular ring under diametrally opposite forces.

58. Circular Ring.—*The Case of Two Opposite Forces* (*Fig.* 203).—From the condition of symmetry, it can be concluded at once that, at the horizontal cross-sections mn, only normal stresses will act and that the magnitude of the longitudinal force at these sections will be equal to $P/2$. The magnitude of the bending moment M_0 at the same section will be found from the condition that the section remains horizontal. Considering one quadrant of the ring (Fig. 203 (b)) and using the principle of least work, the equation for determining M_0 will be

$$\frac{dU}{dM_0} = 0 \tag{a}$$

The bending moment at any cross-section kl (Fig. 203, b) is,

$$M = M_0 - \frac{P}{2}R(1 - \cos \phi) \tag{b}$$

Neglecting the effect of the longitudinal and shearing forces we have from (220)

$$U = \int_0^{\pi/2} \frac{M^2 R d\phi}{2EI}$$

Substituting in (a),

$$\frac{dU}{dM_0} = \int_0^{\pi/2} \frac{\left[M_0 - \frac{P}{2} R(1 - \cos \phi)\right] R d\phi}{EI} = 0.$$

from which,

$$M_0 = \frac{PR}{2}\left(1 - \frac{2}{\pi}\right) = .182PR \tag{228}$$

Substituting this in (b), the following general expression for bending moment will be obtained:

$$M = \frac{PR}{2}\left(\cos \phi - \frac{2}{\pi}\right) \tag{c}$$

The greatest bending moment will be at the top and the bottom of the ring and can be obtained by substituting in (c), $\phi = \pi/2$:

$$M = -\frac{PR}{\pi} = -.318PR \tag{229}$$

In order to obtain the elongation δ of the vertical diameter of the ring, produced by the forces P, the *Castigliano theorem* is used. The potential energy of deformation of the ring is,

$$U = \frac{4R}{2EI}\int_0^{\pi/2} M^2 d\phi.$$

Therefore, the elongation will be,

$$\begin{aligned}\delta = \frac{dU}{dP} &= \frac{4R}{EI}\int_0^{\pi/2} M\frac{dM}{dP}\, d\phi = \\ &= \frac{4R}{EI}\int_0^{\pi/2} \frac{PR}{2} \times \frac{R}{2}\left(\cos \phi - \frac{2}{\pi}\right)^2 d\phi = \\ &= \left(\frac{\pi}{4} - \frac{2}{\pi}\right)\frac{PR^3}{EI} = .149\,\frac{PR^3}{EI}\end{aligned} \tag{230}$$

The same result can be obtained by substituting (c) in equation (223), giving the following differential equation:

$$\frac{d^2u}{ds^2} + \frac{u}{R^2} = \frac{PR}{2EI}\left(\frac{2}{\pi} - \cos\phi\right).$$

A general solution of this equation is:

$$u = A\cos\phi + B\sin\phi + \frac{PR^3}{EI\pi} - \frac{PR^3}{4EI}\phi\sin\phi$$

The arbitrary constants will be determined from the conditions of symmetry:

$$\frac{du}{d\phi} = 0, \text{ for } \phi = 0; \text{ and for } \phi = \frac{\pi}{2}.$$

Then.

$$u = -\frac{PR^3}{4EI}\cos\phi - \frac{PR^3}{4EI}\phi\sin\phi + \frac{PR^3}{EI\pi}.$$

The increase in vertical diameter of the ring is:

$$\delta = -2(u)_{\phi=\frac{1}{2}\pi} = \frac{PR^3}{EI}\left(\frac{\pi}{4} - \frac{2}{\pi}\right) = .149\,\frac{PR^3}{EI}.$$

The decrease in the horizontal diameter is:

$$\delta_1 = 2(u)_{\phi=0} = \frac{PR^3}{EI}\left(\frac{2}{\pi} - \frac{1}{2}\right) = .137\,\frac{PR^3}{EI} \qquad (231)$$

*Stresses in a Flywheel.**—Due to the effect of spokes, the rim of a rotating flywheel undergoes not only extension but also bending.

Let X = tensile force in the spokes,
R = radius of the central line of the rim,
A = cross-sectional area of the rim,
I = moment of inertia of the cross-section of the rim,
2α = the angle between the spokes,
A_1 = cross-sectional area of a spoke,
$\frac{q}{g}$ = mass per unit length of the rim,
$\frac{q_1}{g}$ = mass per unit length of a spoke,
ω = angular velocity of the wheel.

---

* See Bauer, *Dinglers Pol. Jour.*, p. 353, 1908. See also John G. Longbottom, Inst. Mech. Eng. Proc. (London), p. 43, 1924.

Consider an element of the rim (Fig. 204 (b)) between consecutive cross-sections *pl* and *mn*, which bisect the angles between the spokes. Let S_0 and M_0 denote the longitudinal force and the bending moment respectively on these cross-sections. From the condition of symmetry, it follows that the shearing force on these cross-sections will be zero.

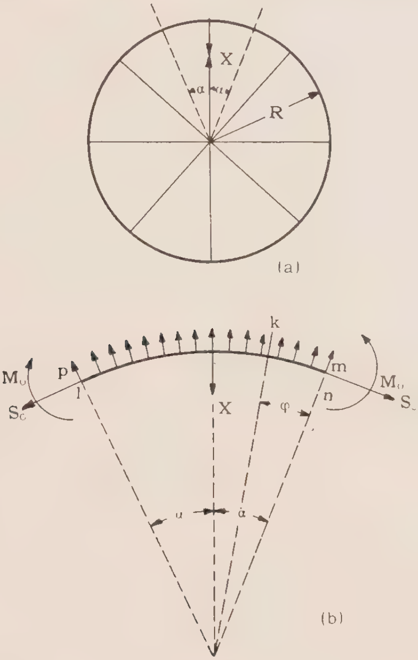

Fig. 204.—Stress distribution in flywheel.

Now the equation of equilibrium of the element *mp* will be,

$$2S_0 \sin \alpha + X - 2R \sin \alpha \cdot \frac{q}{g} \omega^2 R = 0 \tag{a}$$

from which,

$$S_0 = \frac{q}{g} \omega^2 R^2 - \frac{X}{2 \sin \alpha} \tag{b}$$

The longitudinal force at any cross-section k, determined by the angle ϕ (Fig. 204 (b)), is

$$S = S_0 \cos \phi + \frac{q\omega^2 R}{g} 2R \sin^2 \frac{\phi}{2} = \frac{q\omega^2 R^2}{g} - \frac{X \cos \phi}{2 \sin \alpha} \tag{c}$$

The bending moment for the same cross-section will be,

$$M = M_0 - S_0R(1 - \cos\phi) + \frac{q\omega^2R}{g}2R^2\sin^2\frac{\phi}{2}$$

or substituting (b), we have,

$$M = M_0 + \frac{XR}{2\sin\alpha}(1 - \cos\phi) \tag{d}$$

The magnitude of the bending moment M_0 and of the force X can be calculated by using the *principle of least work*. The potential energy of deformation of the element mp of the rim consists of the energy of bending and of tension, therefore,

$$U_1 = 2\int_0^\alpha \frac{M^2Rd\phi}{2EI} + 2\int_0^\alpha \frac{S^2Rd\phi}{2EA} \tag{e}$$

The tensile force in a spoke at a cross-section distant r from the axis of the wheel is,

$$S_1 = X + \frac{q_1\omega^2}{2g}(R^2 - r^2)$$

and the corresponding potential energy is,*

$$U_2 = \int_0^R \frac{S_1^2dr}{2EA_1} \tag{f}$$

Now, equations for determining M_0 and X are:

$$\frac{\partial U_1}{\partial M_0} = 0 \tag{k}$$

$$\frac{\partial U_1}{\partial X} + \frac{\partial U_2}{\partial X} = 0\,. \tag{l}$$

From (k),

$$M_0 = -\frac{XR}{2}\left(\frac{1}{\sin\alpha} - \frac{1}{\alpha}\right) \tag{m}$$

From (l),

$$X = \frac{2}{3}\frac{q\omega^2R^2}{g}\cdot\frac{1}{\frac{AR^2}{I}f_2(\alpha) + f_1(\alpha) + \frac{A}{A_1}} \tag{n}$$

in which,

$$f_1(\alpha) = \frac{1}{2\sin^2\alpha}\left(\frac{\sin 2\alpha}{4} + \frac{\alpha}{2}\right);$$

$$f_2(\alpha) = \frac{1}{2\sin^2\alpha}\left(\frac{\sin 2\alpha}{4} + \frac{\alpha}{2}\right) - \frac{1}{2\alpha}.$$

---

* In this consideration the length of spokes is taken equal to R. In real conditions it will be less than that and X will be somewhat larger than it is by equation (n).

Several values of functions f_1 and f_2 are given in Table XIII, in which n denotes the number of spokes.

TABLE XIII

$n =$	4	6	8	10	12
$f_1(\alpha) =$	.643	.957	1.274	1.592	1.910
$f_2(\alpha) =$	.00608	.00169	.00076	.000395	.000125

By using Table XIII, the force X can be calculated from (n), and the bending moment M_0, from (m). In the usual calculation of the stresses in flywheels, the bending of the rim is neglected. The error involved in this method of calculation, as can be seen from above, will depend on the relative dimensions of the spokes and rim.

The above method can also be used in calculating the stresses produced in locomotive wheels by the shrink fit of the tire.

Stresses in a Plate with a Circular Hole.—As was previously explained, a circular hole produces in a plate submitted to simple tension a high stress concentration. The stress distribution over the cross-section through the center of the hole is as shown in Fig. 13, page 9. An approximate method of determining this stress concentration will now be considered: Let p denote the magnitude of the tensile stresses uniformly distributed over the ends of the plate. At points n-n the stresses will be equal to $3p$, provided that the diameter of the hole is small in comparison with the width of the plate. This disturbance of stress distribution will be produced only in the immediate neighborhood of the hole. If a circle concentric with the hole and of comparatively large diameter D be taken, it can be assumed that the stresses at the points of this circle are not materially affected by the presence of the hole. Let Fig. 205 represent a circular ring cut out of the extended plate by a circle of diameter D. If we now assume that a stress of magnitude $p \sin \phi$ is acting on the outer circumference of the ring

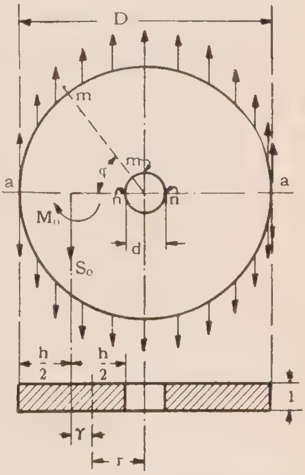

FIG. 205.—Plate with circular hole.

(see equation 4, page 2), the stresses at the points n-n will be approximately the same as in the extended plate. In this manner the problem on stress distribution near the hole is reduced to that of an annular ring* subjected at its outer boundary to the given forces. The stresses over the cross-section a-n of the ring can be reduced to a longitudinal force† $S_0 = pD/2$ and a bending moment M_0.

The longitudinal force at any cross-section mm is

$$S = \tfrac{1}{2} pD \cos^2 \phi \tag{a}$$

The bending moment at this cross-section is

$$M = M_0 + \tfrac{1}{2} pD(1 - \cos \phi)[\tfrac{1}{4} D(1 - \cos \phi) + \tfrac{1}{2} h \cos \phi] \tag{b}$$

The magnitude of M_0 can now be determined from the equation of least work, $dU/dM_0 = 0$. Substituting (218) for U,

$$\int_0^{\pi/2} M d\phi - \gamma \int_0^{\pi/2} S d\phi = 0 \tag{c}$$

from which

$$M_0 = \frac{1}{2\pi} pD^2 \left[(\pi - 2)\frac{R}{D} + \frac{\pi}{2}\frac{\gamma}{D} - (1 - \frac{1}{4}\pi)\frac{h}{D} - \frac{3}{8}\pi + 1 \right] \tag{d}$$

Where,

h = the depth of the cross-section of the ring,
R = the radius of the central line of the ring.

Now the complete stress at the point n consists of two parts: (1) the tensile stress produced by the longitudinal force S_0 and equal to

$$p_1 = \frac{S_0}{h} = \frac{pD}{2h} \tag{e}$$

and (2) the bending stress (Eq. 205)

$$p_2 = \frac{M_0 h_1}{A\gamma(r - h_1)} = \frac{M_0}{\gamma d}\left(1 - \frac{2\gamma}{h}\right) \tag{f}$$

Remembering that, for a rectangular section,

$$\gamma = R - \frac{h}{\log_e \frac{D}{d}},$$

the stresses p_1 and p_2 can be calculated for any value of the ratio D/d. Then, $p_{\max} = p_1 + p_2$. The results of some calculations made in such a manner are given in Table XIV.

---

* See Author's paper, *Jour. of the Franklin Institute*, Vol. 197, p. 505, 1924.

† The thickness of the plate is taken equal to unity.

TABLE XIV.—COEFFICIENTS OF STRESS CONCENTRATION PRODUCED BY CIRCULAR HOLES

$D/d =$	3	4	5	6	8	10
$2\gamma/h =$	.1796	.2238	.2574	.2838	.3239	.3536
$p_1/p =$	1.50	1.33	1.25	1.20	1.14	1.11
$p_2/p =$	2.33	1.93	1.83	1.83	1.95	2.19
$p_{max}/p =$	3.83	3.26	3.08	3.03	3.09	3.30

By comparison with the results of the exact theory, it can be concluded that for $5 < D/d < 8$ the results of approximate calculation agree closely with the exact solution ($p_{\text{max}}/p = 3$) for a small circular hole. When $D/d < 5$, the hole has a perceptible effect on the distribution of the forces acting on the external boundary of the ring, and as a result, some increase of the ratio p_{max}/p is obtained.

The increase of the same ratio for $D/d > 8$ is due to insufficient accuracy in the elementary theory of curved bars for the case where the inner radius is very small in comparison with the outer one.

The approximate method described above can be used also in the case of a hole with a bead (Fig. 206). The calculation worked out for the thickness equal to unity and for $b = 11$, $a/d = .01$, gave the values (shown in Table XV) of the ratio p_{max}/p for various values of D/d:

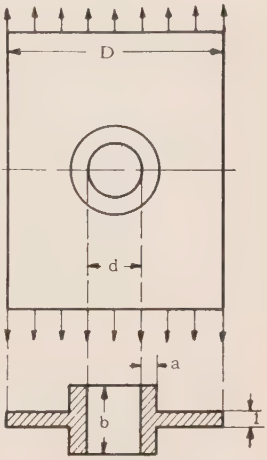

FIG. 206.—Plate with reinforced hole.

TABLE XV.—STRESS CONCENTRATION PRODUCED BY A CIRCULAR HOLE WITH A BEAD

$D/d =$	4	5	6
$p_{\text{max}}/p =$	2.56	2.53	2.56

In Table XV it can be seen p_{max}/p varies but slightly with D/d. Taking this into account, further calculations are made for the case

$D/d = 5$ only. By varying the dimension b, the influence of the area of the cross-section of a bead on the stress concentration can be studied. If $A_1 = d \times 1$ denotes the diametral section of the hole, and $A_2 = (b - 1)a$ the cross-section of the bead, the stress-concentration for several values of the ratio A_2/A_1 will be as given in the Table XVI.

Table XVI.—Effect of the Area of the Cross-section of a Bead on Stress-concentration

$A_2/A_1 =$	.10	.20	.30	.40	.50
$p_{\max}/p =$	2.53	2.17	1.90	1.69	1.53

The results obtained can be used also in the case of other shapes of bead cross-sections, provided that the dimension a of the bead in the radial direction can be considered as small in comparison with the diameter d of the hole. Take, for instance, a plate in tension, $\frac{7}{16}$ in. thick with a circular hole of 40 in. diameter. Let the edge of the hole be stiffened with two iron angles $4 \times 4 \times \frac{7}{16}$ in. In such a case, $A_2/A_1 = .40$ and the Table XVI gives $p_{\max}/p = 1.69$.

The approximate method outlined here can be developed also for any other shape of hole.

Case of Piston Ring.—A piston ring has usually a rectangular cross-section of constant width b and of a variable depth h (Fig. 207). The variation of h with the angle ϕ must be chosen in such a manner as to obtain a ring which, when assembled with the piston in the cylinder, produces a uniformly distributed pressure on the cylinder wall. Let r denote the radius of the cylinder, and $r + \delta$ the outer radius of the ring in the unstrained state. An approximate solution of the problem can be obtained if the outer radius instead of the variable radius of curvature of the central line of the ring be taken. Then by using equation (222) we have

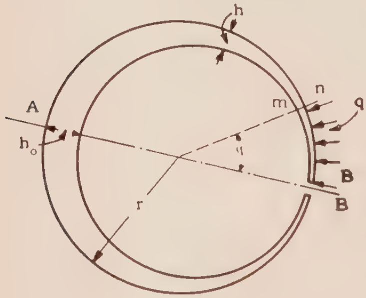

Fig. 207.—Piston ring.

$$\frac{1}{r} - \frac{1}{r + \delta} = -\frac{M}{EI} \tag{a}$$

The bending moment M at any cross-section mn of the ring produced by the pressure q uniformly distributed over the outer surface of the ring will be

$$M = -qb \cdot 2r^2 \sin^2 \frac{\phi}{2}. \tag{b}$$

Substituting this in (a) and taking $bh^3/12$ for I and δ/r^2 instead* of

$$\frac{1}{r} - \frac{1}{r + \delta},$$

the following equation for determining h will be obtained:

$$\frac{\delta}{r^2} = \frac{q}{E} \frac{12 \times 2 \times r^2 \sin^2 \frac{\phi}{2}}{h^3} \tag{c}$$

from which

$$h^3 = \frac{q}{E} \frac{24r^4 \sin^2 \frac{\phi}{2}}{\delta}. \tag{d}$$

A maximum value for h, equal to h_0, will be obtained by substituting $\phi = \pi$ in (d). Then

$$h_0^3 = \frac{q}{E} \frac{24r^4}{\delta}. \tag{e}$$

If the pressure q is given, the magnitude of δ and h_0 can be determined so as to make the maximum stress in the ring equal to a given value p_w. Because, from the known equation

$$p = \frac{M}{S} = \frac{6qb2r^2 \sin^2 \frac{\phi}{2}}{bh^2} = \frac{12qr^2 \sin^2 \frac{\phi}{2}}{h^2}, \tag{f}$$

it can be seen that the maximum stress will occur at the cross-section A opposite to the slot B of the ring. For this cross-section, $h = h_0$ and $\phi = \pi$. Substituting in (f),

$$p_{\max} = \frac{12qr^2}{h_0^2} \tag{g}$$

from which h_0 can be calculated if the working stress p_w for the ring is given. Substituting now h_0 in (e), the value of δ will be obtained.

It must be noted that if two equal and opposite tensile forces P be applied to the ends B-B of the ring, the bending moment at any cross-section mn, produced by these forces, will be

$$Pr(1 - \cos \phi) = 2Pr \sin^2 \frac{\phi}{2},$$

---

* δ is considered as small in comparison to r.

i.e., the bending moment varies with ϕ exactly in the same manner as that given by equation (b). Therefore, if the ends of the open ring be pulled together, and in this condition it be machined such that the outer radius is equal to r, then such a ring when assembled will produce a uniform pressure against the wall of the cylinder.*

59. Symmetrical Ring Submitted to Uniform Pressure.—As an application of the theory of bending of curved bars, we propose to consider here several different problems on the bending of symmetrical rings submitted to uniform hydrostatic pressure. Such kind of problems may be encountered in the design of tanks submitted to internal pressure, in the design of reinforcing rings for submarines, and in other cases.

General.—Let Fig. 208 represent a ring submitted to uniform internal pressure q, X and Y being the axes of symmetry. It can be seen from the condition of symmetry that the cross-sections A and B do not rotate when the ring is deformed by the pressure. Thus, it is only necessary to consider the deformation of one quadrant of the ring. From the equations of statics the tensile forces at A and B are qa and qb respectively. The statically unknown quantity M_0 will be determined by using the *principle of least work* (see Par. 34, p. 123) from the equation

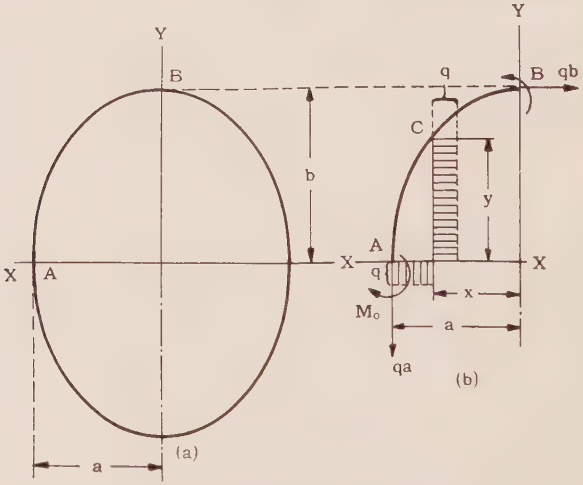

FIG. 208.—Case of symmetrical ring.

$$\frac{dU}{dM_0} = 0. \qquad \text{(a)}$$

---

* The description of a new method of cutting piston rings, see *Zeitschr. d. Ver. D. Ing.*, Vol. 68, p. 254, 1924.

Taking into consideration the potential energy of bending only and assuming that the cross-section of the ring is constant, equation (a) becomes

$$\int_0^l M ds = 0 \tag{b}$$

in which l denotes the length of a quadrant of the ring. It is seen from Fig. 208 (b) that the bending moment at any cross-section C is

$$M = M_0 + \frac{q(a-x)^2}{2} + \frac{qy^2}{2} - qa(a-x) = M_0 - \frac{qa^2}{2} + \frac{qx^2}{2} + \frac{qy^2}{2} \tag{c}$$

Substituting in (b),

$$\left(M_0 - \frac{qa^2}{2}\right)l + \frac{q}{2}(I_x + I_y) = 0,$$

or

$$M_0 = \frac{qa^2}{2} - \frac{q}{2l}(I_x + I_y) \tag{232}$$

where I_x and I_y denote the moments of inertia of the arc ACB about the X and Y axes respectively.

By using equation (232), the diagram of bending moments for any symmetrical ring submitted to the action of a uniform pressure can be obtained.

A Rectangular Frame.—In the case of a rectangle (Fig. 209),

$$I_x = ab^2 + \frac{b^3}{3};$$

$$I_y = ba^2 + \frac{a^3}{3};$$

$$I_x + I_y = \frac{a^3 + b^3}{3} + ab(a + b);$$

$$l = a + b.$$

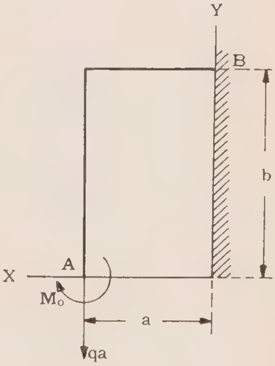

FIG. 209.—Case of rectangular frame.

Substituting in (232),

$$M_0 = \frac{qa^2}{2} - \frac{q}{6}(a + b)^2.$$

The bending moment at B will be

$$M_1 = \frac{qb^2}{2} - \frac{q}{6}(a + b)^2.$$

Now the diagram of bending moment in the usual manner can be obtained.

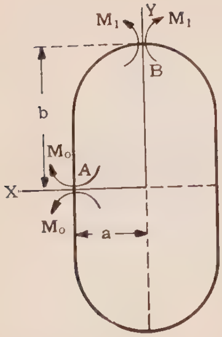

FIG. 210.—Case of symmetrical ring having two parallel sides.

A Ring with Parallel Sides and Semi-circular Ends.—In this case (Fig. 210),

$$I_x = \frac{1}{3}(b-a)^3 + \frac{\pi a}{2}(b-a)^2 + \frac{\pi}{4}a^3 + 2a^2(b-a);$$

$$I_y = (b-a)a^2 + \frac{\pi a^3}{4};$$

$$l = b - a + \frac{\pi a}{2}.$$

Substituting in (232), the bending moment at A becomes

$$M_0 = \frac{qa^2}{2} - \frac{q}{2b + (\pi - 2)a}\left[\frac{1}{3}(b-a)^3 + \frac{\pi}{2}a^3 + 3a^2(b-a) + \frac{\pi a}{2}(b-a)^2\right].$$

The bending moment at B is

$$M_1 = \frac{qb^2}{2} - \frac{q}{2b - (\pi - 2)a}\left[\frac{1}{3}(b-a)^3 + \frac{\pi}{2}a^3 + 3a^2(b-a) + \frac{\pi a}{2}(b-a)^2\right].$$

Taking, for instance, $a:b = 1:2$, then $M_0 = -.76qa^2$ and $M_1 = .74qa^2$.

Elliptical Ring.—In this case (Fig. 208) the calculations are more complicated and the use of tables of elliptical integrals becomes necessary.* The sum of the two moments of inertia can be represented as follows:

$$I_x + I_y = \alpha a^2 b$$

where α denotes a numerical factor calculated for elliptical rings.

The magnitude of the bending moment at A (Fig. 208) will be

$$M_0 = -\beta q a^2$$

where β denotes another numerical factor.

Similarly the bending moment at B will be $M_1 = \gamma q a^2$; here γ denotes the numerical factor.

Table XVII gives the values of the factors α, β and γ for a number of different values of the ratio a/b.

---

* See Ligowsky, "Taschenbuch der Mathematik," p. 64, 1893.

TABLE XVII.—BENDING MOMENT FACTORS FOR ELLIPTICAL RINGS

$a/b =$	1.0	.9	.8	.7	.6	.5	.4	.3
$\alpha =$	1.571	1.663	1.795	1.982	2.273	2.736	3.559	5.327
$\beta =$	0	.057	.133	.237	.391	.629	1.049	1.927
$\gamma =$	0	.060	.148	.283	.498	.870	1.576	3.128

Now the bending moment M at any cross-section of the ring can be obtained by using equation (c), page 243.

60. The Buckling of Circular Rings and Tubes under External Pressure.—*Buckling of a Circular Ring.*—It is well known that a circular ring or tube can be collapsed by external pressure alone; and if the flexural rigidity of the ring is insufficient, such failure can occur at stresses far below the elastic limit of the material. This phenomenon must be taken into consideration for such problems as, for instance, the design of boiler tubes and reinforcing rings for submarines.

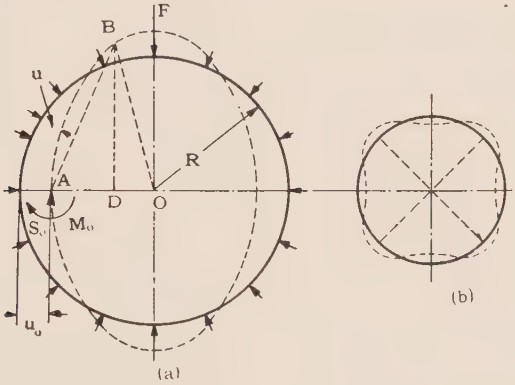

FIG. 211.—Buckling of circular ring under uniform pressure.

The pressure at which the circular form becomes unstable and buckling occurs is known as the *critical pressure.* Its value will be obtained by use of the general equation (223) for the deflection curve.

Assume that under external pressure the ring (Fig. 211) is buckled into an elliptical form as shown by the dotted line. Let:

q = external pressure per unit length.
R = the radius of the central line of the ring.
u = radial displacements during buckling.
u_0 = radial displacement for the cross-section A.
M_0 = bending moment at the cross-section A.
$S_0 = q(R - u_0)$ = Longitudinal compressive force at the cross-section A.

The bending moment at any cross-section B of the buckled ring will be

$$M = M_0 + q \cdot AO \cdot AD - \frac{q}{2} \cdot \overline{AB}^2. \tag{a}$$

Now, from the triangle AOB,

$$\overline{OB}^2 = \overline{AB}^2 + \overline{AO}^2 - 2AO \cdot AD,$$

or

$$\tfrac{1}{2}\overline{AB}^2 - AO \cdot AD = \tfrac{1}{2}(\overline{OB}^2 - \overline{AO}^2) = \tfrac{1}{2}[(R - u)^2 - (R - u_0)^2].$$

Remembering that u is small in comparison to R and neglecting small quantities of higher order,

$$\tfrac{1}{2}\overline{AB}^2 - AO \cdot AD = R(u_0 - u).$$

Substituting this value in (a), we have

$$M = M_0 - qR(u_0 - u).$$

Equation (223), page 231, becomes

$$\frac{d^2u}{d\phi^2} + u = -\frac{R^2}{EI}[M_0 - qR(u_0 - u)],$$

or

$$\frac{d^2u}{d\phi^2} + u\left(1 + \frac{qR^3}{EI}\right) = \frac{-M_0R^2 + qR^3u_0}{EI}. \tag{b}$$

A general solution of this equation will be

$$u = C \sin k\phi + D \cos k\phi + \frac{-M_0R^2 + qR^3u_0}{EI + qR^3} \tag{c}$$

which can be verified by substituting (c) in (b). In this solution, C and D are arbitrary constants to be determined from the conditions at the cross-sections A and F of the buckled ring, and

$$k^2 = 1 + \frac{qR^3}{EI}. \tag{d}$$

From the conditions of symmetry, it follows that

$$\left(\frac{du}{d\phi}\right)_{\phi=0} = 0; \left(\frac{du}{d\phi}\right)_{\phi=\pi/2} = 0. \tag{e}$$

From the first of these conditions it also follows that, in the solution (c), $C = 0$ and from the second,

$$\sin\frac{k\pi}{2} = 0. \tag{f}$$

The smallest root of this equation is

$$\frac{k\pi}{2} = \pi,$$

or

$$k = 2.$$

Substituting this in (d), the value for the critical pressure

$$q_{cr} = \frac{3EI}{R^3} \tag{233}$$

will be obtained.*

Other roots of the equation (f) such as $k\pi/2 = 2\pi$, $k\pi/2 = 3\pi$, and so on correspond to greater values of pressure q and to a larger number of waves of the buckled ring. In Fig. 211 (b) is shown, for instance, the buckled form for $k\pi/2 = 2\pi$. These higher forms of buckling are of interest in studying the stability of short cylindrical tubes with fastened ends.

Buckling of a Circular Arch.—If a circular arch having hinged ends be submitted to uniform pressure, it can buckle as indicated by the dotted line in Fig. 212. The critical value of the pressure depends on the magnitude of the angle α and can be calculated from the equation†

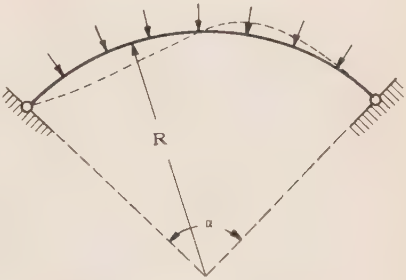

FIG. 212.—Buckled circular arch.

$$q_{cr} = \frac{EI}{R^3}\left(\frac{4\pi^2}{\alpha^2} - 1\right). \tag{234}$$

---

* This equation was obtained by M. Levy, *Jour. d. Math. pure et appl.* (Liouville) Ser. 3, Vol. X, p. 5, 1884. See also A. G. Greenhill, *Mathem. Ann.*, Vol. 52, p. 465, 1899.

† See Author's paper on the stability of elastic systems, *Bulletin of the Polytechnical Institute in Kiew*, 1910. French translation, *Annales des Ponts et Chaussées*, 1913. See also E. Hurlbrink, *Schiffbau*, Vol. 9, p. 640, 1907–1908.

The problem on buckling of the ring in the direction perpendicular to the plane of the ring is also solved.*

Buckling of Circular Tubes.—The theory of buckling developed above for a circular ring can be used also in the case of a long circular tube submitted to uniform external pressure. Considering an elementary ring cut out of the tube by two cross-sections one inch apart, the moment of inertia of the cross-section of this ring will be

$$I = \frac{1 \cdot t^3}{12}$$

where t denotes the thickness of the wall of the tube. In order to take into account that the cross-section of the ring will not be distorted during bending,

$$\frac{E}{1 - \frac{1}{m^2}}$$

instead of E must be taken. Equation (233) for calculating the critical pressure becomes

$$q_{cr} = \frac{Et^3}{4\left(1 - \frac{1}{m^2}\right) R^3}. \tag{235}$$

This equation can be used as long as the corresponding compressive stress in the tube is less than the proportional limit of the material, otherwise the true critical pressure will be less than that obtained from (235).

In order to determine the critical pressure for conditions beyond the elastic limit the following equation can be used.†

$$q_{cr} = \frac{t}{R} \frac{p_y}{1 + 4\frac{p_y}{E} \frac{R^2}{t^2}} \tag{236}$$

in which p_y denotes the stress corresponding to the yield-point of the material in compression. As the thickness is reduced, the critical pressure approaches the limiting value $Et^3/4R^3$, which is slightly less than that given by equation (235) and its value is, in all cases, less than tp_y/R, i.e., less than the pressure corresponding to the yield point.

In the case of short tubes the stability increases due to the fastened ends, and the critical pressure will be greater than that given by equation (235) and will depend on the length l of the tube. The theory of buckling in this case becomes more complicated.* Several values of q_{cr}, expressed in atmospheres, obtained from this theory for steel tubes and for various values of the ratios t/R and R/l are given in Table XVIII.

---

* See E. L. Nicolai, *Zeitschr. f. Angew, Math. u. Mech.*, Vol. 3, p. 227, 1923. See also Author's paper, *Zeitschr. f. Angew, Math. u. Mech.*, Vol. 3, p. 358, 1923.

† See R. V. Southwell, *Phil. Mag.*, Vol. 29, p. 67, 1915.

TABLE XVIII.—CRITICAL PRESSURE IN ATMOSPHERE FOR STEEL TUBES

$100t/R$ = ...	.4	.8	1.2	1.6	2.0	2.4	2.8	3.2
R/l								
0	.035	.28	.95	2.25	4.4	7.6	12	18
.1	.18	1.0	2.9	6.6	12.3	17	23	31
.2	.37	2.1	5.9	13	21	32	47	66
.3	.56	3.2	9.3	18	32	51	76	111
.4	.76	4.5	11.6	25	45	70	101	140
.5	.97	5.5	15	32	55	87	132	190
1.0	2.0							
2.0	4.2							

The figures in the table give the true value of the critical pressure as long as the corresponding compressive stress is below the proportional limit of the material. The pressures are calculated for $E = 28.10^6$ lbs. per sq. in. For a material having a modulus E_1, the figures given in Table XVIII must be multiplied by E_1/E.†

61. Thick Cylinder.—*General.*—If a cylinder be submitted to the action of uniformly distributed internal and external pressures, the deformation will be symmetrical about the axis of the cylinder and there will be no shearing stresses acting on the sides of an element such as *abcd* (Fig. 213) cut out from the wall of the cylinder by two radial planes and two concentric cylindrical surfaces. Let p_ϕ denote the normal stress over the sides *ab* and *cd* of the element, and p_r the normal stress over the side *ad*. Then the stress over the side *bc* will be $p_r + dp_r/dr\ dr$. Taking the sum of the projections in the p_r direction of all the forces acting on the element *abcd*, the following equation of equilibrium will be obtained:

---

* See R. V. Southwell, *Phil. Mag.*, p. 503, 1913. See also R. v. Mises, *Z. d. Ver. deutsch. Ing.*, p. 750, 1914.

† Experiments on the collapse of short tubes by external pressure are given by G. Cook, *Phil. Mag.*, p. 51, 1914. Bibliography of the subject, by the same author: see Brit. Assoc. Rep. (Birmingham), 1913.

$$p_r r d\phi + p_\phi dr d\phi - \left(p_r + \frac{dp_r}{dr}dr\right)(r + dr)d\phi = 0, \tag{a}$$

or, neglecting small quantities of higher order,

$$p_\phi - p_r - r\frac{dp_r}{dr} = 0. \tag{b}$$

In order to obtain stresses p_r and p_ϕ, the deformation of the cylinder must be considered. From the condition of symmetry it can be concluded that during deformation the points in the wall of the cylinder do not undergo displacements in a tangential direction. For all points lying on a cylindrical surface of radius r, the radial displacements will be the same. Let u denote these displacements. Then, for a cylindrical surface of a radius $r + dr$, the radial displacement will be

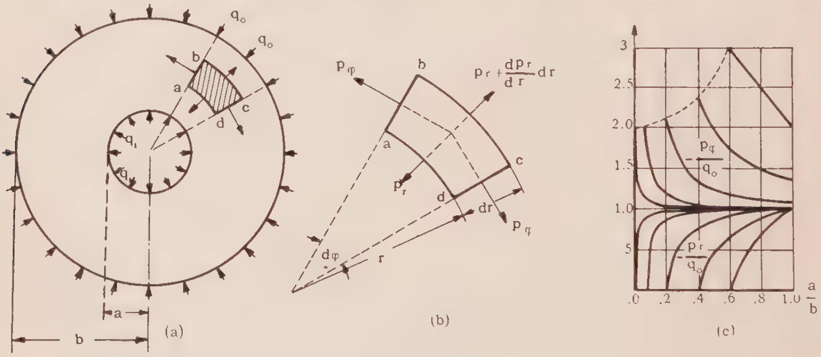

FIG. 213.—Stresses in thick cylinder.

$$u + \frac{du}{dr}dr.$$

Therefore, unit elongation of the element *abcd* in the radial direction will be

$$e_r = \frac{du}{dr} \tag{c}$$

The unit elongation of the same element in a tangential direction will be equal to the unit elongation of the corresponding radius, i.e.,

$$e_\phi = \frac{u}{r}. \tag{d}$$

Using now equations (10a) for combined stresses the following expressions for p_r and p_ϕ will be obtained:

$$\left.\begin{aligned} p_r &= \frac{E}{1 - \frac{1}{m^2}}\left(\frac{du}{dr} + \frac{1}{m}\frac{u}{r}\right), \\ p_\phi &= \frac{E}{1 - \frac{1}{m^2}}\left(\frac{u}{r} + \frac{1}{m}\frac{du}{dr}\right). \end{aligned}\right\} \tag{e}$$

Substituting in (b), the following equation will be obtained:

$$\frac{d^2u}{dr^2} + \frac{1}{r}\frac{du}{dr} - \frac{u}{r^2} = 0. \tag{f}$$

A general solution of this equation is

$$u = Ar + \frac{B}{r}, \tag{g}$$

which can be verified by substituting (g) in (f). A and B, the arbitrary constants, will be determined from the conditions at the inner and outer surfaces of the cylinder. Substituting (g) in (e),

$$p_r = \frac{E}{1 - \frac{1}{m^2}}\left[A\left(1 + \frac{1}{m}\right) - \frac{B}{r^2}\left(1 - \frac{1}{m}\right)\right], \tag{k}$$

$$p_\phi = \frac{E}{1 - \frac{1}{m^2}}\left[A\left(1 + \frac{1}{m}\right) + \frac{B}{r^2}\left(1 - \frac{1}{m}\right)\right]. \tag{l}$$

Let q_i and q_0 denote the internal and external pressures respectively, then the conditions at the outer and inner surfaces of the cylinder will be

$$(p_r)_{r=b} = -q_0 \quad \text{and} \quad (p_r)_{r=a} = -q_i.$$

Substituting (k) in these equations, the following values for the constants will be obtained:

$$A = \frac{1 - \frac{1}{m}}{E}\frac{a^2q_i - b^2q_0}{b^2 - a^2}; \; B = \frac{1 + \frac{1}{m}}{E}\frac{(q_i - q_0)a^2b^2}{b^2 - a^2} \tag{m}$$

Substituting this in (k) and (l),

$$p_r = \frac{a^2q_i - b^2q_0}{b^2 - a^2} - \frac{(q_i - q_0)a^2b^2}{r^2(b^2 - a^2)} \tag{237}$$

$$p_\phi = \frac{a^2q_i - b^2q_0}{b^2 - a^2} + \frac{(q_i - q_0)a^2b^2}{r^2(b^2 - a^2)} \tag{238}$$

Internal Pressure.—In the case where $q_0 = 0$ and an internal pressure alone is acting, equations (237) and (238) become

$$p_r = \frac{a^2 q_i}{b^2 - a^2}\left(1 - \frac{b^2}{r^2}\right), \tag{239}$$

$$p_\phi = \frac{a^2 q_i}{b^2 - a^2}\left(1 + \frac{b^2}{r^2}\right). \tag{240}$$

It is seen from these that p_r is always a compressive stress and p_ϕ a tensile stress. The maximum tensile stress takes place at the inner surface of the cylinder and is equal to

$$(p_\phi)_{r=a} = \frac{q_i(a^2 + b^2)}{b^2 - a^2}. \tag{241}$$

With increase of b this stress approaches the limit equal to q_i the internal pressure. In other words, the maximum stress always remains greater than the internal pressure.

Outer Pressure.—If an outer pressure acts alone on the cylinder, $q_i = 0$; and from equations (237) and (238), we have

$$p_r = \frac{q_0 b^2}{b^2 - a^2}\left(\frac{a^2}{r^2} - 1\right), \tag{242}$$

$$p_\phi = -\frac{q_0 b^2}{b^2 - a^2}\left(\frac{a^2}{r^2} + 1\right). \tag{243}$$

It is seen from these that p_r and p_ϕ are both compressive stresses and that p_ϕ is always greater than p_r. The maximum compressive stress will be at the inner surface of the cylinder, where

$$p_\phi = -\frac{2q_0 b^2}{b^2 - a^2}. \tag{244}$$

With increases of b, this compressive stress approaches the limit $-2q_0$, i.e., it becomes twice as great as the external pressure acting on the cylinder. In Fig. 213 (c) there are given the ratios p_r/q_0 and p_ϕ/q_0 for different values of a/b.

Deformation of the Cylinder.—The displacement u will now be considered. Substituting (m) in (g), the following will be obtained:

$$u = \frac{1 - \frac{1}{m}}{E}\frac{a^2 q_i - b^2 q_0}{b^2 - a^2}r + \frac{1 + \frac{1}{m}}{E}\frac{(q_i - q_0)a^2 b^2}{(b^2 - a^2)r}. \tag{245}$$

When $q_0 = 0$, the increase of the internal radius of the cylinder will be

$$\delta_1 = (u)_{r=a} = \frac{a q_i}{E}\left(\frac{b^2 + a^2}{b^2 - a^2} + \frac{1}{m}\right). \tag{246}$$

When $q_i = 0$, the diminishing of the external radius of the cylinder will be

$$\delta_2 = -(u)_{r=b} = \frac{bq_0}{E}\left(\frac{b^2 + a^2}{b^2 - a^2} - \frac{1}{m}\right). \tag{247}$$

Stresses Produced by Shrink Fits.—By using (246) and (247), the problem on stresses produced by shrink fits can easily be solved. Assume that the external radius of the inner cylinder is larger than the internal radius of the outer cylinder (Fig. 214), and let δ denote the difference of these radii. Then, after assembly, a pressure X will be produced between the cylinders. The value of X will be determined from the condition

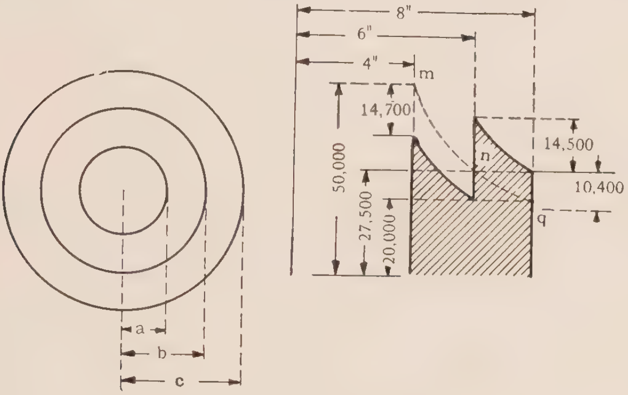

FIG. 214.—Built-up cylinders.

$$\delta = \delta_1 + \delta_2 = \frac{Xb}{E}\left(\frac{b^2 + a^2}{b^2 - a^2} - \frac{1}{m}\right) + \frac{Xb}{E}\left(\frac{c^2 + b^2}{c^2 - b^2} + \frac{1}{m}\right)$$

from which

$$X = \frac{E\delta}{b}\,\frac{(b^2 - a^2)(c^2 - b^2)}{2b^2\ \ (c^2 - a^2)}. \tag{248}$$

This pressure will produce compressive tangential stresses in the inner cylinder and tensile tangential stresses in the outer cylinder. Combining these assembly stresses with the stresses which may be produced by internal pressure, it will be seen that more favorable stress distribution will be obtained than in the case of a solid tube. This is the reason why in cases of very high internal pressures, as for instance, in guns, built-up cylinders consisting of several tubes are used.

Substituting (248) instead of q_i in equations (239) and (240) the stress distribution produced in the outer cylinder* by the shrink fit will be obtained. It is easy to see that the most unfavorable condition takes place at the inner surface of this cylinder.

Taking the maximum shear theory page 502 as the basis for calculating the shrink fit allowances the following equation will be obtained from equations (239) and (240)

$$p_w = p_\phi - p_r = \frac{2Xc^2}{c^2 - b^2} = \frac{E\delta}{b} \frac{c^2(b^2 - a^2)}{b^2(c^2 - a^2)} \tag{s}$$

In the case of a hub and a solid shaft $a = 0$ and we have, from (s),

$$p_w = \frac{E\delta}{b} \tag{t}$$

It is seen that for such a material as steel an allowance of .001 in. per in. makes a maximum difference between the principal stresses equal to .001 E or 30,000 lbs. per square inch.

For annealed medium carbon steel this stress difference approaches the yield point of the material and with further increase of the allowance δ, permanent set may be produced.

For the case of hollow shafts a table of maximum difference $(p_\phi - p_r)$ for different magnitudes of ratios $\frac{a}{b}$ and $\frac{c}{b}$ can easily be calculated from equation (s).

A distribution of initial stresses analogous to those described above can be obtained in a solid tube by applying a high internal pressure sufficient to produce permanent set in the inner part of the tube. It is clear that after removing this internal pressure some stresses will remain in the tube due to permanent set. The inner part will then be in a state of compression, and the outer in a state of tension.†

Example 71.—To determine the stresses in a built up steel cylinder (Fig. 214), submitted to the internal pressure $q_i = 30{,}000$ lbs. per sq. in. Assume that $c = 8$ in., $b = 6$ in., $a = 4$ in. and the shrinkage $\delta = .005$ in.

Solution.—The pressure between two tubes, due to shrinkage, is from equation (248),

$$X = \frac{30 \times 10^6 \times .005(6^2 - 4^2)(8^2 - 6^2)}{6 \times 2 \times 6^2(8^2 - 4^2)} = 4{,}050 \text{ lbs. per sq. in.}$$

---

* Inner cylinder is always in more favorable conditions.

† This method is used in manufacturing guns. See L. Jacob, *Résistance et Construction des Bouches à Feu. Autofretage. Encyclopédie Scientifique*, Paris. See also *A Method of Gun Construction by Radial Expansion*, by S. J. Brown, *United States Naval Institute Proceedings*, Vol. 46, p. 1941, 1920.

The corresponding stresses $p\phi$ for the inner tube are, from equation (243),

$$(p\phi)_{r=a} = -\frac{2Xb^2}{b^2 - a^2} = -\frac{2 \times 4{,}050 \times 6^2}{6^2 - 4^2} = -14{,}700 \text{ lbs. per sq. in.}$$

$$(p\phi)_{r=b} = -\frac{2Xb^2}{b^2 - a^2}\frac{a^2 + b^2}{2b^2} = -10{,}500 \text{ lbs. per sq. in.}$$

The corresponding stresses for the outer tube, from equation (240), are

$$(p\phi)_{r=b} = \frac{X(b^2 + c^2)}{(c^2 - b^2)} = \frac{4{,}050(6^2 + 8^2)}{8^2 - 6^2} = +14{,}500 \text{ lbs. per sq. in.}$$

$$(p\phi)_{r=c} = \frac{2b^2X}{c^2 - b^2} = \frac{2 \times 6^2 \times 4{,}050}{8^2 - 6^2} = +10{,}400 \text{ lbs. per sq. in.}$$

Stresses produced by internal pressure $q_i = 30{,}000$ lbs. per sq. in. calculated as for a solid cylinder with inner radius $a = 4$ in. and outer radius $c = 8$ in. are, from equation 240,

$$(p'\phi)_{r=a} = \frac{q_i(a^2 + b^2)}{b^2 - a^2} = 50{,}000 \text{ lbs. per sq. in.}$$

$$(p'\phi)_{r=c} = \frac{2q_ia^2}{b^2 - a^2} = 20{,}000 \text{ lbs. per sq. in.}$$

$$(p'\phi)_{r=a+c/2} = 27{,}500 \text{ lbs. per sq. in.}$$

The variation of these stresses along the thickness of the cylinder is given by the curve mnq (Fig. 214 (b)). Combining these stresses with stresses due to shrinkage, the stress distribution given by shaded area will be obtained.

It is seen that

$$(p\phi)_{\max} = 27{,}500 + 14{,}500 = 42{,}000 \text{ lbs. per sq. in.}$$

This stress is less than that found above for a solid cylinder.

62. Bending of Curved Tubes.—In the theory of curved bars previously developed it was assumed that during bending the distortion of the shape of cross-sections of the curved bar is very small and has no substantial effect on the stress distribution. An entirely different conclusion will be obtained in the case of bending of thin curved tubes. It is an established fact that curved tubes with comparatively thin walls prove to be more flexible during bending than would be expected by the usual theory of curved bars.* The consideration of the distortion of the cross-section during bending becomes, in such cases, necessary.† Consider an element of a circular curved tube contained between two neighboring cross-sections ac and

---

* Extensive experimental work on the flexibility of pipe bends was done by A. Bantlin, *Z. d. Ver. deutsch. Ing.*, p. 43, 1910. See also *Forschungsarbeiten,* Vol. 96. Some experiments were made also by S. Crocker and S. Sanford, See *Amer. Soc. Mech. Eng. Annual Meeting,* December, 1922.

† The distortion of cross-sections of circular pipes was considered in the paper by Th. Karman, *Zeit. d. Ver. D. Ing.*, Vol. 55, p. 1889, 1911. The case of a rectangular cross-section of curved pipes was considered by the writer. See *Am. Soc. Mech. Eng.*, Spring Meeting, May, 1923.

bd (Fig. 215). It is easy to see that the tensile forces P at the convex side of the tube and the compressive forces P_1 at the concave side have resultants T in the direction towards the neutral axis. Consequently, the previously circular cross-sections become elliptical. The effect this flattening of the section has on the deformation of longitudinal fibers of the tube will now be considered. Let: the outer fiber ab after bending take the position a_1b_1, and its displacement towards the neutral axis be denoted by δ. The extension of the fiber will be

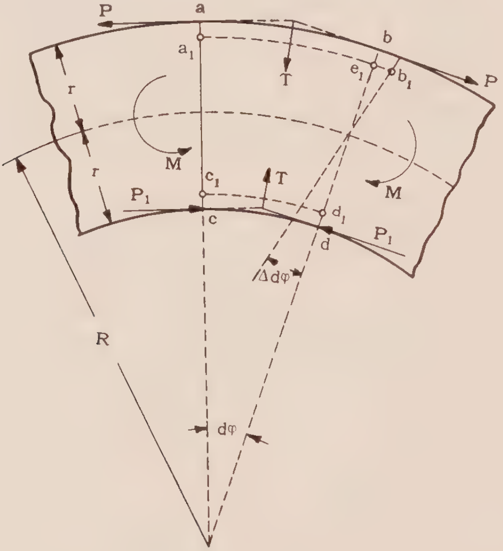

FIG. 215.—Bending of thin tube.

$$\lambda = a_1b_1 - ab = a_1b_1 - a_1e_1 - (ab - a_1e_1). \qquad \text{(a)}$$

Denoting by $d\phi$ the angle between the cross-sections ac and bd, by $\Delta d\phi$ the variation of this angle during bending, by R the radius of the central line of the tube, by r the radius* of the cross-section, and assuming that the neutral axis passes through the center of the section, we obtain

$$a_1b_1 - a_1e_1 = r\Delta d\phi,$$

$$ab - a_1e_1 = (R + r)d\phi - (R + r - \delta)d\phi = \delta d\phi.$$

Substituting in (a),

$$\lambda = r\Delta d\phi - \delta d\phi.$$

---

* The half of the sum of external and internal radii of the cross-section of the tube.

The unit elongation of the fiber ab will be

$$e = \frac{\lambda}{(R+r)d\phi} = \frac{r}{R+r}\frac{\Delta d\phi}{d\phi} - \frac{\delta}{R+r}. \tag{b}$$

The first member on the right side represents the elongation due to the rotation of the cross-section bd with respect to the cross-section ac, during the bending. The second member on the right side represents the effect of the flattening of the cross-section. It is easy to see that this effect may be very marked. Take, for instance, $R + r = 60$ in. and $\delta = .02$ in. Then,

$$\frac{\delta}{R+r} = \frac{1}{3{,}000}.$$

The corresponding stress for steel tubes is

$$E\frac{\delta}{R+r} = \frac{30 \times 10^6}{3{,}000} = 10{,}000 \text{ lbs. per sq. in.}$$

That is, a very small flattening of the cross-section produces a large decrease in the stress in the fiber ab. Similar conditions exist also on the concave side of the bend. The compressive stress of the fiber cd will be substantially diminished by the flattening of the cross-section.

As a result of the flattening of the cross-section as described above, the fibers of the tube most remote from the neutral axis do not share in the stress distribution as required by the ordinary theory of bending. This has an effect on the deformation as if the moment of inertia of the cross-section had been diminished. Instead of the equation (206) for solid curved bars, the following equation for thin tubes must be used:

$$\Delta d\phi = \frac{MRd\phi}{kEI} \tag{249}$$

in which k denotes the factor which takes into account the flattening of the cross-section during bending. This factor depends on the thickness of the wall t and on the magnitude of the radii R and r and can be calculated from the consideration of the energy of deformation. In the case of thin tubes the following approximate formula for calculating k can be used:

$$k = 1 - \frac{9}{10 + 12\left(\frac{tR}{r^2}\right)^2}, \tag{250}$$

i.e., the effect of the flattening of the cross-section on the flexibility of the bend depends on the magnitude of the ratio tR/r^2 only. With decrease of t and R and with increase of r, the factor k decreases, i.e., the effect of the flattening of the cross-section increases. Consider now the effect of the flattening on the stress-distribution. Instead of the simple equation for normal stresses $p = My/I$ in which y denotes the distance from the neutral axis, the following more complicated equation

$$p = \frac{My}{kI}\left(1 - \beta\frac{y^2}{r^2}\right) \tag{c}$$

must be used, in which

$$\beta = \frac{6}{5 + 6\left(\frac{tR}{r^2}\right)^2}.$$

It is seen from (c) that the maximum stress will no longer act in the most remote fibers but in those distant $r/\sqrt{3\beta}$ from the neutral axis. The magnitude of the maximum stress will be

$$p_{\max} = \gamma\frac{MD}{2I} \tag{251}$$

in which D = outer diameter of the pipe, and

$$\gamma = \frac{2}{3k\sqrt{3\beta}}.$$

Several values of γ are given in Table XIX.

TABLE XIX.—MAXIMUM STRESS IN BENDS

tR/r^2 =	.3	.5	1.0
γ =	1.98	1.30	.88

It is seen that in cases where tR/r^2 is small, the real maximum stress is materially greater than that given by the usual theory in which the flattening of the cross-section is neglected.

An analogous theory can be developed also in the case of a rectangular cross-section.* For a thin tube of a square cross-section, for instance, the coefficient k in the equation (249) depends on the magnitude of the quantity

$$\gamma = \frac{b^4}{R^2t^2}$$

in which t = the thickness of the wall,
R = the radius of the central line,
b = the length of the side of the cross-section.

---

* Such problem is to be considered in the design of a Fairbairn crane.

For calculating k the following equation is to be used:

$$k = \frac{49.2 + 1.33\gamma}{49.2 + 3.23\gamma} \tag{252}$$

Taking, for instance,

$$\frac{b}{R} = .1 \text{ and } \frac{b}{t} = 50,$$

it will be obtained: $\gamma = 25$.

Substituting in (252),

$$k = .51.$$

The maximum stress and the maximum deflection will be about twice as great as that given by the usual equations for curved bars.

CHAPTER X

THIN PLATES

63. Bending of a Plate to a Cylindrical Surface.—*General.*—Assuming that a rectangular plate, long in comparison with its width, is loaded in such a manner that the loading does not vary along the length of the plate but may vary in the direction of the width, then at points remote from the short sides of the plate the deflection surface can be taken as a cylindrical one. On this basis, in calculating deflection and bending stresses, the consideration of bending of any strip such as AB of unit width is sufficient (Fig. 216 (a)). Denoting the thickness of the plate by t and the deflection by w and remembering that in the case under consideration (see page 53) $\frac{E}{1 - \frac{1}{m^2}}$ instead of E must be used, the following equation for the deflection curve of the strip AB is obtained:

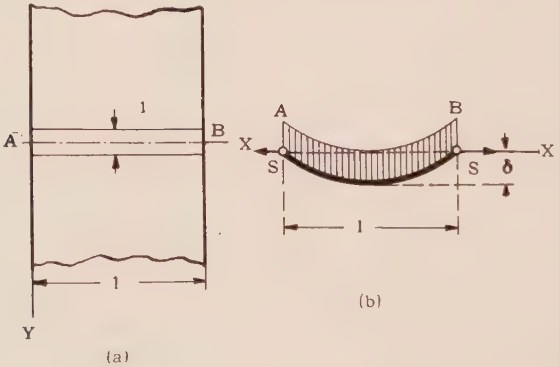

FIG. 216.—Bending of plate into a cylindrical surface.

$$D \frac{d^2w}{dx^2} = -M, \tag{253}$$

in which

$$D = \frac{Et^3}{12\left(1 - \frac{1}{m^2}\right)}. \tag{254}$$

This quantity is called *flexural rigidity* of the plate.

In this manner the problem on bending of a plate into a cylindrical surface is reduced to the solving of equation (253), which has the same form as equation (59) page 71 for deflection curve of a beam. A particular case of the deflection due to the action of a uniformly distributed pressure will now be considered more in detail. This case is of practical importance in design of ships and tanks submitted to hydrostatic pressure.

Simply Supported Edges.—In this case the edges of the plate can freely rotate during bending but do not suffer displacement in the direction of the X axis (Fig. 216). Due to this latter condition, the deflection of an elementary strip AB will be accompanied by an extension in the axial direction, as shown in Fig. 216 (b). The magnitude of the tensile forces S due to this extension will be found from the condition that the extension of the strip is equal to the difference between the length of the deflection curve and the length l of the chord AB. A good approximation* for S will be obtained on the assumption that the deflection curve is a sine curve

$$w = \delta \sin \frac{\pi x}{l} \tag{a}$$

where δ denotes the deflection at the middle.

Then by using equation (138), the extension of the central line of the strip will be

$$\lambda = \frac{1}{2}\int_0^l \left(\frac{dw}{dx}\right)^2 dx = \frac{\pi^2\delta^2}{4l} \tag{b}$$

Taking for the deflection of the middle the approximate equation (see equation (140), p. 163) we have

$$\delta = \frac{\delta_0}{1 + \alpha^2} \tag{c}$$

in which

$$\delta_0 = \frac{5}{384}\frac{ql^4}{D}; \tag{d}$$

---

* An exact solution of the same problem was given by I. Boubnoff. See "Theory of Structure of Ships," Vol. 2, p. 545 (Petersburg), 1914.

and, as before (equation (120)),

$$\alpha^2 = S:S_{cr} = S:\frac{D\pi^2}{l^2} = \frac{Sl^2}{D\pi^2}. \tag{255}$$

Substituting in (b),

$$\lambda = \frac{\pi^2\delta_0{}^2}{4l(1+\alpha^2)^2}. \tag{e}$$

Assuming that any lateral contraction during bending is prevented, the following expression for the extension will be obtained:

$$\lambda = \frac{Sl\left(1-\frac{1}{m^2}\right)}{Et} = \frac{\pi^2\alpha^2t^2}{12l} \tag{f}$$

Equating (e) and (f), an equation for determining α^2 will be obtained as follows:

$$\alpha^2(1+\alpha^2)^2 = \frac{3\delta_0{}^2}{t^2}, \tag{256}$$

or by using (d),

$$\alpha^2(1+\alpha^2)^2 = 3\left(\frac{5}{32}\right)^2\left(1-\frac{1}{m^2}\right)^2\left(\frac{q}{E}\right)^2\left(\frac{l}{t}\right)^8 \tag{257}$$

If the dimensions of the plate and the load q are known, the right side of (257) can be calculated. The solution of (256) can be simplified by letting

$$1+\alpha^2 = x. \tag{g}$$

In this case, (256) becomes

$$x^3 - x^2 = \frac{3\delta_0{}^2}{t^2},$$

i.e., the quantity x is such that the difference between the cube and the square of this quantity has a known value. From a slide rule or a suitable table, x can be determined and then α^2 will be obtained from (g).

The deflection and stresses in the strip AB can now be calculated by using Table VIII, page 161 given for tie rods subjected to lateral loads. It is necessary only to remember that in the case under consideration the equation (123) becomes

$$u = \frac{kl}{2} = \frac{l}{2}\sqrt{\frac{S}{D}} = \frac{\alpha\pi}{2} \tag{258}$$

Taking, for instance, a steel plate of dimensions $l = 45$ in. and $t = 3/8$ in., loaded by a uniformly distributed load $q = 10$ lbs. per sq. in., then

$$\frac{l}{t} = 120,\ \frac{q}{E} = \frac{1}{3}10^{-6},\ \text{and}\ 1-\frac{1}{m^2} = .91.$$

Substituting in (257),

$$\alpha^2(1 + \alpha^2)^2 = 290 \tag{259}$$

from which

$$\alpha^2 = 5.97 \text{ and } u = \frac{\alpha\,\pi}{2} = 3.83.$$

The tensile stress produced by the longitudinal force S will be

$$p_1 = \frac{S}{t} = \frac{\alpha^2 S_{cr}}{t} = \frac{\alpha^2\pi^2 D}{t\ \ l^2} = 11{,}300 \text{ lbs. per sq. in.}$$

and the maximum bending moment at the middle of the strip will be (equation 134, p. 160)

$$M_{\max} = q\frac{l^2}{8}\cdot\psi_1(u) \tag{h}$$

By using Table VIII,

$$\psi_1(u)_{u=3.83} = .131.$$

From this it will be seen that, due to the action of the longitudinal force S, the bending moment is greatly diminished and is only about 13% of that which is produced by the action of transverse loading alone. Using now (h),

$$M_{\max} = \frac{10 \times 45^2}{8} \times .131 = 332 \text{ lbs. in.}$$

The corresponding stress will be

$$p_2 = \frac{6M_{\max}}{t^2} = \frac{6 \times 332}{3^2} \times 8^2 = 14{,}200 \text{ lbs. per sq. in.,}$$

and combining the tensile and bending stresses, the maximum stress during bending of the plate will be

$$p_{\max} = p_1 + p_2 = 11{,}300 + 14{,}200 = 25{,}500 \text{ lbs. per sq. in.}$$

It is easy to show that, due to the action of the longitudinal force, the maximum stress does not increase in the same proportion as the intensity of the load. Taking, for instance, the previous numerical example and assuming that $q = 20$ lbs. per sq. in., then, from (257),

$$\alpha^2(1 + \alpha^2)^2 = 290 \times 4 = 1{,}160,$$

from which

$$\alpha^2 = 9.85;\ u = \frac{\alpha\pi}{2} = 4.93.$$

The stress produced by tensile force S will be

$$p_1 = \frac{S}{t} = 18{,}600 \text{ lbs. per sq. in.}$$

In calculating the bending stress, equation (h) will be used. From Table VIII, for $u = 4.93$,

$$\psi_1(u) = .082.$$

Therefore, the maximum bending stress is

$$p_2 = \frac{6M_{\max}}{t^2} = \frac{6 \times 20 \times 45^2}{8 \times 3^2} \times 8^2 \times .082 = 17{,}900 \text{ lbs. per sq. in.}$$

The complete stress will then become

$$p = 18{,}600 + 17{,}900 = 36{,}500 \text{ lbs. per sq. in.}$$

In other words, due to the action of the longitudinal forces S, the stresses increase less rapidly than the load. In the case considered above, when the load is doubled, the stresses are increased only 43%.

Clamped Edges.—The same method can be used also for the case of a plate with clamped edges. In calculating the tensile forces S, equation

$$w = \frac{\delta}{2}\left(1 - \cos\frac{2\pi x}{l}\right) \tag{k}$$

instead of equation (a) may be used.

It is easy to see that (k) satisfies conditions at the clamped edges because the deflection w and the slope $\frac{dw}{dx}$ at $x = o$ and at $x = l$ become equal to zero. Substituting (k) in (b), the extension of the strip during bending will be

$$\lambda = \frac{1}{2}\int_0^l \left(\frac{dw}{dx}\right)^2 dx = \frac{\delta^2\pi^2}{4l}$$

Remembering that in the case of clamped ends (equation 141, p. 164)

$$\delta = \frac{\delta_0}{1 + \frac{\alpha^2}{4}},$$

equation

$$\alpha^2\left(1 + \frac{\alpha^2}{4}\right)^2 = \frac{3\delta_0^2}{t^2} \tag{260}$$

instead of equation (256) will be obtained for determining α^2.

Taking, as before, $\frac{l}{t} = 120$, $q = 10$ lbs. per sq. in.; and remembering that the deflection δ_0 for clamped ends is five times less than in the case of simply supported ends, the equation for determining α^2 will be (see equation 259)

$$\alpha^2\left(1 + \frac{\alpha^2}{4}\right)^2 = \frac{290}{25} \tag{l}$$

Noting

$$1 + \frac{\alpha^2}{4} = x,$$

equation (l) becomes $x^3 - x^2 = 2.90$, from which $x = 1.849$ and $\alpha^2 = 3.40$.

The tensile force is less than in the case of supported edges considered above in the ratio 3.40/5.97; therefore

$$p_1 = \frac{3.40}{5.97} \times 11{,}300 = 6{,}430 \text{ lbs. per sq. in.}$$

In calculating the bending stresses, Table VIII must be used. In the case under consideration,

$$u = \frac{\alpha\pi}{2} = 2.89.$$

Then from Table VIII,

$$\psi_2 = .686, \quad \psi_3 = .488.$$

The bending moment at the clamped edges will be

$$M = -.686 \cdot \frac{ql^2}{12} = -1{,}150 \text{ lb. ins.}$$

The corresponding bending stress will be

$$p_2 = 49{,}300 \text{ lbs. per sq. in.}$$

Combining the tensile and bending stresses as before,

$$p_{\max} = 6{,}430 + 49{,}300 = 55{,}700 \text{ lbs. per sq. in.*}$$

Comparing this stress with that obtained above for the same plate with simply supported edges it is seen that clamping the edges produces an increase of stress. This result can be explained as follows: Due to the clamping of edges, the deflection of the plate diminishes, and as a result the longitudinal force S is diminished as also is its effect on the maximum bending moment. In the case of simply supported edges the maximum bending moment was only .131 of that produced by transverse load. But in the case of clamped edges the maximum bending moment is .686 of that produced by the transverse load, i.e., the effect of longitudinal force is more pronounced in the case of simply supported edges.

Deflection of Plates Having a Small Initial Cylindrical Curvature.†—In considering this problem the results already obtained for the bending of bars with small initial curvature (Par. 57, p. 230) will be used. Let

$$w_0 = b \sin \frac{\pi x}{l} \tag{m}$$

---

* It is assumed that this stress is below the elastic limit.

† See author's article in the book "Festschrift zum Siebzigsten Geburtstage August Föppl," p. 74 (Berlin), 1923.

represent the small initial deflection of the plate with the maximum deflection at the middle equal to b. If a uniform loading q will now be applied, an additional deflection will be produced, accompanied by an extension of the middle surface of the plate. Let, as before, S denote the tensile force for a strip AB (Fig. 216) of unit width and α^2 the ratio of his force to the critical force (equation (255), p. 262). Then the additional deflection produced during loading will be (see equation (225), p. 262)

$$w_1 = \frac{\delta_0}{1+\alpha^2}\sin\frac{\pi x}{l} - \frac{\alpha^2 b}{1+\alpha^2}\sin\frac{\pi x}{l}. \tag{n}$$

The first member on the right side represents the approximate expression of the deflection for a straight line strip, used above for flat plates; the second member represents the effect of the initial curvature. By adding (m) and (n), the complete deflection will be obtained as follows:

$$w = w_0 + w_1 = b\sin\frac{\pi x}{l} + \frac{\delta_0}{1+\alpha^2}\sin\frac{\pi x}{l} - \frac{\alpha^2}{1+\alpha^2}b\sin\frac{\pi x}{l} = \frac{\delta_0 + b}{1+\alpha^2}\sin\frac{\pi x}{l}. \tag{p}$$

In order to obtain the magnitude of α^2, the extension of the strip AB must be considered. Using the same reasoning as that for flat plates (see equation (b), p. 261), the following expression for the extension of the strip will be obtained

$$\lambda = \frac{1}{2}\int_0^l \left(\frac{dw}{dx}\right)^2 dx - \frac{1}{2}\int_0^l \left(\frac{dw_0}{dx}\right)^2 dx,$$

or substituting (m) and (p) for w_0 and w and integrating,

$$\lambda = \frac{\pi^2}{4l}\left[\left(\frac{\delta_0 - b\alpha^2}{1+\alpha^2}\right)^2 + 2b\frac{\delta_0 - b\alpha^2}{1+\alpha^2}\right].$$

Making this equal to the extension (f), the following equation for determining α^2 will be obtained:

$$\left(\frac{\delta_0 - b\alpha^2}{1+\alpha^2}\right)^2 + 2b\frac{\delta_0 - b\alpha^2}{1+\alpha^2} = \frac{\alpha^2 t^2}{3},$$

from which

$$\alpha^2(1+\alpha^2)^2 = 3\left(\frac{\delta_0 + b}{t}\right)^2 - 3\frac{b^2}{t^2}(1+\alpha^2)^2 \tag{261}$$

If $b = 0$, equation (261) reduces to the equation (256) for a flat plate.

In order to show the effect which an initial curvature produces on the maximum stress, plate of the same dimensions as before will now be considered. Let

$$l = 45 \text{ in.}, \ t = \frac{3}{8} \text{ in}, \ \frac{q}{E} = \frac{1}{3}10^{-6}, \ 1 - \frac{1}{m^2} = .91,$$

and assume that the maximum value of the initial deflection is $b = 3/8$ in. Substituting this in (261) and remembering that

$$\frac{\delta_0}{t} = \frac{5}{384}\frac{ql^4}{Dt} = 9.83 \text{ in.},$$

the following will be obtained:

$$\alpha^2(1 + \alpha^2)^2 = 351.6 - 3(1 + \alpha^2)^2. \tag{r}$$

Denoting, as before,

$$1 + \alpha^2 = x,$$

equation (r) becomes

$$x^3 + 2x^2 = 351.6,$$

from which

$$x = 6.45 \text{ and } \alpha^2 = 5.45.$$

The tensile stress produced by the longitudinal force S will be

$$p_1 = \frac{S}{t} = \frac{\alpha^2 S_{cr}}{t} = \alpha^2\frac{\pi^2 D}{tl^2} = 10{,}200 \text{ lbs. per sq. in.}$$

This stress is somewhat less than the corresponding stress for the flat plate (page 263).

In order to determine the bending stresses, it must be noted that the deflection given by equation (n) consists of two parts, the first being the same as that for a flat plate and the second

$$-\frac{\alpha^2 b}{1 + \alpha^2}\sin\frac{\pi x}{l} \tag{s}$$

representing the effect of the initial curvature. Therefore the maximum stress will be obtained if the stresses due to (s) are added to those for the flat plate (equation (h), p. 263). The first can be calculated as follows:

The bending moment corresponding to (s) is

$$-D\frac{d^2}{dx^2}\left[-\frac{\alpha^2}{1 + \alpha^2}b \sin\frac{\pi x}{l}\right] = -\frac{D\alpha^2\pi^2}{(1 + \alpha^2)l^2}b \sin\frac{\pi x}{l}.$$

Dividing the maximum of this moment by the section modulus $t^2/6$ of the strip, the following stress will be obtained:

$$\frac{-\alpha^2}{1 + \alpha^2}\frac{6D\pi^2 b}{t^2 l^2} = -\frac{6}{1 + \alpha^2}\frac{b}{t}p_1.$$

Substituting here the quantities calculated above for α^2 and p_1, the bending stress due to the effect of the initial curvature will be

$$\frac{-6}{1 + 5.45} \times 10{,}200 = -9{,}500 \text{ lbs. per sq. in.}$$

Combining this with the tensile stress p_1 calculated above and the bending stress previously obtained in the flat plate, (page 263), the following complete stress will be obtained:

$$p_{\max} = 10{,}200 + 14{,}200 - 9{,}500 = 14{,}900 \text{ lbs. per sq. in.}$$

Comparing this with the result obtained for the flat plate of the same dimension, it must be noted that, due to the initial curvature, the tensile forces S are somewhat diminished and the bending stress at the middle is greatly diminished; so that the complete stress $p_{\max}$ is reduced, due to the effect of initial curvature, from 25,500 lbs. per sq. in. to 14,900 lbs. per sq. in. This effect is obtained on the assumption that the initial deflection is equal to the thickness of the plate. By increasing the initial deflection, further reduction in the maximum stress can be obtained.

64. Combination of Pure Bending in Two Perpendicular Directions. *General Consideration.*—The bending of a rectangular plate by moments uniformly distributed along the edges will now be considered (Fig. 217). Let M_1 denote the bending moment per unit length of the edge parallel to the Y axis and M_2 the moment per unit length of the edge parallel to the X axis. In order to obtain the relation between the magnitudes of bending moments M_1 and M_2 and the curvatures of the deflection surface, the same assumption will be taken as for the case of pure bending of beams (page 50). Let Fig. 218 represent an element cut out from the plate by two pairs of planes parallel to the XZ and YZ planes. Then the fundamental assumption is that during the bending produced by moments M_1 and M_2 the lateral sides of the element remain plane and rotate about the n-n axes in such a manner

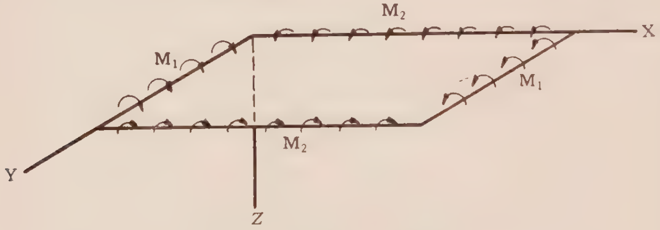

FIG. 217.—Plate under pure bending.

that compression occurs in the upper part of the element and extension in the lower part. The *middle plane nn* does not undergo any deformation during this bending of the plate and becomes a *neutral surface.* Let $1/\rho_1$, and $1/\rho_2$ denote the curvatures of the neutral surface in sections parallel to the ZX and the ZY planes; then the extensions of an elemental sheet abcd, distant z from the neutral surface, in the directions of X and Y axes, will be

$$e_x = \frac{z}{\rho_1},\ e_y = \frac{z}{\rho_2}. \tag{a}$$

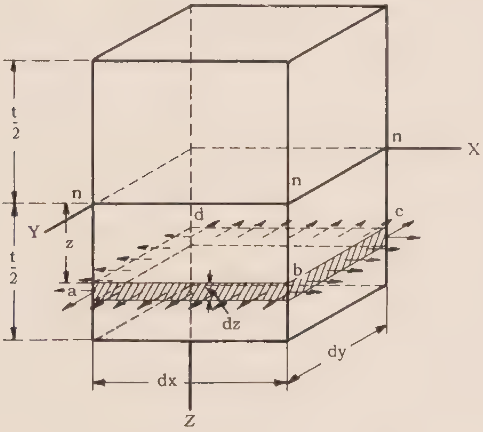

FIG. 218.—Element of bent plate.

Now, by using equation (10) page 12, the corresponding stresses will be

$$p_x = \frac{Ez}{1 - \frac{1}{m^2}}\left(\frac{1}{\rho_1} + \frac{1}{m}\frac{1}{\rho_2}\right), \tag{b}$$

$$p_y = \frac{Ez}{1 - \frac{1}{m^2}}\left(\frac{1}{\rho_2} + \frac{1}{m}\frac{1}{\rho_1}\right). \tag{c}$$

Equaling the moments of the internal stresses (distributed over the sides of the element) to the moments of external couples, the following equations will be obtained:

$$\int_{-\frac{1}{2}t}^{+\frac{1}{2}t} zp_x dydz = M_1 dy, \tag{d}$$

$$\int_{-\frac{1}{2}t}^{+\frac{1}{2}t} zp_y dxdz = M_2 dx. \tag{e}$$

Substituting (b) and (c) for p_x and p_y, and remembering that

$$\frac{E}{1-\frac{1}{m^2}}\int_{-\frac{1}{2}t}^{+\frac{1}{2}t} z^2dz = \frac{Et^3}{12\left(1-\frac{1}{m^2}\right)} = D$$

where D denotes *flexural rigidity*, as before (equation (254), p. 261), the following equations will be obtained:

$$D\left[\frac{1}{\rho_1}+\frac{1}{m}\frac{1}{\rho_2}\right] = M_1, \tag{262}$$

$$D\left[\frac{1}{\rho_2}+\frac{1}{m}\frac{1}{\rho_1}\right] = M_2, \tag{263}$$

which correspond to the equation (48) page 52 for the pure bending of a straight beam.

Denoting the deflections of the plate by w, and using for small deflections the known approximate formula

$$\frac{1}{\rho_1} = -\frac{\partial^2 w}{\partial x^2} \text{ and } \frac{1}{\rho_2} = -\frac{\partial^2 w}{\partial y^2},$$

equations (262) and (263) will be represented in the following form:

$$-D\left(\frac{\partial^2 w}{\partial x^2}+\frac{1}{m}\frac{\partial^2 w}{\partial y^2}\right) = M_1 \tag{264}$$

$$-D\left(\frac{\partial^2 w}{\partial y^2}+\frac{1}{m}\frac{\partial^2 w}{\partial x^2}\right) = M_2 \tag{265}$$

which equations correspond to the equation (59) for the deflection curve of a straight beam.

Deflection to a Spherical Surface.—If $M_1 = M_2 = M$, the curvatures of the deflection surface in two perpendicular directions will be the same:

$$\frac{1}{\rho_1} = \frac{1}{\rho_2} = \frac{1}{\rho},$$

i.e., the deflection surface will be a spherical surface. The radius of the sphere, from (262), will be

$$\frac{1}{\rho} = \frac{M}{D}\frac{1}{1+\frac{1}{m}}. \tag{266}$$

Limitations for the Equations Obtained.—In the considerations above, it was assumed that there is no stretching of the middle surface and that this surface is the *neutral surface* during bending of the plate. It can be shown that this assumption is accurate enough only in cases where the deflection of the plate is small in comparison to its thickness

t. For this purpose consider here the bending of a circular plate produced by the couples M uniformly distributed along the edge. It follows from the previous theory that the deflection surface will be a spherical one the curvature of which is given by equation (266). Let AOB (Fig. 219) represent the diametral section of the bent circular plate, r = the initial radius of the plate, and δ = the deflection at the middle. If there is no stretching of the middle surface in radial direction, then $OB = r$, $\theta = \frac{r}{\rho}$, and $CB = r_1 = \rho \sin \theta$. Therefore, the deflection of the plate will be accompanied by a compressive strain in a direction tangent to the edge. The magnitude of this strain will be

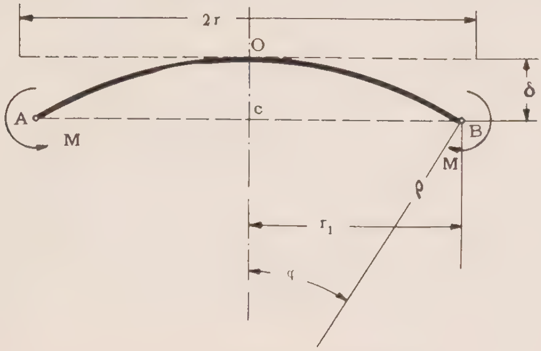

Fig. 219.—Deflection limitations.

$$e = \frac{r - r_1}{r} = \frac{\rho\theta - \rho \sin \theta}{\rho\theta} = \frac{\theta^2}{6}. \tag{g}$$

It will be noted from Fig. 219 that

$$\delta = \rho(1 - \cos \theta) = \frac{\rho\theta^2}{2}. \tag{h}$$

From (g) and (h),

$$e = \frac{\delta}{3\rho} \tag{k}$$

This represents the upper limit* of strain in the middle surface which was neglected in the theory given above. The maximum strain, taken in consideration by the same theory, from (a), is

$$e_x = e_y = \frac{t}{2\rho}. \tag{l}$$

---

* In real conditions there will be some extension in radial direction, and the compression e in the tangential direction will be smaller than that given by equation (k).

It is clear now that the strain (k) can be neglected only in the case if δ is small in comparison to t, and only on this assumption can the tables and equations given below for some special cases of bending of plates be used with sufficient accuracy.

Thermal Stresses in Plates.—Equation (266), obtained above for spherical deflection, can be used also in calculating thermal stresses produced in a plate by non-uniform heating. Let T denote the difference in temperature of the upper and lower sides of the plate, and α the coefficient of linear expansion of the material. Assume that the variation of the temperature through the thickness of the plate follows a linear law. The corresponding expansions will follow the same law, and if the edge of the plate is free, the deflection produced by these expansions will be a spherical one. The difference between the maximum expansion and the expansion at the middle surface is $\alpha T/2$, and the curvature of the spherical surface will be obtained from the equation

$$\frac{\alpha T}{2} = \frac{t}{2\rho},$$

from which

$$\frac{1}{\rho} = \frac{\alpha T}{t}. \tag{267}$$

This bending of the plate will not produce stresses if the edge of the plate is free and the deflection is small in comparison to the thickness.

If, however, the edge of the plate be clamped, bending moments along the edge will be produced during the heating. The magnitude of these moments will be such as to annihilate the curvature (267) produced by non-uniform heating. Because, only in this manner the condition at the clamped edge will be satisfied. Comparing (267) and (266), the following expression for bending moment will be obtained:

$$M = \frac{\alpha D T}{t}\left(1 + \frac{1}{m}\right)$$

The corresponding maximum of thermal stresses will be

$$\begin{aligned} p_{\max} &= \frac{6M}{t^2} = \frac{6\alpha D T}{t^3}\left(1 + \frac{1}{m}\right) \\ &= \frac{\alpha T}{2}\frac{E}{1 - \frac{1}{m}} \end{aligned} \tag{268}$$

This stress is proportional to the coefficient of expansion α, to the difference of temperature on two sides of the plate, and to the modulus of elasticity.

The difference in temperature T* is likely to increase with the thickness of the plate; therefore greater thermal stress can be expected in thick plates than in thin ones.

Equation (268), developed for flat plates, can also be used with sufficient accuracy in cases of spherical and cylindrical thin shells.

65. Bending of Circular Plates.—The simplest case of bending produced in a circular plate by a uniformly distributed load q and by a force P concentrated in the center of the plate will be here considered.† The deflection surface in this case will be symmetrical about the axis which goes through the center and is perpendicular to the plate; therefore a consideration of a diametral section of the plate through this axis will be sufficient for calculating deflections and stresses. Let Fig. 220 represent this diametral section and OZ

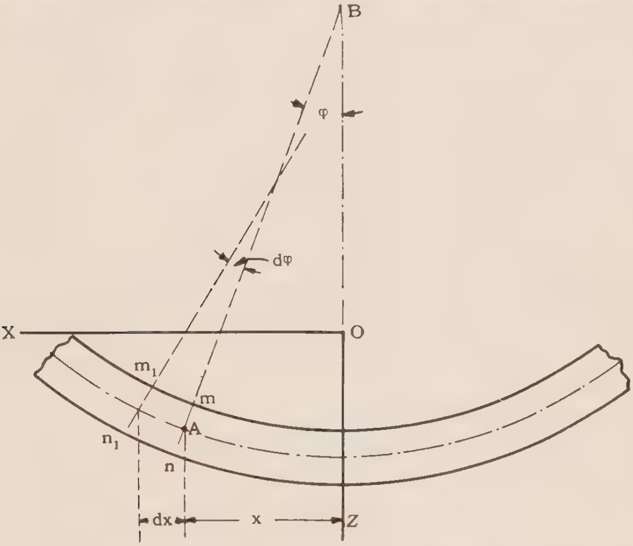

FIG. 220.—Bending of circular plate.

---

* It must be noted that T denotes the difference of temperature between the two sides of the plate and not that between liquids or gases in contact with the plate, for the latter may be much higher than T.

† Bending of a circular plate by a load applied not in the center was considered by Clebsch; see "Théorie de l'élasticité des corps solides," p. 774, published by S. Venant, Paris. A circular plate supported in several points at the edge was considered by A. Nadai; see *Phys. Zeitschr.*, Vol. 23, p. 366, 1922.

represent the axis of symmetry. Let w denote, as before, the deflection of the plate at any point A, and ϕ the slope at the same point. Assuming that the deflection is very small, the curvature of the plate in the diametral section XZ will be

$$\frac{1}{\rho_1} = -\frac{d^2w}{dx^2} = \frac{d\phi}{dx}. \tag{a}$$

In order to find the radius of curvature ρ_2 in the section perpendicular to XZ, it is necessary to note that sections such as nm form, after deformation, a conical surface the apex B of which is obtained by the points of intersection of nm with axis OZ. Then AB represents the radius ρ_2 and from the figure,

$$\frac{1}{\rho_2} = \frac{\phi}{x}. \tag{b}$$

By using (a) and (b) and equation (262) page 270, bending moment* M_1 on the section mn will be obtained as follows:

$$M_1 = D\left(\frac{d\phi}{dx} + \frac{1}{m}\frac{\phi}{x}\right). \tag{269}$$

In the same manner, the bending moment M_2 per unit length of the diametral section XZ will be obtained as follows:

$$M_2 = D\left(\frac{\phi}{x} + \frac{1}{m}\frac{d\phi}{dx}\right) \tag{270}$$

In order to obtain the equation for determining ϕ, the equilibrium of an element *abcd* (Fig. 221) cut out from the plate by two cylindrical sections *ab* and *cd* and by two diametrical sections *ao* and *bo* will now be considered. The couple acting on the side *cd* of the element will be equal to

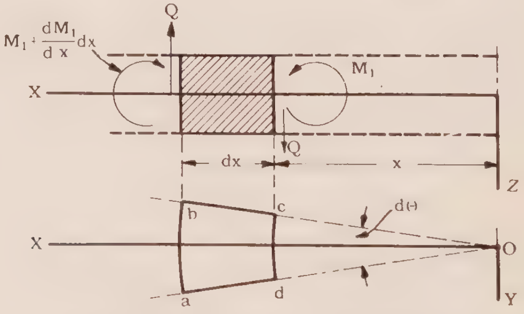

Fig. 221.—Element of bent circular plate.

$$M_1 x d\theta. \tag{c}$$

---

* As before, M_1 and M_2 denote bending moments per unit length.

The corresponding couple on side *ab* is

$$\left(M_1 + \frac{dM_1}{dx}dx\right)(x + dx)d\theta. \tag{d}$$

On the sides *ad* and *bc* of the element couples are acting given by M_2dx, which produce a resultant in the diametral section XZ equal to

$$M_2dxd\theta. \tag{e}$$

In addition to these couples, shearing forces Q will act on the sides *ab* and *cd* of the element. The magnitude of these forces can be found as follows: Consider the side *cd* corresponding to the cylindrical section the axis of which is OZ and the radius of which is x. The shearing force Q per unit length of this section will be found from the condition of equilibrium of the inner part of the plate cut out by the cylindrical surface. The load acting on this part of the plate is $\pi x^2q + P$. This load is statically equivalent to the resultant of shearing forces Q distributed over the cylindrical section; therefore $2\pi xQ = \pi x^2q + P$ from which the shearing force per unit length will be

$$Q = \frac{qx}{2} + \frac{P}{2\pi x}.$$

The shearing force acting on the side *cd* of the element is

$$Qxd\theta = d\theta\left(\frac{qx^2}{2} + \frac{P}{2\pi}\right). \tag{f}$$

Computing the moments of all forces acting on the element *abcd* about an axis perpendicular to the diametral section XZ and using (c), (d), (e), and (f), the following equation of equilibrium will be obtained:

$$\left(M_1 + \frac{dM_1}{dx}dx\right)(x + dx)d\theta - M_1xd\theta - M_2dxd\theta + Qxdxd\theta = 0$$

from which, by neglecting small quantities of higher order, we have

$$M_1 + \frac{dM_1}{dx}x - M_2 + \frac{qx^2}{2} + \frac{P}{2\pi} = 0. \tag{g}$$

Substituting (269) and (270) for M_1 and M_2, equation (g) becomes

$$\frac{d^2\phi}{dx^2} + \frac{1}{x}\frac{d\phi}{dx} - \frac{\phi}{x^2} = -\frac{1}{D}\left(\frac{qx}{2} + \frac{P}{2\pi x}\right),$$

or

$$\frac{d}{dx}\left[\frac{1}{x}\frac{d}{dx}(x\phi)\right] = -\frac{1}{D}\left(\frac{qx}{2} + \frac{P}{2\pi x}\right).$$

By integrating,

$$\frac{1}{x}\frac{d}{dx}(x\phi) = -\frac{1}{D}\left(\frac{qx^2}{4} + \frac{P}{2\pi}\log_e x\right) + C_1,$$

where C_1 = arbitrary constant of integration.

The second integration gives

$$x\phi = -\frac{qx^4}{16D} - \frac{P}{2\pi D}\left(\frac{x^2 \log_e x}{2} - \frac{x^2}{4}\right) + \frac{C_1x^2}{2} + C_2$$

from which

$$\phi = -\frac{qx^3}{16D} - \frac{Px}{8\pi D}(2 \log_e x - 1) + \frac{C_1x}{2} + \frac{C_2}{x}. \tag{271}$$

Substituting

$$\phi = -\frac{dw}{dx}$$

the following equation for deflection will be obtained:

$$\frac{dw}{dx} = \frac{qx^3}{16D} + \frac{Px}{8\pi D}(2 \log_e x - 1) - \frac{C_1x}{2} - \frac{C_2}{x}$$

from which, by integrating,

$$w = \frac{qx^4}{64D} + \frac{Px^2}{8\pi D}(\log_e x - 1) - \frac{C_1x^2}{4} - C_2 \log_e x + C_3. \tag{272}$$

The arbitrary constants C_1, C_2, C_3 must be determined from the conditions at the edge. The method of determining them will now be shown for particular cases.

66. Uniformly Loaded Circular Plate.—*Clamped Edge.*—Let r denote the radius of the plate, and take $P = 0$. Then the arbitrary constants C_1 and C_2 of equation (271) will be determined from the conditions that ϕ must be equal to zero at the edge and at the center of the plate. In this manner the following equations will be obtained:

$$\left(\frac{qx^3}{16D} - \frac{C_1x}{2} - \frac{C_2}{x}\right)_{x=0} = 0,$$

$$\left(\frac{qx^3}{16D} - \frac{C_1x}{2} - \frac{C_2}{x}\right)_{x=r} = 0$$

from which

$$C_2 = 0 \text{ and } C_1 = \frac{qr^2}{8D}. \tag{a}$$

Substituting in (271), we have

$$\phi = \frac{qx}{16D}(r^2 - x^2). \tag{273}$$

Now the bending moments M_1 and M_2, from equations (269) and (270) of the previous paragraph, become

$$M_1 = D\left(\frac{d\phi}{dx} + \frac{1}{m}\frac{\phi}{x}\right) = \frac{q}{16}\left[r^2\left(1 + \frac{1}{m}\right) - x^2\left(3 + \frac{1}{m}\right)\right], \tag{b}$$

$$M_2 = D\left(\frac{\phi}{x} + \frac{1}{m}\frac{d\phi}{dx}\right) = \frac{q}{16}\left[r^2\left(1 + \frac{1}{m}\right) - x^2\left(1 + \frac{3}{m}\right)\right]. \tag{c}$$

At the edge ($x = r$), equations (b) and (c) give

$$M_1 = -\frac{qr^2}{8} \text{ and } M_2 = -\frac{qr^2}{8m}. \tag{d}$$

The corresponding maximum stresses in the radial and tangential directions will therefore be

$$(p_x)_{\max} = \frac{6}{t^2} \cdot \frac{qr^2}{8} = \frac{3}{4}\frac{qr^2}{t^2}, \quad (p_y)_{\max} = \frac{6}{t^2}\frac{qr^2}{8m} = \frac{3}{4}\frac{qr^2}{mt^2} \tag{274}$$

in which, as before, t denotes the thickness of the plate. At the center of the plate ($x = 0$), from (b) and (c),

$$M_1 = M_2 = \frac{qr^2}{16}\left(1 + \frac{1}{m}\right), \tag{275}$$

and the corresponding maximum stresses are

$$(p_x)_{\max} = (p_y)_{\max} = \frac{3}{8}\frac{qr^2}{t^2}\left(1 + \frac{1}{m}\right). \tag{275a}$$

In order to obtain the deflection of the plate, equation (272) will be used. Substituting in it the values for the arbitrary constants given by (a) and making $P = 0$, the following equation will be obtained:

$$w = \frac{qx^4}{64D} - \frac{qr^2x^2}{32D} + C_3. \tag{e}$$

The arbitrary constant C_3 will be found from the condition that at the clamped edge ($x = r$) the deflection is zero. Therefore,

$$C_3 = \frac{qr^4}{64D}$$

and the equation (e) for the deflection becomes

$$w = \frac{q}{64D}(r^2 - x^2)^2. \tag{276}$$

Maximum deflection δ will be at the center ($x = 0$), where

$$\delta = \frac{qr^4}{64D}. \tag{277}$$

Simply Supported Edges.—In order to obtain the deflection for a plate with simply supported edges the principle of superposition will be used. It was shown (equation (d)) that, in the case of clamped edges, negative bending moments $M_1 = -q\frac{r^2}{8}$ are acting along the edge (Fig. 222 (a)). It is easy to see that by combining this case with that of pure bending shown in Fig. 222 (b), thus annihilating the bending moment at the edge, the bending of the plate with simply supported edges will be obtained.

Superimposing the constant bending moment $+qr^2/8$ on the moments (b) and (c), the following expressions for bending moments in the case of a plate with simply supported edges will be obtained:

$$M_1 = \frac{q}{16}\left(3 + \frac{1}{m}\right)(r^2 - x^2),$$

$$M_2 = \frac{q}{16}\left[\left(3 + \frac{1}{m}\right)r^2 - \left(1 + \frac{3}{m}\right)x^2\right].$$

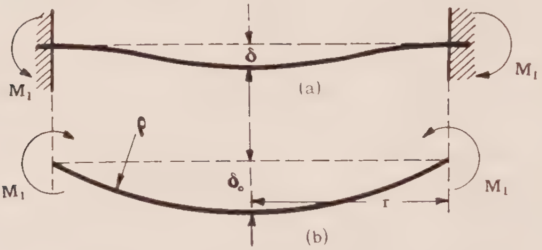

FIG. 222. —Circular plate with built-in edges.

The maximum bending moment will be at the center ($x = 0$) where

$$M_1 = M_2 = \frac{qr^2}{16}\left(3 + \frac{1}{m}\right).$$

The corresponding maximum stresses are

$$(p_x)_{\max} = (p_y)_{\max} = \frac{3}{8}\left(3 + \frac{1}{m}\right)\frac{qr^2}{t^2}. \tag{278}$$

For comparison of $(p_x)_{\max}$ and $(p_y)_{\max}$, for the cases of clamped and simply supported edges, a graphical representation of the variation in these stresses along a radius of the plate is given in Fig. 223. The stresses for the simply supported plates are represented by full lines; those for the clamped plate are represented by dotted lines. It will be seen that due to clamping, more favorable conditions are obtained.

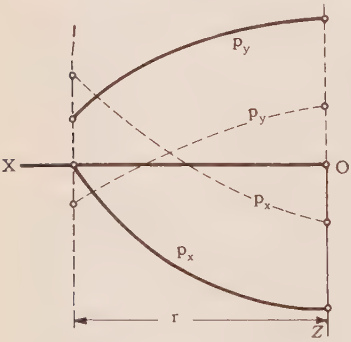

FIG. 223.— Stresses in bent circular plates.

In order to obtain the deflection for the simply supported plate, it is necessary only to add to the deflection (277), found above for the plate with the clamped edge the deflection, δ_0, shown in Fig. 222 (b). The deflection δ_0 can be obtained from the following consideration:

In the case Fig. 222 (b) the deflection surface is a sphere, the radius of which will be found from the equation (266) page 270. Substituting $M = qr^2/8$, the following will be obtained:

$$\rho = 8\left(1 + \frac{1}{m}\right)\frac{D}{qr^2},$$

therefore

$$\delta_0 = \frac{r^2}{2\rho} = \frac{qr^4}{16D\left(1 + \frac{1}{m}\right)}.$$

Adding this to (277), the deflection of the plate with simply supported edges will be obtained as follows:

$$\delta = \frac{qr^4}{64D} + \frac{qr^4}{16D\left(1 + \frac{1}{m}\right)} = \frac{qr^4}{64D}\frac{5 + \frac{1}{m}}{1 + \frac{1}{m}}. \tag{279}$$

For $1/m = .3$, this deflection is about four times as great as that in the case of clamped edges.

67. Circular Plate Loaded in the Center.—*Clamped Edge.*—Substituting in equation (271) $q = 0$, the following equation for ϕ will be obtained:

$$\phi = -\frac{Px}{8\pi D}(2 \log_e x - 1) + \frac{C_1 x}{2} + \frac{C_2}{x}. \tag{a}$$

The arbitrary constants C_1 and C_2 will be found from the conditions that ϕ is equal to zero at the edge and at the center of the plate; therefore

$$\left[-\frac{Px}{8\pi D}(2 \log_e x - 1) + \frac{1}{2}C_1 x + \frac{C_2}{x}\right]_{x=0} = 0, \tag{b}$$
$$\left[-\frac{Px}{8\pi D}(2 \log_e x - 1) + \frac{1}{2}C_1 x + \frac{C_2}{x}\right]_{x=r} = 0$$

from which, taking into consideration that

$$(x \log_e x)_{x=0} = 0,$$

the following values for the arbitrary constants will be obtained:

$$C_1 = \frac{P}{4\pi D}(2 \log_e r - 1),\ C_2 = 0. \tag{c}$$

Substituting in (a),

$$\phi = \frac{Px}{4\pi D}\log_e \frac{r}{x}. \tag{280}$$

Now, from equations (269) and (270),

$$M_1 = \frac{P}{4\pi}\left[\left(1 + \frac{1}{m}\right)\log_e\frac{r}{x} - 1\right], \tag{d}$$

$$M_2 = \frac{P}{4\pi}\left[\left(1 + \frac{1}{m}\right)\log_e\frac{r}{x} - \frac{1}{m}\right]. \tag{e}$$

at the edge ($x = r$) these moments become

$$M_1 = -\frac{P}{4\pi}, \; M_2 = -\frac{P}{4\pi}\frac{1}{m}; \tag{281}$$

and the corresponding maximum stresses will be:

$$(p_x)_{\max} = \frac{3}{2}\frac{P}{\pi t^2}, \; (p_y)_{\max} = \frac{3}{2m}\frac{P}{\pi t^2} \tag{282}$$

Comparing these to equation (274) for a uniform loading, it can be concluded that the load concentrated in the center produces, at the clamped edge of the plate, stresses which are twice as great as the stresses produced by the load of the same magnitude but uniformly distributed over the plate. Applying equations (d) and (e) at the center of the plate ($x = 0$), it will be observed that infinitely large stresses are obtained. This result is due to the assumption made, that the load is concentrated at a point.* By taking the distribution of the load over a small circle, the stresses assume finite values as will be shown later.

Substituting the values (c) for the arbitrary constants in the equation for the deflection surface, the following equation will be obtained:

$$w = \frac{Px^2}{8\pi D}\left(\log_e\frac{x}{r} - \frac{1}{2}\right) + C_3. \tag{f}$$

In order to have $w = 0$ at the edge, it follows that

$$C_3 = \frac{Pr^2}{16\pi D}.$$

Substituting in (f), we have

$$w = \frac{Px^2}{8\pi D}\log_e\frac{x}{r} + \frac{P}{16\pi D}(r^2 - x^2). \tag{283}$$

The deflection at the middle ($x = 0$) will be

$$\delta = \frac{Pr^2}{16\pi D}. \tag{284}$$

Comparing this with (277) it can be concluded that the deflection produced by a concentrated load is four times as great as that produced by a uniformly distributed load of the same magnitude.

---

* Local stresses produced in a circular plate by a concentrated load are considered in the paper by Hencky: *Der Spannungszustand in rechteckigen Platten*, p. 54, Darmstadt, 1913.

Simply Supported Edge.—In order to obtain the deflection for a plate with simply supported edges the same method will be used as for the uniform loading (see Par. 66, p. 277). Superimposing on the deflection (283), found above for the case of a clamped edge, the deflection produced by moments $M_1 = +P/4\pi$ uniformly distributed along the edge, we will have the case of a simply supported edge.

The curvature produced by moments $M_1 = +P/4\pi$ will be (Eq. 266, p. 270)

$$\rho = \frac{4\pi}{P}\left(1 + \frac{1}{m}\right) D;$$

and the corresponding deflection is

$$\delta_0 = \frac{r^2}{2\rho} = \frac{Pr^2}{8\pi D} \cdot \frac{1}{1 + \frac{1}{m}}.$$

Combining this with (284), the deflection at the middle becomes

$$\delta = \frac{Pr^2}{16\pi D} + \frac{Pr^2}{8\pi D}\frac{1}{1 + \frac{1}{m}} = \frac{Pr^2}{16\pi D}\frac{3 + \frac{1}{m}}{1 + \frac{1}{m}}, \tag{285}$$

i.e., about 2.5 times as great as that for the case of clamped edges. The expression for the bending moments can be obtained by adding to the moments (d) and (e) the constant moment $P/4\pi$.

68. Circular Plate Uniformly Loaded along a Concentric Circle.—If the load is uniformly distributed along a circle of radius b (Fig. 224), it is necessary to consider the two parts of the plate separately, the inner part $x < b$, and the outer part $x > b$. By using the same general solution (272) as before and by determining the arbitrary constants so as to satisfy the conditions of continuity between the two parts of the plate and by denoting with P the complete load, the following results can be obtained:* For the clamped edge,

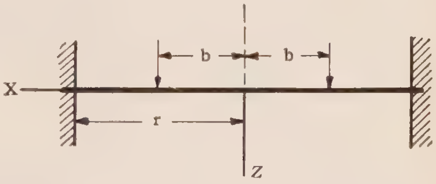

FIG. 224.—Circular plate under concentrated concentric loading.

---

[*] See: Note of Paragraph 45 of Saint-Venant's translation of the book by Clebsch "Theorie der Elasticität fester Körper" (Paris).

$$w_{x<b} = \frac{P}{8\pi D}\left[-(x^2 + b^2)\log_e\frac{r}{b} + (x^2 - b^2) + \frac{1}{2}\left(1 + \frac{b^2}{r^2}\right)(r^2 - x^2)\right], \qquad (286)$$

$$w_{x>b} = \frac{P}{8\pi D}\left[-(x^2 + b^2)\log_e\frac{r}{x} + \frac{1}{2}\left(1 + \frac{b^2}{r^2}\right)(r^2 - x^2)\right]; \qquad (287)$$

For the simply supported edge,

$$w_{x<b} = \frac{w}{8\pi D}\left[-(x^2 + b^2)\log_e\frac{r}{b} + (x^2 - b^2) + \frac{\left(3 + \frac{1}{m}\right)r^2 - \left(1 - \frac{1}{m}\right)b^2}{2\left(1 + \frac{1}{m}\right)r^2}(r^2 - x^2)\right], \qquad (288)$$

$$w_{x>b} = \frac{P}{8\pi D}\left[-(x^2 + b^2)\log_e\frac{r}{x} + \frac{\left(3 + \frac{1}{m}\right)r^2 - \left(1 - \frac{1}{m}\right)b^2}{2\left(1 + \frac{1}{m}\right)r^2}(r^2 - x^2)\right]. \qquad (289)$$

By using these equations together with the principle of superposition, any other case of deflection of a circular plate, by a loading distributed symmetrically about the Z axis, can be found. Consider, for instance, the case shown in Fig. 225, in which the load is uniformly distributed over the inner part of the plate bounded by a circle of radius a.

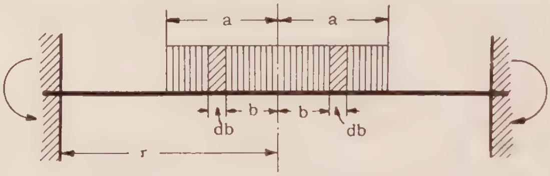

FIG. 225.—Circular plate with uniformly distributed concentric loading.

Substituting in (286) $x = 0$ and $P = 2\pi bdbq$, the deflection produced at the center of the plate by the elemental ring loading, shown in the figure, will be given by

$$dw = \frac{q}{4D}\left[-b^2\log_e\frac{r}{b} - b^2 + \frac{1}{2}\left(1 + \frac{b^2}{r^2}\right)r^2\right]bdb$$

and the deflection produced by the complete load will be

$$\delta = \int_0^a dw = \frac{q}{4D}\int_0^a \left[-b^2 \log_e \frac{r}{b} - b^2 + \frac{1}{2}\left(1 + \frac{b^2}{r^2}\right) r^2 \right] bdb =$$

$$\frac{q}{4D}\left(\frac{-a^4}{4} \log_e \frac{r}{a} - \frac{3}{16} a^4 + \frac{r^2 a^2}{4} \right) \qquad (290)$$

If $a = r$, equation (290) becomes that for a uniformly distributed loading (277).

If we substitute in (290)

$$a = 0 \text{ and } \pi a^2 q = P,$$

we will obtain the deflection (284) for concentrated load P. In order to determine the maximum stress at the center of the plate represented in Fig. 225, the curvature of the deflection surface at this point must be calculated.

Calculating the second derivative of (286) with respect to x and substituting $P = 2\pi b db q$, the curvature at the center, produced by the elemental ring loading (Fig. 225), will be

$$\frac{q}{4D}\left(-2 \log_e \frac{r}{b} + 1 - \frac{b^2}{r^2} \right) bdb$$

from which the curvature produced by the complete loading, distributed over the area of the circle of radius a will become

$$\left(\frac{d^2 w}{dx^2}\right)_{x=0} = \frac{q}{4D}\int_0^a \left(-2 \log_e \frac{r}{b} + 1 - \frac{b^2}{r^2} \right) bdb =$$

$$-\frac{qa^2}{4D}\left(\log_e \frac{r}{a} + \frac{a^2}{4r^2} \right). \qquad (291)$$

The corresponding bending moment at the center will be, from (266),

$$M_1 = M_2 = -D\left(1 + \frac{1}{m}\right)\frac{d^2 w}{dx^2} = \frac{qa^2}{4}\left(1 + \frac{1}{m}\right)\left(\log_e \frac{r}{a} + \frac{a^2}{4r^2}\right), \qquad (292)$$

and the corresponding stresses will be

$$(p_x)_{\max} = (p_y)_{\max} = \frac{3}{2}\frac{qa^2}{t^2}\left(1 + \frac{1}{m}\right)\left(\log_e \frac{r}{a} + \frac{a^2}{4r^2}\right). \qquad (293)$$

Observing that $P = q\pi a^2$, the following equation

$$(p_x)_{\max} = (p_y)_{\max} = \frac{3P}{2\pi t^2}\left(1 + \frac{1}{m}\right)\left(\log_e \frac{r}{a} + \frac{a^2}{4r^2}\right) \qquad (294)$$

for calculating the stresses produced by a load P distributed over the area πa^2 will be obtained. It is seen that these stresses increase with decrease of a, but remain finite as long as a is finite.*

---

* Discussion on stresses produced by a concentrated force in the case of a rectangular plate, see author's paper: *Der Bauingenieur*, p. 51, 1922. See also paper by A. Nadai, in the same periodical, p. 11, 1921.

69. Deflection of a Circular Plate Having a Circular Hole at the Center.—*Bending by Couples.*—In this case the same general equations (271) and (272) for the slope and the deflection can be used.

Substituting in these equations $q = P = 0$, the deflection of the plate by moments M_{1a} and M_{1b} uniformly distributed over the outer and inner edges (Fig. 226) will be obtained.

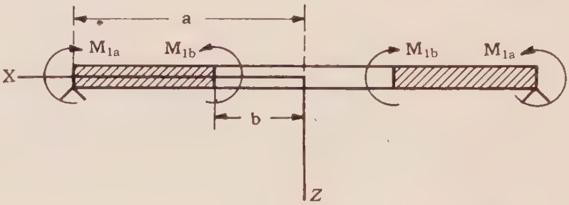

Fig. 226.—Pure bending of circular plate with central hole.

In this case,

$$\phi = \frac{C_1 x}{2} + \frac{C_2}{x}, \tag{a}$$

$$w = -\frac{C_1 x^2}{4} - C_2 \log_e x + C_3. \tag{b}$$

The arbitrary constants will be determined from the condition at the edges.

Substituting (a) in equation (269) page 274,

$$M_1 = D\left[\frac{C_1}{2} - \frac{C_2}{x^2} + \frac{1}{m}\left(\frac{C_1}{2} + \frac{C_2}{x^2}\right)\right]. \tag{c}$$

By putting $x = a$ (and afterwards, $x = b$) we have the following equations for determining C_1 and C_2:

$$D\left[\frac{C_1}{2}\left(1 + \frac{1}{m}\right) - \frac{C_2}{a^2}\left(1 - \frac{1}{m}\right)\right] = M_{1a},$$

$$D\left[\frac{C_1}{2}\left(1 + \frac{1}{m}\right) - \frac{C_2}{b^2}\left(1 - \frac{1}{m}\right)\right] = M_{1b},$$

from which

$$C_1 = 2 \cdot \frac{a^2 M_{1a} - b^2 M_{1b}}{D(a^2 - b^2)\left(1 + \frac{1}{m}\right)}, \tag{d}$$

$$C_2 = \frac{a^2 b^2 (M_{1a} - M_{1b})}{D(a^2 - b^2)\left(1 - \frac{1}{m}\right)}. \tag{e}$$

The constant C_3 will be determined from the consideration of the deflection of the plate.

Assuming, for instance, that the plate is simply supported at the outer edge, the deflection at this edge will be zero and the equation for determining C_3 will be, from (b),

$$-C_1\frac{a^2}{4} - C_2 \log_e a + C_3 = 0.$$

As a second example, consider the case of bending of the plate by the couples M_{1a} when the inner edge is built-in (Fig. 227). In this case,

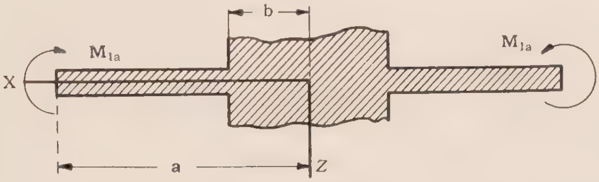

FIG. 227.—Pure bending of flange.

from (a) and (c), the following equations are obtained for determining the arbitrary constants:

$$\frac{C_1 b}{2} + \frac{C_2}{b} = 0,$$

$$\frac{C_1}{2}\left(1 + \frac{1}{m}\right) - \frac{C_2}{a^2}\left(1 - \frac{1}{m}\right) = \frac{M_{1a}}{D},$$

from which

$$C_1 = \frac{2M_{1a}}{D\left[\left(1 + \frac{1}{m}\right) + \frac{b^2}{a^2}\left(1 - \frac{1}{m}\right)\right]},$$

$$C_2 = -\frac{M_{1a}b^2}{D\left[\left(1 + \frac{1}{m}\right) + \frac{b^2}{a^2}\left(1 - \frac{1}{m}\right)\right]}.$$

Substituting in (a),

$$\phi = \frac{M_{1a}}{D\left[\left(1 + \frac{1}{m}\right) + \frac{b^2}{a^2}\left(1 - \frac{1}{m}\right)\right]}\left(x - \frac{b^2}{x}\right). \tag{f}$$

Now the bending moment M_1 (Eq. (269)) at any point will be

$$M_1 = \frac{M_{1a}}{\left[\left(1 + \frac{1}{m}\right) + \frac{b^2}{a^2}\left(1 - \frac{1}{m}\right)\right]}\left[1 + \frac{1}{m} + \left(1 - \frac{1}{m}\right)\frac{b^2}{x^2}\right].$$

Bending by Loading Uniformly Distributed along Inner and Outer Edges.—If bending is produced by a loading uniformly distributed along the edges (Fig. 228 (a)), general equations (271) and (272) can be used, it is neceessary only to put $q = 0$, and P equal to the complete load. The slope will be

$$\phi = \frac{-Px}{8\pi D}(2 \log_e x - 1) + C_1\frac{x}{2} + \frac{C_2}{x}. \tag{a}$$

The arbitrary constants will be determined from the conditions at the edges. Assume, for instance, that the plate is built-in at the edges

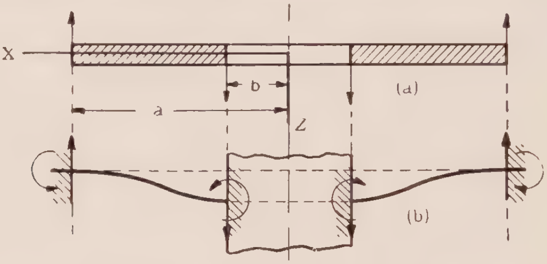

FIG. 228.—Plate with central hole loaded at inner and outer edge.

(Fig. 228 (b)), then the equations for the determination of the arbitrary constants will be

$$(\phi)_{x=a} = \frac{-Pa}{8\pi D}(2 \log_e a - 1) + \frac{C_1 a}{2} + \frac{C_2}{a} = 0,$$

$$(\phi)_{x=b} = \frac{-Pb}{8\pi D}(2 \log_e b - 1) + \frac{C_1 b}{2} + \frac{C_2}{b} = 0.$$

Calculating these constants and substituting in (a), the expression for ϕ will be obtained. The bending moments can then be found from general equations (269) and (270).

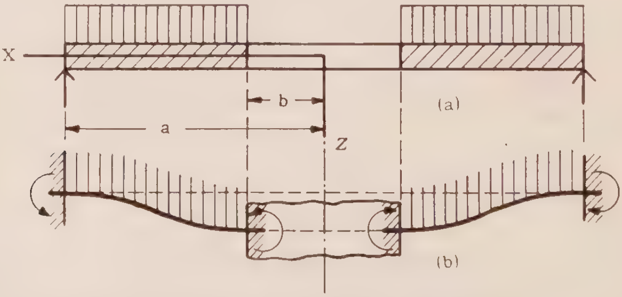

FIG. 229.—Circular plate with central hole uniformly loaded.

Bending by Uniformly Distributed Load.—It is easy to see Fig. 229 (a) that, in this case, shearing force Q at a point distant x from the center will be

$$Q = \frac{q\pi(x^2 - b^2)}{2\pi x} = \frac{qx}{2} - \frac{qb^2}{2x}.$$

Substituting this in place of

$$\frac{qx}{2} + \frac{P}{2\pi x}$$

in the equation of equilibrium (g) page 275, we will have

$$\phi = \frac{-qx^3}{16D} + \frac{qb^2x}{8D}(2 \log_e x - 1) + \frac{C_1x}{2} + \frac{C_2}{x}$$

and

$$w = \frac{qx^4}{64D} - \frac{qb^2x^2}{8D}(\log_e x - 1) - \frac{C_1x^2}{4} - C_2 \log_e x + C_3.$$

The arbitrary constants must be determined as before from the conditions at the edges.

Assuming, for instance, that the plate is built-in at the edges (Fig. 229 (b)), the equations for determining the arbitrary constants C_1 and C_2 will be

$$(\phi)_{x=a} = \frac{-qa^3}{16D} + \frac{qb^2a}{8D}(2 \log_e a - 1) + \frac{C_1a}{2} + \frac{C_2}{a} = 0$$

$$(\phi)_{x=b} = \frac{-qb^3}{16D} + \frac{qb^3}{8D}(2 \log_e b - 1) + \frac{C_1b}{2} + \frac{C_2}{b} = 0;$$

the calculation of the corresponding bending moments can be done without difficulty.

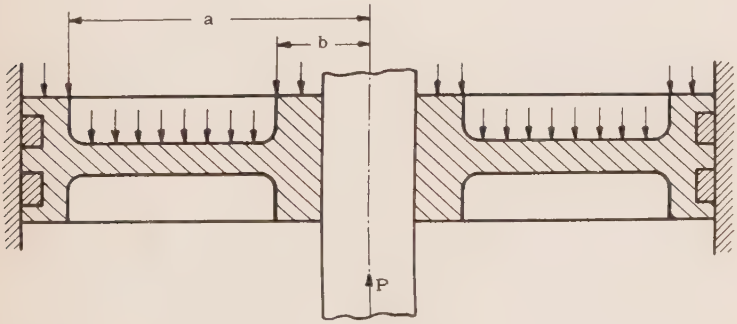

Fig. 230.—Bending of cylinder piston.

By combining the solutions considered in this paragraph, solutions of such problems as the bending in pistons of steam engines and the bending of flanges of cylinders and tubes can be obtained. Combining, for instance, cases represented in Fig. 228 (b) and Fig. 229 (b), an approximate solution of the problem on bending of a piston (Fig. 230) by steam pressure can be obtained.*

70. Bending of Rectangular Plates.—The theory of bending of rectangular plates is more complicated than that for circular plates, and only some final results for the bending moments and deflections are given below which can be used in design.† It is assumed that the deflections are small in comparison with the thickness of the plate, and that the edges during bending can freely displace in the plane of the plate, i.e., there are no forces acting in the *middle plane* of the plate.

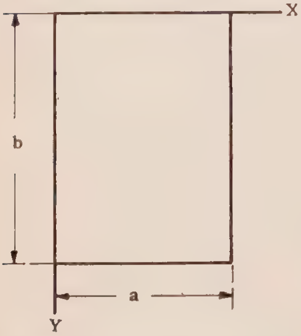

FIG. 231.—Rectangular plate supported at edges.

Simply Supported Edges.—In the case of a uniformily distributed load q the maximum deflection δ will occur at the center of the plate (Fig. 231) and can be represented by the equation

$$\delta = \alpha \frac{qa^4}{Et^3} \tag{295}$$

---

* Several problems of this kind are considered in the following papers: M. Ensslin, *Dinglers Polyt. Journal*, 1904. C. Pfleiderer, *Forschungsarbeiten*, Vol. 97, 1911.

† General theory of bending of plates can be found in the paper by H. M. Westergaard and A. Slater, *Proceedings of the American Concrete Inst.*, Vol. 17, 1921. The tables XX–XXVII are taken from the following books:

I. Boubnov, "Structural mechanics of a Ship," (St. Petersburg) 1913.

S. Timoshenko, "Theory of Elasticity," Vol. 2 (St. Petersburg), 1916.

H. Hencky, "Uber den Spannungszustand in rechteckigen Platten," (Thesis in Darmstadt), 1913.

A. Nadai, "Forschungsarbeiten auf dem Gebiete des Ingenieurwesens," Vol. 170–171 (Berlin), 1915.

Further development of the theory of bending of rectangular plates: See A. Nadai, *Der Bauingenieur*, p. 11, 1921; and p.1, 1924.

H. M. Westergaard, *Ingenioren*, Vol. 32, p. 513, 1923 (Copenhagen).

B. Galerkin, Rectangular Plates, *Bull. of the Polyt. Inst. of St. Petersburg*, 1915, 1918, 1920.

Huber, *Comptes Rendus*, Vol. 170, pp. 511, p. 1305, (Paris), 1920. Further references on the literature; See L. Föppl. *Neure Fortschritte der technischen Elasticitäts-theorie, Zeitschr. f. Angew. Math. & Mech.*, Vol. I, p. 466, 1921.

Very complete study on bending of plates is given in the recently published book by A. Nadai: "Elastische Platten" J. Springer, (Berlin), 1925.

in which

a = the shorter side of the plate,
t = the thickness of the plate,
α = a numerical coefficient depending on the magnitude of the ratio b/a.

Denoting, as before, the bending moments per unit length of the sections perpendicular to X and Y axes respectively by M_1 and M_2, the maximum bending moments will occur at the center of the plate and their magnitudes can be represented as follows:

$$(M_1)_{\max} = \beta_1 q a^2,$$
$$(M_2)_{\max} = \beta_2 q a^2$$

where β_1 and β_2 denote numerical coefficients depending on the magnitude of the ratio b/a.

Several values of coefficients α, β_1, and β_2 are given in Table XX. In calculating these values, Poisson's ratio $1/m$ is taken as 0.3.

TABLE XX.—CONSTANTS FOR CALCULATING UNIFORMLY LOADED RECTANGULAR PLATES WITH SIMPLY SUPPORTED EDGES

b/a =	1.0	1.1	1.2	1.3	1.4	1.5	1.6	1.7	1.8	1.9	2.0	3.0	4.0	5.0	∞
α	0443	.0530	.0616	.0697	.0770	.0843	.0906	.0964	.1017	.1064	.1106	.1336	.1400	.1416	.1422
β_1 =	0479	.0553	.0626	.0693	.0753	.0812	.0862	.0908	.0948	.0985	.1017	.1189	.1235	.1246	.1250
β_2 =	0479	.0494	.0501	.0504	.0506	.0500	.0493	.0486	.0479	.0471	.0464	.0404	.0384	.0375	.0375

It is seen from Table XX that maximum deflection and maximum bending moment for $b/a = 4$ nearly coincide with those for $b/a = \infty$. This means that for long rectangular plates ($b/a \geqq 4$) the effect of the short sides can be neglected and the deflection surface at the middle can be considered as a cylindrical one.

Built-in Edges.—For this case the maximum deflection takes place at the center of the plate and can be expressed by the same equation (295) as was used for supported edges.

The maximum bending moment occurs at the middle of the longer sides and can be expressed by the equation

$$(M_1)_{\max} = \beta q a^2.$$

Several values of the coefficients α and β are given in the Table XXI. From this table it is seen that for built in edges the deflection is much smaller than that for supported edges.

Table XXI.—Constants for Uniformly Loaded Rectangular Plates with Clamped Edges

$b/a =$	1.00	1.25	1.50	1.75	2.00	∞
$\alpha =$	.0138	.0199	.0240	.0264	.0277	.0284
$\beta =$	.0513	.0665	.0757	.0817	.0829	.0833

It is seen also that for $b/a = 2$ the maximum deflection and the maximum bending moment nearly coincide with those obtained for $b/a = \infty$. Therefore in calculating long rectangular plates ($b/a >$ 2) with built in edges, the results, obtained in Par. 63 for cylindrical bending can be used with very high accuracy.

Two Opposite Sides ($x = 0$, $x = a$) *Simply Supported, Third Side* ($y = 0$) *Built-in and the Fourth Side Free. Fig.* 232.—It is clear that in the case of uniformly distributed loading the maximum deflection will be at the middle of the free side at the point A. This deflection can be represented by the equation

$$\delta = \frac{\alpha q b^4}{E t^3} \qquad (296)$$

in which α is a numerical coefficient depending on the magnitude of the ratio b/a. Several values of this coefficient are given in Table XXII.

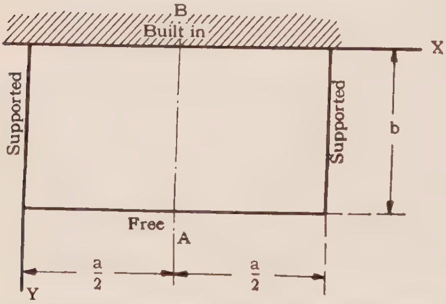

Fig. 232.—Rectangular plate having different edge conditions.

The maximum bending moment M_1 takes place also in the point A, and its magnitude can be represented by

$$(M_1)_{\max} = \beta_1 q a^2.$$

Maximum bending moment M_2 takes place at β the middle of the built-in side, and can be represented by the equation

$$(M_2)_{\max} = \beta_2 q b^2.$$

Several values of the coefficients β_1 and β_2 are given in the Table XXII.

TABLE XXII.—CONSTANTS FOR UNIFORMLY LOADED RECTANGULAR PLATES SHOWN IN FIG. 232

$b/a =$	0	$\frac{1}{3}$	$\frac{1}{2}$	$\frac{2}{3}$	1
$\alpha =$	1.37	1.03	.635	.366	.123
$\beta_1 =$	0	.0078	.0293	.0558	.0972
$\beta_2 =$	.500	.428	.319	.227	.119

Uniformly Loaded Plate Supported at Many Equidistant Points.—If a uniformly loaded plate be supported at many equidistant points (Fig. 233), a good approximation for the maximum stress and the stress distribution near to a support will be obtained if a part of the plate near the support bounded by a circle of radius $r = .22a$* be considered as a circular plate simply supported at the edge, loaded at the center by a load $P = -qa^2$, and uniformly loaded by the load q. The loads acting on the plate, on the basis of this assumption, are given in Fig. 233 (b). Equations for calculating the stresses produced by such a load were developed in paragraphs 66, 67, and 68.

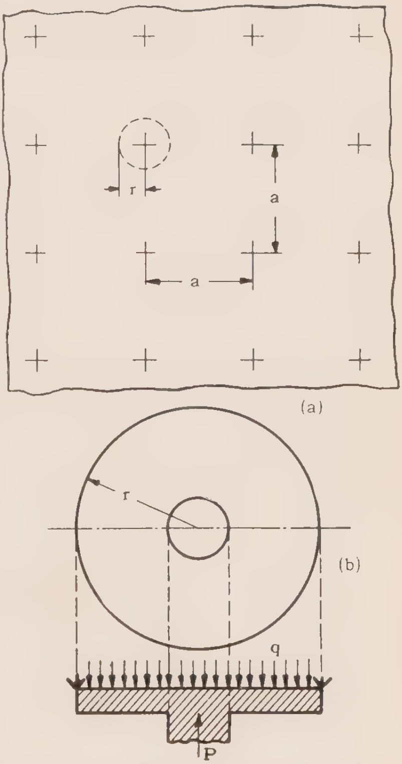

FIG. 233.—Plate on many equidistant supports.

71. Buckling of Rectangular Plates.—*Simply Supported Rectangular Plate under a Uniform Compression.*—If a rectangular plate supported on four sides undergoes a uniform compression in the direction of the X axis (Fig. 234), a certain limit for the compressive stress p_{cr} can be established,* beyond which the flat form of compressed plate becomes unstable and lateral buckling of the plate may occur.

---

* See A. Nadai, *Der Bauingenieur*, Vol. V, p. 1, 1924. See also the paper by H. M. Westergaard and A. Slater mentioned in the footnote page 288.

This *critical* value of the compressive stress is given by the equation

$$p_{cr} = kp_e \tag{297}$$

in which

$$p_e = \frac{\pi^2 D}{b^2 t} \tag{298}$$

denotes the critical compressive stress as obtained by Euler's formula (equation (143), p. 164) for a strip having the length b and the thickness t equal to the thickness of the plate, and where

$$k = \left(\frac{a}{mb} + \frac{mb}{a}\right)^2 \tag{a}$$

denotes a coefficient depending on the magnitude of the ratio a/b and on the integer m, which must be so chosen that k becomes a minimum. Several values of this coefficient are given in the Table XXIII.

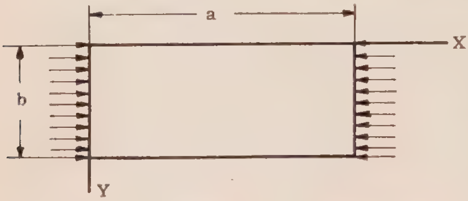

FIG. 234.—Buckling of compressed plate.

TABLE XXIII.—CONSTANTS FOR CALCULATING CRITICAL COMPRESSIVE STRESS FOR SIMPLY SUPPORTED RECTANGULAR PLATES

$a/b =$	.4	.6	.8	1.0	1.2	1.4	1.6	1.8	2.0	2.2	2.4	2.7	3
$k =$	8.41	5.14	4.20	4.00	4.13	4.47	4.20	4.04	4.00	4.04	4.13	4.04	4.00

For longer plates $(a/b > 3)$ $k = 4$ always represents a good approximate.

Three Sides of the Plate Supported, and the Fourth Free.—The same equation (297), for calculating the critical value of the compressive stress, can be used. The scheme is shown in Fig. 234. In this case the side $y = b$ is considered as free. Several values of the coefficient k are given in the Table XXIV.

---

* The solution of this problem belongs to G. H. Bryan; see *London Math. Soc. Proc.*, Vol. XXII, p. 54, 1891. Other cases of buckling of rectangular plates were considered by the writer. See author's papers: (1) On the stability of compressed plates, *Bull. of the Polyt. Inst. in Kiev*, 1907; (2) *Z. f. Mathematik und Physik*, Vol. 58, 1910; (3) *Der Eisenban*, Vol. 12, 1921. See also H. Reissner, *Zentralbl. d. Bauverw.* (Berlin), p. 93, 1909.

TABLE XXIV.—CRITICAL COMPRESSIVE STRESS FOR A RECTANGULAR PLATE WITH THREE SUPPORTED EDGES AND THE FOURTH ($y = b$) FREE

$a/b = \dots\dots$	.5	1.0	1.2	1.4	1.6	1.8	2.0	2.5	3.0	4.0	5.0
$k = \dots\dots$	4.40	1.440	1.135	.952	.835	.755	.698	.610	.564	.516	.506

Two Opposite Sides Simply Supported, the Third Built-in, and the Fourth Free.—The same equation (297) can be used. In this case sides ($x = 0$, $x = a$) in Fig. 234 are considered as simply supported and side $y = 0$ as built in. The values of the coefficient k are given in the Table XXV.

TABLE XXV.—CRITICAL COMPRESSIVE STRESS FOR A RECTANGULAR PLATE WITH TWO OPPOSITE SIDES SIMPLY SUPPORTED, THE THIRD BUILT-IN, AND THE FOURTH ($y = b$) FREE

$a/b = \dots\dots$	1.0	1.1	1.2	1.3	1.4	1.5	1.6	1.7	1.8	1.9	2.0	2.2	2.4	2.6	2.8	3
$k = \dots\dots$	1.70	1.56	1.47	1.41	1.36	1.34	1.33	1.33	1.34	1.36	1.38	1.45	1.47	1.41	1.36	1.34

For larger values of the ratio a/b, a good approximation is $k = 1.33$.

Two Opposite Sides Simply Supported, and Two Others Built in.—The sides $x = 0$ and $x = a$ are considerd as simply supported. The corresponding values of the coefficient k in equation (297) are given in Table XXVI.

TABLE XXVI.—CRITICAL COMPRESSIVE STRESS FOR A RECTANGULAR PLATE, TWO OPPOSITE SIDES OF WHICH ARE SIMPLY SUPPORTED, AND TWO OTHERS BUILT-IN

$a/b = \dots\dots$	.4	.5	.6	.7	.8	.9	1.0	1.2	1.4	1.6	1.8	2.1
$k = \dots\dots$	9.44	7.69	7.05	7.00	7.29	7.83	7.69	7.05	7.00	7.29	7.05	7.00

Rectangular Plate Supported on Four Sides and Submitted to the Action of Shearing Stresses Uniformly Distributed along the Sides. The critical value of the shearing stress which may produce buckling of the plate can be represented by the equation

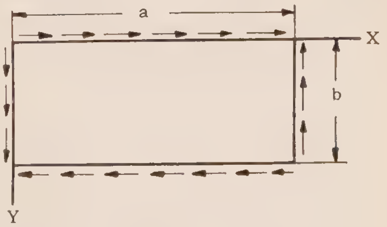

FIG. 235.—Buckling of plate due to shear.

$$(p_t)_{cr} = \frac{k\pi^2 D}{b^2 t} \tag{299}$$

The values of the numerical coefficient k are given in Table XXVII.

TABLE XXVII.—CRITICAL STRESS FOR A RECTANGULAR PLATE SUPPORTED ON FOUR SIDES AND SUBMITTED TO THE ACTION OF A UNIFORM SHEAR

$a/b =$	1	1.2	1.4	1.5	1.6	1.8	2.0	2.5	3
$k =$	9.42	8.0	7.3	7.1	7.0	6.8	6.6	6.3	6.1

This table can be useful in choosing the thickness of the web of a plate girder. Near the supports the shearing force is the most important factor. Therefore the part of the web between two stiffeners can be considered as a rectangular plate with supported edges, subjected only to the action of shearing stresses. Taking, for instance, the distance between the stiffners equal to 5 ft. and assuming for structural steel $E = 30 \times 10^6$ lbs. per sq. in. and $1/m = .3$ the following values of critical stress in lbs. per sq. in. for different thicknesses t and different depths h of girders have been obtained by using Table XXVII.

$t =$ h	⅜″	7⁄16″	½″	9⁄16″
5′	9,980	13,600	17,700	22,400
7′	7,730	10,500	13,700	17,400
10′	6,990	9,510	10,400	15,700

By using the Tables XXIII–XXVI, the necessary thickness of steel sheets to be used in built-up sections (Fig. 236) can easily be obtained. It must be noted that the critical stress is proportional to the square of the thickness t, and inversely proportional to the square of the width b. Considering, for instance, the sides of the tubular

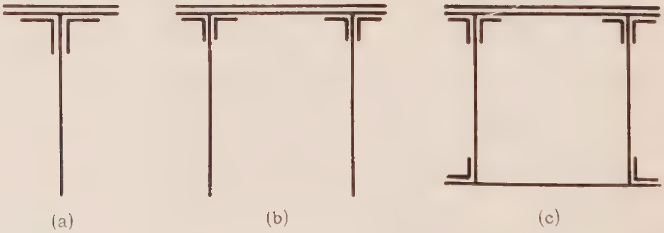

FIG. 236.—Case of built-up sections.

section Fig. (c) as long rectangular plates simply supported, the corresponding critical compressive stress will be

$$p_{cr} = \frac{4\pi^2 D}{b^2 t} = \frac{\pi^2}{3}\frac{t^2}{b^2}\frac{E}{1 - \frac{1}{m^2}}. \tag{a}$$

Taking, for instance, $t/b = .01$, we will have

$$p_{cr} = 10{,}800 \text{ lbs. per sq. in.}$$

This stress is far below the proportional limit of structural steel.

In the cases (a) and (b) (Fig. 236) the compressed vertical steel sheets may be considered as long plates built in* along the upper edge and free along the lower edge. In such case Table XXV must be used. The critical stress will be

$$p_{cr} = 1.33\frac{\pi^2 D}{b^2 t} = \frac{1.33\pi^2}{12}\frac{t^2}{b^2}\frac{E}{1 - \frac{1}{m^2}}. \tag{b}$$

It is seen that the stability of the plate depends again on the magnitude of the ratio b/t. Assuming that the yield point of structural steel is 30,000 lbs. per sq. in. and taking p_{cr} equal to this stress, it will be found from (b)

$$\frac{b}{t} = \sqrt{\frac{1.33\pi^2}{12 \times 30{,}000} \times \frac{30 \times 10^6}{.91}} = \text{about } 35.$$

It is seen from this that when $b/t > 35$, lowering of working stress or reinforcement of lower edge of the compressed vertical sheets becomes necessary.

---

[*] This assumption gives for the critical stress an upper limit. The true critical stress will be somewhat lower due to the fact that the fastening of the upper edge is not absolutely rigid.

CHAPTER XI

STRESSES PRODUCED BY DYNAMICAL CAUSES

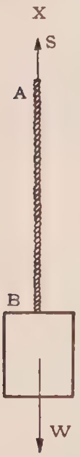

FIG. 237.—Tensile stress from moving load.

72. Effect of Inertia Forces.—*General.*—If an elastic body is in motion, the stress distribution will depend not only on the external forces acting on the body but also on the inertia forces. In many cases in modern engineering high speeds are used, hence the stresses produced by the inertia forces may be very large and cannot be neglected. If the conditions of the problem are such that the effect of elastic deformation on the motion of the body can be neglected, the problem on stresses produced by inertia forces is a comparatively simple one. Considering in this case a moving machine element as absolutely rigid, the acceleration at any point can be found from the known motion of the machine, and the inertia forces can easily be calculated in the usual manner. Then, by adding these forces to the known external forces, the complete solution will be obtained exactly in the same manner as in a statical problem. Consider, for instance, stresses in a rope AB produced by a weight W, when in motion along the vertical axis X (Fig. 237). During motion at constant speed the conditions will be the same as in a static problem. There will be no inertia forces, and the tensile force S in the rope must be equal to the weight W. A different condition will be obtained if the motion is not uniform. Assume, for instance, the weight is moving upwards with an acceleration a, the corresponding inertia force will act in an opposite direction, and its magnitude will be

$$\frac{W}{g}a. \qquad \text{(a)}$$

This force must be added to the weight of the body so that the tensile force in the rope becomes

$$S = W + \frac{W}{g}a, \qquad \text{(b)}$$

where g = acceleration due to gravitation.

It is seen that the additional stress, produced by the inertia force, may become very high in cases where a large acceleration takes place. In the case where retardation occurs, the quantity a in equation (b) becomes negative and the tensile stress in the rope becomes less than that produced by a static load W.

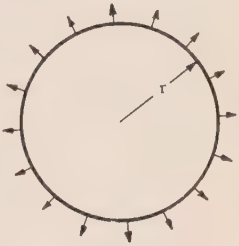

FIG. 238.—Stress in rotating ring.

Stresses in a Rotating Circular Ring.—If a thin circular ring is rotating at constant angular velocity ω about the axis through the center and perpendicular to the plane of the ring, the inertia forces (centrifugal forces) are uniformly distributed around the ring and are directed radially outward. Their amount per unit length of the ring will be

$$\frac{q}{g}\omega^2 r,$$

where q = weight of the ring per unit length,
r = the radius of the center line of the ring.

The tensile stress produced by these forces in the ring becomes

$$p = \frac{q\omega^2 r^2}{Ag} = \frac{\gamma v^2}{g}, \tag{300}$$

in which γ = weight per unit volume of the material,
$v = \omega r$ = circumferential velocity.
A = cross-sectional area.

It is seen that for a given material this stress (Eq. 300) depends only on the velocity v.

For a steel ring these stresses become as follows:

v ft. per sec. = ...	100	200	300	400	500	600	800	1,000
p lbs. per sq. in. = ...	1,060	4,200	9,500	17,000	26,500	38,000	68,000	106,000

The above conclusion on stresses produced by inertia forces in rings can be generalized as follows: For two geometrically similar bodies of the same material rotating with the same circumferential speed the stresses in similarly situated points are the same, which can be explained as follows. Let M and m denote the masses of two similar and similarly situated elements cut out from two bodies under consideration. These masses will be in the same ratio as the cubes of the corresponding linear dimensions of the bodies. The centrifugal forces acting on the masses will be Mv^2/ρ and mv^2/ρ_1 respectively, where v denotes the velocity of each of the masses ρ and ρ_1 the distances from the axis of rotation which are proportional to the corresponding linear dimensions of the bodies. It is seen that the centrifugal forces acting on the two elements are proportional to the squares of their respective linear dimensions, i.e., proportional to the areas of the sides of the elements. Therefore, the stresses distributed over these sides, and balancing the inertia forces, must be equal.

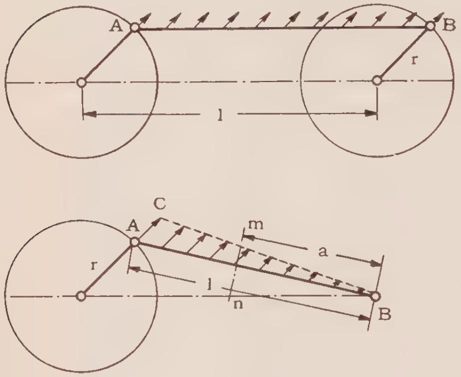

Fig. 239.

Example 72.—Determine bending stresses produced by inertia forces in a side rod and in a connecting rod, both of constant cross-section, if the driving wheels have a constant angular velocity ω (Fig. 239).

Solution.—In the case of the side rod the inertia forces act in a radial direction and are uniformly distributed along the rod. If q denotes the weight per unit length of the rod, the corresponding inertia force will be

$$\frac{q}{g}\omega^2 r.$$

At high speed this force may be very large in comparison with the weight q. Take, for instance, $r = 15$ in., and assume that the wheels make five revolutions per second. Then $\omega = 10\pi$, and the inertia force per unit length will be

$$q \cdot \frac{100\pi^2}{386} \cdot 15 = 38.3q \text{ per unit length.}$$

The maximum bending moment in the side rod corresponds to the inertia forces in a vertically downward direction and is equal to

$$M_{\max} = q\left(\frac{38.3 + 1}{8}\right)l^2,$$

from which the bending stresses can be found.

In the case of a connecting rod, a good approximation will be obtained on the assumption that the inertia forces are represented by the triangle ACB (Fig. 239). The maximum bending moment produced by such loading will be at the section mn distant $a = l/\sqrt{3}$ from the end B, this is equal to about

$$M_{\max} = \frac{1}{9\sqrt{3}}q(38.3 + 1)l^2.$$

Example 73.—A bar OC with a weight W at the end C (Fig. 240) is rotating with a constant angular velocity ω about the axis O perpendicular to the plane of the figure. How will the cross-sectional area of the bar vary if the tensile stress produced by the inertia forces in all the cross sections is the same and equal to p_w?

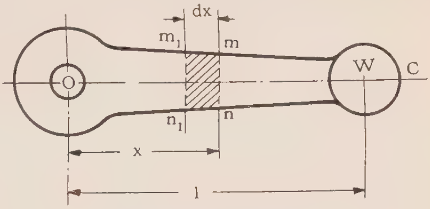

FIG. 240.

Solution.—The difference in tensile forces in the two cross-sections mn and m_1n_1, due to the centrifugal force acting on the element dx of the bar, is

$$\frac{A\gamma}{g}\,\omega^2\,x\,dx,$$

in which A = cross sectional area of the bar at section m_1n_1,
γ = weight per unit volume of the material.

In order to have the same stress in both sections, the difference dA of the cross sectional areas must satisfy the equation

$$dA\;p_w = -\frac{A\gamma}{g}\omega^2\,x\,dx,$$

or

$$\frac{dA}{A} = -\frac{\gamma\omega^2\,x\,dx}{gp_w}.$$

Integrating this equation, we have

$$A = Ce^{-\gamma\omega^2x^2/2gp_w} \tag{a}$$

For determining the arbitrary constant C, the condition at the end $x = l$ must be considered. Here the centrifugal force of the weight W is $W/g\omega^2 l$. Therefore, the cross-sectional area at this end of the bar must be equal to

$$A_1 = \frac{W\omega^2 l}{gp_w}. \tag{b}$$

From (a), for the same cross-section, will be obtained

$$A_1 = Ce^{-\gamma\omega^2l^2/2gp_w}. \tag{c}$$

Comparing (b) and (c),

$$C = \frac{W\omega^2 l}{gp_w}e^{\gamma\omega^2l^2/2gp_w}$$

Substituting this in (a),

$$A = \frac{W\omega^2 l}{gp_w}e^{\frac{\gamma\omega^2(l^2-x^2)}{2gp_w}} \tag{d}$$

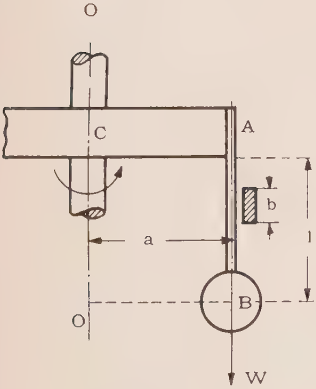

FIG. 241.

Example 74.—Determine the deflection of the governor spring AB (Fig. 241) rotating about the axis O-O with a constant angular velocity ω. Consider the bar AC as absolutely rigid and neglect the mass of the spring AB.

Solution.—Let δ denote the deflection, then the centrifugal force of the weight W is

$$\frac{W}{g}\,\omega^2(a + \delta).$$

Considering AB as a cantilever, the equation for determining δ will be

$$\delta = \frac{W}{g}\omega^2(a + \delta)\frac{l^3}{3EI},$$

from which

$$\delta = \frac{W\omega^2 a l^3}{3gEI}\,\frac{1}{1 - \dfrac{W\omega^2 l^3}{3gEI}}.$$

It is seen that the deflection increases indefinitely when ω is such that

$$1 - \frac{W\omega^2 l^3}{3gEI} = 0. \qquad \text{(a)}$$

This value of ω is called *critical speed.*
It will be shown later (see Par. 75, p. 313) that

$$2\pi\sqrt{\frac{Wl^3}{3EIg}} = T$$

is the period of free vibration of the load W on the spring AB.

Remembering also that the period of one revolution of the governor is $T_1 = 2\pi/\omega$ equation (a) can be written in such a form:

$$1 - \frac{T^2}{T_1^2} = 0,$$

from which

$$T = T_1.$$

The *critical speed* of the governor is that at which the time of one revolution is equal to the period of free vibration of the governor.

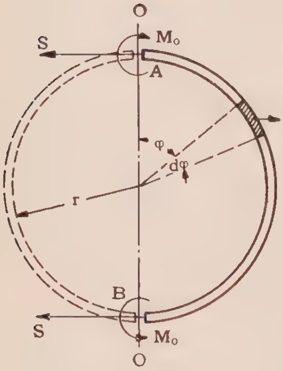

FIG. 242.

Example 75.—A thin circular ring of constant cross-section is rotating with a constant angular velocity about the vertical diameter O-O (Fig. 242). Determine the maximum bending moment and the increase of the horizontal diameter produced by inertia forces, if the radius of the center line of the ring is r and the weight of the ring per unit length is q.

Solution.—Let S and M_0 denote the tensile force and bending moment respectively at the vertical cross-sections A and B. Noting that the centrifugal force acting on an element of the ring is

$$\frac{qr\,d\phi}{g}\omega^2 r \sin\phi,$$

the following equation for determining S will be obtained:

$$S = \int_0^{\pi/2}\frac{qr^2\omega^2}{g}\sin\phi\,d\phi = \frac{qr^2\omega^2}{g}$$

For determining M_0 the *theorem of least work* (see Par. 34, p. 123) will be used.

The bending moment at any cross-section determined by the angle ϕ is

$$M = M_0 - Sr(1 - \cos\phi) + \frac{q\omega^2 r^2}{g}\int_0^{\phi} r\,(\cos\psi - \cos\phi)\sin\psi\,d\psi = M_0 - \frac{q\omega^2 r^3}{2g}\sin^2\phi. \qquad \text{(a)}$$

Substituting this in the expression for the potential energy

$$U = \frac{1}{EI}\int_0^{\pi} M^2 r d\phi$$

and concluding from the condition of symmetry that section A does not rotate during the bending of the ring,

$$\frac{dU}{dM_0} = \frac{2}{EI}\int_0^{\pi} M \frac{dM}{dM_0} r d\phi = 0,$$

or, substituting (a),

$$M_0 = \frac{q\omega^2 r^3}{4g}.$$

For determining the increase δ of the horizontal diameter, Castigliano's theorem may be used.

This will give*

$$\delta = \frac{qr^5\omega^2}{6gEI}.$$

The vertical diameter of the ring will be decreased by the same amount.

73. Rotating Discs.—*Circular Disc of a Uniform Thickness.*—The problem on stresses produced in a thin rotating disc by inertia forces can be solved approximately by making a simple assumption that the stresses do not vary through the thickness of the disc. This thickness is assumed in further calculations equal to unity.

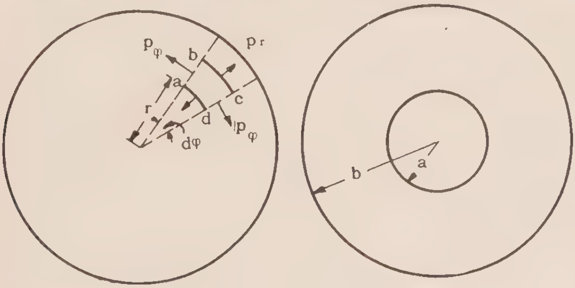

(a) (b)

FIG. 243.—Stresses in rotating disc.

Cutting out from the disc an element *abcd* (see Fig. 243), it can be concluded from the conditions of symmetry that there will be no shearing stress on the sides of this element. The equation for determining normal stresses p_r and p_ϕ, acting in radial and tangential directions, can be obtained from the condition of equilibrium of the element *abcd* exactly in the same manner as it was done in consideration of stresses in thick cylinders (see Eq. (a) p. 250). It is necessary only to add to the forces considered before, the inertia force acting on the element, equal to

---

* See G. A. V. Peschka, *Z. f. Math. u. Phys.* (Schlömilch), Vol. 13, 1868.

$$\frac{\gamma\omega^2}{g} r^2 dr d\phi. \tag{a}$$

Here

γ = the weight per unit volume,
ω = the angular velocity of the disc,
r = the distance of the element from the center of the disc.

Then the equation of equilibrium becomes

$$p_r + r\frac{dp_r}{dr} - p_\phi + \frac{\gamma\omega^2 r^2}{g} = 0. \tag{b}$$

The stresses p_r and p_ϕ can be expressed by the radial displacement u (see equation (e), p. 251) as follows:

$$p_r = \frac{E}{1 - \frac{1}{m^2}}\left(\frac{du}{dr} + \frac{1}{m}\frac{u}{r}\right) \tag{c}$$

$$p_\phi = \frac{E}{1 - \frac{1}{m^2}}\left(\frac{u}{r} + \frac{1}{m}\frac{du}{dr}\right)$$

Substituting (c) in equation (b), the following equation for determining u will be obtained:

$$\frac{d^2u}{dr^2} + \frac{1}{r}\frac{du}{dr} - \frac{u}{r^2} + \left(1 - \frac{1}{m^2}\right)\frac{\gamma\omega^2 r}{gE} = 0. \tag{301}$$

Denoting

$$\left(1 - \frac{1}{m^2}\right)\frac{\gamma\omega^2}{gE} = N, \tag{302}$$

equation (301) may be represented in the following form:

$$\frac{d}{dr}\left[\frac{1}{r}\frac{d}{dr}(ur)\right] + Nr = 0, \tag{301'}$$

A general solution of this equation gives

$$u = \frac{-Nr^3}{8} + \frac{C_1 r}{2} + \frac{C_2}{r}, \tag{d}$$

in which C_1 and C_2 are arbitrary constants which must be determined in such a manner as to satisfy the conditions at the edges of the disc. Consider first a disc with a hole at the center (Fig. 243 (b)) and assume that there are no pressures on the edges of the disc. In such a case the conditions for determining the constants C_1 and C_2 become

$$(p_r)_{r=a} = 0; \quad (p_r)_{r=b} = 0. \tag{e}$$

Substituting (d) in the first of the equations (c) we have

$$p_r = \frac{E}{1 - \frac{1}{m^2}}\left[- \frac{3 + \frac{1}{m}}{8} N r^2 + \frac{1}{2}\left(1 + \frac{1}{m}\right)C_1 - \left(1 - \frac{1}{m}\right)C_2 \frac{1}{r^2}\right] \tag{f}$$

Substituting in (e), we obtain

$$\begin{aligned} - \frac{3 + \frac{1}{m}}{8} N a^2 + \frac{1}{2}\left(1 + \frac{1}{m}\right)C_1 - \left(1 - \frac{1}{m}\right)\frac{1}{a^2}\, C_2 &= 0. \\ - \frac{3 + \frac{1}{m}}{8} N b^2 + \frac{1}{2}\left(1 + \frac{1}{m}\right)C_1 - \left(1 - \frac{1}{m}\right)\frac{1}{b^2}\, C_2 &= 0, \end{aligned} \tag{g}$$

from which

$$C_1 = \frac{3 + \frac{1}{m}}{4\left(1 + \frac{1}{m}\right)}(a^2 + b^2)N; \; C_2 = \frac{3 + \frac{1}{m}}{8\left(1 - \frac{1}{m}\right)} a^2 b^2 N. \tag{h}$$

Substituting in (d) and using (c), we obtain

$$p_\phi = \frac{3 + \frac{1}{m}}{8\left(1 - \frac{1}{m^2}\right)} EN \left[- \frac{1 + \frac{3}{m}}{3 + \frac{1}{m}} r^2 + a^2 + b^2 + \frac{a^2 b^2}{r^2}\right], \tag{303}$$

$$p_r = \frac{3 + \frac{1}{m}}{8\left(1 - \frac{1}{m^2}\right)} EN \left[- r^2 + a^2 + b^2 - \frac{a^2 b^2}{r^2}\right]. \tag{304}$$

Substituting (302) for N and denoting

$$\frac{a}{b} = \alpha, \; \frac{r}{b} = \phi, \; v = b\omega,$$

equations (303) and (304) become

$$p_\phi = \frac{\gamma v^2}{g} \frac{3 + \frac{1}{m}}{8} \left[- \frac{1 + \frac{3}{m}}{3 + \frac{1}{m}} \phi^2 + 1 + \alpha^2 + \frac{\alpha^2}{\phi^2}\right]; \tag{305}$$

$$p_r = \frac{\gamma v^2}{g} \frac{3 + \frac{1}{m}}{8} \left[- \phi^2 + 1 + \alpha^2 - \frac{\alpha^2}{\phi^2}\right]. \tag{306}$$

It is seen that the radial stress p_r becomes equal to zero at the edges ($\phi = 1$ and $\phi = \alpha$) and is positive (tensile stress) in other points. Maximum value of p_r occurs at points where

$$\phi = \sqrt{\alpha}, \quad \text{or } r = b\sqrt{\alpha} = \sqrt{ab}. \tag{i}$$

Substituting this in (304),

$$(p_r)_{\max} = \frac{\gamma v^2}{g} \frac{3 + \frac{1}{m}}{8} (1 - \alpha)^2 \tag{307}$$

Stress p_ϕ in a tangential direction becomes maximum at the inner edge of the disc where $\phi = \alpha$. Then, from (305),

$$(p_\phi)_{\max} = \frac{\gamma v^2}{g} \frac{3 + \frac{1}{m}}{4} \left[1 + \frac{1 - \frac{1}{m}}{3 + \frac{1}{m}} \alpha^2 \right]. \tag{308}$$

It is seen that $(p_\phi)_{\max}$ is always larger than $(p_r)_{\max}$ and it increases with the increasing of α^2, i.e., with the increasing of the hole. For a very small hole the second term in the brackets on the right side of equation (308) may be neglected, and we have

$$(p_\phi)_{\max} = \frac{\gamma v^2}{g} \frac{3 + \frac{1}{m}}{4}. \tag{309}$$

When the inner radius approaches the outer radius of the disc, α^2 approaches unity, and (308) becomes

$$(p_\phi)_{\max} = \frac{\gamma v^2}{g}. \tag{j}$$

This coincides with equation (300) previously obtained for a thin rotating ring.

In the case of a solid disc, the arbitrary constants of general solution (d) will be obtained as follows: From the condition of symmetry it can be concluded that $u = 0$ for $r = 0$; therefore, in solution (d) $C_2 = 0$. The constant C_1 will be found from the condition that $p_r = 0$ at the outer edge. Then from (g),

$$-\frac{3 + \frac{1}{m}}{8} N b^2 + \frac{1}{2}\left(1 + \frac{1}{m}\right) C_1 = 0,$$

from which

$$C_1 = \frac{3 + \frac{1}{m}}{4\left(1 + \frac{1}{m}\right)} N b^2. \tag{k}$$

Then, from (c), the expressions for stresses become

$$p_\phi = \frac{\gamma v^2}{g}\frac{3+\frac{1}{m}}{8}\left[-\frac{1+3\frac{1}{m}}{3+\frac{1}{m}}\phi^2 + 1\right], \tag{310}$$

$$p_r = \frac{\gamma v^2}{g}\frac{3+\frac{1}{m}}{8}[-\phi^2 + 1]. \tag{311}$$

Both stresses remain always positive and increase with the decrease of ϕ, i.e., as we approach the center. At the center $\phi = 0$ and

$$(p_\phi)_{\max} = (p_r)_{\max} = \frac{\gamma v^2}{g}\frac{3+\frac{1}{m}}{8}. \tag{312}$$

This stress is one-half of that stress equation (309) found above for a disc with a very small hole. It must be noted also that stress equation (312) does not depend on the dimensions of the disc but only on the circumferential velocity v and on the density of material. In the case of discs with holes (Eq. 308) the maximum stresses will be equal if circumferential velocities and α are equal, i.e., if the discs are geometrically similar.

In the previous considerations it was assumed that the edges of the discs are free from external forces. If tensions or compressions uniformly distributed around the edges are acting on the disc, the corresponding stresses will be found by using the theory of thick cylinders. (See Par. 61, p. 249.) These stresses can be represented in the following form: (See equations (237 and 238, p. 251.)

$$p_r = k - \frac{n}{r^2}$$

$$p_\phi = k + \frac{n}{r^2}, \tag{l}$$

in which k and n are constants depending on the dimensions of the disc and on the magnitude of the external forces.

Stresses (l) must be superimposed on stresses given by equations (303) and (304) if the edges of the disc are not free. Then the combined stresses will be:

$$p_r = A + \frac{B}{r^2} - \delta\omega^2 r^2$$

$$p_\phi = A - \frac{B}{r^2} - \beta\omega^2 r^2 \tag{313}$$

$$A = \left[k + \frac{(a^2+b^2)(3+1/m)\gamma\omega^2}{8g}\right]$$

$$B = -\left[\frac{a^2b^2(3+1/m)\gamma\omega^2}{8g} + n\right]$$

in which

$$\delta = \frac{\gamma}{8g}\left(3 + \frac{1}{m}\right), \quad \beta = \frac{\gamma}{8g}\left(1 + \frac{3}{m}\right), \tag{314}$$

and A and B denote the constants which can be calculated for every particular disc by using equations (303), (304), (237), and (238).

By using notations

$$\begin{aligned} s &= p_r + \delta\omega^2 r^2 \\ t &= p_\phi + \beta\omega^2 r^2 \end{aligned} \tag{315}$$

and

$$w = \frac{1}{r^2} \tag{316}$$

equations (313) become $s = A + Bw$, $t = A - Bw$. (317)

If s and t are known for any point of the disc, the magnitudes of these quantities for any other point can easily be obtained by using the following graphical method:* Let s_1 and t_1 denote the magnitudes of s and t for a point in which $w = w_1$ (see Fig. 244). Then the magnitudes s_2 and t_2 of s and t for another point ($w = w_2$) will be obtained by intersection of the vertical line through w_2 with the straight lines s_1-s_2 and t_1-t_2 having their point of intersection on the vertical axis of the coordinate and equally inclined to this axis. It is easy to see that these lines represent graphically equations (317). They have the common ordinate A on the ordinate axis ($w = 0$) and equal and opposite slopes ($\pm B$).

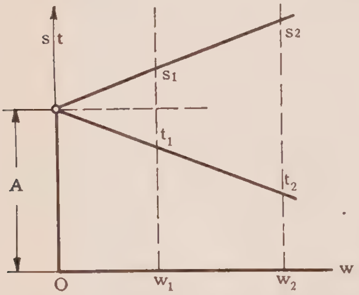

Fig. 244.—Graphical determination of stresses in discs.

Circular Disc of a Variable Thickness.—A general equation for this case, together with considerations of different methods of its solution can be found in the well-known book by Stodola.† A simple method based on replacement of the actual profile by a system of discs of uniform thicknesses (see Fig. 245) will here be considered.* For calculating stresses in these discs, the equations given above for discs of a uniform thickness may be used. It is only necessary to consider the variation of stresses at sections such as 2, 3, 4 (see Fig. 245) where abrupt changes of the thickness occur.

---

* This method was developed for calculating stresses in rotating discs by Dr. R. Grammel; see his paper *Ein Neues Verfahren zur Berechnung Rotierender Scheiben Dinglers Pol. Jour.*, Vol. 338, p. 217, 1923.

† A. Stodola "*Dampf-und Gasturbinen*" 6th ed., pp. 312–340, 1924. *Rotating Disc of Conical Profile* was considered by H. M. Martin, *Engineering*, Vol. CXV, p. 1, 1923; see also B. Hodkinson, *Engineering*, Vol. CXVI, p. 274, 1923.

If y and $y + \Delta y$ denote two different thicknesses, then the corresponding change Δp_r in the magnitude of the radial stress p_r will be found from the following equation of statics:†

$$yp_r = (y + \Delta y)(p_r + \Delta p_r)$$

from which

$$\Delta p_r = -\frac{\Delta y}{y + \Delta y}\, p_r. \tag{a}$$

The change Δp_ϕ of the stress p_ϕ will be found from the condition that unit elongation in the circumferential direction remains the same for both thicknesses, i.e.,

$$p_\phi - \frac{1}{m}\, p_r = p_\phi + \Delta p_\phi - \frac{1}{m}\,(p_r + \Delta p_r)$$

from which

$$\Delta p_\phi = \frac{1}{m} \Delta p_r.$$

Now, from equation (315),

$$\begin{aligned} \Delta s &= \Delta p_r = -\frac{\Delta y}{y + \Delta y}\, p_r \\ \Delta t &= \Delta p_\phi = \frac{1}{m}\, \Delta s. \end{aligned} \tag{318}$$

Equations (314), (315), (316), and (318) together with the graphical solution given in Fig. 244 are sufficient for calculating any disc of a variable thickness.

Consider, as an example, the disc, represented in Fig. 245, rotating at a speed of 3,000 R.P.M. (The dimensions are given in Table XXVIII.) Assume also that the centrifugal forces due to the blades are such that at the outer edge

$$(p_r)_1 = 100\, \frac{kg}{cm^2}$$

---

* This method was developed by M. Donath, "Die Berechnung rotierender Scheiben und Ringe" (Berlin), 1912. Further development of the method was given by R. Grammel; see paper mentioned above. From this latter paper is taken the numerical example given below.

† It is assumed, as before, that the stresses are uniformly distributed through the thickness of the disc.

and that

$$\frac{1}{m} = .3, \quad \gamma = .00785\frac{\text{kg}}{cm^3}$$

Then, by using equation (314),

$$\delta\omega^2 = .327\,\frac{kg}{cm^4}; \quad \beta\omega^2 = .188\,\frac{kl}{cm^4}$$

From these data and from Fig. 245 the first eight columns of Table XXVIII are obtained.

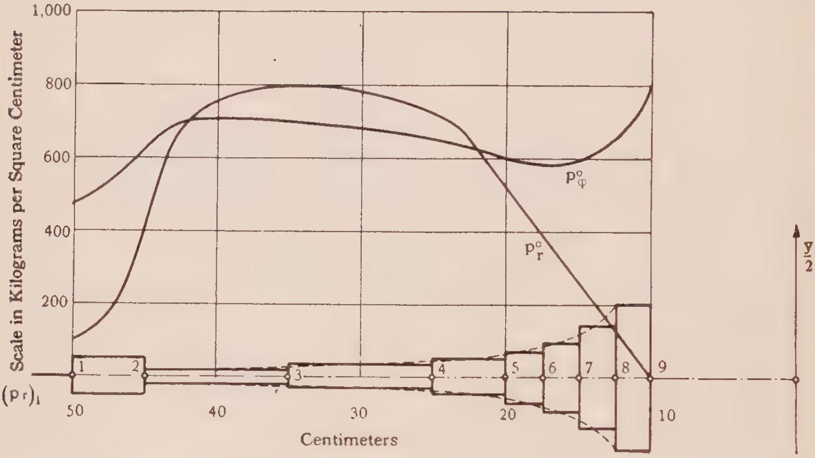

FIG. 245.—Disc of variable cross section.

We start the calculation of stresses from the outer edge of the disc where $(p_r)_1$ is known. The magnitude of the stress $(p_\phi)_1$ is usually unknown (usually the pressure on the inner edge, due to shrinkage, is given) and an arbitrary magnitude of this stress must be taken for the beginning. The simplest way is to take $(p_\phi)_1$ such as to make s and t equal, i.e. (from equation 315),

$$(p_\phi)_1 = (p_r)_1 + \delta\omega^2 r_1^2 - \beta\omega^2 r_1^2,$$

or, by using the figures of the fifth and sixth columns of the table above,

$$(p_\phi)_1 = 100 + 817 - 470 = 447\frac{kg}{cm^2}$$

Now, from equations (315),

$$s_1 = (p_r)_1 + \delta\omega^2 r_1^2 = 100 + 817 = 917\frac{kg}{cm^2}$$

$$t_1 = (p_\phi)_1 + \beta\omega^2 r_1^2 = 447 + 470 = 917\frac{kg}{cm^2}.$$

TABLE XXVIII.—STRESS CALCULATION IN ROTATING DISCS

Cross section	r, centimeters	r^2	$\frac{10^4}{r^2}$	$\delta\omega^2r^2$, kilogram per square centimeter	$\beta\omega^2r^2$ kilogram per square centimeter	y, centimeters	$-\frac{\Delta y}{y+\Delta y}$	p_r, kilogram per square centimeter	Δ_s kilogram per square centimeter	Δ_t kilogram per square centimeter	p_ϕ, kilogram per square centimeters	p_r^0	p^0_ϕ
1	50	2 500	4.00	817	470			100 0			447 50	100	479
						2.5							
2	45	2 025	4.94	662	381		+1.50	255 −6	+383 −9	+115 −3	536 56	440	628
						1.0							
3	35	1 225	8.16	401	230		− .333	984 −36	−328 +12	− 98 +4	705 75	801	705
						1.5							
4	25	625	16.00	204	118		− .400	950 −72	−380 +29	−114 +9	626 128	724	653
						2.5							
5	20	400	25.00	131	75		− .286	682 −94	−195 +27	− 58 +8	514 186	534	605
						3.5							
6	17.5	306	32.63	100	58		− .263	532 −109	−140 +29	− 42 +9	459 232	402	688
						4.75							
7	15	225	44.44	74	42		− .321	421 −140	−135 +45	− 40 +14	430 300	280	604
						7.0							
8	12.5	156	64.00	51	29		− .300	294 −182	− 88 +55	− 26 +16	419 402	152	666
						10.0							
9	10	100	100.00	33	19			178 −281			447 570	0	808

Due to the fact that $s_1 = t_1$, the s and t straight lines (the construction of which was explained in Fig. 244) coincide. In Fig. 246 they are represented by the line *a-a* prallel to the w axis.

In this manner, s_2 and t_2 for the section 2 are obtained; giving

$$s_2 = t_2 = 917\frac{kg}{cm^2}.$$

Now, by using equation (315),

$$(p_r)_2 = s_2 - \delta\omega^2 r^2{}_2 = 917 - 662 = 255\frac{kg}{cm^2}$$

$$(p_\phi)_2 = t_2 - \beta\omega^2 r^2{}_2 = 917 - 381 = 536\frac{kg}{cm^2}$$

In order to take into account an abrupt change of the thickness of the disc at section (2), equations (318) and the numbers of the eighth column of the table will be used, then

$$(\Delta s)_2 = (\Delta p_r)_2 = 1.50 \times 255 = 383\frac{kg}{cm^2}$$

$$(\Delta t)_2 = (\Delta p_\phi)_2 = .3 \times 383 = 115\frac{kg}{cm^2}$$

The corresponding points b and c on the vertical through the point 2 are given in Fig. 246, and the lines *b-b* and *c-c* are constructed as explained in Fig. 244. In such a manner s_3 and t_3 for the section 3 are obtained. By repeating the same reasoning as above, all necessary data for the third section can be obtained, and so on. By this method, all numbers* of the columns nine to twelve, of the table above, are calculated.

Due to the fact that the stress $(p_\phi)_1$ was taken arbitrarily, the condition at the inner edge usually will not be satisfied, and the stress $(p_r)_9$ obtained by the method described will be different from that which actually exists on the inner edge of the disc.

In order to satisfy the condition at the inner edge, an additional calculation is required, since it is necessary to have the stresses produced in the disc by a radial pressure uniformly distributed around the inner edge.

Assuming $(p_r)_1 = 0$, $\omega = 0$, and taking for $(p_\phi)_1$ an arbitrary value (in our calculation we take $(p_\phi)_1 = 50$ kg/cm^2) the stress distribution required can be obtained exactly in the same maner as explained above. (In this case, from equation 315, $s = p_r$ and $t = p_\phi$.) The results of calculations are given in columns nine to twelve in light type, and the corresponding constructions, in Fig. 246, by the lines s' and t'.

---

* The only numbers considered are those printed in heavy type.

By combining the two stress distributions calculated, a solution corresponding to the real condition at the inner edge of the disc can be obtained as follows:

If $(p_r)_9$ and $(p_r)_9'$ are the radial stresses at the inner edge of the disc, obtained in the first and the second calculations respectively, and if $(p_r)_9^\circ$ denotes the stress which actually exists at the inner edge, then multiplying the stresses of the second stress-distribution by

$$k = \frac{(p_r)_9^\circ - (p_r)_9}{(p_r)_9'}$$

and superimposing the results obtained on the first stress-distribution, the solution for the actual condition will be obtained.

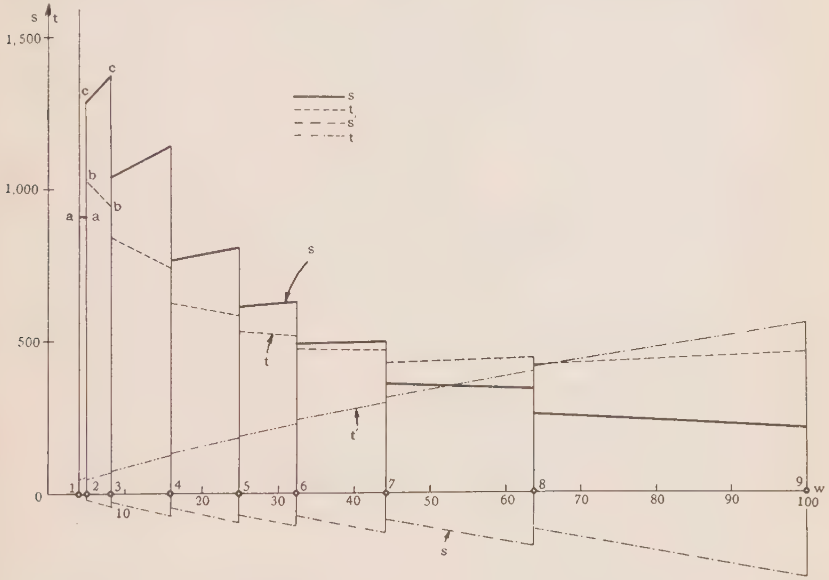

FIG. 246.—Application of graphical method of stress determination to case of variable cross section.

The average stresses at the sections where the thickness changes abruptly will be calculated by using equations

$$(p_r)^\circ = \left(p_r + \frac{\Delta s}{2}\right) + k\left(p_r' + \frac{\Delta s'}{2}\right),$$

$$(p_\phi)^\circ = \left(p_\phi + \frac{\Delta t}{2}\right) + k\left(p_\phi' + \frac{\Delta t'}{2}\right).$$

The results of such calculations are given in the two last columns of Table XXVIII and are represented graphically in Fig. 245.

74. Vibrations of Elastic Systems.—If an *elastic system,* for instance, a loaded beam, twisted shaft or a deformed spring is disturbed from its *position of equilibrium* by an impact or by the sudden application and removal of an additional force, the elastic forces of the member in the *disturbed position* will no longer be in equilibrium with the loading, and vibrations will ensue. Such vibration, maintained by the elastic forces of the system alone, is called *free* or *natural* vibration.

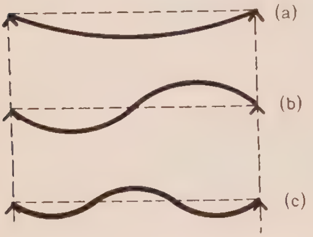

Fig. 247.—Different modes of beam vibration.

Generally an elastic system can perform vibrations of different modes, for instance, the deflection curve of a vibrating beam may have a shape as shown in Fig. 247 (a), or it can have one point of inflection, i.e., one node, as shown in Fig. 247 (b), or two points of inflection as in Fig. 247 (c), etc. Usually the slowest or *fundamental* type of vibration is the most important. In many cases the higher types of vibrations can be completely neglected and the system can be considered as having one type of vibration. The motion in this case will be determined by one coordinate only. Such a system is called a system with *one degree of freedom.* Take, for instance, the case shown in Fig. 248. If the arrangement be such that only vertical displacements of the weight W are possible and the mass of the spring be small in comparison with W, the system can be considered as having one degree of freedom. Its configuration will be determined completely by the vertical displacement of the weight.

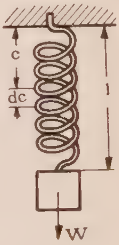

Fig. 248.—System having one degree of freedom.

It will be shown later that if an elastic system be acted upon by a *periodic disturbing force,* vibrations of the same frequency as that of the force will be set up. This gives an entirely different condition from that previously discussed because the amplitude of these *forced vibrations* and the stresses caused by them will depend on the relation between the *frequency* of the disturbing force and that of the natural vibration of the system. If these two frequencies are equal, a condition of *resonance* takes place. Under this condition even a small disturbing force may be all that is necessary to cause very large vibrations and produce serious stresses.

In machines running at constant speed, periodic disturbing forces, for instance, such as those arising from lack of *balance,* are always present, and if the number of revolutions per second is equal to the frequency of the natural vibration of the machine, large vibrations and serious stresses may be expected. It is clear, therefore, that there are many cases in service where a preliminary study of these natural vibrations of systems is of great practical importance.

In the case of a system having one degree of freedom the determination of the frequency of natural vibration offers no particular difficulty. In the more complicated cases the determination of this frequency can also be made with sufficient accuracy for designers by using an approximate method developed by Lord Rayleigh and W. Ritz.

75. Free Vibrations.—*A System with One Degree of Freedom.*—In coming to a detailed discussion of the different types of vibration, free vibrations of the system shown in Fig. 248 will be considered as an example. Let k denote the load which produces unit extension of the spring. Then the static deflection of the spring under the action of the weight W will be

$$\delta_{st} = \frac{W}{k}. \tag{a}$$

Denoting a vertical displacement of the weight from its position of equilibrium by x and considering this displacement as positive if it is in a downward direction, the expression for the tensile force in the spring corresponding to any position of the weight becomes

$$S = W + kx. \tag{b}$$

During vibration, this force is always in equilibrium with the load W, together with the inertia force $-W/gx''$, in which x'', the second derivative of the displacement x with respect to time t, represents the acceleration of the moving load W. Therefore

$$W - \frac{W}{g}x'' = W + kx, \tag{319}$$

or

$$x'' + p^2x = 0, \tag*{(319)$'$}$$

where

$$p = \sqrt{\frac{kg}{W}} = \sqrt{\frac{g}{\delta_{st}}}. \tag{320}$$

A general solution of equation (319)$'$ can be written as follows:

$$x = A \cos pt + B \sin pt, \tag{c}$$

and the velocity of the weight becomes

$$x' = -Ap \sin pt + Bp \cos pt \tag{d}$$

It is seen that the motion of the natural vibration is a *simple harmonic*, one having a period given by

$$T = \frac{2\pi}{p} = 2\pi\sqrt{\frac{\delta_{st}}{g}}. \tag{321}$$

The period is the same as that of a mathematical pendulum, the length of which is equal to δ_{st}. This conclusion always holds for any elastic system with one degree of freedom, and if the static deflection produced by the load be known, the natural period of vibration will be determined from equation (321). It increases with increase of δ_{st}, i.e., (see equation (a)) with increase of the load W and of the flexibility of the spring.

In order to determine the arbitrary constants A and B, the initial conditions must be considered. Assume, for instance, that at the initial moment ($t = 0$) the weight W has a displacement x_0 from its position of equilibrium, and that its initial velocity is x'_0. Substituting these conditions in (c) and (d), we have from (c)

$$A = x_0,$$

and from (d)

$$B = \frac{x'_0}{p}.$$

Equation (c) then becomes

$$x = x_0 \cos pt + \frac{x'_0}{p} \sin pt. \tag{322}$$

It is seen that the vibration consists of two parts; one due to the initial displacement x_0, and another due to the initial speed x_0'.

Effect of the Mass of the Spring.—In our previous calculations the mass of the spring was completely neglected. In order to determine its effect on the period of the natural vibration an approximate method based on the consideration of the energy of the system will now be developed. Consider again the arrangement shown in Fig. 248 and neglect first the mass of the spring. The kinetic energy of the system during vibration will be

$$\frac{W}{2g}(x')^2. \tag{e}$$

The potential energy of the system consists of two parts; one part due to the potential energy of the deformation of the spring, and another part due to the potential energy of the load by virtue of its position. The tensile force in the spring corresponding to any displacement x will be $(\delta_{st} + x)k$, and the corresponding energy of the spring is

$$k\frac{(\delta_{st} + x)^2}{2}.$$

The energy of the spring in the equilibrium position $(x = 0)$ is

$$\frac{\delta_{st}^2 k}{2};$$

so that the energy stored in the spring during the displacement x will be

$$k\frac{(\delta_{st} + x)^2}{2} - \frac{k\delta_{st}^2}{2} = kx\delta_{st} + \frac{kx^2}{2} = Wx + \frac{kx^2}{2}. \tag{f}$$

The energy of the load W during the displacement x will vary by the quantity

$$-Wx. \tag{g}$$

Now, on the basis of the principle of conservation of energy, the sum of the kinetic and potential energies of the system remains constant. Therefore, from (e), (f), and (g) we have

$$\frac{W}{2g}x'^2 + \frac{kx^2}{2} = \text{constant}. \tag{h}$$

The magnitude of the constant on the right side of the equation (h) depends on the initial conditions. Take, for instance, that at $t = 0$ the displacement is equal to x_0 and the initial velocity is zero, then equation (h) becomes

$$\frac{W}{2g}x'^2 + \frac{kx^2}{2} = \frac{kx_0^2}{2}. \tag{i}$$

This means that during vibration the sum of the kinetic and potential energy remains constant. When during vibration x becomes equal to x_0, the velocity becomes equal to zero and the energy of the system consists of the potential energy only. When x becomes equal to zero, as occurs when the load, during vibration, passes through its middle position, the velocity has its maximum value and the corresponding magnitude of the kinetic energy, from (i), becomes

$$\frac{W(x'^2)_{\max}}{2g} = \frac{kx_0^2}{2}. \tag{j}$$

This means that the total kinetic energy is equal to the potential energy stored in the system during the initial displacement x_0 from the position of equilibrium.

In considering the effect of the mass of the spring, assume that this mass is small in comparison with the mass of the load W and that it does not change the type of vibration.* This means that if x is the displacement of the load, the displacement of any cross-section of the spring distant c from the fixed end (Fig. 248) is the same as that of a massless spring, i.e., equal to

$$\frac{xc}{l} \tag{k}$$

where l = the length of the spring.

If the displacements are not affected by the mass of the spring, the potential energy in equation (i) remains unchanged, and it is only necessary to consider the kinetic energy of the system. Let q denote the weight of the spring per unit length. Then the mass of an element of the spring per length dc will be qdc/g, and the corresponding kinetic energy, by using (k), becomes

$$\frac{q}{2g}\left(\frac{x'c}{l}\right)^2 dc.$$

The complete kinetic energy of the spring will be

$$\frac{q}{2g}\int_0^l \left(\frac{x'c}{l}\right)^2 dc = \frac{qx'^2}{2g}\cdot\frac{l}{3}.$$

This must be added to the energy of the weight W; so that equation (i) becomes

$$\frac{x'^2}{2g}\left(W + \frac{ql}{3}\right) + \frac{kx^2}{2} = \frac{kx_0^2}{2}.$$

This means that in order to estimate the effect of the mass of the spring on the period of the natural vibration it is only necessary to add one-third of the weight of the spring to the weight W of our previous calculation. Therefore, equation (a) must be modified so that

$$\delta = \frac{W + \tfrac{1}{3}ql}{k}. \tag{l}$$

This latter value of δ must then be substituted in the equation (321) in order to determine the effect of the weight of the spring on the period T of the natural vibration. This conclusion, obtained on the assumption that the weight of the spring is very small in comparison with that of the load, can be used with sufficient accuracy† even in cases where the weight of the spring is of the same order as W. For instance, for $ql/W = .5$ the error of the approximate solution is about ½%. For $ql/W = 1$ the error is about ¾%. For $ql/W = 2$, the error is about 3%.

---

* This method was developed by Lord Rayleigh. See his famous book "Theory of Sound," 2nd Ed., Vol. I, p. 111, 287.

† The exact solution of the problem was obtained first by Poisson. See also author's paper Die Erzwungene Schwingungen von Prismatischen Stäbe, *Z. f. Math. u. Phys.*, Vol. 59, 1911.

In our considerations the arrangement shown in Fig. 248 was taken. The approximate method developed can, however, be used in other cases, such as shown in Fig. 249. Assuming, for instance, that the deflection curve during vibration of the beam represented in Fig. 249 (a) has the same shape as the statical deflection curve and denoting by x the displacement of the load W during vibration, the displacement of any element qdc of the beam will be*

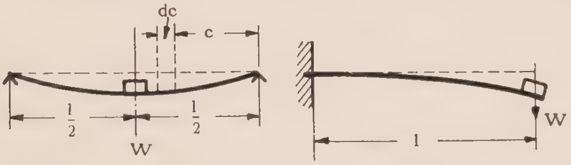

(a) (b)

Fig. 249.—Approximate calculation of fundamental frequency.

$$x\frac{3l^2c - 4c^3}{l^3}.$$

The kinetic energy of the beam itself will be

$$2\int_0^{l/2}\frac{q}{2g}\left(x'\frac{3l^2c - 4c^3}{l^3}\right)^2 dc = \frac{17}{35}ql\frac{(x')^2}{2g}. \tag{323}$$

This additional energy equal to that arising from $^{17}\!/_{35}$ of the beam weight must be added to the energy $Wx'^2/2g$ of the load concentrated at the middle in order to estimate the effect of the weight of the beam on the period of vibration T.

It must be noted that equation (323), obtained on the assumption that the weight of the beam is small in comparison with that of the load W, can be used in all practical cases. Even in the extreme case where $W = 0$ and where the assumption is made that $^{17}\!/_{35}ql$ is concentrated at the middle of the beam, the error from the approximate solution $2\pi\sqrt{\delta_{st}/g}$ will be less than 1%.

Applying the same reasoning to the case represented in Fig. 249 (b) it can be concluded that $^{33}\!/_{140}ql$ must be added to W in calculating δ_{st}.

The further development of these approximate methods and their application to technical problems will be discussed below in paragraphs 76 and 77.

---

* It can be obtained from the equation 61, page 72.

76. Approximate Methods for Calculating the Frequency of Natural Vibrations of a System. -*Vibrations of Loaded Beams.*—From the consideration of forced vibration given above it must be appreciated that the investigation of natural periods of vibration of machines is of great practical importance. In designing a machine it is necessary to consider not only the stresses which may be produced during operation but also to consider the flexibility of the separate parts of the machine.

With these factors in mind, the proportions must be so chosen as to avoid resonance conditions.

In considering free vibrations of a system with one degree of freedom, an approximate method for calculating frequencies of natural vibration in the more complicated cases was described. This method is based on the consideration of the energy of a vibrating system and can easily be applied if the mode of vibration, i.e., the deflection form of the system during vibration, be known.

As an example, a beam loaded in several points will now be considered (Fig. 250). Let w_1, w_2, w_3 denote the loads and y_1, y_2, y_3 denote the corresponding deflections. Then the potential energy of deformation stored in the beam during bending will be

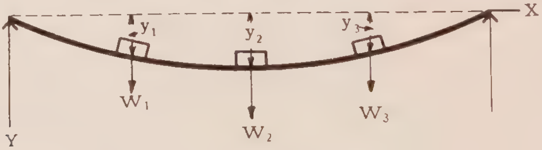

Fig. 250.—Vibration of loaded beam.

$$U = \frac{w_1y_1}{2} + \frac{w_2y_2}{2} + \frac{w_3y_3}{2}. \tag{a}$$

In calculating the period of the fundamental type of vibration, the static deflection curve given in Fig. 250 can be taken as a good approximation* for the deflection curve of the beam during vibration. The vertical displacements of the loads w_1, w_2, w_3, during vibration, can be taken in such a form:

$$y_1 \cos pt, \qquad y_2 \cos pt, \qquad y_3 \cos pt \tag{b}$$

Then the maximum deflections of the beam, from the position of equilibrium, are the same as those given in Fig. 250; therefore, the increase of the potential energy of deformation of the system during the deflection of the beam from the position of equilibrium to the extreme position will be given by equation (a). The maximum kinetic energy of the system takes place at the moment when the beam, during vibration, passes through its middle position. The corresponding velocities of the load, from (b), are

---

* See page 317.

$$py_1, \quad py_2, \quad py_3$$

and the kinetic energy of the system becomes

$$\frac{p^2}{2g}(w_1y_1^2 + w_2y_2^2 + w_3y_3^2) \tag{c}$$

Equating (a) and (c), the following expression for p^2 will be obtained:

$$p^2 = \frac{g(w_1y_1 + w_2y_2 + w_3y_3)}{w_1y_1^2 + w_2y_2^2 + w_3y_3^2} \tag{324}$$

For the period of vibration we have

$$T = \frac{2\pi}{p} = 2\pi\sqrt{\frac{w_1y_1^2 + w_2y_2^2 + w_3y_3^2}{g(w_1y_1 + w_2y_2 + w_3y_3)}} \tag{325}$$

In the case where only one load is acting on the beam, equation (325) reduces to (321) obtained above for a system with one degree of freedom.

It is seen from (325) that for calculating T the statical deflections y_1, y_2, y_3, of the beam only are necessary. These quantities can easily be obtained by the usual methods (see Chapter IV). If the beam has a variable cross-section, graphical or grapho-analytical methods may be very useful for this calculation.

Critical Speed of a Rotating Shaft.—The method described above is used very often in calculating *critical speeds* of rotating shafts.* It is a well-known fact that rotating shafts at certain speeds become dynamically unstable and very large vibrations are likely to develop. This phenomena is due to resonance effect. The *critical speed* for a shaft is that speed at which the number of revolutions per second of the shaft is equal to the frequency of the natural vibration of the shaft. Determining this frequency as explained above, the critical speed for a machine can easily be established.

Due to the fact that the effect of a disturbing force on the amplitude of the vibration increases rapidly as the condition of resonance is approached, it is a common practice to design a shaft so as to obtain its critical speed far above† the operating speed of the machine.

---

* This subject is considered in detail in the book by A. Stodola, "Dampf-und Gasturbinen," Berlin, 1924, p. 357–398.

† A lower limit of the ratio of the speed of the machine to its critical speed is taken sometimes equal to 1:1.5.

It must be noted that in Fig. 250 rigid supports were assumed. In certain cases the rigidity of the supports is not sufficient. This may produce a substantial effect on the magnitude of the critical speed. In order to take this into account it is only necesary to add in the previous calculations the vertical displacements due to the deformation of the supports under the action of the loads w_1, w_2, w_3, to the deflections y_1, y_2, y_3 of the shaft (Fig. 250).

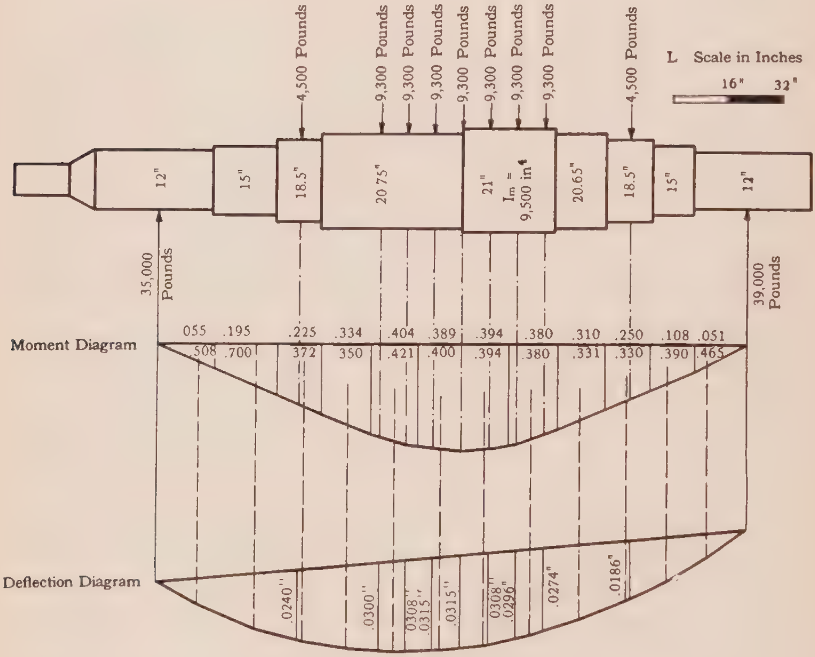

Fig. 251(a).—Determination of critical speeds for shaft.

In all previous calculations the weight of the shaft was neglected. In order to take this into consideration, the shaft must be divided into several parts, the weights of which, applied at their respective centers of gravity, must be considered as concentrated loads w_1, w_2 . . .

In Fig. 251(a) the deflection diagram of the shaft of a 15,000 K.V.A. synchronous condenser is given. Necessary calculations are given in Table XXIX. (Figure 251 (b) represents polygons of forces acting on the shaft.)

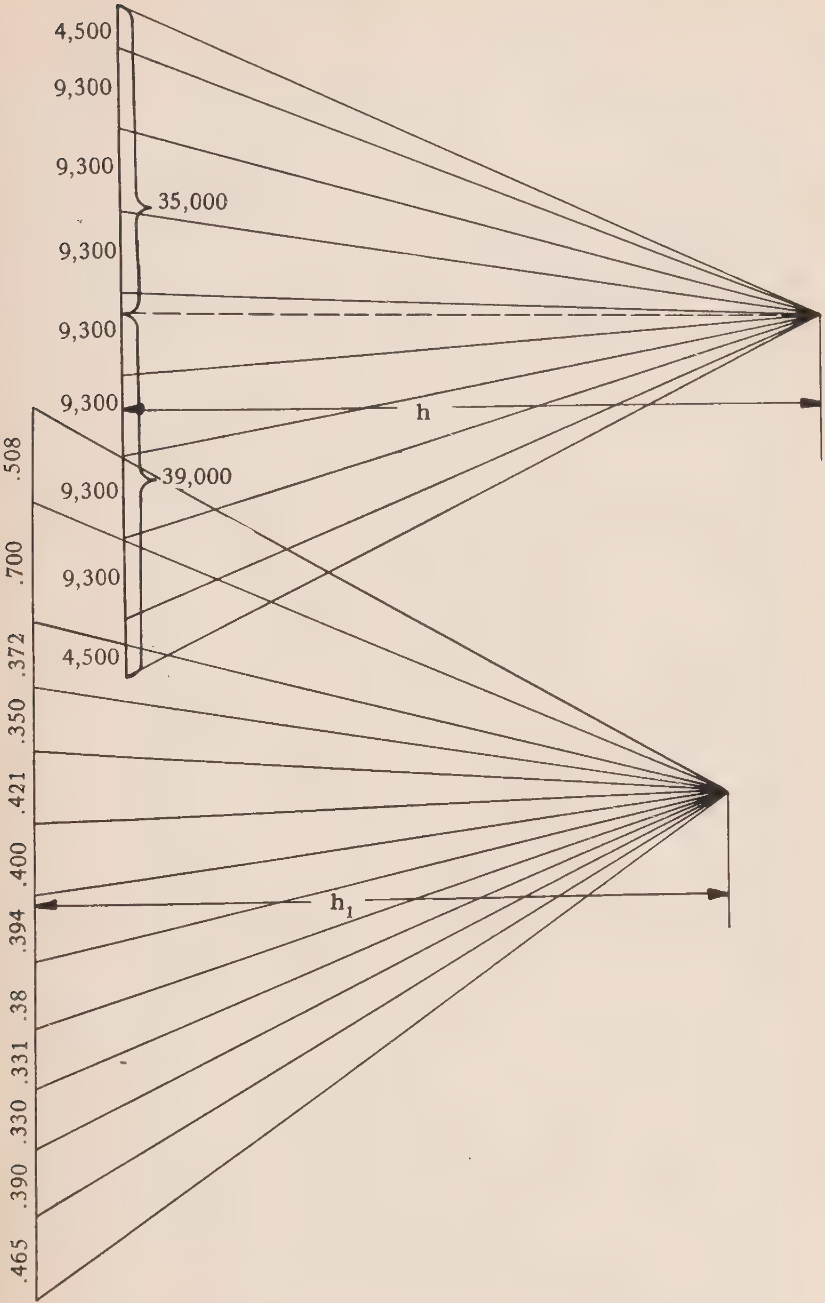

FIG. 251(b).—Polygons of forces shown in Fig. 251(a).

TABLE XXIX.—CALCULATION OF CRITICAL SPEED

w pounds	$y \times 10^2$ inches	$y^2 \times 10^4$ square inches	wy inch pounds	wy^2 square inch pounds
4,500	2.40	5.76	108	2.59
9,300	3.00	9.00	279	8.37
9,300	3.08	9.48	287	8.86
9,300	3.15	9.83	293	9.15
9,300	3.15	9.83	293	9.15
9,300	3.08	9.48	287	8.86
9,300	2.96	8.76	275	8.15
9,300	2.74	7.50	255	6.98
4,500	1.85	3.42	83	1.54
			$\Sigma wy = 2,160$	$\Sigma wy^2 = 63.65$

The critical number of revolutions per minute will be obtained, from equation (324), as follows:

$$N_{cr} = \frac{60}{T} = \frac{30}{\pi}\sqrt{\frac{g\Sigma\, wy}{\Sigma wy^2}} = \frac{30}{\pi}\sqrt{\frac{386 \times 2,160}{63.65}} = 1,090 \text{ cycles per minute.}$$

77. Rayleigh-Ritz Method.—It has been shown by Rayleigh that proceeding as explained above (see Par. 76), the calculated frequency of the fundamental type of vibration will always become greater than is actually the case. In order to obtain an exact solution, it is necessary to choose from all possible deflection curves such a one as will make the frequency a minimum. This is a problem of variational calculus which represents in many cases great analytical difficulty. In order to avoid this, a method of calculating successive approximations will now be discussed. As an example, the case of vibration of a beam of variable cross-section will be considered.

Let y denote the deflection of a beam in its extreme position. Then the potential energy of deformation will be

$$U = \frac{1}{2}\int_0^l EI\left(\frac{d^2y}{dx^2}\right)^2 dx \qquad \text{(d)}$$

Assuming that during vibrations the deflections vary as $y \cos pt$, the kinetic energy of the beam when it passes through its position of equilibrium will be

$$T = \frac{p^2}{2g}\int_0^l qy^2dx \qquad \text{(e)}$$

where q denotes the weight per unit length of the beam. Equating (d) and (e) we have

$$p^2 = \frac{g\int_0^l EI\left(\frac{d^2y}{dx^2}\right)^2 dx}{\int_0^l qy^2dx}. \tag{f}$$

The exact expression for the deflection curve will be that which makes the right side of (f) a minimum. In order to obtain an approximate solution, the expression for the deflection curve with several parameters $\delta_1, \delta_2, \ . \ . \ .$ is to be taken, and these parameters are to be chosen in such a manner as to satisfy the equations:*

$$\frac{\partial p^2}{\partial \delta_1} = 0, \ \frac{\partial p^2}{\partial \delta_2} = 0, \ . \ . \ . \ \text{etc.},$$

or, substituting for p^2 its expression (f),

$$\frac{\partial}{\partial \delta_1}\left[\int_0^l EI\left(\frac{d^2y}{dx^2}\right)^2 dx - \frac{p^2}{g}\int_0^l qy^2dx\right] = 0 \tag{g}$$

$$\frac{\partial}{\partial \delta_2}\left[\int_0^l EI\left(\frac{d^2y}{dx^2}\right)^2 dx - \frac{p^2}{g}\int_0^l qy^2dx\right] = 0 \tag{h}$$

. . . .

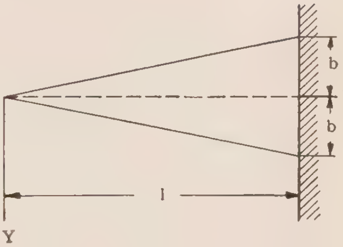

FIG. 252.—Vibration of wedge.

As an example, the fundamental type of vibration of a wedge having a constant thickness equal to unity, built in at the right end (Fig. 252) will be considered. The exact solution for this case is†

$$p = 5.315\frac{b}{l^2}\sqrt{\frac{Eg}{3\gamma}} \tag{i}$$

in which l = the length of the beam,

$2b$ = the depth of the beam at the built-in end,

γ = the weight per unit volume of the beam,

$$I = \frac{1}{12}\left(\frac{2bx}{l}\right)^3, \ q = \gamma\frac{2bx}{l}$$

In order to satisfy the conditions at the built-in end,

$$(y)_{x=l} = 0, \left(\frac{dy}{dx}\right)_{x=l} = 0,$$

---

* This method was developed by W. Ritz, see *Annalen d. Phys.*, Vol. XXVIII, 1909.

† It was obtained by Kirchhoff, "Berliner Monatsberichte," p. 815, 1879.

the following expression for the deflection curve can be taken:

$$y = \left(\frac{x}{l} - 1\right)^2\left(\delta_1 + \delta_2\frac{x}{l} + \delta_3\frac{x^2}{l^2} + \ . \ . \ . \ \right) \tag{j}$$

Taking only terms with δ_1 and δ_2 and substituting (j) in (g) and (h), the following two equations for determining δ_1 and δ_2 will be obtained:

$$\left(\frac{Eg}{\gamma}\frac{b^2}{3l^4} - \frac{p^2}{30}\right)\delta_1 + \left(\frac{2}{5}\frac{Eg}{\gamma}\frac{b^2}{3l^4} - \frac{p^2}{105}\right)\delta_2 = 0,$$

$$\left(\frac{2}{5}\frac{Eg}{\gamma}\frac{b^2}{3l^4} - \frac{p^2}{105}\right)\delta_1 + \left(\frac{2}{5}\frac{Eg}{\gamma}\frac{b^2}{3l^4} - \frac{p^2}{280}\right)\delta_2 = 0.$$

These linear homogeneous equations give for δ_1 and δ_2 solutions different from zero only in the case if the deteminant of these equations becomes equal to zero, i.e., if

$$\left(\frac{Eg}{\gamma}\frac{b^2}{3l^4} - \frac{p^2}{30}\right)\left(\frac{2}{5}\frac{Eg}{\gamma}\frac{b^2}{3l^4} - \frac{p^2}{280}\right) - \left(\frac{2}{5}\frac{Eg}{\gamma}\frac{b^2}{3l^4} - \frac{p^2}{105}\right)^2 = 0$$

From this latter equation, p^2 can be calculated. The smaller of the two roots gives

$$p = 5.319\frac{b}{l^2}\sqrt{\frac{Eg}{3\gamma}}. \tag{k}$$

The difference between this result and the exact solution (i), is only .1%.

Further approximations can be obtained by increasing the number of parameters δ_1, δ_2 . . .

The method developed above is very useful in calculating the periods of natural vibrations of such structures as bridges and ships.*

78. Damped Vibrations.—*Damping Proportional to the Velocity.*—In the previous consideration the frictional resisting forces were neglected, and, as a result, vibrations of constant amplitude were obtained. In actual conditions, however, resisting forces, though small in some cases, are always present and, due to their action, the vibrations generated originally will be gradually damped. These *damping forces* may arise from several sources of different nature, such as air, fluid friction, internal friction of the material of the vibrating body, and friction between sliding surfaces.† For small velocities the resisting force of the air or fluid may be assumed to vary as the velocity.* For larger velocities a damping proportional to the second power of the velocity must be taken;† while, for sliding, the friction between the two surfaces may be taken as a constant if the pressure between the surfaces remains constant during motion. The simplest case of damping proportional to the velocity will first be considered.

---

* See Author's book, "Theory of Elasticity," Vol. II, pp. 222–231 (Petersburg), 1916. The principal results obtained by the writer are given also in the paper by N. Akimoff: On the Vibrations of Beams of Variable Cross-Section, *Trans. of the Society of Naval Architecture* (London), Vol. XXVI, 1918.

† The bibliography on friction may be found in the article by R. v. Mises, Dynamische Probleme der Maschinenlehre. *Encyklopaedie d. Mathem. Wiss.*, Vol. IV, 1, II, p. 153.

Taking the same arrangement as before (see Fig. 248) and adding to the forces acting on the weight W during vibration, the friction force $-\alpha x'$, where α is a constant depending on the conditions, the following equation of motion from equation (319) will be obtained:

$$W - \frac{W}{g} x'' - \alpha x' = W + kx, \tag{a}$$

or

$$x'' + 2nx' + p^2 x = 0 \tag{326}$$

in which, as before (Eq. 320),

$$p = \sqrt{\frac{kg}{W}}$$

and

$$2n = \frac{\alpha g}{W}. \tag{327}$$

The solution of equation (326) is‡

$$x = e^{-nt}(A \sin \sqrt{p^2 - n^2}\, t + B \cos \sqrt{p^2 - n^2}\, t) \tag{b}$$

The arbitrary constants will now be determined from the initial conditions. Let x_0 and x_0' denote the displacement from the position of equilibrium and the velocity at the moment $t = 0$ respectively, then from equation (b), by using denotation

$$p_1 = \sqrt{p^2 - n^2}, \tag{328}$$

we obtain

$$A = \frac{1}{p_1}(x_0' + nx_0), \quad B = x_0$$

and solution (a) becomes

$$x = e^{-nt}\left[\frac{x_0'}{p_1} \sin p_1 t + x_0 \left(\cos p_1 t + \frac{n}{p_1} \sin p_1 t\right)\right] \tag{329}$$

---

* See experiments of A. Stodola, *Schweiz. Bauz,* Vol. 22, p. 113, 1893.

† Damping proportional to the square of the velocity is considered in the book by W. Hort, "*Technische Schwingungslehre,*" 2nd Ed., p. 44, 1922. This book contains discussion of many vibration problems of practical importance.

‡ It is assumed that n is small, so that $\sqrt{p^2 - n^2}$ is real, otherwise a periodic motion takes place.

When there is no damping, $n = 0$; then solution equation (329) reduces to (322) previously obtained.

The period of damped vibration, from (329), is

$$T = \frac{2\pi}{p_1} = \frac{2\pi}{\sqrt{p^2 - n^2}}. \tag{330}$$

Comparing this with equation (321) it can be concluded that, due to damping, the period increases, but if n is small in comparison to p, the effect of damping on the period is a small quantity of the second order and usually can be neglected. Due to the factor e^{-nt} the amplitude of vibrations gradually decreases with the time. It is represented graphically in Fig. (253) for the simplest case.*

$$x = e^{-nt}x_0 \cos p_1 t \tag{c}$$

The curve representing displacements from the position of equilibrium is tangent to the curve x_0e^{-nt} at points $m_1(t = 0)$, $m_2(t = T)$, and to the curve $-x_0e^{-nt}$ at $m_1'(t = \frac{1}{2}T)$, $m_2'(t = \frac{3}{2}T)$. These points do not coincide with the points of maximum and minimum displacement and it is easy to see that due to the damping, the time interval necessary for displacement of the system from a middle position to the subsequent extreme position is less than that necessary to return from the extreme position to the subsequent middle position.

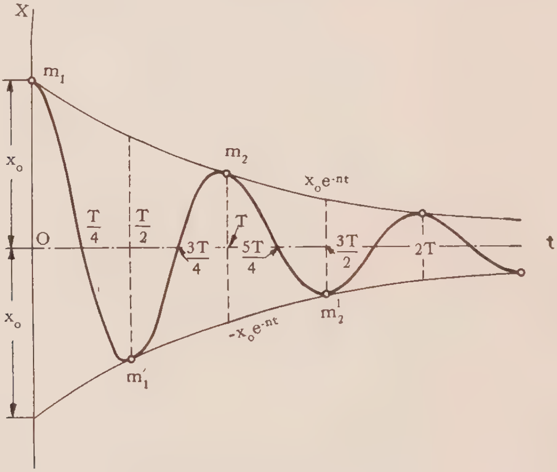

Fig. 253.—Vibration with damping proportional to velocity.

---

* i.e. for the case (see equation 329) when the initial conditions are such that

$$\frac{x_0'}{p_1} + \frac{x_0 n}{p_1} = 0.$$

The rate of damping depends on the magnitude of the constant n. It is seen from general solution (329) that the amplitude of the vibration diminishes after every cycle in the ratio

$$e^{-nT}:1, \tag{d}$$

i.e., it decreases following the law of geometrical progression. Equation (d) can be used for an experimental determination of the coefficient of damping n. It is necessary only to determine by experiment in what proportion the amplitude of vibration is diminished after a given number of cycles.

Constant Damping.—As an example of constant damping, the arrangement shown in Fig. 254 will be considered. Assume that the weight W is brought in its extreme right position $x = x_0$ and released; then motion towards the left begins. The following forces are acting on the load during this motion: (1) a tensile force in the spring equal to kx;* (2) an inertia force $-W/gx''$; and (3) a constant friction R between the load and the sliding rod, in a direction opposite to that of motion. The equation of motion will be

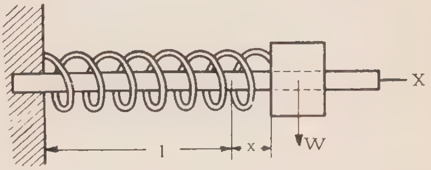

FIG. 254.—Vibration with constant damping.

$$-kx - \frac{W}{g}x'' + R = 0, \tag{e}$$

or

$$x'' + p(x - a) = 0 \tag{331}$$

here, as before (Eq. 320),

$$p = \sqrt{\frac{kg}{W}}$$

and

$$a = \frac{R}{k}. \tag{332}$$

This latter quantity has a simple physical meaning. It is the extension of the spring produced by the frictional force R. Making

$$x_1 = x - a,$$

equation (331) reduces to

$$x_1'' + p^2x_1 = 0.$$

This equation is in complete agreement with the equation (319)′ previously considered, and the following conclusions may be drawn:

---

* x is measured from the position of unstrained condition of the spring.

(1) A constant friction does not change the period of vibration. (2) The middle position about which the simple harmonic vibration takes place is displaced in the direction of the friction by the distance a (Eq. 332). Due to this latter fact, the extreme left position of the load will be distant only $x_0 - 2a$ from the position corresponding to the unstrained condition of the spring. This means that a diminishing of the amplitude produced by constant damping during half a cycle is equal to $2a$.

Considering now the motion from the extreme left position to the right, and applying the same reasoning, it can be shown that during the second half of the cycle a further diminishing of the amplitude of the quantity $2a$ will be produced. Therefore we see that in this case considered the decrease of the amplitude follows the law of arithmetical progression. The load W will remain in one of its extreme positions as soon as the amplitude becomes less than a. It is clear that in this position the friction will be sufficient to balance the tensile force of the spring.

79. Forced Vibrations.—*Particular Case.*—Taking again the arrangement shown in Fig. 248, assume that, in addition to the forces previously considered (see Eq. a, p. 325), a periodic force $Q \sin mt$ is acting in a vertical direction on the load W. Then using the notation

$$\frac{gQ}{W} = q, \tag{a}$$

the equation of motion becomes

$$x'' + 2nx' + p^2x = q \sin mt. \tag{333}$$

A general solution of this equation will be obtained if, to the solution of the corresponding homogeneous equation (see Eq. b, p. 325), a particular solution of Eq. 333 will be added. The latter will have the form

$$x = M \sin mt + N \cos mt.$$

Substituting this in equation (333), the following equations for determining constants M and N will be obtained:

$$\begin{gathered} -Nm^2 + 2Mmn + Np^2 = 0. \\ -Mm^2 - 2Nmn + Mp^2 = q, \end{gathered}$$

from which

$$N = -\frac{2qmn}{(p^2 - m^2)^2 + 4m^2n^2}, \quad M = \frac{q(p^2 - m^2)}{(p^2 - m^2)^2 + 4m^2n^2}.$$

Now the general solution of (333) becomes*

$$x = e^{-nt}(A \sin p_1t + B \cos p_1t) - \frac{2qmn}{(p^2 - m^2)^2 + 4m^2n^2} \cos mt + \frac{q(p^2 - m^2)}{(p^2 - m^2)^2 + 4m^2n^2} \sin mt. \tag{334}$$

The first member on the right side having the factor e^{-nt} represents the *damped vibrations* studied in the previous paragraph. The two other terms, proportional to q, represent the *forced vibrations*. They are maintained by the periodical external force and will not be damped with the time. Their period $T_1 = 2\pi/m$ is the same as that of the disturbing force and their amplitude is proportional to the magnitude of this force. This amplitude depends also on the relation between the period T of the natural vibration of the system and the period T_1 of the disturbing force.

The expression for the forced vibration can be simplified by using the following notations:

$$\frac{-2qmn}{(p^2 - m^2)^2 + 4m^2n^2} = -C \sin \alpha \tag{b}$$

$$\frac{q(p^2 - m^2)}{(p^2 - m^2)^2 + 4m^2n^2} = C \cos \alpha. \tag{c}$$

The expression for the forced vibrations becomes

$$C (\cos \alpha \sin mt - \sin \alpha \cos mt) = C \sin (mt - \alpha). \tag{335}$$

The amplitude C of forced vibrations, from (b) and (c), is

$$C = \frac{q}{\sqrt{(p^2 - m^2)^2 + 4m^2n^2}}. \tag{336}$$

The angle α in equation (335) represents the *difference in phases* between the *forced vibration* and the *disturbing force*.

Dividing (b) by (c) we have

$$\tan \alpha = \frac{2mn}{p^2 - m^2}. \tag{337}$$

If $p > m$, as occurs when the period of the natural vibration of the system is less than that of the disturbing force, α becomes positive and less than $\pi/2$. For the case $p < m$ we have $\alpha > \pi/2$. It can also be concluded from equation (335) that the forced vibration is behind the disturbing force $q \sin mt$.

When $p = m$, i.e., in the case of resonance, $\tan \alpha$ in equation (337) becomes infinite and the difference of the phases becomes equal to $\pi/2$. This means that during such vibratory motion the system assumes its middle position at the very moment when the disturbing force attains its maximum value.

---

* The notations of the previous paragraph are used here.

The amplitude C of this forced vibration will now be considered. Remembering that

$$q = \frac{gQ}{W}$$

and

$$p^2 = \frac{kg}{W}$$

it will be concluded that

$$\frac{q}{p^2} = \frac{Q}{k} = a, \tag{d}$$

where a denotes the deflection which would be produced by the maximum disturbing force if this were to be applied statically.

By using (d) the expression of the amplitude of the forced vibrations (equation (336)) becomes

$$C = \frac{a}{\sqrt{\left(1 - \frac{m^2}{p^2}\right)^2 + \frac{4m^2n^2}{p^4}}} = \frac{a}{\sqrt{\left(1 - \frac{T^2}{T_1^2}\right)^2 + \frac{T^2\gamma^2}{T_1^2}}}, \tag{338}$$

in which $T = \frac{2\pi}{p}$ = period of the natural vibration of the system,

$T_1 = \frac{2\pi}{m}$ = period of the disturbing force $Q \sin mt$,

$\gamma = \frac{2n}{p}$ = quantity depending on the magnitude of the damping forces.

It is easy to see that if the disturbing force has a very large period T_1, C approaches the value a. This means that in such cases the deflections of the system can be calculated on the assumption that the disturbing force $Q \sin mt$ is acting statically. Another extreme case will be obtained on the assumption that T_1 is a very small quantity, as occurs when the disturbing force has a very high *frequency*. In such case the denominator of equation (338) becomes very large and the amplitude of forced vibrations approaches the zero value. For instance, the load W will remain practically immovable in the space when the upper end A of the spring (see Fig. 248) will perform oscillations with a frequency much larger than that of the natural vibration of the system. On the basis of this phenomena many instruments for recording vibrations are built, such as seismographs for recording vibrations of earthquakes, and different types of vybrographs, for recording vibrations in machines and foundations.

If T_1 approaches T and the damping forces are small, the denominator in expression (338) becomes very small. This means that in the case of resonance a comparatively small disturbing force may produce very large forced vibrations, and very serious stresses in a vibrating structure.

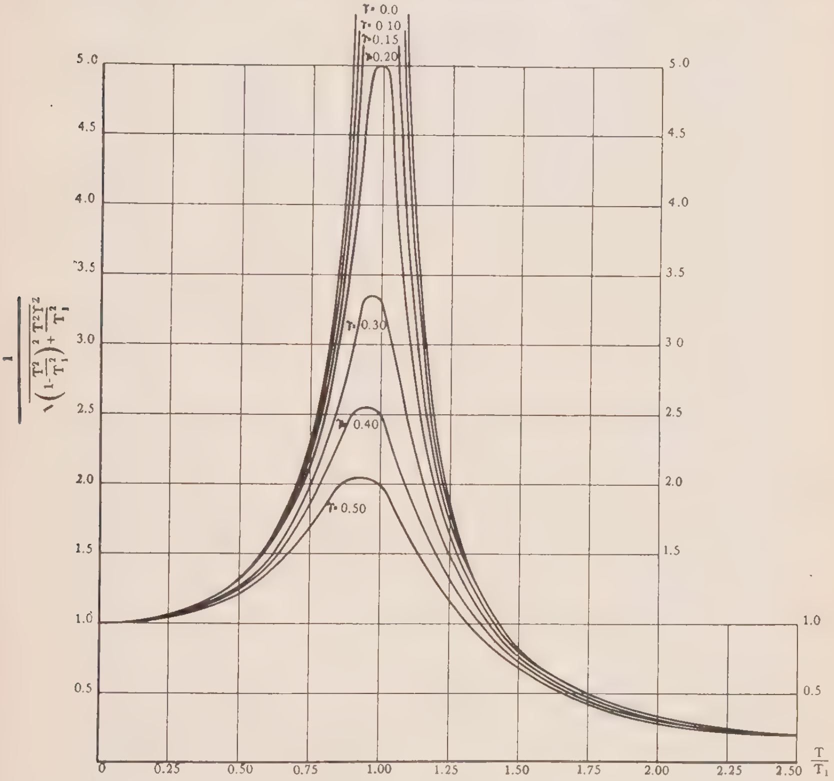

FIG. 255.—Curves showing amplitudes of forced vibrations.

In order to give a clear picture of the variation of the amplitude C with the variation of the ratio T/T_1 and of the quantity γ, several curves representing the quantity

$$\frac{1}{\sqrt{\left(1 - \frac{T^2}{T_1^2}\right)^2 + \frac{T^2\gamma^2}{T_1^2}}} \tag{e}$$

as a function of the ratio T/T_1 are plotted in Fig. (255) for different values of the quantity γ. It is seen from these curves that the points of maximum amplitude do not coincide exactly with the condition of resonance, but that the magnitude of the ratio T/T_1, corresponding to the maximum amplitude, is somewhat less than unity and approaches this limit with the decrease of damping. In the case of a small damping the difference between the maximum amplitude of the forced vibration and the amplitude of this vibration at resonance is very small, and the latter amplitude will be used as a basis for calculating the maximum stress during forced vibration.

General Case.—In the previous consideration the simple assumption was made that the disturbing force varies with the time as sin mt. In general, a periodic disturbing force can be represented by a trigonometrical series such as

$$Q = q_1 \sin\left(\frac{2\pi t}{T_1} + \alpha_1\right) + q_2 \sin\left(\frac{4\pi t}{T_1} + \alpha_2\right) + q_3 \sin\left(\frac{6\pi t}{T_1} + \alpha_3\right) + \dots \quad \text{(f)}$$

in which the first term has the same period T_1 as that of the disturbing force; the period of the second term as half as great; the period of the third term one-third as great, etc. α_1, α_2, α_3 denote the corresponding phases. If the period of one of these terms is identical with the period of the natural vibration of the system the condition for resonance takes place, and forced vibrations of large amplitude may be expected.

In the case of engines with reciprocating masses, the disturbing force, due to lack of balance, has usually the form given by (f), and if the number of free vibrations per minute of the system supporting the engine is equal to or a multiple of the R.P.M. of the machine, large forced vibrations may occur in the system.

Another Method of Calculating Forced Vibrations.—From general solution (334) page 329 it is seen that at the moment of application of the disturbing force not only forced vibrations of the system are produced, but also free vibrations. The latter vibrations will be gradually damped due to different kinds of resisting forces, but at the beginning of motion they may be of importance. In order to obtain the complete displacement of the system at starting, a method based on solution (329) page 325 will be considered. It is seen from this solution that the displacement from the position of equilibrium at any moment t produced by the initial velocity x_0' is

$$x = e^{-nt}\frac{x_0'}{p_1} \sin p_1 t. \quad \text{(g)}$$

Assume that a variable force $F(t)$ is acting on the system, and let

$$f(t) = \frac{gF(t)}{W}$$

be the force per unit mass of the weight W. The variation of this force in the interval from 0 to t_1 is represented in Fig. 256 by a curve MN. In order to obtain the displacement of the system at any moment t_1 imagine the continuous action of the force divided into short intervals such as dt (see Fig. 256). Due to the action of the force $f(t)$ during this interval, the velocity of the weight W is increased a small amount, which can be found from the equation

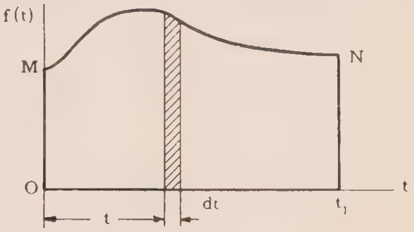

FIG. 256.—General case of disturbing force.

$$\frac{dx'}{dt} = f(t),$$

from which

$$d(x') = f(t)dt. \tag{h}$$

Now from (g) it can be concluded that any addition to the velocity at time t such as given by (h) will produce at time t_1 a displacement given by

$$dx = e^{-n(t_1-t)}\frac{f(t)dt}{p_1} \sin p_1(t_1 - t). \tag{i}$$

This expression represents the displacement due to the action of the force during an infinitely small interval dt only. In order to obtain the displacement produced by a continuous action of the force, the summation of such elemental displacements as (i) must be made. The displacement at the moment t_1 then becomes

$$x = \frac{1}{p_1}\int_0^{t_1} e^{-n(t_1-t)}f(t) \sin p_1(t_1 - t)dt. \tag{339}$$

This expression represents the complete displacement produced by the force acting from $t = 0$ to $t = t_1$. It includes both forced and free vibrations and may become very useful in studying the motion of the system at starting. It can be used also in cases where an analytical expression for the disturbing force is not known and where the force $f(t)$ is given graphically or numerically. It is necessary in such a case only to determine the magnitude of the integral (339) by using one of the approximate methods* of integration.

As an example of the application of this method, vibrations of a locomotive wheel produced by a low† spot on the rail or a flat spot on the wheel will now be considered.

Stresses Produced in Railway Track by the Effect of Low Spots.—Let η = the variable depth of the *low spot*‡ produced either by wear or permanent deflection (Fig. 257), y = the deflection of the rail, W/g = the mass of a wheel, α = the concentrated force necessary to produce a deflection of the rail equal to unity. This quantity α can easily be calculated from equation (105) page 137 if the dimensions of the rail and the modulus of foundation are known.

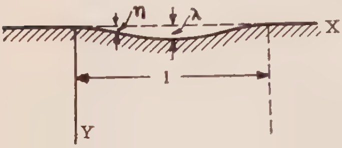

Fig. 257.—Low spot on rail.

If $\delta = W/\alpha$ = the deflection of the rail under the static action of the weight of the wheel, then the period of free vibrations of the wheel supported by the rail, from equation (321), will be

$$T = 2\pi\sqrt{\frac{\delta}{g}}. \tag{340}$$

For a 100 lb. rail $EI = 30 \times 44 \times 10^6$, lbs. × in. square, and taking the modulus of elastic foundation k = 1,500 lbs. per sq. in., W = 3,000 lbs., and this period will be .0483 sec., that is, the wheel performs about 20 vibrations per second.

The period will not be changed substantially by the force transmitted to the wheel by the spring, because the latter force can be considered as constant.

Consider now the forced vibrations of the wheel produced by the low spot. The vertical displacement of the wheel in an ideal condition is equal to the deflection of the rail, but due to the low spot of variable depth η this displacement becomes equal to $y + \eta$. Therefore, the inertia force is

$$-\frac{W}{g}\frac{d^2(y + \eta)}{dt^2}.$$

---

* Several methods of approximate integration are described in the books by v. Sanden, "Praktische Analysis" (Berlin), 1914, and in the book by Prof. C. Runge, "Vorlesungen u. numerisches Rechnen, J. Springer," (Berlin), 1924.

† This low spot can be due to a wearing of the rail or to a permanent depression.

‡ Effect of a flat spot on the wheel produces exactly the same effect as a low spot on the rail and all results obtained below can be used also in this case.

The reaction of the rail corresponding to the deflection y is $-\alpha y$. The equation of motion of the wheel in a vertical direction becomes

$$\frac{W}{g}\frac{d^2(y+\eta)}{dt^2} + \alpha y = 0,$$

or

$$\frac{W}{g}\frac{d^2y}{dt^2} + \alpha y = -\frac{W}{g}\frac{d^2\eta}{dt^2}. \tag{a}$$

When the shape of the low spot and the speed of the locomotive are known η can easily be expressed as a function of the time. Assuming, for instance, that the shape of the low spot is determined by the equation

$$\eta = \frac{\lambda}{2}\left(1 - \cos\frac{2\pi x}{l}\right), \tag{b}$$

in which l = the length of the low spot,

λ = the depth of the spot at the middle of its length.

Assume that at the initial moment ($t = 0$) the point of contact of the wheel coincides with the beginning of the low spot, and denote by v the constant speed of the locomotive, we have $x = vt$, and from (b),

$$\eta = \frac{\lambda}{2}\left(1 - \cos\frac{2\pi vt}{l}\right)$$

$$-\frac{W}{g}\frac{d^2\eta}{dt^2} = -\frac{W}{g}\frac{\lambda}{2}\frac{4\pi^2v^2}{l^2}\cos\frac{2\pi vt}{l}. \tag{c}$$

In the general case we will have

$$-\frac{W}{g}\frac{d^2\eta}{dt^2} = F(t),$$

where $F(t)$ is a certain function of t, depending on the shape of the low spot; and the equation (a) becomes

$$\frac{W}{g}\frac{d^2y}{dt^2} + \alpha y = F(t).$$

This coincides with the equation of forced vibrations when damping is absent.

A general solution (339) for this case becomes

$$y = \frac{g}{W}\frac{T}{2\pi}\int_0^{t_1} F(t)\sin\frac{2\pi}{T}(t_1 - t)dt. \tag{d}$$

This gives the general expression for the additional deflection of the rail produced by a low spot. In the particular case when the shape of the spot is given by equation (b) the disturbing force $F(t)$ is given by (c). Substituting this in (d), performing the integration, and denoting

$$T_1 = \frac{l}{v}$$

as the time required for the wheel to pass over the flat spot, we will have

$$y = \frac{\lambda}{2} \frac{1}{1 - \left(\frac{T_1}{T}\right)^2} \left(\cos \frac{2\pi t}{T_1} - \cos \frac{2\pi t}{T}\right). \tag{e}$$

It is seen that the *additional deflection** is proportional to the depth of the spot λ and depends on the magnitude of the ratio

$$\frac{T_1}{T}.$$

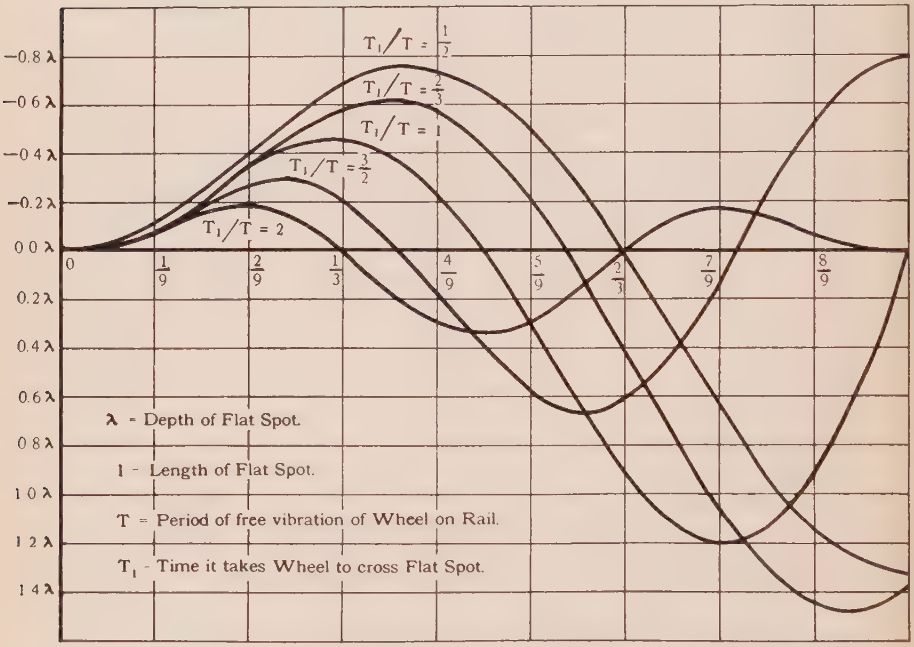

FIG. 258.—Curves showing dynamical effect of low spots on rail.

The variation of this deflection of the rail under the wheel in the interval $0 < t < T_1$ for different values of the ratio T_1/T is represented in Fig. 258.

It should be noted that at the instant the wheel reaches the edge of the low spot the pressure on the rail and the deflection begin to diminish while the wheel begins to accelerate in a downward direction. Then, the retardation of this movement begins and with it the increase in pressure and deflection, as seen from the figure. The values of the maximum deflection, calculated from equation (e) for different values of the ratio T_1/T, are given in the Table XXX.

---

* This deflection must be added to the statical deflection $\delta = W/\alpha$.

TABLE XXX.—MAXIMUM DEFLECTION PRODUCED BY THE FLAT SPOT

$T_1/T =$	2	$3/2$	1	$4/5$	$2/3$	$3/5$	$1/2$
$y_{\max}/\lambda =$	.33	.65	1.21	1.41	1.47	1.45	1.33

The maximum deflection, equal to about 1.47λ, occurs at the speed corresponding to $T_1/T = 2/3$. Taking, for example, $\lambda = 1/16$ in., equation (105) page 137 shows that the additional pressure on the rail, corresponding to the additional maximum deflection $1.47 \times 1/16$ in., is about 12,000 lbs. for the numerical data taken above. Thus, a comparatively small low spot produces, at certain speeds, very appreciable dynamic effect. Similar results can be obtained for low spots of different shapes.* In all the considerations presented the mass of the vibrating part of the rail was neglected in comparison with the mass of the wheel. The error involved in this simplification of the problem is not great if the time T_1 required for the wheel to pass over the spot is long enough in comparison with the period of the fundamental type of free vibration of the rail. With the train's increasing speed the error increases and the elementary solution given above may be then considered as a first approximation only.†

80. Torsional Vibrations.—*General.*—The problem on torsional vibrations in shafts is of great practical importance in the field of engineering. If the dimensions of the system are such that the frequency of natural vibration is equal to or a multiple of the number of revolutions per second of the machine, the condition of resonance occurs. The amplitude of forced vibration in such cases may become very large,‡ and the corresponding dynamical stresses of the alternating type may finally produce failure of the shaft due to the fatigue of material.

---

* See the author's paper On the Stresses in Railway Track, *Transactions Inst. of Eng. of Ways of Communication*, (S. Petersburg), 1915.

† Solutions of several problems on vibrations of rails are given in the author's paper On the Vibration of Rails. *Bulletin of the Electrotechnical Inst.*, Vol. XIII, p. 555, 1915 (Petersburg). Abstract of the paper in French, see "Le Genie Civil," p. 551, 1921.

‡ For instance, H. Frahm, see *Neue Untersuchungen uber dynamischen Vorgänge in den Wellenleitungen v. Schiffsmaschinen, Z. d. Ver. Deutsch. Ing.*, p. 797, 1902, found experimentally that in the case of a propeller shaft designed on the basis of a working stress equal to 3,200 lbs. per sq. in. app., the maximum stress at certain speeds varied during one revolution within the limits 8,500 lbs. per sq. in., − 2,400 lbs. per square inch.

Single Disc.—When a shaft with one end fixed carries at its free end (see Fig. 259) a disc the moment of inertia of which is large in comparison with that of the shaft, the moment of inertia of the shaft can be neglected, and the system becomes that with one degree of freedom. Then the period of natural vibration can easily be obtained.

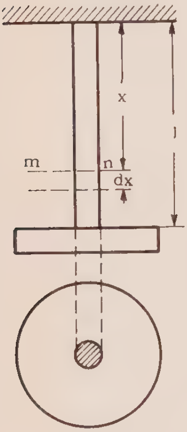

Fig. 259.—Shaft with single disc.

Let l = the length of the shaft,

$I_p = \frac{\pi d^4}{32}$ = polar moment of inertia of the cross-section of the shaft,

I = moment of inertia of the disc about the axis of the shaft,

ϕ = variable angle of twist during torsional vibrations.

Then the moment of the inertia forces about the axis of the shaft during vibration is $-I\phi''$, and the moment of twist is

$$-\frac{GI_p}{l}\phi.$$

The differential equation of free vibration of the rotating disc becomes

$$I\phi'' + \frac{GI_p}{l}\phi = 0. \tag{a}$$

Using the notation

$$\frac{GI_p}{lI} = p^2, \tag{341}$$

we have

$$\phi'' + p^2\phi = 0. \tag{b}$$

This equation is in the same form as the equation (319′) page 313 previously considered. Its general solution is

$$\phi = A \cos pt + B \sin pt.$$

The period of free vibration becomes

$$T = \frac{2\pi}{p} = 2\pi\sqrt{\frac{lI}{GI_p}}. \tag{342}$$

This period increases with increase in the length of the shaft and in the moment of inertia of the disc, and decreases with the increase of torsional rigidity of the shaft. It is seen that in the case of long shafts the frequency of free vibrations may become low and conditions of resonance may be likely to occur.

In this case it was assumed that the shaft had a constant diameter d. When the shaft is of different diameters in different parts, such a shaft can easily be reduced to one having a constant diameter. It is only necessary to bear in mind that the angle of twist of a shaft is proportional to its length and inversely proportional to the fourth degree of the diameter. Therefore, without changing the angle of twist, a part of the shaft having a length a_1 and a diameter d_1 may be replaced by an equivalent part having a length a_2 and a diameter d_2. It is only necessary to satisfy the condition

$$\frac{a_1}{a_2} = \left(\frac{d_2}{d_1}\right)^4. \tag{c}$$

By using (c) a shaft of variable cross-section can be reduced to one of constant cross-section as considered above.

The effect of the mass of the shaft itself on the period of vibration can easily be obtained by using the *Rayleigh method.* Assume that the type of vibration is not changed, then the angle of rotation for any cross-section mn distant x from the fixed end is (Fig. 259)

$$\phi\frac{x}{l}.$$

Let I_0 denote the moment of inertia of the shaft per unit length, then the kinetic energy of an element of the shaft of length dx will be

$$\frac{1}{2}\phi'^2\frac{x^2}{l^2}I_0 dx.$$

The total kinetic energy of the shaft becomes

$$\frac{1}{2}\int_0^l \phi'^2\frac{x^2}{l^2}I_0 dx = \frac{1}{2}\phi'^2 I_0\frac{l}{3}. \tag{343}$$

This means that in order to take into account the moment of inertia of the shaft itself it is only necessary to add one-third of its moment of inertia to the moment of inertia of the disc.*

---

* The manner of calculating further approximations by using the Rayleigh method is developed in the author's paper On the Resonance in Shafts, *Bull. of the Polytechnical Inst. in S. Petersburg*, 1905.

Two Discs.—During free vibration of such a system as shown in Fig. 260 the two discs are always rotating in opposite directions, so that somewhere between them is a *nodal* section mn which does not rotate. Let I_1 and I_2 denote the moments of inertia of the discs; let a and b denote the distances of the nodal section from the ends of the shaft. Considering the nodal section as fixed and using equation (342), the lengths a and b will be obtained from the equation

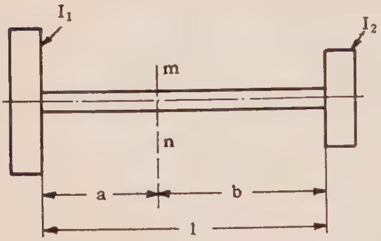

FIG. 260.—Shaft with two discs.

$$2\pi\sqrt{\frac{aI_1}{GI_p}} = 2\pi\sqrt{\frac{bI_2}{GI_p}}. \tag{d}$$

which means that both parts of the shaft have the same period of vibration. From this equation it follows that

$$\frac{a}{b} = \frac{I_2}{I_1}. \tag{e}$$

Remembering that

$$a + b = l,$$

we have from (e)

$$a = \frac{I_2 l}{I_1 + I_2}, \quad b = \frac{I_1 l}{I_1 + I_2}.$$

Substituting in (342),

$$T = 2\pi\sqrt{\frac{I_1 I_2 l}{GI_p(I_1 + I_2)}}. \tag{344}$$

In order to take into account the moment of inertia of the shaft itself, the quantities

$$\frac{aI_0}{3} \text{ and } \frac{bI_0}{3}$$

must be added to I_1 and I_2 respectively.

*Three Discs.**—Let I_1, I_2, and I_3 represent the moments of inertia of the discs (Fig. 261), and ϕ_1, ϕ_2, and ϕ_3 their maximum angular displacements. Let C_1 and C_2 be constants depending on the rigidity of the shaft, such that $C_1(\phi_1 - \phi_2)$ and $C_2(\phi_2 - \phi_3)$ represent the maximum torque moments on the left and right part of the shaft respectively.

---

* See paper by Roth, *Z. d. Ver. deutsch. Ing.*, 1904. See also Morley's paper, *Eng.*, p. 785, 1910.

The angular displacements of the discs during vibration can be taken as follows:

$$\phi_1 \cos pt, \quad \phi_2 \cos pt, \quad \phi_3 \cos pt;$$

then the inertia moments of each of the discs will be:

$$I_1p^2\, \phi_1 \cos pt, I_2p^2\phi_2 \cos pt, I_3p^2\phi_3 \cos pt.$$

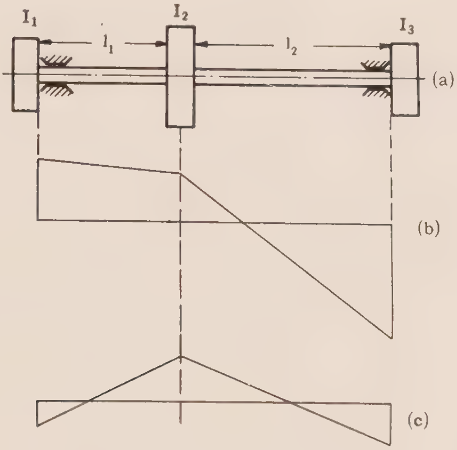

FIG. 261.—Shaft with three discs.

We can now consider the inertia moment of each of the discs as balanced by the moments of the elastic forces of the adjacent shaft sections. The corresponding equations become

$$I_1p^2\, \phi_1 - C_1(\phi_1 - \phi_2) = 0 \tag{f}$$
$$I_2p^2\phi_2 - C_2(\phi_2 - \phi_3) + C_1(\phi_1 - \phi_2) = 0 \tag{g}$$
$$I_3p^2\, \phi_3 + C_2(\phi_2 - \phi_3) = 0. \tag{h}$$

The quantity p^2 determining the frequency of the system can now be obtained as follows:

Adding the three equations (f), (g), and (h), we have

$$I_1\phi_1 + I_2\phi_2 + I_3\phi_3 = 0. \tag{i}$$

Now from (f),

$$\phi_1 = \frac{-C_1\phi_2}{I_1p^2 - C_1}, \tag{j}$$

and from (h),

$$\phi_3 = \frac{-C_2\phi_2}{I_3p^2 - C_2}. \tag{k}$$

Substituting (j) and (k) in (i),

$$-\frac{I_1C_1}{I_1p^2 - C_1} + I_2 - \frac{I_3C_2}{I_3p^2 - C_2} = 0, \tag{l}$$

or

$$\frac{I_1I_2I_3}{C_1C_2}p^4 - \left(\frac{I_1I_2 + I_1I_3}{C_1} + \frac{I_2I_3 + I_1I_3}{C_2}\right)p^2 + (I_1 + I_2 + I_3) = 0, \tag{345}$$

from which p^2 can easily be obtained if the dimensions of the system are known.

Two roots of this equation correspond to two types of vibrations shown diagrammatically in Fig. 261 (b) and (c).

General Case.—If a shaft carries n discs, the above method can be used for determining the frequencies of natural vibrations. By using previous notations the following system of equations will be obtained:

$$\begin{aligned} &I_1p^2\,\phi_1 - C_1(\phi_1 - \phi_2) = 0, \\ &I_2p^2\,\phi_2 - C_2(\phi_2 - \phi_3) + C_1(\phi_1 - \phi_2) = 0, \\ &I_3p^2\,\phi_3 - C_3(\phi_3 - \phi_4) + C_2(\phi_2 - \phi_3) = 0 \\ &\cdot\ \cdot\ \cdot\ \cdot\ \cdot\ \cdot\ \cdot\ \cdot\ \cdot\ \cdot\ \cdot\ \cdot\ \cdot\ \cdot\ \cdot\ \cdot\ \cdot\ \cdot \\ &I_np^2\,\phi_n + C_{n-1}(\phi_{n-1} - \phi_n) = 0. \end{aligned} \tag{m}$$

Proceeding as in the case of three discs, an equation of the degree $(n - 1)$ for determining p^2 can be obtained from (m). The $n - 1$ roots of this equation correspond to $n - 1$ different types of natural vibrations of a shaft with n discs. The numerical solution of such an equation may present some difficulty and if only one or two of the lower types of vibrations are of interest, the corresponding frequencies can be obtained directly from the system (m) by successive approximations* as follows:

The system of equations (m) can be written in such a form:

$$\phi_2 = \phi_1 - \frac{I_1p^2}{C_1}\phi_1, \tag{n}$$

$$\phi_3 = \phi_2 - \frac{p^2}{C_2}(I_1\phi_1 + I_2\phi_2), \tag{o}$$

$$\phi_4 = \phi_3 - \frac{p^2}{C_3}(I_1\phi_1 + I_2\phi_2 + I_3\phi_3). \tag{p}$$

Making a rough estimate of the value p and taking an arbitrary value for ϕ_1, the angular deflection of the first disc, the corresponding value of ϕ_2 will be found from equation (n); then, from equation (o), will be found ϕ_3; from equation (p), ϕ_4, and so on. If the magnitude of p^2 was chosen correctly, the last of the equations (m) will be satisfied. Otherwise, the angles ϕ_2 and ϕ_3 must be calculated again with a new estimate for p^2.

---

* Several examples of this calculation can be found in the book by H. Holzer, "Die Berechnung der Drehschwingungen," (Berlin), J. Springer, 1921.

Another manner of calculating p^2 will be obtained by considering the kinetic and potential energy of the vibrating system.

The maximum kinetic energy of the system is

$$T = \tfrac{1}{2}p^2(I_1\phi_1^2 + I_2\phi_2^2 + I_3\phi_3^2 + \ . \ . \ .) \qquad \text{(q)}$$

The maximum potential energy is

$$U = \tfrac{1}{2}C_1(\phi_1 - \phi_2)^2 + \tfrac{1}{2}C_2(\phi_2 - \phi_3)^2 + \tfrac{1}{2}C_3(\phi_3 - \phi_4)^2 + \ . \ . \ . \qquad \text{(r)}$$

By comparing (q) and (r)

$$p^2 = \frac{C_1(\phi_1 - \phi_2)^2 + C_2(\phi_2 - \phi_3)^2 + \ . \ . \ .}{I_1\phi_1^2 + I_2\phi_2^2 + \ . \ . \ .} \qquad (346)$$

By making a rough estimate of p while assuming an arbitrary value for ϕ_1, the angles ϕ_2, ϕ_3, ϕ_4 can be calculated from (n), (o), (p). Substituting their values in equation (346) a better approximation for p^2 will be obtained. Repeating the calculations with this new value of p^2 further approximations will be found.

Equation (346) is of the same type as equation (324) considered before (see paragraph 76); therefore the Rayleigh-Ritz method can also be used here in the same manner as in studying the vibrations of beams, which was explained above.

A system of equations such as (m) will also be obtained in the case of vibration of a geared system such as shown in Fig. 262. This kind of vibration problem has a practical interest in connection with geared drives for ships.*

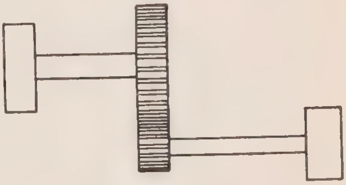

FIG. 262.—Vibration of geared system.

Example 76.—Take, for instance, motor generator set with four rotating masses, The moments of inertia of rotating masses are,

$I_1 = 51{,}000$ lbs. in. sec.^{2}
$I_2 = 52{,}000$ lbs. in. sec.^{2}
$I_3 = 71{,}000$ lbs. in. sec.^{2}
$I_4 = 51{,}000$ lbs. in. sec.^{2}

---

* See H. Reissner, Uber die Kraftschlussigkeit von Zahnradgetrieben insbesondere für Schiffspropeller, *Ztschr. f. Angw. Math. u. Mechanik*, Vol. 4, p. 53, 1924. See also T. H. Smith, Nodal arrangements of geared drives, *Engineering*, 1922, pp. 438 and 467.

The dimensions of the shafts are such that

$$C_1 = 1{,}020 \times 10^6 \text{ in. lbs.}$$
$$C_2 = 350 \times 10^6 \text{ in. lbs.}$$
$$C_3 = 1{,}150 \times 10^6 \text{ in. lbs.}$$

Assuming roughly $p_1 = 100$ and taking $\phi_1 = 1$, it will be found from equations (n), (o) and (p) $\phi_2 = .5$, $\phi_3 = -1.7$, $\phi_4 = -1.32$.

Substituting in equation 346, $p_1 = 78$ will be obtained.

The further approximation gives $\phi_1 = 1$, $\phi_2 = .73$, $\phi_3 = -.70$, $\phi_4 = -.89$ and p_1 about 74.

This solution corresponds to the fundamental type of vibrations with one node near the middle of the shaft. For the second mode of vibrations with two nodes it will be obtained, by using the same equations (n), (o), (p) and (346).

$$p_2 = 199.$$

81. Impact.—The problems on stresses produced by suddenly applied loads or by a falling weight are of great practical importance. The exact solution of such problems involves the study of vibrations of the structures and presents great analytical difficulties.[*] In cases where the mass of the structure is negligible an approximate solution can be obtained by considering the energy of the system.

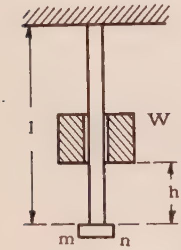

FIG. 263.—Tension by impact.

Impact Producing Tension.—A simple example of impact producing tension in a prismatical bar will now be considered. Taking the arrangement shown in Fig. 263, assume that a weight W falls through a height h on to a stop mn in such a manner as to produce a simple tension in a bar of length l. Let $\lambda_{st} = Wl/EA$ represent the statical extension of the bar under the action of the weight W, and λ the extension produced during impact so that the complete vertical displacement of the weight W at the moment its velocity becomes zero is equal to $h + \lambda$; then the work done by this load during falling becomes

$$W(h + \lambda). \tag{a}$$

If the mass of the bar is small in comparison to the mass of the falling weight, the loss of energy during impact will be negligible and it can be assumed with a sufficient accuracy that the work done during impact (a) will be completely transformed into the potential energy of the bar extension,* provided the limit of proportionality of the material is not exceeded. The expression for this energy is

---

[*] The problem on the longitudinal impact of prismatical bars was solved by S. Venant. Further simplifications in solution of this problem were made by Sebert and Hugoniot (C. R., 1882, p. 213, 278, 338, 382). Experimental study of longitudinal impact, see W. Voigt, *Wied. Ann.*, 19, p. 43, 1883. See also C. Ramsauer, *Ann. d. Phys.*, Vol. 30, 1909.

Impact of bars with spherical ends was studied by T. E. Sears, *Cambridge Phil. Soc. Trans.*, Vol. XXI, p. 49, 1908.

$$U = \frac{\lambda^2 EA}{2l},$$

and the equation for determining λ becomes

$$\frac{\lambda^2 EA}{2l} = W(h + \lambda) \tag{b}$$

from which

$$\lambda = \lambda_{st} + \sqrt{\lambda_{st}^2 + 2\lambda_{st}h}. \tag{347}$$

If

$$h = 0,$$
$$\lambda = 2\lambda_{st}.$$

It means that a suddenly applied load produces twice as great an extension as that due to a statical loading of equal magnitude.

If h is large in comparison with λ_{st} equation

$$\lambda = \sqrt{2\lambda_{st}h} \tag{348}$$

instead of equation (347) can be used.

The maximum tensile stress in such a case is

$$p_{\max} = \frac{E\lambda}{l} = E\sqrt{\frac{2\lambda_{st}h}{l^2}}. \tag{c}$$

This result can be represented in another form if we remember that the velocity of the weight at the beginning of impact is $v = \sqrt{2gh}$, from which

$$h = \frac{v^2}{2g}. \tag{d}$$

Substituting in (c),

$$p_{\max} = E\sqrt{\frac{\lambda_{st}v^2}{gl^2}} = \sqrt{\frac{E}{Al}\,\frac{Wv^2}{g}}. \tag{349}$$

This means that the stress produced by impact depends not on the cross-sectional area but on the volume Al of the bar and on the kinetic energy of the falling weight.

Impact Producing Bending.—The same method, as above, can also be used in the case of bending. A simple case of a beam supported at the ends and struck midway between supports by a falling weight W will now be considered. Let δ denote the dynamical deflection of the beam, and P the pressure of the weight W on the beam, corresponding to this deflection; then

---

* This approximate solution was given in the book "A Course of Lectures on Natural Philosophy," p. 135, by Th. Young, 1807.

$$\delta = \frac{Pl^3}{48EI}, \tag{e}$$

or

$$P = \frac{48EI\,\delta}{l^3}. \tag{f}$$

The potential energy of bending will be

$$U = \frac{P\delta}{2} = \frac{24EI}{l^3}\delta^2,$$

and the equation for determining δ becomes

$$W(h + \delta) = \frac{24EI}{l^3}\delta^2, \tag{g}$$

where h has the same meaning as before (see Fig. 263). Now, from (g),

$$\delta = \frac{Wl^3}{48EI} + \sqrt{\left(\frac{Wl^3}{48EI}\right)^2 + \frac{2Wl^3h}{48EI}} = \delta_{st} + \sqrt{\delta_{st}{}^2 + 2\delta_{st}h}, \tag{350}$$

where δ_{st} denotes the statical deflection of the beam under the action of the load W.

This equation is of the very same form as equation (347) obtained above, and it can be concluded at once that a load suddenly applied produces a deflection twice as great as that in the case of a statical loading.

If h is large in comparison with δ_{st}, equation

$$\delta = \sqrt{2\delta_{st}h} = \sqrt{\frac{Wl^3}{48EI}\,\frac{v^2}{g}} \tag{351}$$

instead of equation (350) can be used.

The maximum bending moment during impact will be (see equation f)

$$M_{\max} = \frac{Pl}{4} = \frac{12EI\delta}{l^2}$$

and the corresponding maximum stress

$$p_{\max} = \frac{12aE\delta}{l^2} \tag{352}$$

in which a denotes the distance from the neutral surface to the most remote fiber of the beam. By using equation (351),

$$p_{\max} = \frac{12aE}{l^2}\sqrt{\frac{Wl^3}{48EI}\,\frac{v^2}{g}}$$

from which

$$\frac{Wv^2}{2g} = p^2_{\max}\frac{lI}{6a^2E}. \tag{353}$$

Taking, for instance, a rectangular cross-section

$$\frac{I}{a^2} = \frac{1}{3}A \tag{g}$$

where A is the area of the cross-section, substituting (g) in (353),

$$\frac{Wv^2}{2g} = p^2_{\max}\frac{lA}{18E}. \tag{354}$$

It is seen that for a given value of $p_{\max}$ the limiting value of the kinetic energy of the falling weight is proportional to the volume lA of the beam. Taking, for instance, the length of the beam four times as great, other conditions for impact remaining the same, the maximum stress, from equation (354), will be one-half as great.

Impact Producing Twist.—Assume that a flywheel mn (Fig. 264), having a moment of inertia I about the axis of rotation AB, rotates with a constant angular velocity ω. If the motion at the end A of the shaft is suddenly stopped, an impact twist of the shaft will be produced. By using the same reasoning as before and assuming that the kinetic energy of the rotating flywheel during impact will be completely transformed into the potential energy of twist of the shaft, the equation for the determination of the corresponding torque moment becomes (see Eq. 33, p. 29).

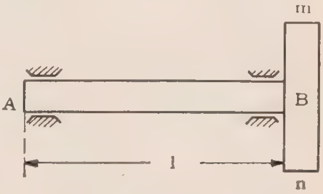

FIG. 264.—Twist by impact.

$$\frac{M_t^2 l}{2GI_p} = \frac{I\omega^2}{2}$$

from which

$$M_t = \sqrt{\frac{IGI_p\omega^2}{l}}. \tag{k}$$

The corresponding maximum stress becomes

$$(p_t)_{\max} = \frac{M_t d}{2I_p} \tag{l}$$

where d = the diameter of the shaft.

From (k) and (l),

$$(p_t)_{\max} = \sqrt{\frac{8IG\omega^2}{\pi l d^2}}. \tag{355}$$

It is seen that in this case again the maximum stress depends on the volume of the structure. For instance, by increasing the length of the shaft four times, the maximum stress at impact will be reduced to one-half.

The Effect of the Mass of the Structure.—In our previous considerations of impact the mass of the structure was always neglected and it was assumed that the kinetic energy of the falling weight W will be completely transformed in the potential energy of deformation of the structure. In actual conditions a part of the kinetic energy will be lost during the impact and calculations made above will give an upper limit for the dynamical deflection and the dynamical stresses. In order to obtain a more accurate solution the mass of the structure submitted to the action of impact must be taken into consideration.

If a moving body, having a mass W/g and a velocity v, strikes a resting body of a mass w/g centrally, and if the deformation at the point of contact is perfectly unelastic, the final velocity c, after impact (equal for both bodies), may be determined from the known equation

$$\frac{W}{g} v = \frac{W + w}{g} c,$$

from which

$$c = \frac{W}{W + w} v. \tag{m}$$

Considering rods or beams submitted to impact by a falling weight W, it must be noted that only at the point of contact some common velocity c of the weight W and of the rod will be established at the first moment of impact, and that other points of the structure may have velocities different from c. For instance, at the supports of a beam these velocities will be equal to zero. Therefore, not the actual mass of the elastic structure but some *reduced mass* must be used in equation (m) for calculating the velocity c. The magnitude of this reduced mass will depend on the shape of the deflection curve of the structure and can be approximately determined by using the method of calculation previously explained (see paragraph 75). Taking a suitable shape for the deflection curve, the kinetic energy of the structure can be replaced by the kinetic energy of a mass concentrated at the point of impact. This mass must be substituted in equation (m) for w/g in calculating c.

Consider, for example, a simply supported beam submitted to an impact midway between supports.

Let W = the weight of the falling weight,
w = the weight of the beam.

Assuming that the deflection curve of the beam during impact has the same shape as the statical deflection curve produced by the action of a uniformly distributed load, the reduced mass of the beam becomes (see equation 323, p. 317)

$$\frac{17}{35}\frac{w}{g}.$$

Then from (m),

$$c = \frac{W}{W + \frac{17}{35}w}v.$$

The corresponding magnitude of the kinetic energy of the system will be

$$\frac{\left(W + \frac{17}{35}w\right)c^2}{2g} = \frac{Wv^2}{2g}\frac{1}{1 + \frac{17}{35}\frac{w}{W}}.$$

This quantity must be substituted for

$$\frac{Wv^2}{2g} = Wh$$

in the previous equations (350) and (351) in order to take into account the effect of the mass of the beam. The dynamical deflection becomes, from (350),

$$\delta = \delta_{st} + \sqrt{\delta_{st} + 2\delta_{st}h\frac{1}{1 + \frac{17}{35}\frac{w}{W}}}.$$

By using the same reasoning we obtain for impact, producing tension (Fig. 263),

$$\lambda = \lambda_{st} + \sqrt{\lambda^2_{st} + 2\lambda_{st}h\frac{1}{1 + \frac{1}{3}\frac{w}{W}}}$$

in which $\frac{1}{3}w$ represents the reduced weight of the rod for this case (see paragraph 75).

The same method can be used in all other cases of impact in which the displacement of the structure at the point of impact is proportional to the pressure. The expression for the dynamical displacement λ has always the form

$$\lambda = \lambda_{st} + \sqrt{\lambda_{st}^2 + 2\lambda_{st}h\frac{1}{1 + k\frac{w}{W}}}$$

in which kw denotes the *reduced weight* of the structure. It can be calculated if a suitable deflection curve is chosen. The method described* gives sufficiently accurate results in cases of thin rods and beams if the mass of the falling weight is large in comparison to the mass of the beam. Otherwise the consideration of vibrations of the system and of local deformations at the point of impact becomes necessary to obtain a satisfactory solution of the problem.†

If all the dimensions of the bodies submitted to the action of impact are of the same order, for instance, in the case of an impact of two spherical bodies, a satisfactory solution can be obtained by neglecting vibrations and considering only local deformations at the point of contact.‡

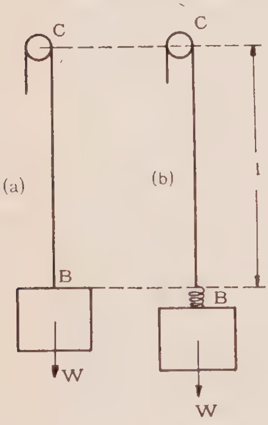

Fig. 265.

Example 77.—The weight W attached to the end of the wire rope CB is moving downwards with a velocity v. What stresses will be produced in the rope if the end C of the rope is suddenly stopped during the motion of the load? What diminishing of the stress can be obtained by putting a spring between the rope and the weight as shown in (b). Make the calculations for the following data

W = 10,000 lbs.
v = 3 feet per sec.
l = the free length of the rope in the moment of the sudden stop = 60 feet.
A = the cross-sectional area of the rope = 2.5 sq. ins.
E = modulus of elasticity for the wire rope = 10.10^6 lbs. per sq. in.
k = 2,000 lbs. = the force producing extension of the spring equal to 1 in.

Solution.—Neglecting the mass of the rope, assume that at the moment of stop the kinetic energy of the moving weight will be completely transformed into the potential energy of deformation of the rope. Then the equation for determining the maximum extension λ of the rope becomes

$$\frac{\lambda^2 EA}{2l} - \frac{\lambda^2_{st} EA}{2l} = \frac{W}{2g} v^2 + W(\lambda - \lambda_{st})$$

---

* This method was developed by H. Cox, *Cambridge Phil. Soc. Trans.*, p. 73, 1849. See also Todhunter and Pearson, *History*, Vol. I, p. 895. Further Development of the theory see, Clebsh, "Théorie de l'élasticité," traduite par S. Venant, note finale du paragraph 61, p. 490.

† See author's paper, Zur Frage nach der Wirkung eines Stosses auf einen Balken, *Z. f. Math. u. Phys.*, Vol. 62, p. 198, 1913.

‡ See Hertz, *J. f. Math.* (Crelle), Vol. 92, 1881. See also Lord Rayleigh *Phil. Mag.* (6 ser), Vol. 77, 1916.

from which

$$\frac{AE}{2l}(\lambda - \lambda_{st})^2 = \frac{Wv^2}{2g}.$$

The maximum extension becomes

$$\lambda = \lambda_{st} + v\sqrt{\frac{Wl}{AEg}}.$$

Therefore, due to the sudden stop of the motion, the tensile stress in the rope will increase in the ratio

$$\frac{\lambda}{\lambda_{st}} = 1 + \frac{v}{\lambda_{st}}\sqrt{\frac{Wl}{AEg}} = 1 + \frac{v}{\sqrt{\lambda_{st} g}}. \qquad (r)$$

In our case

$$\lambda_{st} = \frac{Wl}{AE} = \frac{10{,}000 \times 60 \times 12}{2.5 \times 10^7} = .288 \text{ in.}$$

Therefore, the stress during impact will increase in the ratio

$$\frac{\lambda}{\lambda_{st}} = 1 + \frac{v}{\sqrt{\lambda_{st} g}} = 1 + \frac{36}{\sqrt{.288 \times 386}} = 1 + 3.41 = 4.41.$$

Its magnitude will be 10,000/2.5 × 4.41 = 17,600 lbs. per sq. in.

It is seen that with the increase of λ_{st} the effect of impact decreases.

By putting the spring between the weight and the rope the statical extension becomes

$$\lambda_{st} = .288 + \frac{10{,}000}{2{,}000} = 5.29 \text{ in.}$$

In such case the increase during impact will be in the ratio [(from eq. (*r*)]

$$\frac{\lambda}{\lambda_{st}} = 1 + \frac{v}{\sqrt{\lambda_{st} g}} = 1 + \frac{36}{\sqrt{5.29 g}} = 1.80$$

Example 78.—A circular spring of a constant cross-section (Fig. 266) is submitted to the action of impact. Determine the maximum deflection and the maximum stress if the magnitude *W* of the falling weight, the height *h*, and the dimensions of the spring are known.

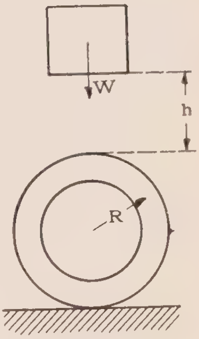

FIG. 266.

Solution.—The statical compression of the spring under the action of the load *W*, from equation (230) will be

$$\lambda_{st} = \frac{WR^3}{EI}\left(\frac{\pi}{4} - \frac{2}{\pi}\right).$$

For determining the dynamical deflection λ we have, by neglecting the mass of the spring,

$$\lambda = \lambda_{st} + \sqrt{\lambda_{st}^2 + 2h\lambda_{st}}.$$

The maximum bending moment, from equation 229, is

$$M_{\max} = .318\frac{\lambda}{\lambda_{st}} WR.$$

APPLIED ELASTICITY

PART II

CHAPTER XII

TENSION AND COMPRESSION

TENSION

82. General.—As mentioned in the introductory remarks, the term "Strength of Materials" used in its widest sense, has two sides, a mathematical one, which deals with the different kinds of stresses imposed on structures, and an experimental one, which deals with the mechanical properties of the materials of which these structures are composed. The following chapters deal only with the experimental side.

The application of forces to a solid body causes a deformation corresponding to the nature of the applied force, for instance, a pull causes an extension while a push causes a shortening. If these forces be of sufficient magnitude, permanent deformation of the body may be seen when the forces are removed, even supposing these forces have not been sufficient to cause fracture. When these forces are of less intensity, the body may so recover its original form, on removal of such forces, that very delicate instruments are required to measure permanent set, should any exist. In the mathematical treatment of the subject, this property, which bodies possess of recovering their original form provided the stresses causing deformation are removed after reaching a certain limit, forms the whole basis for the analysis. It readily will be seen that this fact, which can be proved experimentally, becomes of vital importance to the engineer. It is therefore proposed to discuss in detail certain experimental evidence related to such phenomena.

If a bar of material be subjected to a gradually increasing tensile stress it will experience progressive extension. If this bar is disposed in such a manner that the stress and corresponding extension can be measured accurately, such as for instance, by employing a machine as shown in Fig. 267 and an extension measuring apparatus as in Figs. 268* and 269,* it will be found that within certain limits the extension is proportional to the applied stress.

---

* The Ewing extensometer in Fig. 268 enables extensions of .00002 inch to be measured, which on a 2 inch gauge length corresponds to that produced by a stress of 300 lbs. per sq. inch on steel. The Martens extensometer, Fig. 269 enables extensions of .0002 millimeter to be read, which on a 2 inch gauge length corresponds to that produced by a stress of 120 lbs. per sq. inch on steel.

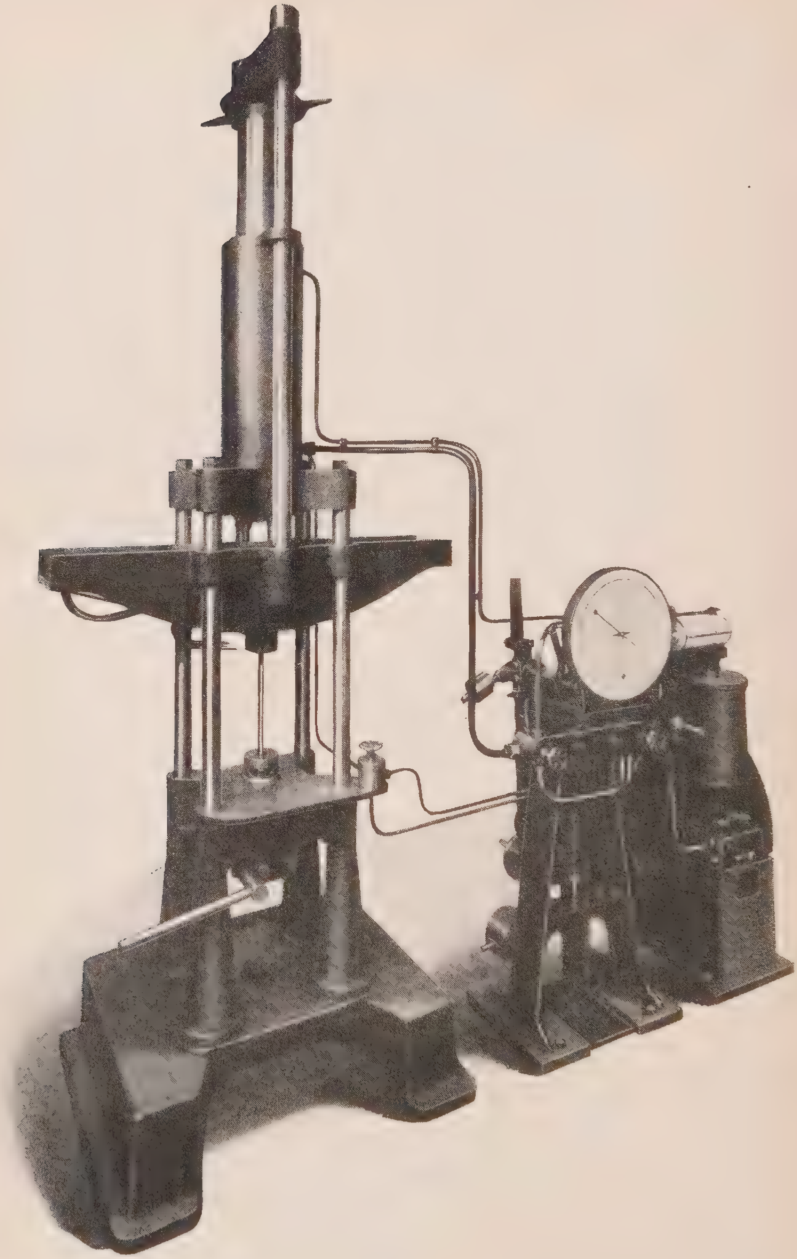

FIG. 267.—Hydraulic tensile testing machine. 100,000 lb. capacity.

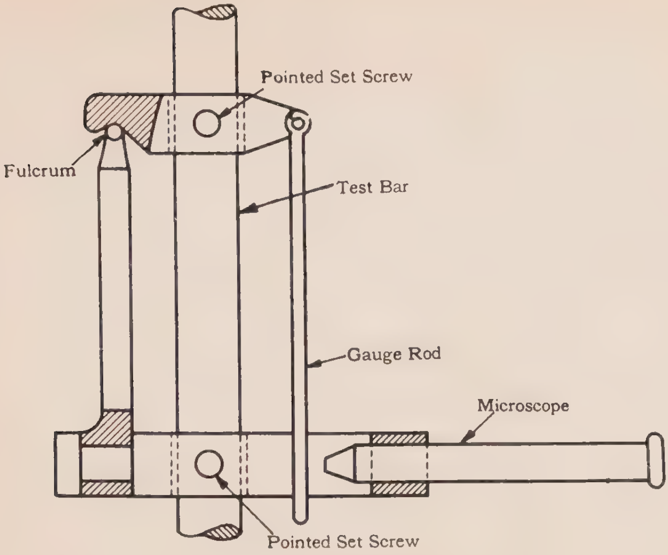

FIG. 268.—Ewing extensometer.

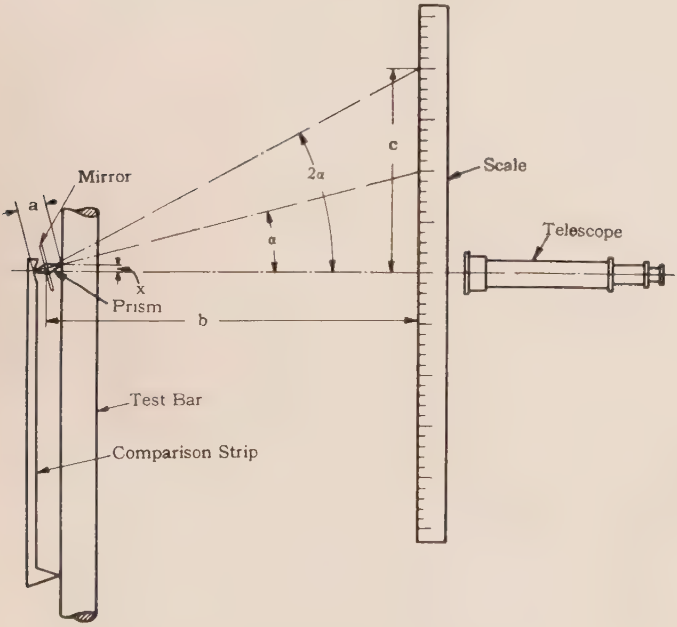

FIG. 269.—Marten's extensometer.

Robert Hooke in 1676 was the first to publish this statement. It may be noted that this law with few exceptions is in general true within certain limits, for structural materials.

Referring to Fig. 270 Hooke's law will be true up to the point A, which point is called the *limit of proportionality* of the material. For a low carbon steel the extension of a 2 inch length corresponding to the stress at A will be of the order of .002 inch. It will be seen, therefore, that sensitive apparatus for measuring these deformations is necessary.

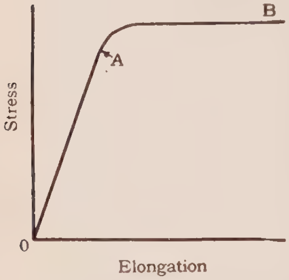

FIG. 270.—Elastic stage of tensile test.

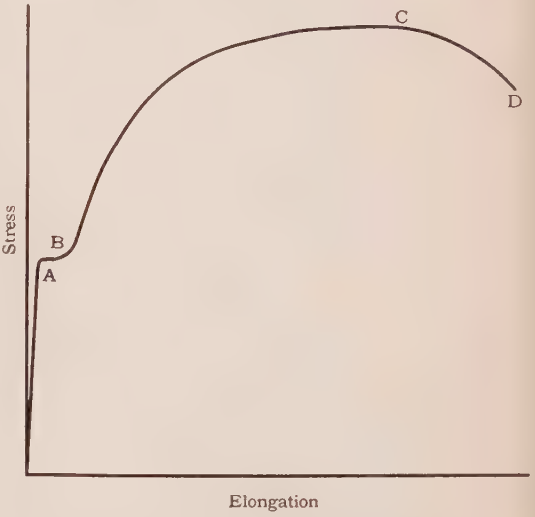

FIG. 271.—Complete tensile test diagram.

If for this steel the stress be continued beyond the point A, the extension will take place more rapidly; and at a value of stress corresponding to B there will be a considerable extension without further increase of stress. This point is called the *yield point* of the material. If the loading be still continued, the stress will again commence to increase, but the extensions will now be more rapid than during the stage from O to A. At the point C in Fig. 271, the maximum force will occur and the bar will then commence to contract locally to the point D where fracture will occur. The stage from O to A is called the *elastic stage* and that from A to C and C to D the *plastic stage*. From A to C the deformation is uniformly distributed over the length of the piece being tested, but beyond C concentration of deformation occurs.

Every material has a characteristic tensile test diagram, the shape of which will depend on the chemical analysis of the material and on the treatment which this material has received. Consideration will now be made of the definitions of terms associated with the work so far discussed.

83. Definitions: Elastic and Transition Stages. (a) *Elastic Limit.*—The *elastic limit* is the maximum stress to which a material can be subjected without this material, on removal of such stress, showing permanent deformation however small. It will be noted that a material may still possess an elastic limit while not necessarily obeying Hooke's law.

The determination of this value will, as previously stated, depend on the accuracy of the measuring apparatus. In order that the *elastic limit* may have a practical significance, it is necessary in its measurement to agree as to the magnitude of the allowable permanent set. Bach,* as will be seen later, takes this permanent extension as equal to .0003 of gauge length. Referring to Fig. 272 the lines (which in certain cases may be curves) OA and OA_1 are obtained by successive loading and unloading for small stress increments. When the permanent set x is equal to .0003 of the gauge length, the corresponding stress is called the elastic limit of the material.

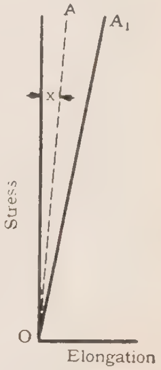

Fig. 272.—Method of determining elastic limit.

b. *Limit of Proportionality.*—The limit of proportionality is that stress at which the extension ceases to be proportional to the load (point A in Fig. 270). For certain materials such as low carbon steel the elastic limit and proportional limit coincide. This is of course not necessarily a general rule. As in the case of the elastic limit, the accuracy of determination of this value will depend on the sensitivity of the measuring apparatus. When this sensitivity is of a high order, cast iron† may be shown to possess a proportional limit, provided the stress limitation is sufficiently small. For the determination of this value the author prefers to use precision apparatus and take the stress corresponding to the point of tangency as to A in Fig. 270.

For commercial purposes, however, it is necessary to use some other method for its determination. The first one which will be discussed is the Johnson‡ method. By this, the proportional limit is taken as that stress corresponding to a point on the diagram at which the rate of deformation is 50% greater than that at the origin. Referring to Fig. 273 the curve *OAB* represents the diagram of the initial stage of a tensile test. *OE* is the line through the origin. The line *OD* is drawn with a slope 50% greater than *OE*, i.e., $DF = 1.5\ FE$. A tangent parallel to *OD* is then drawn to the curve. This locates the point *C*. The stress at this point is the proportional limit, according to this method. The proportional limit thus found has the advantage that it is always governed by the slope at the origin. On the other hand, it is an arbitrary value and has no real physical meaning.

---

* Bach, "Elastizität und Festigkeit," p. 27, 1920.

† Grueneisen, *Berichte der Deutschen Phys. Gesellschaft*, 1906.

‡ Johnston, "Materials of Construction," 5 Edit., p. 10.

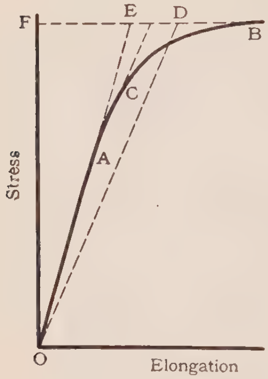

Fig. 273.—Method of determining proportional limit.

A second method of determination is that used by certain German laboratories.* By this method, the limit of proportionality is defined as that stress corresponding to a permanent extension of 0.0003 of the gauge length, determined as shown in Fig. 274. This method again gives an arbitrary value, but since the yield point, as will be seen later, is determined in a similar manner, it has the good feature of correlating these two values.

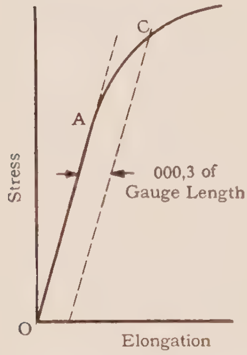

Fig. 274.—Method of determining proportional limit.

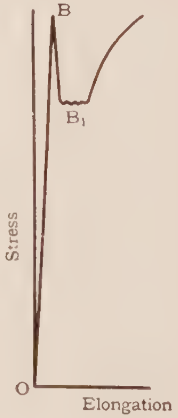

Fig. 275.—Upper and lower yield points.

---

* Bach, "Elastizität und Festigkeit," 1920.

A third method is that used by Moore* in which the Johnston method is modified so that the slope of the line OD (Fig. 273) is only 25% greater than OE. This value is again arbitrary.

c. *Yield Point.*—The yield point is that stress at which an appreciable extension occurs without further increase in stress.

If low carbon steel is being tested and an autographic record is being taken, it will be found that as the point B (Fig. 275) is reached a very striking phenomenon makes itself felt. The load will decrease from B to B_1 and then the material will extend considerably without further increase in load. If a lever type machine is being employed, the beam will drop at point B; if the machine is hydraulic the pointer registering the load will remain stationary. Meanwhile, the test piece is seen to undergo a visible change. If scale previously adhered to the material, it will now be observed to flake off, frequently in lines inclined about 45° to the direction of stress. Furthermore, if the material is polished, it will be observed that lines appear on the material, running also about 45° to the axis of stress and of such magnitude that they can be felt. These lines are called Lueders' lines; their occurrence may be employed for determining, in the absence of a stress measuring apparatus, this yield point of the material. These have a practical application† and are discussed later.

Referring again to Fig. 275, the reduction of stress at B may be considerable: for instance, this was found by Bach to be 13.8% Dalby‡ found this to be 13%, and Cook§ obtained as much as 27% reduction. Bach called B the *upper yield point* where the sliding begins, and B_1 the *lower yield point* where extension occurred without increase in stress.

It will be appreciated, therefore, that the yield point for such a material is a definite physical phenomenon, showing in a visible manner the end of the elastic stage and the commencement of the stage where large permanent or plastic extensions occur. Its determination in such a case is simple. On the other hand there are many materials which do not have any such well defined yield point, and it will now be shown that for such materials it is advisable to consider an imaginary one.

---

* Moore and Kommers, Investigation of Fatigue of Metals, *University of Illinois Bull.*, No. 124, p. 50.

† Timoshenko & Dietz, Proc. of Amer. Soc. Mech. Eng., 1925.

‡ Dalby, *Roy. Soc. Proc.*, Vol. 86, p. 414.

§ Robertson & Cook, Transition from Plastic to Elastic Stage in Mild Steel. *Roy. Soc. Proc.*, Vol. 88, 1913.

Referring to Figs. 276 and 277 which represent the initial stage of the tensile test diagram for copper in the annealed and in the cold worked conditions respectively, it will be seen that no well defined yield point exists. If, however, the loads or the stresses corresponding to a given extension (in these diagrams this is taken as .004 inch on a 2 inch gage length) be considered, then these diagrams convey much information to the designing engineer, and show that the annealed material is inferior.

It is this conception which has given rise to the adoption by German* laboratories of the yield point as that stress corresponding to a permanent extension of .002 to .005 of the gauge length. For low carbon steel this value will coincide with the yield point observed.

Another method very similar to the previous one is used in certain English laboratories whereby the yield point, called the *proof stress*, is determined as that stress corresponding to an extension on unloading of .005 of the gauge length. They are both arbitrary, but from what has been said they are valuable to the engineer. Furthermore, the discussion by Charpy* on this same subject makes it appear that there is a general agreement in such adaptation. Accordingly, it is from this angle that discussion will subsequently be made of certain phases of this work.

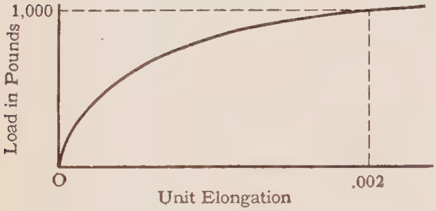

FIG. 276.—Stress-strain diagram for annealed copper.

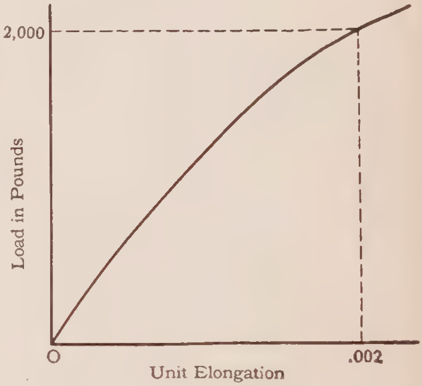

FIG. 277.—Stress-strain diagram for cold worked copper.

d. *Elasticity.*—As has been seen, a material is said to be elastic if the strain imposed by an applied stress entirely disappears on removal of such stress. Most materials can be considered, within certain limits, as perfectly elastic.

The factor characterizing extensibility or compressibility is measured, for materials which possess a proportional limit, by the

* G. Charpy, "Reception des Metaux," p. 80, 1917.

slope of the line OA in Fig. 270, where the ordinates represent stress and abscissae unit elongation. This factor is called the *modulus of elasticity*.

If p = stress in lb. per sq. inch,
x = extension in inches,
l = length over which extension is measured,
$e = \frac{x}{l}$ = strain,

then, $$\frac{p}{e} = E, \tag{356}$$

and since e is a number, it will be apparent that the slope as a measure of the elasticity has the same dimensions as stress.

84. Definitions—Plastic and Breaking Stage.—*General.*—So far only the terms associated with the elastic and transition stage have been considered. It will now be necessary to discuss the chief characteristics of the subsequent stage where permanent deformations leading up to actual fracture of the material occur.

As stated previously, a material such as low carbon steel will, when the stress is in excess of the yield point, continue to extend with increasing stress until a state is reached at which the extension becomes unstable: necking begins and further extension continues with decrease in load. This continues until fracture occurs. The final form which the test piece assumes is made use of to give a measure of the ductility of the material.

This property, which all structural materials possess in more or less degree, is of great significance to the designer. As has been shown (p. 70 on Stress Concentration), certain types of construction such as that having fillets, holes, etc. may be subjected to very high local stresses. Material which has the property of ductility can yield in these overstressed points and in such manner can so redistribute the stresses as to permit of a more favorable condition being obtained.

Any physical value which gives a measure of such a property must therefore be of importance. This leads to a consideration of the ultimate stress, elongation, and reduction of area values.

a. *Ultimate Strength.*—The *ultimate strength* is that stress, calculated on the maximum value of the force and on the original area of the cross section, which causes fracture of the material. It should be noted that, due to the contraction of area which occurs in all ductile materials before fracture, this calculated stress is considerably lower than the actual maximum stress value. Taken alone, it has very little significance for the designer, but in conjunction with the elastic properties it has quite an important place in our conception of physical values. For instance, to say that the ultimate stress of 0.37 carbon steel in the normalized state is 74,000 lbs. per sq. inch means very little, but, due to the mine of experimental data which has been accumulated round such a test value, it is known that an ultimate stress of 74,000 lbs. per sq. inch for such a steel implies also a limit of proportionality of approximately 35,000 lbs. per sq. inch.

In other words, the ultimate stress is valuable chiefly in so far as it helps toward an estimation of some other more important characteristic.

Elongation.—The *elongation* is the ratio of increase in length of test bar when fractured to the original length. It is usually expressed as a percentage and is one of the two factors employed to give a measure of ductility.

It has been found,[*] however, that this value depends on the geometrical form of specimen, and therefore for strictly comparable results adherence must be made to this similarity law. It was Barba who first discussed the importance of form, his statement being that geometrically similar test bars deform similarly. In applying this law to the case of cylindrical test pieces, if

l = gauge length in inches,
d = diameter of test bar in inches, then

$$\frac{l}{d} = C, \text{ a constant.}$$

The value of C adopted on the European continent in general is 10.

$$\frac{l}{d} = 10, \text{ or}$$

$$l = 11.3\sqrt{a}$$

where a = area of cross section in sq. cm.
l = gauge length in cms.

In England the values given in Table XXXI have been adopted having been recommended by the British Engineering Standard Association[†] (B.E.S.A.).

---

[*] Barba, *Mem. Soc. des Ing. Civ.*, 1880.
Batson & Hyde, "Mechanical Testing," p. 98, 1922.

[†] See *Report No.* 18, *of B.E.S.A.*

TABLE XXXI

d inches	a inches^2	l inches
0.564	0.25	2
0.798	0.500	3
0.977	0.750	3½

These values correspond approximately to the law

$$l = 4\sqrt{a} \tag{358}$$

In this country the standard recommended by the American Society for Testing Materials (A.S.T.M.) is $d = 0.5$ in. and $l = 2$ in. which gives

$$l = 4.5\sqrt{a}. \tag{359}$$

So that for cylindrical test pieces, while different dimensions have been chosen for d and l, there is more or less agreement with the law.

Where rectangular test pieces are employed, such as for plate material, the case is not so simple because this gives rise to the practical difficulty of adopting a varying gauge length for different cross sections. Considerable divergence from the fundamental law is sometimes found for such cases. The British Engineer's Standards Assn. prescribe the sizes given in Table XXXII for plate material.

TABLE XXXII

Thickness of plate, inches	Width of test bar, inches	Gauge length, inches	Relation between l and a
Under ⅜	2½	8	$l = 8.25\sqrt{a}$
⅜ to ⅞	2	8	$l = 9.24\sqrt{a}$ to $6\sqrt{a}$
Over ⅞	1½	8	$l = 7.0\sqrt{a}$

It will be appreciated that these values are far removed from the similarity law however much their adoption may have been influenced by the practical aspect. This fact appears to be important; because in investigation work these secondary causes should not necessitate divergence from the fundamental law in the choice of dimensions.

Another point worthy of consideration is that of the position where the test bar fractures; since this also may considerably influence the results obtained. If the fracture occurs anywhere within the middle third of the gauge length the error is of such a small magnitude that no correction appears to be necessary. When, however, this occurs outside this region such a correction must be made if the results are to be strictly comparable. According to the notation adopted if l is divided off into n parts of equal length before testing, and if

dl = total extension required,
x = extension on the division containing the fracture;

then, if the fracture occurs outside the middle third and the number of divisions n is even, the extension is given by dl, the measurement being always made on the longer part of the test piece.

$dl = x +$ extension on $(n/2 - 1)$ divisions + extension on $n/2$ divisions. If n is odd, this will become $dl = x +$ extension on $\frac{1}{2}(n - 1)$ divisions + extension on $\frac{1}{2}(n - 1)$, where the measurement is again made on the longer part of the test piece. This correction will be found to give consistent values of elongation for such special cases.

Considerable discussion has been made of this elongation factor, and it is felt that, due to such divergencies in result, certain discrepancies may have arisen. This fact has engendered a feeling of doubt as to the significance of the value obtained. When it is borne in mind that a low elongation value in the presence of other confirmatory evidence obtained from the same location may determine (as indicative of segregation) the acceptance or the rejection of large forgings weighing many thousands of pounds, it will be appreciated that there must be no doubt in the mind of the engineer as to what this value signifies. There need be no doubt whatever if due cognizance be taken of Barba's work.

Reduction of Area.—The *reduction of area* is the ratio of decrease in cross sectional area of the test bar after fracture to the original area. It is usually expressed in percentage and does not depend on the geometrical form to such a degree as the elongation value. Hence it is considered by some authorities to be a better measure of ductility than the elongation value previously discussed. There arises, however, the difficulty of measuring this value accurately, especially for the rectangular form of test piece. The author has devised a method which appears to possess some good features: the fractured ends of the test bar are photographed alongside a standard form of test piece. A photograph* of such is shown in Fig. 278.

---

* This was used by Pilling in his work in the Westinghouse Research Laboratory on the ductility of copper.

By the use of a planimeter the respective areas can be computed from the photograph. Provided the fracture is approximately at 90° to the direction of stress so that good focus can be obtained for the photograph this method appears to possess certain advantages over that in which direct measurement is made from the test piece.

FIG. 278.—Photograph showing reduction of area in copper.

Sometimes the reduction in width may also be used to measure the property of ductility on cold-worked material.

TABLE XXXIII.—DUCTILITY OF COPPER

	Annealed %	Cold worked %
Elongation on 2 in.	50	5
Reduction in area	60	50
Reduction in width	30	6

In Table XXXIII are given these ductility properties for copper in the annealed and cold-worked conditions, the section of test bar being 0.625″ × 0.078″.

85. Significance of the Tensile Test to Designers.—Summarizing these definitions it is seen that they can be divided into two classes: first, those dealing with the elastic properties of the material, and second, those deailing with the non-elastic or ductile properties. On the first depends entirely the possibility of structures withstanding the designed loads without permanent set occurring and on the second depends the possibility of their being able to carry, in emergency, local stresses in excess of those pertaining to elastic conditions.

COMPRESSION

86. General.—It has been seen that the tensile test gives values for metals used in construction which are of great significance to the engineer. It is now proposed to discuss the characteristics of constructional materials subjected to a compressive load. This test is a fundamental one for such materials as concrete, wood, cast iron, and stone, and is so widely used that certain standard forms of test pieces have been adopted for these tests. On the other hand, while not being a basic test for steels, certain data is often required by the engineer on such material. A general discussion is therefore necessary.

In conducting the test there is a possibility of errors arising in the results due to the form of test piece, and observance of such must be made before a true analysis can be expected. If the test piece is too short in comparison with the lateral dimensions the friction occurring at the ends will invalidate the results. (Foeppl* found that for concrete in the form of cubes when the ends were dry the strength was 50% higher than that obtained when the ends were greased.) On the other hand if the test piece is too long buckling will occur. For accurate measurement of elastic deformations a sensitive extensometer is necessary. This requires a reasonably long length of test piece, for instance,

$$l = 4 \text{ to } 6d.$$

Further discussion will be divided into two parts: ductile materials and brittle materials.

87. Compression of Ductile Materials.—When low carbon steel is subjected to a compressive load it will be found, as in tension, that the deformation, in this case a shortening, will be proportional to the applied stress. In other words, the material will, within limits, obey Hooke's law. The value of the proportional limit will approximately coincide with that obtained for tension although Morley† for low carbon steel and Moore‡ for iron show slightly higher values for compression. With further increase in stress the yield point will be reached, which again will more or less coincide with the value obtained in tension. With further continuation of loading the test bar will commence to increase rapidly in area due to the metal spreading under the action of the applied load. This spreading will increase with increase in load and for such a material as here considered failure will seldom occur. The shape of the test piece when taken from the machine will usually be as shown in Fig. 279.

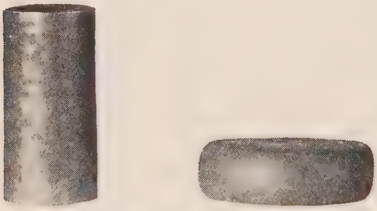

FIG. 279.—Photograph of compression failure of low carbon steel.

The modulus of elasticity can again be determined from the slope of the line for the elastic stage as described under tension.

These remarks can be applied in general to all steels possessing a fairly high degree of ductility. It will therefore be seen that the more important characteristics of ductile material, such as proportional limit, yield point and modulus of elasticity, can be determined in compression. A typical diagram obtained by the author is shown in Fig. 280.

---

* Foeppl, *Mitt. a. d. Mech. Tech. Lab. Munchen,* Vol. 27.

† Morley, "Theory of Structures," pp. 34 and 37, 1912.

‡ Moore & Kommers, Fatigue of Metals, *University of Illinois Bull. No.* 124, pp. 55 and 57.

If the material tested is very soft (such as copper or aluminum), the test bar will commence to increase in area very rapidly and will ultimately assume the shape of a flat disc as shown in Fig. 279. For these tests on ductile material the cylindrical form of test bar is usually chosen. The ratio of length to diameter must be at least four if a mirror extensometer has to be employed; otherwise this ratio is usually 2. In the case of material such as babbitt metal, Freeman* has found that the deformation is independent of this ratio provided this is not greater than 3. Using special equipment the deformation was determined on varying gauge lengths, the minimum being ½ inch.

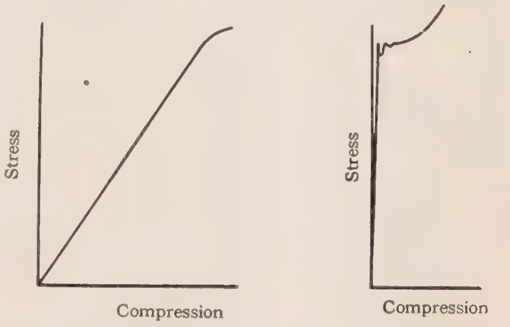

Elastic stage of compression test.

Complete compression test diagram.

FIG. 280.

These results seem to indicate that a ratio of 1:2 is quite satisfactory for all ductile materials, and where extra length is necessary that a ratio of 1:4 is good for loads up to and slightly beyond the elastic stage.

88. Compression of Brittle Materials.—If a test piece of cast iron be subjected to a compressive load so that a sensitive extensometer may be used for measuring the deformations, precautions being taken that an axial load is obtained, it will be found that for any but very small stresses the stress is no longer proportional to the strain, i.e., Hooke's law is not obeyed. The relation between stress and strain is in such cases no longer a simple one. An exponential relation† has been suggested as follows:

$$eE = p^n \qquad (360)$$

---

[*] Influence of Ratio of Length to Diameter in Compression Tests of Babbitts, by Freeman & Brandt. Amer. Soc. Test. Mat. Proc., 1923.

[†] Bach, "Elastizitat und Festigkeit," p. 36, 1920.

where n = a constant greater than unity,
E = modulus of elasticity in lbs. per sq. in.,
e = strain,
p = stress in lbs. per sq. in.

This is now generally applied to the testing of such material as cast iron, stone, and concrete. It will be observed, however, that this exponential law is not satisfactory for zero stresses. For a material which does not possess a proportional limit, the modulus can be expressed as the slope of the stress-strain curve, then from equation (360)

$$p = (eE)^{\frac{1}{n}}$$

$$\frac{dp}{de} = \frac{1}{n} E^{\frac{1}{n}} e^{\left(\frac{1}{n}-1\right)} \tag{361}$$

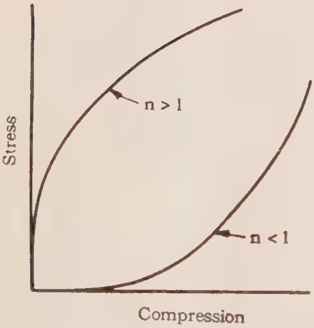

FIG. 281.—Graphical representation of exponential stress-strain relation.

An examination of this relation will show that for $n > 1$, as the stress approaches zero, the slope approaches infinity, i.e., the stress-strain curve coincides with the axis of stress. For $n < 1$, as the stress approaches zero, the curve will coincide with the axis of strain. These will give the forms of stress-strain curves shown in Fig. 281.

The work of Grüneisen (see p. 356) showed, however, that for small stresses cast-iron does obey Hooke's law. A modification of this law has been suggested which is known as the *parabolic relation.*

$$e = \frac{1}{E}(p + b_1p^2 + b_2p^3 + \ . \ . \ . \ ) \tag{362}$$

It will be seen that if p is small the equation (362) can be written $e = p/E$, which signifies obedience to Hooke's law.

Therefore, the relation given in equation (362) seems to satisfy entirely the stressed condition of cast iron because, when the stresses are small, it becomes Hooke's law and gives for higher stress values a straight line merging into the characteristic curve for such a material.

In Fig. 282 is shown a curve for cast iron according to Bach. If the load be continually increased, fracture will ultimately occur, and for such a material as is being considered the plane of this failure will be inclined at an angle to the axis of stress, due to the shearing action on this inclined face. A typical fracture is shown in Fig. 283.

The manner in which brittle materials fracture under compression is similar in that the effect of shearing action is more or less always in evidence. Cement usually fails by double shearing as shown in Fig. 284, while wood fails by the fibres becoming kinked in form as shown in Fig. 285. The dimensions of the test piece will, however, largely determine how this fracture will occur.

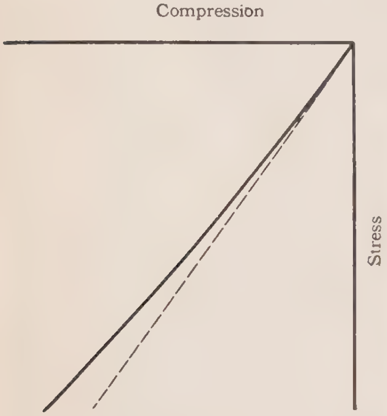

FIG. 282.—Compression test curve for cast iron.

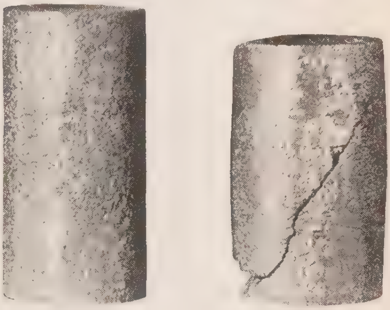

FIG. 283.—Photograph of compression failure of cast iron.

In compression tests on cast iron the cylindrical form of test piece is usually employed. This is taken such that the length is equal to two diameters. For such materials as stone and concrete the cube form has been adopted. It has been shown* that if rectangular test pieces are chosen, the effect of frictional forces can be considered as eliminated if the length is three times the minimum lateral dimension, and that if it is expedient to increase the length further the ultimate strength should retain the same ratio to the cubical strength provided buckling does not intervene. These results may have important applications where a divergence from standard form is necessary.

In general it will be appreciated from the preceding discussion that the most important value obtained for brittle materials is the ultimate stress to fracture. In reinforced concrete work, however, it may be necessary to take into consideration the deformation of such materials under small stresses. It seems opportune therefore to finish the discussion by emphasizing that for such materials the ratio of stress to strain will be greater for small stresses than for larger ones,

---

* Bauschinger, *Mitt. a. d. Mech. Tech. Hochsch. Munchen*, Vol. 6, 1876.

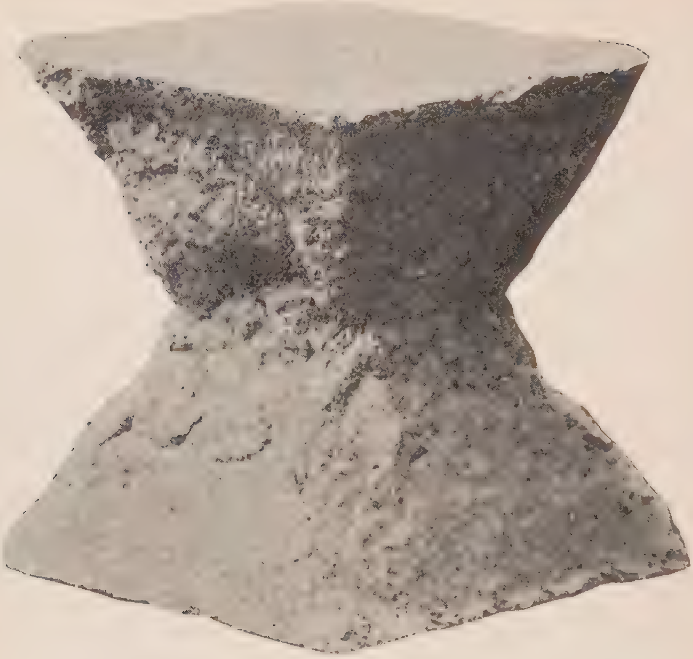

Fig. 284.—Photograph of compression failure of concrete. Reproduced from Elastizität and Festigkeil. Bach—1920.

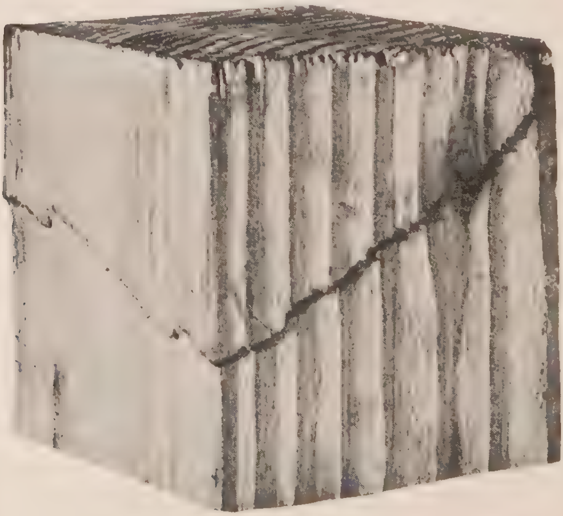

Fig. 285.—Photograph of compression failure of wood.

and that if the modulus of elasticity* is used in design calculations, it seems imperative to define the stress at which this modulus value was obtained.

CHEMICAL ANALYSIS

89. General.—The influence which various elements, either in the form of added alloys or impurities, have on the tensile properties of metals belongs more or less to the domain of metallurgy. It seems, however, that the general effects of the chief elements must be briefly considered because it is important for the engineer to know how the properties of the materials he uses can be improved.

For this purpose the discussion will be divided into three parts: carbon steels, alloy steels and nonferrous metals.† Reference will be made again, however, in later chapters to this part of the work.

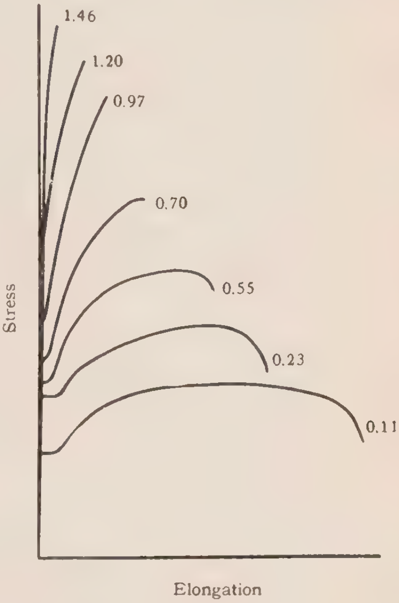

FIG. 286.—Diagram showing effect of carbon content on tensile properties.

90. Carbon Steel.—*Annealed or Normalized.*—As the percentage of carbon in steel is increased the proportional limit and ultimate strength increase while the elongation and reduction of area values decrease. Certain empirical methods‡ have been devised for showing this change, but a better understanding can be obtained from a consideration of actual test diagrams.

In Fig. 286 are shown such diagrams for steels with carbon content varying from 0.11 to 1.46, according to Goodman.|| It will be seen that these confirm the general statement that increase in carbon

---

* According to the definition of modulus of elasticity it will be appreciated that this can be applied in a general way for all materials obeying or disobeying Hooke's law. In this latter case it will become the slope at any point on the stress strain curve and therefore will be a variable quantity.

† NOTE.—Unless otherwise stated a diameter of 0.505 inch and gauge length of 2 inches was adopted for all tensile tests made by the author.

‡ Guillet et Portevin, "Metallographie," p. 172, 1918.

§ Goodman, "Mechanics Applied to Engineering," p. 300, 1908.

|| Aitchison, "Engineering Steels," p. 140, 1921.

content increases the elastic properties as indicated by the proportional limit and yield point values, but decreases the ductility as shown by the gradual reduction in the elongation and also in the necking effects, the latter being entirely suppressed for the higher carbon steels. An increase in the elastic properties is only accompanied by a decrease in the ductility. In Table XXXIV where the tensile test values* for steels varying in carbon content from 0.06 to 0.89 in the normalized condition are given, further confirmation of this generalization is evident.

Means other than an increase in carbon content alone have therefore to be adopted if higher elastic and ductility values are necessary. This is usually done by thermal treatment.* The steel as it leaves the rolls, or the mould if a cast material, is more or less in a coarse granular condition. Any thermal treatment which this material undergoes will, if properly conducted, break up this coarse structure and give higher tensile values. The treatments generally adopted for this purpose are those of annealing and normalizing. *Annealing* consists in heating the steel above its critical range, holding it there for a length of time, depending on the mass of material, and allowing it to cool in the furnace. *Normalizing* consists in heating the steel above upper critical temperature and allowing the material to cool rapidly in the air. In Table XXXV are given values obtained by the author on a 0.37 carbon steel for three different states. In this case the annealing was carried out by heating the material in bar form (2¼ inch dia.) to 850°C. and cooling in the furnace; the normalizing was done by a similar heating, but a cooling in air.

TABLE XXXIV.—THE EFFECT OF CARBON CONTENT UPON TENSILE PROPERTIES OF CARBON STEELS

Carbon %	Yield point pounds per square inch	Ultimate strength pounds per square inch	Elongation % on 2 inches	Reduction of area %
0.06	29,000	47,000	46	75
0.21	38,000	56,000	42	68
0.38	45,000	67,000	35	56
0.60	53,700	94,000	20	40
0.89	56,000	117,000	13	15

The advantages gained by the treatment in this case, while considerable, are not so great as these would be had the material been worked at a lower temperature in the last stages of rolling. This

---

* For a complete discussion of thermal treatment, reference should be made to such work as "Physical Metallurgy," Rosenhain, 2nd Edition, Chap. XII, 1919.

Table XXXV.—Tensile Properties of 0.37 Carbon Steel (Rolled)

State	Proportional limit, pounds per square inch	Yield point, pounds per square inch	Ultimate strength, pounds per square inch	Elongation, %	Reduction of area, %
Rolled............	27,000	31,000	74,000	32	48.6
Annealed..........	36,500	37,800	70,000	32	49.
Normalized........	38,000	41,500	79,200	29	46.

would have given a cold worked material possessing, as will be seen later, a low proportional limit and would have shown a greater improvement in tensile properties by the subsequent treatment.

In Table XXXVI are given results obtained from such a material, in this case a 0.32 carbon steel plate in the rolled and normalized conditions. The normalizing consisted in heating the material in plate form to 875°C. and in cooling in air. The advantages in this case of the normalizing operation are very striking.

Table XXXVI.—Tensile Properties of 0.32 Carbon Steel (Rolled)

State	Proportional limit, pounds per square inch	Yield point, pounds per square inch	Ultimate strength, pounds per square inch	Elongation, %	Reduction of area, %
Rolled............	None	37,300	73,000	35	46
Normalized........	25,500	30,000	73,600	30	49

In Table XXXVII are given the same values obtained by the author from steel castings. The annealing was carried out by heating the material in coupon form to 925°C. and in cooling in the furnace; the normalizing was done by heating to 925°C. and cooling in air.

Table XXXVII.—Tensile Properties of 0.33 Carbon Steel (Cast)

State	Proportional limit, pounds per square inch	Yield point, pounds per square inch	Ultimate strength, pounds per square inch	Elongation, %	Redution of area, %
Cast..............	20,000	33,500	76,200	26	34
Annealed..........	37,000	41,200	80,000	27	39.5
Normalized........	40,500	46,000	85,000	27.6	45.6

In Figs. 287, 288, and 289 are shown the photo-micrographs (100 diameters) of this latter steel in these conditions. It will be appreciated

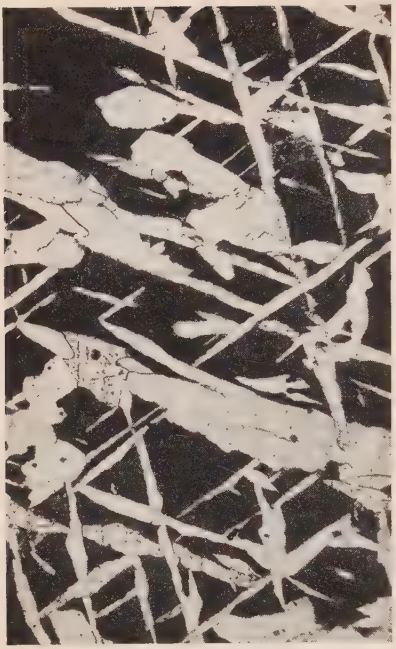

FIG. 287.—Photo micrograph of .33 steel as cast.

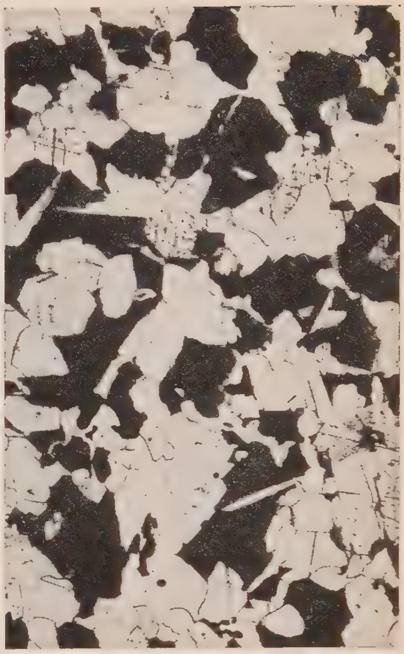

FIG. 288.—Photo micrograph of .33 steel as annealed.

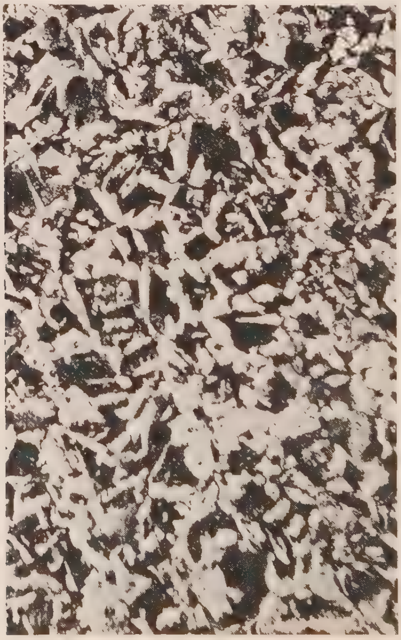

FIG. 289.—Photo micrograph of .33 steel as normalized.

from an examination of such that the improvement in elastic properties, characterised by the position of the proportional limit, obtained without sacrifice in ductility, has been due to a removal of the previously coarse condition by the thermal treatment.

Heat-treated.—Further refinement of structure of carbon steel, with corresponding increase in elastic properties can only be obtained by *heat-treatment.* This consists in two operations: (1) heating the steel up to a temperature depending on the carbon content, holding at this temperature and then quenching in oil or water, and (2) tempering. In the quenched state the material has very little ductility and the proportional limit may be very low with, in certain cases, an entire suppression of the yield point. In this state the material is of very little value for constructional purposes. To impart ductility the material is then tempered by heating to a temperature depending on the degree of ductility required and either cooled in air or again quenched in oil or water. This steel will now be found to possess high elastic properties and, provided the tempering temperature has been high enough, high ductility values also. In Table XXXVIII are given results obtained by the author on a 0.37 carbon steel, and in Table XXXIX are shown those obtained on a 0.45* carbon steel.

TABLE XXXVIII.—TENSILE PROPERTIES OF 0.37 CARBON STEEL HARDENED IN WATER 850°C. (2¼ DIA. BAR) AND TEMPERED

Tempering temperature	Proportional limit, pounds per square inch	Yield point, pounds per square inch	Ultimate strength, pounds per square inch	Elongation, %	Reduction of area, %
100°C.	68,000	80,000	116,000	16.6	41
450°C.	65,000	74,000	114,000	18	49
550°C.	65,000	69,000	105,000	22	56

TABLE XXXIX.—TENSILE PROPERTIES OF 0.45 CARBON STEEL HARDENED IN WATER 870°C. (1⅛ DIA. BAR) AND TEMPERED

Tempering temperature	Yield point pounds per square inch	Ultimate strength pounds per square inch	Elongation %	Reduction of area %
	100,000	146,000	11	28
300°C.	98,500	146,000	11	23
400°C.	103,000	134,000	15	46
500°C.	87,000	123,000	22	56
600°C.	74,000	110,000	26	64
700°C.	67,000	94,000	27	66

---

* Aitchison, "Engineering Steels," p. 147, 1921.

It will be seen by comparing the results given in Tables XXXV and XXXVIII that this heat-treatment, by imparting a further refinement of structure, does considerably improve the elastic and ductility properties over those obtained when the same steel is annealed or normalized. It will be noted, on the other hand, that as the tempering temperature is reduced the ductility decreases so that there is a limit at which such treatment ceases to be beneficial. Furthermore, for carbon steels of lower carbon content than 0.25 these beneficial effects are not so pronounced. Finally, there is the most important question of mass effect.

In an annealed or normalized material the beneficial effects of the treatment are apparent at the center of bars at least 6 inches in diameter.* It is different, however, with a heat-treated steel. With methods in use at present when a carbon steel is quenched, due to the immersing medium not being able to extract heat sufficiently rapid, the structure on the outside of large sized material will be entirely different from that at the center. Aitchison† has found that the ultimate stress at the center of a $\frac{9}{16}$ inch diameter bar of 0.85 carbon steel when quenched in water from 850°C. was 217,000 lbs. per sq. in. while from the same location in a 2 inch diameter bar the ultimate strength was only 125,000 lbs. per sq. in., the treatments being identical.‡

Since these treatments appear to be limited in their application (1) by the decrease in ductility as the temperature of tempering is reduced, and (2) by the mass of the material treated, other means have to be considered for improving the tensile test characteristics. This leads to a discussion of alloy steels.§

91. Alloy Steels.—*Annealed or Normalized.*—The advantages to be gained by alloying elements are best seen by an examination of the test data obtained. The comparison should be made, however, on the basis of steels possessing as near as possible similarity in microstructure. In Table XL are given the tensile properties of a steel of carbon 0.35 and nickel 3.4, obtained by the author. The material was normalized by being heated to 840°C. and cooled in air. The third series was given a similar treatment but was tempered at 730°C. and cooled in the furnace.

---

* See the author's paper published in the *Trans. Amer. Soc. Steel Treating*, Vol. 11, No. 9, p. 812–816, 1922.

† Aitchison, "Engineering Steels," p. 72, 1921.

‡ For further data on mass effect, see the *Report of the Steel Research Committee, Inst. of Automobile Eng., Proc.* (London), 1920.

§ This term is used in reference to such alloying elements as nickel, chromium, vanadium, etc. Strictly speaking, carbon steels may be considered as alloy steels containing carbon and manganese.

The advantage gained by the addition of nickel in the carbon steel previously discussed (see Table XXXV) can be seen in the higher proportional limit obtained while retaining a relatively high ductility as compared with the carbon steel having a similar treatment.

TABLE XL.—TENSILE PROPERTIES OF 3½% NICKEL STEEL

State	Proportional limit, pounds per square inch	Yield point, pounds per square inch	Ultimate strength, pounds per square inch	Elongation, %	Reduction of area, %
Rolled	47,000	60,000	105,000	21	42
Normalized	52,000	60,000	104,000	22	49
Normalized and drawn	52,000	56,000	95,000	25	49

If in addition to nickel, chromium be added, the advantages over carbon steels are even more apparent. Such data obtained for a steel containing carbon 0.23, nickel 3.0, chromium 0.53 are given in Table XLI, after this material had received the following treatment: heated to 850°C., cooled in the air, and tempered at 670°C.

TABLE XLI.—TENSILE PROPERTIES OF NICKEL CHROME STEEL

State	Yield point, pounds per square inch	Ultimate strength, pounds per square inch	Elongation, %	Reduction of area, %
Normalized	86,000	110,000	22	68
Normalized	90,000	112,000	23	67.5

Heat-treated.—Although alloy steels possess advantages over carbon steels in the annealed and normalized conditions, it is held by certain authorities that alloy steels are only used to advantage when in the heat-treated condition. In other words, full advantage should be taken of the alloying element. It is found that this treatment can be applied more readily to alloy steels, because, due to the metallurgical condition obtaining in such steels at high temperature, the material is much more uniform in structure after quenching than that of plain carbon steels. In Table XLII are given the comparative tensile results on a .31 carbon steel hardened from 850°C. in water and the highest form of constructional alloy steels (of carbon 0.30, nickel 4.3 and chromium 1.44, air hardened from 800°C., the tempering temperatures being as indicated). It will be apparent that the increase in the elastic properties in the case of the alloy steel far outweighs the slight decrease obtained in ductility values.

TABLE XLII.—COMPARATIVE TENSILE PROPERTIES OF PLAIN CARBON AND AIR-HARDENED NICKEL CHROME STEELS

Material	Tempering temperature	Proportional limit, pounds per square inch	Yield point, pounds per square inch	Ultimate strength, pounds per square inch	Elongation, %	Reduction, %
Carbon............	200°C.	....	79,000	110,000	19	44
Nickel chrome......	200°C.	81,000	174,000	226,000	13	42
Carbon............	400°C.	....	80,000	113,000	17	44
Nickel chrome......	400°C.	120,000	180,000	220,000	10	36
Carbon............	600°C.	....	59,000	96,000	26	60
Nickel chrome......	600°C.	92,000	141,000	157,000	18	55

TABLE XLIII

Material	Treatment	Proportional limit, pounds per square inch	Yield point, pounds per square inch	Ultimate strength, pounds per square inch	Elongation, %	Reduction of area, %
1.0 carbon.......	Quenched in oil at 825°C.; drawn at 400°C.	102,000	118,000	187,000	8	18.5
0.5 carbon....... 2.0 silicon....... 0.69 manganese...	Quenched in oil at 850°C.; drawn at 425°C.	128,000	170,000	201,000	6	20
0.43 carbon....... 1.0 chrome...... 0.41 molybdenum.	Quenched in oil at 860°C.; drawn at 450°C.	170,000	186,000	196,000	14	52

In Table XLIII are given the tensile data for carbon, silico-manganese, and chrome-molybdenum steels obtained by the author.

While it is seen from these considerations that improved tensile test properties are obtained by the use of alloying elements, this does not imply that such should always be used in preference to carbon steels. The fact that alloy steels are more sensitive to heat-treatment may also make the question of surface defects and sharp corners a more vital one in heat-treated alloy steels. In other words, the penalty for mal-practice in the use of alloy steels may be of quite a higher order than that for carbon steels. It is unquestionable at any rate that the possibility and causes of flaws in steels have received much more attention since the advent of the alloy material. It appears that it is only in cases where high stresses are encountered that their use can be justified. While their application in such cases is logical, no plea can be advanced to defend those cases where alloy steels are used entirely to the exclusion of carbon steels. Furthermore it must be appreciated that discussion has only so far been made of tensile tests. An advantage in such a test may be real; it may also be imaginary. The truth of such will only be appreciated when examination has been made of the dynamic forms of testing.

92. Light Alloys.—It is felt that this subject should not be closed without saying a word or two regarding the application of light alloys in engineering design. The development of the aircraft engine has made it necessary to demand materials which will give maximum strength with the minimum of weight. Recent research development now appears to have satisfied this demand because aluminum alloys can now be produced which have a strength equal to that of low carbon steel.

In Table XLIV are given the results obtained from the Alloys Research Committee's report,* in which is shown specific tenacity for different materials. This quanity, being defined as the tensile strength in tons per sq. in. (1 ton = 2,240 lbs.) divided by the weight of one cubic inch of the material, is a very important design characteristic where the maximun strength per lb. weight is important, as in aircraft construction. The values for copper and bronze have been added by the writer for comparison.

TABLE XLIV.—RELATIVE STRENGTHS OF LIGHT ALLOYS AS COMPARED WITH HEAVY ALLOYS

Material	Condition	Specific tenacity
Low carbon steel	Annealed	105
Bronze	Rolled	80
Copper	Rolled	50
Aluminum alloy (Y)	Rolled and heat treated	268

It will be seen from this table that these light alloys are much superior to low carbon steel on this basis of strength per cubic inch. Their extended application is therefore to be expected.

---

* For complete information on this subject reference should be made to *Eleventh Report Alloys Research Committee, Inst. Mech. Eng. Proc.*, 1921.

EFFECT OF SPEED

93. General.—The speed at which loading is applied in the testing of constructional materials in tension and compression appears to affect one class of materials more than another, being greater for ductile materials. This will appear to be logical when the more detail consideration, given to this subject in the next chapter, has been considered.

94. Brittle Material.—The speed effect on brittle material such as cast iron has been found by Bauschinger* to be negligible. Since the extensions of brittle materials† are small they are usually never measured and the time effect for such is of no practical importance.

95. Ductile Material.—For such material as steel, copper, phosphor bronze, and brass, Bauschinger* found a difference due to the effect of time but this was believed to be masked by the differences in the material. This appears to be supported by the results obtained by Bach‡ shown in Tables XLV and XLVI.

TABLE XLV.—TIME EFFECT ON TENSILE PROPERTIES OF MEDIUM CARBON STEEL

Time of test	Ultimate strength, pounds per square inch	Elongation, %	Reduction of area, %	Remarks
1 sec..................	......	28.7	60.3	Diam. of T.P. 8 mms.
6 secs.................	79,000	28.6	59.1	
20 mins...............	75,600	29.3	60.9	

TABLE XLVI.—TIME EFFECT ON TENSILE PROPERTIES OF LOW CARBON STEEL

Time of test	Ultimate strength, pounds per square inch	Elongation, %	Reduction of area %	Remarks
20 secs................	56,800	35	70.4	Diam. of T.P. 20 mms.
2 min. 14 sec...........	56,400	31.4	70.1	
23 min. 53 sec..........	54,800	33.8	70.4	

Results made by the author on 0.32 carbon to determine the effect of speed on the proportional limit values are shown in Fig. 290. In the first test the speed was such that an extension of 0.01 inch on a 2-inch gauge length was obtained in 2 min. 46 secs., and in the second this extension was obtained after an elapse of 17 mins. 28 secs. It will be noted that within the limits of accuracy to be expected for such tests on a rolled material, the time effect is negligible. These results, however, only apply to tests having the durations as stated. Where the differences in time duration are very great in comparison with those given, there appears to be a marked change. Results obtained by Bottomley* and also by Ewing† show that these effects may be considerable.

---

* Bauschinger, *Mitt. a. d. Mech. Tech. Labor. Muenchen*, Vol. XX, 1891.

† Referred to in Bach, *Elastizitat und Festigkeit*, p. 172 & 173, 1920.

‡ Bach, Elastizitat und Festigkeitlehre, 1920, p. 170.

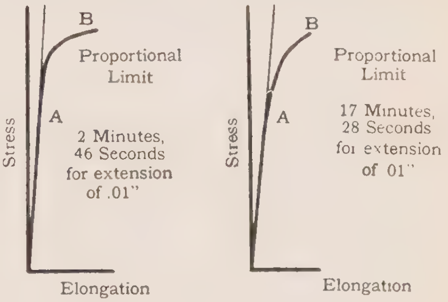

FIG. 290.—Diagrams showing time effect.

Bottomley found that an iron wire loaded at the rate of 1 lb. in 5 minutes broke at 44½ lbs. and stretched 27%, but this changed to 47 lbs. and 7% when the rate of loading was altered to 1 lb. in 24 hours. The results of Ewing for soft iron wire are given in Fig. 291. The fast rate in this case was such that rupture occurred in 4 minutes and the slow rate took a period 5,000 times as long for rupture. It will be appreciated from such results that the time effect for such material does appear to influence the values obtained when such time is of exceptional duration, either very long or very short, but this is not a contradiction of Bach's work because the times in his case were comparatively short.

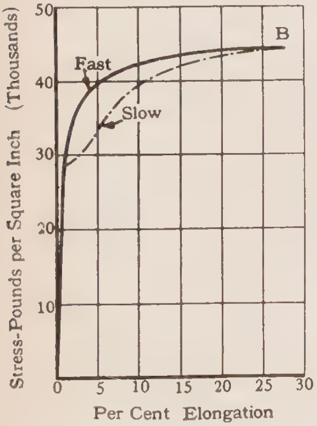

FIG. 291.—Diagrams showing time effect.

96. Very Ductile Materials.—With very ducitle materials such as lead or tin the effects of time were found by Bauschinger to be very marked, the extension increasing with the time of testing.

---

* Bottomley, *Roy. Soc. Proc.*, p. 221, 1879.

† Ewing, "Strength of Materials," p. 42, 1914.

97. Conclusions.—It can be concluded from these results that in general for speeds adopted in practice there will be no great effect on the values obtained in a tensile test due to a change in speed, subject of course to the following reservations: With very slow speeds of testing extending over many hours a reduction in elongation may in some cases be expected from that value obtained by a higher testing speed. Furthermore, the phenomena of yield requires, as has been seen, a definite period of time to complete. In tests where the proportional limit is being determined the speed of machine must be sufficiently slow to allow extensometer readings being taken, and in such cases the yield point is usually determined at the same comparatively slow speed. In many cases, however, the yield point alone is required and in such cases the testing speed may be considerably higher than the maximum possible for proportional limit determinations. In such cases due to this period of time being necessary when the material yields, it is conceivable that this value may be considerably higher than would be obtained at a slower speed, which appears to have been confirmed by Ewing's tests. Again these remarks are only true for tests at normal temperature. In tests at elevated temperatures a large variation of values may be expected with comparatively small changes in speed.

Bach* found large differences in the values obtained when testing at temperatures varying from 300°C. to 400°C. In Table XLVII are shown these variations for the usual speed and a considerably slower speed for medium carbon steel.

TABLE XLVII.—THE EFFECT OF TIME AND TEMPERATURE ON THE TENSILE PROPERTIES OF CARBON STEEL CASTINGS

Physical value	300°C.		500°C.	
	Usual speed	Much slower	Usual speed	Much slower
Ultimate strength lbs. per sq. in.	60,400	58,500	29,000	22,200
Elongation %	19.0	23.8	51.3	41.4
Reduction of area %	49.4	52.8	75.7	57.0

These results have also been confirmed by the author for medium carbon steel (0.37 C.). Three diagrams obtained from such tests are shown in Figs. 292 to 294 and are self-explanatory in showing speed effects.

---

* Bach, "Elastizitat und Festigkeit," p. 170, 1920.

It is therefore necessary to bear in mind that, while speed of testing may not be important for tests at normal temperature, at higher temperature this factor becomes fundamentally so and it appears to the author that where speed is not recorded for high temperature investigations, this omission tends towards making the results invalid.

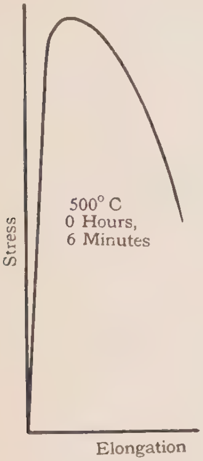

FIG. 292.—Diagram showing time effect.

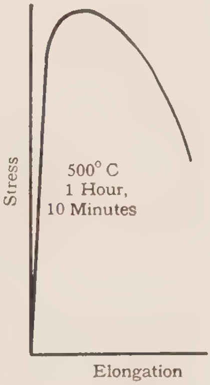

FIG. 293.—Diagram showing time effect.

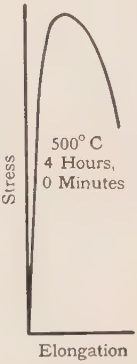

FIG. 294.—Diagram showing time effect.

EFFECTS OF HIGH TEMPERATURE

98. General.—Tests for determining the strength of materials at high temperature have been carried out since the early part of the nineteenth century,* and have by different investigators been continued until the present time.† Modern research, however, has supplied us with more information on this subject and it is now generally known that the elastic and ductile properties of metals are considerably modified by temperature effects. It will even be seen in the following chapter that in certain cases material, even when exposed for a short time to moderate temperatures, will show entirely different elastic characteristics. We are not concerned with the effects of mere exposure here, however, but rather with those values obtained when the material is tested at those elevated temperatures.

99. Steels.—*Effect on the Elastic Properties of Steel.*—The effect of high temperature on the elastic properties of steels is such that in general these are reduced. In Fig. 295 are shown the variations in yield point and modulus of elasticity for low carbon steel from temperatures of 20°C. to 600°C., which were obtained by Lea* on 0.75 in. diam. test bars. It will be noted that at a temperature in the region of 570°C. the yield point, determined in this case by the drop of the beam, and modulus of elasticity values have become approximately half of what these were at normal temperature. This general decrease in yield point is also confirmed by Bach,† curves of which tests are given in Figs. 296 to 299. In this case the yield point as obtained from the autographic record is suppressed entirely, at a temperature of 400°C.

---

* Fairbairn, *Brit. Assoc. Rep.*, p. 405, 1856.

† Martens, *Mitt a. d. Tech. Versuchsamstahlten* (Berlin), 1890.

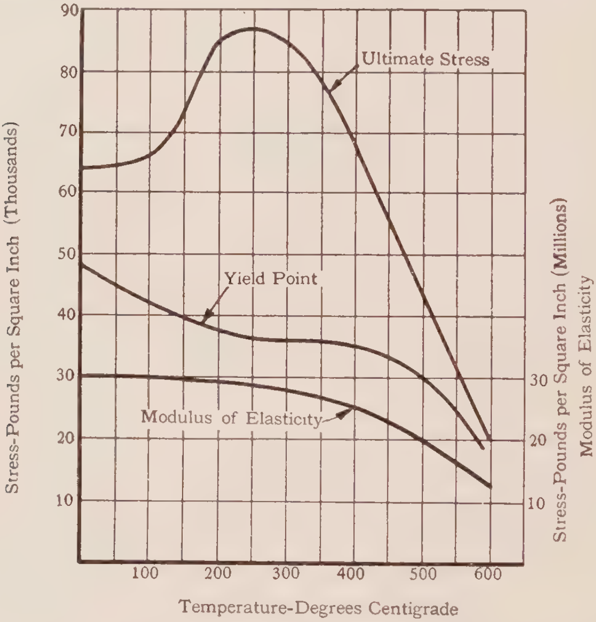

FIG. 295.—Tensile test properties of low carbon steel at high temperatures.

This suppression of yield point for a low carbon steel (.19C.) was found by Carrington‡ to occur at a lower temperature on test bars (0.5 inch dia. by 2 inch gauge length), but this discrepancy may have been due to a difference in chemical analysis or to a variation in the speed of testing, which, as we have seen, is very important in such work.

---

* Lea, *Engineering*, p. 487, October 16, 1914.

† Bach, "Elastizitat und Festigkeit," p. 174–175, 1920.

‡ Carrington, *Engineering*, p. 69, Jan. 18, 1924.

Carrington also concluded that the proportional limit values for such a material followed very closely the yield point values. These proportional limits however were in his case obtained like the yield points, from autographic diagrams and not from precision instruments. A contribution to the subject by Welter,* which is a very good and comprehensive one, discusses in detail the variation of elastic limit,

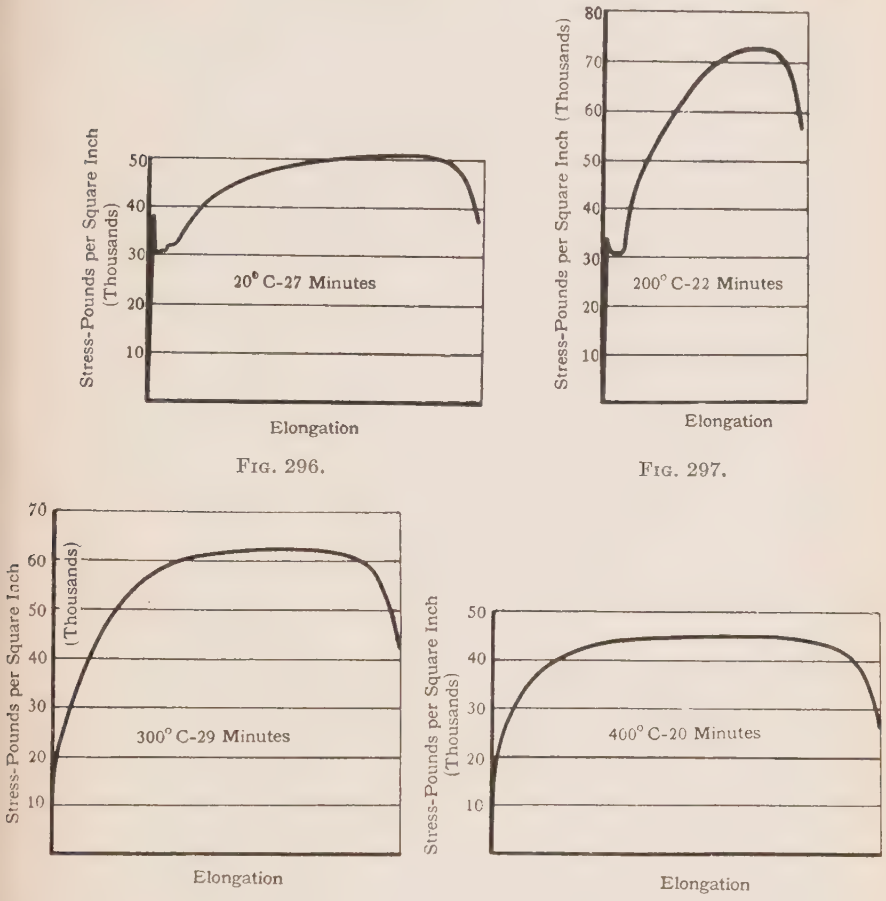

FIG. 296. FIG. 297.

FIG. 298. FIG. 299.

FIGS. 296, 297, 298 and 299.—Tensile test diagrams for low carbon steel at various temperatures.

---

* Welter, Elastizitat und Festigkeit von Spezialstahlen bei hohen Temperaturen. *Forschungsarbeiten*, Vol. 230.

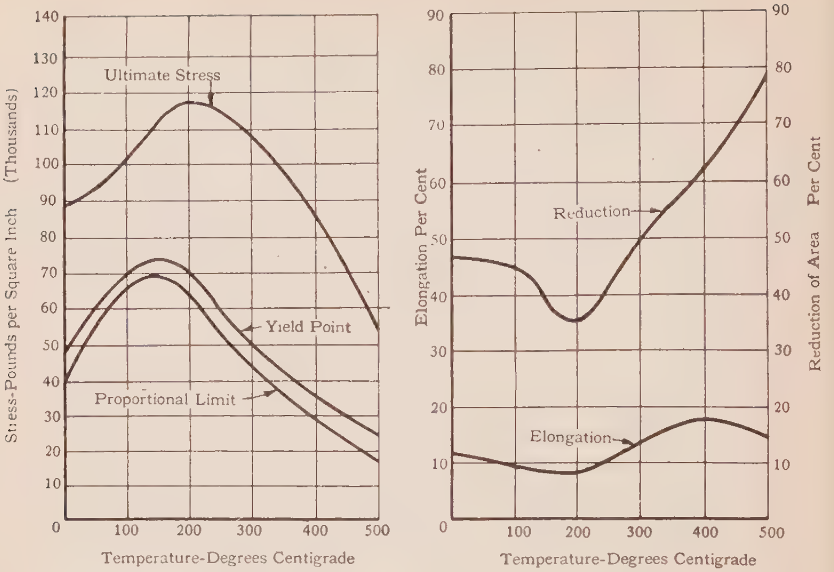

FIG. 300.—Tensile test properties of steels at high temperature C 0.37 Mn 0.76 Si 0.4.

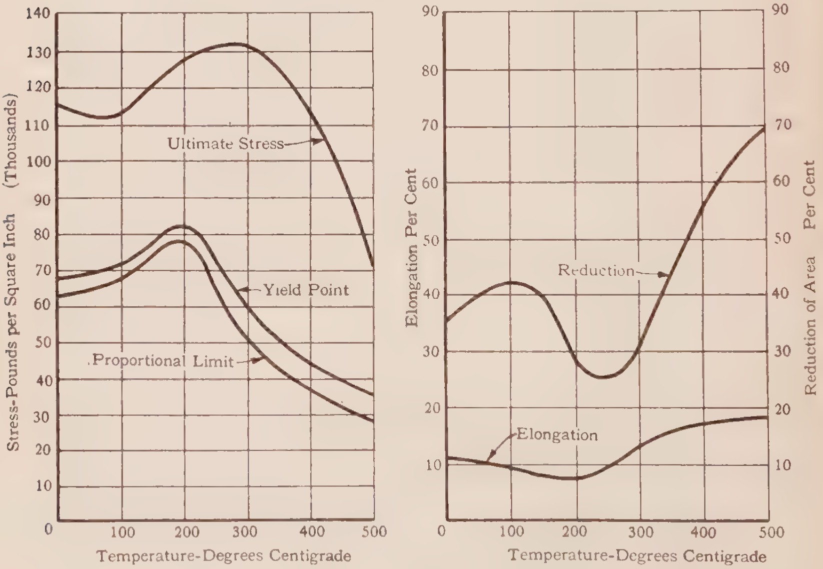

FIG. 301.—Tensile test properties of steels at high temperature C 0.49 Mn 1.05 Si 0.58.

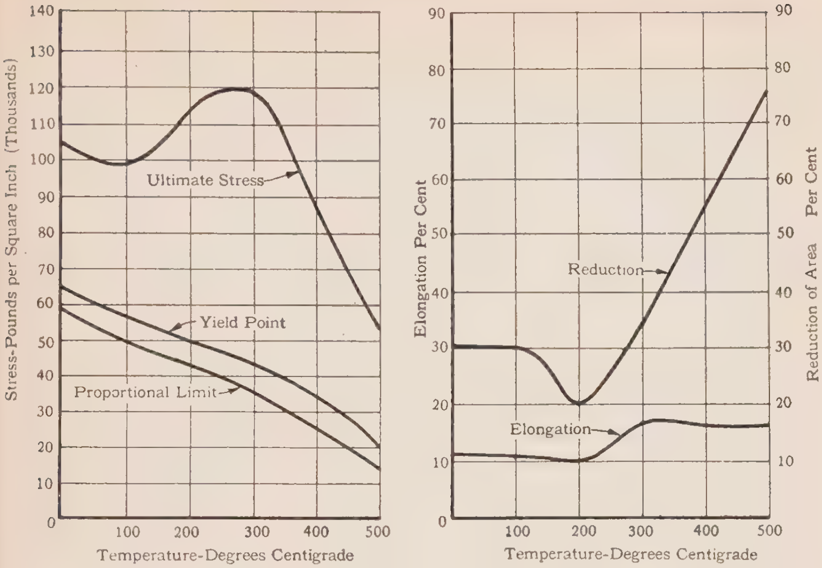

Fig. 302.—Tensile test properties of steels at high temperature C 0.74 Mn 0.78 Si 0.04.

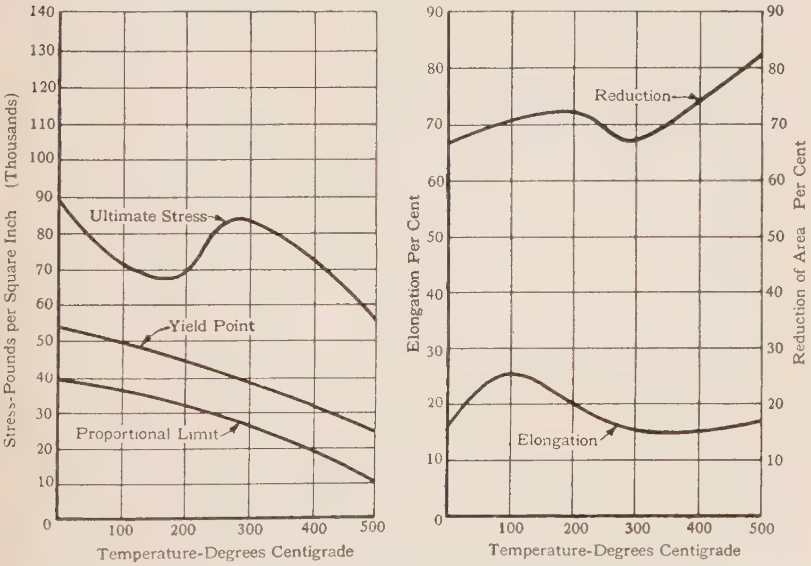

Fig. 303.—Tensile test properties of steels at high temperature. C 0.13 Mn 0.48 Si 1.1 Cr 0.29 Ni 4.2.

proportional limit, yield point, and modulus values for medium carbon, high carbon, and alloy steels. In all the tests, precision apparatus was used for measuring extensions and the yield point was always determined as that stress corresponding to a given extension. Certain characteristic curves from this work are given in Figs. 300 to 303 for a test piece, diameter of 8 mm. It will be noted that for the higher carbon and alloy steels there is a general reduction in the elastic properties for increase of temperature, but that for the medium carbon steel there is first an increase up to approximately 200°C. and then a continuous decrease. These exceptions to the general rule have not yet been confirmed by other investigators.

Effect on the Ultimate Strength and Ductility of Steel.—The effect of high temperature on the ultimate strength of steels is in general an increase with increase in temperature up to a certain limit, beyond which further increase in temperature will result in reduction of the ultimate stress. The results of Lea* on test bars 564 dia. by 2 inch gauge length and Bach† confirm this for low carbon steels, (see Figs.

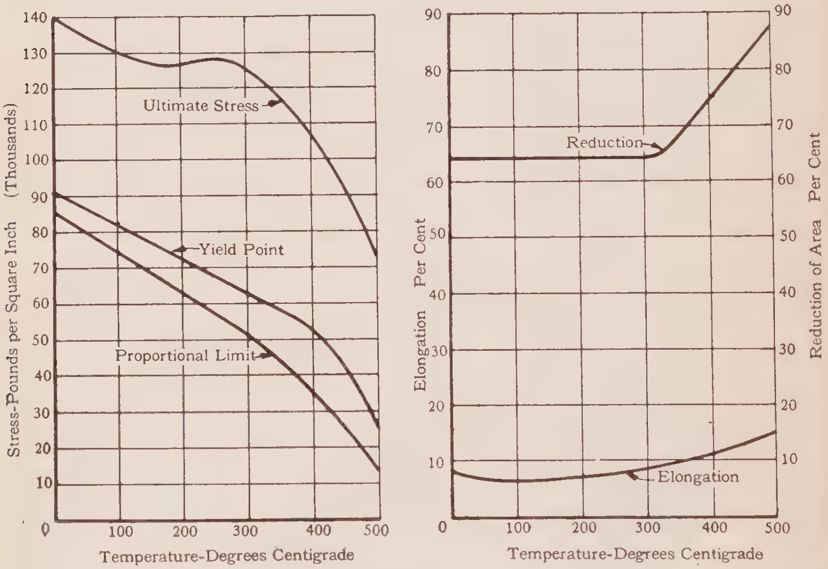

FIG. 304.—Tensile test properties of steels at high temperature. C 0.33 Mn 0.58 Si 0.18 Cr 1.01 Ni 3.18.

---

* Lea, *Engineering*, p. 487, Oct. 16, 1914.

† Bach, "Elastizitat und Festigkeit," p. 174, 1920.

295 and 298) and those of Welter* add confirmation for medium carbon steels. An examination of Welter's results show however that, for the higher carbon steels, small increments of temperature cause in general a slight reduction in the ultimate strength values, but further increase in temperature will increase this value to a maximum which will then, as explained above, cause a decrease with further temperature increase. In the case of certain alloy steels it appears that no increase in this value takes place as shown in Fig. 304 for nickel chrome steel, but that the strength continues to fall away as the temperature is increased for the normal.

The ductility properties as characterised by the elongation and reduction of area values generally commence to decrease up to a temperature of approximately 150°C. and then commence to increase with further temperature rise. The minimum elongation does not necessarily coincide with the minimum reduction of area nor does either of these coincide necessarily with the maximum value of the ultimate stress, according to Welter and Carrington. It seems to be conclusive that the variation in these ductility properties largely depends on the analysis of the steel, as an examination of Figs. 302 and 303 will undoubtedly show. For instance, the alloy steel given in Fig. 303 shows an increase in both these values up to 100°C., which is a contradiction of the general rule.

100. Non-ferrous Alloys.—We have seen in the previous paragraph the general reduction, with increase of temperature, in the elastic and strength properties of steels. It has been seen that for steels this can be of a high order and it will now be shown that for non-ferrous material the effects of temperature may be more striking.

Effect on the Elastic Properties.—The results obtained by Lea† on manganese bronze and gun-metal are shown in Figs. 305 and 306. It will be noted that the proportional limit of the manganese bronze at 350°C. has nearly decreased to zero while for the gun-metal at 450°C. it has become only half its original value at 20°C. The modulus of elasticity at this temperature meanwhile decreased 35% for this latter material.

Effect on the Ultimate Strength and Ductility.—A glance at Figs. 305 and 306 will show that temperature has a much greater effect on the strength of these alloys than upon carbon or alloy steels, and at a temperature of 450°C. the ultimate stress value may only be a small percentage of what it was at normal temperature. The loss in ductility as measured by the drop in elongation with rise in temperature is also very marked in the region of 300°C. Since the results obtained by Bach* for bronze confirms this fact, it appears to be a

---

* Welter, *Forschungsarbeiten*, Vol. 230.

† Lea, *Engineering*, p. 294, August 27, 1920.

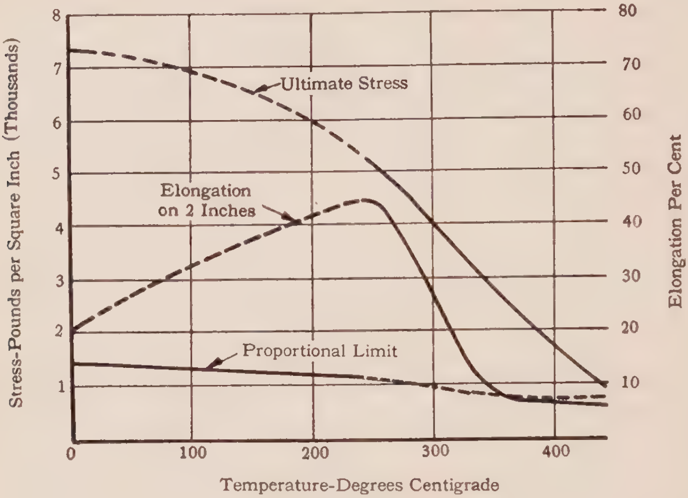

Fig. 305.—Tensile test properties of manganese bronze at high temperature.

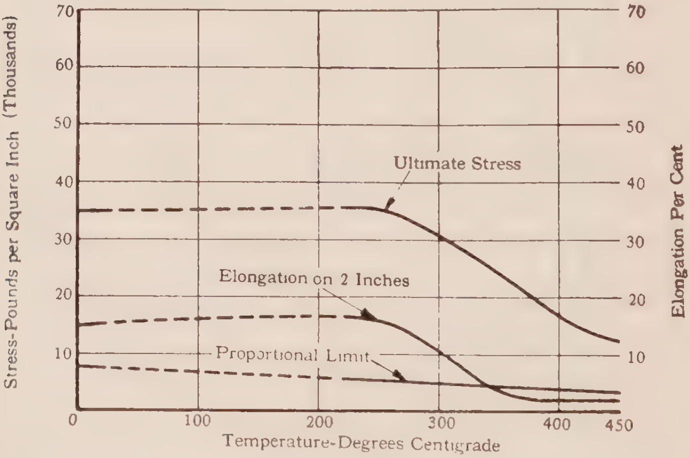

Fig. 306.—Tensile test properties of gun-metal at high temperature.

---

* Bach, "Elastizitat und Festigkeit," p. 179 and 180, 1920.

characteristic of these materials. Bach found the drop in elongation between 200°C. and 300°C. to be 67%, and at 400°C. the elongation was so small that it was impossible to record. This loss in ductility for such material seems from the designer's point of view to be of more than passing interest. It appears only to be applicable to the alloys discussed, for in the case of aluminium alloys* there may be an increase of elongation with rise in temperature from 250°C. to 350°C.

101. Cast Iron.—It is interesting to note, in view of what has been said on steels and non-ferrous alloys, that the ultimate strength for cast iron† remains practically constant up to 300°C., while even at a temperature of 570°C. the strength is more than half its value at normal temperature.

102. Conclusions.—In general, the fact we have been endeavoring to emphasize is that from the designer's point of view the calculations which he has made applicable to normal temperature conditions will in no wise apply to those cases where high temperatures prevail. A structure which is just strong enough at 20°C. may be too weak at 400°C. For example, in cases where vibration is to be expected it is necessary to observe that critical speed values, depending as they do on the modulus of elasticity, are liable to change with increase in temperature. Due recognition of these facts is essential. Another point is evident from this discussion, which will be developed in more detail later, namely, that it is vitally important that the designer should know the factors which influence the properties of the materials he uses. This is true for all conditions but more especially for those of high temperature. What is peculiarly characteristic for one material may or may not hold for another. As the subsequent chapters are developed, it will be appreciated that the possibility of good design rests entirely on these fundamental conceptions.

---

* *Eleventh Report of Alloys Research Com. Inst. Mech. Eng. Proc.* (London), p. 31, 1921.

† Bach, "Elastizitat und Festigkeit," p. 180, 1920.

CHAPTER XIII

THE ELASTIC STAGE MODIFICATIONS

103. Overstrain.—*General.*—In the previous chapter it was shown that the first stage of the tensile test, embracing as it does the proportional limit and yield point values, where these exist, is of the utmost importance to the engineer. So far, general forms of the diagram have been considered, but it will now be necessary to discuss in detail how these forms become modified by a variety of factors.

Low and Medium Carbon (0.1 to 0.6 C) *Steels.*—If a test bar of low carbon steel be loaded in tension to a point in excess of the yield point, as at A in Fig. 307, and the load be removed, then if the reloading be immediately carried out, it will be found, first, that the proportional limit is either entirely *suppressed,* the material not obeying Hooke's law at all, or will be very low and, second, that the yield point is much higher than before, corresponding approximately to the value of stress which was reached in the first loading. Ewing* found that the proportional limit for carbon steel occurred at 57,400 lbs. per sq. inch for the first loading, and the yield point occurred at 62,600 lbs. per sq. inch when a permanent extension of 0.14 inch on a 9 inch gauge length took place. On the first reloading the proportional limit had dropped to 11,500 lbs. per sq. inch. If after the unloading an interval of time is allowed to elapse, then, on reloading, a still higher value of the yield point will be obtained as at C in Fig. 307 and the material may be found to again obey Hooke's law and possess a proportional limit, the magnitude of which will depend on the time elapsing between

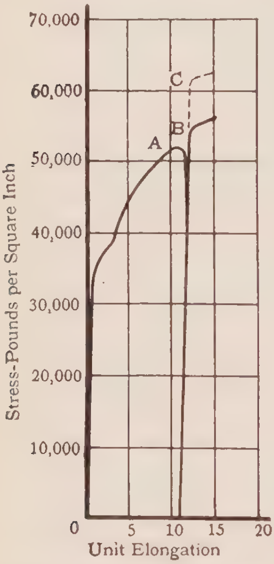

Fig. 307.—Diagram of overstrain for low carbon steel.

---

* Ewing, "Strength of Materials," p. 35, 1914.

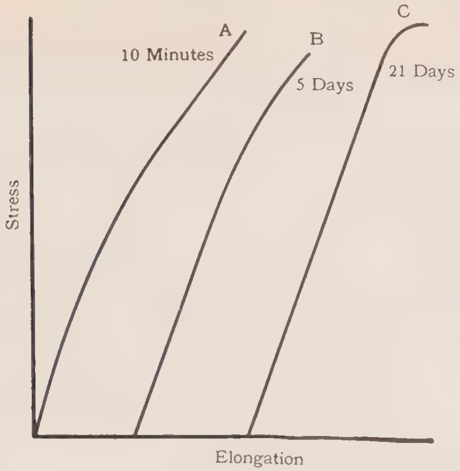

FIG. 308.—Diagrams of overstrain and recovery for low carbon steel.

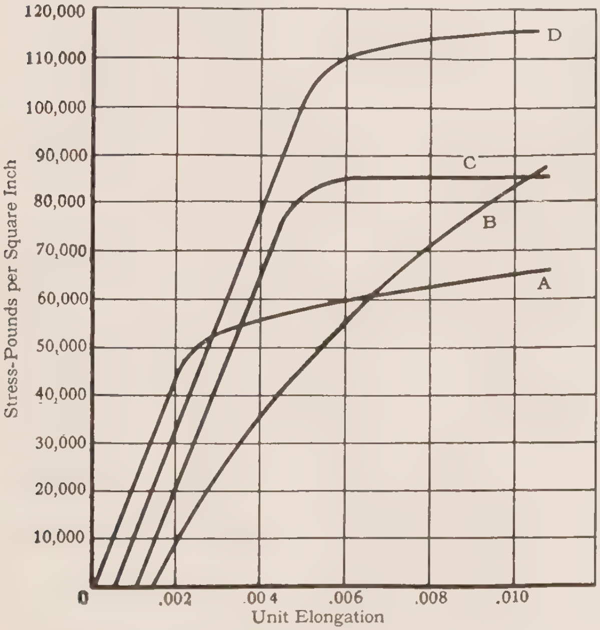

FIG. 309.—Diagrams of overstrain and recovery for medium carbon steel.

the unloading and reloading and upon the material. It will therefore be appreciated that a *hardening or stiffening* process has been going on in the material during this period of rest. In Fig. 308 are shown three curves plotted by the author from the results of Ewing obtained on the material previously mentioned. It will be seen that 10 minutes after straining, the material ceases to obey the proportionality law, but after 5 days it has recovered in part its elasticity, and after 21 days has nearly completely recovered. It has also been shown that material of this same class can have its *recovery* hastened by exposure to a temperature of boiling water (100°C.). This is shown very clearly in Fig. 309 which is again according to Ewing.

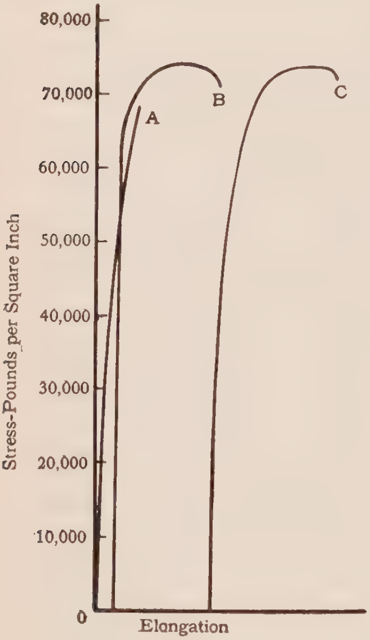

Fig. 310.—Diagrams of overstrain and recovery for medium carbon (.35 C) steel.

The curve *A* was obtained from medium carbon steel on the primary test. *B* was obtained 10 minutes after *A*. The material was then subjected to a temperature of 100°C. for 4 minutes and curve *C* was obtained. It will be seen that the material has recovered its elasticity, having a definite proportional limit and yield point both occurring at much higher stress values than in the first test. Curve *D* was gotten after further stressing and exposure to 100°C. This straining and recovery can be continued until the test bar will finally fracture in a manner resembling hard steel with low elongation and reduction of area, and at a stress value considerably in excess of the ultimate strength of the material obtained in an ordinary test.

In Fig. 310 are shown results obtained by the author on a cold worked medium carbon steel. Curve *A* was the primary test, the loading being continued until a stretch of 0.11 inch on an original 2 inch test piece was obtained. The test bar was then unloaded, and after 15½ hours the curve *B* was obtained. It will again be seen that whereas in the first test the material did not appear to possess a proportional limit, after *straining* and *resting* it continued to obey Hooke's law up to a stress of 64,000 lbs. per sq. inch. Curve *C* was obtained on another test bar of the same material without resting, the elongation and reduction of area in this case being slightly higher. This then is the general principle of *overstrain* and recovery from such. It must clearly be understood, however, that so far discussion has only been made of low and one medium carbon (.35 C) steels.

High Carbon and Alloy Steels.—It is now known that while this principle of overstrain can be applied to all steels, the recovery after resting is not general in its application. In some cases the boiling water treatment will even show no tendency to make the material recover. This refers to high carbon and alloy steels. Dalby* has shown that a lapse of 6 days had a negligible effect on an overstrained 0.8 carbon steel. This is true likewise with a nickel steel.

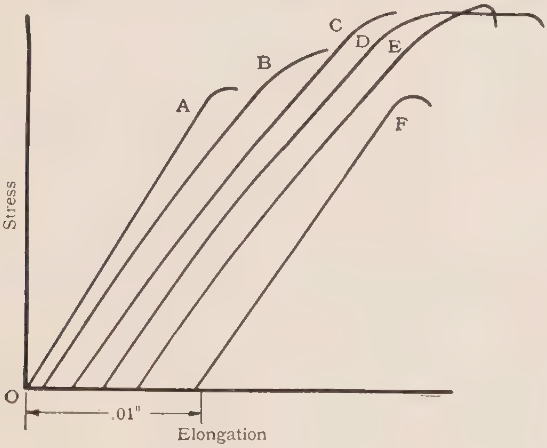

FIG. 311.—Diagrams of overstrain and recovery for 3.7% nickel steel.

In Fig. 311 curves† are given for a 3.7% nickel steel. Curve *A* was obtained from the primary test and gave the limit of proportionality at 58,000 lbs. per sq. inch and yield point at 67,000 lbs. per sq. inch. Curve *B*, taken after a 2% stretch on a 5 inch gauge length, showed that the proportional limit had disappeared. Curve *C* was obtained after a 6% stretch, and *D* was obtained after turning the bar to a slightly reduced diameter, the time interval between *C* and *D* being 24 hours. The piece was then boiled for one hour and curve *E* was obtained, which showed no elastic recovery. Finally the bar was heated to 550°C. and kept there for 30 minutes. The subsequent curve F showed complete recovery of elasticity due to *re-crystallization,* with a slight raising of the proportional limit and yield point values.

---

* Dalby, *Phil. Trans. Roy. Soc.*, Series A, Vol. 221, 1920.

† Dalby, "Strength and Structure of Metals," p. 137, 1923.

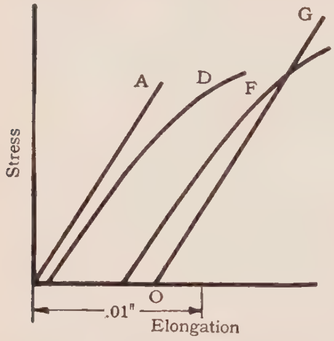

Fig. 312.—Diagrams of overstrain and recovery for low carbon steel.

In Fig. 312 are shown results obtained by Dalby on a low carbon steel. A was the first pull. D was taken after a stretch of 2%; F after a stretch of 4.2%, while after 15 days the curve G was obtained showing complete elastic recovery.

Conclusions.—These results can be summarized by stating that straining a steel beyond its yield point will make the material partially lose its elasticity. In the case of low and medium carbon steels the new strained state of the material will be more or less *unstable* because its recovery takes place either slowly or rapidly, depending on external conditions. In the case of alloy and high carbon steels, on the other hand, this strained state appears to be more *stable,* and recovery is only possible after the elapse of very long periods of time or by the subjection to higher temperatures. In all cases, however, the material after recovery has assumed new characteristics, namely, higher proportional limit and yield point values in tension and will if fractured show less ductility. Excluding annealing of the material at temperatures above the critical range, the material is permanently changed by this stressing from what it was originally. These facts have an important bearing on the theory surrounding such phenomena, which will be discussed later.

104. Cold Work and Quenching Effects.—*Cold Work Effects.*—If a material in the process of manufacture is being deformed while the temperature is gradually falling from a previously high temperature, the effect of this deformation will at first not be shown, because the temperature will be sufficient to enable the material to anneal itself. If deformation is continued, however, a point will be reached at which the temperature will be insufficient for this annealing and if cooled, the effects of deformation will not be obliterated. Such a material is said to be *cold-worked* and will exhibit the same tensile properties as an overstrained material previously discussed. Subsequent annealing will however remove these effects. The temperature at which this cold working will begin will depend on the material; for instance, 400°C. can be considered as hot working for aluminum alloy but as cold working for steel.

From what has been said previously on the effects of overstrain it can be assumed that cold working will increase the ultimate stress and reduce the ductility. Examination of Fig. 313, which is according to Aitchison,* will prove this to be the case, the abscissa of these curves representing the reduction of initial cross-section in percent, which is considered to be a *measure* of the intensity of cold work.

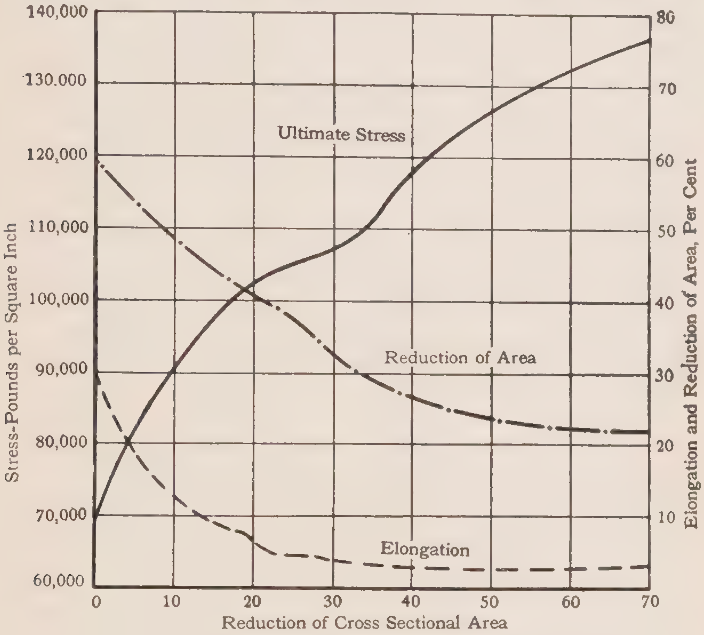

FIG. 313.—Tensile properties of cold worked steel.

It will therefore be seen that the loss in ductility determines to what extent this cold working can be carried out. Similar to an overstrained material, a cold worked material shows decided changes in the form of the tensile test diagram, when subjected to low temperature effects. According to Rosenhain† the effects of this annealing are as follows: First, there is a mechanical softening leaving the strained structure unaltered; then there is a process of gradual re-crystallization from the previously deformed structure. The point which requires emphasis is that according to expert metallurgical opinion the change occurs in these two steps. A very important paper on the effect of annealing on cold drawn steels was contributed by Rees.* Tests were carried out on low carbon and high carbon steels, the former being cold worked until the area was reduced 14.8% and the latter 8.1%. Curves in Figs. 314 and 315 are reproduced from this work.

---

* Aitchison, "Engineering Steels," p. 267, 1921.

† Rosenhain, "Introduction to Metallurgy," p. 268, 2nd Ed., 1919.

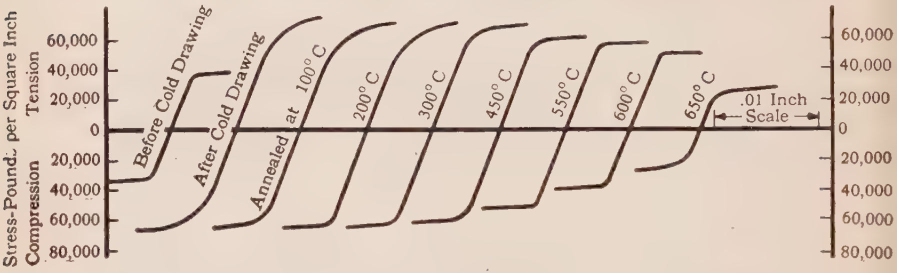

Fig. 314.—Load extension diagrams—low carbon steel (.04 C). Annealed for 1 hr. at temperature stated.

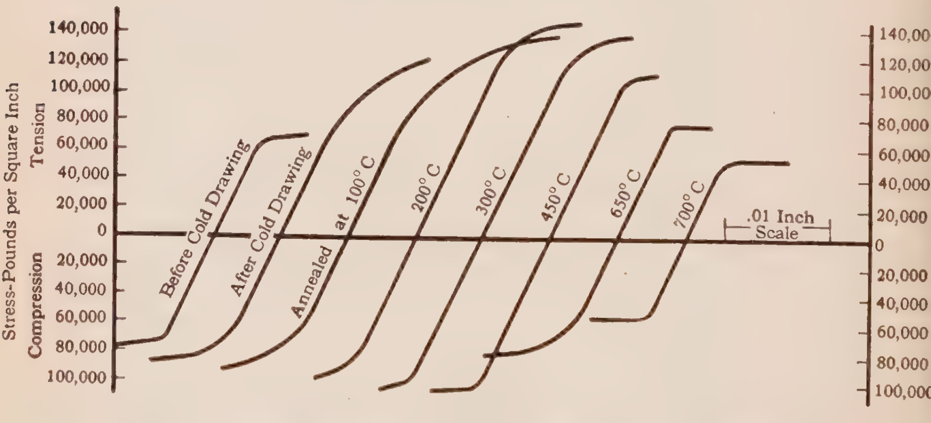

Fig. 315.—Load extension diagrams—high carbon steel (.85 C). Annealed for 1 hr. at temperature stated.

It is seen from these diagrams that the effect of the low temperature annealing is to increase the value of the proportional limit while the yield point remains more or less unchanged up to a temperature of 300°C. The increase in the tensile properties due to the cold work was also accompanied by a decrease in the compression properties; although both were increased by the annealing operation as shown in Fig. 316.

---

* Rees, Effect of Low Temperature Annealing on the Mechanical Properties of Cold Drawn Steels, *Iron & Steel Inst. Jour.*, 1923.

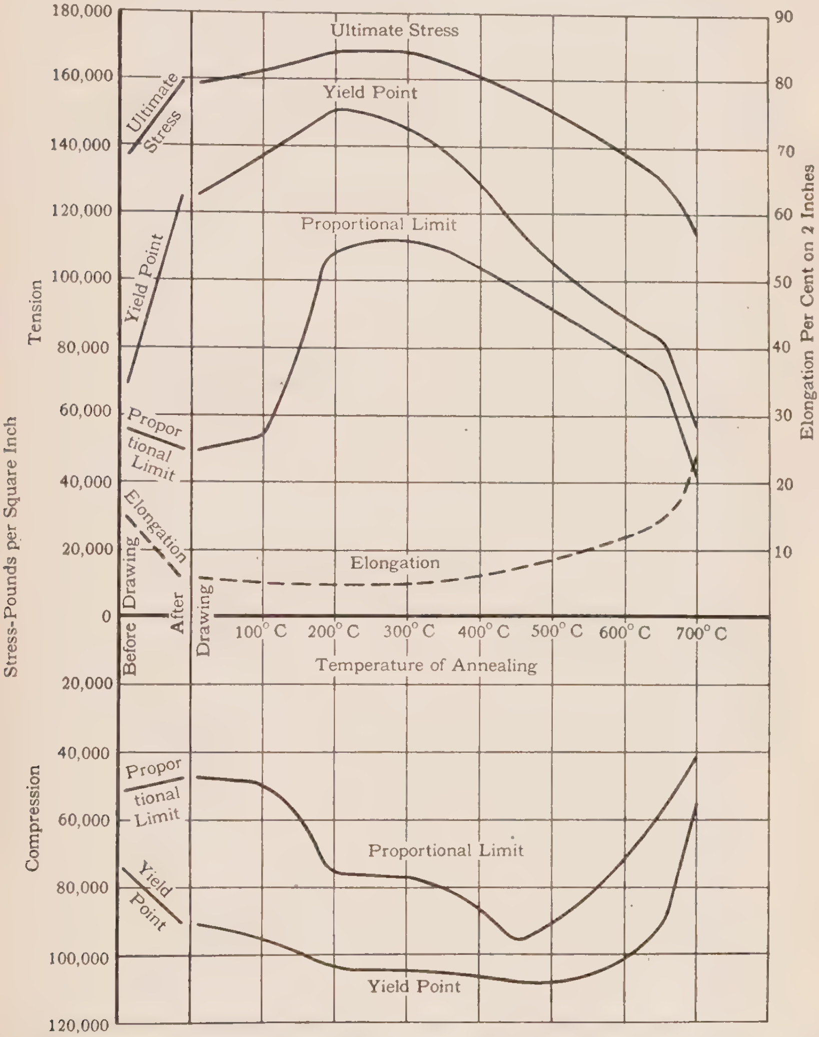

FIG. 316.—Tensile and compressive test characteristics of cold worked steels showing annealed effects.

In other words, the cold working produced a *directional effect* on the material similar to overstrain.

In Fig. 316 is also shown, in diagrammatic form, the results of the complete tests obtained on high carbon steel. This diagram is decidedly interesting in that it shows very clearly that as the annealing temperature is increased, the distance separating the yield point and proportional limit decreases. In other words, the form of the elastic stage of the tensile test diagram becomes more *sharp* (see Fig. 315). What has been said about the high carbon steel applies more or less to the other materials tested.

QUENCHING EFFECTS

Modification of the tensile test diagram does not belong entirely to materials which have been mechanically strained. This can also be produced by *thermal* effects and it is generally accepted that the low proportional limit occurring in strained material is also met with in *untempered* quenched steels, the treatment of which was discussed in Chap. XII, paragraph 90. Steels possessing a proportional limit and yield point when fully annealed may have both suppressed when quenched from above the critical range. In a recent contribution to the literature of the subject, Aitchison* has shown that the quench hardened steel and the cold worked steel are not the same in that stressing slightly above the proportional limit in the work hardened steel will lower the proportional limit value, while a similar stressing in the case of the *air hardened* material will raise it. The explanation advanced for this difference, which appears to be logical, was that the cold working had so deformed the material that further stressing tended to increase this deformation. Another very striking difference was found between the two steels. The quenched steel tempered for a long time at a temperature of 100°C. had substantially the same enhanced properties as when tempered for a short time at a higher temperature. In the cold worked material a prolonged heating at 100°C. did not produce such a large alteration in the proportionality limit. The fact that cold worked material appears to offer more stability than quenched steels is not strange when it is remembered that an overstrained material is in some cases unstable and in others stable.

PRACTICAL APPLICATION OF COLD WORKED MATERIAL

Cold worked material is in certain applications very useful in engineering practice, being applied in such cases as banding for gun barrels and hydraulic cylinders. Its use in the case of wire is furthermore well known. The beneficial effect of cold working of the light alloys of aluminium are fully discussed in the eleventh Report of the Alloys Research Committee, previously mentioned. The danger incurred is that the advantage of cold working can disappear if the material is subjected to a high temperature. Referring to Figs. 276 and 277 the curves thus obtained by the author on pure copper are shown. In the cold worked condition the extension corresponding to a load of 2,100 lbs. was .04 inch on a 2 inch gauge length, but after the material had been subjected to a temperature of 400°C. the load for the same extension was only 1,000 lbs. Furthermore, as will be discussed later, the advantages only persist if the applied loads are static. Alternating loads appear to dissipate at least in part the cold working effects. In short it is important to bear in mind that *strain hardness* produced by cold work is at best not a particularly reliable factor in design work.

---

* Aitchison, The Low Apparent Elastic Limit of Quenched or Work Hardened Steels, *Carnegie Mem. of Iron & Steel Inst.*, Vol. 12, 1923.

105. Time Effect Stresses within Elastic Limit.—*General.*—As discussed at the beginning of Chap. I, the mathematical treatment of the subject of elasticity is simplified by assuming that the form of a body depends only on the forces which, within the limits of elasticity, act on it at the time, and not upon those which have ceased to act. Since this is a very important assumption it is necessary to examine it in certain detail in order to determine as far as possible its justification since it leads us directly into a consideration of *time effects,* which, as we have seen in Chap. XII, paragraph 97, may be of real significance for a true knowledge of the physical properties of materials.

Elastic after Effects.—In our previous consideration of this subject it was assumed that for a steel test bar loaded and unloaded within the limit of elasticity, which for such a material is also taken, as we have seen, as coinciding with the limit of proportionality, no retardation in the strain takes place, but that the strain obtained after unloading always remains the same. This is not rigidly true because it is now known that constructional materials when stressed within the range of elasticity will show a change of strain with the time due to what is termed *after effect.* These effects may either be of a thermal or an electrical nature. Much work has been done by various investigators* on this subject. It is our intention to discuss in some detail those after-effects due to temperature.

---

* Weber, De Fili Bombycini vi elastica, *Poggendorf's, Annalen,* Vol. LIV, 1835, An Abstract is given in "History of Theory of Elasticity," Vol. I, p. 389. Todhunter & Pearson, 1886.

Kelvin, Elasticity, "Ency. Brit.," 9th Edit.

Gough, Properties of Indian Rubber, *Manchester Phil. Mem.,* Vol. 1, 1805.

A graphical illustration of the temperature effect is shown in Fig. 317. If a test bar be loaded quickly in tension from O to A, then at A the temperature will be lower than the surrounding medium and after a certain time it will absorb heat and expand to B. On unloading to C, it will now be at a higher temperature than the surrounding medium and it will complete the cycle of operations by cooling down and contracting to O the original value. The line OA gives the *adiabatic modulus* of elasticity and OB gives the *isothermal modulus.*[*] Due to this thermal effect it will be appreciated that *looping* is obtained within the elastic conditions of the material. This looping is of course very small and, while its magnitude is of no practical significance to the engineer, still it is present. Lord Kelvín gave an explanation of this from a *thermo-dynamic* standpoint by stating that any solid has its temperature reduced by straining in opposition to its own elastic forces and raised by yielding to these forces, provided the strength of such would decrease with increase in temperature. Certain after-effects of an electrical nature[†] have also been observed when there is stressing within the limits of elasticity, and it appears that there is a more or less complete analogy between the action of an electric current and a force mechanically applied.

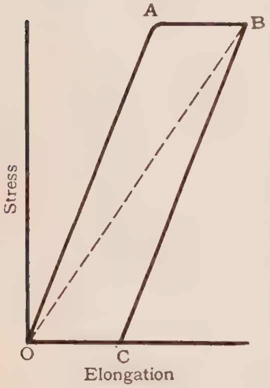

Fig. 317.—Diagram of elastic after-effect.

We are only interested, however, in recording these various effects and referring to the various literature on the subject. In general, they are only of passing interest to the designer. What concerns us, however, is that in a recent contribution to this subject by Joffe[‡] all after-effects of ideal elastic crystals can be explained if such phenomena as temperature and electrical effects be considered. This will be developed in more detail in a subsequent paragraph and appears to be fundamental with regard to our conception of elastic and proportional limits.

106. Time Effect Stresses beyond the Elastic Limit.—*General.*—From the previous discussion of the subject it will have been gathered that the various factors, elastic limit, proportional limit, and yield point are liable to undergo decided modification, due to a variety of causes. Since these values are vital to the designer as an index of the material, it is important that as much enlightenment as possible should be given of the underlying causes and possible explanation of these changes. On the basis of recent research, an attempt will therefore be made, in the remainder of this chapter to discuss these in more detail with the view of arriving at some conclusions regarding them.

---

[*] Searle, "Experimental Elasticity," p. 20, 1920.

[†] Wertheim, Les sons produits par le courant electrique, *Ann. de Chimie,* Vol. XXIII, 1848.

[‡] Joffe, Elektrizitätsdurchgang durch Kristalle, *Ann. d. Physik,* Sept., 1923 This contains references to all previous work by the same author on this subject.

Geiss Theory.—To begin with, the question might be asked, why certain materials do not obey the proportionality law in one condition, but yet may do so in another condition. This is a very important matter for the designer and appears worthy of our attention. According to a recent contribution to the literature by Geiss* it seems that the extension of all crystalline materials can be completely explained if the time factor alone be taken into account. In other words, the relation between stress and strain can be written in the form

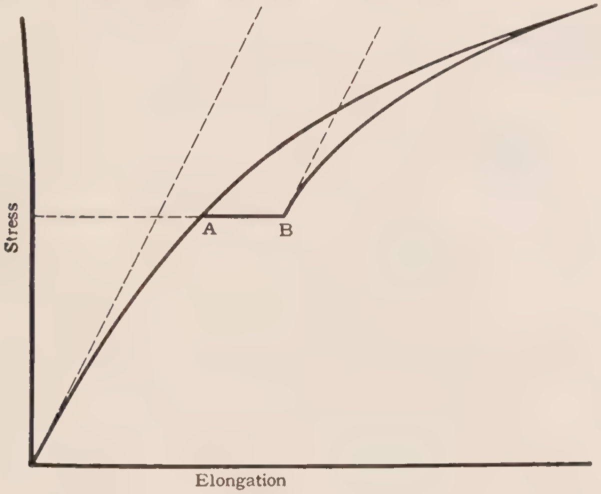

FIG. 318.—Tensile test diagram for cast iron showing time effect.

$$e = \phi(p) + \phi_1(p_1t_1)$$

where e, p, and t represent the strain, stress, and time, respectively. Geiss assumed that the first term was linear in p, and a material which showed no time effect would therefore follow Hooke's law. Conversely

* Geiss, Zur Elastizität der Metalle, *Z. f. Metallkunde*, Nov., 1923.

if it did not do so, then this could only be explained on the grounds of time effect. To support these conclusions, certain experimental evidence was given of which the curves shown in Fig. 318 and Fig. 319 form a part. The figures given represent part of the stress-strain diagrams obtained for cast iron when tested in tension. If the stress be increased to a value as represented by *A* and maintained constant at this point, the line *AB* represents the time effect, and on continuation of loading, the tangent to the new stress-strain line is found to be parallel to the one through the origin. In other words, if the time effect be excluded there will be no deviation at all in a horizontal direction and the material will obey the proportionality law in line with his statement.

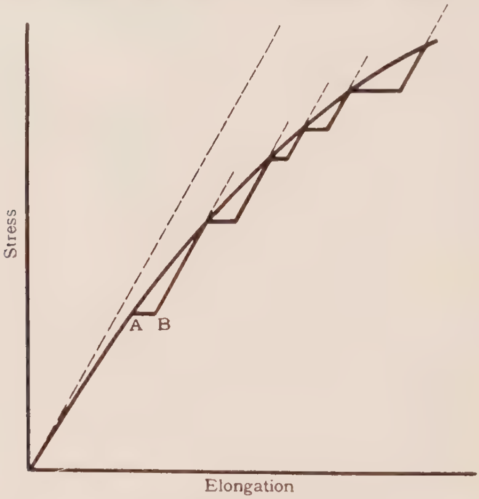

FIG. 319.—Tensile test diagram for cast iron showing time effect.

This reasoning can be further widened to give the general statement that for a *crystal* the proportional limit will also be the elastic limit, but for a *crystalline material* the proportional limit becomes the elastic limit of the more *unfavorably situated* crystals or the point at which such crystals experience permanent set.

Effect of Internal Stress.—These conclusions provide a means of explaining why a steel may in one state have no proportional limit, while in another it may possess this property of proportional extension. We have seen (page 355) that a medium carbon steel (and this can be generally applied to all steels) in the annealed condition, will possess this property up to a stress value approximately coinciding with the yield point as represented in Fig. 320. It can therefore be inferred that in such a condition there are comparatively few unfavorably situated crystals but that all are equally stressed.

On the other hand, it has also been observed that a steel which has undergone mechanical deformation or one which has been quenched may have a very low proportional limit or even in some cases may have this value entirely suppressed as in Fig. 321. This means that in such cases certain of the crystals are unfavorably situated and may experience permanent set more readily. This naturally leads us to inquire why the one steel has no unfavorably situated crystals while the other does appear to have such. In the present state of the knowledge the most reasonable explanation of the presence of these unfavorable crystals is due to the action of stress. And since up to the present we have been considering the action of externally applied stress on the extension or compression of metals, it is logical to assume that for steels in the state indicated by Fig. 321 that we are also witnessing the effects of stress, but this time the stress is of an internal nature. There appears to be plenty of evidence to support this theory. For example, certain air-cooled alloy steels show no proportional limit, or on the basis of our hypothesis have become internally stressed, making certain of the crystals unfavorably situated. Tempering at a comparatively low temperature allows these internal stresses to be relieved, thus giving a favorable crystal formation and allowing the material to show a definite proportional limit. This appears also to be con-

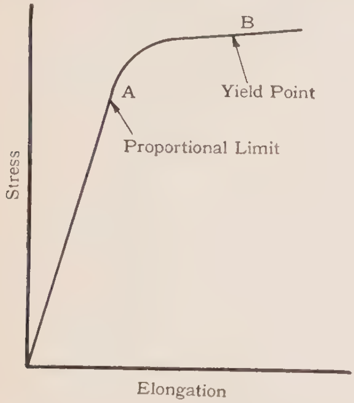

FIG. 320.—Elastic stage of tensile test for medium carbon steel, annealed.

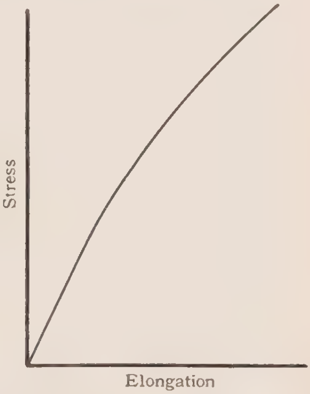

FIG. 321.—Elastic stage of tensile test for medium carbon steel, cold worked.

firmed by the experimental evidence obtained from cold-worked material. We have seen that annealing at temperatures far below that necessary for metallurgical changes to occur (see pages 396 and 399) causes quite a definite increase in the proportional limit value while leaving the yield point practically unaltered. This can only be explained, it appears, on the ground of release of internal stress. It is very interesting also to note that Ewing,* in commenting on Hodgkinson's experiments on cast iron, expressed the belief that the disobedience to the proportionality law in such a material for stresses of a small but reasonable magnitude may have been due to internal stress in the material. On this basis we are therefore advancing the thought that material, which in the annealed condition obeys the proportionality law, possesses in such a state minimum internal stress, and if by a mechanical or thermal treatment the obedience to this law is disturbed, then internal stresses are present. In leaving to a future paragraph the consideration of a method whereby the magnitude of such stresses may be indicated, it is important to note that by internal stress the stress due to the material alone is implied and this term is not intended to include those internal stresses which might be developed, for instance, in a casting due to geometrical form.

107. Hysteresis.—*Hysteresis Looping in Metals.*—We have seen, in the previous paragraph, if materials are loaded and unloaded within the elastic limit that due to certain after-effects the line for the unloading will not coincide with that for loading, but that looping will occur. It has also been observed that this is, in general, of little significance to the engineer. It is now proposed to discuss in the following paragraph an entirely *different* kind of looping obtained when the stresses are in excess of those pertaining to elastic conditions, which is of real importance to the designer.

If a metal be stretched beyond its elastic limit, then on unloading, the recovery of elasticity may be partial or complete, as discussed in paragraph 103. It is in this state of non-recovery imperfectly elastic.

Referring to Fig. 322 which represents a diagram for 3½% nickel steel obtained by Dalby† with his special recorder the initial loading took place from *O* to *B*. At *A*, the limit of proportionality, the strain commenced to increase more rapidly than the stress, and at *B* the yield point was reached. At *C* the test bar was unloaded and the line

---

* Ewing, "Strength of Materials," pp. 31 and 60, 1914.

† Dalby, The Elastic Properties of Metals, *Phil. Trans. Roy. Soc.*, Series A. Vol. 221, p. 117–138.

Dalby, "Strength and Structure of Metals," 1923.

CD was obtained. On reloading, the line obtained formed an enclosed area with that obtained for the unloading. This phenomenon is generally termed *hysteresis looping* and applies in general to all metals.*

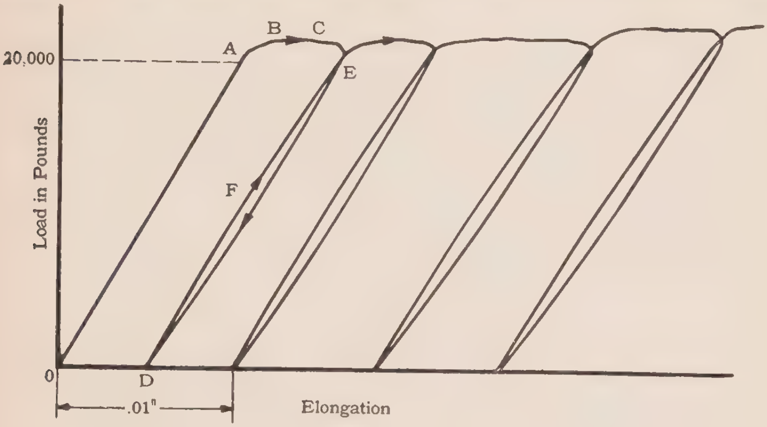

FIG. 322.—Hysteresis looping of 3½ % nickel steel.

This looping is of a much larger order than the hysteresis effects obtained within the elastic limit and previously mentioned. It will also be noted that if the looping is continued the yield point becomes higher with successive loadings, which is in agreement with the discussion of overstrain in paragraph 103. Furthermore the material at

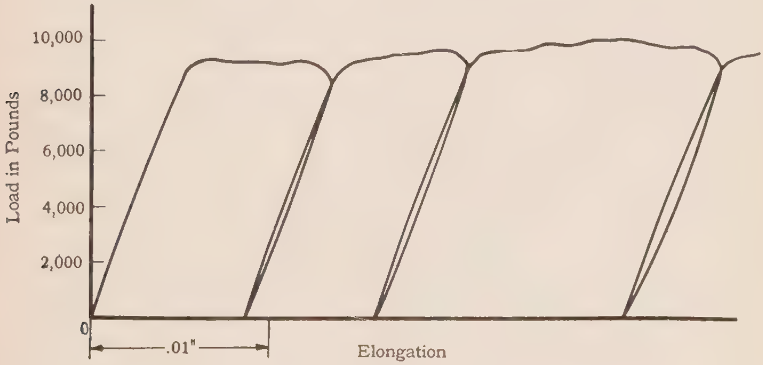

FIG. 323.—Looping in iron.

---

* This also refers to the looping which is obtained in metals at stress values below the elastic limit and which is in addition to after effects mentioned.

C, while no longer elastic, is nevertheless not *plastic* in a true sense because it always possesses during unloading, as shown by the curve *CD*, Fig. 322 the elastic property to a certain degree. It is plastic under loading but partially elastic during unloading. Dalby concluded that the elastic extension plus the plastic extension after passing beyond the proportional limit were about equal to the imperfect elastic shrink plus the permanent set *OD*.* In Figs. 323, 324, and 325 are given further diagrams according to Dalby. It will be noted that each material gives a characteristic diagram. For soft iron (Fig.

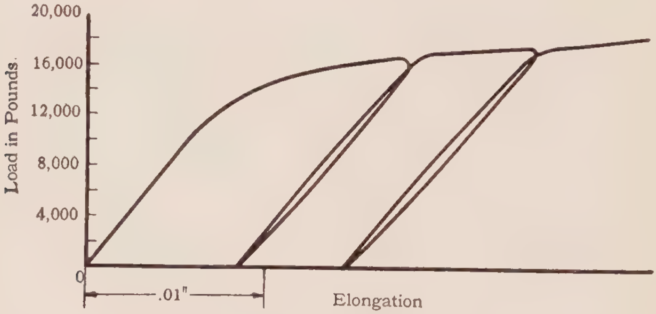

Fig. 324.—Looping in carbon steel.

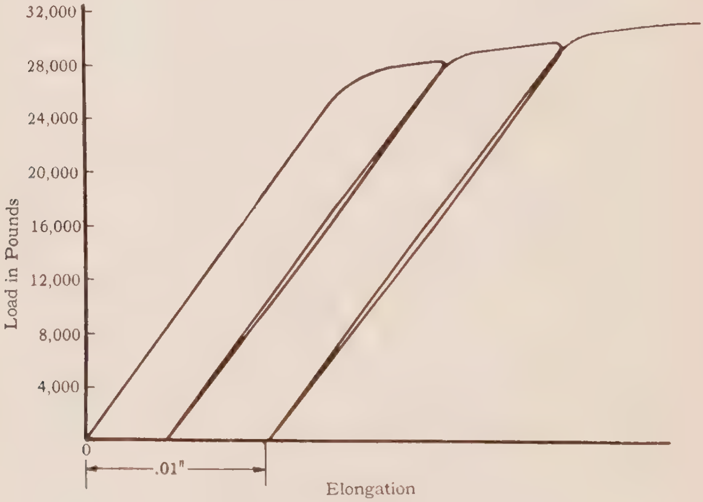

Fig. 325.—Looping in nickel chrome steel.

---

*See p. 409 for different conditions as in non-ferrous metal.

323) the looping is small, while for carbon steel it is larger. The curved boundaries of the areas enclosed by the loop appear to follow generally the slope of the elastic line and this appears to be true even when this looping is continued up to the point of fracture. With other materials such as zinc or tin, an entirely different form of diagram is obtained as shown in Figs. 326 and 327. In these cases, on removal of the load, the material continues to shrink. In other words we are observing another manifestation of time effect on the stressing of metals.

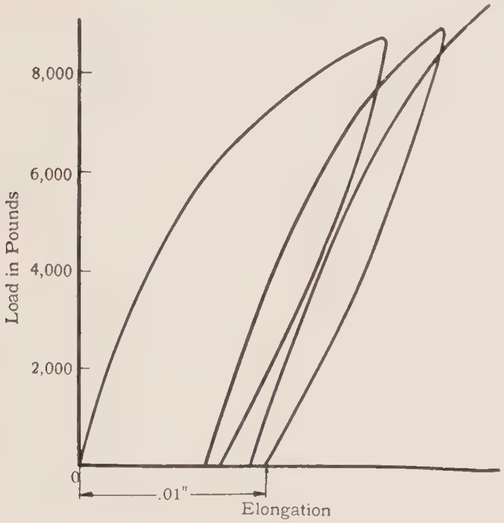

FIG. 326.—Looping in zinc.

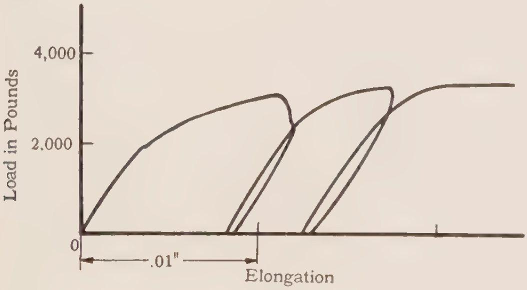

FIG. 327.—Looping in tin.

Hysteresis Looping in Crystals.—It is undoubtedly true that a great amount of information will be gained with reference to the behavior of metals by research into the characteristics of single crystals. To date much has been accomplished and a certain amount of data has now been published on the subject. According to Dalby* and Carpenter† the crystals (in this case, of aluminium) showed an elastic condition merging at yield point into a plastic one, also that loading and unloading beyond the yield point gave the same characteristic looping as for a crystalline material. One of the points mentioned was that the strength of the crystalline material was not much in excess of the pure crystal, while Dalby mentioned that the yield load of the single crystal was lower than that of the multi-crystal test piece. In stating these facts, however, it is necessary to bear in mind that the tensile properties of crystals vary widely according to the direction in which they are stressed. This was observed by Carpenter and also later by Czochralski‡ on copper crystals. Since this latter work showed that the ratio of maximum to minimum strength could be in the neighborhood of three in discussing the physical properties of single crystals, it appears to be necessary to specify direction. This will in turn give rise to some difficulty in endeavoring to obtain relative data between single crystals and multi-crystal test bars. But, nevertheless the whole study of single crystals promises to throw more light on the behavior of the crystal aggregates. The important point to note from this discussion is that modern research indicates this looping effect is not a property of the crystalline structure but is inherent in the crystals themselves.

Conclusions.—Summarizing these various points we can conclude that after the material has been stressed up to or beyond the yield point, the response of a metal to the removal and re-application of stress is an *absorption of energy* represented by an area such as *EDF* in Fig. 322. On repeated applications of this looping it will be found that, provided the stresses are sufficiently high, there is a general increase of loop area which appears to tend toward a maximum value and which remains more or less constant for a given material. Furthermore, it will have been inferred from the information already given that the curve form, the loop area and the rate of increase in area are all characteristic not only of a material but of the state of that material. It appears therefore that if records be made of the elastic line and a few loops that these may have a real significance in the selection of materials. In stating that further consideration of this phenomena will be made in the chapter on fatigue we can well close this paragraph with the remark that a study of these looping affects gives additional information to what can be expected from the ordinary tensile test previously described, and on this basis has rightly earned a place in our discussion.

---

* Dalby, "Strength and Structure of Metals," p. 152, 1923.

† Carpenter and Elam, Production of Single Aluminium Crystals and Their Tensile Properties, *Roy. Soc. Proc.*, Vol. 100, Sec. A, Dec., 1921.

‡ Czochralski, Die Grundlagen der Verfestigungsvorgänge, *Z. d. Ver. deutsch. Ing.*, June, 1923.

108. Internal Stress.—*General.*—We have seen in a preceding paragraph how the position of the proportional limit appears to be affected by the magnitude of the internal stress. It is now proposed to advance a method of comparing the magnitudes of these internal stresses by using the ratio of yield point* to proportional limit. In choosing the ratio the author's chief thought is to make it dependent on the shape of the elastic and transition stages of the tensile test diagram because this conception of diagram shape is put forward as fundamental. Possibly other ratios such as the difference between the yield point and proportional limit expressed as a percentage of the yield point would express this quite as well. At present we are only concerned with discussing the one given.

In the development of this theory we will adhere to the principle that comparisons will be made as far as possible on steels possessing approximately similarity in micro-structure.

Annealed State.—Taking the case of a fully annealed low or medium carbon steel, it has been seen that in this condition the material has minimum internal stress. This being the case it is cogent to inquire what effect this has on the form of the curve up to the yield point for this state. As we have seen in Fig. 270 experimental evidence indicates that the diagram shows a sharp break off at the yield point. This latter point for the particular condition appears to coincide with the proportional limit value. In other words the ratio of yield point to proportional limit assumes a minimum value for this condition of minimum internal stress, and for such is approximately equal to unity.

Rolled, Cast, and Normalized States.—Reasoning on this basis the author believes that, since for the condition of minimum internal stress this ratio is also minimum, this method can be further applied to indicate the degree of internal stress present in the same material for other states. As has been shown, steel as it leaves the rolls, or the mould if a cast material, is in a coarse condition, and due to the uneven cooling must possess a greater degree of internal stress than an annealed material. Again, a normalized steel, since it is cooled rapidly in air, must also possess a greater degree of internal stress than the annealed material. On the basis of the previous hypothesis the stress strain diagrams for such conditions must be more rounded than the diagram for the annealed condition. In other words, the ratio of yield point to proportional limit, denoted from now on by k, should be greater for such states. In Table XLVIII and XLIX are given the results reproduced from Table XXXV on medium carbon steel (0.37 C) in the rolled, annealed, and normalized conditions and on carbon steel castings (0.34 C) from Table XXXVII for the cast, annealed, and normalized conditions, respectively.

---

* For materials which do not possess a yield point, see discussion on p. 358.

TABLE XLVIII.—RATIO k FOR MEDIUM CARBON STEEL (.37 C)

State	Proportional limit, pounds per square inch	Yield point, pounds per square inch	Ratio k
Rolled	27,000	31,000	1.15
Annealed	36,500	37,800	1.03
Normalized	38,000	41,500	1.10

TABLE XLIX.—RATIO k FOR MEDIUM CARBON STEEL (.34 C)

State	Proportional limit, pounds per square inch	Yield point, pounds per square inch	Ratio k
Cast	20,000	33,500	1.67
Annealed	37,000	41,200	1.10
Normalized	40,500	46,000	1.13

In Table L are given the values of k from the results on the nickel steel previously discussed in Table XL. The effects of normalizing and tempering operation are included in this case.

TABLE L.—RATIO OF k FOR A 3½% NICKEL STEEL

State	Proportional limit, pounds per square inch	Yield point, pounds per square inch	Ratio k
Rolled	47,000	60,000	1.27
Normalized	52,000	60,000	1.15
Normalized and tempered	52,000	56,000	1.07

It will be seen that these experimental results support the theory that internal stress can be at least indicated by the ratio k. If the material is in a coarse structural condition then the ratio k is large as indicated by the values of 1.15, 1.67, and 1.27 from Tables XLVIII to L, respectively. If, on the other hand, a more uniform structure is obtained, then this ratio will decrease by the release of these internal stresses. The more gradual the cooling is, the less will this ratio be, as is shown by a comparison of the results for the normalized, and for the normalized and tempered states, respectively.

Heat-treated States.—In the case of heat-treated steels this method of reasoning can also be applied, but since the structure has in such cases been changed the comparison of the internal stress must be made taking this fact into consideration. A medium carbon steel (0.37 C) when heat-treated by quenching and tempering will have, if the tempering has been carried far enough, what metallurgists name a *sorbito-pearlitic* structure, as compared with *pearlitic structures* for the annealed and normalized conditions. Like a pearlitic steel, a sorbitic steel can show a value of k approximately unity. As the temperature of tempering is reduced, however, this ratio rapidly increases due to the effects of the internal stresses which with the reduced temperature of tempering have not been removed. In Table LI are shown these values of k obtained for the steel of Table XXXVIII.

TABLE LI.—RATIO OF k FOR A HEAT-TREATED 0.37 CARBON STEEL

Tempering temperature °C.	Proportional limit, pounds per square inch	Yield point, pounds per square inch	Ratio of k
550	65,000	69,000	1.06
450	65,000	74,000	1.14
100	68,000	80,000	1.18

Overstrained States.—It will now be necessary to investigate how this reasoning can be applied to steels other than those having undergone thermal treatment above the transformation points. As shown in paragraph 103, a steel if loaded beyond the yield point, will on reloading indicate either no proportional limit or at least a very low value for such. The author admits some difficulty in applying the ratio k for a steel with no proportional limit because in such a case this ratio k taken as a measure of internal stress would be infinite. It is to be hoped that the further tests now in progress will help to clear up this particular case. In other words, in the material an internal stress has been developed, as shown by the high ratio of yield point to proportional limit. This internal stress can be released in the case of low and medium carbon steels by the effects of time or the subjection of the material to low temperature annealing. The higher proportional limit obtained on recovery of elasticity can then be explained on the grounds of the *amorphous theory,* which will be developed in the subsequent paragraph.

For cold worked material the same reasoning can be applied. In this case the deformation of the crystal structure has gone so far that higher temperatures are necessary to diminish these internal stresses. This fact is shown rather strikingly in the results obtained by Rees (see Figs. 315 and 316) because as the temperature of annealing is increased the ratio of yield point to proportional limit progressively decreases. When recrystallization occurs, the ratio may continue to decrease. If, however, in the first stages of tempering, a minimum value of k is observed this is not necessarily a contradiction of our hypothesis; because the steel is a modified one, the crystals being still in a state of deformation. This agrees with Rosenhain's findings that the *transformation* can be divided into two parts (see p. 397). It is also supported by the fact that the strength of materials as will be shown later, when subjected to the action of repeated stresses does not appear to have been increased by this cold working.

Conclusions.—There appears, therefore, to be sufficient experimental data to warrant the advancing of the thought that this ratio of yield point to proportional limit can be used as an indication of internal stress in steels of similar micro-structure on the understanding that further data must be forthcoming before definite conclusions are made. It will be left to a further chapter, namely, that dealing with the characteristics of materials under cyclic variations of stress, to show the effects of these internal stresses. There we will give further experimental data which appear to substantiate, in large measure, the theory outlined here.

109. Amorphous Theory.—It will now be necessary to advance certain theories regarding the stressing effects on metals, with the view of explaining the various characteristics observed in a tensile test. This again will lead us into the field of metallurgy, but in general the engineer's point of view will be maintained. When a bar of ductile material such as low carbon steel be polished and etched on one side, and suitably arranged so that this side can be observed through a microscope, then if tensile stress be applied the following observations may be made. As long as the metal is being deformed elastically then there is no visible change. As soon, however, as the proportional limit is passed definite changes are seen. Across the previously polished faces of the crystal fine black lines appear which increase in number as the stress is increased and finally form a very close network. The approximate depth of these *minute lines* may be of the order of 1/50,000 of an inch. In the case of a ductile material, as the yield point is approached, another phenomenon will appear in the form of *Lueders' lines* (see p. 358), the difference being, however, that whereas these minute lines are of microscopic dimensions the Lueders' lines are visible to the naked eye. They are similar in the respect that both seem to be caused by slip, but whereas the strain lines can be removed by etching and occur on all crystalline materials when stressed, the lines of Lueder are not removed by etching and are best seen with materials possessing a well defined yield point. The true nature of these minute lines is now well understood, and the name "*slip bands*" has been applied to them. According to Rosenhain* their origin lies in the fact that when a crystal of such a material is forcibly altered in shape it adapts itself to the new configuration imposed upon it by a process of sliding on certain of its *crystallographic planes.* This crystal formation before and after straining is indicated in Figs. 328 and 329, respectively, which have been reproduced from the above work.

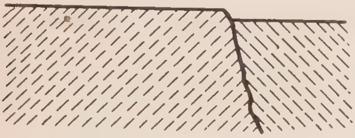

Fig. 328.—Unstrained crystal.

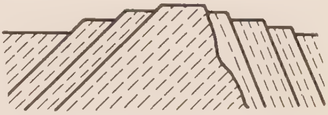

Fig. 329.—Crystal with slip bands.

If slip were the only result from applied stress then the crystalline structure of the metal would remain unaltered by such. It has been shown, however, that a metal is hardened by strain (paragraph 103), either applied by cold working or by successive loading and unloading in a testing machine. There must be something more, and this is where we encounter the amorphous theory first put forward by Beilby,† and developed by Rosenhain. Just as the rubbing action of polishing

* Rosenhain, "Introduction to Metallurgy," p. 243, 2nd Ed., 1919.

† Beilby, *Roy. Soc. Proc.*, No. 72, 1903; No. 82, 1909. *Inst. Met. Jour.*, Vol. 2, 1911.

Beilby, "Aggregation and Flow of Solids," p. 123, 1921.

produces on metal surfaces a thin layer of *amorphous material* so a similar disturbance of the molecules may be expected to occur on the adjacent slip planes of a crystal. This amorphous material will increase with the degree of stress applied. At first these layers will possess mobility but after a time the disturbed molecules will have had time to set, so that on each slip plane a layer of hard non-plastic amorphous metal is present. As long as the amorphous material possesses mobility, deformation may be caused much easier, which is to be expected. This is in complete agreement with what we have seen regarding the lowering of proportional limit by overstrain. This material, being like a *cement*, will set after elapse of a period of time, and this will explain the recovery of elasticity in an overstrained material. Furthermore, since it is assumed to be a hard non-plastic material, when in this condition, it will require higher stress values to cause yielding. This is in accord with the higher yield point obtained after recovery. It can also be expected that the temperature will affect greatly the conditions of solidification of this cement.

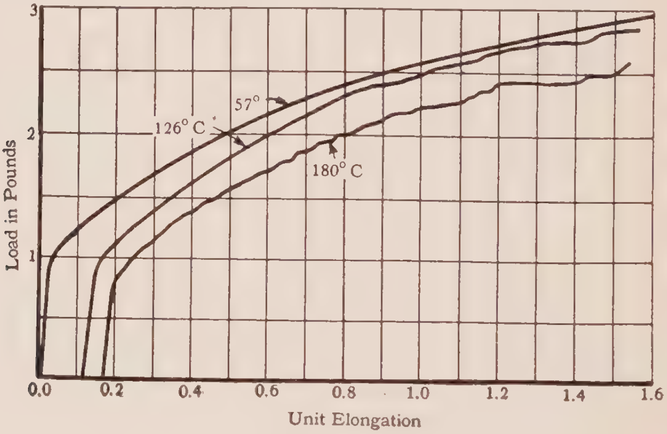

Fig. 330.

A very interesting paper confirming this setting process was contributed by deForest,* in which it was shown that if plastic deformations are made at temperatures above the normal, the amorphous material by "setting" faster, together with the high temperature reducing the *viscosity* of the amorphous material, will produce a wavy diagram, while at normal temperature it will be smooth. In Fig. 330 is shown this effect for annealed phosphor bronze wire, the time of loading being the same for each test, 3½ minutes.

---

* deForest, Some Experiments on the Plastic Elongation of Wire, *Amer. Soc. Test. Mat. Proc.*, 1916.

In Fig. 331 are shown the diagrams for the same material, the time of testing being increased to 16½ minutes.

This therefore represents the explanations put forward by the metallurgist as an explanation of the effects of overstrain. It is difficult for the engineer to comment on such a subject because even in best informed metallurgical circles there is divergence of opinion regarding them. All that can be done is to discuss the subject in the light of physical test results. On this basis there seems to be experimental evidence to support the theory that a material after overstraining has suffered a change in the crystal *orientation*, which makes it more and more difficult for slip to occur due to stress applications. The amorphous theory appears to be a logical explanation of this phenomenon shown by the tensile test.

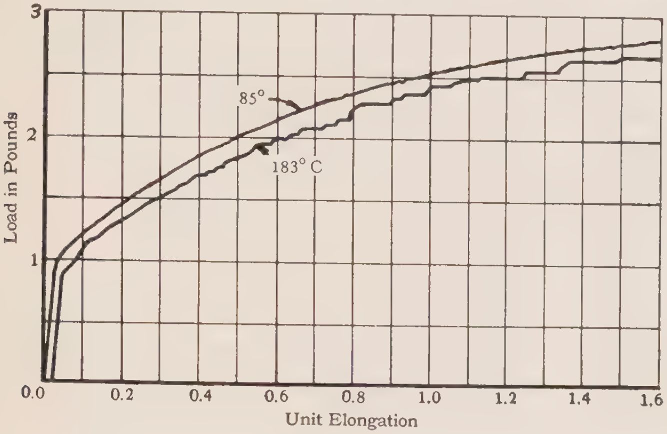

Fig. 331.

CHAPTER XIV

IMPACT TESTS

110. *Importance of Dynamic Tests.*—In the preceding chapters discussion was made of the testing of materials under *static* conditions only. In order to have a true perspective in the application of materials a knowledge of the static characteristics is not sufficient and in this chapter we come to a discussion of one of the *dynamic* forms of testing, namely, that of impact.

It was shown in paragraph 95 of Chap. XII that while the time of duration of the tensile test, for the ordinary speeds adopted, appears to have little influence yet when the time factor is varied in great degree, a decided change in the characteristics of materials could be expected. Since this is true for different speeds of testing in tension, it can be safely assumed that when the time effect is shortened in an enormous degree as in the impact test, characteristics not shown by the tensile test will stand revealed. This is in accordance with actual experimental fact, and while there is great divergence of opinion as to what high resistance to impact really means to the designer, it is generally accepted that the impact test shows characteristics which the static forms fail to do.

Un-notched Bar Tests.—A certain amount of investigation has been done on impact by using *un-notched* specimens. Hatt* in his contribution concluded that for steels there is very little difference in the total elongation and the *unit work* to fracture, whether this occurs in 10 minutes or 0.01 seconds. Stanton† and Velikhow‡ have since shown that the results obtained under unnotched tensile impact are substantially the same as those obtained under static tensile tests. The important fact is that this test enables a study of the material under impact to be made without recourse, as will be seen later, to a *notch* or *groove* in the specimen. While tests of such nature will, when developed, be expected to yield beneficial results, as far as stress measurement is concerned, the fact is at present they are not extensively used commercially. One point is that they require very large machines which raises the possibility of errors appearing in the results. This fact was discussed by Davidenkoff[*] who suggested a special method of supporting the test bar in order to lessen this possibility of error.

---

* Hatt, Tensile Impact Tests, *Amer. Soc. Test. Mat. Proc.*, Vol. IV, p. 282, 1904.

† Stanton & Bairstow, Resistance of Materials to Impact, *Inst. Mech. Eng. Proc.*, Nov., 1908.

‡ Velikhow, Notes on Rupture under Longitudinal Impact, *Inter Assoc. Test. Mat. Proc.*, 1909.

Importance of Stress Measurement.—It will be shown fully in the next paragraph that the shock testing of constructional materials has been developed in an empirical manner and consequently the results obtained are not strictly comparable for different materials. This is undoubtedly due to the fact that very little if anything is known regarding the magnitude of the stresses occurring during impact. Development along this line is now receiving attention, however, and several interesting contributions have been made to the literature. Plank[†] in his work discussed the fundamentals of the subject. He showed that the phenomenon of rupture in the tensile est was entirely different from that in the impact tensile test. In

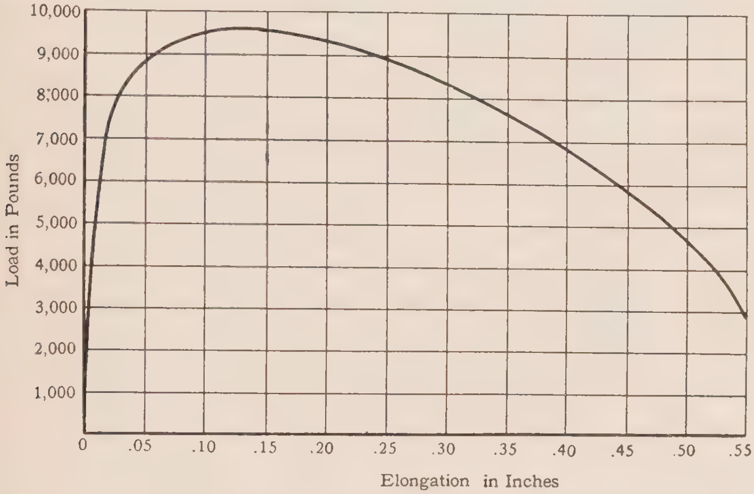

Fig. 332.—Impact tensile test diagram.

---

[*] Davidenkoff, Investigation on Tensile Impacts, *Inter. Assoc. Testing Mat. Proc.*, 1912.

[†] Plank, Betrachtungen uber dynamische Zugbeanspruchung, *Forschungsarbeiten*, Vol. 133, 1913.

the static test there is a gradual increase of force while in the dynamic test the force increases suddenly to a maximum and then decreases. In Fig. 332, a typical stress strain diagram obtained by him is shown. The weight in this case was 25 kg. and the drop 2 metres, the bar 235 mm. long over the gauge length and 10 mm. diameter not being fractured.

He also made measurements of the forces occurring in the material by obtaining, from a suitably arranged chart mounted on a rotating drum attached to the impact machine, a *space time diagram.* A double differentiation of this diagram gave the magnitudes of the forces occurring during impact, as shown in Fig. 333.

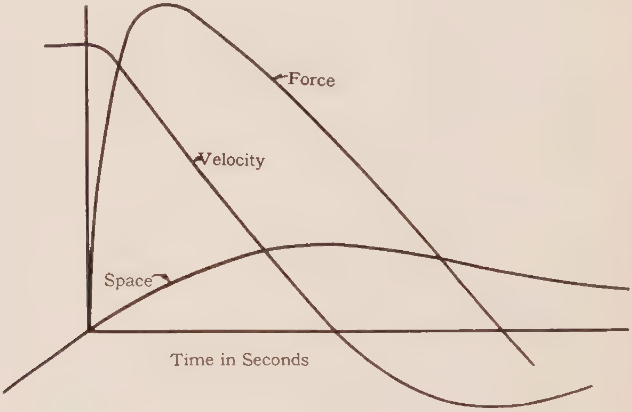

FIG. 333.

He found in this manner that the yield point under dynamic loading was 4,000 kg. per sq. cm. for low carbon steel, whereas under a static tensile test it was 3,000 kg. per sq. cm. with an ultimate stress of 4,500 kg. per sq. cm.

He further concluded that the tensile force in the bar could be stated completely by two terms, one representing the *elastic force* calculated in the usual manner and the second depending on the rate of deformation which he called the *friction effect.*

$$P = p + \Phi \frac{dx}{dt},$$

where P = force in kgs. per sq. cm.
p = elastic force in kgs. per sq. cm.
x = elongation in cms.
Φ = constant, depending on the properties of material.

At the beginning when the velocity is high the second term seems to explain that the friction has a great effect in assisting the material to resist deformation. This indicates further that due to the friction the maximum elastic force is less than the complete tensile force and gives some explanation of the discrepancy between the static and dynamic yield point previously mentioned. Seehase* made also a contribution to the subject along similar lines. It will be observed that this method of measuring forces requires the differentiating of space-time, and velocity-time curves. Since the velocity varies rapidly during the test it is therefore to be expected that large errors are possible. Margerum† dwelt on this point and sugggested a method whereby the maximum load might be found by obtaining indentations on a *calibration bar* attached to the moving head of the impact machine, and suggested using this in conjunction with an autographic stress strain diagram. Elmendorf‡ also appreciated this fact because in his experiments on the impact of wooden beams under transverse loading he employed a special type of instrument to obtain the necessary differential curves. While this may be an improvement, the method of obtaining force from a space time curve is open to criticism.

Some work has been done on the method of measuring directly the maximum forces occurring at impact, and in this respect Kreuger's§ work is worthy of consideration. In this case the falling weight strikes the test bar through the medium of a steel ball suitably located on a calibration bar. From a measurement of the diameter of the circle of contact the maximum forces can be computed. Very few results have, however, been obtained by this method.

It is therefore apparent that no really satisfactory method of measuring stresses at impact has yet been developed and while it will have been appreciated from this discussion that much has been done, a great deal of development still remains to be done before we understand all about the impact test.

111. Notched Bar Tests.—*Scope.*—In the preceding paragraph some consideration was made of impact tests made on unnotched bars but now we come to a study of an entirely different type in which the position of fracture is predetermined by a notch or groove cut in the specimen. The presence of the notch has given rise to the thought* that this form of shock testing is an attempt to determine how easily a crack may be propagated through a material. The fact that in such tests fracture is obtained in a definite location and with practically the entire localization of the contraction to the region of fracture a *new field* is at once opened up whereby we are able to study the characteristics of materials.

---

* Seehase, Die experimentelle Ermittlung des Verlaufes der Stosskraft, *Forschungsarbeiten*, Vol. 182, 1915.

† Margerum, Measurement of Pressures Caused by Impact, *Amer. Soc. Test. Mat. Proc.*, 1922.

‡ Elmendorf, Stress in Impact. *Jour. Franklin Institute*, p. 771, Dec., 1916.
Elmendorf, *Amer. Soc. Test. Materials Proc.*, 1922.

§ Kreuger, Apparat zum Messen von Stossen, *Bauingenieur*, Vol. 4, 1921.

The development of this form of test has been largely the work of French investigators. Barba in 1900 was the first to contribute to the literature, certain of his tests being confined to flat specimens. By fixing the test bars in a horizontal position and using a falling weight of 18 kilograms, certain conditions of *brittleness* were detected. It was then generally agreed that this form of test gave results which were not observed by the tensile test. In 1901 LeChatelier, Charpy, and Fremont† made further contributions to the subject. In 1903 Izod‡ introduced his impact testing machine. In 1907 the German Association for Testing Materials recommended the adoption of the Charpy form of test with a test bar 30 mm. × 30 mm. × 160 mm., the notch being as shown in Fig. 334. This was discussed at the Interna-

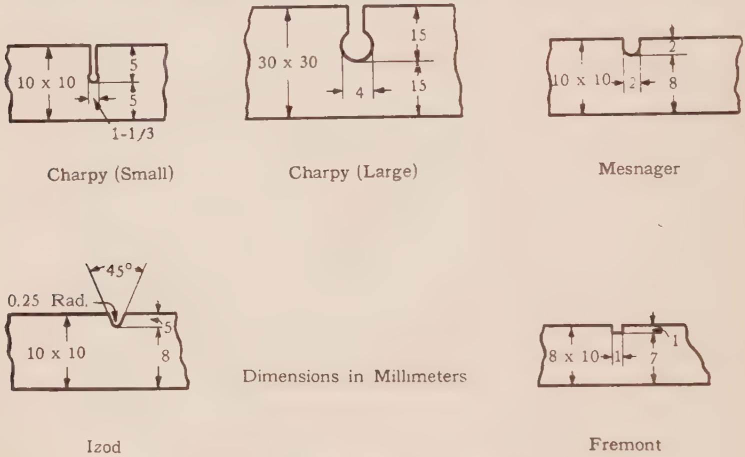

Charpy (Small) Charpy (Large) Mesnager

Izod Fremont

Fig. 334.—Standard notch forms.

---

* Hadfield, Shock Tests and Their Standardization, *Inst. Civ. Eng. Proc.*, p. 127, 1920.

† *Proc. Inter. Assoc. Test. Mat. Proc.*, 1901.

‡ Izod, *Engineering*, Sept. 25, 1903.

tional Association of Testing Materials in Copenhagen in 1909, where a smaller specimen being one-third of the size of the larger but *geometrically similar* to it was also suggested as an alternative. The notch of this smaller test bar is also shown in Fig. 334. Confirmation of the acceptance of these forms was made at the New York meeting of this Congress in 1912. Today the Izod and the Charpy types are standardized in England and in Germany, respectively.

In Fig. 334 the standard notch forms for the chief *notched bar* tests are given. It will be noted that all the notches excepting the Charpy forms must be produced by milling. The question of choice of a particular type of notch must largely depend on the accuracy with which the form can be reproduced. In all these tests two values are usually recorded, namely, the amount of *energy* required to fracture the test bar and, in the cases where the fracture is not complete, the *angle* through which the bar is bent. It will therefore be seen that in its present form the test does not give fundamental data which can be applied directly to design. Too little is known regarding the fundamentals of the test. The theory of Fillunger* in this direction however forms a very important contribution. According to this authority the total energy to fracture can be completely expressed by two terms, one containing a value of 2ω depending on the resistance of the material to *fracture*, and another containing a value δ involving its resistance to *deformation* together with a value y, the eccentricity of the notch (see Fig. 335). He concluded from this work that structural steels which are exposed rarely to high stresses and which do not have sharp corners should have a high δ. If, however, sharp corners cannot be avoided then a high value of 2ω is important. This work emphasizes the importance of geometrical form which will be subsequently considered. While the test, with our present knowledge, is only a relative one this does not mean that it has not a real value, although it may be an

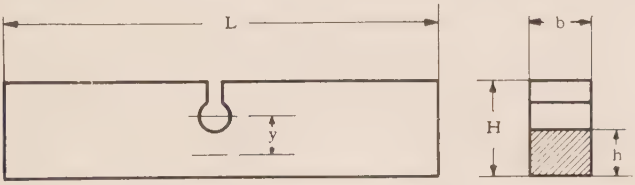

FIG. 335.

---

* Fillunger, Notched Bar Impact Tests, *Testing*, Vol. 1, Jan., 1924.

indirect one to the designer. The fact that the test is in its present form, however, has laid it open to certain criticisms. Hatfield,* on the basis that most of the energy is absorbed after the proportional limit has been passed, seemed to believe that it was of very little use in the selection of material. This of course seems to be an entirely false premise, since on this basis the ductility values obtained from the tensile test would be likewise of no value. We do know that these ductility characteristics in the case of localized stresses are of great value, and this must also be true of the notched bar test results.

We therefore come to a consideration of these notched bar tests and will discuss in the first place some of the governing factors which influence the results, and then review some of the available numerical data.

Effect of Dimensions.—The dimensions of the test bar play a very important role in the values obtained from notched bar tests. It is now well known that the energy to fracture does not depend on the square of the linear dimensions nor does it depend on the cube of these dimensions. The relation is more complex and the energy seems to depend on some intermediate value between the square and the cube.† Referring to Table LII which represents data obtained by Batson‡ on geometrically similar test bars it will be seen at once that for both steels the energy per square centimeter is too high for the larger test pieces, while the energy per cubic centimeter is too low. The variation appears to be different, however, for each steel.

TABLE LII.—IMPACT TESTS ON GEOMETRICALLY SIMILAR TEST BARS

Size of bar in millimeters	Energy					
	Steel A			Steel B		
	Kilogram-meters	Kilogram-meters per square centimeter	Kilogram-meters per cubic centimeter	Kilogram-meters	Kilogram-meters per square centimeter	Kilogram-meters per cubic centimeter
10 × 10 × 53.33	4.77	5.96	0.89	1.28	1.60	0.24
30 × 30 × 160	60	8.33	0.42	36.3	5.04	0.25
63 × 63 × 336	296	9.32	0.22	197	6.20	0.15

---

* Hatfield, Discussion of Notched Bar Tests, *Inst. of Automobile Eng. Proc.*, Vol. 12, p. 346, 1917.

† Stribeck, Kerbschlagprobe, *Z. d. Ver. deutsch. Ing.*, Jan., 1915.

‡ Batson & Hyde, "Mechanical Testing," Vol. 1, p. 318, 1922.

The original belief that the resilience of different specimens followed strictly the similarity law allowed the standardization of two forms of Charpy* test bars (see Fig. 334). It now appears that this was scarcely justifiable because, in line with the above results, we now know that the values obtained from these two types are not strictly comparable.

Hadfield† has stated the belief that the fact that the energy does not depend on the cube of the linear dimensions is probably due to speed effect. In making tests it therefore seems necessary to conform to the same dimensions of test bar if strictly comparable results are required. Further development in the subject will be necessary before we can afford to go very far from this method of determination.

Effect of Speed.—There appears to be a difference in opinion in regard to the effect which speed of impact has on the results obtained. Charpy,‡ in an elaborate series of tests, showed that the velocity of impact has no effect, but this was not entirely accepted by Hadfield§ who believed that in order to detect brittleness in low carbon steels a higher velocity of impact than is usually met with in commercial machines is necessary. In the contribution by Hadfield he showed that at velocities of 1,700 ft. per sec. even unnotched badly treated steel will show a crystalline fracture, whereas properly treated steel will not.

McAdam‖ appears to believe that the results of Charpy settle the question of speed effect and that within the limits used in ordinary testing the striking velocity has no influence on the results. Further data given by Batson¶ seems to confirm this belief. With these conclusions the author agrees.

It therefore appears that in making impact tests on materials all that is necessary is to keep the velocity of impact constant. In the Table LIII below are given these velocities for the standard machines used.

---

* *Inter. Assoc. Test. Mat. Proc.*, 1909.

† Hadfield and Main, Shock Tests and Their Standardization, *Inst. Civ. Eng. Proc.*, 1920.

‡ Charpy and Cornu-Thenard, New Experiments on Shock Tests, *Iron & Steel Inst. Jour.*, 1917.

§ Hadfield and Main, Shock Tests and Their Standardization, *Inst. Civ. Eng. Proc.*, 1920.

‖ McAdam, Impact Tests of Metals, *Amer. Soc. Test. Mat. Proc.*, 1922.

¶ Batson & Hyde, "Mechanical Testing," Vol. 1, p. 309, 1922.

TABLE LIII.—IMPACT VELOCITIES

Type of machine	Velocity at impact,* meters per second	Energy, kg.m.
Charpy (small)	5.3	30
Izod	3.5	16.6
Fremont	8.85	60
Guillery	8.85	60

* NOTE: It must also be observed that the velocity of fracture is of importance.

Effect of High Temperature.—There is considerable data available on the effect of high temperature on the impact values of steels. Charpy* has shown that for steel the energy absorbed in fracture increases with increase of temperature and reaches a maximum at about 150°C. It then decreases to a minimum between 400°C. and 500°C. and then rises again. By far the most important contribution to the literature, however, was that made by Langenberg.† The curves given in Figs. 336 and 337 are reproduced from this work.

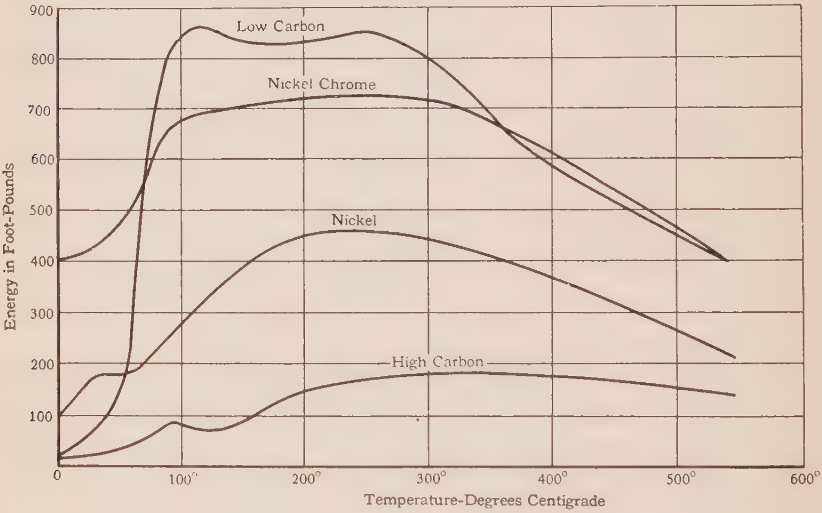

FIG. 336.—Impact test properties of annealed steels at high temperature.

---

* Charpy, *Bull. Soc. Ing. Civ.*, Vol. II, p. 562.

† Langenberg, Behavior of Certain Steels under Impact at Different Temperatures, *Carnegie Mem. Iron & Steel Inst.*, p. 75, 1923.

In this case the larger Charpy type of test bar (see p. 422) was employed and tests were made on six different steels, three of which were plain carbon, the other three being alloy steels. It will be apparent from an examination of these curves, four of which are shown, that the impact value increases with increase in temperature for all the steels although, between certain ranges of temperatures, decreases were observed. Langenberg concluded that for the annealed condition the alloy steels were more susceptible to this increase for the lower ranges of temperature than the carbon steels. Furthermore the impact values between 0°C. and 40°C. for the alloy steels, as annealed, were uniformly higher than those for the annealed carbon steels.

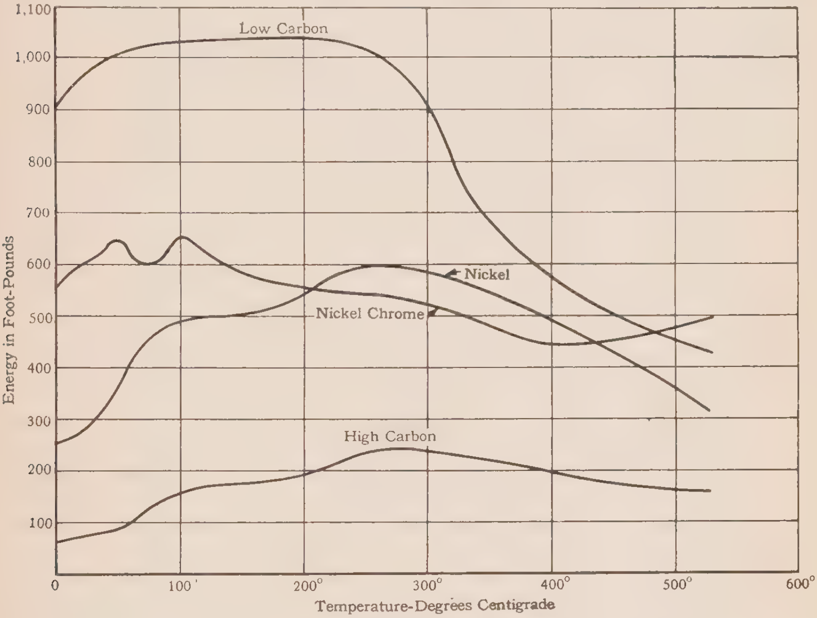

Fig. 337.—Impact test properties of heat-treated steels at high temperature.

Carbon Steel Results.—A great deal of information is now available on the results obtained from notched bar single blow tests. Those given here refer entirely to the Izod type of test (see Fig. 334).

In Fig. 338 are shown the impact values for a low carbon steel hardened in water at 900°C. and tempered as indicated according to Aitchison.* The corresponding tensile test results for the quenched material and also when drawn at 600°C. being given in Table LIV.

* Aitchison, "Engineering Steels," 1921.

TABLE LIV.—TENSILE PROPERTIES OF 0.14 CARBON STEEL QUENCHED IN WATER 900°C. (1⅛ INCH) AND TEMPERED

Tempering temperature °C.	Yield point, pounds per square inch	Ultimate stress, pounds per square inch	Elongation, %	Reduction, %
. . .	56,000	76,000	33	70
600	53,700	71,500	37	73

In Fig. 339 the results for a medium carbon steel are given. This steel had been hardened in water at 850°C. and tempered at various temperatures. The corresponding tensile test results are given in Table LV. The characteristics of another carbon steel of still higher carbon content are shown in Table LVI and in Fig. 340.

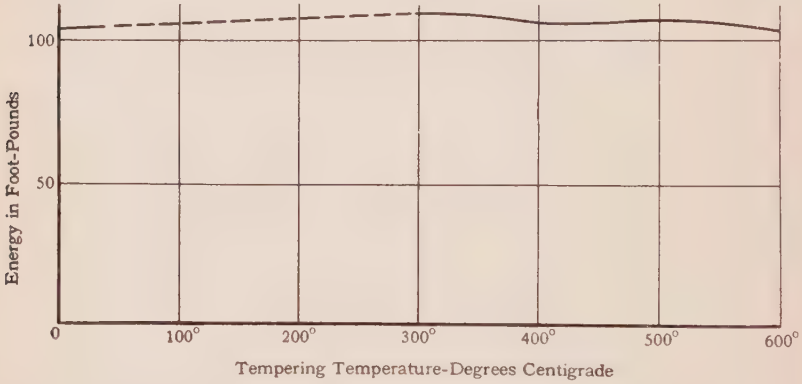

FIG. 338.—Notched bar properties of low carbon steel. C 0.14 Si 0.07 Mn 0.44.

TABLE LV.—TENSILE PROPERTIES OF 0.31 CARBON STEEL HARDENED IN WATER 850°C. (1⅛ INCH) AND TEMPERED

Tempering temperature	Yield point, pounds per square inch	Ultimate stress, pounds per square inch	Elongation, %	Reduction, %
. . . . . .	79,000	114,000	16	42
700°C.	58,000	84,400	28.7	62

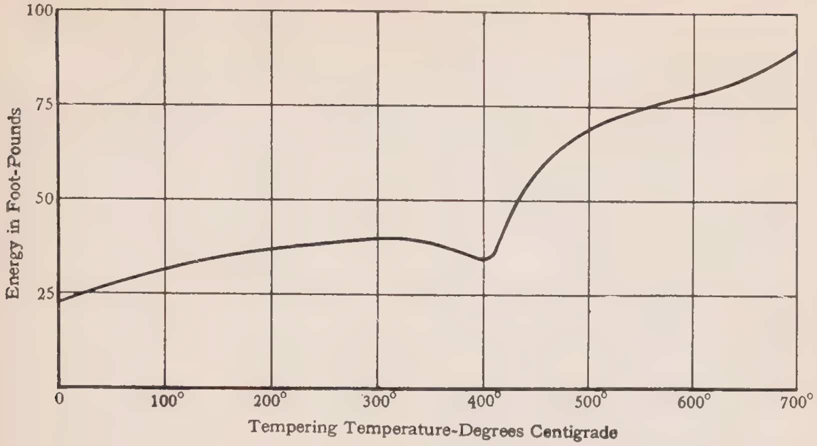

FIG. 339.—Notched bar properties of medium carbon steel. C 0.31 Si 0.11 Mn 0.58.

TABLE LVI.—TENSILE PROPERTIES OF 0.45 CARBON STEEL HARDENED IN WATER 870°C. (1⅛ INCH DIA.) AND TEMPERED

Tempering temperature	Yield point, pounds per square inch	Ultimate stress pounds per square inch	Elongation, %	Reduction, %
. . . . . .	100,000	145,000	11	28
700°C.	67,200	94,000	27	66

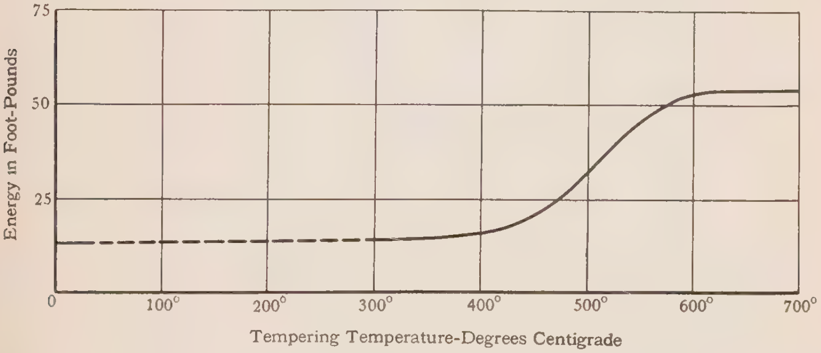

FIG. 340.—Notched bar properties of medium carbon steel. C 0.45 Si 0.25 Mn 0.75.

These results are, in general, characteristic for carbon steels. It will be noted that for the low carbon steel the impact value is more or less constant and that this is high compared with those for the other steels. This fact shows that there is no advantage obtained by heat-treating such material, a point which has been previously considered in Chap. XII, p. 375. For the other two steels considered the increase in impact value with increase in tempering temperature arising from a reduction in hardness is very appreciable. Another important point to note is that while increase in impact value, in general, corresponds to increase in ductility, as measured by reduction of area, there is no simple relation existing between them. For the low carbon steel a reduction of area value of 73% corresponds to an impact value of 104 ft. lbs.; whereas for the 0.45 carbon steel the reduction of area is 66% for an impact value of only 54 ft. lbs. This fact emphasizes the importance of Fillunger s* work previously discussed and shows that the impact values, obtained from the test in its present form for different steels, cannot be compared if these steels differ widely in chemical analysis.

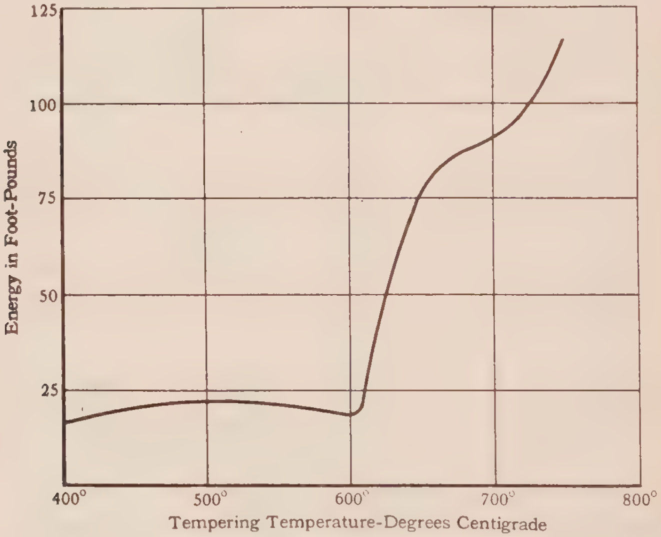

Fig. 341.—Notched bar properties of chrome-vanadium steel. C 0.42 Cr 1.04 Va 0.15 Mn 0.75.

Alloy Steel Results.—Having considered the characteristic carbon steels we now come to a discussion of certain alloy steels. In Fig. 341 are shown the impact values for a chrome vanadium steel and in Table LVII are given some of the corresponding tensile test results.

---

* Fillunger, Notched Bar Impact Tests, *Testing*, Vol. 1, Jan., 1924.

TABLE LVII.—TENSILE PROPERTIES OF CHROME-VANADIUM STEEL HARDENED IN OIL 870°C. (1⅛ INCH DIAMETER) AND TEMPERED

Tempering temperature	Yield point, pounds per square inch	Ultimate stress, pounds per square inch	Elongation, %	Reduction, %
400°C.	154,000	186,000	13.5	55
750°C.	90,000	103,000	30.5	70

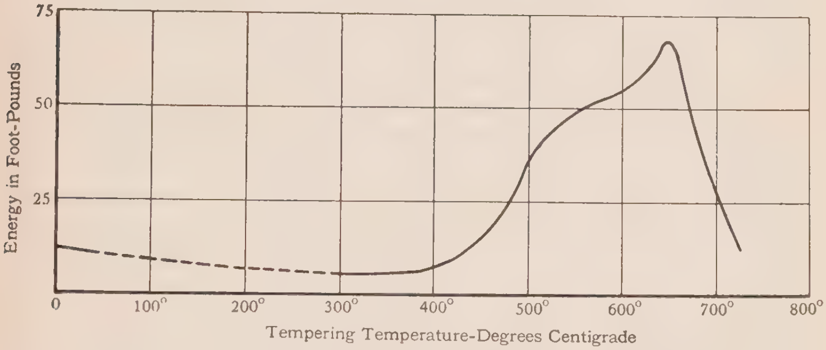

FIG. 342.—Notched bar properties of nickel chrome steel. C 0.32 Ni 3.37 Cr 0.93 Mn 0.48.

Figure 342 shows the impact values for an oil-hardened nickel chrome steel, certain tensile test results being given in Table LVIII.

TABLE LVIII.—TENSILE PROPERTIES OF NICKEL CHROME STEEL HARDENED IN OIL 820°C. (1⅛ INCH DIAMETER) AND TEMPERED

Tempering temperature	Yield point, pounds per square inch	Ultimate stress pounds per square inch	Elongation, %	Reduction, %
....	242,000	255,000	13	29
650	107,000	134,000	21	62

These curves have all been plotted from the data obtained by Aitchison.* In Fig. 343 and Table LIX are shown the impact and tensile results, respectively, obtained for an air hardened nickel chrome steel according to the Steel Research Committee Report† to which further reference should be made, since the work is a comprehensive one.

---

* Aitchison, "Engineering Steels," 1921.

† *Report of Steel Research Comm. Inst. of Automobile Eng.*, 1920.

TABLE LIX.—TENSILE PROPERTIES OF NICKEL CHROME STEEL HARDENED IN AIR 820°C. (1⅛ INCH DIAMETER) AND TEMPERED

Tempering temperature	Yield point, pounds per square inch	Ultimate stress pounds per square inch	Elongation, %	Reduction, %
......	200,000	244,000	10	39
650°C.	103,000	125,000	25	66

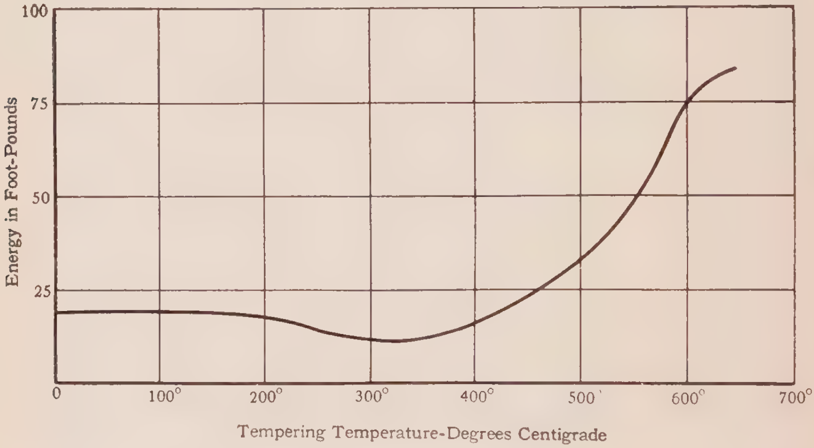

FIG. 343.—Notched bar properties of nickel chrome steel. C 0.32 Ni 3.7 Cr 1.42 Mn 0.46.

A comparison of Figs. 342 and 343 will show that what was true as regards the test as a basis of comparison for different carbon steels is also true for alloy steels, because at 650°C. the ductility properties are substantially the same whereas the impact values are much higher for the air-hardening steel. There is another point which is evident from these curves, namely, the drop in impact value which occurs when the tempering temperature is in the region of 350°C. This is a very important phenomenon, to the consideration of which, we now come.

Notch-brittleness.—Another characteristic shown by the notched bar test (and this test appears to be the only one which does show it) is that now known as *notch-brittleness.* Referring to Figs. 342 and 343 for nickel chrome steels it will be observed that there is a *critical range* of temperature within which the impact figure falls considerably. This phenomenon is now well known and has been observed on other steels by various investigators, many contributions having been made to the literature of the subject. If the material be quickly cooled through this range of temperature, instead of being slowly cooled, this notch brittleness entirely disappears. Hadfield* stated that it is met with in low carbon steel (0.12 carbon) and showed that in the one case where the steel was quenched and drawn the test bar which was of the Fremont type bent double, but yet when this same material was overheated and slowly cooled from 1,200°C. it only bent 1° before fracture. A very good contribution on this subject was that made by Greaves and Jones.† In this the authors stated, what is generally known, that this phenomenon of temper-brittleness is not shown by the tensile test or by a slow bending test. In other words, the stresses applied to the steel have to be highly localized. They further concluded that if a minute flaw or inclusion exists in a test bar stressed uniformly even in tension, a steep gradient of stress will result, giving a low elongation value. In other words, the low impact value obtained on such temper brittle steels, which show normal ductility tested in tension, could conceivably be very dangerous if localized stresses due to machining or impurities are encountered in service. Other published data on the subject‡ have shown that in certain cases forgings which had fractured in a very peculiar manner gave very low impact values from subsequent tests. Again, in commenting on certain failures which had occurred in boiler plate, Rosenhain§ stated that experience had repeatedly shown that materials which gave a low figure under impact were liable to fail under apparently static conditions.

It can readily be seen that this characteristic of the notched bar test in being able to detect brittle materials must on this basis alone go a long way to making the test a standard one.

Appearance of Fractures.—Due to the method of fracturing in a notched bar test a new means is provided for examining the structure of the material. It is well known that the appearance of a fractured tensile test bar is a valuable adjunct to the numerical data obtained from the test. Nevertheless, due to the fact that large deformation occurs before fracture, the appearance of the crystals is entirely masked. This is otherwise in the notched bar test. Here the fracture is highly localized and an opportunity can be had of examining the crystalline state of the material. Any slight variation in the heat-treatment might only cause a slight reduction in the tensile test results and pass unnoticed. It is otherwise with the notched bar fractures because any slight change in the heat-treatment will be readily seen from the fractured ends of the broken test bar. It has been noted by the author that certain nickel chrome steels when properly heat-treated would give say 17% elongation on a 0.5 inch diameter test bar having a gauge length of 2 inches, when tested in tension, and would show a non-crystalline notched bar fracture, but if defectively treated the elongation would drop by 1 or 2% while the impact test bar would then show a decided crystalline center. Langenberg* in his work gave some interesting notched bar fractures. He also observed that a low carbon steel at 200°F. showed a notched bar fracture with a crystalline center. Nevertheless at 250°F. the crystalline structure had entirely disappeared; the energy absorbed in fracture had meanwhile only increased from 800 ft. lbs. to 840 ft. lbs. These points have been emphasized previously by the author† who feels that a very valuable tool is in this manner put into our hands for selecting materials. Although it is qualitative, and can only be applied strictly to tests on the same material, it is none the less valuable.

---

* Hadfield & Main, Impact Tests and their Standardization, *Inst. Civ. Eng. Proc.*, p. 127. 1920,

† Greaves and Jones, Temper-Brittleness of Nickel Chrome Steels, *Iron & Steel Inst. Jour.*, Vol. CII, p. 171, 1920.

‡ Rosenhain, Discussion on Mechanical Properties of Steel, *Inst. Mech. Eng. Proc.*, p. 472, May, 1919.

§ Rosenhain & Hanson, A Cause of Failure in Boiler Plates, *Iron & Steel Inst. Jour.*, Vol. XCVII, p. 316, 1918.

112. Repeated Blow Tests.—*General.*—Having dealt with those types of impact tests where fracture is carried out by a single blow we now come to the consideration of an entirely different form of test in which the characteristics of material, when subjected to the action of *repeated blows,* are examined. In this test the test bar is supported horizontally at two points and is subjected to blows from a hammer over a notch cut in the bar mid-way between the supports. The test piece is rotated 180° between successive blows which are continued until fracture occurs, the number of blows to cause failure being recorded.

* Langenberg, Behavior of Certain Steels under Impact, *Iron & Steel Inst. Jour.*, Vol. XII, 1923.

† See paper by the author: Impact Testing Methods, *Trans. Amer. Soc. Steel Treaters*, May, 1922.

In some cases,* however, the number of blows to begin the fracture are also noted. By a suitable arrangement the height of drop or weight of the hammer can be altered so that *varying* energies of blows can be obtained. Making a series of tests on different bars by altering the height of drop for each, and plotting the number of blows to fracture as abscissae and the height of drop or energy as ordinates, a curve can be obtained which gives useful information to the designer.

Certain† extensive investigations have been carried out on this method of testing. The conclusions were that with the conditions chosen, provided the number of blows was less than 500 for the particular test bar employed, the results seemed to agree with those obtained from the single blow test, and when the number exceeded 100,000 the results seemed to agree with those for *fatigue* conditions. It can therefore be concluded that this test gives impact and fatigue characteristics depending on the energy of the blow.

Results.—In this paragraph the results obtained by the author on the Stanton type of machine are discussed. In this machine the weight of the hammer is 4.71 lbs. and the form of test bar used is shown in Fig. 344. The results given in Table LX were obtained from medium carbon steel,‡ for the rolled, annealed, and normalized conditions for hammer drops varying from 2 inches to 0.4 inch. It will be noted that as the height of drop decreases, the life of the test bar, as determined by the number of blows to fracture, increases. This is in accordance with the statement given in the preceding paragraph.

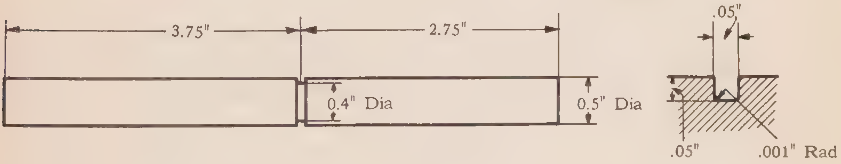

Fig. 344.—Repeated impact test bar.

---

* Müller and Leber, Beanspruchungshöhe, Korngrösse und Temperatur bei Ermüdungserscheinungen, *Z. d. Ver. deutsch. Ing.*, Apr. 14, 1923.

† Stanton and Bairstow, Resistance of Materials to Impact, *Inst. Mech. Eng. Proc.*, Nov., 1908.

‡ See Table XXXV, p. 372 for the corresponding tensile test results.

TABLE LX.—IMPACT (REPEATED) PROPERTIES OF 0.37 CARBON STEEL (ROLLED)

Height of drop in inches	Number of blows to fracture		
	Rolled	Annealed	Normalized
2	1,120	708	1,040
1½	1,690	1,070	1,560
1	3,750	2,770	4,170
0.6	11,730	7,460	12,300
0.4	28,650	65,900	32,140

In Table LXI the results obtained for the same steel* in different heat-treated conditions are given.

TABLE LXI.—IMPACT (REPEATED) PROPERTIES OF 0.37 CARBON STEEL, HARDENED IN WATER AT 850°C. (2¼ INCHES DIA. BAR) AND TEMPERED AS INDICATED

Height of drop in inches	Number of blows to fracture			
		100°C.	450°C.	550°C.
2	. . . . . .	3,430	3,000	1,490
1.5	. . . . . .	7,730	4,370	3,890
1	14,000	16,000	10,030	9,460
0.6	. . . . . .	48,500	32,200	29,660
0.4	. . . . . .	90,000	112,000	82,300

---

* See table XXXVIII, p. 375 for the corresponding tensile test results.

In Table LXII the results obtained on a carbon-vanadium steel ($C = 0.52$, $Va = 0.19$) are given, and in Fig. 345 these results are shown plotted, while in Table LXIII those obtained from steel* castings are shown.

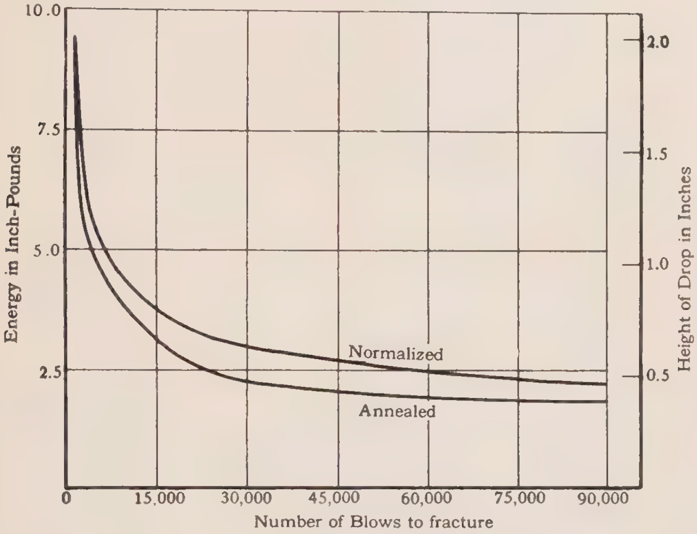

FIG. 345.—Curves of repeated impact test for carbon-vanadium steel (annealed and normalized).

TABLE LXII.—IMPACT (REPEATED) PROPERTIES OF 0.52 CARBON, 0.19 VANADIUM STEEL (FORGED)

Height of drop in inches	Number of blows to fracture	
	Annealed at 870°C.	Normalized at 870°C.
2	1,230	1,140
1½	2,290	2,780
1	4,830	7,320
0.6	17,900	37,950
0.4	69,000	132,700

---

* See Table XXXVII, p. 373 for the corresponding tensile results.

TABLE LXIII.—IMPACT (REPEATED) PROPERTIES OF 0.33 CARBON STEEL (CAST)

Height of drop in inches	Number of blows to fracture		
	Cast	Annealed	Normalized
2	676	980	2,000
1½	1,743	1,277	2,481
1	3,847	2,590	4,467
0.6	11,000	17,500	17,500
0.4	23,000	43,000	60,000

Due to the fact that when the height of drop is large the test approximates single blow conditions, and when small, fatigue conditions, it is to be expected that an examination of the fractured ends of test bars will show these conditions. Experimental results obtained by the author give confirmation to this statement; because in examining Figs. 346 to 348 which represent photographs (2¾ diameters) of test bars of medium carbon steel annealed (see Table LX) for drops of 2 inches, 1 inch, and 0.4 inch, respectively, it will be noted that each differs entirely from the others. For a 2 inch drop the fracture is almost entirely crystalline; whereas for the 1 inch drop this crystalline area takes the form of an *ellipse* surrounded by a differently orientated material. The area of the ellipse gradually decreases with decrease in drop until for the 0.4 value it has become almost a straight line. Müller,* in his contribution to the subject, examined cross-sections

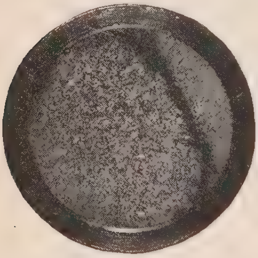

FIG. 346.—Photograph of fractured repeated blow impact test bar.

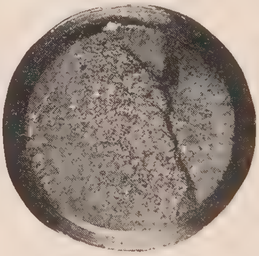

FIG. 347.—Photograph of fractured repeated blow impact test bar.

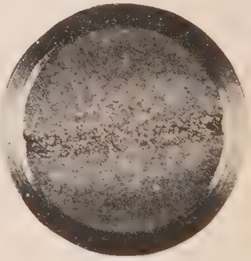

FIG. 348.—Photograph of fractured repeated blow impact test bar.

---

* Müller and Leber, Beauspruchungshöhe, Korngrösse und Temperatur bei Ermüdungserscheinungen, *Z. d. Ver. deutsch. Ing.*, Apr., 14, 1923.

of the test bars after these had been subjected to a given number of blows, and thereby determined the number to just cause commencement of breakdown. With our present knowledge, however, these fracture observations have only a *qualitative* value, being in this respect similar to those obtained from the single blow test previously discussed. This investigator realized this fully, because in the experiments mentioned the principal thought was to derive fundamental data, namely, the magnitude of the stresses occurring during impact, rather than the observing of fractures which gave supplementary information only.

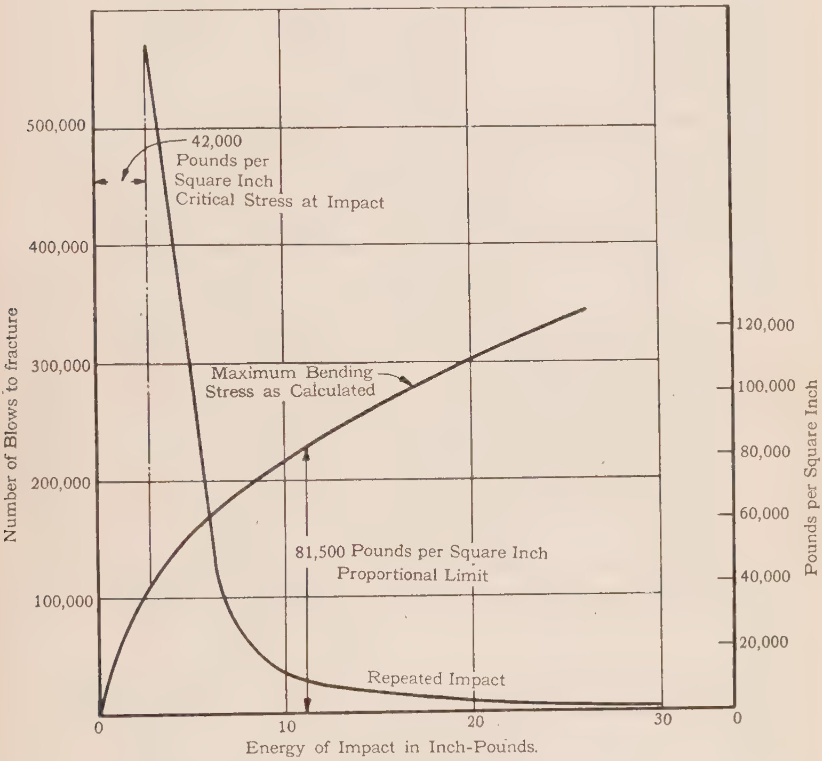

FIG. 349.—Curve of stress in a repeated blow impact test.

In Fig. 349 is shown one of the curves reproduced from this work for a nickel-chrome steel. It will be noted that the limiting stress as obtained by impact is about half of the proportional limit. This comparatively low limiting stress can be explained by the fact that the stress concentration at bending was not taken into account in the stress calculation. The important point to note is that some idea of the stresses can be obtained, and it is believed that along these lines development must take place before the test can become fundamental. These remarks do not mean that the test is not a valuable one but rather that the results, in view of our limited knowledge, must be properly interpreted. In the next paragraph we shall come to a discussion of the test results in the light of our present knowledge.

Discussion of Results.—There are several points of interest to the designer in the results of these tests. In the first place, as previously mentioned, from the ordinate of the curve (Fig. 345) some measure of the stress imposed on the material can be obtained, and if this measurement be made at a point towards the right hand side where the curve becomes approximately horizontal, then this value will represent in some measure the sresss which the material will withstand indefinitely. This point, as previously observed, was stated by Stanton, and although this will be more fully discussed in Chap. XVI, it appears proper to mention that the data given here proves this to be the case. A second point worthy of note is the fact that for intermediate heights of drop the annealed material (see Tables LX, LXII, and LXIII, and Fig. 345 for carbon-vanadium steel) always requires a *smaller* number of blows to fracture than the same material subjected to more rapid cooling. In all the materials examined by the author the only contradiction to the above was found in very low carbon steel castings. Annealing in this case raised the shock resisting properties for medium heights of drop.

Further light may be thrown on these points when more information is available on the magnitudes of the stresses occurring during impact. In making the previous statement it will be observed that the comparison was made on the same material in different states possessing more or less similarity in microstructure. This is very important because if different steels be compared on the basis of the number of blows to fracture for any single arbitrary drop without taking into consideration the region of the curve (see Fig. 345) to which this drop corresponds, very misleading conceptions may be obtained. For example, referring to Table LX, supposing we choose a drop of 0.4 inch, then on the basis of the number of blows to fracture, the annealed material will be more than 100% stronger than the rolled material. Of course the results do not imply this at all, but rather that for a 0.4 inch drop on this material we are on the part of the curve which is approaching the *asymptote*, and any small irregularity will materially change the values obtained. A similar condition will be observed in the results given in Table LXII for the same drop. In the very interesting contribution made to the subject by Müller,[*] where the relative values of different steels subjected to different energies were discussed, he concluded that the order in which the materials were put remained approximately unchanged, although the energy of the blow was, within limits, modified. This of course is a coincidence and does not in any way whatsoever change the statements previously made. In certain other contributions to the literature[†] it was concluded that there was no relation between the results of the repeated impact test and the fatigue test. Since these conclusions were made without having obtained the curve of repeated impact, as previously described, it appears that there is nothing contradictory to our previous statements.

These remarks must not be taken as inferring that repeated impact tests undertaken at a single arbitrary drop are of no value. On the contrary, if the drop be chosen so that we are working on the portion of the curve of impact corresponding to a high energy value and low number of blows, they have a very decided value as a control test for the heat-treatment of a single material, the general impact characteristics of which have been previously determined. This value as a check on the heat-treatment of steel has in the author's opinion not yet been fully appreciated. Another valuable characteristic of the repeated impact test is shown in the testing of heat-treated steels. It has been indicated by Moore[‡] that for certain heat-treated steels as the tempering temperature is reduced below 400°F., there is little change in the tensile properties with further decrease in tempering temperature and from this it can be concluded that the tensile test is not sensitive enough to detect small changes. This does not appear to apply to repeated impact because it has been shown[§] that for a nickel-chrome steel the material can withstand a maximum number of blows when it possesses an indentation hardness of 360, and further increase or decrease in the value of tempering temperature lowers the number of blows. From certain results obtained by the author on the steel of Table LXI, it appears that this is confirmed for carbon steels. With this steel, when it had been subjected to a more severe quenching effect, it was found that for the 1 inch drop the number of blows to fracture decreased from the 16,000 given in the table to 14,000. In other words, the decrease in ductility for decrease in tempering temperature is not compensated by an increase in the impact properties. The data available on this question is again meagre but the question seems to be worthy of further study.

---

[*] Müller and Leber, Beanspruchungshöhe, Korngrösse und Temperatur bei Ermudungserscheinungen. *Z. d. Ver. deutsch. Ing.*, Apr. 14, 1923.

[†] Moore and Jasper, Investigation on Fatigue of Metals, *Univ. of Illinois, Bull.*, No. 136, p. 56.

[‡] Moore and Jasper, Investigation on Fatigue of Metals, *Univ. of Illinois Bull.*, No. 136, pp. 61 and 62.

[§] Hatfield, Mechanical Properties of Steel, *Inst. Mech. Eng. Proc.*, May, 1918, p. 383.

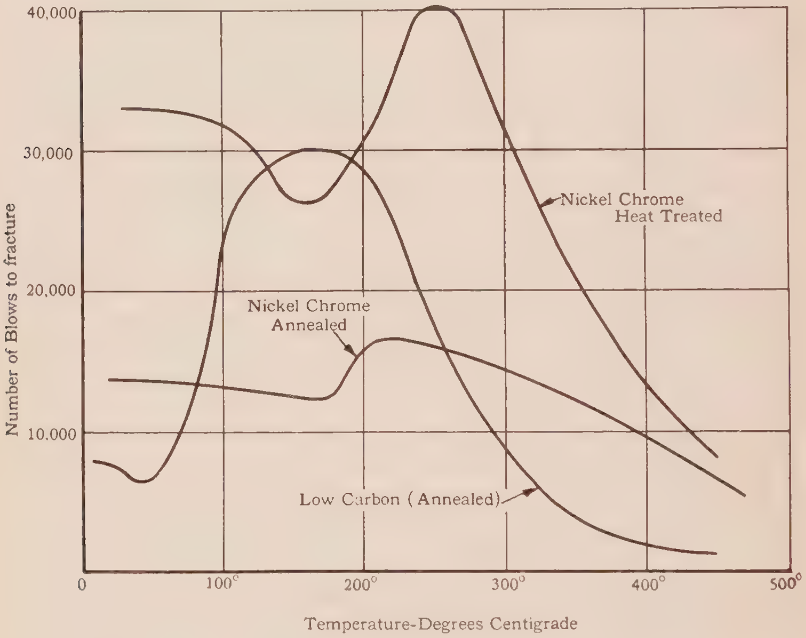

Fig. 350.—Results of repeated impact tests at different temperatures.

Effect of Temperature.—Very little information is available as to the effect of temperature on the characteristics of materials subjected to repeated blows. Müller* in his work gives some data on the subject, and the curves given in Fig. 350 are reproduced from it. The striking fact which is evident from these results is that a small increase in temperature, as has been seen for the tensile properties, may suffice to change in large measure the repeated impact properties.

---

* Müller and Leber, Beanspruchungshöhe, Korngrösse und Temperatur bei Ermüdungserscheinungen, *Z. d. Ver. deutsch. Ing.*, Apr. 14, 1923.

113. Significance of the Impact Test to the Designer.—From the consideration of impact tests it therefore appears that several important points are brought out for the designer.

The results obtained from unnotched bars are in substantial agreement with those from the static tensile test although by such a test we are able to study the deformation of materials at high speed without recourse to notches or grooves. Further development therefore is to be expected with this form of test only so far as measurement of stresses is concerned. Its development as a commercial test is not to be expected.

On the other hand, the single blow notched bar test has been reviewed in more detail. This test in its present form gives results, which, while not being like those obtained from the tensile test capable of being directly applied in design are of great relative value in the control of materials. Particularly is this true as regards the ability of the test to show such phenomenon as notch brittleness or the assistance derived in heat-treatment control by the possibility which it gives of examining the fractures themselves. The tensile test is valuable not only because it is a *fundamental test*, but also because it is the *repository* of a great deal of information acquired from its extended use. There is no doubt that when the notched bar test has been further developed and sufficient data have been accumulated, its place in all our more important material specifications will also have to be considered.

Similar with the repeated blow test, the results obtained are only of a *relative* nature. Nevertheless, in its present form the test does provide a very good method of controlling materials, and when precautions are taken to associate the results for a single height of drop with the curve of repeated impact, the value is a very real one indeed. Müller in his work suggested 12.5 kg.-cm. and Rolls Royce used 9.4 lbs. ins. as the most suitable energy for this control. Then again we have seen that when the height of drop is sufficiently small the test becomes a fatigue test. This of course is again an important point, but the discussion of this will be made in more detail in Chap. XVI.

In general, it is a safe conclusion that even in its present state of being able to provide relative data only, the notched bar test is a very valuable one to the designer and its development is important.

CHAPTER XV

HARDNESS

114. Introduction.—The term *hardness* is extremely vague in its meaning. In his Hawksley lecture, Unwin* expressed the thought that physicists doubted the existence of a definable quality such as hardness. Be this as it may, the fact remains that the term is often loosely applied. For instance we have *indentation* hardness, *cutting* hardness, and *abrasion* hardness. Unless this fact be borne in mind, there is likely to be confusion. Manganese steel, as is well known, possesses abrasion hardness in great degree, yet according to indentation methods it is relatively soft. This discrepancy apparently lies in the fact that our conceptions of hardness are not based on fundamental data. Like the impact tests previously discussed, we have in our hardness tests an unknown stress distribution, and our measurement of hardness is based on the consequences of these stresses. In other words, hardness tests are only *relative*, and since it will always be impossible to measure the unknown stresses they are likely to remain relative. Comparison of relative test data must, on these grounds, always be accompanied by decided reservations. Of course this does not mean that the hardness of materials as determined by present methods has no real value. It has a very decided value to the designer for controlling his materials and in the following paragraphs we will come to a consideration of its importance. For this purpose the discussion will be divided into three distinct parts: *indentation tests*, *dynamic tests*, and *scratch tests*, each being separately considered.

115. Indentation Hardness.—*Material Tested with Itself.*—A considerable amount of work has been done on the measurement of hardness of materials from the consideration of the volume of indentation produced in a material by a piece of the same material being pressed into it. Reaumur† did work on the subject using right-angled prisms (see Fig. 351 (a)). The axes of the prisms were arranged at right angles and the relative hardness was measured by the depth of the indentation. Foeppl* used the same method only he changed the form of the test bars from prisms to cylinders (see Fig. 351 (b)). He defined hardness as the pressure per unit area of flattened surface. Haigh† has since made a contribution to the literature in which he used square prisms (see Fig. 351 (c)).

---

* Unwin, Mechanical Properties of Material, *Inst. of Mech. Eng. Proc.*, October, 1918.

† Reaumur, "L'Art de Convertir," 1722.

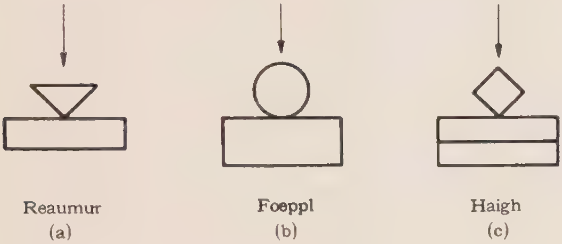

Fig. 351.

In this case, if P is the load in tons (1 ton = 2,240 lbs.) and X the width of the indentation along the edge as shown in Fig. 352, then *prism hardness* (PH) is defined as $PH = P/X^2$.

Using the ends of broken Izod notched bar test pieces, Haigh found that the prism hardness of annealed carbon steel increased from about 50 tons per sq. in. for 0.18 carbon content to 100 tons per sq. in. for 0.9 carbon content. He also found that in certain cases of hardened carbon steels fracture occurred in the process of testing, showing evidence of brittleness, the material which fractured not

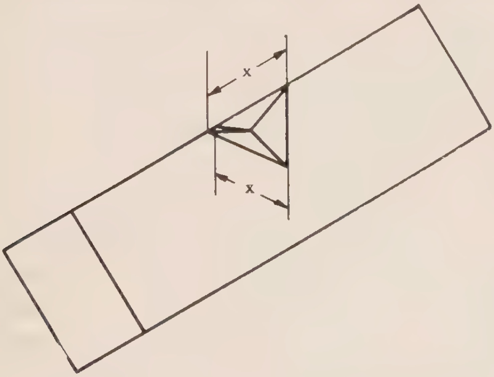

Fig. 352.—Indentation in prism test bar.

---

* Foeppl, *Ann. Phy. Chem.*, Vol. I, pp. 103 to 108.

† Haigh, Prism Hardness, *Instit. Mech. Eng. Proc.*, October, 1920.

necessarily showing the highest value of prism hardness. This evidence of brittleness may yet prove serviceable. The value in this method of hardness testing however seems to lie in the fact that it gives a uniform hardness scale in tons per sq. in. or in kg. per sq. cm. and appears to be less dependent on the incidental test conditions than in other forms, as will be seen later. Furthermore, the test appears to possess the possibility of being readily extended to give data on the hardness of metals at elevated temperatures.

Ball Method.—Hardness indentation tests were made towards the middle of last century, although it is at a comparatively recent date that they have come into general use. In 1856 the U. S. Ordinance Department* published data on the hardness of metals, based on the volume of indentation produced by a pyramidal point under a load of 10,000 lbs. It was not until 1901 when Brinell† published his work that the hardness of metals by indentation measurement commenced to receive attention from a practical standpoint. In the Brinell method, now extensively used, the hardness of a material is determined from the dimensions of the indentation produced by a steel ball being pressed into it under a given load. Brinell used the *spherical area* of the indentation as the basis, consequently if

D = diameter of ball in millimeters,
d = diameter of impression in millimeters,
P = load applied in kilograms,
h = depth of impression in millimeters,
N_b = hardness indentation number,

then $A = \text{spherical area} = \pi Dh = 1.57D(D - \sqrt{D^2 - d^2})$,

and $N_b = \frac{P}{A}$.

The load and diameter of ball specified by Brinell were:

P = 3,000 kg. for hard material,
P = 500 kg. for soft material,
D = 10 mm.

In Fig. 353 are given curves of indentation numbers for different steels according to the Steel Research Committee Report‡ previously mentioned. These values are in general what may be expected. Due to the fact that such a test measures some property of the material analogous to *flow*, the question of time of duration of test might appear important. Main* has shown however that for steels there is no difference in hardness number whether the time be 10 seconds or 2 minutes. In Table LXIV are given some of his results for steels, and it will be apparent that within the limits given the time effect is negligible. It should be noted that these remarks only apply to steels for with softer metals the case might be entirely different.

---

* U. S. Ordinance Dept., *Report on Tests for Cannon*, 1856.

† Brinell, Methods of Testing Steel, *Inter. Assoc. Test. Mat. Proc.*, 1901.

‡ *Report of Steel Research Comm. Inst. of Automobile Eng. Proc.*, pp. 10, 27, 35, 47, 1920.

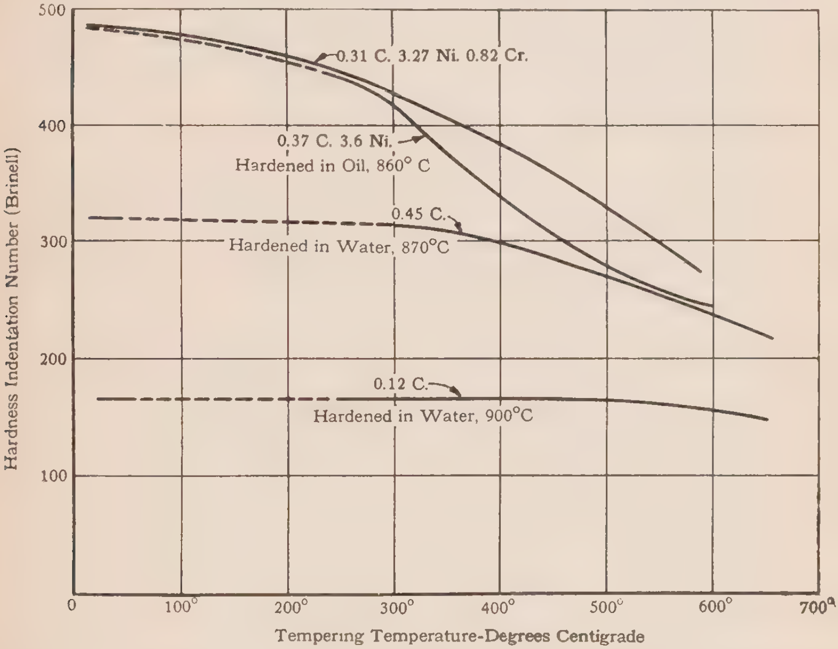

FIG. 353.—Indentation numbers for different steels quenched and tempered as indicated.

TABLE LXIV.—TIME EFFECT ON HARDNESS

Material	Pressure in kilograms	10 seconds	30 seconds	2 minutes
		Indentation hardness numbers		
Swedish Iron	3,000	86.6	86.6	86.6
Ni-Cr steel annealed	3,000	217	217	215
Ni-Cr steel hardened and tempered	3,000	340	340	335
Ni-Cr steel hardened and tempered	5,000	548	548	545

---

* Main, Discussion of Paper on Hardness Tests, *Inst. Mech. Eng. Proc.*, p. 511, Oct., 1918.

It has now been found that the hardness number is affected by the diameter of the ball and also by the pressure, and that for strict comparisons fixed values of D and P must be adopted. The contribution of Meyer* to this subject, in the light of the above statements, is a fundamental work. He concluded that the mean pressure per unit area was constant for the same material irrespective of the ball diameter, provided that d/D was kept constant. This means that the pressure per unit area was constant when indentations were geometrically similar i.e.,

$$\frac{4P}{\pi d^2} = K_1.$$

It follows that for geometrical similarity P/D^2 must be constant for the same material. This therefore enables us to extend the test on a strictly comparable basis to materials whose thickness is insufficient to enable the standard load of 3,000 kgs. to be used. Baker† using this relation has carried out some tests using balls varying in diameter from 10 mm. to 1.19 mm. A few of his results are given in Table LXV.

TABLE LXV.—COMPARISON OF BRINELL INDENTATION NUMBERS WITH DIFFERENT DIAMETER BALLS

Steel	Diameter of ball in millimeters	Load in kilograms	Brinell No.
A	10	3,000	85
	7	1,470	85
	5	750	87
	1.19	42.5	86
B	10	3,000	159
	7	1,470	158
	5	750	163
	1.19	42.5	158
C	10	3,000	306
	7	1,470	308
	5	750	310
	1.19	42.5	311

It will be observed from these results that the accuracy obtained by using this relation is sufficiently good for practical purposes.

---

* Meyer, *Z. d. Ver. deutsch. Ing.*, p. 645, 1908.

† Baker, Discussion of Batson's Paper, *Inst. Mech. Eng. Proc.*, Oct., 1918.

Batson* has since carried out tests with ball diameters up to 50.8 mm., and from these concluded that the law of comparison, $P/D^2 = K_2$, for use in accurate testing practice was sufficiently reliable. In the Table LXVI below are given the ball diameters required for different loads.

TABLE LXVI.—STANDARD LOAD FOR DIFFERENT SIZES OF BALLS

Standard 3,000 kilograms		Standard 500 kilograms	
Diameter of ball mm.	Load in kilograms	Diameter of ball	Load in kilograms
1	30	1	5
2	120	2	20
5	750	5	125
10	3,000	10	500
15	6,750	15	1,125
20	12,000	20	2,000

Although Meyers' work has broadened the scope of the ball test, the *geometrical dissimilarity* for different materals still remains. Much attention has been given the subject in order to obviate this difficulty. A very good contribution on this subject was made by Devries.† He has shown that if the depth of the ball indentation below the original surface of the specimen be taken as the basis of spherical area computation, the hardness numbers derived from this become independent of the load. Batson‡ has made use of this fact to indicate the difference in hardness obtained on four different materials by basing the hardness computations on the diameter and on the depth of the impression calculated from the original surface.

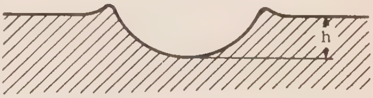

FIG. 354.—Ball impression.

Batson calculated his values as follows: $N_b = P/\pi Dh = P/31.416h$, for a ball 10 mm. diameter, where h is as shown in Fig. 354.

In Fig. 355 and 356 are given the curves obtained for the four materials for the two methods respectively.

---

* Batson, Static Indentation Tests, *Inst. Mech. Eng. Proc.*, p. 401, April, 1923.

† Devries, Methods of Hardness Measurement, *Amer. Soc. Test. Mat. Proc.*, Vol. XI, p. 717.

‡ Batson, Static Indentation Tests, *Inst. Mech. Eng. Proc.*, April, 1923.

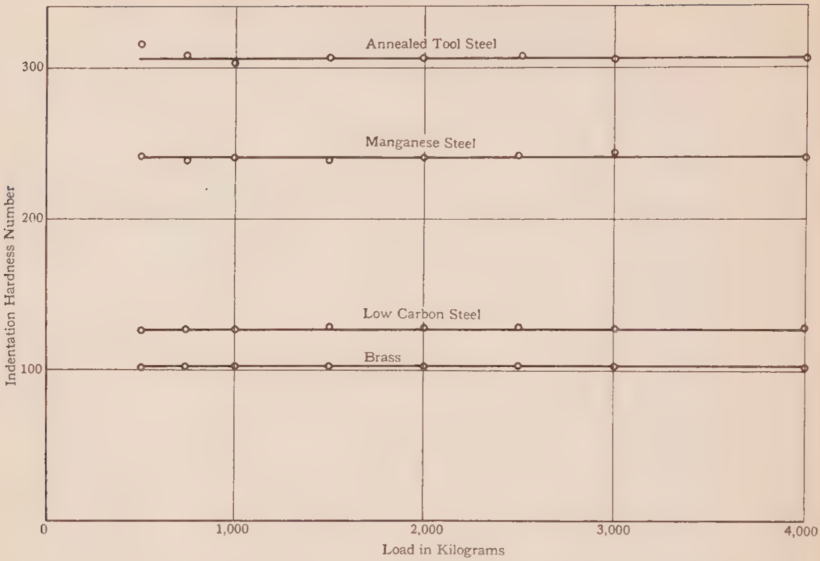

FIG. 355.—Curves of hardness numbers (based on depth *h*) for different materials.

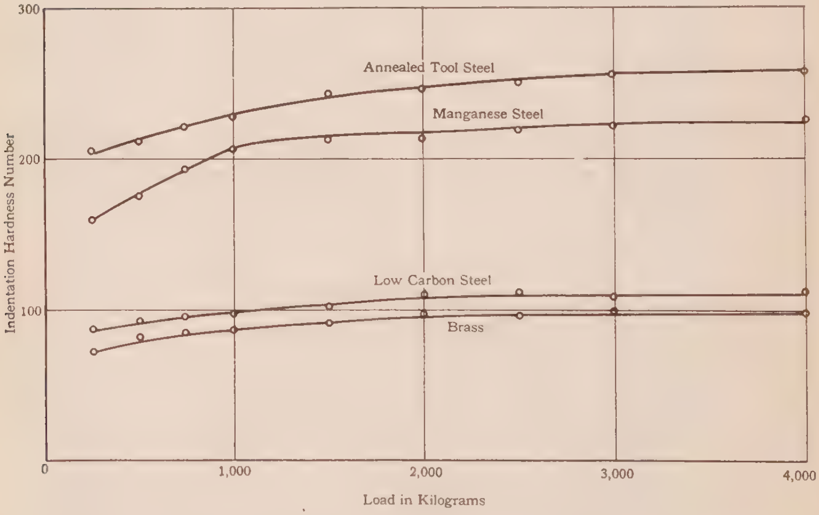

FIG. 356.—Curves of hardness numbers (based on diameter *D*) for different materials.

It will be noted from Fig. 355 as compared with Fig. 356, that the measurement of the depth h in this manner appears to make the test more uniform.

Carrington* has now extended this work to other materials and finds there is a general agreement although certain exceptions were noted.

It appears safe to conclude however that the area computed from the net depth will be more in accordance with the law of geometrical similarity than when computed from the diameter. The hardness number derived from the net depth therefore cannot be affected by load to the same degree and appears to be worthy of our consideration.

Cone Method.—We have seen that hardness values deduced from the indentation of a ball are influenced by the magnitude of the load and the diameter of the ball. This variation is due to the fact that the indentations are geometrically dissimilar. In order to overcome this defect, Ludwick† recommended the use of a right angled cone instead of a ball. The indentations from the cone are geometrically similar, and hence the hardness numbers are to a large extent independent both of the load and indentation radius.

Using the previous notation, if

P = load applied in kgs.,
d = diam. of impression,
N_c = hardness number,

then

$$N_c = \frac{P}{\frac{\pi d}{2} \times \frac{d}{\sqrt{2}}} = 0.9 \frac{P}{d^2} \text{ (approximately).}$$

The hardness number in this case, due to the impressions being geometrically similar, are said to be independent of the load employed. There is a difficulty encountered however with hard materials, due to the point of the cone not being able to withstand the pressure. This led Unwin‡ to suggest a truncated cone which, although giving dissimilar indentations, would still with moderate truncation be better than the ball test. In the contribution by Batson§ in which he discussed the results obtained from the cone test, he concluded that the hardness number calculated from the conical area of impression was approximately constant, but those obtained from the net depth of the impression varied with the load. This, as we have seen, is the opposite from what was obtained by him for the ball tests, and shows that it is impossible to fix a definite ratio between the results of the ball and of the cone for all materials.

---

* Carrington, Brinell Identations, *Engineering*, May 9, 1924.

† Ludwick, Hardness Tests, *Inter. Assoc. Test. Mat. Proc.*, 1908.

‡ Unwin, Ludwick Hardness Test, *Inst. Mech. Eng. Proc.*, October, 1918.

§ Batson, Static Indentation Tests, *Inst. Mech. Eng. Proc.*, April, 1923.

116. Dynamic Tests.—*General.*—So far, consideration has been made of static indentation tests. Much work has, however, been done on dynamic methods, and we now come to a discussion of this phase of the subject.

Martel[*] in 1895 communicated a very interesting paper to the literature. He used a pyramidal point as the indenting tool and allowed the fall of a ram to produce the necessary indentation. By so arranging the height of drop that the rebound was negligible he concluded that the work done by the ram was proportional to the volume of the indent and the hardness was therefore expressed as the work necessary to produce unit volume of indentation, or if

P = weight of ram in kg.,
V = volume of indentation in cubic mm.,
F = height of fall in mm.,
H = hardness number $= \dfrac{PF}{V}$ kg. per sq. mm.

He further concluded that for equal energies of blow the volume of indentation was nearly the same when using indenting tools of slightly different form. Batson[†] has since extended this work by using a 10 mm. diam. ball. He found that for materials having a range of Brinell numbers from 20 to 680 the ratio of the dynamic hardness number to the Brinell number was approximately 1.5; whereas Martel found it to be in the neighborhood of 1.25.

Unwin,[‡] however, had previously shown that theoretically the Martel and Brinell numbers should agree, and in commenting on Batson's work he indicated that time effect was the reason for the divergence from the theoretical value. The chief advantage in the use of such a method appears to be in the fact that it is applicable for the determination of indentation hardness values at high temperature. The time interval is so short that the heat does not affect the indenting tool.

Scleroscope.—The best known form of dynamic hardness test is that made by means of the scleroscope. In this test the hardness is determined by the height of rebound of a small diamond pointed hammer about $\frac{3}{4}$ inch long and $\frac{1}{4}$ inch diam. When this falls freely on the material, the hardness of which is desired, the height of rebound is measured against a graduated scale suitably situated. A more or less proportional relation has been found to exist between the scleroscope number and the Brinell hardness number. The author has found that a Brinell hardness of 440 corresponds approximately to 75 scleroscope. Stanton has carried out extensive comparative tests of both methods of testing. It appears that any relation which does exist is however not a constant one, but changes with the hardness of the material tested. The results from this method of testing are affected by the size of the test bar and also by the method of support. The scleroscope is usually employed in cases where the static indentation method cannot be applied, such as the case hardened surfaces of cam-shafts. In this respect therefore it is of considerable value for the control of the heat-treatment of materials. It possesses the advantage also that it leaves no indentation.

---

[*] Martel, *Commission des Methods d'Essais*, Sect. A, p. 261 (Paris), 1895.

[†] Batson, Hardness Tests, *Inst. Mech. Eng. Proc.*, p. 493, 1918.

[‡] Unwin, Definition of Hardness, *Engineering*, p. 535, May, 17, 1918.

Pendulum Tester.—Recently a new instrument* has been put into the hands of the engineer whereby another method is employed for measuring hardness by means of indentations.

A ball one millimeter in diameter is used in this instrument, the latter being in the form of a pendulum such that the ball can be put into contact with the material, the hardness of which is desired. The pendulum is made to oscillate, the time required for a given number of oscillations being taken as the measure of the time hardness. In most cases the time of a single or double swing is sufficient for this determination, but in soft materials where the oscillations are rapid the time of 10 swings is taken. Calling the time hardness T, typical scale readings for different materials are given in Table LXVII, the diameter of ball being one millimeter.

It appears that there is a simple relation between the time hardness number T and the Brinell hardness number H. The time hardness number, if above $33\frac{1}{3}$, multiplied by 10 gives the Brinell hardness number.

$$H = 10T \text{ where } T > 33\tfrac{1}{3}.$$

In cases where T is less than $33\frac{1}{3}$ the relation becomes

$$H = 0.3T^2.$$

---

* Pendulum Hardness Tester, p. 390, *Engineer*, April 13, 1923. For Theory of Instrument, see discussion by S. Timoshenko in *Engineer*, July 6, 1923, p. 21 also Sept. 7, 1923, p. 248

TABLE LXVII.—PENDULUM HARDNESS NUMBERS

Material	Time hardness (T)
Glass	97
Very hard carbon steel	93
Hard carbon steel	88
Tempered high speed steel	75
Annealed high speed steel	54
Annealed carbon steel	41
Rolled brass	14
Cast brass	4

In Fig. 357 are given the curves of Brinell indentation hardness and time hardness for a variety of materials on the basis of the above equations.

It should be noted that the weight of the instrument is either two or four kilograms and therefore it can be used to determine the hardness of thin and fragile materials that otherwise could not be tested.

The instrument is a new one and while there is not sufficient data at present to make definite conclusions as to its practicability, nevertheless further work with such an instrument can conceivably yield valuable results.

117. Scratch Tests.—The conception of hardness determination by means of the scratch test is not modern. In 1722 Reaumur* made tests of this nature by using a standard bar, the hardness of which increased from end to end. The metal under test was used as the tool for scratching the standard, and the position on the bar where a scratch was possible indicated the hardness. Mohs† as the first to give, for mineralogists, a scratch hardness scale, talc being taken as the one extremity and diamond as the other. Turner‡ did further work on the subject: he used a diamond suitably located in a lever which could be rotated over the surface of the specimen. He defined hardness as the smallest weight in grams on the diamond (computed from the position of a sliding weight) which would produce a visible scratch on the test bar. Martens§ further extended this and defined the

---

* Reaumur, "L'Art de Convertix," 1722.

† Mohs, "Grundriss der Mineralogie," 1822.

‡ Turner, *Birmingham Phil Soc. Proc.*, Vol. V, 1887.

§ Martens, Sitzungsberichte des Vereines. Zur Beforderung des Gewerbfleisse. 1888.

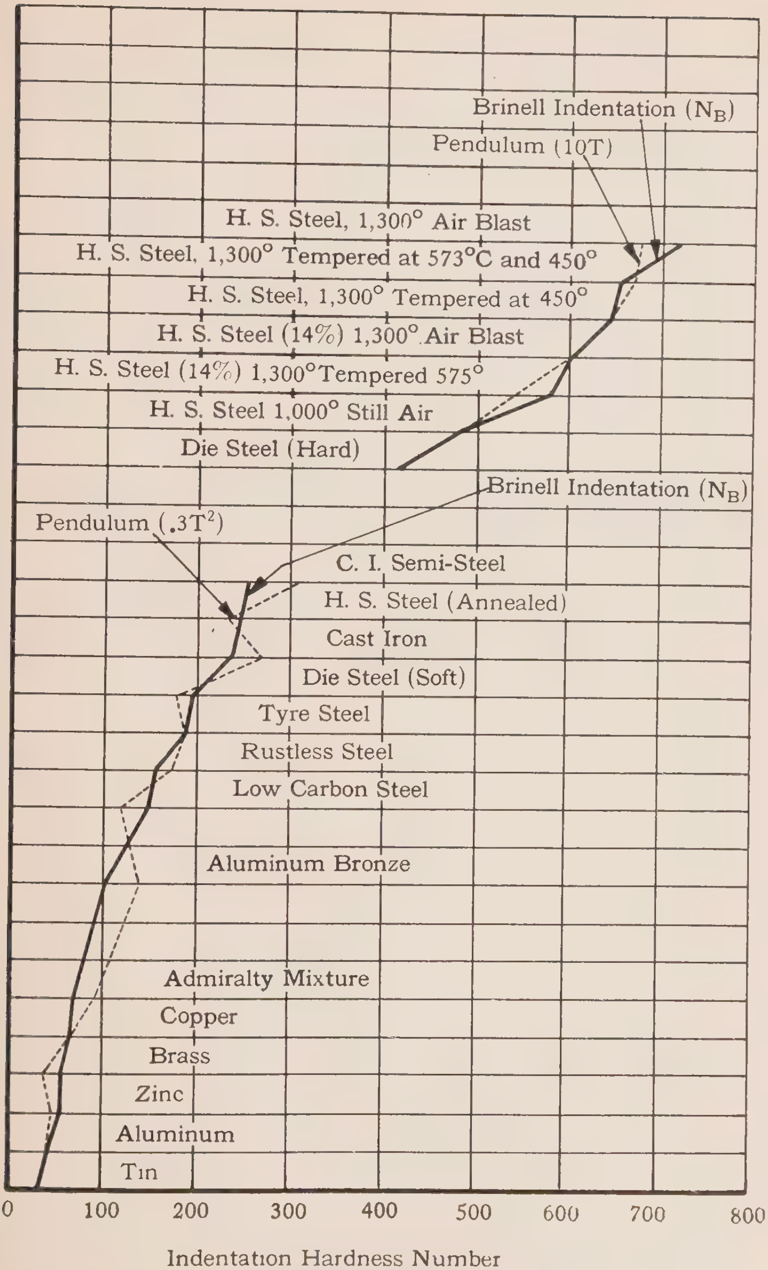

FIG. 357.—Relation between Brinell hardness and time hardness.

hardness as the load in grams under which a conical diamond would produce a scratch .01 mm. wide.

In recent years the subject of scratch hardness has been receiving more attention. Hadfield* contributed a paper on the subject in which he showed that there was a general relation between the Brinell indentation hardness and the scratch hardness, the Brinell indentation number being found equal to the ratio .02675/(width of scratch in mm.)^3 for the experiments made. A notable exception was found for very hard steels, where the Brinell value was very much lower than the scratch hardness. This led him to conclude that for material with an indentation hardness of 640 Brinell, the ball indentation test is of no value due to the flattening of the ball.

A very comprehensive contribution was made to the literature by Hankins.† In this case the diamond was fixed and the test bar was drawn across the face by means of a screw. Using three types of diamonds he found that in all cases a straight line law was obtained when the square of the width of the scratch was plotted against the load on the diamond. In Fig. 358 is given the relation obtained for various materials, varying from lead to hardened chromium steel when using the diamond shown in Fig. 359. It will be noted that all the lines tend to meet at a common point near to, but not coinciding with, the origin.

Hankins suggested the following relation for defining scratch hardness:

P = load on diamond
w = width of scratch
k = constant for material

$$k = \frac{P - p}{w^2 - q},$$

q and p being the co-ordinates of the point of intersection. While the values p and q appear to be useful in determining the position of the lines, it can not be concluded that these lines represent any real physical meaning near to the point of intersection. The lines can only be used within the limits of the experiments and can not be extrapolated to zero width of scratch.

The ratio of the scratch hardness to the Brinell indentation number has been plotted by the author in Fig. 360 from the results given in the paper. It will be noted that a minimum value for this ratio occurs in the region of 450 Brinell, and the upward trend of the curve towards the right hand probably indicates the breakdown of the ball test.

---

* Hadfield & Main, Brinell and Scratch Tests, *Inst. Mech. Eng. Proc.*, p. 581, Oct., 1919.

† Hankins, The Relation between Width of Scratch and Load on Diamond in Scratch Hardness Test, *Inst. Mech. Eng. Proc.*, p. 423, April, 1923.

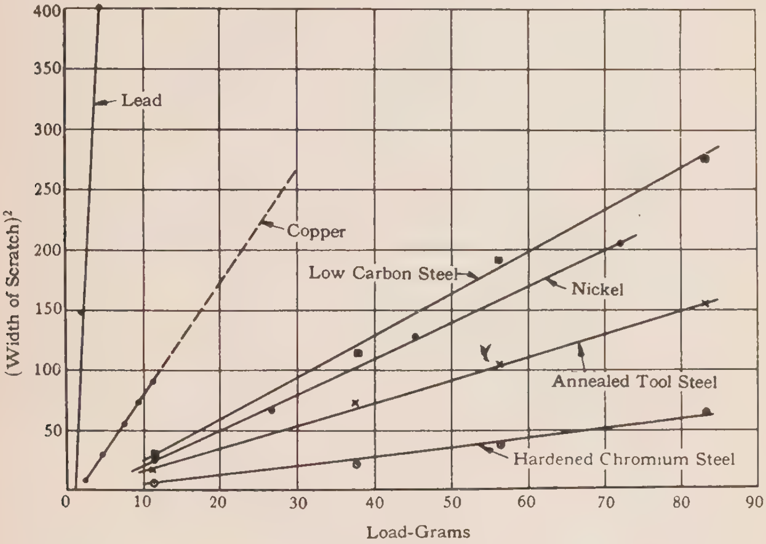

FIG. 358.—Relation between load and width of scratch.

The value of k/H for copper does not lie on this line. Hankins, commenting on this fact, mentioned Turner's statement that hardened copper may show a greater hardness than low carbon steel yet no amount of cold rolling would enable copper to cut steel. On the other

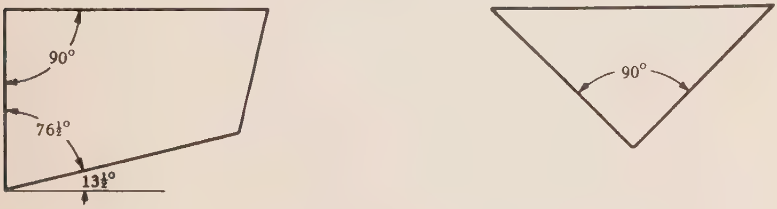

FIG. 359.—Diamond used in test.

hand, this steel will always cut copper. From these results he concluded that the scratch test gives some property of the material slightly different from that obtained by the indentation test. O'Neil* in discussing these results pointed out the similarity between the relation the load bears to the width of scratch and Meyers' law. Because, if p and q be zero the relation becomes $P = kw^2$, and corresponds to Meyers' data. There is no doubt that an extension of such work as this will be valuable to the engineer, particularly for those materials whose hardness lies above 640, where, as we have seen, the indentation test appears to fail.

---

* O'Neil, *Inst. Mech. Eng. Proc.*, p. 479, April, 1923.

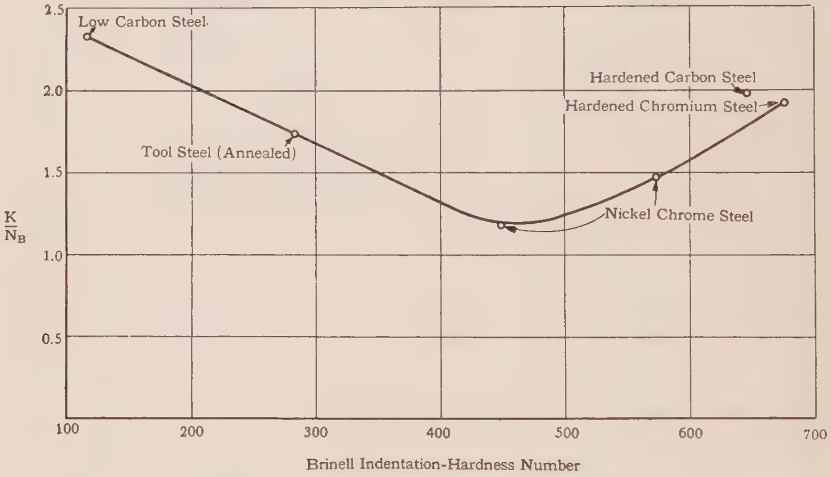

FIG. 360.—Curve of Brinell and scratch hardness.

118. Significance of Hardness Test to the Designer.—It will have been appreciated from the previous discussion that, with indentation tests, there are arguments for both the ball and the cone method of conducting the test, and the final selection must depend on how much geometrical similarity in indentation, as obtained in the cone test, outweighs ease of replacement and uniformity of form in the ball test. Whatever method is selected will not, however, affect in any degree our argument that the indentation test as a relative test has become invaluable towards facilitating a better control of materials. By itself it means very little, its real place being as a *subsidiary* test to the tensile test; it has there a true meaning. It is known that if

$p_{\max}$ = ultimate stress in tons per sq. in. (1 ton = 2,240 lbs.)
H = Brinell hardness number
k = constant = 0.23 for steel, then $p_{\max} = kH$.

Since such a relation enables us to calculate the tensile strength of steels with a reasonable degree of accuracy, this is of great practical significance to the engineer. Because, consider for an instant that it is necessary to know something regarding the physical properties of a piece of fractured material which is in itself insufficient for supplying the necessary test bars. Then if the Brinell hardness number be taken and data be available both on the chemical analysis of the material and the heat-treatment, then a fair approximation can be obtained regarding the ultimate stress in tension and from this some further information on the elastic and ductility properties are possible. It will therefore be seen that the test, although a relative one, loses none of its importance if the data which it provides is properly applied. As we have seen, the scleroscope has also its proper place in assisting in the control of materials. The other forms discussed however are only valuable in the fact that they are assisting us to determine the fundamentals of hardness. They are still in the process of development and even when more knowledge has been gained concerning them it is doubtful whether they will ever be able to displace the indentation test from its present position.

CHAPTER XVI

FATIGUE

119. General.—In this chapter the characteristics of material under another form of dynamic test will be considered, namely those relating to conditions where the stress is continually *alternating*. Such characteristics are very important to the designer because it is well known that materials under these conditions can be made to fail under stresses considerably *lower* than the ultimate stress in tension. In this respect it does not matter whether the stress be made to vary between a maximum and zero or be completely reversed varying between a positive maximum and a negative maximum, the same statement will be true. For the purpose of our consideration we will suppose a compressive stress as a negative tensile stress, and the difference between these stresses as the *range of stress*. Obviously, with this understanding, if a test bar be loaded as a beam such that the maximum stress be p lb. per sq. inch and if, in this loaded condition, the bar be rotated such that the direction of the load remains fixed, then in each revolution the material will be subjected to a *cyclic variation* of stress varying from $+p$ lb. per sq. inch to $-p$ lb. per sq. inch, giving a range of stress as $2p$. Although much experimental work has been done on this subject it is only in the last few decades that an intensive study has been made. In 1864 Fairbrain* published the results of certain tests made on wrought iron girders and concluded that the safe stress for complete cyclic variation should not be greater than one third of the ultimate stress in tension. That is to say that a material having an ultimate stress of 90,000 lbs. per sq. inch could only be safe provided the stress varied within the limits of +30,000 lbs. per sq. inch and −30,000 lbs. per sq. inch. This work was followed in 1870 by that of Wöhler.† These tests were very comprehensive, and while the results of later investigators have enlarged somewhat the state of the knowledge regarding the *mechanism of fatigue*, still the original conclusions of Wöhler remain unchallenged. These stated that a stress below the ultimate stress would fracture material if repeated a sufficient number of times, that the range of stress together with the maximum stress determines the number of cycles to fracture, and that for a given maximum or minimum stress the number of cycles to fracture increases with diminishing of the range of stress, and at a certain stress called now the *endurance limit* the number will become infinite. Spangenberg* continued this work, and in 1874 published results obtained on the original machines of Wöhler. Bauschinger† in 1886 made a further fundamental contribution to the literature. The theory advanced by him, which extended further the work of Wöhler, has attracted great attention. Since we may have to refer to this later on in the chapter it seems well that we should state here the chief points of this work. He concluded that by the action of gradually increasing cyclical stresses on low carbon steel, the proportional limit for compression could be lowered only provided the tensile stress exceeded the proportional limit in tension; and correspondingly the proportional limit in tension could be lowered only provided the compressive stress exceeded the proportional limit in compression, the proportional limits in tension and compression being usually different for such material. If the proportional limit in tension were lowered by a previous compression beyond the proportional limit, as explained above, it could again be raised by the action of gradually increasing *cyclical tension* and compression but would always have a considerably lower value than the previous proportional limit. He further concluded that if there were no *artificial raising* of the proportional limit then the endurance limit would coincide with the proportional limit. Furthermore that if the proportional limit were raised artificially by some previous stressing or by cold working effects then it will be lowered by the action of cyclical stresses to a certain limit which Bauschinger proposed to call the *natural elastic limit* of the material. This limit would have exactly the same value as that to which the proportional limit could be raised by the action of cyclical stresses, after having been previously lowered, as explained above by excess stresses of an opposite kind.

---

* Fairbrain, The Effect of Impact Vibratory Action on Wrought Iron Girders, *Phil. Trans. Roy. Soc.*, 1864.

† Wöhler, Über die Festigkeitversuche mit Eisen and Stahl, *Z. f. Bauwesen*, 1870; and see also *Engineering*, 1871.

It will be seen later that this work has been supported by the results of modern investigators to the consideration of which we will now come.

---

* Spangenberg, Uber das Verhalten der Metalle, *Z. f. Bauwesen,* 1874.

† Bauschinger, Die Veranderungen der Elasticitätsgrenze. *Mitt. a. d. Mech. Tech. Labor* (München) 1886. See also abstract in *Dingl. Polyt. Jour.*, Vol. 266, 1886.

120. Looping during Cyclical Stress.—The greatest step towards a better knowledge of the phenomenon of fatigue has been, in part at least, largely made by a study of the variation in looping as a test bar is fatigued. We have seen in chapter XIII that every material when loaded beyond a certain point and unloaded will show hysteresis effects on reloading and that this looping will depend on the composition and state of this material. It can be assumed at once that these statements will also apply to materials where, instead of the stress varying between zero and a maximum in tension, this is varied from tension to compression. Experimental evidence has now shown this to be true. Bairstow,* by measuring the variations in strain, made a complete study of this looping for different ratios of tensile and compressive stresses. In Fig. 361 are shown some of the results obtained by him on low carbon steel.

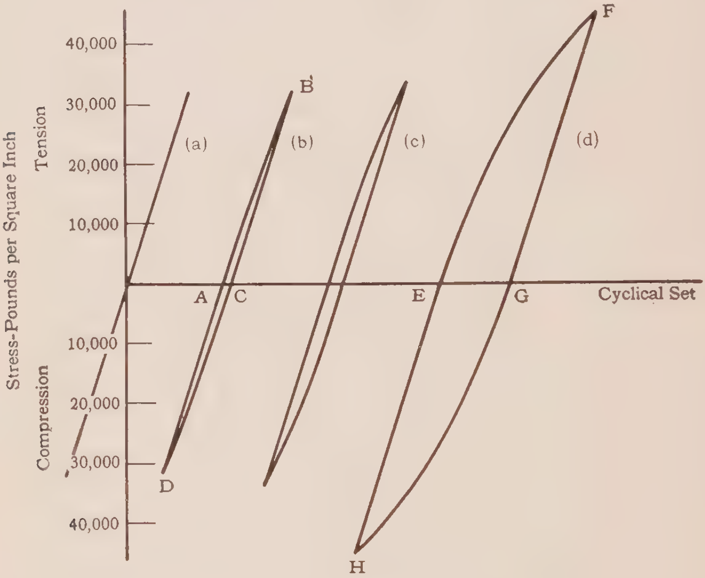

FIG. 361.—Hysteresis looping under cyclic stress variation.

Commencing with a direct stress of 31,600 lbs. per sq. in. the elastic line shown in Fig. 361 (a) was obtained. This shows no looping, and at such stress values any looping that might occur, as we have seen, would be so small that it could be neglected. The machine was then set in motion such that the cyclic variation of stress was at the rate of two per minute. After 18,730 cycles under these conditions the line for unloading no longer corresponded to that for loading, the material having experienced a *cyclical set* of approximately 11% of the original elastic extension. This of course assumes that this set produced by tension would be annihilated by compression and that the length of the test bar remains the same. The loop obtained is shown in Fig. 361 (b), AC being this cyclical set. An important point to note is that the lines BC and DA for the unloading remained parallel to the original elastic line Fig. 361 (a). The stress was then raised to 33,600 lbs. per sq. inch and the cyclic set immediately increased, having approximately 50% greater width after 23,200 cycles than at 18,730 cycles, giving the loop shown in Fig. 361 (c). Increasing the stress to 45,500 lb. per sq. inch, the width of the loop increased greatly as shown in Fig. 361 (d), which was obtained after 29,300 cycles. The increase in width for this condition was approximately ten times greater than that for Fig. 361 (b). Even in this condition of large cyclic set the lines for unloading, FG and HE, remained parallel to the original elastic line. While the width of the loop increased with the stress there was found to be a definite range of stress where the width tended towards a limiting value, and subsequent stressing did not materially change the width even when this range of stress was sufficient to finally cause fracture. These results led Bairstow to conclude that the width of the loop EG as in Fig. 361 (d) depended on the elastic extension being equal to the change in length from E to F minus the elastic extension, and that the range between the natural elastic limits as defined by Bauschinger coincides with the range of stress which a material will withstand indefinitely. This work is therefore of great importance to the designer since it substantiates Bauschinger's work, and emphasizes the fact that the elastic characteristics of material play a role in fatigue phenomena, a point which in some quarters appears to have been neglected. In chapter XIII, paragraph 107 a discussion was made of the work done by Dalby* on hysteresis effects where the stress was varied from zero to maximum in tension. This work has been considerably extended and we are now able to discuss it further. The published data on the subject supports the work of Bairstow in that the looping obtained is characteristic of the material, and the area of such loops tends towards a constant value. In Fig. 362 are shown loop characteristics for different materials, according to Dalby. The areas are plotted as ordinates, and in this case the permanent set as abscissae.

---

* Bairstow, Elastic Limits of Iron and Steel under Cyclic Variation of Stress, *Phil. Trans. Roy. Soc.*, 1911.

---

* Dalby, "Strength and Structure of Metals," 1923.

A further study of the effects of cyclic straining of materials was made by Mason.* In this case the stresses were produced by torsion of the test bar. By suitably arranging the machine so that the speed of alternation could be changed from 2 per minute to 200 per minute while the stress remained unchanged he obtained very interesting results. The material, after being fatigued, showed an increase in *angular strain* when frequency of alternation was decreased, and showed a decrease when this frequency was increased. This change was explained on the basis of the fact that at the lower speed there is more time for the crystal slipping to operate, and consequently the strain increased. This is in line with what was said previously on page 420 in that at high speeds the friction will be large, and due to this fact the strain can be decreased. The fact that after running at 200 cycles per minute the strain, previously decreased as explained above, commenced to increase was concluded by Mason to be due to the increased production of mobile material (see Chap. XIII) by the increased rate of slipping to-gether with the decrease in the time for

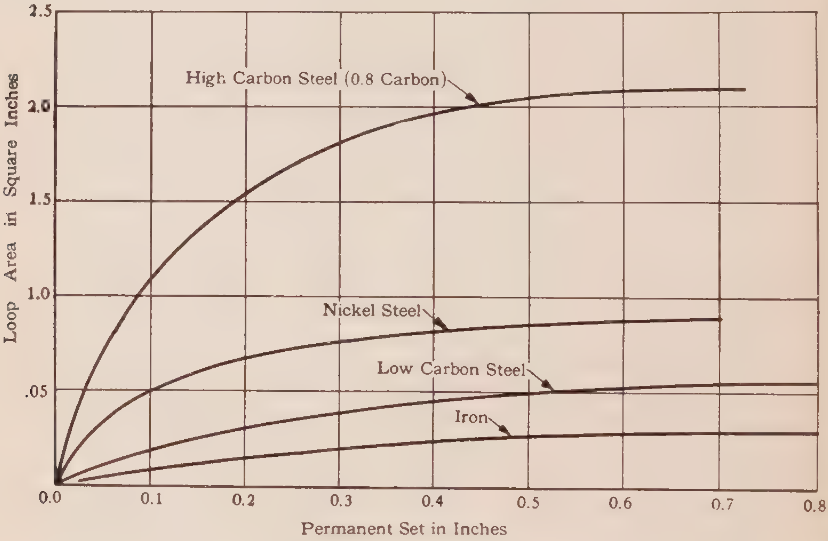

FIG. 362.—Variation of loop area for different materials.

---

* Mason, Speed Effect and Recovery in Slow Speed Alternating Stress Tests, *Roy. Soc. Proc.*, p. 373, 1916.

hardening arising from the speed increase. It appears safe to conclude that, from these various contributions, a material possessing perfect elasticity will suffer no deterioration from stress changes lying within these limits of perfect elasticity. If a material be strained beyond these limits then a loop will be formed indicating that the material is under viscous flow arising from the internal stresses produced by the surrounding material. It will be clear from this reasoning that the endurance limit cannot be a fraction of the yield point, nor can it be a fraction of the ultimate stress, but will depend on the internal condition of the material. With this consideration we will come to the presentation and discussion of some experimental data obtained.

121. Changes in Crystals.—It has been observed (p. 414) that when a material such as low carbon steel is being stressed, definite changes can be seen in the crystals as the stressing proceeds. These changes, as we have seen, are due to slip* occurring on certain planes within the crystalline grains. This slip imparts plasticity to the crystal grain, and allows it to adapt itself to the new conditions imposed on it. As long as the stress is static then the appearance of these slip bands may not be the indication of a dangerous condition only evidencing local yielding of the material. If, however, the stress be a cyclical one then, as has been clearly indicated by Ewing,† these bands can become the *nucleus* of the failure of the material, provided the straining is carried sufficiently far. It must be clearly understood that while, in the author's opinion, the appearance of these bands must precede failure their appearance may occur at stresses considerably below the endurance limit. Ewing observed this in his work but concluded that it only required time to bring about failure at stress values corresponding to their first appearance. Further work has now been done by Gough‡ who concludes that the appearance of slip bands can occur, on certain materials at least, at stresses well below their true endurance values. For a certain class of iron these slip bands were first observed at a reversed stress of 21,000 lb. per sq. inch, but the endurance value for this material only occurred after a stress of 28,600 lb. per sq. inch was reached. It appears, therefore, that it is only when the straining is carried sufficiently far after the appearance of the first slip that failure will occur. Of course since the yielding of the material under this slipping action must be closely associated with the ductility of the material, it can be inferred that the difference of stresses between the first appearance of slip bands and the endurance limit will depend on the ductility possessed by the particular materials. So far, investigations have only been made on ductile materials. Moore* appears to think that with harder materials there is no clear evidence that slip always precedes failure. This, of course, may be due to the fact that in material such as hardened steel the examination of slip bands is impossible or at least very difficult due to the fineness of the crystals. At present no definite experimental data are available to support the contention.

---

* Ewing and Rosenhain, Crystalline Structure of Metals, *Phil. Trans. Roy. Soc.*, Vol. 193, 1899.

† Ewing and Humfrey, Fractures of Metals under Repeated Stresses, *Phil. Trans. Roy. Soc.*, 1903.

‡ Gough and Hansen, Behaviour of Metals Subjected to Repeated Stresses, *Roy. Soc. Proc.*, Vol. 104, Nov., 1923. Moore and Kommers, *Univ. of Illinois Bull. No.* 124.

We can, therefore, conclude that the appearance of slip bands in the crystals of materials is the direct result of the applied stresses. If this stressing is sufficiently increased the material will ultimately fail although the first appearance of these slip bands may not indicate a dangerous stress condition. While the endurance limits of certain materials occur at higher stress values than those relative to elastic conditions in tension there is evidence that the appearance of these slip bands does depend on the elastic properties and that the difference in stress value between their first appearance and fatigue depends not entirely on these properties but rather more on those of ductility. It therefore cannot be inferred that the breakdown by fatigue on the basis of this work is not connected in some manner with the elastic and plastic properties of the material. In other words, even from this new point of view, we cannot get far away from Bauschinger's fundamental work.

122. Cycles of Complete Stress Reversal.—*Preliminary Statements.* From the discussion in the preceding pages it will have been appreciated that fatigue stresses can either be imposed on the material by tension and compression produced either by direct method, or by bending, or by torsional shear. Here we are more concerned with the results obtained rather than the means adopted, but nevertheless a few words on the method will be necessary. In the results obtained by the author the cantilever type of machine in which the stress is produced by bending has been used, and, unless otherwise stated, the form of test bar employed is as shown in Fig. 363, operating at a speed of 1,300 revolutions per minute.

---

* Moore and Jasper, Investigation of Fatigue of Metals, *Univ. of Illinois Bull.*, No. 142, p. 22, 1924.

This test bar being similar in form to that used by another investigator* possesses the advantage that the maximum stress is not concentrated at a given section but is approximately constant over a portion of the length, the variation in stress between AA' and BB' being of the order of 1%. In determining the endurance limit of steels by such a method, usually eight test bars of the same material are chosen. Commencing with the first bar the machine is set in motion and the load is so adjusted that the maximum stress is about 0.7† of the ultimate stress in tension. The number of revolutions to fracture is recorded. The second test bar is then stressed at a lower value and the revolutions for fracture again recorded. This is continued on successive bars until the stress is of such a value that after a chosen number of cycles of stress fracture does not occur. The values obtained in this manner are plotted as shown in Fig. 364 such that the ordinates represent stresses and the abscissae represent the corresponding number of cycles to fracture. It will be seen that the curve is of such a form that it seems to be *asymptotic* to a line drawn parallel to the horizontal base line, which means that the material would withstand the action of the stress, corresponding to this asymptote, indefinitely. Accepting this hypothesis, it is assumed that if the material is steel and it withstands 20×10^6 cycles‡ of stress without fracture, the asymptote is well determined and that the material

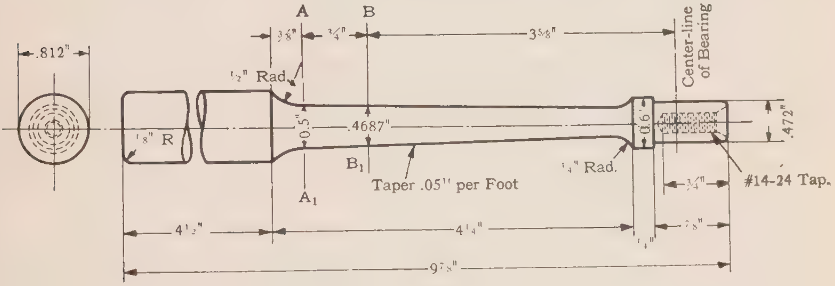

Fig. 363.—Cantilever form of fatigue test bar.

---

* McAdam, Endurance of Steel under Repeated Stress, *Chemical and Met. Engr.*, December 14, 1921.

† Note.—For non-ferrous metals and cast iron the commencing stress will require to be less than 0.7 of the ultimate stress.

‡ Note.—This is more conservative than certain other investigators such as Stanton and Reynolds who determined the endurance limit for fewer repetitions.

under such conditions would withstand an infinite number of cycles of stress. The stress value corresponding to the asymptote is called the endurance limit of the material for complete stress reversal. It will be seen later that, although 20×10^6 cycles is satisfactory for steel, the number must be materially increased for non-ferrous metals before satisfactory results can be expected.

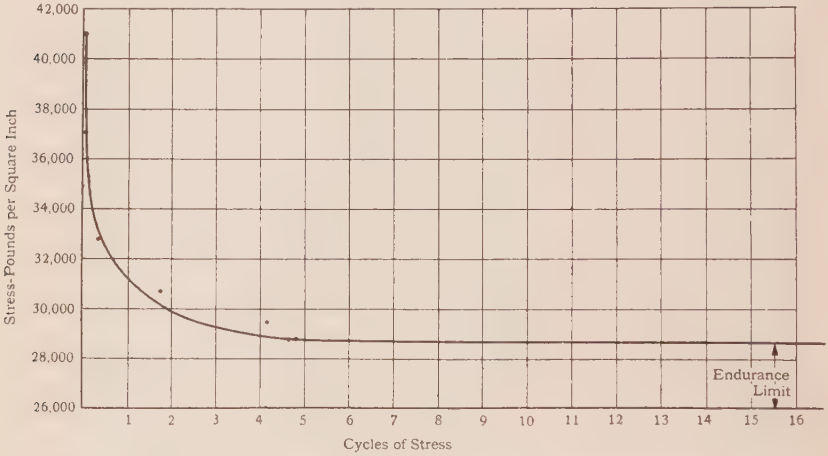

Fig. 364.—Endurance curve for 0.37 carbon steel as annealed.

B. *Carbon Steel*.—The results obtained for a medium carbon (0.37) steel in the rolled, annealed, and normalized conditions are shown in Table LXVIII.* For the purpose of discussion, the values for the ultimate strength in tension and also for the ratio k have been reproduced from Tables XXXV and XLVIII respectively.

Table LXVIII.—Fatigue Properties of 0.37 Carbon Steel (Rolled)

State	Endurance limit, pounds per square inch	Ultimate strength, pounds per square inch	Ratio: $\frac{\text{Endurance limit}}{\text{Ultimate strength}}$	Ratio k
Rolled	28,000	74,000	0.38	1.15
Annealed	29,000	70,000	0.42	1.03
Normalized	29,300	79,200	0.38	1.10

As we have seen in Chap. XIII, page 405, the value k being the ratio of yield point to propotional limit appears to be indicative of the

* See Table XXXV for Tensile Properties.
See Table LX for Repeated Shock.

magnitude of the internal stress and it is included in the table for the purpose of our discussion.

The first point to note from these results is that the endurance limit value is approximately the same as the proportional limit in tension. This is in general true for the majority of carbon steels although certain exceptions have been noted on other materials. Moore* found for instance that, for commercially pure iron, the proportional limit was 16,000 lb. per sq. inch whereas the endurance limit under reversed bending was 26,000 lb. per sq. inch. Moore, in commenting on these values, felt that the homogeneity of structure had some influence on this result. This appears to be a reasonable conclusion because the same phenomenon has been observed when testing commercially pure nickel† where structural homogeneity is to be expected. In this case the endurance limit was found to be ± 29,000 lb. per sq. inch whereas the proportional limit in tension was only 12,800 lb. per sq. inch. The author‡ has also observed similar characteristics when testing this material, the values for the endurance limit being about ± 38,000 lb. per sq. inch and 16,000 lb. per sq. inch for the proportional limit. We therefore see that the endurance limit does not depend directly on the value of the proportional limit in tension, it is sometimes equal to or slightly less than the proportional limit, as in annealed carbon steels; it is sometimes in excess of the proportional limit, as in pure nickel and iron, and we shall see later in heat treated steels it is usually less, sometimes to a considerable degree, than the proportional limit.

While the proportional limit has not a direct effect, it appears to have an indirect one on the endurance limit value. As we have seen (p. 460) from Fairbairn and Wöhler's work it appeared that the endurance limit was approximately one third of the ultimate stress in tension. This ratio is however not a constant one, as an examination of Table LXVIII will show. It appears to be influenced by the internal stress present in the material, and since, as we have seen, the value k seems to be an indication of the magnitude of this internal stress it is to be expected that a relatively high value for k will result in a low value for the ratio of endurance limit to ultimate strength. The results given in Table LXVIII show this to be the case. In Table LXIX are given values obtained by Moore* for a variety of carbon steels, a pure iron also being included. The values for k and those for the ratio of endurance limit to ultimate have been added by the author.

---

* Moore and Kommers, Investigation of Fatigue of Metals, *Univ. of Illinois, Bull. No.* 124, 1921.

† Hankins, Properties of Commercially Pure Nickel, *Aeronautical Res. Comm. Rep. No.* 789, November, 1921.

‡ See the Author's Paper, The Elastic Limit in Tension, *Inst. Mech. Eng. Proc.*, Dec., 1924.

TABLE LXIX.—FATIGUE PROPERTIES OF ROLLED CARBON STEELS

Carbon content	State	Endurance limit, pounds per square inch	Ultimate strength, pounds per square inch	Ratio: $\frac{\text{Endurance limit}}{\text{Ultimate strength}}$	Ratio k
.02	Received	26,000	42,400	0.61	1.18
.52	Normalized	42,000	98,000	0.42	1.05
.93	Normalized	30,500	84,000	0.36	1.20
1.20	Normalized	50,000	117,000	0.42	1.04

Excluding the values for the pure iron where, as we have already observed, the endurance limit was in excess of the proportional limit, it will again be noted that a low value of k corresponds to a high value of the ratio of endurance limit to ultimate strength. While, therefore, the author feels, like other investigators, that the endurance limit is related to the ultimate stress in tension, he also feels that the internal stress as given by k materially affects such a relation. Furthermore, since the value k depends on the elastic properties of the material, he concludes that these characteristics must also be considered when fatigue resisting properties are being considered.

So far we have been discussing steels possessing more or less similarity in microstructure, namely pearlitic steels. We now come to another class of steels where the microstructure is entirely changed, namely heat-treated steels. As we have seen in Chap. XII (p. 373), the heat-treatment imparts a refined structure to the material and it will now be seen that this refinement has a distinct bearing on the fatigue characteristics. For instance, referring to Table LXX† which repre-

TABLE LXX.—FATIGUE PROPERTIES OF 0.37 CARBON STEEL HARDENED IN WATER 850°C. (2¼ INCH DIA. BAR) AND TEMPERED

Tempering temperature	Endurance limit, pounds per square inch	Ultimate strength, pounds per square inch	Ratio: $\frac{\text{Endurance limit}}{\text{Ultimate strength}}$	Ratio k
100°C.	52,000	116,000	0.45	1.18
450°C.	50,000	114,000	0.44	1.14
550°C.	51,000	105,000	0.49	1.06

---

* Moore and Kommers, Investigation of Fatigue of Metals, *Univ. of Illinois, Bull. No.* 124.

† See Table XXXVIII for the corresponding tensile test results.

sents the fatigue results obtained for a 0.37 carbon steel, it will be observed that the ratio of endurance limit to ultimate stress is now higher than the ratio for the same steel normalized (see Table LXVIII). Similar conclusions can be deduced from Moore's* results, as an examination of Table LXXI, which represents some values obtained by him for several carbon steels will show. In this case each steel, in the particular heat treated condition chosen, shows higher values for this ratio than the same steel normalized. It appears, therefore, that when we base endurance limit values on ultimate stress this fact also must be taken into consideration.

Table LXXI.—Fatigue Properties of Various Carbon Steels (Moore)

Carbon	State	Endurance limit, pounds per square inch	Ultimate strength, pounds per square inch	Ratio: $\frac{\text{Endurance limit}}{\text{Ultimate strength}}$
1.20	Normalized	50,000	116,900	.43
1.20	Sorbitic	92,000	179,900	.51
.93	Normalized	84,000	30,500	.36
.93	Sorbitic	115,000	56,000	.48
.49	Normalized	33,000	91,500	.36
.49	Sorbitic	48,000	96,900	.50
.37	Normalized	33,000	71,900	.46
.37	Sorbitic	45,000	94,000	.48

Reasoning on the same basis as before, it can also be expected that when the tempering temperature is low the internal stress in the material will be higher than when it is tempered at a higher temperature. The results in Table LXX indicate this to be the case because the minimum value of k corresponds to a maximum value of the ratio of endurance limit to ultimate strength.

We have indicated previously that the endurance limit usually is equal to or less than the proportional limit in tension for annealed carbon steels. In general, with heat treated steels the endurance limit is less than the proportional limit value, and by a greater amount than for the same steel simply annealed. This is an important point for the designer because the increase which is obtained on the tensile test properties by heat-treatment may not be a measure of the increase to be expected on the fatigue properties. Another point arising from these results is the influence of the ductility properties. Referring to the tensile test characteristics given in Table XXXVIII for the heat-treated medium carbon steel, it will be observed that there is a marked difference in the elongation and the reduction of area values with change in tempering temperature. Since the endurance values for this particular steel are substantially the same irrespective of these large differences in ductility it appears that the conclusions arrived at on p. 360, in that these ductility properties are only of value in cases of stress concentration, are amply justified.

---

* Moore and Jasper, Investigation of Fatigue of Metals, *Univ. of Illinois, Bull. No.* 136, 1923.

Alloy Steels.—It has been shown in Chap. XII, par. 91, that alloy steels possess decided advantages over plain carbon steels as far as tensile characteristics are concerned. This fact is probably still more true if the fatigue characteristics be chosen as the basis for comparison. In Table LXXII are given the fatigue values for a 3½% nickel steel.

TABLE LXXII.—FATIGUE PROPERTIES OF 3½% NICKEL STEEL

State	Endurance limit, pounds per square inch	Ultimate strength, pounds per square inch	Ratio: $\frac{\text{Endurance limit}}{\text{Ultimate strength}}$	Ratio k
Rolled	41,000	105,000	0.39	1.27
Normalized	44,000	104,000	0.42	1.15
Normalized and drawn	47,500	95,000	0.50	1.07

It will be noted that the endurance limit for a normalized and drawn material has now assumed the value of 0.5 of the ultimate strength, a phenomenon which, as we have seen, required a heat-treating operation in order that this condition might be brought about in a carbon steel. Similar results have also been noted by the author on steels where vanadium is the alloying element. In this case the carbon content was 0.5, the vanadium 0.19 and the manganese 0.81. In the annealed condition this gave an endurance limit of 45,000 lbs. per sq. in. with an ultimate stress in tension of 96,000 lbs. per sq. in.

Moore's results confirm this, because for a 3½% nickel steel quenched in oil at 1,450°F. and drawn at 1,200°F. virtually an annealed material, the endurance limit was 0.54 of the ultimate strength. It appears, therefore, that the addition of an alloying element, by assisting to refine the structure of the material, manifests its effect in making it more difficult for the cyclic varying stresses to cause breakdown, and thereby in raising the ratio of the endurance limit to ultimate stress. Heat-treatment of the material unlike carbon steels does not appear to raise this ratio, and this may, in part at least, be due to the fact that with heat-treated alloy steels, unless tempered at sufficiently high temperatures, the internal stress as indicated by k is high. This appears to be borne out by reference to Fig. 365 which represents further data from Moore's* work. In this case the ratio of endurance to ultimate is very low for tempering temperatures below 300°C.

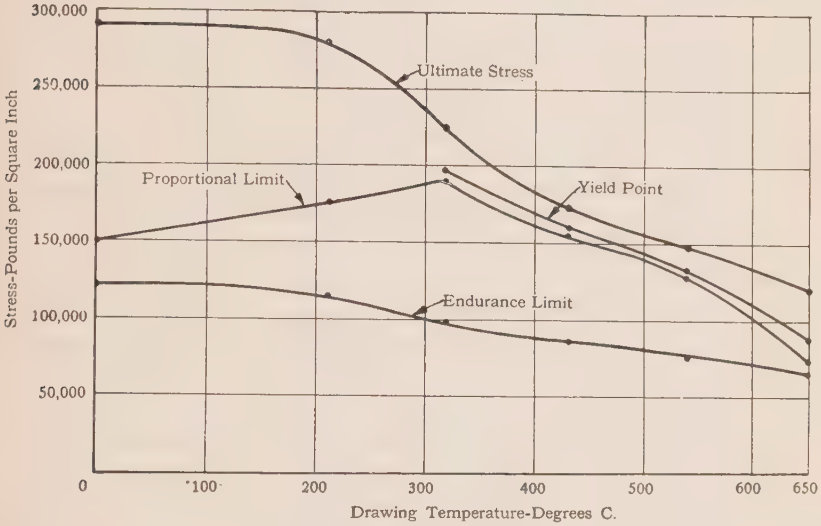

Fig. 365.—Tensile and fatigue properties of 3½ % nickel steel.

Steel Castings.—Very little published data is available on the fatigue properties of steel castings. Some knowledge of such characteristics is of course valuable to the designer, and it is proposed briefly to discuss certain values obtained. In those cases where no previous discussion has been made of a particular material, the tensile test results will also be given for comparison purposes. The first material to be examined is a low carbon steel (0.18 carbon; 0.82 manganese). This was tested by the author in two different states, the first being as cast and the second after being annealed in bar form approximately 1 inch diameter at 900°C. and cooled in the furnace. In Table LXXIII are given the tensile test results and in Table LXXIV the fatigue test results.

---

* Moore and Jasper, Investigation of Fatigue of Metals, *Univ. of Illinois, Bull.* 136, page 64, 1923.

TABLE LXXIII.—TENSILE PROPERTIES OF LOW CARBON STEEL (CAST AND ANNEALED)

State	Proportional limit, pounds per square inch	Yield point, pounds per square inch	Ultimate strength, pounds per square inch	Elongation, % on 2 inches	Reduction, %
Cast	22,000	28,000	60,000	33	49
Annealed	28,500	32,000	63,000	34	61

TABLE LXXIV.—FATIGUE PROPERTIES OF LOW CARBON STEEL (CAST AND ANNEALED)

STATE	ENDURANCE LIMIT, LBS. PER SQ. IN.
Cast	26,000
Annealed	26,500

NOTE.—The points on fatigue test curves were almost as regular for steel castings as for rolled or for forged steel.

It will be noted that the annealing operation improved considerably the tensile properties but left the fatigue characteristics unchanged. This might seem to indicate that there is very little benefit to be derived from annealing such material as far as improvement in endurance limit is concerned. It should, however, be borne in mind that the repeated impact values were improved by the annealing operation.

Coming now to steel castings of higher carbon content we find more striking advantages in subjecting the material to thermal operations. The analysis of this material was 0.3 carbon, 0.70 manganese. In coupon form, approximately 2 in. × 1¼ in. × 32 in. this material was annealed by being heated to 925°C. and cooled in the furnace; and was normalized by being heated to 925°C. and cooled in the air.

In Table LXXV* are given the fatigue test values obtained for the three conditions mentioned above. It was previously noted on page

TABLE LXXV.—FATIGUE PROPERTIES OF MEDIUM CARBON STEEL (0.33 C) (CAST)

State	Ratio k	Ultimate strength, pounds per square inch	Endurance limit, pounds per square inch
Cast	1.67	76,200	30,500
Annealed	1.1	80,000	35,000
Normalized	1.14	85,000	35,000

* See Table XXXVII for the tensile test values.

373 that the advantage to be gained by annealing and normalizing such material on the tensile test values was evident. This fact, as an examination of results in Table LXXV shows, is none the less true for the fatigue properties.

Some results are also available on carbon vanadium castings, carbon −0.3, vanadium −0.18, manganese −0.78, the test bars being machined from coupons similar in dimensions to those described for the previous material. The annealing and normalizing operations were also carried out in a similar manner and at the same temperature. In Table LXXVI are given the tensile test values and in Table LXXVII the fatigue test values for the three states.

Table LXXVI.—Tensile Properties of Carbon-vanadium Steel (Cast)

State	Proportional limit, pounds per square inch	Yield point, pounds per square inch	Ultimate stress, pounds per square inch	Elongation, %	Reduction, %
Cast	22,500	37,000	80,800	23.6	29.6
Annealed	32,000	40,000	80,000	27.5	43
Normalized	50,500	52,500	89,000	26.4	46.7

Table LXXVII.—Fatigue Properties of Carbon-vanadium Steel (Cast)

State	Endurance limit, pounds per square inch	Ratio: $\frac{\text{Endurance limit}}{\text{Ultimate strength}}$
Cast	39,000	.48
Annealed	42,000	.52
Normalized	42,000	.47

These results lend confirmation to the previous statements that the addition of an alloying element raises considerably the ratio of endurance limit to ultimate strength. For the case given, this ratio is approximately .5. An examination of the tensile and fatigue characteristics of these steel castings* will show that the values appear to be as good as those obtained for forged material. It should be remembered, nevertheless, that with steel castings there must always be present the possibility of blow holes and unsound material. Slag inclusions of course are liable and do occur with forged material, but the expectancy is of a higher order with steel castings. Furthermore we have seen that an annealing or normalizing operation is vitally necessary with a casting, and it must be borne in mind that the benefits which we have indicated were obtained on relatively small coupon test bars. Where the masses of cast material are large, these beneficial effects might not be so pronounced, in which case the cast material could conceivably be decidedly inferior to a rolled or forged material.

---

* See author's paper, Carbon and Carbon-vanadium Steel Castings, *Trans. Amer. Soc. Steel Treating*, Feb., 1924.

It seems, therefore, on this basis that the designer must approach the subject. After all it is on the least favorable conditions that all designs must be contemplated, and these for a cast material diverge more from the average than for a rolled or forged material.

Cold Worked Material.—Very little information is available on the effects of cold work on the fatigue properties of materials. In tests made by Moore* it appeared that a cold worked 0.2 carbon steel showed a higher endurance limit than the same material annealed. This was not confirmed however by later results† which he published, where it was shown that overstressing by simple tension in the case of 0.49 carbon steel reduced the endurance limit 23%. Other workers‡ do not appear to confirm these results because in some cases it has been found that the endurance limit bears the same relation to the ultimate strength whether the material be cold worked or subsequently tempered. While sufficient data is lacking on this subject, it appears that overstressing by simple tension lowers the endurance limit. Therefore, the statement that the endurance limit is not affected by cold work appears sound; because, as shown fully in Chap. XIII, the material in a cold worked state is in such a condition that it can be altered by subjecting it to reversal of stress and to temperatures lower than that necessary for metallurgical changes to occur. The point for the designer to note is that, pending further evidence, the advantages gained by cold working on the elastic properties in tension should not be taken as an inference that the endurance limit values will have been correspondingly raised.

Non-ferrous.—Very little work has been done on the fatigue testing of non-ferrous metals. From the results published, however, it appears that the endurance limit of such metals is not so easily determined as that of steel, and whereas 20×10^6 cycles of stress may suffice for steel for this determination, a much higher number appears to be necessary for non-ferrous metals. On certain results obtained by Moore* on manganese bronze, electron metal, and duralumin, he concluded that it might be necessary to run 200×10^6 cycles of stress before the endurance limit could be determined. In a more recent contribution to the literature† it appears from preliminary results that it is even doubtful whether such materials as annealed copper, annealed brass, or annealed bronze have an endurance limit. When this is taken in conjunction with the fact that Haigh‡ obtained, as will be seen later in Fig. 368, very peculiar results on brass, it appears that insufficient data is at present available in order to make definite conclusions possible. Further development of fatigue testing of non-ferrous metals is therefore of prime importance.

---

* Moore and Kommers, An Investigation of Fatigue of Metals, *Univ. of Illinois, Bull.* 124, p. 55, 1921.

† Moore and Jasper, An Investigation of Fatigue of Metals, *Univ. of Illinois, Bull.* 136, p. 66, 1923.

‡ Aitchison, "Engineering Steels," p. 280, 1921.

123. Cycle of Stress Variation.—In the previous paragraph consideration has been given to those conditions of stressing where complete reversal is obtained. We now come to a discussion of those characteristics of materials under cyclic varying stresses other than those obtaining when the stresses are completly reversed.

In Wöhler's original conclusions it has been noted that the range of stress together with the maximum stress determined the failure of the material. In the bending tests previously discussed, the stresses varying from a positive maximum to a negative maximum gave the maximum possible range of stress variation. According to the conclusions of Wöhler, confirmed later by Bauschinger, it can be expected that, if the test bar be loaded such that the compressive stress can be decreased while the tensile stress is increased, any decrease in compressive stress will immediately result in an increase of endurance limit. In other words the results when plotted will give a general relation such as shown in Fig. 366. Any material stressed in such a manner that the maximum stress imposed on the material falls within the shaded area will withstand an infinite number of stress reversals without failure. From these conceptions it can be assumed that the range of stress, of which *ac* represents the maximum value, not only will decrease as the tensile stress is increased but also will decrease if the maximum stress instead of being a tensile one becomes a compres-

---

* R. Moore, Resistance of Manganese Bronze, Electron Metal and Duralumin to Alternating Stresses, *Amer. Soc. Test Mat. Proc.*, 1923.

† H. F. Moore and T. M. Jasper, An Investigation into Fatigue or Metals, *Univ. of Illinois, Bull.* 142, 1924.

‡ Haigh, The Fatigue of Brass, *Inst. Met. Jour.*, Sept., 1917.

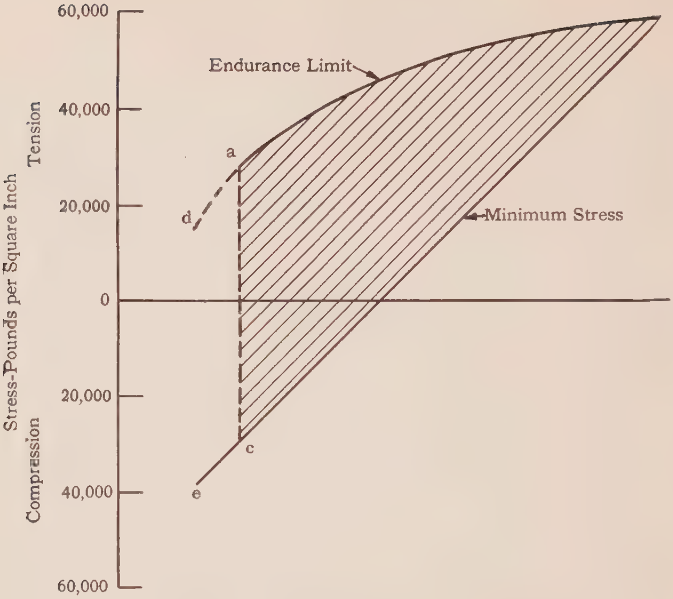

FIG. 366.—Curve of repeated stress showing the change in safe range.

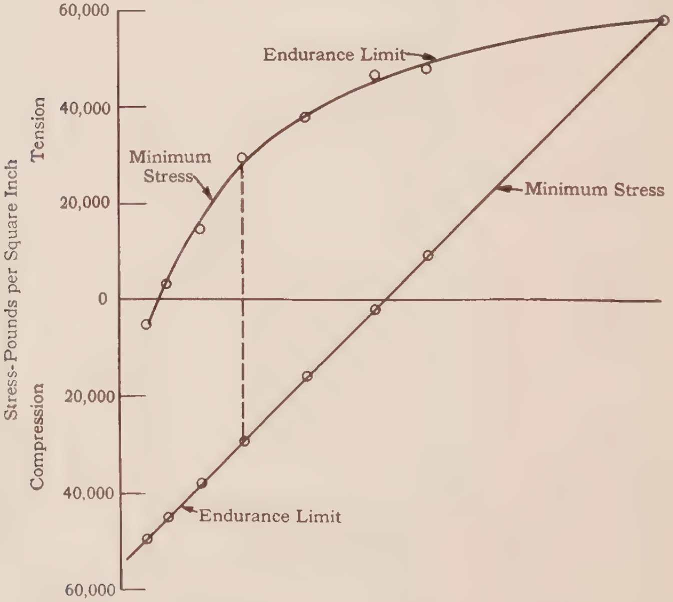

FIG. 367.—Curve of repeated stress for low carbon steel.

sive one. Some results, however, show that the lines *da* and *ec* are approximately parallel. More recent tests* seem to indicate that different materials behave in different ways with changes in the ranges of cyclic stresses. For example, in Fig. 367 is shown the results obtained on low carbon steel. It will be noted that these results are in agreement with the general statements of Wöhler. Coming now to the results shown in Fig. 368 for naval brass,† it will be observed that these lie approximately on a straight line, and that the range of stress increases with increase of compressive stress. Further data must be required before we can afford to get very far away from the fundamental conclusions regarding the fatigue range.

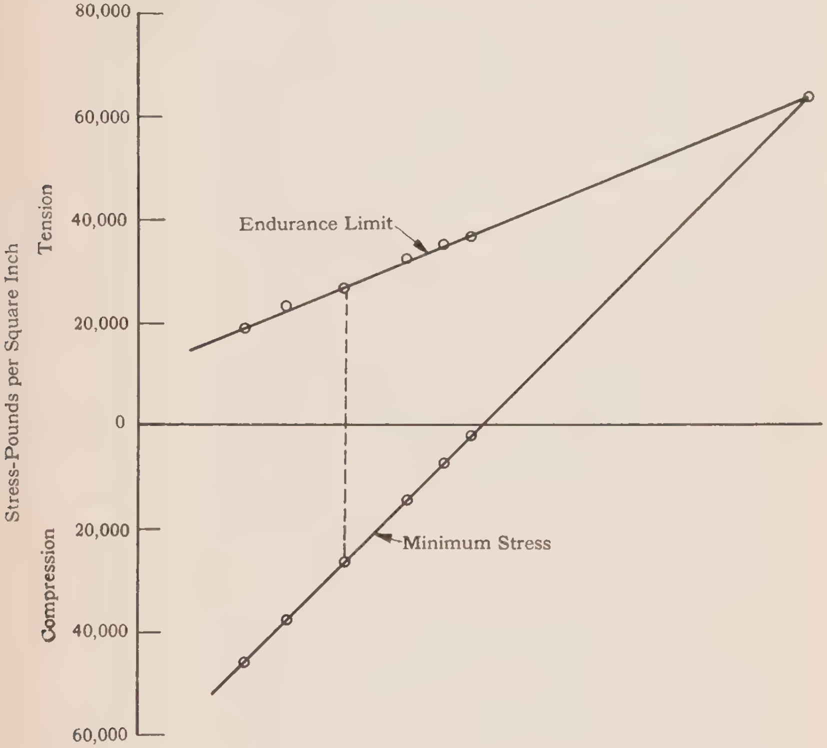

FIG. 368.—Curve of repeated stress for brass.

The important point for the designer to observe in these results is the fact that material can be made to fail under the action of unidirectional stresses at values less than the ultimate stress in tension. In many structures this stress variation might conceivably arise due to temperature changes, and if the member in question be subjected say to a tensile load assumed to be static, such changes may set up a condition which might lead to failure in view of the fact that as the maximum stress is increased the safe range is rapidly decreased.

---

* Haigh, Stress Distribution in Engineering Materials, *Brit. Assoc. Rep.*, 1915.

† Haigh, The Fatigue of Brass, *Inst. Met. Jour.*, Sept., 1917.

124. Effect of Form.—While the importance of providing machine parts subjected to reversal of stress with adequate fillets has been probably well known for a long time, it appears that in certain quarters it is not yet fully appreciated. It is therefore proposed to emphasize, by the presentation of available data on the subject, the importance to the designer of the avoidance, as far as is possible, of excessive stress concentration due to such rapid changes in section.

Stanton* worked on the subject and experimented with three forms of test bars; namely, one having a Whitworth thread (.375 in. diam.), another having a minimum diameter of .295 in. and neck radius of .062 in., and the third having the same minimum diameter but instead of the radius, having a square shoulder. The stress, as we have previously noted, was tensile and compressive. His results showed that for low carbon steel the stress at the endurance limit computed by the common formulae was reduced 30% by the thread, 30% by the .062 inch radius, and approximately 45% by the square shoulder. These endurance values are therefore far below the maximum possible if no concentration of stress is present. Eden† made tests also on V-grooved specimens and found a reduction of approximately 25%

TABLE LXXVIII.—EFFECT OF CHANGE IN SECTION ON FATIGUE PROPERTIES OF MEDIUM CARBON (0.49 C) STEEL

Radius of fillet in inches	Minimum diameter of test bar in inches	ρ/d	Endurance limit, pounds per square inch	Reduction in endurance limit, %
9.85	.275	36	49,000	
1.0	.275	3.5	47,500	3
.275	.275	1	44,500	9
0	.275	0	24,000	51
V notch.....	.275	0	19,000	61

---

* Stanton and Bairstow, On Resistance of Iron and Steel to Reversals of Stress, *Inst. Civ. Eng. Proc.*, 1906.

† Eden, Rose, and Cunningham, The Endurance of Metals, *Inst. Mech. Eng. Proc.*, 1911.

for low carbon steel. Moore* has since extended the work on medium carbon steels for different forms of test bars. In Table LXXVIII are given the results obtained on heat-treated medium carbon steel.

Some results obtained by the author in co-operation with S. Timoshenko on medium carbon steel (C 0.33, Mn 0.65) after annealing at 850°C. and cooling in the furnace are given in Tables LXXIX and LXXX. In this case the test bars were of the cantilever type as shown in Fig. 369, the standard form of bar for obtaining the endurance limit exclusive of stress concentration being as shown in Fig. 363.

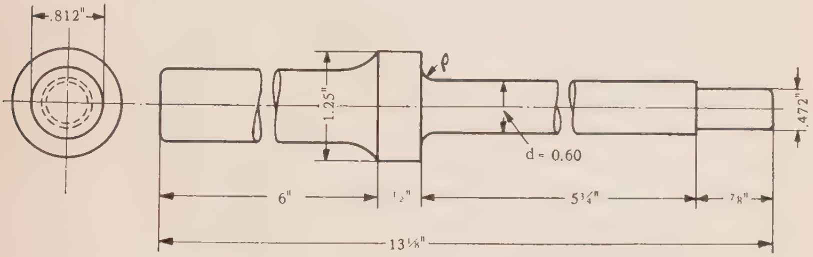

Fig. 369.—Special form of fatigue test bar.

Table LXXIX.—Tensile Test Properties of Medium Carbon (0.33) Steel

Proportional limit, pounds per square inch	Yield point, pounds per square inch	Ultimate strength, pounds per square inch	Elongation, %	Reduction, %
40,600	41,500	73,000	35.5	57

Table LXXX.—Effect of Change in Section on Fatigue Properties of Medium Carbon (0.33) Steel

Radius of fillet in inches	Minimum diameter of bar	ρ/d	Endurance limit, pounds per square inch	Reduction in endurance limit, %
Standard form.	. . .	. . .	32,000	
.15	0.6	¼	29,900	9.7
.05	0.6	1⁄12	21,000	31

From these and previous results it will be appreciated that the endurance limit undergoes a very big reduction when the ratio of

---

* Moore and Kommers, An Investigation of Fatigue of Metals, *Univ. of Illinois, Bull.* 124, 1921.

ρ/d has a value less than 0.25; this reduction for a very square shoulder may become as much as 50% for the class of steel considered, while for harder steels it can conceivably be much higher. The fact that this is no greater is undoubtedly due to the ability which the material has of being able to adapt itself to the new conditions. It has been shown (Part I, paragraphs 2 and 19 B) that in certain cases the maximum stress produced by a rapid change in section may be two or three times as high as the average stress on the section,* and the fact that this stress concentration does not affect the endurance limit in the same ratio is due entirely as mentioned on p. 360 to the ductility properties of the material. In view of the fact that the endurance limit has been shown to depend on the other properties shown by the tensile test rather than on the ductility properties, the importance of these latter values is liable to be neglected. Therefore, where changes in section are necessary on members subjected to cyclical stresses it is not enough to ensure that the endurance value be sufficiently high, but precaution must be taken to ensure that the ductility properties are sufficiently great to allow local yielding of the material under the concentrated stresses and thereby enable a redistribution of the stresses in the best possible manner.

125. Effect of Surface Finish.—So far a discussion has been made of the characteristics of materials when subjected to alternating stresses without reference having been made to the influence of any of the secondary effects such as surface finish, speed, or geometrical form. Since it is to be expected that this influence must have a bearing on the subject, it is proposed to come in this paragraph to a study of the effects of surface finish on the endurance limit, leaving to a subsequent paragraph the consideration of speed and form effects.

Possibly the first contribution to the subject of the effect of surface finish was that made by Eden, Rose, and Cunningham.† They showed that the endurance limit of low carbon steel is materially reduced if the surface is scratched with an ordinary needle. These results also showed that a ground finish did not give maximum resistance, a very important fact to which we will return later. Moore‡ has since made a study of the subject of surface finish, and since he endeavored to standardize the various methods of producing these finishes, his results are valuable. The finish he classified as standard was that obtained by final polishing with No. 0 and No. 00 emery cloth. In Table LXXXI are given the results obtained on a medium carbon (0.49 C) steel in the sorbitic state, and also on a low carbon (0.02 C) material for different degrees of finish.

---

* Wilson and Haigh, Influence of Rivet Holes on Steel Structures, *Brit. Assoc., Rep.*, Sec. A, Sept., 1922. See Abstract in *Engineering*, Sept. 8, 1922.

† Eden, Rose, and Cunningham, *Inst. Mech. Eng. Proc.*, Oct., 1911.

‡ Moore and Kommers, An Investigation of Fatigue of Metals, *Univ. of Illinois Bull.* 124, p. 108.

TABLE LXXXI.—EFFECT OF SURFACE FINISH ON ENDURANCE LIMITS OF STEELS

MATERIAL	FINISH	ENDURANCE LIMIT IN POUNDS PER SQUARE INCH
.49 Carbon	Standard	49,000
.49 Carbon	Rough	50,000
.49 Carbon	Ground	45,000
.49 Carbon	Smooth turned	43,000
.49 Carbon	Rough turned	41,500
.02 Carbon	Standard	26,000
.02 Carbon	Smooth turned	24,000
.02 Carbon	Rough turned	23,000

It will be noted from these results that there is a decided drop in the endurance limit value; this drop for the 0.49 carbon material in the rough turned condition is in the neighborhood of 18%. Another point evident from these results is that the ground finish is not the strongest, being about 10% weaker than the standard finish. This, as we have seen, is in accordance with the results of Eden. A further very interesting contribution to the subject was that made by Thomas.* In Table LXXXII are given the results obtained by this investigator who used a medium carbon (0.33) steel.

TABLE LXXXII.—EFFECT OF SURFACE FINISH ON THE ENDURANCE LIMIT OF STEEL

TYPE OF FINISH	ESTIMATED REDUCTION IN ENDURANCE LIMIT, %
Turned	12
Coarse file	18 to 20
Bastard file	14
Smooth file	7½
No. 3 emery	6
No. 1 emery	4
No. 0 emery	2 to 3
Fine carborundum	2 to 3
Fine ground	4
Accidental scratches	16

These values were put forward as a rough indication yet they agree in general with previous results. Again, the ground finish is not the

---

* Thomas, Effect of Scratches and of Finish on the Fatigue Strength of Steel, *Engineering*, p. 449, Oct. 12, 1923.

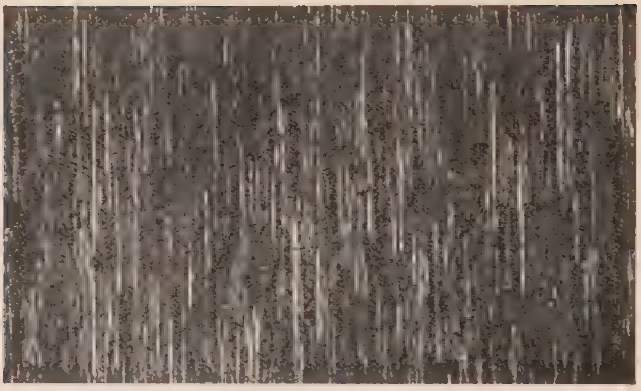

FIG. 372.—Ground.

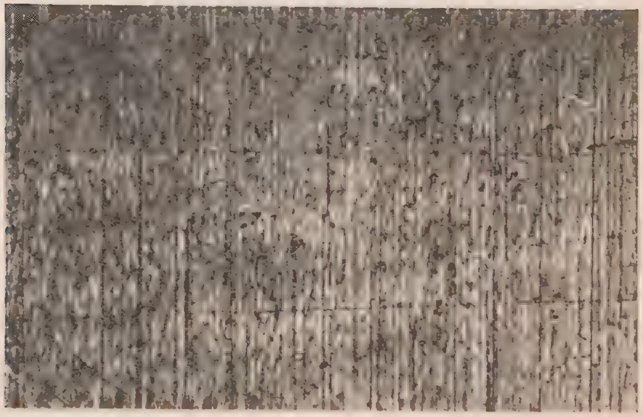

FIG. 371.—Fine emergy and oil.

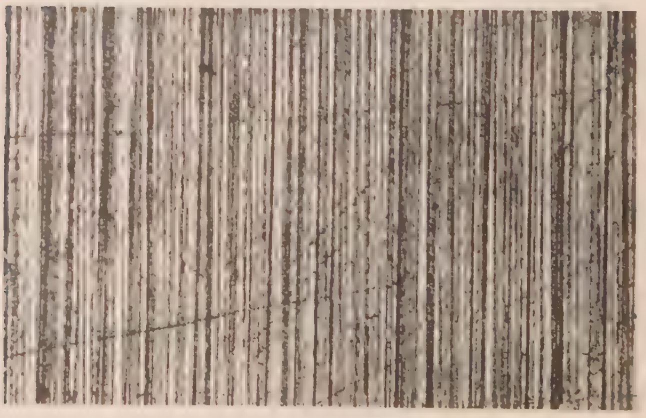

FIG. 370.—No 000 emery.

strongest material. The author has carried this work a little further and from his results has concluded that the final polishing of a material can be carried to too great a degree. In Figs. 370 to 372 are shown photographs of 100 diameters of three finishes namely 000 emery and oil, fine emery and oil, and grinding respectively. It will be noted that the surface shown in Fig. 371 is entirely different from that of the standard finish in Fig. 370. This is felt to be due to oxydation arising from the heat developed by the intensive polishing pressure. While exhaustive tests have not so far been made, a reduction of endurance limit was observed. These results, in general, indicate that there is one finish which gives most favorable results. The ground finish shown in Fig. 372 shows very strikingly the discontinuity in the lines due undoubtedly to chattering effects of the grinding wheel. This in the author's opinion is why previous investigators have found that the ground finish is not the best for maximum resistance.

The conclusions to be drawn from these considerations are that surface finish on machine members is of importance and must be taken into consideration in design.

126. Effect of Speed.—In this paragraph the effect of speed of stress reversal on the value of the endurance limit will be considered. The tests made by Wöhler* were carried out at a very slow speed of reversal, namely 60 per minute. It was not until a comparative recent date, however, that a real study of this speed effect was made. In 1902 Reynolds† contributed to the literature of the subject an interesting paper. In these tests the stress was alternating tension and compression and the speed of alternation was carried as high as 2,500 per minute. These results appeared to show that the high speed had a great effect on the endurance limit. The value obtained for low carbon steel was 13,400 lbs. per sq. inch, while the result obtained on an approximately similar material by Wohler was 26,800 lbs. per sq. inch. Rose‡ made a further contribution for intermediate speeds, and showed that although low carbon steel in the untreated state and with a ground finish gave an endurance limit of 22,000 lbs. per sq. inch when speed of reversal was 280 per minute, yet when this speed was increased to 1,300 per minute the endurance value was unaltered.

---

* Wöhler, Uber die Festigkeitversuche mit Eisen und Stahl, *Z. f. Bauwesen*, 1870.

† Reynolds and Smith, A Throw Testing Machine for Reversals of Stress, *Phil. Trans. Roy. Soc.*, Vol. 199, 1902.

‡ Eden, Rose, and Cunningham, The Endurance of Metals, *Inst. Mech. Eng. Proc.*, 1911.

Moore* has recently found that on five different steels tested by him varying from low carbon to high carbon there was no difference in the endurance limit when the speed was changed from 200 reversals† per minute to 5,000 reversals per minute. This as we have seen is in contradiction to the results of Reynolds, but since the latter investigator used a machine in which the stresses were produced by a reciprocating weight while Moore used a machine having a negligible inertia effect, the chances are that the machine defects in the inertia type would serve to explain these discrepancies. On the other hand, Hopkinson‡ made tests on low carbon steel in tension and compression at a speed of 7,000 cycles per minute. He found that the endurance limit was increased 10% with this increased speed, but his tests do not appear to be comprehensive enough for us to draw definite conclusions. It has been shown (Chap. XIV, page 420) that, according to Plank, when the velocity is high the internal friction of the material has a great effect in assisting the material to resist deformation; the higher endurance limit found by Hopkinson may on these grounds be explained. This investigator, although he did not conceive the friction effect, believed that as the time per cycle was diminished the effect produced might diminish in greater proportion. While, therefore, the question of the effects of speed is still more or less undetermined, it appears safe to conclude that for ordinary speeds of testing which are usually less than 2,000 cycles per minute there is no great effect produced by a change in speed. In order to obtain strictly comparable results, however, a constant speed of operation is desirable.

127. Effect of Temperature.—Very little work has been done on the effects of high temperature on the fatigue characteristics of metals. Batson§ made some tests on medium carbon steel at 250°C. and found the endurance limit decreased to ±37,000 lbs. per sq. inch, being ±47,000 lbs. per sq. inch at 20°C. Lea|| however found that low carbon steel at 390°C. had an endurance limit at least 16% higher than that at 16°C. No conclusions can, however, be drawn from such

---

* Moore and Jasper, An Investigation of the Fatigue of Metals, *Univ. of Illinois, Bull.* 136, p. 59.

† Note.—The idea of recovery from overstrain at such a low speed must not be excluded.

‡ Hopkinson, The Endurance of Metals under Alternating Stresses of High Frequency, *Roy. Soc. Proc.*, Vol. 86, 1912. See also paper by Jenkin, *Report of British Assn.*, (Toronto), 1924.

§ Batson and Hyde, "Mechanical Testing," Vol. 1, p. 339, 1922.

|| Lea, Effect of Repetition of Stresses, *Engineering*, Feb. 16, 1923.

tests.* In a previous chapter the importance of the tensile characteristics at high temperatures was emphasized. This is no less true for the fatigue characteristics and it is to be hoped that in the near future this phase of the subject will receive much more attention than in the past.

128. Short Time Methods.—From the results given in the preceding paragraphs it will be clearly understood that the determination of the endurance limit by the ordinary methods described is a very long process. In the machines, for instance, used by the author the speed is 1,300 R.P.M., and since 20×10^6 cycles is taken as the limiting value, the time required for the making of one test for such a number of reversals is at least 11 days, and as we have seen several other tests are necessary. Due to this fact the development of *short time* methods is of practical importance. These short time methods fall into three classes as:

A. Strain method
B. Rise of temperature method
C. Repeated blow method

which will now be considered in sequence.

Strain Method.—We have already seen that, according to Bauschinger,† when the cycle of stress is from zero to a maximum, if the maximum stress is gradually raised higher than the proportional limit, then the proportional limit will increase with the number of cycles but will not go beyond a certain limit. If the cyclic stress be lower than this limit then fracture will not take place. This led Bauschinger to conclude that this could be made the basis of a short time test, by establishing through a comparatively small number of cycles the limit to which a material could be stressed to maintain an infinite number of cycles.

The development of this idea of a *strain method* for determining the endurance limit was due to Gough.‡ He experimented with torsion tests and, in addition to applying the rise of temperature method previously discussed, he arranged mirrors on the test bar so that the strain imposed on the bar could be read from the movement of a spot of light on a scale after reflection at the mirror. Observations made in this manner showed that at a given value of stress the amplitude of the motion of this spot of light suddenly increased. The stress corresponding to this sudden yielding of the material was found to correspond also to the endurance limit of the material. He concluded that in most cases the break in the curve was more clearly shown than that obtained by the thermal method. In Fig. 373 is shown a curve obtained by him for a 0.65 carbon steel, this data being obtained at the same time as the thermal data shown later in Fig. 376. It will be observed that the break in the curve is very sharp. In the report results obtained from a variety of steels are given, to which further reference can be made. Gough* also appplied this strain method to those cases where the material was subjected to reversed bending stresses. He fitted the mirror in the end of the rotating test bar and, by so arranging the lamp filament (see Fig. 374 for author's modified form) so that it could be moved along a scale until it coincided with the cross wires in a telescope, accurate measurements of the deflection of the test bar corresponding to a given load could be obtained. By gradually increasing the load on the test bar and taking scale readings for each increment a point was reached at which the deflection suddenly increased. The stress corresponding to this load was found to be in

---

* Note.—See Rep. of Brit. Assoc., 1924 for further data by Lea.

† Bauschinger, *Dingler's Poly. Journal*, Vol. 266, 1886.

‡ Gough, Some experiments on the Fatigue of Material, *Aeronautical Res. Comm., Rep.* No. 743, 1922.

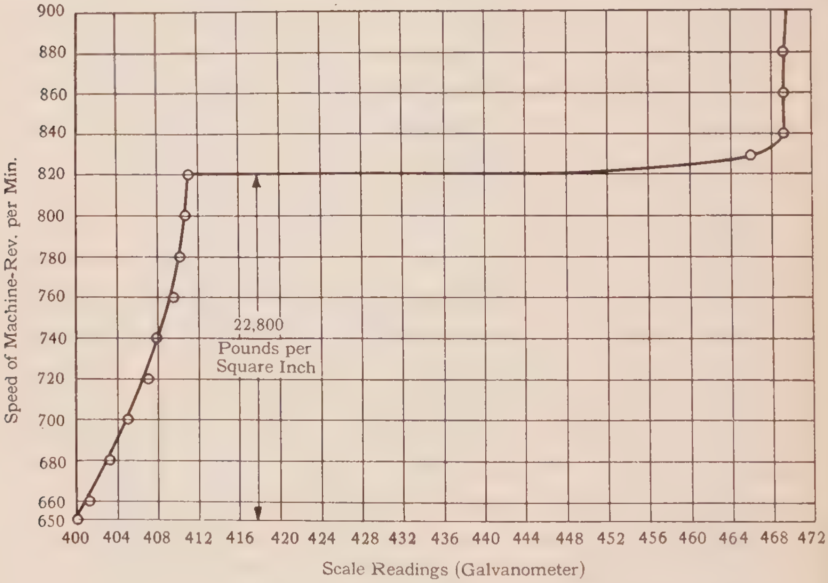

Fig. 373.—Curve of stress and strain for torsion fatigue of 0.65 carbon steel.

---

* Gough, Some Experiments on the Fatigue of Metals, *Aeronautical Res. Comm., Rep.* No. 743, 1922. See also Batson and Hyde, "Mechanical Testing," Vol. 1, p. 258, 1922.

good agreement, for the materials examined, with the endurance limit as found by long time tests. Another very important point brought out was that the value of endurance limit found in this manner on solid specimens agreed well with the results obtained for hollow specimens. This point is very important since it eliminates the necessity of machining hollow specimens. This method has also been applied by Lea,* who made tests on several carbon steels. The results led this investigator to conclude that this method of determining the endurance limit is one which requires great care; he pointed out that the material should not be overstressed and then retested.

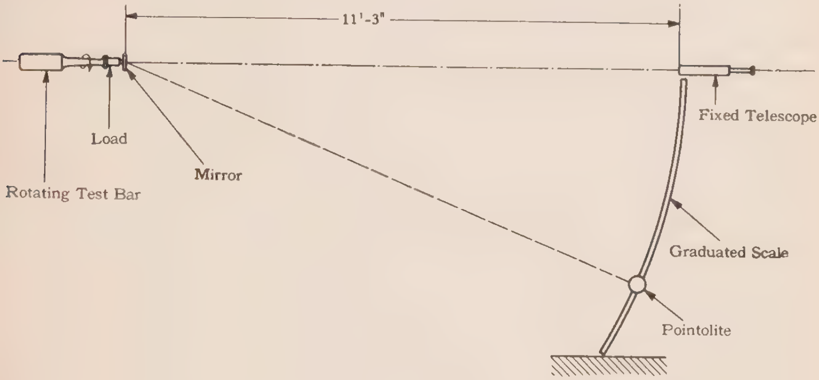

FIG. 374.—Arrangement of apparatus for determining endurance limit by deflection method.

A considerable amount of investigation work has been done by the author on this type of testing. The apparatus employed being an adaptation of that used by Gough is shown in diagrammatic form in Fig. 374. In Fig. 375 are shown the curves obtained for 0.37 carbon steel annealed and heat-treated respectively. For purposes of comparison the endurance limit obtained by the long time method is shown at *A* in each diagram. The short time method is therefore in good agreement with the long time tests. Referring to these figures it will be noted that the proportional limit in tension marked by *B* is in excess of the endurance limit obtained either by the short or long time methods. This fact seems to be important because, in work done by the author on a variety of steels, provided the proportional limit is less than the value of stress obtained by the short time method, then the results given by this latter method are not in good agreement with the results of the long time tests and may give entirely misleading results. This was mentioned by the author* previously, and in a recent contribution he† discusses this fact in more detail.

---

* Lea, The Effects of Repetition Stresses on Materials, *Engineering*, Feb. 23, 1923.

It appears therefore advisable to apply this method with a great deal of caution especially in the cases of new and more or less unknown materials. There is no doubt that such a short time method as this has advantages over the rise in temperature method, but this does not justify us, at this stage in its development, in applying it blindly to all materials.

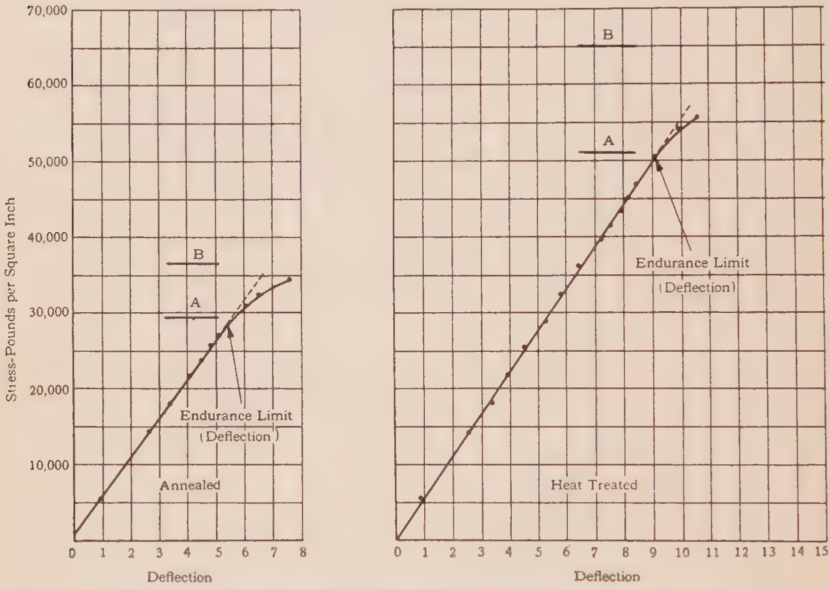

FIG. 375.—Stress-deflection curves for medium carbon steel.

Rise in Temperature Method.—The *rise in temperature method* is based on the fact that when a material is repeatedly stressed beyond a certain limit, definite thermal phenomena appear which can be measured. The work done on the material by the repeated application of stress appears in the form of heat energy and by studying the change in temperature of the test bar under stress, data on the effect of this stress can be readily observed. In order to determine the endurance limit all that is necessary is to so arrange the test bar that accurate temperature measurements can be made corresponding to any stress value commencing from zero. Usually these temperatures are measured for the plane of maximum stress. If, starting from zero, these measurements are made allowing sufficient time between readings to have temperature equilibrium, which time must be constant, then on plotting stress as ordinate and temperature as abscissae it will be found that the temperature increases with increase in stress up to a certain value, when the increase becomes much more rapid. The stress corresponding to this point has been called the endurance limit of the material. Stromeyer* was the first to use this method for endurance limit determination. He experimented with torsion fatigue tests and measured the temperature of the specimen by two thermometers, one placed at the inlet and the other at the outlet of a water jacket surrounding the test bar the jacket allowing water to pass

---

* See the author's Discussion of McAdam's Paper on Fatigue, *Amer. Soc. Test. Mat. Proc.*, 1923.

† See the author's Paper: *Inst. Mech. Eng. Proc.*, Dec., 1924.

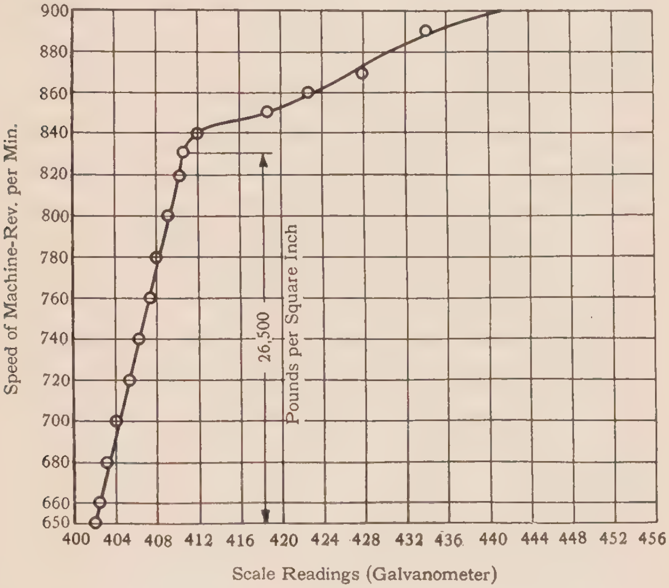

FIG. 376.—Curve of stress and temperature rise for torsion fatigue of 0.65 carbon steel.

---

* Stromeyer, Determination of Fatigue Limits, *Roy. Soc. Proc.*, p. 114, 1914.

slowly along the surface of the bar. He concluded that the torsional endurance limit occurred at that temperature corresponding to a given rise in temperature. Gough* has since extended this method by employing more delicate temperature measuring apparatus. Instead of the thermometers he used thermocouples and obtained in this manner greater accuracy in temperature measurements. In Fig. 376 is shown a curve for medium carbon steel reproduced from his results. It will be noted that the break in the curve is well defined and that the endurance limit occurs at a stress of 26,500 lbs. per sq. inch, whereas the endurance limit obtained by the long time tests was also 26,500 lbs. per sq. inch; so the agreement is very close. The results were also in good coincidence with those found by the strain method previously described. Putnam† has also contributed to the literature of the subject, having made tests on many different steels. In Fig. 377 are shown curves reproduced from their work for material varying from iron to 1.2 carbon steel. In this case the speed of the machine was 1,000 R.P.M., and for the first three curves the period between successive readings was 30 seconds, but this of course will depend both on dimensions and material. It was found for instance that this period was too short for the heat-treated steels and a period of 2 minutes was adopted for such. The author feels that this question of time interval between successive readings is important and must be considered. The endurance limit in these tests was taken as that point where the curve showed a sharp break. The author has added in Fig. 377 horizontal lines marked *A* representing the endurance limit as determined from the long time tests and it will be seen that there is agreement between the two methods. It will also be observed however that the curves do show a break at points considerably below that chosen as the endurance limit. These workers felt that this point might be the *real endurance limit* of the material. The fact remains that such a method as this requires very accurate temperature determination otherwise grave errors may arise. This test, used as a check test, has useful application but in our present state of knowledge it would be dangerous to let this test entirely displace the long time tests.

Repeated Blow Tests.—It has been previously mentioned under repeated impact tests page 410) that the results obtained from

---

* Gough, Some Experiments on the Fatigue of Materials, *Aeronautical Res. Comm. Rep.*, No. 743, 1922.

† Putnam and Harsch, Rise of Temperature Method of Determining Endurance, *Univ. of Illinois, Bull. No.* 124, p. 119, 1921. Putnam's work was apparently prior to that of Gough.

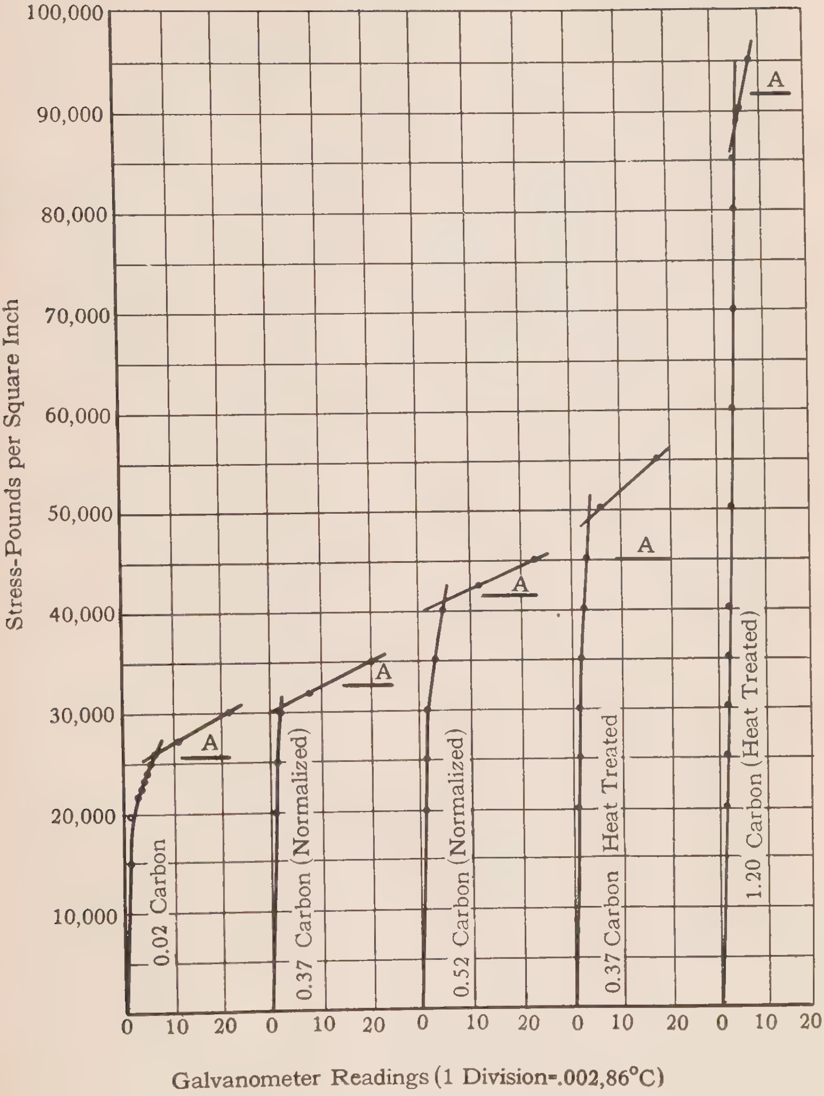

Fig. 377.—Curves of stress and temperature rise for bending fatigue of carbon steels.

such tests can be closely associated with the fatigue properties. As we previously noted, Stanton* discussed this question in detail and, when using a test bar form as shown in Fig. 378, he concluded that when the number of blows to fracture exceeded 100,000,† the conditions represented by this height of drop approximated to fatigue conditions. In other words, the ordinate at that point represented to some scale the endurance limit of the material. If, therefore, these heights are available for different materials not differing widely in microstructure, and the endurance limit has been determined by long time methods for one material, then a good approximation for the endurance limits of the others can be obtained from the ratio of the heights obtained from the curve of repeated impact. The author, using the Stanton type of machine, has carried out many tests on this phase of the subject. As has been seen in Chap. XIV, the test bar used is shown in Fig. 344 which, as previously mentioned, is a modification of the original one of Stanton. In Table LXXXIII are given the results obtained for a 0.37 carbon steel in the rolled, the annealed, and the normalized conditions. Choosing as the basis the height of drop corresponding to 80,000 blows, the values in the second column were obtained from the respective curves of repeated impact. The endurance values given in the third column were taken from Table LXVIII and represent the endurance limits obtained by the long time methods. In the last column are given the endurance limits calculated on the basis of the material in the rolled condition, in which case 28,000 lbs. per sq. inch obtained from the fatigue test corresponds to 0.26 drop obtained from the repeated impact test. The error, it will be noted, by this calculation is within that obtained

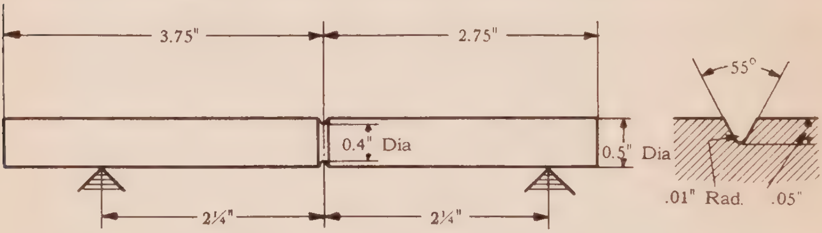

Fig. 378.—Sketch of Stanton test bar.

---

* Stanton, Resistance of Material to Impact, *Inst. Mech. Eng. Proc.*, Nov., 1908.

† Note.—On this basis, the repeated blow test can scarcely be classified as a short time test, but since it requires shorter time than the ordinary tests it is included here.

Table LXXXIII.—Repeated Shock and Fatigue Properties of 0.37 Carbon Steel

State	Height of drop for 80,000 blows	Endurance limit, pounds per square inch*	
		By experience	Calculated
Rolled	0.26	28,000	28,000
Annealed	0.25	28,600	27,000
Normalized	0.27	29,300	29,000

* Note.—It was assumed in these calculated values that the asymptote of the repeated impact test curve was reached at 80,000 blows and that this corresponded to 28,000 lbs. per sq. in., as obtained from the fatigue test. The other endurance limit values were then calculated on this basis.

in usual experiments. In Table LXXXIV are given the results for a carbon-vanadium forged material for two states, the first being obtained after the steel had been normalized in bar form (5 in. dia.) by being heated to 870°C. and cooled in air, and the second after being annealed at 870°C. and cooled in the furnace.

Table LXXXIV.—Repeated Shock and Fatigue Properties of 0.52 Carbon 0.19 Vanadium Steel

State	Height of drop for 80,000 blows, inches	Endurance limit, pounds per square inch	
		By experiment	Calculated
Normalized	0.46	54,000	54,500
Annealed	0.38	45,000	45,000

The results shown in Table LXXXV are for the 0.37 carbon steel of Table LXXXIII after heat-treatment. Further data on other material has been published by the author.* Probably sufficient has

Table LXXXV.—Repeated Shock and Fatigue Properties of 0.37 Carbon Steel Hardened in Water 850°C. (2¼ Inch Diameter) and Tempered

Tempering temperature	Height of drop for 80,000 blows, inches	Endurance limit, pounds per square inch	
		By experiment	Calculated
100°C.	.43	52,000	52,200
450°C.	.42	50,000	51,000
550°C.	.42	51,000	51,000

---

* See the author's Paper—Static and Dynamic Tests for Steel, *Trans. Amer. Soc. Steel Treaters*, Oct., 1923.

been said of this method to enable us to conclude that the application of the data given by the repeated shock test enables us to predetermine the endurance limit of the material provided the above mentioned procedure is adopted. This will make the running of long time endurance tests unnecessary in all cases, and hence gives a comparatively short time method. The results therefore are of practical importance to the designer, and the discussion of this test is fully justified.

129. Significance to the Designer.—The importance of the fatigue test characteristics to the designer cannot be too strongly emphasized. Like the tensile test, the fatigue test provides him with *fundamental* data which can be used directly in design. As we have seen the static tensile test may be able to give a good indication of the fatigue characteristics, nevertheless it appears that more evidence must be forthcoming before the tensile test can always be used as the only guide, unless for the common grade carbon steels on which much data is now available. With special steels, cold worked steels, and non-ferrous metals there is little or no data, and fundamental tests must be made if a rational design is to result therefrom.

Fatigue tests also are valuable in that they enable a picture to be made of the effects of stress concentration. By their further application in conjunction with stress analysis to a study of fillets, keyways, and holes we will yet be able to obtain a true measure of the value of ductility.

The test as it stands at present has the decided drawback that it requires long periods of time to accomplish; nevertheless it is to be hoped that the discussion of short time tests may be further developed so that this difficulty can be overcome.

That the importance of this form of dynamic testing has been appreciated by engineers in general is evident from the amount of activity in this line of testing. That this importance will tend to increase, once the significance of test has been truly appreciated, is the only logical conclusion to make by those who are interested in the advancement of better and more economical designs.

CHAPTER XVII

THEORY OF STRENGTHS

130. General.—*Simple Stress.*—In the design of members to withstand the action of *simple stresses* such as tension, compression or shear there is no difficulty in arriving at suitable dimensions. The state of stress in any single element whether this be tension, compression, or shear, shown in Fig. 379 can be reproduced experimentally, and all necessary data such as proportional limit, yield point, or ultimate strength can be obtained from the stress strain diagram as shown in Fig. 380, from which the dimensions necessary can be calculated.

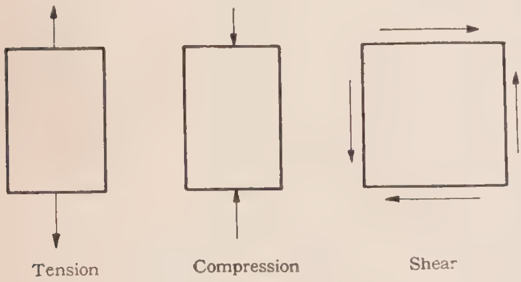

FIG. 379.—States of simple stress.

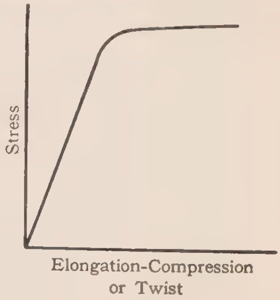

FIG. 380.—Stress—strain—diagram for tension, compression or shear.

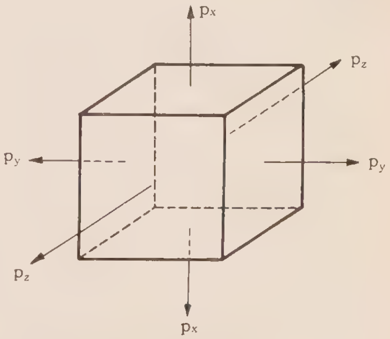

FIG. 381.—State of combined stress.

Combined Stress.—For the *general case* of state of stress represented by three principal stresses as shown in Fig. 381 the determination of values such as proportional limit, yield point, or ultimate strength cannot be determined by a single test, and since it is impossible to make experiments to suit all the varieties of relations between the principal stresses met with in service, it is therefore necessary to inquire into fundamental facts underlying *failure.** This can only be done by conducting tests on certain general cases and from these tests developing a *theory* or theories and applying these conclusions to all conditions. The problem before us in this chapter is therefore to discuss these various theories which have been developed from time to time by various investigators, and so place before the designer as clear a conception as the subject will allow.

131. Variety and Scope of Theories.—From the consideration given in the first part of the book to the subject of combined stresses (see paragraph 3, page 11) it will have been appreciated that the form of the final design to withstand the action of such stresses will depend in large measure on the manner in which it is assumed the structure will fail. This may be either due to a given value of the maximum tensile stress, or a given value of the maximum strain, or a given value of the maximum shear stress, from which conceptions the four well known theories for such failures have their genesis.

Before we begin to consider in detail these various theories it seems advisable to specify what is meant by failure. This raises some slight difficulty because, from previous considerations, it has been seen that there are two classes of materials, one, such as low carbon steel, which possesses a proportional limit and yield point and the other, such as cast iron or copper, which does not. Guest† in his work on low carbon steel takes the yield point as the criterion of failure and it is proposed here for such material to take the *point of failure* as that point where permanent set begins, namely the proportional limit, and for such material as cast iron, the ultimate stress to fracture.

132. Maximum Stress Theory.—The *maximum stress* theory assumes that regardless what the ratio of the stresses acting on mutually perpendicular planes may be, whether these stresses are like or unlike, failure will occur when, and only when, one of the stresses reaches the value corresponding to the limiting stress in tension or compression as the case may be. It takes no account of the fact that the material may be strengthened or weakened due to the action of the two other principal stresses acting at right angles to the one considered.

---

*NOTE.—By failure as will be seen later is meant the proportional limit for ductile materials such as low carbon steel, and the ultimate stress for material such as cast iron.

† Guest, Strength of Materials under Combined Stress, *Philosophical Magazine,* July, 1900.

In other words, referring to Fig. 381 which represents three like stresses acting on mutually perpendicular planes, if $p_x > p_y > p_z$ and if the stress just to cause failure under simple tension or compression be p, then failure will occur only when $p_x \geq p$. In Fig. 382 is given a representation of this theory, according to Becker.[*] If a tensile stress *OB* or a compressive stress *OD* be applied to a material then if these represent the limiting stresses to just cause failure and if a further tensile stress such as *OE* be applied at right angles to the direction of the previous stresses provided that *OE* is less than *OA*, this second stress will not contribute to failure.

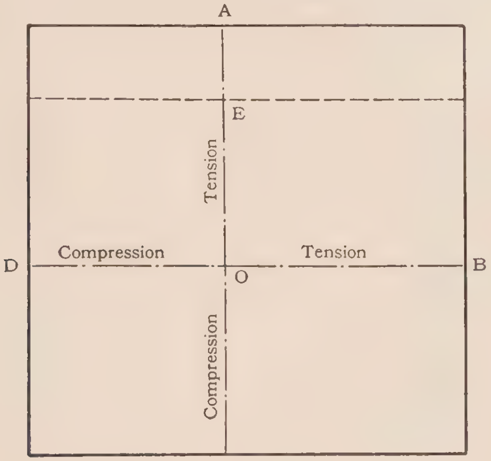

FIG. 382.—Representation of maximum stress theory.

If such a theory were strictly true then all materials would be expected to fracture in a direction at right angles to the maximum stress.[†] But reverting again to simple tension we know that while a brittle material such as cast iron will so fracture as shown in Fig. 383, ductile materials such as low carbon steel do not show such characteristics. For example we have the appearance of Lueders lines on the surface of such material (page 358). These lines as we have seen are inclined at 45° approximately to the axis of stress and indicate, at this stage at least, the predominating effect of tangential stresses. We have further evidence in the fractured ends of tensile test pieces from such ductile material. The fracture plane is not at right angles to the stress as in the previous case but is inclined to it at an angle giving rise to the cup type of fracture shown in Fig. 384 (a).

---

[*] Becker, The Strength and Stiffness of Steel under Bi-axial Loading, *Bulletin No.* 85, *University of Illinois.*

[†] NOTE.—By fracture is meant the breakdown of the material. If we speak of permanent set, it can be assumed that this will occur in the weakest plane perpendicular to the maximum stress.

In many cases the type of fracture obtained on ductile materials is represented by a truncated cone as in Fig. 384 while for brittle material the fracture plane will, as we have seen in Fig. 383, be at right angles to the axis of stress. Taking again the ultimate stress instead of the proportional limit as the point of failure it will be found that test bars of low carbon steel, tested in torsion, will fracture in a plane at right angles to the axis, i.e., in the plane of maximum shearing stress.

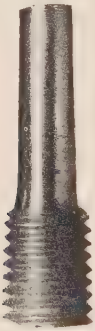

Fig. 383.—Fractured end of cast iron test bar.

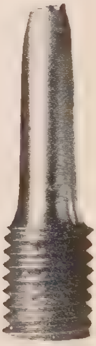

Fig. 384.—Fractured ends of low carbon steel.

The strongest factor contradicting this theory is, however, the well known fact that *homogeneous* materials withstand hydrostatic pressures in excess of their simple breaking stress values. This could not be so were the theory to be rigidly true. On these two points, therefore, the theory, while apparently true for such a material as cast iron, cannot be generally applied.

133. Maximum Strain Theory.—The *maximum strain* theory (or St. Venant theory) holds that when the state of stress in any single element is given by two or three principal stresses the strength is increased if the stresses are like in sign, and that the maximum strain due to such stresses is the criterion of failure. This conception appears to take into consideration the forces existing between the molecules composing the crystals since these must, in large measure, determine the extent to which strain in one direction will result in strain in a direction at right angles. Referring again to Fig. 381 which represents the stresses acting, and taking

$\frac{1}{m}$ = Poisson's ratio,
E = Modulus of elasticity,
e = Strain in direction x corresponding to a simple tension p,
p = Limiting stress to cause failure in simple tension,

then the limiting value of e will be

$$e = \frac{p}{E},$$

and in order that failure must not take place,

$$\frac{p_x}{E} - \frac{1}{mE}(p_y + p_z) \overset{=}{<} e,$$

or

$$p_x - \frac{1}{m}(p_y + p_z) \overset{=}{<} p$$

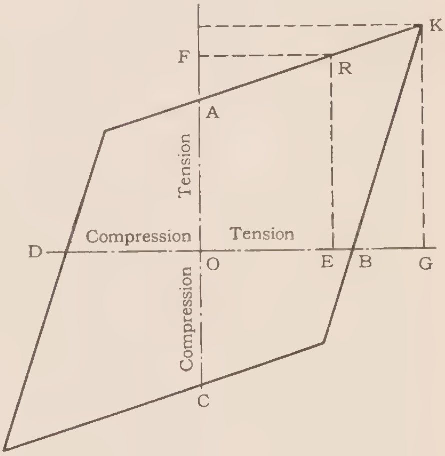

Fig. 385.—Representation of maximum strain theory.

In Fig. 385 is given the graphical representation of this theory according to Becker. *OA* and *OB* represent the limiting stresses in tension, and *OC* and *OD* those for compression. A tensile stress of magnitude *OE* would require a tensile stress equal to *OF* acting at right angles to cause failure. For two equal tensile stresses, failure would not occur until a stress value corresponding to *OG* be reached.

This theory is not supported by experimental results, because, as shown by the known experiments of Wehage,* the strength of a material in one direction is not increased by a tension in a direction at right angles.

134. Maximum Shear Theory.—The *maximum shear* or Coulomb theory holds that when a material is subjected to the action of two or three stresses on mutually perpendicular planes, failure will occur only when the maximum tangential stress reaches a certain limiting value.

Referring to Fig. 381, if

$$p_x > p_y > p_z,$$

---

* Wehage, *Mitteilungen d. Techn. Versuchsanstalten*, (Berlin), p. 89, 1888.

the maximum value of the tangential stress will be

$$\frac{1}{2}(p_x - p_z),$$

(see p. 16) the intermediate stress having no effect; and in order that failure will not occur,

$$\frac{1}{2}(p_x - p_z) \overline{\overline{<}} \frac{p}{2},$$

where p denotes the limiting stress in simple tension, or

$$\frac{p_{\max} - p_{\min}}{2} \overline{\overline{<}} \frac{p}{2},$$

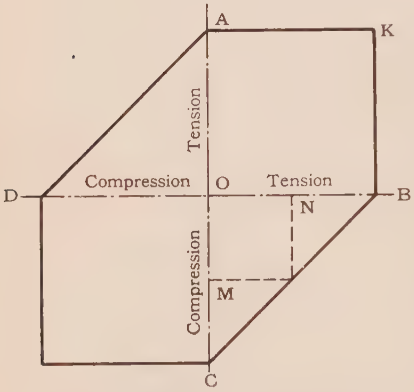

FIG. 386.—Representation of maximum shear theory.

Bearing in mind the fact that the *intermediate* stresses have no effect, then a graphical representation may be given of these shear stresses.

In Fig. 386 is again shown this representation according to Becker. For the case of two tensile stresses the intermediate stress is evidently the lesser of these stresses, and for such conditions we have maximum shear stress

$$\frac{p_x - 0}{2} = \frac{p}{2}$$

giving $p_x = p$ = limiting stress in tension, and this will be represented by a rectangle *OAKB*, which corresponds to the maximum stress condition. If the two stresses be tension and compression then the intermediate stress will be zero, and the maximum shearing stress will be determined by the lines *AD* and *BC*, inclined at 45°, due to the fact that

$$\tfrac{1}{2}(p_x - p_z) = \text{constant} = p_t.$$

Referring to Fig. 386, a tensile stress, represented by *ON*, combined with a compression stress, represented by *OM*, will cause yielding of the material.

This theory seems for ductile materials to be in better coincidence with experimental fact than the other two theories previously discussed. A very important contribution was made in support of this theory by

Guest.* His experiments were all made on ductile materials, low carbon steel, copper, and brass. While the tests on the non-ferrous metals were insufficient to enable definite conclusions to be made, the tests on steel substantiated the theory in that the maximum tangential stress appeared to be the cause of failure.

It will have been understood from the previous statements that it is presupposed the proportional limit in tension and compression are the same. We know that this is only approximately true for such ductile materials as low carbon steel and for these materials the maximum shear theory can be used. With a material like cast iron where the properties in tension and compression are vastly different some allowance for these facts is necessary. Such is provided by the Mohr theory and to the consideration of this we will now come.

135. Mohr Theory.—We now come to a theory which, as an extension of the maximum shear theory, appears to have received too little attention in English engineering text books, namely the *Mohr theory*.

As we have seen the maximum shear theory presupposes that the limiting stress in tension and compression are alike. As is generally known this is approximately true only for steels. Any theory which makes allowance for this difference is therefore more valuable since it can be generally applied. Such is the Mohr† theory, being in reality an extension of the maximum shear theory.

As has been discussed in (paragraph 5, page 16) the state of stress at a point in a body can be represented by the Mohr circles as shown in Fig. 387. In the case as shown

$$p_x > p_y > p_z.$$

The theory of Mohr is based on the following statement:

If a point be taken in a stressed body, then an infinite number of planes can be traced through it, such that these will have the same normal stress. From all these planes the weakest will be that which has the maximum tangential stress. Supposing all planes with normal stress equal to p be taken as shown in Fig. 387, the shearing stress will vary from B to A and the maximum shear stress will correspond to point A. This means that from all the planes having the same normal stress the maximum shear will act on that going through the intermediate stress, i.e., considering the condition of safety at this point, it is necessary only to consider the outer Mohr's circle. This is equivalent to saying that the intermediate stress has no effect on the condition of failure. Due to the fact that the limiting stress may be different for different ratios of p_x and p_z the corresponding Mohr's circles may have different radii. This therefore leads to a general diagram as shown in Fig. 388 for the Mohr theory. In this diagram the curve such as *AB* represents the *enveloping curve* for all possible circles representing different limiting states of stress. Every circle tangent to this envelope will give one of the possible limiting states of stress, and by drawing this circle the radius will then be the limiting shear stress and the points of intersection of the circle with the axis of abscissae will then represent the corresponding maximum principal stresses. On the other hand when the conditions of failure for tension and compression are alike, limiting circles become equal and the Mohr theory becomes the maximum shear theory as shown in Fig. 389 provided that the enveloping curve is assumed for such conditions to be a straight line. Since this theory is general in its application it is to be recommended in preference to those already mentioned.

---

* Guest, Strength of Materials under Combined Stress, *Philosophical Magazine*, July, 1900.

† Mohr, Die Elastizitatsgrenze und den Burch eines Materials, *Zeit. d. Ver. Deut. Ing.*, p. 1530, 1900.

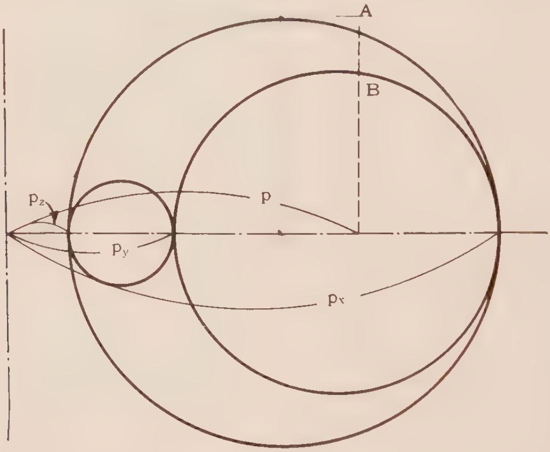

FIG. 387.—Graphical representation of three mutually perpendicular stresses.

136. Other Theories.—In addition to the theories already discussed there are certain other ones which must be mentioned.

Becker,* due to certain experimental work which he carried out, concluded that neither the maximum strain theory nor the maximum shear theory were true, but that a combination of both agreed with his experimental results. The strength at the yield point follows the maximum strain theory until the shearing stress reaches the value of the shearing yield point, after which failure occurs according to the maximum shear theory. Reyto* suggested a further modification of the maximum shear theory which took into consideration *internal friction.* This theory would appear to explain why the Lueders' lines in tension and compression have different inclinations to the axis of stress. If the friction angle is zero the internal friction theory becomes the maximums shear theory.

---

* Becker, The Strength and Stiffness of Steel under Bi-axial Loading, *Bulletin No.* 85 *of University of Illinois.*

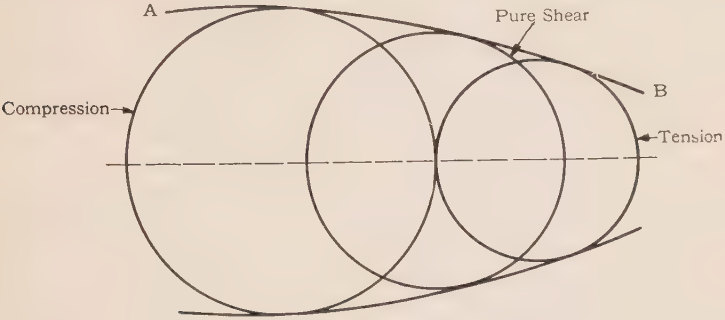

Fig. 388.—Graphical representation of Mohr theory.

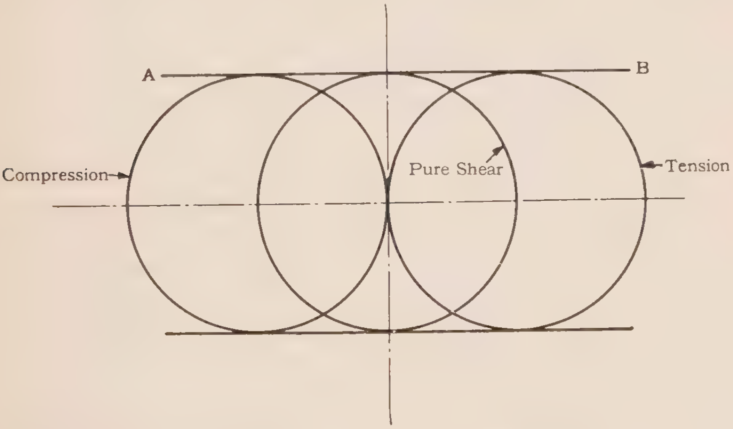

Fig. 389.—Particular case of Mohr theory—maximum stress theory.

---

* Reyto, "Die Innere Reibung," 1897.

Still a further theory was put forward by Beltrami* which has now been discussed by Haigh.† In this, account is taken of the maximum resilience stored in the material under stress and failure is explained as the critical amount of energy stored per unit volume. Quantities of work are done on the metal in a strictly reversible manner; this may be expressed in terms of the applied stresses and elastic constants. If W is the work done, then if the material be isotropic,

$$W = \frac{1}{2E}(p_x^2 + p_y^2 + p_z^2) - \frac{1}{mE}(p_xp_y + p_yp_z + p_xp_z)$$

or

$$C^2 = p_x^2 + p_y^2 + p_z^2 - \frac{2}{m}(p_xp_y + p_yp_z + p_xp_z).$$

where C = a constant. This relation on being plotted gives an ellipsoid shown in Fig. 390 where it is drawn superimposed on that for the maximum strain theory.

It appears from this representation that the maximum strain theory overestimates the critical stress value when the two stresses are equal and like. In general it will be observed that none of these modifications get very far away from the maximum shear theory, and do not appear to change the basis of the conclusions already made regarding it.

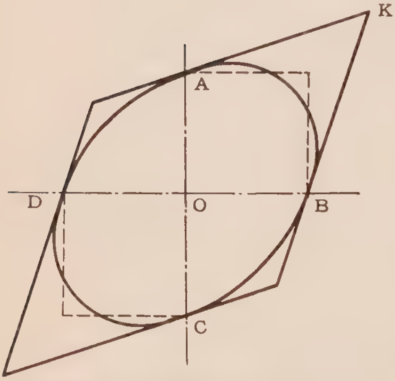

FIG. 390.—Graphical representation of Haigh theory.

137. Limitations.—In the consideration given to these various theories it has been assumed that the material is homogeneous and isotropic. In reality it is not so and a word of caution is therefore necessary in order that these limitations may be observed.

According to the maximum shear theory it is to be expected that the proportional limit in torsion will be 50% of that in tension. If solid test bars are being employed in torsion, then, due to the stress varying over the cross section, it is difficult to detect deviation from the proportionality law, and consequently the indicated proportional limit in torsion will usually be higher than 50% of that in tension.

* Beltrami, *Rendiconti*, p. 704, 1885; *Math. Annalen*, p. 94, 1903.
Girtler, Wien Berichte, Vol. 116, 1907.

† Haigh, The Strain Energy Function and the Elastic Limit, *Rep. of Brit. Assoc. for Advancement of Science*, p. 324, 1921.

From tests made by the author, it is evident that lack of homogeneity of material may lower considerably this ratio from the 50% according to the maximum shear theory. In one case this ratio was observed to be 40%, the material on being examined microscopically showing decided nonhomogeneity in structure.

The point we are emphasizing is that there is the possibility of considerable variation arising in a particular design depending on the theory adopted as a criterion of failure, but that these variations may be no greater and may even be less than those arising from nonhomogeneity in the material itself. It is therefore very necessary, in applying such theories as have been discussed, to know just how far the material is homogeneous and in this respect the microscope can be of great value to the engineer.

138. Conclusions.—In concluding this discussion of the strength theory it is proposed to take certain cases* of simple and complex loading and apply the theories to their solution. By this means the divergence in the results obtained can be seen at once. In the consideration of numerical examples we will only be concerned with the first four theories discussed namely maximum stress, maximum strain, maximum shear and Mohr theories.

Simple Torsion.—In the case of simple torsion it has been shown (paragraph 8, page 26) that the material is in a state of pure shear and that this is equivalent (page 14) to tension in one direction combined with compression in a direction at right angles. If p_x and p_y represent these stresses respectively and using the adopted notation, then

$$p_x = -p_y = \frac{16M_t}{\pi d^3},$$

and

$$p_x - (p_y) = 2p_x = \frac{32M_t}{\pi d^3}.$$

In order to show the variation which can be expected according to the theory adopted, the three theories will be applied in this case.

Maximum Shear Theory.—This theory implies that the difference between the principal stresses must not be larger than the *working stress*† in simple tension. Accordingly, if p be the value of this working stress, then

$$d^3 \gtreqless \frac{32M_t}{\pi p},$$

---

* Roth, Die Festigkeitstheorien, *Zeit. f. Mathematik und Physik*, Volume 48, p. 285, 1902.

† Note.—See Chapter XVIII for a discussion of working stresses.

and

$$d \approx \sqrt[3]{\frac{10M_t}{p}} \approx 2.15\sqrt[3]{\frac{M_t}{p}},$$

Maximum Strain Theory.—This theory requires that the maximum strain corresponding to the combined stresses must not be greater than that due to the working stress in simple tension. Therefore

$$\frac{p_x}{E} - \frac{1}{m}\frac{p_y}{E} \overline{\underset{}{<}} \frac{p}{E}$$

$$\frac{p_x}{E}\left(1 + \frac{1}{m}\right) \overline{\underset{}{<}} \frac{p}{E}$$

$$p_x = \frac{p}{1 + \frac{1}{m}}$$

or

$$\frac{16M_t}{\pi d^3} = \frac{p}{1 + \frac{1}{m}}$$

and taking $\frac{1}{m} = 0.3$

$$d^3 \overline{\underset{}{>}} \frac{6.5M_t}{p}$$

$$d \approx \sqrt[3]{\frac{6.5M_t}{p}} = 1.86\sqrt[3]{\frac{M_t}{p}}$$

where p is the value of the working stress.

Maximum Stress Theory.—This theory requires that the maximum principal stress shall not be greater than the working stress in simple tension therefore:

$$p_x = \frac{16M_t}{\pi d^3} \overline{\underset{}{<}} p$$

$$d^3 \approx \frac{5M_t}{p}$$

$$d \approx \sqrt[3]{\frac{5M_t}{p}}$$

$$\approx 1.71\sqrt[3]{\frac{M_t}{p}}$$

It will be noted, from these considerations, that the diameter depends on the theory selected for the design. Taking the maximum shear theory as the basis this variation in diameter due to the three theories is shown in Table LXXXVI below.

Table LXXXVI.—Relative Values from Different Theories (Torsion)

Maximum Shear	Maximum Strain	Maximum Stress
1	0.87	0.79

Bending and Twist.—For the case of a member subjected to the action of bending and twisting we have seen (paragraph 50 page 184) that the principal stresses are given by

$$p_x = \frac{16}{\pi d^3}(M_b + \sqrt{M_b^2 + M_t^2})$$

$$p_y = \frac{16}{\pi d^3}(M_b - \sqrt{M_b^2 + M_t^2}).$$

Maximum Shear Theory.—In this case the maximum shear stress will be given by $\frac{1}{2}(p_x - p_y)$, therefore,

$$p_x - p_y = \frac{16}{\pi d^3}(2\sqrt{M_b^2 + M_t^2}) \leqq p$$

or

$$\frac{32}{\pi d^3}\sqrt{M_b^2 + M_t^2} \leqq p$$

$$d^3 \geqq \frac{32}{\pi p}\sqrt{M_b^2 + M_t^2}$$

$$d \approx \sqrt[3]{\frac{10}{p}\sqrt{M_b^2 + M_t^2}}$$

Maximum Strain Theory.—From this theory we have

$$\frac{p_x}{E} - \frac{p_y}{mE} = \frac{16}{E\pi d^3}\left[M_b\left(1 - \frac{1}{m}\right) + \left(1 + \frac{1}{m}\right)\sqrt{M_b^2 + M_t^2}\right]$$

and taking $1/m = .3$

$$\frac{p_x}{E} - \frac{p_y}{mE} \approx \frac{10}{Ed^3}\left(.35M_b + .65\sqrt{M_b^2 + M_t^2}\right) \leqq \frac{p}{E}$$

$$d^3 \geqq \frac{10}{p}(.35M_b + .65\sqrt{M_b^2 + M_t^2})$$

$$d \approx \sqrt[3]{\frac{10}{p}(.35M_b + .65\sqrt{M_b^2 + M_t^2}}$$

Maximum Stress Theory.—Since p_x is greater than p_y from this theory we have

$$p_x = \frac{16}{\pi d^3}(M_b + \sqrt{M_b^2 + M_t^2}) \leqq p$$

$$d^3 \geqq \frac{16}{\pi p}(M_b + \sqrt{M_b^2 + M_t^2})$$

$$d \approx \sqrt[3]{\frac{5}{p}(M_b + \sqrt{M_b^2 + M_t^2})}$$

In this case the discrepancy between the values obtained for (d) by each theory will depend on the relation of M_t to M_b. In Table LXXXVII below are given the relative values of each for three different values of M_t to M_b.

TABLE LXXXVII.—RELATIVE VALUES FROM DIFFERENT THEORIES (TORSION AND BENDING)

	Maximum shear, theory	Maximum strain, theory	Maximum stress, theory
$M_t = M_b$..........	1	.96	.95
$M_t = 2M_b$.........	1	.93	.90
$M_b = 0$	1	.87	.79

It will be seen that in the case of pure torsion the design made according to the maximum strain theory would be 13% weaker and that made according to the maximum stress would be 21% weaker than the one obtained by the maximum shear theory.

Thick Cylinder.—The case of a thick cylinder of internal and external radii r and R respectively subjected to an internal pressure q lbs./sq. in. will now be considered.

At a point on the inner circumference where the tension is maximum

$$p_y = -q,$$

$$p_x = q\frac{R^2 + r^2}{R^2 - r^2}.$$

Maximum Shear Theory

$$p_x - p_y = q\left(\frac{R^2 + r^2}{R^2 - r^2} + 1\right) \overline{<} p$$

or

$$\frac{2qR^2}{R^2 - r^2} \overline{<} p$$

$$R \overline{>} r\sqrt{\frac{p}{p - 2q}}$$

Maximum Strain Theory

$$\frac{p_x}{E} - \frac{p_y}{mE} = \frac{1}{E}\left(q\,\frac{R^2 + r^2}{R^2 - r^2} + \frac{q}{m}\right) \overline{<} \frac{p}{E}$$

or $(p - q/m)(R^2 - r^2) = q(R^2 + r^2)$ and taking $1/m = 0.3$

$$R^2 \overline{>} \frac{r^2\,(p + .7q)}{p - 1.3q}$$

$$R \overline{>} r\sqrt{\frac{p + .7q}{p - 1.3q}}$$

Maximum Stress Theory

$$p_x = q\,\frac{R^2 + r^2}{R^2 - r^2} \leqq p$$

$$R^2 \geqq \frac{r^2(p + q)}{p - q}$$

$$R \geqq r\sqrt{\frac{p + q}{p - q}}$$

As before the discrepancy between the values obtained will depend on the ratio which p bears to q. If this ratio be $p = 3q$, then R has the values for the three theories respectively as follows

$$1.0 : 0.85 : 0.81.$$

Application of Mohr Theory to Simple Torsion.—It will now be necessary to give an example of a more complex case, where the limiting stress for the material in tension and compression are entirely different. In such cases the maximum shear theory cannot be used, and therefore the Mohr theory must be applied. In order to simplify the application the assumption is made that the theory between the limits of simple tension and simple compression can be represented with sufficient accuracy by a straight line DC, drawn as indicated in Fig. 391, as tangent to the two limiting circles mentioned above.

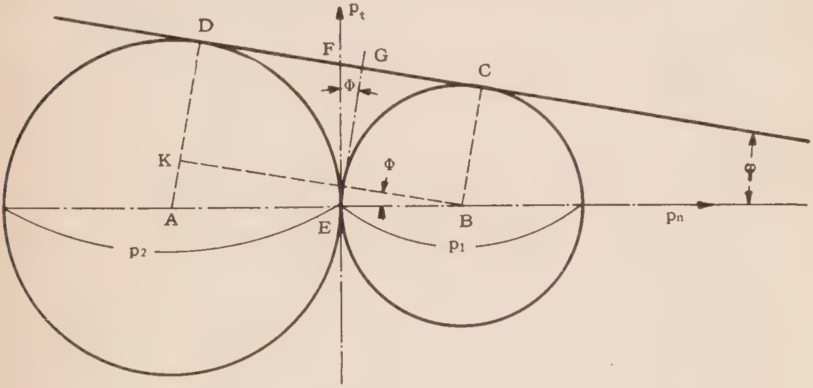

FIG. 391.—Graphical representation of special case of Mohr theory.

The problem in this case is to determine the limiting value of the stress p_t under pure shear represented by EG provided the limiting tensile and compressive stresses be p_1 and p_2 respectively.

$$EF = FD = FC = \frac{1}{2}DC = \frac{1}{2}AB\cos\phi = \frac{1}{2}\left(\frac{p_1 + p_2}{2}\right)\cos\phi \qquad \text{(a)}$$

and

$$p_t = EG = EF \cos \phi \qquad \text{(b)}$$

from (a) and (b)

$$p_t = \frac{1}{4}(p_1 + p_2) \cos^2 \phi \text{ and } \cos \phi = \frac{\sqrt{\overline{AB}^2 - \overline{AK}^2}}{AB} = \frac{\sqrt{p_1 p_2}}{\frac{1}{2}(p_1 + p_2)}$$

$$\therefore \quad p_t = \frac{1}{4}(p_1 + p_2)\left[\frac{4p_1p_2}{(p_1 + p_2)^2}\right]$$

$$= \frac{p_1\, p_2}{p_1 + p_2} \qquad \text{(c)}$$

Provided the limiting stresses in tension and compression be known the limiting pure shear stress can easily be determined.

As an application of this theory the case of cast iron will be considered. According to results given by Bach* if p_1 = breaking stress in tension in lbs. per sq. inch p_2 = breaking stress in compression in lbs. per sq. inch then $p_2 = 4p_1$

from (c) therefore

$$p_t = \tfrac{4}{5}p_1$$

and

$$\frac{\text{breaking stress in pure shear}}{\text{breaking stress in tension}} = \frac{p_t}{p_1} = 0.8$$

This value is in good agreement with that given by Bach* for the strength of hollow test bars and therefore the simplification of the Mohr theory on the lines we have discussed seems to be justifiable.

* Bach, "Elastizität und Festigkeit," 7th Edition, p. 362.

CHAPTER XVIII

WORKING STRESSES

139. Introduction.—In the initial chapters of this volume consideration was given, in more or less complete detail, to the theoretical side of design, while in the latter chapters the characteristics of the materials commonly employed in constructional work have been discussed. Coming, as we do, in this chapter to a consideration of *working stresses*, it will be shown how these two phases of the subject are inseparably connected, each being part of a complete whole.

The selection of working stresses is of the utmost importance to the engineer, and if the design is to be sound, it is essential that we have very clear ideas regarding them. It can be said that there are at least four *factors* to be considered, each of which influence the choice of working stresses, namely *accuracy of formulae, characteristics of materials, dimensions of members,* and lastly, *estimation of forces.*

It is not the intention to give here working stresses for different branches of design, since it is generally accepted that this choice must more or less depend on the feeling of the engineer. Modern practice has accumulated much *empirical data* on the basis of previous experience, and while it is necessary to sometimes criticize some of this data, it is not the author's intention to depreciate their value. The employment of such information in conjunction with the results of analysis seems however to be a sound policy toward the proper selection of working stresses, and that is the course which is strongly advocated here.

The thought is to give, therefore, in this chapter, on the basis of the theory discussed in the first part of this volume and on the physical characteristics given in the second part, *some fundamental ideas* which, it is felt, must form a guide for engineers who, as previously stated, must always decide the question of working stresses.

In developing the various factors which control the selection of working stresses we will first discuss the role of analysis in the solution of technical problems. This we consider as fundamentally necessary if proper and logical development has to be made. The question then arises as to the accuracy of the formulae derived. We believe that in many cases these formulae represent in an accurate manner the actual conditions, although it is also our opinion that there are others which do not accurately represent the actual conditions. In the various chapters in the first part of this work, therefore, not only, is discussion of the accuracy of formulae made but also criticism is given of the actual basis on which these were developed. Consequently, it is felt that in this volume there is sufficient information to develop the basis for sound criticism of any particular analysis. Coming now to a consideration of the properties of materials we again find that these play a very important role in the selection of working stresses. In the latter chapters an idea of the characteristics of some materials have been given. From such discussion, a knowledge of the elastic properties of material so very important to the designer can be obtained. The question however must always be present as to how far such characteristics represent the material as a whole. This *factor of reliability* is a very important point since on this entirely depends how far the values obtained in the laboratory can be in general applied. It seems, only by a proper selection of control tests in conjunction with the fundamental data, that the necessary assurance can be provided for the designer. Of course, as we have seen, the properties of material undergo very radical changes when the material is subjected to high temperature, and therefore, for material under such conditions, the working stresses must be chosen not on the characteristics at normal temperature but on those corresponding to the working temperature. As regards the question of dimensions of the various members, there should be no difficulty because, although they control the final working stress, they are easily determined. In many members, however, the original dimensions are liable to undergo considerable change due to the effects of corrosion, or abrasion, and in such cases these factors must have a place in the designer's consideration.

Having emphasized these various points there only remains the question of the magnitude of the forces acting. Due to the fact that it is usually difficult to determine the magnitudes of such forces acting on a structure, an additional reason arises for diminishing these working stresses. There are of course, in addition, other cases where very high stresses may occur without even the action of external forces. In constructional work these may be caused by statically indeterminate systems, due either to a variation in temperature or due to inaccuracy in assembly. The same can be said possibly in greater measure as regards the stresses in machine parts produced by non-uniform heating or the residual stresses produced by quenching or by casting. In many cases it is impossible to determine the magnitude of those stresses and in those cases the only precaution consists in a lowering of the working stresses.

From all these considerations it follows that the working stress must be adopted so that it is much less than the stress at which failure of the material is to be expected. In selecting working stresses a *factor of safety* is therefore employed which is defined as the factor by which the working stress must be multiplied to give the stress which will result in failure. Due to the reasons which make it necessary, the term *factor of ignorance* has very aptly been applied to this term. Since this is by far the most important phase of the subject, it is proposed in the remaining part of the chapter to develop some of these working stresses for different conditions, depending on the manner in which the forces act, always with the fundamental thought in view, that once these forces have been chosen and a design agreed on, then the structure must be so designed that all parts have as near as possible equal strength.

140. Static Loading.—In the discussion of working stresses for static conditions there are two distinct types to be considered, namely, that in which the member is subjected to simple stress, and that in which it is subjected to combined stresses.

Simple Stress.—In the case of simple stress which may be either tension or compression a further subdivision is necessary depending, as we have seen, on the characteristics of the material employed. One group will include such material as steel possessing distinct elastic properties, i.e., as proportional limit and yield point, and the other will include materials such as cast iron and concrete, which do not possess these characteristics. These two groups will now be separately considered.

With regard to the former there is no great difficulty because from the various discussions which have been made in this work, it will have been appreciated, that it is necessary to base working stress values on the elastic properties. Therefore for such cases if:

p_w = working stress in lbs. per sq. inch
p = proportional limit in simple tension, compression or shear
n = factor of safety

then

$$p_w = \frac{p}{n}.$$

In general, n is usually taken as 2, and, under these conditions, provided the requirements concerning accuracy of formulae, characteristics of material, dimensions of members, and estimation of forces have been satisfied, a conservative design will be the result. It is necessary to observe, however, that in cases where the most unfavorable loading has been selected, the factor n can be decreased and may have an intermediate value between 2 and unity. For conditions where, due to holes or notches, high local stress concentration occurs, this coefficient n may have this lower value because, since the conditions considered are static, such stress concentration is not detrimental provided the material be sufficiently ductile. Such reduction near to the unity value, however, must require the exercise of great judgment on the part of the designer. On the other hand for cast iron or concrete some other basis must be chosen for the selection of working stresses. For the lack of a better method this is usually taken as a factor of the ultimate stress. In order to make some allowance for the change from the proportional limit to the ultimate stress as the basis, a value of n is adopted which can usually have a value between 4 and 8. In the cases where the factors previously mentioned such as accuracy of formulae, etc. have been well determined, the lower limit may be taken.

Combined Stress.—For the case of combined stress a complete discussion has been made in the previous chapter. Adopting the maximum shear theory as the criterion of failure for ductile materials, and the Mohr theory for such materials as cast iron, there will be no difficulty in making a satisfactory design. In other words, we have shown in that chapter the limiting stresses for characteristic types of loading and in such cases we have as before

$$p_w = \frac{p}{n}$$

where p is now the limiting stress prescribed by the maximum shear or Mohr theories respectively. The reservations regarding the value of n are similar to those discussed in the previous paragraph. It may have a value of 2 for a conservative design provided the conditions previously discussed have been satisfied. Similarly it may, in cases of stress concentration, have the value approaching unity.

141. Dynamic Loading.—*General.*—In this paragraph we come to a consideration of those cases where the member is subjected to changing stress conditions, arising either from complete cyclical variation of stress as occurs in piston rods or locomotive axles, or from stress variation from zero to a maximum.

Reversal of Stress.—As we have seen in the chapter on fatigue these cyclical stresses may be either completely reversed, or may vary between a maximum and minimum. Considering first the case of complete stress reversal, there is no difficulty in arriving at a satisfactory design because the results of experiment for many materials, as we have seen, are directly available to the designer. In the latter part of this chapter, values of endurance limits so found for some materials are tabulated.

Before the results of such a wide variety of materials were available, various empirical relations were established between the tensile test results and fatigue test results, so that in the absence of actual experimental values for the endurance limits, an estimation of such could be made from the tensile test data. The object in compiling such empirical relations was probably due to the fact, that as we have seen, the determination of endurance values take a very long time. The author feels that due to the amount of actual data now available on complete stress reversal the use of such relation for these cases where data is available is no longer justified. Since, however, there is very little data available on endurance limit values for those cases other than complete stress reversal some theory is necessary and it is proposed at this time to discuss these theories. The best known one is that of Gerber.[*] Based on the results of Wöhler's tests he concluded that if

p_e = endurance limit lbs. per sq. inch
r = range of stress lbs. per sq. inch
k = constant depending on the material
p_{max} = ultimate stress in tension lbs. per sq. inch

then

$$p_e = \frac{r}{2} + \sqrt{p^2{}_{\text{max}} - krp_{\text{max}}}$$

This equation on being plotted on a base of minimum stress gives a curve shown in Fig. 367. For the case under consideration, of complete stress reversal $r = 2p_e$ and $p_e = \frac{p_{\text{max}}}{2k}$.

The values given by Unwin[†] for k vary from 1.5 for ductile steels to 2 for harder steels. From our previous discussion on the subject it will have been appreciated that k depends on the elastic properties and also on the microstructure and while the use of such a relation may, in the absence of actual experimental data, be permissible, it is

[*] Gerber, *Z. f. Baukunde*, (München), 1874.

[†] Unwin, "Testing of Materials of Construction," Third Edition, p. 389, 1910.

not in general, in the state of our present knowledge, to be recommended since much test data is now available. Another empirical relation has been suggested by Goodman* in which

$$p_e = p_{\max} - \frac{1}{2}r$$

but since this does not consider the conditions of the material it is doubtful if its application can be justified.

Using the value of the endurance limit so found then if

p_e = endurance limit in lbs. per sq. inch
p_w = working stress in lbs. per sq. inch
n = factor of safety

$$p_w = \frac{p_e}{n}$$

With regard to the choice of a value for n it is necessary to observe that the endurance limit is more like the static ultimate stress than the proportional limit because to exceed the proportional limit will only mean the occurrence of permanent set. As we have seen however the exceeding of the endurance limit will mean fracture of the material. Furthermore stress concentration is always present, more or less, in actual designs and while this is not detrimental for static conditions it always lowers the endurance limit value. Due to these points the factor of safety cannot be chosen on the same basis as for static loading.

For cases where all the conditions such as, accuracy of formulae, etc. and where stress concentration is not present in great degree n can have a value 3. Therefore

$$p_w = \frac{1}{3}p_e$$

As we have seen, stress concentration becomes very important in dynamic conditions. The effect of notches, sharp fillets or holes is to materially reduce the endurance limit of the material and should the endurance values be obtained from tables as previously discussed, it is important to observe that these do not include stress concentration effects. The only way to determine these reduction factors is to make tests on geometrically similar models as discussed in paragraph 124 page 480, or to take values from available published data. Since, however, there is not at present sufficient of this available it is necessary to propose some value. On the basis of the results of Stodola† and Stanton* for ductile materials a safe limit can be reached if the working stresses for such material be reduced 30%. The value of n will therefore be taken as 4 for conditions of stress concentration. It must be noted, however, that for the case of harder material there is no data available and for this the reduction in working stress must be of a higher order. This means that for such types of structures the stress concentration must be avoided as far as possible and, if this is impossible, a more detailed study of the effect of such concentration becomes necessary. Since as we have seen the factor of surface finish may lower still further the endurance limit it is our opinion that these values of 3 and 4 for normal, and stress concentration conditions, respectively, are not in any sense, conservative, like the value 2 for static loading, and can only be reduced after very serious consideration on the part of the designer.

---

* Goodman, "Mechanics Applied to Engineering," 1908.

† Stodola & Schüle, Hohlkehlenschärfe und Dauerbiegung. Schweiz, Bauz., p. 145, 1918.

Variation of Stress.—So far consideration has been given to the cases where the member is subjected to complete stress reversal. There are many cases in service where the stress is not completely reversed but is subject to variation only. For such cases as we have seen, due to the absence of experimental data, reliance has to be made on theory alone and Gerbers seems to be the best. According to this if the stress varies from zero to a maximum, and k be taken as 1.5 then if p = ultimate stress lbs. per sq. in. and p_e = endurance limit in lbs. per sq. in. (0 to max.) then p_e is about $2/3p$. In other words the endurance limit for stress varying from zero to a maximum is twice that for complete stress reversal. Using the values previously given as 3 for normal conditions and 4 for stress concentration, satisfactory designs can be made. It must be clearly understood, however, that the values of the working stress, calculated on this basis, may become higher than that for static conditions. In this case the working stress for static conditions must be taken.

Combined Stress.—As we have seen for ductile materials subjected to combined static stresses, application of the maximum shear theory for failure appears to be justifiable. Although very little data is available on the subject of combined dynamic stresses there are certain results available from which we can infer that the maximum shear theory can also be applied for those dynamic cases. Mason† has shown that the endurance limit of low carbon steel in alternating torsion is half the value of the endurance limit in bending. In other words the safe range of shear stress is sensibly the same whether the stress be induced by bending or twisting. Batson* in the discussion of this paper added confirmation for higher carbon steels. On this basis, therefore, it can be inferred that for ductile material, the maximum shear theory can be applied in order to determine the limiting stress for members subjected to the action of combined dynamic stresses. The working stress p_w will therefore be determined as before by value of p/n where p is the value of the limiting shear stress, being in other words the value of the endurance limit for torsional shear conditions. As discussed previously for fatigue conditions, the value of n will be 3 where stress concentration is not present in great degree. For cases where such concentration obtains a value of 4 will be adopted.

---

* Stanton and Bairstow, On Resistance of Iron and Steel to Reversals of Stress, *Inst. Civ. Ing. Proc.*, 1906.

† Mason, Alternating Stress Experiments, *Inst. Mech. Eng. Proc.*, p. 121, 1917.

142. Other Types of Loading.—*Buckling.*—In all previous considerations, it has been assumed that the structure is in the condition of *elastic stability.* If this is not the case then it is necessary to lower the working stresses still further.

Such cases of elastic instability arise when one or two dimensions of a member are small in comparison with the others, such as, for example in the compression of thin plates and thin struts.

In the analytical part some formulae were given for determining the critical values of the loads at which sidewise buckling of the member will occur. This *critical load* must be considered as the ultimate stress for failure, therefore, the working stress must be based not on the proportional limit nor on the ultimate stress but on the critical load. Some data regarding the choice of such working stresses are given in Chaps. VII and IX.

Vibrations.—Just as we have referred to the statical stability of compression members it is necessary also to speak of the *dynamical stability* of moving parts of machines.

For example, it is well known that under conditions of resonance, vibration alone may completely destroy a machine. The determination of the critical speed in such cases is very necessary and the question of *flexibility* becomes of prime importance. Due to the fact that the critical speed depends on the flexibility of the system, it is clear that in such cases the problem is not one of stress but one of flexibility. In order to exclude the possibility of large vibrations the working speed must not approach near to the critical speed and a ratio of working speed to critical speed of 1: 1½ must be considered as the upper limit for working conditions. Some problems of vibration and critical speeds have been considered in Chap. XI and such data, it is felt, will materially assist the designer.

---

* Batson, *Inst. Mech. Eng. Proc.*, p. 182, 1917.

Impact.—Lastly, there is the question of effects produced by impact. The satisfactory design which takes into consideration such effects is difficult and, it is felt, a proper method of computing the forces caused by such impacts can alone help to properly choose the working stresses for these cases. Methods of calculating impact stresses are given in Chap. XI, par. 81 and there, it is shown, that provided the mass of the falling weight be large in comparison with the mass of the structure, the accuracy of the calculations can be considered as satisfactory. So that, if the other elements such as accuracy of formula, reliability of material, etc. be known, the same coefficient can be used for single blow impact as for static loading. If the blows be repeated then the coefficient for dynamic loading must be taken.

TABLE LXXXVII.—TENSILE* PROPERTIES OF CARBON STEELS

Number	Material	State	Proportional limit pounds per square inch	Yield point, pounds per square inch	Ultimate stress, pounds per square inch	Elongation on 2 in. %	Reduction of area, %	Brinell number	Modulus of elasticity, pounds per square inch	Authority †	Remarks
1	.02 C .03 Mn	Normalized	16,100	19,000	42,400	48.3	76	69	....	1	Bar 1 in. diameter.
2	.37 C .55 Mn	Annealed at 850°C.	36,500	37,800	70,000	32	49	131	30×10^6	2	Bar 2¼ in. diameter.
3	.37 C .55 Mn	Normalized at 850°C.	38,000	41,500	79,200	29	46	142	....	2	Bar 2¼ in. diameter.
4	.37 C .55 Mn	Heat-treated Water at 850°C. Temp. at 550°C.	65,000	69,000	105,000	22	56	205	....	2	Bar 2¼ in. diameter.
5	.49 C .46 Mn	Normalized at 910°C.	44,700	47,100	91,500	26.5	39.5	164	....	1	Bar 1 5/16 in. square.
6	.49 C .46 Mn	Heat-treated Oil at 790°C. Temp. at 430°C.	75,800	78,800	121,800	11.3	51	217	....	1	Bar 1 5/16 in. Square
7	.93 C .38 Mn	Annealed at 870°C.	28,000	33,400	84,100	25	37	162	....	1	Bar 2 in. × ⅞ in.
8	.93 C .38 Mn	Heat-treated Oil at 790°C. Temp. at 650°C.	60,000	67,600	115,000	23	40	227	....	1	Bar 2 in. × ⅞ in.

* NOTE.—For Fatigue Test Results See Corresponding Number in Table XCII.

† For authority, refer to p. 531.

TABLE LXXXVIII.—TENSILE* PROPERTIES OF ALLOY STEELS

Number	Material	State	Proportional limit, pounds per square inch	Yield point, pounds per square inch	Ultimate stress, pounds per square inch	Elongation on 2 in., %	Reduction of area, %	Brinell number	Modulus of elasticity, pounds per square inch	Authority	Remarks
1	.35 C .45 Mn 3.4 Ni	Rolled	47,000	60,000	105,000	21	42	206	27 × 10⁶	2	Plate 3 ft. 6 in. × 2 ft. 0 × 3 in.
2	.35 C .45 Mn 3.4 Ni	Normalized at 840°C.	52,000	60,000	104,000	21.5	49	212	27 × 10⁶	2	Plate 3 ft. 6 in. × 2 ft. 0 × 3 in.
3	.35 C .45 Mn 3.4 Ni	Normalized at 840°C. Temp. at 730°C.	52,000	56,000	94,000	25	48	184	27 × 10⁶	2	Plate 3 ft. 6 in. × 2 ft. 0 × 3 in.
4	.35 C .45 Mn 3.4 Ni	Heat-treated Water at 800°C. Temp. at 600°C.	72,000	77,000	107,000	23	56	220	27 × 10⁶	2	Plate 3 ft. 6 in. × 2 ft. 0 × 3 in.
5	.41 C .75 Mn 3.4 Ni	Annealed at 780°C.	61,000	64,600	101,000	25.5	52	194	....	1	Bar 1 in. square.
6	.41 C .75 Mn 3.4 Ni	Heat-treated Oil at 830°C. Temp. 590°C.	108,000	108,000	123,000	22.6	59	248	....	1	Bar 1 in. square.
7	.24 C .37 Mn 3.3 Ni .87 Cr	Annealed at 780°C.	56,700	60,000	87,000	33	67	167	....	1	Bar 2 in. × 1 in.
8	.24 C .37 Mn 3.3 Ni .87 Cr	Heat-treated Oil 830°C. Oil 370°C.	115,000	128,000	138,000	18	62	291	....	1	Bar 2 in. × 1 in.
9	.30 C .56 Mn 4.3 Ni 1.4 Cr	Air-hardened from 800°C.	45,000	177,000	244,000	10.8	37	...	....	3	Bar 1⅛ in. diameter.
10	.30 C .56 Mn 4.3 Ni 1.4 Cr	Air-hardened from 800°C. Temp. 600°C.	92,000	142,000	157,000	17.5	55	...	....	3	Bar 1⅛ in. diameter.
11	.43 C .57 Mn 2.4 Si 3.0 Ni .24 Zr	Heat-treated Oil 860°C. Temp. at 370°C.	219,000	....	281,000	7.5	31.5	510	....	4	

* NOTE.—For Fatigue Test Results See Corresponding Number in Table XCIII.

TABLE LXXXIX.—TENSILE* PROPERTIES OF STEEL CASTINGS

Number	Material	State	Proportional limit pounds per square inch	Yield point, pounds per square inch	Ultimate stress pounds per square inch	Elongation on 2 in., %	Reduction of area, %	Brinell number	Modulus of elasticity, pounds per square inch	Authority	Remarks
1	.18 C .82 Mn .36 Si	Cast	22,000	28,000	60,000	33	49	118	26×10^6	2	Bar 1 in. × 1 in. × 14 in.
2	.18 C .82 Mn .36 Si	Annealed at 900°C.	28,500	32,000	63,000	34	61	117	26×10^6	2	Bar 1 in. × 1 in. × 14 in.
3	.32 C .74 Mn .32 Si	Cast	20,000	33,500	76,000	26	34	141	30×10^6	2	Bar 2¼ in. × 1¼ in. × 32 in.
4	.32 C .74 Mn .32 Si	Annealed at 925° C.	37,000	41,000	80,000	27	39.5	143	30×10^6	2	Bar 2¼ in. × 1¼ in. × 32 in.
5	.32 C .74 Mn .32 Si	Normalized at 925°C.	40,500	46,000	85,000	27.6	45.6	163	30×10^6	2	Bar 2¼ in. × 1¼ in. × 32 in.
6	.32 C .77 Mn .18 V	Cast	22,500	37,000	81,000	23.6	30	156	28×10^6	2	Bar 2¼ in. × 1¼ in. × 32 in.
7	.32 C .77 Mn .18 V	Annealed at 925°C.	32,000	41,000	80,000	27.5	43	152	28×10^6	2	Bar 2¼ in. × 1¼ in. × 32 in.
8	.32 C .77 Mn .18 V	Normalized at 925°C.	51,000	52,000	89,000	26.5	46.7	162	28×10^6	2	Bar 2¼ in. × 1¼ in. × 32 in.

* NOTE.—For Fatigue Test Results See Corresponding Number in Table XCIV.

TABLE XC.—TENSILE PROPERTIES OF WIRE

Number	Material	State	Ultimate stress, pounds per square inch	Elongation, %	Authority	Remarks
1	Copper	Annealed	36,000	35 on 10 in.	7	.46 in. diameter.
2	Copper	Annealed	40,000	20 on 10 in.	7	.003 in. diameter.
3	Copper	Hard-drawn	49,000	3.7	7	.46 in. diameter.
4	Copper	Hard-drawn	60,000	88 on 60 in.	7	.04 diameter.
5	Steel	Hard-drawn	360,000	....	7	.029 in. diameter.
6	Steel	Hard-drawn	290,000	....	7	.063 in. diameter.

TABLE XCI.—TENSILE PROPERTIES OF MISCELLANEOUS MATERIALS

Number	Material	State	Proportional limit, pounds per square inch	Yield point, pounds per square inch	Ultimate stress, pounds per square inch	Elongation on 2 in. %	Reduction of area, %	Brinell number	Modulus of elasticity, pounds per square inch	Authority	Remarks
1*	Manganese Bronze 56.8 Cu 1.5 Fe .20 Mn Rem. Zn	Cast	13,000	......	70,000	33	41	93	14×10^6	5	Bar ⅝ in. diameter
2*	Electron Metal .41 Cu .25 Fe 4.4 Zn Rem. Mg.	Rolled	6,300	......	36,500	17.5	20.5	64	6×10^6	5	Bar 2 in. diameter.
3*	Duralumin 3.2 Cu .70 Mg Rem. Al	Heat-treated Water 500°C.	18,500	......	51,000	29.3	47.5	100	11×10^6	5	Bar ¾ in. diameter.
4*	Duralumin 3.2 Cu .70 Mg Rem. Al	Annealed 370°C.	6,800	......	25,000	25	61	50	10.7×10^6	5	Bar ¾ in. diameter.
5*	Aluminum Alloy 3.0 Cu 20.0 Zn Rem. Al	Hot rolled	......	41,000	60,000	21	36	...	....	6	Bar ⅞ in. diameter.
6	Aluminum Alloy 3.0 Cu 20.0 Zn Rem. Al	Annealed at 250°C.	20,400	......	58,500	19	21.4	...	....	6	Bar ⅞ in. diameter.
7	Aluminum Alloy 4.0 Cu 2.0 Ni 1.5 Mg Rem. Al	Hot rolled	......	27,000	39,500	20	30	...	....	6	Bar ⅞ in. diameter.
8*	Brass 61.0 Cu 38.3 Zn	Hard-drawn	.....	34,700†	60,000	40	73	...	....	4	Bar .4 in. diameter.

TABLE XCI.—TENSILE PROPERTIES OF MISCELLANEOUS MATERIALS (*Continued*)

Number	Material	State	Proportional limit, pounds per square inch	Yield point, pounds per square inch	Ultimate stress, pounds per square inch	Elongation on 2 in. %	Reduction of area, %	Brinell number	Modulus of elasticity, pounds per square inch	Authority	Remarks
9*	Copper 99.75 Cu .24 O	Drawn	......	20,000†	41,000	26	48	.....	....	4	Bar .4 in. diameter.
10	Cast Iron 2.5 to 4.0 C	....	......	......	12,000 to 35,000	....	....	90 to 200	12 × 10⁶	7	
11	Cast Iron 3.0 C 1.3 Si .6 Mn	....	......	......	25,000 to 38,000	Negligible	....	100 to 150	....	7	Bar .75 diameter.
12	Semi Steel 3.50 C (total) 2.89 (graph) 1.37 Si	....	......	......	10,000 to 38,000	....	....	100 to 200	....	7	
13	Cast Iron (White)	....	......	......	40,000 to 50,000	....	....	...	....	7	
12	Malleable Iron	....	......	......	40,000	5	....	...	....	7	
13	Wrought Iron	Rolled	......	24,000	48,000	26	40	...	....	7	

* NOTE.—For Fatigue Test Results See Corresponding Number in Table XCV.

† NOTE.—Yield Point Corresponding to a Given Extension Was Determined by Dividers.

Table XCII.—Fatigue* Properties of Carbon Steels

Number	Material	State	Endurance limit, pounds per square inch	Authority	Remarks
1	.02 C .03 Mn	Normalized	±26,000	1	Bar 1 in. diameter.
2	.37 C .55 Mn	Annealed at 850°C.	±29,000	2	Bar 2¼ in. diameter.
3	.37 C .55 Mn	Normalized at 850°C.	±29,300	2	Bar 2¼ in. diameter.
4	.37 C .55 Mn	Heat-treated Water 850° C. Temp. 550°C.	±51,000	2	Bar 2¼ in. diameter.
5	.49 C .46 Mn	Normalized at 910°C.	±33,000	1	Bar $\frac{15}{16}$ in. square.
6	.49 C .46 Mn	Heat-treated Oil at 790°C. Temp. at 430°C.	±64,000	1	Bar $\frac{15}{16}$ in. square.
7	.93 C .38 Mn	Annealed at 870°C.	±30,500	1	Bar 2 × ⅞ in.
8	.93 C .38 Mn	Heat-treated Oil at 790°C. Temp. at 650°C.	±56,000	1	Bar 2 × ⅞ in.

* Note.—For Tensile Test Results See Corresponding Number in Table LXXXVII.

TABLE XCIII.—FATIGUE* PROPERTIES OF ALLOY STEELS

Number	Material	State	Endurance limit, pounds per square inch	Authority	Remarks
1	.35 C .45 Mn 3.4 Ni	Rolled	±41,000	2	Plate 3 ft. 6 in. × 2 ft. 0 × 3 in.
2	.35 C .45 Mn 3.4 Ni	Normalized at 840°C.	±44,000	2	Plate 3 ft. 6 in. × 2 ft. 0 × 3 in.
3	.35 C .45 Mn 3.4 Ni	Normalized at 840°C. Temp. at 730°C.	±47,500	2	Plate 3 ft. 6 in. × 2 ft. 0 × 3 in.
4	.35 C .45 Mn 3.4 Ni	Heat-treated Water at 800°C. Temp. at 600°C.	±52,000	2	Plate 3 ft. 6 in. × 2 ft. 0 × 3 in.
5	.41 C .75 Mn 3.4 Ni	Annealed at 780°C.	±54,000	1	Bar 1 in. square.
6	41 C .75 Mn 3.4 Ni	Heat-treated Oil at 830°C. Temp. at 590°C.	±64,000	1	Bar 1 in. square.
7	.24 C .37 Mn 3.3 Ni .87 Cr	Annealed at 780°C.	±49,000	1	Bar 2 in. × 1 in.
8	.24 C .37 Mn 3.3 Ni .87 Cr	Heat-treated Oil at 830°C. Oil at 370°C.	±68,000	1	Bar 2 in. × 1 in.
9	.30 C .56 Mn 4.3 Ni 1.4 Cr	Air-hardened From 800°C.	±102,000	3	Bar 1⅛ in. diameter.
10	.30 C .56 Mn 4.3 Ni 1.4 Cr	Air-hardened From 800°C. Temp. 600°C.	± 80,000	3	Bar 1⅛ in. diameter.
11	.42 C .57 Mn 2.41 Si 3.0 Ni .24 Zr	Heat-treated Oil 860°C. Temp. at 370°C.	±109,000	4	

* NOTE.—For Tensile Test Results See Corresponding Number in Table LXXXVIII.

TABLE XCIV.—FATIGUE* PROPERTIES OF STEEL CASTINGS

Number	Material	State	Endurance limit, pounds per square inch	Authority	Remarks
1	.18 C .82 Mn .36 Si	Cast	±26,000	2	Bar 1 in. × 1 in. × 14 in.
2	.18 C .82 Mn .36 Si	Annealed at 900°C.	±26,500	2	Bar 1 in. × 1 in. × 14 in.
3	.32 C .74 Mn .32 Si	Cast	±30,500	2	Bar 2¼ in. × 1¼ in. × 32 in.
4	.32 C .74 Mn .32 Si	Annealed at 925°C.	±35,000	2	Bar 2¼ in. × 1¼ in. × 32 in.
5	.32 C .74 Mn .32 Si	Normalized at 925°C.	±35,000	2	Bar 2¼ in. × 1¼ in. × 32 in.
6	.32 C .77 Mn .18 V	Cast	±39,000	2	Bar 2¼ in. × 1¼ in. × 32 in.
7	.32 C .77 Mn .18 V	Annealed at 925°C.	±42,000	2	Bar 2¼ in. × 1¼ in. × 32 in.
8	.32 C .77 Mn .18 V	Normalized at 925°C.	±42,000	2	Bar 2¼ in. × 1¼ in. × 32 in.

* NOTE.—For Tensile Test Results See Corresponding Number in Table LXXXIX.

TABLE XCV.—FATIGUE* PROPERTIES OF MISCELLANEOUS MATERIALS

Number	Material	State	Endurance limit, pounds per square inch	Authority	Remarks
1	Manganese Bronze 56.8 Cu 1.5 Fe .20 Mn Rem. Zn	Cast	±15,000	5	Bar ⅝ in. diameter.
2	Electron Metal .41 Cu .25 Fe 4.4 Zn Rem. Mg	Rolled	±17,000	5	Bar 2 in. diameter.
3	Duralumin 3.2 Cu .70 Mg Rem. Al	Heat-treated Water 500°C.	±12,000	5	Bar ¾ in. diameter
4	Duralumin 3.2 Cu .70 Mg Rem. Al	Annealed 370°C.	±10,800	5	Bar ¾ in. diameter.
5	Aluminum Alloy 3.0 Cu 20.0 Zn Rem. Al	Hot rolled	±19,500	6	
8	Brass 61.0 Cu 38.3 Zn	Hard-drawn	Less than ±20,000	4	Bar .4 diameter.
9	Copper 99 75 .24 O	Drawn	Less than ±17,500	4	Bar .4 diameter.

* NOTE.—For Tensile Test Results See Corresponding Number in Table XCI.

TABLE OF REFERENCES

Number	Authority
1	Bulletin of Univ. of Illinois—H. F. Moore and T. Jasper, No. 136 p. 33.
2	Tests by Author.
3	Engineering Steels—L. Aitchison (Van Nostrand 1921) P. 209.
4	Notes on Endurance Tests—H. Gillet and E. Mack, Proc. A.S.T.M. 1924.
5	Resistance of Mang Bronze. Duralumin and Electron. Metal to Alternating Stresses. R. R. Moore, Proc. A.S.T.M. 1923.
6	Eleventh Alloys Res. Rep. Instit. of Mech. Eng. 1921 P. 143, 146.
7	Physical Prop. of Materials—Circ. 101 Bur. of Stds. 1924.

LIST OF AUTHORS

A

Aitchison, L., 371, 375, 376, 399, 400, 427, 431, 476
Akimoff, N., 324
Anthes, H., 46

B

Bach, C., 54, 357, 358, 367, 370, 380, 382, 384, 388, 390, 391, 512
Bairstow, L., 418, 435, 462, 480, 519
Baker, 448
Bantlin, A., 255
Barba, 362, 424
Batson, R. G., 362, 424, 449, 451, 452, 486, 487, 520
Bauer, H., 234
Bauschinger, J., 369, 380, 461, 487
Bauschlicher, A., 23
Becker, 499, 504
Beilby, Sir G. T., 415
Beltrami, 506
Bottomley, J. T., 381
Boubnoff, J., 261, 288
Boussinesq, J., 230
Brandt, 367
Bredt, R., 47
Brinell, 446
Brown, S. J., 254
Bryan, G. H., 292

C

Carpenter, H. C., 410
Carrington, 384, 451
Castigliano, A., 92, 119
Charpy, G., 360, 425, 426
Coker, E. G., 9
Cook, 249, 359
Cornu-Thenard, 425
Cox, H., 350
Crocker, S., 255
Cunningham, F. L., 480, 482, 485
Czochralski, J., 410

D

Dalby, W. E., 359, 395, 406, 410, 463
Davidenkoff, 419
deForest, A. V., 416
Devries, 449
Dietz, W., 11, 359
Dinnik, A., 35, 176
Donath, M., 307

E

Eden, E. M., 480, 482, 485
Elam, 410
Elmendorf, 421
Engesser, F., 176
Ensslin, M., 288
Euler, L., 164
Ewing, Sir. J. A., 381, 392, 406, 465

F

Fairbairn, Sir W., 383, 460
Fillunger, 423, 430
Filon, L. N., 62, 66
Flamant, A., 62
Foeppl, A., 11, 16, 24, 35, 366, 445
Foeppl, L., 288
Frahm, H., 337
Freeman, J. R., 367
Fuchs, S., 21
Fuller, C. E., 168

G

Galerkin, B., 288
Geiss, 403
Gerber, 517

Girtler, 506
Golovin, H., 219
Goodman, J., 371, 518
Gough, H. J., 401, 465, 487, 488, 492
Grammel, R., 214, 306
Greaves, R. H., 433
Greenhill, A. G., 247
Griffith, A. A., 11
Griffith, H. H., 46
Grueneisen, 357
Guest, J. J., 498, 503
Guillet, 371

H

Hadfield, Sir R. A., 422, 425, 433, 456
Haigh, B. P., 445, 477, 479, 482, 506
Hankins, G. A., 456, 469
Hansen, 433, 465
Harsch, J. W., 492
Hatfield, W. H., 424, 441
Hatt, W. K., 418
Heerwagen, F., 21
Hencky, H., 280
Herbert, H., 54
Herz, H., 21, 23, 350
Hodkinson, B., 306
Holzer, H., 342
Hooke, 2, 356
Hopkinson, B., 486
Hort, W., 325
Huber, M. T., 288
Humfrey, J. W., 465
Hurlbrink, E., 247
Hyde, J. H., 362, 486, 487

I

Inglis, C. E., 9
Izod, 422

J

Jacob, L., 254
Jasper, 441, 466, 471, 473, 476, 477, 486
Joffe, 402
Johnston, J. B., 357
Jones, 433
Jouravski, 63

K

Karman, T., 167, 255
Kelvin, Lord (Sir W. Thompson), 401
Kirsch, 9
Kirschhoff, G., 323
Kolosoff, G., 9
Kommers, J. F., 11, 359, 366, 465, 469, 470, 476, 481, 482
Kreuger, 421

L

Landau, D., 92
Langenberg, F. C., 426, 434
Larmour, J., 43
Lea, F. C., 384, 388, 389, 486, 487, 489
Leber, 435, 438, 441, 442
Levy, M., 247
Loewe, 92
Longbottom, J. A., 234
Lorenz, H., 47
Love, A. E., 172
Ludwik, 451

M

Main, S. A., 425, 433, 447, 456
Margerum, C. E., 421
Martel, 452
Martens, A., 383, 454
Martin, H. M., 306
Mason, W., 464, 519
Maxwell, C., 126
Mayer, R., 230
McAdam, D. J., 425, 467
Mesnager, A., 62
Meyer, 448
Michell, J. H., 35, 68
Mises, R., 249, 324
Mohr, O., 13, 503
Mohs, 454
Moncrieff, J. M., 167
Moore, H. F., 11, 359, 366, 441, 465, 466, 469, 470, 471, 473, 476, 477, 481, 482, 486
Moore, R. R., 477
Morley, A., 156, 340, 366
Müller, 435, 438, 441, 442

N

Nadai, A., 273, 283, 288, 291
Nicolai, E. L., 248

O

O'Neill, 457

P

Palmgren, A., 21
Pearson, 401
Peschka, G. A., 301
Petrenko, S. N., 22
Pfleiderer, C., 288
Pilling, N. B., 364
Plank, 419
Poeschl, T., 35
Poisson, S. D., 2
Portevin, A. M., 371
Prandtl, L., 45, 176, 219
Prescott, J., 47
Preuss, E., 10
Putnam, W. J., 492

R

Ramsauer, C., 344
Rankine, 168
Rayleigh, Lord, 126, 316, 350
Reaumur, 444, 454
Rees, 398
Reissner, H., 292, 343
Reynolds, O., 467, 485
Reyto, 505
Ritz, W., 322, 323
Robertson, 359
Rose, W. N., 480, 482, 485
Rosenhain, W., 372, 397, 415, 433, 465
Roth, 340, 507
Runge, C., 334

S

Sanden, K., 146, 334
Sanford, S., 255
Schüle, 518
Schwinning, 23
Searle, G. F. C., 402
Sears, T. E., 344
Seehase, 421
Smith, J. H., 485
Smith, T. H., 343
Southwell, R. V., 166, 248, 249
Spangenberg, 461
Stanton, T. E., 418, 435, 467, 480, 494, 519
Stodola, A., 306, 319, 322, 325, 518
Stribeck, G., 23, 424
Stromeyer, 491
St. Venant, 33, 62, 273, 281, 344, 350, 500
Sundberg, K., 21

T

Tanaka, Y., 92
Taylor, G. T., 46
Tetmayer, L., 167
Thomas, W. N., 11, 483
Todhunter, 33, 401
Trefftz, E., 47
Turner, T., 454

U

Unwin, W. C., 444, 451, 452, 517

V

Van der Fleet, A. P., 156
Velikhow, P. A., 418
Voight, W., 344

W

Weber, 401
Wehage, 501
Welter, 385, 389
Wertheim, 402
Westergaard, H. M., 161, 288, 291
Whittemore, H. L., 22
Willers, F. A., 36
Wilson, 482
Winkler, E., 216
Wöhler, 460, 485

Z

Zacharais, L., 31
Zimmermann, A., 136

INDEX

A

Alloy steel, effect of heat-treatment on fatigue test results of, 473
  effect of heat-treatment on impact test results of, 430
  effect of heat-treatment on tensile test results of, 377
  fatigue tests on, 472
  hardness tests on, 447
  high temperature impact tests on, 427
  high temperature tensile tests on, 387
  hysteresis in, 408
  impact tests on, 430
  overstrain of, 395
  tensile tests on, 376
Alloys, light, 379
Amorphous, theory, 414
Amplitude, of vibrations, 330
Approximate method of determining critical load, 169
  of figuring frequency of vibrations, 318
Arches, buckling of circular, 247
Assembly stresses in built-up cylinders, 254

B

Ball, hardness, 446
Balls and rollers, 21
Barba's Law, 362
Bars, curved, Chap. IX, 216
  on elastic foundations, Chap. VI, 133
Beams, Chaps. III, IV, V, VI
  cantilever, 74
  continuous, 112
  deflection of, Chap. IV, 71
  normal stresses in, 62
  of variable cross-section, 68, 90, 105
  on elastic foundation, 133
Beams on three supports, 110
  one end built-in, the other simply supported, 99
  principal stresses in, 67
  shearing stresses in, 63
  simply supported, 71
  stresses in, Chap. III, 50
  with built-in ends, 102, 105
  with overhanging ends, 87
Bending, and direct stresses, Chap. VII, 153
  and twist, combined, Chap. VIII, 183
  beyond elastic limit, 54, 57
  moment, 59
  of bars on elastic foundation, Chap. VI, 133
  of bi-metallic strip, 58
  of continuous beams, 112
  of crankshafts, 188
  of curved bars, Chap. IX, 216
  of frames, 105, 124, 125, 169, 243
  of T beam, 56
  of thin plates, Chap. X, 260
  of thin strips, 52
  potential energy of, 53
  principle of superposition for, 77
  pure, 50
  theory of, Chaps. III, IV, V, VI
Buckling, approximate theory of, 169
  of a circular ring, 246
  of bars of variable cross-section, 175
  of built-up sections, 294
  of circular arch, 247
  of circular tubes, 248
  of compression member, 165
  of effect of shearing force on, 176
  of latticed struts, 176
  of pillar uniformly loaded, 171
  of rectangular frame, 169
  of rectangular plates, 291
  of tubular sections, 166

C

Cantilever, beam, 74
  deflection of, 81, 86, 88, 90, 93
Carbon steel, effect of annealing and normalizing on tensile properties of, 372
  effect of carbon on the tensile properties of, 371
  effect of heat-treatment on tensile properties of, 375
  fatigue tests on, 468
  hardness tests on, 447
  high temperature impact tests on, 427
  high temperature tensile tests on, 383
  impact tests on, 428, 436
  limitation of, 376
  overstrain of, 392
  structure of, 374
  tensile tests on, 371
Castings, steel (*see* Steel castings).
Cast iron, compression tests on, 367
  effect of high temperature on the tensile strength of, 391
  fracture of, 368, 500
  tensile tests on, 500
Castigliano, theorem of, 119
Chemical analysis and tensile tests results, 371
Circular hole, in rotating discs, 305
  in tension member, 9, 237
  in twisted shafts, 43
  with a bead, 239
Circular plate, loaded in the center, 279
  symmetrically loaded, 273
  uniformly loaded with clamped edge, 276
  uniformly loaded with supported edge, 277
  with concentric loading, 281
  with a hole at the center, 284
Circular ring, bending by two opposite forces, 232
  buckling of, 245
  deflection curve of, 229
  stresses in rotating, 297, 300
Clapeyron's theorem of three moments, 113
Cold work effects, 396, 476
Collapse of tubes under external pressure, 248
Column empirical formulae, 167
  Rankin formula, 168
  theory, 164
Combined bending and direct stresses, Chap. VII, 153
  bending and twist, 183
  stresses, 11
  stresses represented by Mohr's circle, 13
Compound cylinders, 253, 254
Compression, eccentric, 153
  of balls and rollers, 23
  of prismatical bars, 1
Compression, failure of cast iron, 369
  failure of concrete, 370
  failure of steel, 366
  failure of wood, 370
  of brittle material, 367
  of ductile material, 366
Compression test, Chap. XII, 365
  stages of the, 367
Concrete, compression of, 370
Cone hardness, 451
Conical, spring, 32
  tank, 19
Continuous beam, 112
  with the supports not on the same level, 113
Contraction lateral, 2
Crankshaft, bending in the plane of the throw, 190
  bending in the plane perpendicular to the throw, 193
  multi-throw, 199
  multi-throw under bending, 207
  multi-throw under twist, 204
  single throw, 188
  twist of simply supported throw, 195
  twist of throw clamped at journals, 198
Critical load, 155
  determination by energy method, 169
Critical pressure for a circular ring, 245
  compressive stress, 165
Critical speed, 300
  of rotating shafts, 319
Curvature of beams, 51, 71

Curved bars, bending stresses in, 218
  deflection of, 226
  neutral axis in, 223
  of circular cross-section, 222
  of rectangular cross-section, 220
  of trapezoidal cross-section, 222
  T and I cross-sections, 223, 226
  theory of bending, Chap. IX, 216
  with circular axis, 229
  with small initial curvature, 230
Curved tubes, of circular cross-section, 255
  of rectangular cross-section, 258
  theory of bending, 255
Cylinder, built-up, 253, 254
  deformation of, 252
  shrink fit pressure in, 253
  stresses in, 251
  thick, theory of, 249
Cylinder, thin, 19
Cylindrical boiler, 19
Cylindrical tube, buckling under external pressure, 245
  deformation symmetrical about the axis, 143
  thermal stresses in, 146
  with reinforcing rings, 145

D

Damping, proportional to velocity, 324
  constant, 327
Deflection curve, approximate expressions, 156, 163, 164
  as funicular polygon, 82
  of a bar on elastic foundation, 133
  of a bar with small initial curvature, 230
  of a circular ring, 229
  represented by a trigonometrical series, 129
Deflection of beams, Chap. IV, 71
  cantilever, 74, 81, 86, 88
  due to impact, 346
  due to shearing force, 94
  from bending moment diagram, 84
  graphical determination of, 82
  of variable cross-section, 90
  on elastic foundation, Chap. VI, 133
  under direct and bending load, Chap. VII, 153
Deflection of beams uniformly loaded, 78
  with overhanging ends, 87
  with supported ends, 71, 89
Deflection of helical springs, 31, 32, 209, 214
  of leaf-type spring, 92
Deflection of plates, circular having central hole, 284
  circular with clamped edge, 277
  circular with supported edge, 279
  rectangular, 288
Deflection of rails, 141, 336
Diagrams of bending moment, 60, 61
  of shearing force, 60, 61
Discs, rotating, constant thickness, 301
  varying thickness, 306
Ductility and fillets, 361
Dynamical effect of loading (*see* Impact).

E

Eccentric longitudinal loading, 153
Elastic after effects, 401
Elastic limit, definition of, 357
  determination of, 357
Elastic properties, effect of speed and temperature on the, 383
  effect of speed on the, 381
  effect of temperature on, of alloy steel, 387, 388
  effect of temperature on, of carbon steel, 383, 386
  effect of temperature on, of non-ferrous metal, 389
  of alloy steel, 377
  of carbon steel, 372
  tables of, 522, 523, 524
Elastic stage of tensile test, 356
Elastic strain, energy of twist, 29
  of bending, 53, 117
Elasticity, 360
  effect of temperature on modulus of, 384, 388, 389
  modulus of, 1, 361
Elliptical cross-section, shaft of, 33
  ring, 244
Elliptical hole in tension member, 9
  in twist, 43

Elongation in simple tension, 2, 352
  definition of, 362
  effect of high temperature on the values of 386, 387, 388
  measurement of, 362
  of cylindrical bars, 362
  of rectangular bars, 363
  under combined stress, 12, 17
  value, influence of position of fracture on the, 364
Endurance limit, definition of, 468
Energy method in column theory, 169
Energy, potential, of bending, 53, 117
  of twist, 29
Equation of three moments, 113
Euler's column formulae, 164
  limitations, 165
Exponential law, 368
Extensometer, Ewing, 355
  Martens, 355

F

Factor of safety, 168, 515
Fatigue, Chap. XVI, 460
  hysteresis and, 462
  phenomenon of, 465
  properties, of carbon steel, 528
    alloy steel, 529
    non-ferrous metal, 531
    steel castings, 530
  tests on carbon steel, 468
    cold worked material, 476
    effect of form of test bar on, 480
    effect of speed on, 485
    effect of surface finish on, 482
    effect of temperature on, 486
    non-ferrous metal, 476
    on alloy steel, 472
    on steel castings, 473
    short time, by impact method, 492
    short time, by strain method, 487
    short time, by temperature method, 490
    significance of, 496
  with complete stress reversal, 466
  with variation of stress, 477
Flattening of the section of thin tube, 256
Flexural rigidity, 53
Flywheel rim, stress in, 234
Forced vibrations, 328
  amplitude of, 330
Frames, 105, 124
  buckling of rectangular, 169
  symmetrically loaded, 106
  under uniform pressure, 243
  unsymmetrically loaded, 108
Frequency of vibrations, 312
Funicular curve, equation of, 83

G

Geiss theory, 403
Generalized force, 118
Graphical representation of combined stress, 13
  determination of deflection curve, 82
Grapho-analytical method of calculating deflections, 84
Grooves, in bending, 70
  in tension member, 9
  in twist, 42

H

Haigh theory, 506
Hardness, Chap. XV, 444
  ball method of determining, 446
  cone method of determining, 451
  impact method of determining, 452
  indentation, 444
  pendulum method of determining, 453
  prism method of determining, 444
  scratch method of determining, 454
  test, significance of, 458
    time effect on, 447
Helical springs, close-coiled, 30, 31
  open-coiled, 209
Hole, circular, in tension member, 9, 237
  circular or elliptical, in twisted shaft, 43
  elliptical tension member, 9
  reinforced, 239
Holes and grooves in bending, 70
Hollow shaft, 30
Hook, stress in, 225
Hooke's law, 2, 356

Hydrodynamical analogy in torsion, 42
Hysteresis looping in metals, 406
  in crystals, 409

I

Imaginary loading in the theory of bending, 83
Impact, effect of the mass of the structure, 348
Impact hardness, 452
Impact in bending, 345
Impact in tension, 344
Impact in twist, 347
Impact test, Chap. XIV, 418
  effect of dimensions of test bar in the, 424
  effect of heat-treatment in, 429
  form of test bar for, 422–435
  fractures in, 433, 438
  friction effect in the, 420
  notch brittleness in the, 433
  notched bar, 421
  repeated blow, 434
  significance of, 443
  single blow, 427
  speed effects in, 425
  stress measurement in the, 419
  temperature effects in, 426, 442
  unnotched bar, 418
Inertia, moment of, 52
Influence line, 128
Internal stress, 404, 411

L

Lame's theory of thick cylinders, 249
Lateral contraction, 2
Lateral loads on struts, 156
  on tie rods, 159
Least work, theorem of, 123
Line of influence, 128
Local stress, due to concentrated force, 62
  due to shearing force, 66
Long columns, 164

M

Membrane analogy in torsion, 44
Middle plane of a plate, 269
Modes of vibration, 312
Modulus of elasticity, 1, 360
  of foundation, 133
  of rigidity, 15
  of section, 52
Mohr circle, 13, 504
  theory, 503
Moment, bending, 59
  of inertia, 52

N

Natural vibration, 312
Neutral axis, 50
  in curved bars, 224, 225
Neutral surface, 50, 269
Non-ferrous alloy, effect of temperature on the tensile results of, 389
  fatigue tests of, 476
  hysteresis in, 409
  tensile tests on, 379

O

Overstrain, discussion of, 392
  in high carbon steel, 395
  in low carbon steel, 392
  recovery after, 393

P

Parabolic law, 368
Pendulum test, 453
Period of vibration, 314
Photo-elastic method, 9
Pillars, 164
Pipes, circular, 143
  bending of, 255
  buckling of, 248
  reinforced, 144
Piston, ring, 240
  bending of, 287
Plastic stage of tensile test, 356
Plate, bending into a cylindrical surface, 260
  buckling of, 291
  circular, loaded in the center, 279
  circular, symmetrically loaded, 273
  circular, with a central hole, 284
  circular, with concentric loading, 281

Plate, rectangular, 288
Plate, uniformly loaded, with clamped edge, 276
Plate, uniformly loaded, with supported edge, 277
Poisson's ratio, 2
Potential energy of deformation, 29, 53, 117
Principal axes of inertia, 53
  flexural rigidity, 53
  planes of flexure, 53
  stresses in beams, 67
  stresses in shafts, 184
Principle of superposition in bending. 77, 137
  of least work, 123
Proof stress, 360
Proportional limit, definition of, 357
  determination of, 357

Q

Quenching effects, 400

R

Railroad track stresses, 141
  dynamical, 334
Rankine's formula for struts, 168
Reciprocal theorem, 126
Rectangular plates, 288
  bucking of, 291
Reduction of area, definition of, 364
  effect of high temperature on the value of, 386, 387, 388
  measurement of, 364
Redundant fastening, 118
  reactive element, 98, 118
Resistance to shock, 344
Rigidity, modulus of, 15
Rings, circular, bending by two opposite forces, 232
  circular, buckling of, 245
  elliptical, 244
  stresses in rotating ring, 297, 300
  symmetrical, submitted to uniform pressure, 242
  with parallel sides and semi-circular ends, 244
Rollers and balls, 21
Rotating discs, 301
  of variable thickness, 306
  solid, 304
  with a hole in the center, 302

S

Scleroscope, 452
Scratch hardness, 454
Shafts, of circular cross-section, 26
  of non-circular cross-section, 32
  of tubular sections, 47
  of variable cross-section, 35
  under bending and twist, 183
Shear, pure, 14
  in beams, 63
Shear theory, 498
  application to thick cylinders, 254, 510
    to bending and twisting of shafts, 184, 509
Shearing forces in bending, 60
  effect on the deflection of, 94
Shells, 17
Shocks, resistance to, 344
Shrink-fit stresses, 254
Simple bending, 50
Spherical shell, thin, 20
Spring, helical close-coiled, 30
  helical open-coiled, 209
  leaf-type, 92
Square plates, 288
  shafts, 33
Stability, elastic, 170, 520
Steel castings, fatigue tests on, 473
  tensile tests on, 373
Strain method of fatigue testing, 487
Stress strain relations, 12, 17, 356
  energy, 117
Stresses, combined, 11, 497
  concentration of, 9, 40, 43, 44, 70, 480
  due to change of temperature, 2, 3, 4, 5, 58, 102, 146, 272
  oblique, 2
  principal, 67, 183
  shear, 14, 507
  shearing in bending, 63
  simple, 1, 497

Struts, approximate solution, 161
  laterally loaded, 156
  with eccentric load, 153

T

Temperature effects on the elastic properties of non-ferrous metal, 389
  on the elastic properties of steel, 383
  on the fatigue properties of steel, 486
  on the impact properties of steel, 426, 429, 442
  on the strength of cast iron, 391
  on the strength properties of non-ferrous metals, 389
  on the strength properties of steel, 388
Temperature stresses, 2, 3, 4, 5, 58, 102, 146, 272
Tensile failure of cast iron, 500
  of steel, 500
Tensile tests, at high temperature, 383
  effect of carbon on the results of the, 371
  effect of speed and temperature on the results of the, 382
  effect of speed on the results of the, 380
  effect of temperature on the results of the, 383
  on alloy steel, 376, 523
  on carbon steel, 371, 522
  on cold worked steel, 397
  on non-ferrous metal, 379, 526
  on steel castings, 373, 524
  on wire, 525
  significance of the, 365
  stages of the, 356
Tension, Chap. XII, 353
Test bar proportions in tensile test, 362, 372
  fatigue test, 467
  in compression test, 367
  in impact test, 424
Theory of strengths, Chap. XVIII, 397
  application to bending and twist, 509
  application of Mohr theory, 511
  application to simple tension, 507
Theory of strengths, application to thick cylinder, 510
  limitations of the, 506
  maximum strain, 500
  maximum stress, 498
  Mohr, 503
  other, 504
  shear, 501
Theorem of three moments, 113
  of least work, 123
  reciprocal, 126
Thick cylinder, 249
Thin cylinders, 19, 143, 245
  curved tubes, 255
Thrust on columns, 164
Tie rods laterally loaded, 159
Time effect, 401
Torque moment, 26
Torsion, Chap. II, 26
  beyond elastic limit, 28
  hydrodynamical analogy in, 42
  of shafts of circular section, 26
    of non-circular section, 32
    of tubular section, 47
    of variable cross-section, 35
  potential energy of, 29
Torsional rigidity, 34
  vibrations, 337
Twisting moment, 26

U

Ultimate strength, definition of, 361
  effect of high temperature on, 388
  in shear, 29
  measurement of, 361
  relation between hardness and, 458
  significance of, 362

V

Vessels subjected to internal pressure, 17
Vibrations of elastic systems, 312
Vibrations, approximate method of figuring frequency of, 318
  damped, 324
  forced, 328
  of bridges and ships, 324

670126697

Vibrations of elastic systems of rails, 334
  of a system with one degree of freedom, 313
  of a wedge, 323
  Rayleigh-Ritz method of figuring frequency of, 322
  torsional, 337

W

Whirling (critical speed) of shafts, 319
Working stress for buckling, 520
  dynamic loading, 516
Working stress for impact, 521
  static loading, 515
  vibration, 520
Working stresses, Chap. XVIII, 513

Y

Yield point, arbitrary, 359
  definition of, 359
  determination of, 359
  effect of high temperature on, 384
  phenomenon, 359
  upper and lower, 359

TA 350
T58
c.3

1 670126697

BEVIER ENGINEERING LIBRARY

DATE DUE

~~V.613358~~33
~~Apr.16~~
SEP 3 0 1993
OCT 2 8 1993
DEC 2 1993
DEC 1993
APR 1 2 1994
JAN 2 1995
APR 0 1997

DEC 2 2 1997
JAN 0 8 1999
9/5/06
DEC 1 6 2008
JAN 1 2 2011
APR 2 7 2011
APR 3 0 2011

GAYLORD
PRINTED IN U.S.A.